Technische Universität Kaiserslautern
Fachbereich Chemie
Fachrichtung Lebensmittelchemie / Toxikologie

Effects of Polychlorinated Dibenzo-*p*-Dioxins, Polychlorinated Dibenzofurans, and Polychlorinated Biphenyls in Human Liver Cell Models (*in vitro*) and in Mice (*in vivo*)

Vom Fachbereich Chemie der Technischen Universität Kaiserslautern
zur Verleihung des akademischen Grades
„Doktor der Naturwissenschaften“
genehmigte

Dissertation
(D386)

vorgelegt von
Diplom-Lebensmittelchemikerin
Christiane Lohr

Betreuer der Arbeit: Prof. Dr. Dr. D. Schrenk

Kaiserslautern 2013

Eröffnung des Promotionsverfahrens: 27. Juni 2012

Tag der wissenschaftlichen Aussprache: 25. Oktober 2013

Promotionskommission:

Vorsitzender: Prof. Dr. W. Thiel
1. Berichterstatter: Prof. Dr. Dr. D. Schrenk
2. Berichterstatter: Prof. Dr. M. van den Berg

Der experimentelle Teil der vorliegenden Arbeit entstand im Zeitraum von Mai 2009 bis Juli 2012 im Fachbereich Chemie, Fachrichtung Lebensmittelchemie und Toxikologie an der Technischen Universität Kaiserslautern im Arbeitskreis von Prof. Dr. Dr. Dieter Schrenk.

Table of Contents

Abstract

Polychlorinated dibenzo-*p*-dioxins, dibenzofurans, and polychlorinated biphenyls are persistent environmental pollutants which ubiquitously occur as complex mixtures and accumulate in the food and feed chain due to their high lipophilic properties. Of the 419 possible congeners, only 29 share a common mechanism of action and cause similar effects, the so called dioxin-like compounds. Dioxin-like compounds evoke a broad spectrum of biochemical and toxic responses, i.e. enzyme induction, dermal toxicity, hepatotoxicity, immunotoxicity, carcinogenicity as well as adverse effects on reproduction, development, and the endocrine system in laboratory animals and in humans. Most, if not all, of the aforementioned responses, are mediated by the aryl hydrocarbon receptor. In the present work, the elicited biochemical effects of a selection of dioxin-like compounds and the non dioxin-like PCB 153 were examined in mouse (*in vivo*) and in human liver cell models (*in vitro*). Emphasis was given to the main contributors to the total toxic equivalents in human blood and tissues TCDD, 1-PnCDD, 4-PnCDF, PCB 118, PCB 126, and PCB 156, which likewise contribute about 90 % to the dioxin-like activity in the human food chain.

Three mouse *in vivo* studies were carried out aiming to characterize the alterations in hepatic gene expression as well as the induction of hepatic xenobiotic metabolizing enzymes after single oral dose. Based on the results obtained from mouse 3-day and 14-day studies, the seven test compounds can be categorized into three classes; the ones which are 'pure' AhR ligands (TCDD, 1-PnCDD, 4-PnCDF, and PCB 126) or solely CAR inducers (PCB 153), and the ones which are AhR/CAR mixed-type inducers (PCB 118, PCB 156). Moreover, the analysis of hepatic gene expression patterns after a single oral dose of either TCDD or PCB 153 revealed that the altered genes fundamentally differed. Profiling of significantly altered genes led to the conclusion that changes in gene expression were associated with different signalling pathways, in fact by AhR and CAR.

For investigating the role of the AhR in mediating biological responses, several experimental approaches were carried out, such as the analysis of blood plasma metabolites in *Ahr* knockout and wild-type mice. Genotype specifics and similarities were determined by HPLC-MS/MS analysis. Several plasma metabolites could be identified in both genotypes, but also differences were detected. Furthermore, an *in vivo* experiment was performed aiming to characterize AhR-dependent and -independent effects in female *Ahr* knockout and wild-type mice. For this purpose, mice received a single oral dose of TCDD and were killed 96 h later. Microarray analysis of mouse livers revealed that although the *Ahr* gene was knocked out in $Ahr^{-/-}$ mice, the quantity of affected genes were in the same order of magnitude as for $Ahr^{+/+}$ mice, but the pattern of altered genes distinctly differed. In addition, the relative liver weights of TCDD-treated $Ahr^{+/+}$ mice were significantly increased which led to the conclusion, that TCDD induced the development of hepatic steatosis in female *Ahr* wild-type.

The performed *in vitro* experiments aimed to characterize the effects elicited by selected DLCs and PCB 153 in human liver cell models by the use of HepG2 cells and primary human hepatocytes. In general, primary human hepatocytes were less responsive than HepG2 cells. This was not only observed in EC values derived from EROD assay, but also regarding microarray analysis in terms of differently regulated genes. *In vitro* REPs gained from both

liver cell models widely confirmed the current TEFs, but some deviations occurred. The comparison of the TCDD-altered genes in both human cell types revealed that only a considerably small number of genes was in common up regulated by both human liver cell models, such as the established AhR-regulated highly inducible cytochrome P450s *1A1*, *1A2*, and *1B1* as well as other AhR target genes. Although the overlap was rather small, the TCDD-induced genes could be consistently associated with the broad spectrum of established dioxin-related biological responses. The gene expression pattern in primary human hepatocytes after treatment with selected DLCs (TCDD, 1-PnCDD, 4-PnCDF, and PCB 126) and PCB 153 was additionally characterized by microarray analysis. The highest response in terms of significantly altered genes was determined for TCDD, followed by 4-PnCDF, 1-PnCDD, and PCB 126, whereas exposure to PCB 153 did not evoke any significant changes in gene expression. The pattern of significantly altered genes was very homogenous among the four congeners. Genes associated with well-established DLC-related biological responses as well as novel dioxin-inducible target genes were identified, whereby an extensive overlap in terms of up regulated genes by all four DLCs occurred. In conclusion, the results from the *in vitro* experiments performed in primary human hepatocytes provided fundamental insight into the congeners' potencies and caused alterations in gene expression patterns. The obtained findings implicate that although the extent of enzyme inducibilities varied, the gene expression patterns are coincidental. Microarray analysis identified species-specific (mouse vs. human) as well as model-specific (*in vitro* vs. *in vivo* and transformed cells vs. untransformed cells) differences. In order to identify novel biomarkers for AhR activation due to treatment with dioxin-like compounds, five candidates were selected based on the microarray results i.e. *ALDH3A1*, *TIPARP*, *HSD17B2*, *CD36*, and *AhRR*. Eventually, *ALDH3A1* turned out to be the most reliable and suitable marker for exposure to DLCs in both human liver cell models eliciting the highest mRNA inducibility among the five chosen candidates. In which way these species- and cell type-specific markers are involved in the dioxin-elicited toxic responses should be further characterized *in vivo* and *in vitro*.

Deutsche Zusammenfassung

Polychlorierte Dibenzo-*p*-Dioxine, Dibenzofurane und polychlorierte Biphenyle sind persistente Umweltkontaminaten, welche als komplexe Gemische ubiquitär vorkommen und sich aufgrund ihrer lipophilen Eigenschaften in der Nahrungskette anreichern. Von den 419 möglichen Kongeneren teilt nur eine verhältnismäßig kleine Gruppe von 29 Verbindungen den gleichen Wirkmechanismus und das gleiche biologische Wirkspektrum, die sogenannten Dioxin-artigen Verbindungen. Dioxin-artige Verbindungen verursachen eine Vielzahl von biochemischen und toxischen Effekten, z. B. die Induktion von Enzymen, dermale Toxizität, Lebertoxizität, Immuntoxizität, und Kanzerogenität. Aber auch die Beeinträchtigung der Fortpflanzung, der normalen Entwicklung und des Hormonhaushalts konnten im Tiermodell und am Menschen beobachtet werden. Die meisten, wenn nicht sogar alle Wirkungen werden durch die Bindung der Dioxin-artigen Kongenere an den Arylhydrocarbon Rezeptor hervorgerufen. In der vorliegenden Arbeit, wurden die biochemischen Effekte durch Behandlung mit einer Auswahl Dioxin-artiger Verbindungen sowie von PCB 153, ein nicht Dioxin-artiges polychloriertes Biphenyl, im Mausmodell (*in vivo*) und in humanen Leberzellmodellen (*in vitro*) untersucht. Im Mittelpunkt standen sieben Kongenere, TCDD, 1-PnCDD, 4-PnCDF, PCB 118, PCB 126, PCB 153 und PCB 156, welche mit ca. 90 % den größten Anteil zur gesamten Dioxin-Aktivität in der Nahrungskette beisteuern. Im Vordergrund der *in vivo* Mausstudien stand die Untersuchung der Veränderungen in der Expression hepatischer Gene sowie die Überprüfung der möglichen Induktion hepatischer fremdstoffmetabolisierender Enzyme nach einmaliger oraler Gabe der Testsubstanzen. Die sieben getesteten Kongenere können aufgrund der erhaltenen Resultate aus den 3-Tage und 14-Tage Mausstudien in drei Klassen eingeteilt werden: „reine“ AhR Liganden (TCDD, 1-PnCDD, 4-PnCDF, PCB 126), CAR Induktoren (PCB 153) sowie diejenigen, die sowohl den AhR als auch CAR aktivieren können (PCB 118, PCB 156). Zusätzlich wurde der mögliche Einfluss auf die Expression hepatischer Gene nach einmaliger oraler Gabe von TCDD und PCB 153 mit Hilfe der Microarrays untersucht. Es konnte gezeigt werden, dass die Art und die Anzahl der beeinflussten Gene sich grundlegend unterscheiden und unterschiedlichen Signalwegen (AhR und CAR) zugeordnet werden konnten. Des Weiteren wurde die physiologische Rolle des AhR sowie dessen Einfluss auf die TCDD-induzierten Veränderungen des Genexpressionsmusters in der Mausleber näher untersucht. Durch die HPLC-MS/MS-gestützte Untersuchung des Blutplasmas von *Ahr* Wild-Typ und Knockout Mäusen konnten Genotyp-spezifische Besonderheiten und Gemeinsamkeiten bestimmt werden. Mit Hilfe der etablierten Analysemethode war es möglich einige Plasmametabolite in beiden Genotypen zu identifizieren, aber auch spezifische Unterschiede konnten nachgewiesen werden. Darüber hinaus, wurde eine *in vivo* Mausstudie durchgeführt, um AhR-abhängige und AhR-unabhängige Effekte zu charakterisieren. *Ahr* Knockout und Wild-Typ Mäusen wurde TCDD einmalig oral verabreicht und die Tiere nach 96-stündiger Exposition getötet. Die anschließende Microarrayanalyse der Mauslebern zeigte, dass obwohl das *Ahr* Gen in den *Ahr* Knockout Mäusen nicht exprimiert war die Anzahl der durch TCDD-Behandlung beeinflussten Gene in derselben Größenordnung lag als bei den Wild-Typ Mäusen, jedoch das Genexpressionsmuster in der Leber sich grundlegend unterschied. Die TCDD-induzierten Veränderungen auf hepatischer Genexpressionsebene von *Ahr* Wild-Typ

Mäusen sowie das erhöhte relative Lebergewicht der Tiere ließen die Schlussfolgerung zu, dass TCDD im vorliegenden Fall zu Entwicklung einer Fettleber in Wild-Typ Mäusen geführt hat. In den *in vitro* Versuchen sollten die Auswirkungen einer Reihe Dioxin-artiger Verbindungen und PCB 153 in menschlichen Leberzellmodellen (HepG2 Zellen und primäre humane Hepatozyten) untersucht werden. Allgemein konnte gezeigt werden, dass primäre humane Hepatozyten weniger sensitiv auf die Behandlung mit den Testsubstanzen reagiert haben als die immortalisierte Leberkarzinomzelllinie HepG2. Das wurde nicht nur anhand der EC-Werte aus dem EROD Assay beobachtet, sondern auch anhand der Anzahl veränderter Gene, welche mittels Microarray analysiert wurden. Die *in vitro* REPs, abgeleitet aus den Versuchen in den Leberzellmodellen, bestätigten überwiegend die aktuellen TEFs, jedoch wurde in einigen Fällen Abweichungen beobachtet. Der Vergleich TCDD-induzierter Veränderungen auf Genexpressionsebene in beiden Leberzellmodellen zeigte, dass nur eine verhältnismäßig kleine Anzahl von Genen übereinstimmend hoch reguliert wurde u. a. die etablierten AhR-regulierten, hoch induzierbaren Cytochrom P450 *1A1*, *1A2*, und *1B1* sowie weitere etablierte AhR Zielgene. Diese hoch regulierten Gene konnten mit den vielfältigen etablierten biologischen Wirkungen von Dioxinen in Verbindung gebracht werden. Weiterhin wurde die Veränderungen der Genexpression in primären humanen Hepatozyten nach Behandlung mit ausgewählten Kongeneren (TCDD, 1-PnCDD, 4-PnCDF und PCB 126) sowie PCB 153 untersucht. TCDD verursachte die größte Anzahl an Veränderungen auf Genexpressionsebene, gefolgt von 4-PnCDF, 1-PnCDD und PCB 126, wohingegen die Behandlung mit PCB 153 keinen Einfluss auf die Genexpression zeigte. Ein Vergleich der durch die vier Kongenere hoch regulierten Gene lieferte ein homogenes Bild mit einer großen Anzahl übereinstimmend induzierter Gene, wobei sowohl Gene, welche mit den biologischen und toxischen Wirkungen von Dioxinen in Zusammenhang gebracht werden, als auch neue Dioxin-induzierbare Gene identifiziert werden konnten. Zusammenfassend konnte gezeigt werden, dass obwohl das Ausmaß der CYP1A1 Induzierbarkeit abhängig vom Leberspender interindividuell stark variierte, die Veränderungen auf Ebene der Genexpression eine enorme Übereinstimmung aufwiesen. Weiterhin konnten mittels Microarrayanalyse Spezies-Abhängigkeiten (Maus vs. Mensch), als auch Modell-Abhängigkeiten (*in vitro* vs. *in vivo* sowie transformierte Zellen vs. nicht-transformierte Zellen) nachgewiesen werden. Die Suche nach neuen Biomarkern für die Exposition gegenüber Dioxin-artigen Verbindungen bildete einen weiteren Schwerpunkt der vorliegenden Arbeit. Der Vergleich der Microarrays führte zu fünf Spezies- und Zelltyp-spezifischen potentiellen Biomarker-Kandidaten, *ALDH3A1*, *TIPARP*, *HSD17B2*, *CD36* und *AhRR*. Von diesen, stellte sich *ALDH3A1* als der am besten geeignete Marker gegenüber der Exposition mit Dioxin-artigen Verbindungen in beiden humanen Leberzellmodellen heraus, welcher die höchste mRNA Induzierbarkeit unter den ausgewählten Kandidaten besaß. Auf welche Weise diese spezifischen Marker möglicherweise zu den Dioxin-vermittelten toxischen Wirkungen beitragen, sollte anhand weiterer *in vivo* und *in vitro* Experimente untersucht werden.

List of Abbreviations

A	colour intensity
AhR	aryl hydrocarbon receptor
AhRR	aryl hydrocarbon receptor repressor
ALDH	aldehyde dehydrogenase
amu	atomic mass unit
ANOVA	one-way analysis of variance
ARNT	aryl hydrocarbon nuclear translocator
ATSDR	Agency for Toxic Substances and Disease Registry
BCA	bicinchoninic acid
BfR	Bundesinstitut für Risikobewertung
bHLH/PAS	basic-helix-loop-helix Per-ARNT-Sim
BSA	bovine serum albumin
bw	body weight
CAR	constitutive androstane receptor
CCRP	cytoplasmic CAR retention protein
cDNA	complementary DNA
CD36	cluster of differentiation 36
cRNA	complementary RNA
C_T	threshold cycle
CTP	cytidine-5'-triphosphate
CYP	cytochrome P450-dependent monooxygenase
DBD	DNA binding domain
DCC/FBS	dextran-coated charcoal fetal bovine serum
ddH_2O	double-destilled water
DEN	diethyl-N-nitrosamine
DL	dioxin-like
DLCs	dioxin-like compounds
DMBA	7,12-dimethylbenz[a]anthracen
DMEM	Dulbecco's modified Eagle's medium
DMF	dimethylformamide
DMSO	dimethylsulfoxide
DNA	deoxyribonucleic acid
dNTP	desoxynucleotide triphosphate
DTT	dithiothreitol
EDTA	ethylenediaminetetraacetate

EFSA	European Food Safety Authority
e.g.	*[exempli gratia]* for example
EGTA	ethylene glycol tetraacetic acid
EGF	epidermal growth factor
ER	estrogen receptor
EROD	7-ethoxyresorufin-O-deethylase
ESI	electronic spray ionization
et. al	*[et aliae]* and others
ETOH	ethanol
FCS	fetal calf serum
FDR	false discovery rate
g	acceleration of gravity
g	gram
GO	gene ontology
GSH	glutathione
GST	glutathione-S transferase
h	human
h	hour
HEPES	2-[4-(2-hydroxyethyl)piperazin-1-yl] ethanesulfonic acid
hHeps	primary human hepatocytes
HPLC	high performance liquid chromatography
HSD	hydroxysteroid dehydrogenase
HSP	heat shock protein
i.e.	that is
i.p.	intraperitoneal
i.v.	intravenous
I3C	indole-3-carbinol
IARC	International Agency for Research on Cancer
ICZ	indolo-[3,2,-b]-carbazole
kDa	kilodalton
LBD	ligand binding domain
lfc	logarithmic (base 2) fold change
kg	kilogram
m	mouse
mA	milliampere
MeOH	methanol
min	minute

ml	milliliter
MNNG	N-methyl-N9-nitro-N-nitrosoguanidine
mM	millimolar
µM	micromolar
µm	micrometer
µmol	micromol
mRNA	messenger RNA
MS	massspectrometry
n	number of independent experiments
NADH	nicotinamide adenine dinucleotide
NADPH	nicotinamide adenine dinucleotide phosphate
NDL	non dioxin-like
NDMA	N-nitrosodimethylamine
NES	nuclear export signal
ng	nanogram
NLS	nuclear localization signal
nm	nanometer
nM	nanomol
NOAL	no observed adverse effect level
NR	nuclear receptor
NTP	National Toxicology Program
NTP	nucleotide triposphate
oligo(dT)	oligodeoxythymidylic acid
PAGE	polyacrylamide gel electrophoresis
PB	phenobarbital
PBREM	PB responsive enhancer module
PBS	phosphate buffered saline
PCAH	polychlorinated aromatic hydrocarbons
PCB	polychlorinated biphenyls
PCDD	polychlorinated dibenzo-*p*-dioxins
PCDF	polychlorinated dibenzofurans
PCR	polymerase chain reaction
pg	picogram
pH	potential hydrogenii
pM	picomolar
PP2A	protein phosphatase 2A
ppt	parts per trillion

P/S	penicillin/streptomycin
PTFE	polytetrafluorethylene
PVDF	polyvinylidene fluoride
PXR	pregnane X receptor
RT-PCR	quantitative real-time polymerase chain reaction
REP	relative effect potency
RNA	ribonucleic acid
ROS	reactive oxygen species
RP	reversed phase
rpm	revolutions per minute
RT	reverse transcription
RXR	retinoid X receptor
SCF	Scientific Committee on Food
SD	standard deviation
SDS	sodium dodecyl sulfate
sec	second
TAE	tris-acetate-EDTA
Taq	thermus aquaticus
TBS	tris buffered saline
TEF	toxic equivalency factor
TEQ	toxic equivalent
TDI	tolerable daily intake
TIC	total ion current
TIPARP	TCDD-inducible poly (ADP-ribose) polymerase
Tris	tris(hydroxymethyl)aminomethane
UGT	UDP glucoronosyltransferase
UV	ultraviolet radiation
WHO	World Health Organization
w/o	without
wt	wild-type
XAP2	hepatitis B virus X associated protein 2
XRE	xenobiotic responsive element
XREM	xenobiotic responsive enhancer module

Figures

Tables

I Introduction

Humans are daily exposed to a myriad of chemicals either by inhalation, ingestion, or dermal absorption. A class of chemicals, which is in focus of the public attention and research objectives due to industrial incidents and various food scandals are polychlorinated aromatic hydrocarbons (PCAHs).
The family of structurally-related compounds consists of three groups, the polychlorinated dibenzo-*p*-dioxins (PCDDs), dibenzofurans (PCDFs), and biphenyls (PCBs). A total of 419 possible congeners exist, whereas only 7 PCDDs, 10 PCDFs, and 12 non-ortho and mono-ortho PCBs (dioxin-like PCBs) share a common mechanism of action and cause similar biochemical and toxic effects. These 29 dioxins and dioxin-like compounds bind to a transcription factor, the aryl hydrocarbon receptor. It has been established that the aryl hydrocarbon receptor mediates most, if not all, biological and toxicological effects of dioxins and dioxin-like compounds (Holsapple et al., 1991) (Birnbaum, 1994) (IARC, 1997) (Schmidt et al., 1996) (Fernandez-Salguero et al., 1996) (Gonzalez et al., 1998) (Nebert et al., 2000) (Schrenk et al., 1995).
Since dioxins and dioxin-like compounds are highly lipophilic and persistent, they ubiquitously occur as complex mixtures in the environment and in the human food chain, whereby humans are predominantly exposed by food of animal origin such as meat, fish, eggs, milk, and other dairy products (EFSA, 2010). The establishment of emission limit values for dioxins and furans, binding limits for the 29 congeners in food and feed products as well as the monitoring of food and environmental matrices led to the remarkably reduction of exposure levels in most European countries (Liem et al., 2000) (Malisch et al., 2003) (EFSA, 2010) (EFSA, 2012). Nevertheless, various populations such as newborns and infants or humans that are exposed to higher amounts of dioxin-like compounds by occupation or accidents exhibit higher exposure levels than the established tolerable daily intake of 1-4 pg TEQ/kg bw (WHO, 1998) (IARC, 1997) (IARC, 2012).

For improvement of the human risk assessment the European project SYSTEQ was initiated in 2009 which aimed to derive and establish *in vitro* TEFs (REPs) based on data from human and animal *in vitro* systems after exposure to a selection of PCDD/Fs and dioxin-like PCBs. These *in vitro* REPs/TEFs will be compared to novel systemic REPs/TEFs obtained from *in vivo* mouse and rat experiments to clarify species differences and provide important knowledge in extrapolation from the *in vitro* to the *in vivo* human situation. The present thesis provides essential research data about a myriad of congener's potencies, as the available data for most of the 29 dioxin-like compounds is insufficient in human liver cell models. The current work predominantly deals with SYSTEQ research objectives, but also aspires to elucidate the role of the aryl hydrocarbon receptor in mediating the toxicity of dioxin-like compounds in mouse. The presented doctoral thesis has been performed under the supervision of Prof. Dr. Dr. D. Schrenk in the Department of Food Chemistry and Toxicology at the University Kaiserslautern.

II Theoretical Background

II.1 Polychlorinated Dioxins, Furans, and Biphenyls

Polychlorinated dibenzo-*p*-dioxins, polychlorinated dibenzofurans and polychlorinated biphenyls are widespread persistent environmental pollutants. In total possible 75 PCDDs, 135 PCDFs, and 209 PCBs exist depending on the number and position of chlorine atoms-bound to the respective molecule. Amongst the 210 PCDD/F congeners, only 7 PCDDs and 10 PCDFs, with chlorine atoms in the lateral ring positions 2, 3, 7, and 8 of the molecule, cause dioxin-like biological and toxic effects.

All 209 PCBs have the ability to rotate around the phenyl-phenyl-axis. The 209 PCBs are categorized into two groups based on the respective elicited toxicological responses, the small group of 12 dioxin-like PCBs and the large group of 198 non dioxin-like PCBs. 8 mono-ortho and 4 non-ortho substituted PCBs are categorized as dioxin-like compounds because they exhibit a dioxin-like activity and similar toxic responses.

All 29 structurally-related dioxin-like compounds are persistent and bioaccumulate as well as they share a common mechanism of action by binding to the aryl hydrocarbon receptor (AhR) and evoke the same spectrum of biological and toxic responses. The most toxic congener and reference compound for the class of dioxin-like compounds is 2,3,7,8-Tetrachlorodibenzo-*p*-dioxin (TCDD) (IARC, 1997) (Fiedler, 2003) (van den Berg et al., 2006). TCDD represents the best studied congener among the group of dioxin-like compounds.

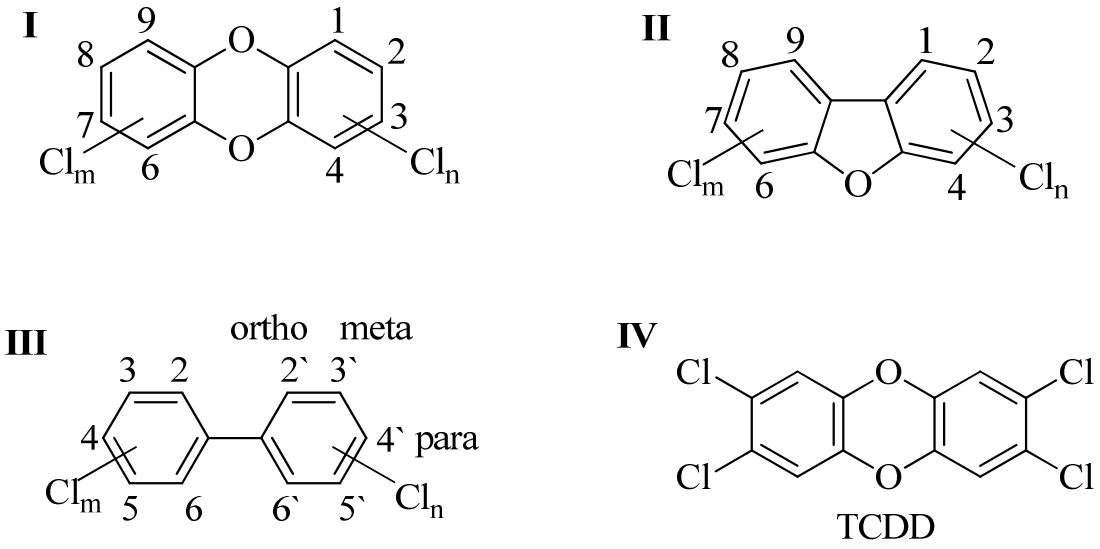

Figure 1. Molecular structures of PCDDs (I), PCDFs (II), and PCBs (III).
Molecular structure of 2,3,7,8-Tetrachlorodibenzo-*p*-dioxin (TCDD) is featured in (IV).

II.1.1 Toxic Equivalency Factors and Total Toxic Equivalence (TEF/TEQ Concept)

Polychlorinated aromatic hydrocarbons (PCDD/Fs and PCBs) usually occur as complex mixtures of congeners in environmental and biological matrices. Therefore, the toxic equivalency concept was developed during the 1980's (OMEA et al., 1985) (NATO, 1988). Each dioxin-like compound is assigned a toxic equivalency factor (TEF) which expresses the relative effect potency (REP) derived from *in vivo* and *in vitro* studies of individual dioxin-like compounds to 2,3,7,8-Tetrachlorodibenzo-*p*-dioxin (TCDD). TCDD is the most toxic compound of the group of dioxin-like congeners and serves as prototype which was assigned a TEF value of 1.0. A compound must fulfil several requirements to be attributed with a TEF value; it has to exhibit structural similarities to PCDD/Fs and bind to the aryl hydrocarbon receptor. Furthermore it must evoke AhR-mediated biochemical and toxic effects and be persistent and accumulate in the food chain (Birnbaum, 1994) (van den Berg et al., 1998) (van den Berg et al., 2006) (Haws et al., 2006). The total toxic equivalent (TEQ) concept was developed for risk assessment and is based on the assumption that the toxic responses elicited by all dioxin-like compounds (DLCs), existing in the examined sample, are additive. The formula for TEQ value calculation is featured in the following equation. The concentration of each DLC is multiplied by its respective TEF and the products are ultimately summed up to obtain the TEQ value of the environmental or biological matrix. The resulting TEQ value estimates the TCDD-like activity of the compound mixture in the analyzed sample.

$$\mathrm{TEQ} = \sum_{i=1}^{n} (C_i \times \mathrm{TEF}_i)$$

With: TEF_i = toxic equivalency factor of the individual congener
n = total numbers of congeners present in the sample
i = individual congener
C_i = concentration of individual congener

During the last three decades the TEF values were evaluated respectively re-evaluated by WHO expert meetings taking into account new published *in vivo* and *in vitro* experiments (Ahlborg et al., 1994) (van den Berg et al., 1998) (van den Berg et al., 2006). Therefore, it is essential for risk assessment that publications state which TEF values were used for calculation of the total TEQ concentration in the given samples.
An overview of the human and mammalian WHO-TEFs of the year 1998 and the current TEF values, re-evaluated by the WHO in 2005, for PCDDs, PCDFs, and dioxin-like PCBs are summarized in Table 1. Publications on the relative effect potencies of dioxin-like compounds often feature significant differences in REP values of the same congener. These differences can be due to various reasons, for instance, they can be based on different study designs (e.g. acute, subchronic, or chronic), species, and addressed endpoints. In publications methods for calculation of relative effect potencies (REPs) differ. Therefore, the WHO expert panel gave general guidelines and criterias for *in vivo* and *in vitro* studies in which REP values are determined (van den Berg et al., 2006).

Table 1. TEF values of PCDDs, PCDFs, and dioxin-like PCBs re-evaluated by WHO in 1998 and 2005. (van den Berg et al., 1998) (van den Berg et al., 2006)

Compound		TEF (WHO, 1998)	TEF (WHO, 2005)
Chlorinated dibenzo-*p*-dioxins			
2,3,7,8-TetraCDD	TCDD	1.0	1.0
1,2,3,7,8-PentaCDD	1-PnCDD	1.0	1.0
1,2,3,4,7,8-HexaCDD	1,4-HxCDD	0.1	0.1
1,2,3,6,7,8-HexaCDD	1,6-HxCDD	0.1	0.1
1,2,3,7,8,9-HexaCDD	1,9-HxCDD	0.1	0.1
1,2,3,4,6,7,8-HeptaCDD	1,6-HpCDD	0.01	0.01
1,2,3,4,6,7,8,9-OctaCDD	OCDD	0.0001	0.0003
Chlorinated dibenzofurans			
2,3,7,8-TetraCDF	TCDF	0.1	0.1
1,2,3,7,8-PentaCDF	1-PnCDF	0.05	0.03
2,3,4,7,8-PentaCDF	4-PnCDF	0.5	0.3
1,2,3,4,7,8-HexaCDF	1,4-HxCDF	0.1	0.1
1,2,3,6,7,8-HexaCDF	1,6-HxCDF	0.1	0.1
1,2,3,7,8,9-HexaCDF	1,9-HxCDF	0.1	0.1
2,3,4,6,7,8-HexaCDF	4,6-HxCDF	0.1	0.1
1,2,3,4,6,7,8-HeptaCDF	1,4,6-HpCDF	0.01	0.01
1,2,3,4,7,8,9-HeptaCDF	1,4,9-HpCDF	0.01	0.01
1,2,3,4,6,7,8,9-OctaCDF	OCDF	0.0001	0.0003
Non-ortho substituted PCBs			
3,3',4,4'-TetraCB	PCB 77	0.0001	0.0001
3,4,4',5-TetraCB	PCB 81	0.0001	0.0003
3,3',4,4',5-PentaCB	PCB 126	0.1	0.1
3,3',4,4',5,5'-HexaCB	PCB 169	0.01	0.03
Mono-ortho substituted PCBs			
2,3,3',4,4'-PentaCB	PCB 105	0.0001	0.00003
2,3,4,4',5-PentaCB	PCB 114	0.0005	0.00003
2,3',4,4',5-PentaCB	PCB 118	0.0001	0.00003
2',3,4,4',5-PentaCB	PCB 123	0.0001	0.00003
2,3,3',4,4',5-HexaCB	PCB 156	0.0005	0.00003
2,3,3',4,4',5'-HexaCB	PCB 157	0.0005	0.00003
2,3',4,4',5,5'-HexaCB	PCB 167	0.00001	0.00003
2,3,3',4,4',5,5'-HeptaCB	PCB 189	0.0001	0.00003

II.1.2 Physicochemical Properties

The physicochemical properties vary widely among polychlorinated dibenzo-*p*-dioxins, furans, and biphenyls (Mackay et al., 2006). Nevertheless, in general they are poorly water soluble, but soluble in organic solvents (for instance dimethyl sulfoxide). Furthermore, they exhibit high oil and fat solubility. They are chemically very stable and are low-flammable compounds. PCBs exhibit a low electrical and high thermal conductivity. Due to their resistance to chemical and biological degradation under normal conditions PCDD/Fs and dioxin-like PCBs are highly persistent and accumulate in the feed and food chain (Lohmann et al., 1998) (Jones et al., 1999) (Cornell, 2005).

II.1.3 Production, Occurrence, and Exposure

PCDDs and PCDFs were never synthesized for commercial purposes, except in small scale for scientific research. Predominantly, they are unintendedly generated in chemical combustion processes such as waste and sewage sludge incinerations as well as in other chemical processes such as paper pulp bleaching or metal smelting and subsequently are released into the environment. PCDD/PCDFs are also unwanted by-products during the synthesis of chlorinated phenols. In particular, TCDD is formed during the manufacturing of 2,4,5-trichlorophenol. 2,3,4-tricholorphenol was utilized to synthesize the herbicide and defoliant 2,4,5-trichlorophenoxyacetic acid being a component of Agent Orange which was used for weed control and defoliation during the Vietnam War (Poland et al., 1982a) (ATSDR, 1998) (Pereira et al., 2004). Additionally, PCDD/Fs are formed as inadvertent by-products during the synthesis of polychlorinated biphenyls. To a lesser extent, they are formed by natural causes such as the partial combustion of organic material, e.g. in forest fires (ATSDR, 1998).

Polychlorinated biphenyls were commercially synthesized due to their physicochemical properties and applied in a wide variety of industrial products such as transformators and capacitors, hydraulic lubricants, heat transfer fluids, adhesives, plasticisers and sealants. PCBs were marketed as mixtures referring to the percentage of the respective chlorine content under several trade names such as Aroclor (Monsanto, USA), Clophen (Bayer, Germany), Kanechlor (Kanegafuchi, Japan), Santotherm (Mitsubishi, Japan) as well as Phenaclor and Pyralene (Prodolec, France). About 55 years after the first manufacturing of PCBs the production, distribution well as the usage was banned in Europe and the USA during the mid 1980's (Alcock et al., 1998) (Fiedler et al., 1995) (Pereira et al., 2004). Due to their widespread usage in various technical applications, PCBs are still released into the environment by leaks of transformators and capacitors as well as from improper waste disposal (Pereira et al., 2004).

Humans are predominantly exposed to TCDD and related compounds primarily through diet, which contributes more than 90 % to the total human exposure. Since PCDD/Fs and PCB accumulate in fat-rich organisms, main sources of PCDD/Fs and DL-PCBs contaminants are lipid-rich food of animal origin; the highest levels were determined in fish, meat, eggs, milk, and other dairy products (EFSA, 2010). Other routes of exposure are by inhalation of air or ingestion of water contaminated with PCDD/Fs and DL-PCBs (Liem et al., 2000).

An overview of the average estimated dietary intakes of PCDD/Fs and DL-PCBs for adults in different countries is presented in Table 2. Estimated dietary intakes presented in Table 2 vary about a factor of three. TEQ values for PCDD/Fs range from 0.5 pg TEQ/kg bw/day in the Netherlands to 1.67 pg TEQ/kg bw/day in the USA, whereby highest PCB-TEQ values were estimated in Japan (1.36 pg TEQ/kg bw/day) and lowest dietary intake levels were assessed for the Netherlands (0.5 pg TEQ/kg bw/day). The differences can be attributed to different calculation methods, different statistical analysis, and different DL-compounds analyzed. Additionally, the dietary habits in food consumption in the countries also contribute to the aforementioned variations of the estimated daily human intakes of TCDD and related compounds (Fattore et al., 2006).

Table 2. Average estimate daily human intakes of PCDD/Fs and DL-PCBs expressed as pg TEQ/kg bw/day. TEQs calculated with WHO_{1998}-TEFs. Thereby, (a) upper bound estimates (b) lower bounds estimates (c) medium bound estimates (d) only non-ortho PCBs analyzed

Country	PCDD/Fs	DL-PCBs	Reference
Italy[(a)]	0.96	1.30	Fattore et al. 2006
Germany	0.7	1.3	Mathar et al., 2003
Belgium[(a)(d)]	1.00	1.04	Focant et al., 2002
Finland[(b)]	0.79	0.74	Kiviranta et al., 2004
The Netherlands[(a)]	0.6	0.5	Baars et al., 2004
France[(a)]	0.5	1.2	Tard et al., 2007
Japan[(a)]	0.89	1.36	Tsutsumi et al., 2001
USA[(c)]	1.67	0.65	Schecter et al., 2001

In 1998 the World Health Organization established a tolerable daily intake (TDI) for dioxins and dioxin-like compounds of 1-4 pg TEQ/kg bw/day. The TDI was calculated by applying an uncertainty factor of 10 to the range of lowest adverse effect levels (LOAELs) 14-37 TCDD pg/kg bw/day for the most sensitive adverse effects from different experimental species. In addition, the animal body burden was included in the TDI calculation. The upper limit of 4 pg TEQ/kg bw/day should be regarded as maximal tolerable intake, whereas the aspired aim is to decrease the human intake levels below 1 pg TEQ/kg bw/day (WHO, 1998).

In all studies presented in Table 2 the estimated TEQs are within the range of established WHO-TDI. Though the tolerable daily intake established by the Scientific Committee on Food (SCF) of 2 pg TEQ (PCDD/Fs and DL-PCBs)/kg bw/day is slightly exceeded in some cases. Recently published results from health monitoring studies revealed that the dioxin intake levels further decreased resulting in estimated dietary intake levels for PCDD/Fs and

DL-PCBs ranging between 0.57 to 1.64 pg TEQ_{WHO05}/kg bw/day for adults in 15 European studies (EFSA, 2012).

The studies summarized in Table 2 only represent the estimated daily intake of an average adult human. Other subpopulations such as newborns and children are exposed to higher PCDD/F and PCB levels due to the maternal body burden and consumption of fat-rich products such as milk and other dairy products. In 2012, the European Food Safety Authority published data from the two monitoring surveys in which the dietary exposure of dioxins and DL-compounds in infants, toddlers, and other children were analyzed. The estimated infant exposure level was 1.17 pg TEQ/kg bw/day in a Bulgarian survey and 1.08 pg TEQ/kg bw/day in an Italian study. Levels for toddlers ranged from 1.25 to 2.54 pg TEQ/kg bw/day assessed in 9 surveys, whereas the daily exposure of the sum of PCDD/Fs and DL-PCBs in older children was in the same order of magnitude (1.08 - 2.49 pg TEQ/kg bw/day) (EFSA, 2012). In all the aforementioned studies human milk was not taken into account. Several studies demonstrated that the TEQ exposure in nursing infants is several orders of magnitude higher than in infants feed with formula (Ulaszewska et al., 2011). The estimated average intake levels of PCDD/Fs and DL-PCBs by human milk was 77 pg TEQ/kg bw/day for an three month-old German infant in the year 2009 (BfR, 2011). This value exceeds the TDI by far, but with the increasing age and body weight the infant exposure levels decrease quickly. Furthermore, since the 1980's levels of dioxins and dioxin-like compounds are steadily declining in human milk in most European countries, whereby a decrease of more than 80 % for the average PCDD/Fs contamination in milk fat was examined in Germany up until 2009 (van Leeuwen et al., 2002) (BfR, 2011) (Focant et al., 2013). This affirmative development could be attributed to the decreased PCDD/F emission, the strict food and feed monitoring and furthermore to a change in human dietary habits.

Since July 2002, maximal limits for PCDDs and PCDFs expressed as WHO-PCDD/F-TEQ using WHO_{1998}-TEFs in food and feed became effective which were set by the Council of the European Commission (IP/02/1669 andIP/02/1670). In addition to the maximum limits for the sum of PCDD/Fs in food and feed, maximum levels for the sum of PCDD/Fs and DL-PCBs were settled as well as recommended action levels, in 2006. In 2011, established maximum levels were adjusted using WHO_{2005}-TEFs and maximum limits for NDL-PCBs expressed as the sum of six indicator PCBs (PCB 28, 52, 101, 138, 153, and 180) were set.

Besides the exposure by food and feed, humans are exposed to dioxins and related compounds by occupation or by industrial accidents (IARC, 2012). In 1976, an explosion of a trichlorophenol reactor led to the release of a cloud containing up to 30 kg TCDD and other toxic components on a chemical plant in Italy. Seveso was the municipal mostly affected by the aerosol cloud, whereupon the tragic incident was called 'Seveso disaster'. The Seveso disaster resulted in the highest known TCDD exposure levels in humans, whereat a median TCDD level of 56 ppt (ranging between 2.5-56000 ppt) was measured in a large female cohort in the most contaminated zones A and B (Eskenazi et al., 2004) (Mocarelli et al., 2008).

II.1.4 Toxicokinetics and Metabolism

The toxicokinetics of PCDD/Fs and dioxin-like PCBs is based on the congener's lipophilicity, metabolism, and binding to CYP1A2 in the liver. TCDD and related compounds are predominantly absorbed through the gastrointestinal tract and to a much lesser extent by inhalative and dermal absorption. Distribution in the organism is mediated by binding of congeners to serum lipids and lipoproteins (van den Berg et al., 1994). TCDD and related compounds are highly lipophilic, whereby lipophilicity increases with chlorination and has impact on the compound's absorption as well as tissue partitioning. Metabolism acts as the rate-limiting step for elimination of these environmental contaminants. Since they are highly persistent, they are slowly metabolized and eliminated. Subsequently they accumulate in liver and adipose tissues of humans and animals (WHO, 1998).

CYP1A2 induction results in the hepatic sequestering of TCDD and related compounds which has been demonstrated among others by the use of transgenic mouse model. *Cyp1a2* knockout mice treated with a single dose of 25 µg [^{3}H] TCDD/kg bw or 300 µg [^{14}C] 4-PnCDF/kg bw exhibited high amounts of the radiolabelled compounds in the adipose tissue, but not in liver four days after administration. In contrast, C57BL/6N mice, which were exposed to the same dosages of the radiolabelled chemicals, featured higher compound concentrations in the liver than in the adipose tissue (Diliberto et al., 1999). Metabolism of PCDD/Fs correlates with the number and position of chlorination. Higher chlorinated congeners are metabolized to a lesser degree than less chlorinated ones (van den Berg., 1994). The toxicity of dioxins and dioxin-like compounds depends on the parent compound and the slow formation of metabolites contributes to the fatal toxic responses as well. Biotransformation of several PCDD/Fs and PCBs has been demonstrated in various animal species in which congeners are primarily epoxidized and subsequently hydroxylated polar metabolites are formed which can be readily glucoronidated and in the following be excreted by bile or kidney (van den Berg et al., 1994) (Peirera et al., 2004).

TCDD is the most toxic congener among the group of dioxins and related compounds, whereas little is known about its metabolism in humans. Sorg and co-workers identified two TCDD metabolites (2,3,7-trichloro-8-hydroxydibenzo-*p*-dioxin and 1,3,7,8-tetrachloro-2-hydroxy-dibenzo-*p*-dioxin) in feces, urine, and serum of a patient after acute TCDD intoxication (Sorg et al., 2009).

The apparent body half-life depends on several factors such as dose, body composition, age, and sex (van Leeuwen et al., 2000). Different PCDDs, PCDFs, and PCBs have different persistence in humans and animals which is reflected in their different reported half-lives (Milbrath et al., 2009). The elimination half-life of TCDD in rodents is normally 2-4 weeks (Rose et al., 1976) (Birnbaum, 1986). In humans, the TCDD elimination half-life has been estimated to range between 7-11 years (Pirkle et al., 1989) (Wolfe et al., 1994) (Milbrath et al., 2009).

II.1.5. Toxicity and Carcinogenicity of TCDD and Related Compounds

TCDD and related compounds evoke a spectrum of biochemical and toxicological responses in different species such as enzyme induction, dermal toxicity, immunotoxicity, hepatotoxicity and carcinogenicity as well as adverse effects on reproduction, development, and the endocrine system has been demonstrated (Holsapple et al., 1991) (Birnbaum, 1994) (Schmidt et al., 1996) (Fernandez-Salguero et al., 1996) (Gonzalez et al., 1998) (Nebert et al., 2000) (Schrenk et al., 1995) (IARC, 1997). Most, if not all, of these biological and toxic effects are mediated by the aryl hydrocarbon receptor (AhR). Elicited responses of DL-compounds range species-, gender-, age-, strain-, organ-, and tissue-dependent. TCDD is the most toxic member of the class of DL-compounds and features the most extensive toxicological database from all DL-compounds (DLCs).
Hence, the following chapters primarily deal with the biochemical and toxic effects of TCDD, preferentially in liver, but studies of other DLCs as well as NDL-PCB 153 are additionally presented.

II.1.5.1. TCDD in Rodents

II.1.5.1.1 Toxicity

One-time administration of TCDD at high doses (lethal or near lethal) causes in rodents a severe body weight loss (up to 50 % of the original body weight) which contributes to the lethality of animals (Moffat et al., 2010). This effect is called wasting syndrome. Up to the present day, the mechanism of the TCDD-induced wasting is still not clarified, but it has been demonstrated that the aryl hydrocarbon receptor is involved in the excessive weight loss, since TCDD does not evoke 'wasting' in *Ahr* knockout mice (Seewald et al., 1984) (Fernandez-Salguero et al., 1996) (Gonzalez et al., 1998).

In rodents, the liver is the organ predominantly affected by TCDD and related compounds. TCDD induces extremely enlarged liver (hepatomegaly) based on hyperplasia and hypertrophy of parenchymal cells in rodents and in various other species (Poland et al., 1982a). Further hepatotoxic effects include alterations in hepatic genes and enzyme induction as well as shift in serum enzyme activities, increased liver weight, hepatic inflammation, necrosis, hepatic steatosis, disruption of hepatic energy metabolism, decreased vitamin A levels, porphyria as well as the impairment of the membrane function, hyperbilirubinemia and hypercholesterolemia in mice and rats (Shen et al., 1991) (Smith et al., 1998) (Niittynen et al., 2002) (Angrish et al., 2011) (Angrish et al., 2013).

The TCDD-induced toxic responses have been associated with AhR-mediated alterations in hepatic gene expression. These changes occur rather quickly, whereas TCDD-elicited toxic effects in rodents such as the wasting syndrome, hepatotoxicity, and lethality usually are developed after a delay period.

One of the established TCDD-induced biochemical responses in rodent livers is the induction of xenobiotic metabolizing enzymes such as CYP1A1, CYP1A2, and CYP1B1 (Nebert et al., 2000). The induction of CYP1A1 is the most sensitive and earliest indicator for exposure to dioxins and DL-congeners (Vanden Heuvel et al., 1993) (Drahushuk et al., 1996). In which way the induction of CYP1A isoenzymes contribute to the adverse effects of TCDD is still not completely clarified. The induction of CYPs could lead to the generation of reactive oxygen species and oxidative stress which has been linked to oxidative DNA damage (Park et al., 1996). CYP1A1 is required for the generation of TCDD-induced cardiovascular superoxide anions in mice livers resulting in endothelial dysfunction as well as hypertension (Kopf et al., 2010).

In addition, TCDD induces the AhR-mediated transcriptional up regulation of other genes linked to phase I and II of the xenobiotic metabolism, summarized as the classical murine AhR gene battery including *Nqo1*, *Aldh3a1*, *Gsta1*, and *Ugt1a6* in liver (Nebert et al., 2000). The respective enzymes are involved in detoxifying processes, i.e. biotransformation of exogenous and endogenous compounds. Furthermore, TCDD alters genes associated with cell development, growth, and differentiation. It has been proven that these processes are regulated by the aryl hydrocarbon receptor (Bock et al., 2006). By the establishment of a new toxicogenomic approach during the last decades, the microarray analysis, it has been possible to identify a large number of genes altered by TCDD in different cell types and tissues which can be linked to TCDD-elicited adverse responses (Boverhof et al., 2006) (Kim et al., 2009) (Dere et al., 2011).

Many recently published toxicogenomic studies aimed to identify the mechanism of the TCDD-induced hepatotoxicity in rodents. In a study performed by Forgacs and co-workers, female ovariectomiced C57BL/6 mice and immature female Sprague-Dawley rats were treated with a single dose of either sesame oil as vehicle or 30 µg/kg bw TCDD for mice and 10 µg/kg bw for rats by gavage and were sacrificed 24, 72, 120, or 168 h post-treatment. Comparative toxicogenomic profiling revealed that the TCDD-caused hepatic steatosis in mice is due to down regulation of genes associated with the *de novo* fatty acid synthesis and triglyceride biosynthesis as well as the up regulation of genes linked to the hepatic lipid uptake and the metabolism of saturated fatty acids to mono-unsaturated fatty acids and poly-saturated fatty acids. Histopathological examinations of mouse livers were consistent with the toxicogenomic findings. The vacuolization of the hepatic mouse tissue was a result of triglyceride and fatty acid accumulation as well as inflammatory cell accumulation and apoptosis. TCDD also induced an increase of the relative liver weight in rats, but no hepatic steatosis was detected 168 h after single dose treatment. Histopathology of rat livers unveiled a moderate lipid accumulation which was on account of the evolved hepatocellular hypertrophy. These findings were in accordance with the alterations in gene expression linked to cellular growth and lipid metabolism (Boverhof et al., 2006) (Forgacs et al., 2012) (Angrish et al., 2012) (Forgacs et al., 2013).

II.1.5.1.2 Carcinogenicity and Tumour Promotion

Toxic effects presumably contribute to the TCDD-evoked carcinogenesis and tumour promotion in rodents. A multitude of carcinogenicity studies were conducted with TCDD in animals. It was demonstrated that TCDD caused tumours in various organs and tissues, e.g. liver, lung, skin, thyroid, hard palate, nasal turbinates, and tongue in rodents and hamsters (IARC, 2012).

Toth et al. analyzed the carcinogenic potential of TCDD in male Swiss/H/Riop mice which were treated with 0.007, 0.7, 7 µg TCDD /kg bw by gavage once a week over a period of one year. Afterwards animals were observed over a life span. The overall incidence of hepatocellular adenomas and carcinomas was increased in the selected mouse strain (Toth et al., 1979). In a long-term carcinogenicity study performed by the National Toxicology Program, male and female B6C3F1 mice were treated by gavage with 0.01, 0.05, or 0.5 µg TCDD/kg bw (males) and 0.04, 0.2, or 2 µg TCDD/kg bw (females) twice a week for 104 weeks (NTP, 1982). The incidences of hepatocellular adenomas and carcinomas were dose-related increased relative to the respective vehicle controls in both sexes. In female mice, the incidences of follicular adenomas of the thyroid gland were also dose-related elevated as well as lymphomas in the hematopoietic system and fibrosarcomas in the subcutaneous tissues. Furthermore, a dose-related increase in alveolar/bronchial adenomas and carcinomas was observed in male mice.

Della Porta et al. performed two mouse studies in which the carcinogenic potential of TCDD has been characterized. In the first study, male and female C57Bl/6J x C3Hf mice were given 2.5 or 5 µg TCDD/kg bw by gavage once a week for 52 weeks. Animals were observed until week 104. A dose-related increase of hepatocellular adenomas and carcinomas was determined in both sexes. The incidence of other tumour types was low and not related to TCDD treatment (Della Porta et al., 1987). In a second study, 10-days old male and female B6C3 and B6C mice were treated intraperitoneally once a week with 1, 3, or 60 µg TCDD/kg bw for five weeks. Animals were observed until 78 weeks of age. Hepatocellular carcinomas occurred dose-dependently in male B6C3 mice only, whereas hepatocellular adenomas were observed in both sexes in a dose-dependent manner. Thymic lymphomas were determined at 60 µg/kg bw in both hybrids and sexes and at 30 µg/kg bw in all but female B6C3 mice (Della Porta et al., 1987).

In a study performed by Wyde et al. TCDD was topically applied three times a week at doses of 5, 17, 36, 76, 121, 166, 355, or 760 ng TCDD/kg bw (equivalent to average daily doses of 2.1, 7.3, 15, 33, 52, 71, 152, or 326 ng TCDD/kg bw/day) or by gavage five times a week at doses of 105, 450, or 1250 ng TCDD/kg body weight (equivalent to average daily doses of or 0, 75, 321, and 893 ng TCDD/kg/day) for 26 weeks. The incidence of squamous cell papillomas and carcinomas has been dose-dependently increased compared to the respective vehicle control animals by dermal and oral administration of TCDD, but the response of TCDD-induced cutaneous papillomas was greater in mice by dermal route than by oral administration (Wyde et al., 2004).

TCDD acts as tumour promoter during the process of carcinogenesis, meaning that the administration of TCDD after the initial treatment with a known carcinogen (such as diethylnitrosamine (DEN), 7,12-dimethylbenz[a]anthracen (DMBA), or N-methyl-N9-nitro-N-nitrosoguanidine (MNNG)) increases the incidences of multiple tumour types such as lung and liver adenomas, hepatoblastomas, or skin papillomas in mice. Furthermore, TCDD is also a tumour promoting agent in several rat strains (Knerr et al., 2006).

In a tumour promotion study, 5 weeks old male C57BL/6, DBA/2, and B6D2F1 mice were initially given a single dose of 90 mg DEN/kg bw intraperitoneally. Three weeks later, TCDD-treatment started and mice received 0.05 µg TCDD/kg bw per week for 20 weeks. Animals did not receive any further chemical treatment and were observed until week 52 of age. TCDD increased the liver tumour incidences (all types of tumours) in B6D2F1 mice, relative to mice only treated with DEN. In the two other strains, liver tumour incidences were not significantly elevated. No significant increase in lung tumours was observed after TCDD treatment in all three mice strains. However, mice treated with DEN alone had a high incidence of lung tumours which excluded the determination of TCDD-mediated responses in the mouse lung (Beebe et al., 1995a). In a second study performed by Beebe et al. the tumour promoting potential of TCDD in the lung was investigated. 5 weeks old male Swiss mice were given either a single dose i. p. (1.6, 16, or 48 µg/kg bw) or repeated doses (0.05 µg/kg bw/week for 20 weeks) of TCDD following tumour initiation with N-nitrosodimethylamine (25 mg NDMA/kg bw). Animals were observed until 52 weeks of age. Alveolar-cell adenomas and carcinomas were observed in all mice and in all treatment groups. In addition, lung tumour multiplicity was significantly enhanced by low dose TCDD treatment (1.6 µg/kg bw) and repeated TCDD administration (0.05 µg/kg bw (x 20)) (Beebe et al., 1995b).

In a study performed by Poland and co-workers, female haired and hairless HRS/J mice were initially treated with a single application of DMBA (200 nM) followed by applications of 20 ng TCDD/mouse twice a week for eight weeks, followed by 50 ng TCDD/mouse for another 17 weeks. Skin tumours (papillomas) were only determined in hairless HRS/J mice, but not in haired mice (Poland et al., 1982b). In a second study, female hairless HRS/J mice were given single applications of 5 µmol MNNG (N-methyl-N9-nitro-N-nitrosoguanidine) followed by doses of 3.75, 7.5, 15, or 30 ng TCDD/mouse twice a week for another 20 weeks. Skin tumour incidences were increased in all TCDD treatment groups compared to mice solely exposed to MNNG (Poland et al., 1982b).

II.1.5.2. TCDD in Humans

Toxic and carcinogenic effects of TCDD are summarized in the following section. The presented toxicological data is mainly based on case reports and epidemiologic studies which describe effects linked to the exposure to materials contaminated with TCDD. Humans are exposed to high doses of TCDD mainly by occupation or accident. It has to be considered that humans are in particular not only exposed to TCDD, but also to other chemicals such as organic solvents or herbicides. However, toxic responses are dependent on exposure level and period.

II.1.5.2.1 Toxicity

In humans, the most commonly observed effect after acute and chronic exposure to TCDD (and other polychlorinated aromatic compounds) is chloracne (Jirasek et al., 1976) (ATSDR, 1996). Chloracne is an acne-like condition which is distinguished by follicular hyperkeratosis (comedones) with or without cystsand papules (Crow, 1978) (Crow, 1981). Chloracne occurs on the face and neck, but may extend to other body regions (for example upper arms, back or chest). Other acute dermatologic responses associated with TCDD exposure include hypertrichosis and hyperpigmentation (Jirasek et al., 1976) (ATSDR, 1998). Acute hepatic effects reported in case or cohort studies implied liver cirrhosis, enlargement, or elevated hepatic enzyme levels (lactate dehydrogenase (LDH), aspartate transaminase (AST), and alanine transaminase (ALT)) (Reggiani et al., 1980) (Caramaschi et al., 1981) (Ideo et al., 1982) (Ott et al., 1994) (ATSDR, 1998). Other acute responses observed in humans were elevated lipid levels (triglycerides and cholesterol), porphyria (porphyria cutea tarda and uroporphyria), impairment of the thyroid function, as well as renal, neurologic and pulmonary disorders (Suskind et al., 1984) (Zober et al., 1994) (ATSDR, 1998).

Long-term effects examined in adults were again chloracne as well as increased serum gamma-glutamyl transferase concentrations (Calvert et al., 1992). In addition, exposure of humans to TCDD has been connected to other adverse effects such as cardiovascular disease, diabetes, and perturbation of the glucose metabolism, as well as reproductive and developmental disturbances and impairment of the immune system, but further research is required to confirm the correlation between these disorders and TCDD exposure (Moses et al., 1984) (USAF, 1991) (Egeland et al. 1994) (Flesch-Janys et al. 1995) (Huisman et al., 1995) (Mocarelli et al. 1996) (Henriksen et al., 1997) (ATSDR, 1998) (U. S. EPA, 2006).

II.1.5.2.2 Carcinogenicity

The International Agency for Research on Cancer (IARC) evaluated the evidence for the carcinogenic potential of TCDD in humans based on several studies in which humans were accidentally or occupationally exposed to high TCDD levels. Cohort studies of herbicide producers from the USA, the Netherlands, Germany, a cohort from Seveso (Italy), and a multicountry study from the IARC formed the basis for this evaluation. An increased risk for incidence of lung cancer, non-Hodgkin lymphomas, and soft-tissue sarcomas was reported, though the increase was mostly not significant compared to control groups. Other malignant neoplasms were also observed such as breast and rectal cancers as well as myeloid leukaemia in the Seveso cohort, bladder cancer and several types of myeloma in the US cohort, bladder and genital cancers in the Dutch cohort, several cancer types of the oral cavity and pharynx in the German cohort studies as well as kidney cancer in the IARC study (IARC, 1997) (IARC, 2012).

Altogether, an elevated risk for all cancers combined has been determined, though the increase was rather small with the relative risk being 1.4 in the subcohorts. It has to be taken into consideration that the general population is exposed to TCDD levels several magnitudes lower than the aforementioned industrial populations (IARC, 1997) (IARC, 2012).
Based on the evidence from the animal carcinogenicity data as well as the carcinogenicity data from humans exposed to TCDD, the IARC classified TCDD as carcinogenic to humans (Group 1) in 1997 (IARC, 1997).

II.1.5.3 DLCs and NDL-PCB 153

The TEF concept is based on the fact that dioxin-like compounds share a common mechanism of action by binding to the AhR and evoke the same pattern of biological and toxic effects. They only differ in their respective potencies (expressed as the congener's TEF value). In the following chapter, studies are presented in which rodents were exposed to DLCs or NDL-PCB 153 with emphasis on tumour promoting and carcinogenic effects.

The induction of xenobiotic metabolizing enzymes as immediate response to the exposure to PCDD/Fs and PCBs *in vivo* and *in vitro* is an established biochemical response. The induction of CYP1A isoenzymes are the earliest indicators for exposure to DLCs (Vanden Heuvel et al., 1993) (Nebert et al., 2000). Dioxin-like PCBs are classified into subgroups as a result of their respective CYP isoenzyme inducibility. For instance, PCB 77 and 126 are solely CYP1A inducers (TCDD-like inducers), whereas PCB 105, 118, and 156 are mixed-type congeners (phenobarbital (PB)- and TCDD-like inducers) which induce CYP1A and CYP2B isoenzymes levels (McFarland et al., 1989). NDL-PCB 153 has been characterized as a PB-type congener which only induces CYP2B enzyme activities (McFarland et al., 1989) (van Birgelen et al., 1994) (Martin et al., 2010) (Roos, 2011).

Several lifetime (2-year) carcinogenicity studies in rats were conducted by the National Toxicology Program (NTP) during the last decades to evaluate carcinogenicity of dioxin-like compounds (amongst others TCDD, 4-PnCDF, PCB 118, PCB 126) and NDL-PCB 153 (NTP, 2006a) (NTP, 2006b) (NTP, 2006c) (NTP, 2006d) (NTP, 2010).

Female Harlan Sprague-Dawley rats were treated with TCDD (3, 10, 22, 46, or 100 ng/kg bw), 4-PnCDF (6, 20, 44, 92, or 200 ng/kg bw), PCB 126 (30, 100, 175, 300, 550, or 1000 ng/kg bw), or PCB 118 (100, 220, 460, 1000, or 4600 µg/kg bw) by gavage 5 days a week for a period of 104 weeks. Histopathological findings after 104 weeks included non-neoplastic effects in various organs such as liver, lung, pancreas, adrenal cortex, thyroid gland, and kidney after treatment with all four compounds. Various types of neoplastic lesions were determined in different organs after exposure to the DLCs. Three specific neoplasms were reported in all four rat studies: cholangiocarcinomas and hepatocellular adenomas of the liver as well as cystic keratinizing epitheliomas (CKE) of the lung. A dose-dependent increase of tumour incidences was obtained for all aforementioned tumour types except for CKEs. Additionally, squamous cell carcinomas of the oral mucosa were determined in the TCDD, 4-PnCDF, and PCB 126 carcinogenicity studies (NTP, 2006a) (NTP, 2006b) (NTP, 2006c) (NTP, 2010).

Waern and co-workers conducted a study to evaluate the tumour promoting activity of 1-PnCDD and 4-PnCDF compared to TCDD in rat. Partially hepatoectomized female Sprague-Dawley rats were initially treated with NDEA (30 mg/kg bw). After five weeks, rats were administered either vehicle, 1-PnCDD (0.088, 0.35, or 1.4 pg/kg bw), 4-PnCDF (0.16, 0.64, or 2.6 pg/kg bw) or TCDD (0.044, 0.175, or 0.7 pg/kg bw) each week by subcutaneous injections for 20 weeks. Determined effects included the dose-dependent increase of the relative liver weight, thymus weight, EROD activity, and plasma protein levels (ALT and AST). The dose-dependent decrease of the hepatic vitamin A concentration was additionally determined. The dose-dependent increase of altered hepatic γ-glutamyltranspeptidase positive (GGT^+) foci (per cent foci in liver and number of foci per liver) were examined in the rat liver, indicating that all three congeners are potent liver tumour promoters in female SD rats. The obtained results suggest that 1-PnCDD is as potent as TCDD, while 4-PnCDF reaches about ten per cent of the other two congeners' potencies (Waern et al., 1991).

In a study performed by Hemming and co-workers, the tumour promoting potential of PCB 126 was investigated, while TCDD was used as established tumour promoting agent in the performed animal experiment. Partially hepatoectomized female rats were intraperitoneally treated with the tumour initiator nitrosoethylamine (30 mg/kg bw). After 5 weeks, rats were given PCB 126 (0.316, 1, 3.16, or 10 µg PCB 126/kg bw) or TCDD (0.1, 0.316, or 1 µg TCDD/kg bw) or vehicle by weekly subcutaneous injections for 20 weeks. Both substances induced a dose-related thymic atrophy which has been detected in a decreased relative thymus weight as well as the dose-dependent increase of the relative liver weight. Comparing the liver tumour activity of both chemicals, PCB 126 caused about 10 % of the TCDD`s tumour promoting activity in relation to the administered doses which was determined as the formation of γ-glutamyl-transpeptidase-positive altered hepatic foci in the rat liver (Hemming et al., 1995).

PCB 153 belongs to the group of non dioxin-like PCBs and is commonly used as representative of NDL-PCBs in both *in vivo* and *in vitro* studies. Diverse toxic responses were determined for NDL-PCBs such as neurological and reproductive toxicity, as well as alterations in the endocrine system (Giesy et al., 1998). Additionally, Umannova and co-workers showed that PCB 153 affects the intercellular communication in rat liver progenitor cells. PCB 153 led to the release of arachidonic acid in WB-F344 cells. Earlier studies performed by Marks et al. and Telliez et al. demonstrated that the interference in arachidonic acid signalling could conduce to toxic responses, including tumour promotion, of NDL-PCBs (Marks et al., 2000) (Telliez et al., 2006) (Umannova et al., 2008).

The National Toxicology Program performed a 2-year study in female Sprague-Dawley rats in which PCB 153 was administered by gavage (10, 100, 300, 1000, or 3000 µg/kg bw) 5 days a week for 105 weeks. Increased incidences of non-neoplastic lesions of the liver, thyroid gland, ovary, oviduct, and uterus were reported. Non-neoplastic liver lesions included hepatocyte hypertrophy, diffuse fatty change, and bile duct hyperplasia which increased in a dose-dependent manner. Neoplastic lesions were not reported, but two cases of cholangioma of the liver were observed in the 1000 µg/kg bw dose group. Based on these findings the NTP working group concluded that there is only equivocal evidence of carcinogenic activity of PCB 153 in female SD rats (NTP, 2006d).

The International Agency for Research on Cancer classified the entire group of polychlorinated biphenyls as probably carcinogenic to humans (Group 2A) in 1987 based on the available data at that time (IARC, 1987).

In 1997, polychlorinated dibenzo-*p*-dioxins (other than 2,3,7,8-Tetrachlorodibenzo-*p*-dioxin) and polychlorinated dibenzofurans were categorized as Group 3 carcinogens by the IARC, implying that they are not classifiable as to their carcinogenicity in humans due to the published data up to this IARC evaluation (IARC, 1997).

Since then, new data on carcinogenicity of DLCs was published resulting in the re-evaluation of two congeners (4-PnCDF and PCB 126) by the IARC in 2012. The International Agency for Research on Cancer classified 4-PnCDF and PCB 126 as carcinogenic to humans (Group 1) based on the carcinogenic effects obtained in laboratory animals and because both congeners exhibit activities similar to TCDD for all stages of the mechanism which was reported for the TCDD-mediated carcinogenesis in humans (IARC, 2012).

II.2 Xenobiotic Metabolism

Organisms are daily exposed to substances which cannot be used as either physiological component or as energy supply. These 'unusable' xenobiotics must be rapidly eliminated to prevent their accumulation in the organism. Main routes of elimination are the kidney and bile, whereas the lung and breast milk represent minor elimination routes. Usually, xenobiotics are highly lipophilic substances. Due to the lipophilic properties they can be easily resorbed in the gastrointestinal tract and would be only slowly eliminated from the organism. The xenobiotic metabolism is a multi-phase mechanism in which lipophilic substances are transformed into hydrophilic conjugates which subsequently can be more readily excreted. The liver is the major organ for biotransformation of xenobiotics in higher organisms, but also other tissues such as the gut, kidney, and lung express xenobiotic metabolizing enzymes (Forth et al., 2001) (Marquardt et al., 2004).

The xenobiotic metabolism is distinguished into three consecutive phases:
In phase I, functional groups (e.g. OH, SH, or NH_2) are introduced into substrates, whereupon more hydrophilic metabolites are formed. Several enzymes participate in these functionalization reactions such as oxidoreductases of the cytochrome P450-dependent monooxygenases (CYPs), aldehyde dehydrogenases (ALDHs) flavin-dependent monooxygenases (FMOs), and monoamine oxidases (MAOs) (Forth et al., 2001) (Marquardt et al., 2004).
In phase II, functionalized metabolites are conjugated with highly hydrophilic, negatively charged endogenous molecules (e.g. glutathione, glucuronic acid, and sulphate). Conjugation reactions are catalyzed by 'transferase' enzymes such as the glutathione S-transferase (GST), UDP-glucuronosyl-transferase (UGT) or sulfotransferases (ST) (Forth et al., 2001) (Marquardt et al., 2004).

In phase III, the highly hydrophilic conjugated metabolites are transported out of the cell to the excretion organs. Active transport systems are the ABC transporter (ATP-binding cassette) as well as solute carrier transport systems such as the organic anion and cation transporters (OATs, OCTs) and organic anion transport polypeptides (OATPs) (Forth et al., 2001) (Marquardt et al., 2004) (Omiecinski et al., 2011).

II.2.1 Cytochrome P450 Enzymes

Cytochrome P450 monooxygenases play key roles in the oxidative phase I xenobiotic metabolism. CYPs catalyze a wide variety of functionalization reactions, among others the aliphatic and aromatic hydroxylation, epoxidation or N-oxidation. The number '450' is derived from the wavelength of the absorption maximum of the enzymes when they are in their reduced state and complexed with carbon monoxide. Cytochrome P450 enzymes are hemeproteins that consist of heme B as prosthetic group which is anchored to cysteine in the active centre of the enzyme. CYPs are located in the membrane of the endoplasmatic reticulum and are associated with the NADPH cytochromes P450 reductase to a reactive complex. The monooxygenase reaction additionally requires molecular oxygen, NADPH, and phospholipids, especially phosphatidylcholine. During the monooxygenase reaction one oxygen atom is transferred onto the substrate, and the other oxygen atom is reduced to water by proton absorption. The equation of the monooxygenase reaction is summarized in the following equation:

$$RH + O_2 + NADPH + H^+ \rightarrow ROH + H_2O + NADP^+$$

The scheme of the monooxygenase reaction is featured in Figure 2 below. The monooxygenase reaction is a multistep mechanism. The substrate (RH) binds to the resting enzyme which is in its ferric state. The NADPH-dependent cytochrome P450 reductase transfers a single electron to the heme iron (Fe^{III}) of the cytochromes P450. Afterwards, the resulting oxidized heme iron (Fe^{II}) is able to bind molecular oxygen, whereupon the ferric superoxide complex is formed. The transfer of a second electron by the NADPH reductase results in the ferric peroxy anion, which is subsequently protonated resulting in the formation of the ferric hydroperoxo complex. The obtained ferric hydroperoxo intermediate is unstable and after the further protonation a porphyrin radical cation is formed. The ferryl intermediate reacts with the substrate, whereupon the hydroxylated metabolite is released. The enzyme returns in its resting ferric state after re-equilibration with water (de Montello et al., 2010).

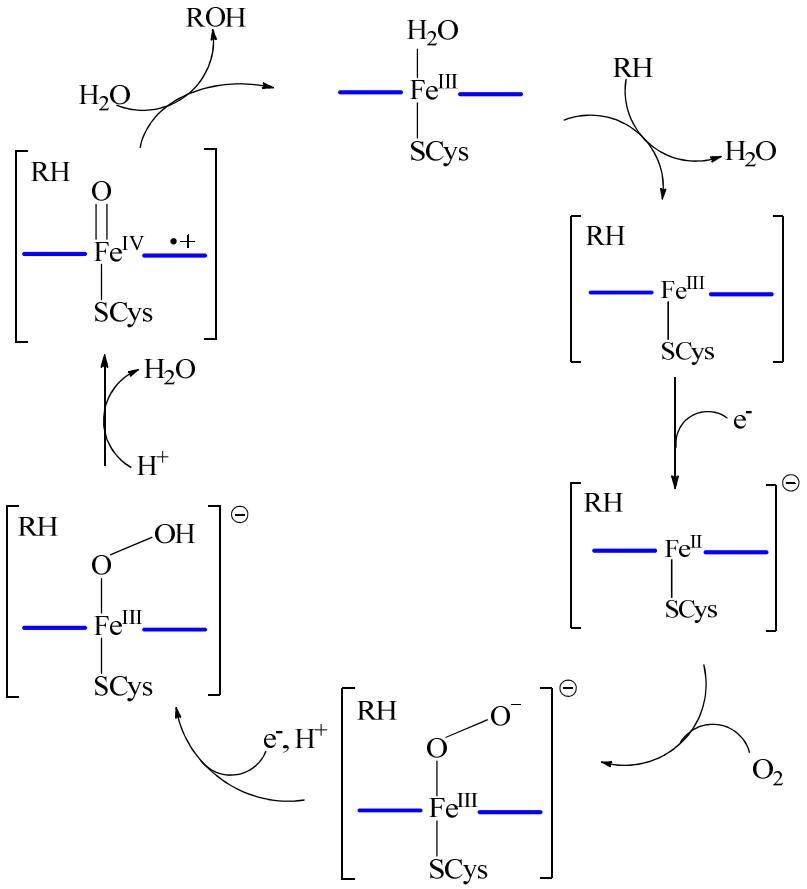

Figure 2. **Scheme of the monooxygenase reaction (according to de Montello et al., 2010).**
The heme group is featured as two solid blue bars with the iron (Fe) in between.
The cysteine thiolate provided by the protein is represented as SCys.
The abbreviation RH represents the substrate hydrocarbon and ROH is the hydroxylated product.

According to the official international guidelines, cytochromes P450 enzymes are designated with the abbreviation CYP, followed the Arabic numeral for the family (> 40 % amino acididentity), then the Latin numeral for the subfamily (> 55 % amino acid identity), and the Arabic numeral for the isoenzyme (Danielson et al., 2002) (Forth et al., 2001).

In mammals, 18 CYP gene families exist, and about 60 individual CYP genes can be found in the different species. CYPs are involved in various metabolic processes of in the metabolism of endogenous lipophilic compounds such as steroids, bile acids, eicosanoids, and retinoids but also play key roles in the metabolism of exogenous xenobiotics such as environmental pollutants, drugs, and carcinogens. The enzymes of the CYP1-4 families predominantly catalyze phase I reactions of xenobiotics (Honkakoski et al., 2000) (Forth et al., 2001) (Nebert et al., 2002).

II.2.1.1 CYP1 Family

II.2.1.1.1 CYP1A1, CYP1A2, and CYP1B1

In humans and rodents the CYP1 subfamily consists of CYP1A1, CYP1A2, and CYP1B1. They are able to catalyze the metabolic activation of polycyclic aromatic hydrocarbons, heterocyclic and aromatic arylamines, which leads to the formation of ultimate carcinogens (Murray et al., 1988) (Honkakoski et al., 2000). *CYP1A1/Cyp1a1* and *CYP1B1/Cyp1b1* are predominantly expressed in extrahepatic tissues such as lung, kidney, and placenta. CYP1A2 is a liver-specific enzyme. The human *CYP1A2* gene is constitutively expressed and contributes 13 % to the total CYP content in the human liver (Guengerich, 2010). In humans, *CYP1A2* is only expressed in the adult liver (Xu et al., 2000). They are inducible by polyhalogenated aromatic hydrocarbons such as TCDD and related compounds as well as dioxin-like polychlorinated biphenyls. Ligands, such as TCDD, bind to the aryl hydrocarbon receptor (AhR) resulting in the activation of the AhR signalling pathway. Several studies performed in immortalized cell lines and primary cultured cells demonstrated that the inducibility of human hepatic CYP1A enzymes by DLCs was weaker than the inducibility of CYP1A enzymes in rat liver. However, distinctive differences in responsiveness based on donor health status or genetic background (polymorphism) were determined (Murray et al., 1988) (Honkakoski et al., 2000) (Shimada et al., 2002a) (Silkworth et al., 2005) (Connor et al., 2006) (Budinsky et al., 2010) (Black et al., 2012). A recently published study by Forgacs and co-workers demonstrated that mouse primary hepatocytes are as sensitive as rat hepatocytes in terms of *Cyp1a1* mRNA inducibility (Forgacs et al., 2013).

II.2.1.1.2 CYP1 Induction by AhR Signalling Pathway

The induction of CYP1 enzymes by exposure to dioxins and related compounds is regulated by the aryl hydrocarbon receptor (AhR) which belongs to the group of the basic helix-loop-helix/Per-ARNT-Sim (bHLH/PAS) transcription factors. The mechanism of the AhR signal transduction is featured in Figure 3 below.

In the absence of a ligand, the inactive AhR forms together with two molecules of HSP90 (heat shock protein with 90 kDa), XAP2 (hepatitis b virus X-associated protein 2, also known as AhR-interacting protein), and p23 (23-kDa co-chaperone protein) a cytosolic multiprotein complex. Upon ligand binding to the AhR (such as TCDD), the AhR supposedly undergoes a conformational change resulting in the exposure of a nuclear localization sequence which leads in the following to the translocation of the complex into the nucleus. It is most likely that XAP2 dissociates from the AhR/ligand complex prior to the nuclear translocation of the activated AhR complex (Fujii-Kuriyama et al., 2010) (Denison et al., 2011). After the release of the co-chaperones HSP90 and p23, the AhR dimerizes with ARNT (AhR nuclear translocator), another member of the bHLH/PAS family.

Subsequently, the ligand/AhR/ARNT complex binds to its specific DNA recognition site, the so called xenobiotic responsive element (XRE) also known as dioxin responsive element (DRE) and recruits in the following coactivators such as CBP/p300, SCR-1, or NCoA2/GRIP1/TIF2 resulting in the transcription of *CYP1A/Cyp1a* genes and other AhR-responsive genes (Denison et al., 2002) (Denison et al., 2003) (Mimura et al., 1999) (Fujii-Kuriyama et al., 2010). Detailed information about the AhR and AhR-regulated target genes are featured in II.3 Aryl hydrocarbon receptor (AhR).

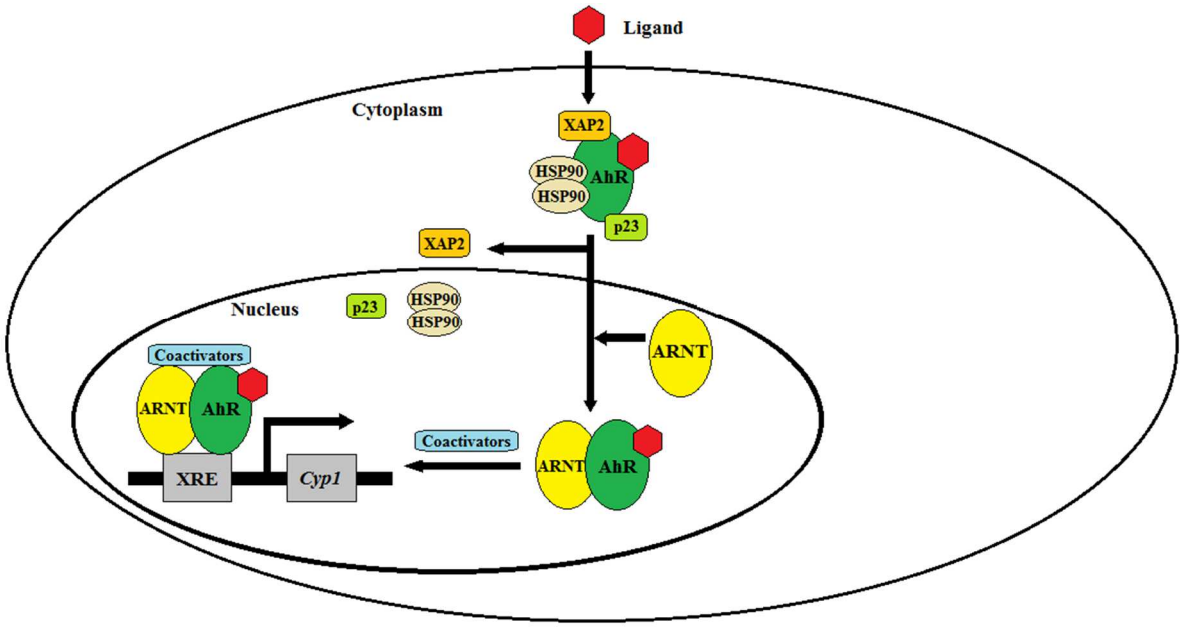

Figure 3. Molecular mechanism of activation of *Cyp1* by AhR (according to Denison et al., 2011).

II.2.1.2 CYP2B Subfamily

II.2.1.2.1 Mouse and Human CYP2B Isoenzymes

In mouse, the CYP2B subfamily consists of the isoenzymes CYP2B9, CYP2B10, CYP2B13, CYP2B19, and CYP2B23. *Cyp2b9* and *Cyp2b10* are the major mouse *Cyp2b* genes. *Cyp2b9* is only expressed in the female mouse liver. *Cyp2b10* is predominantly expressed in both mouse genders in extrahepatic tissues such as lung, duodenum, ileum, and colon (Renaud et al., 2011). In humans, the CYP2B family consists of the *CYP2B6* gene and the *CYP2B7P1* pseudogene (Nelson et al., 2004). *CYP2B6* is primarily expressed in liver, but also to a lesser degree in extrahepatic tissues such as kidney, brain, intestine, and lung. The relative expression levels of *CYP2B6* range between 2 to 10 % of the total hepatic CYP content. The pseudogene *CYP2B7P1* is only expressed in the human lung (Ding et al., 2003) (Wang et al., 2003). CYP2B enzymes catalyze the hydroxylation of various xenobiotics and steroids. CYP2B isoforms are inducible by industrial solvents, barbiturates, antimycotics and NDL-

PCBs. Phenobarbital (PB) belongs to the group of barbiturate and is the prototype of xenobiotics which specifically induce CYP2B isoforms by the constitutive androstane receptor signalling pathway (Honkakoski et al., 1996) (Kawamoto et al., 1999) (Honkakoski et al., 2000) (Cheng et al., 2005).

II.2.1.2.2 CYP2B Induction by CAR Signalling Pathway

The induction of cytochromes P450 2B isoforms is mediated by the constitutive androstane receptor (CAR). CAR belongs to the group of orphan nuclear receptors and is predominantly expressed in the liver where it primarily regulates the transcriptional up regulation of *CYP2B*/*Cyp2b* genes and to a lesser extent the *CYP3A/Cyp3a* transcription.

In the absence of an inducer CAR is located in the cytoplasm associated with HSP90 (heat shock protein with 90 kDa) and CCRP (cytoplasmic CAR retention protein) forming a complex. CAR can be indirectly activated in the presence of an activator such as phenobarbital (Figure 4) or directly by ligand binding such as TCPOBOP (1,4-bis[2-(3,5-dichloropyridyloxy)]benzene) (Figure 5). Upon activation, the protein phosphatase 2A (PP2A) is recruited which leads to the dephosphorylation of CAR, resulting in the release of HSP90 and CCRP. In the following, CAR translocates into the nucleus where it forms a heterodimer with the retinoid X receptor (RXR). The CAR-RXR heterodimer binds with the aid of coactivators (such as the steroid receptor coactivator 1 (SRC-1) or glucocorticoid receptor-interacting protein 1 (GR-interacting protein 1)) to the PB-responsive enhancer module (PBREM) resulting in the transcription of *CYP2B/Cyp2b* isoforms (Kawamoto et al., 1999) (Swales et al., 2004) (Hernandez et al., 2009) (Timsit et al., 2006).

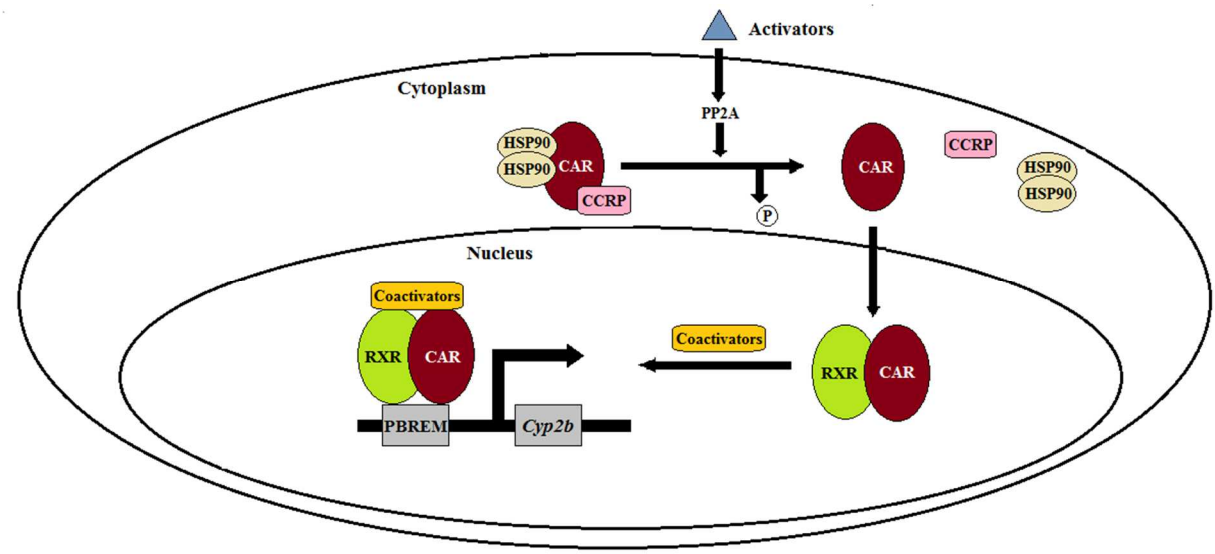

Figure 4. Molecular mechanism of activation of *Cyp2b* by CAR activators (according to Timsit et al., 2006).

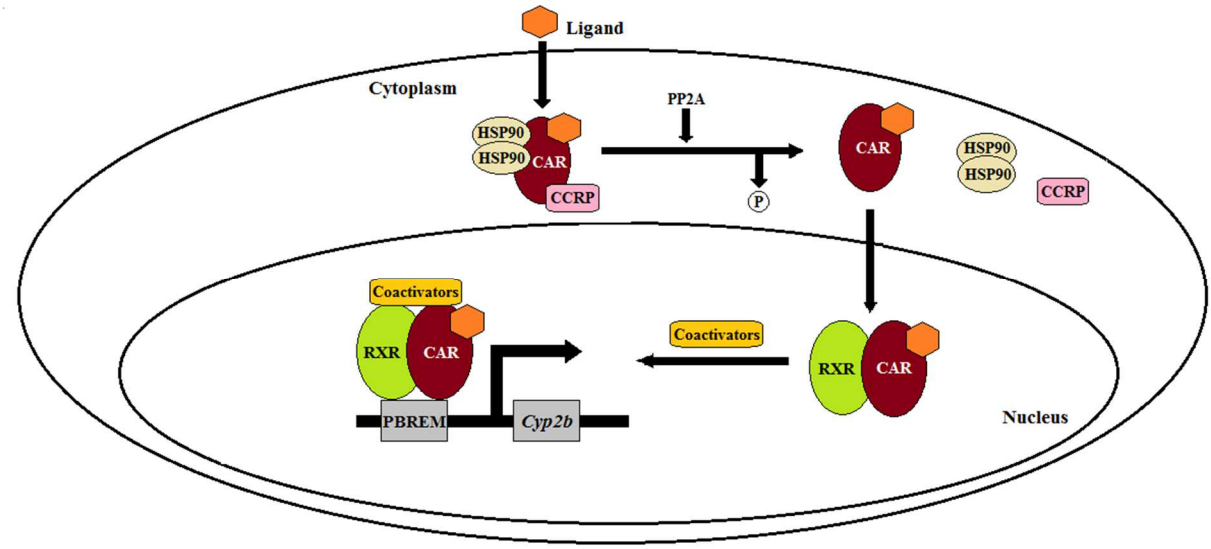

Figure 5. Molecular mechanism of activation of *Cyp2b* by CAR ligands (according to Timsit et al., 2006).

Furthermore, CAR additionally regulates genes that are involved in metabolic detoxification processes such as sulfotransferases, glucoronosyl transferases, glutathione S-transferases, and transporters as well as hepatic genes associated with the energy metabolism in presence of an CAR activator such as phenobarbital (Ueda et al., 2001) (Assem et al., 2004) (Konno et al., 2008) (Gao et al., 2010).

II.2.1.3 CYP3A Subfamily

II.2.1.3.1 Mouse and Human CYP3A Isoenzymes

The CYP3A subfamily consists of eight isoenzymes CYP3A11, CYP3A16, CYP3A25, CYP3A41, CYP3A44, CYP3A57, and CYP3A59 in the mouse. Mouse *Cyp3a* isoforms are primarily expressed in liver and intestine. *Cyp3a41* and *Cyp3a44* are predominatly expressed in livers of female mice (Sakuma et al., 2002). The human *CYP3A* subfamily consists of *CYP3A4, CYP3A5, CYP3A7,* and *CYP3A43*. As in mouse, they are predominantly expressed in the adult liver and intestine. In humans, the CYP3A isoenzymes contribute about 30 % to the total hepatic CYP content. CYP3As metabolize endogenous substrates such as steroids (testosterone and progesterone) and bile acids, but the subfamily plays also an important role in metabolization of xenobiotics. More than 50 % of all available prescriptive drugs are metabolized by CYP3A4 such as antimycotics, antibiotics, and contraceptive steroids as well as antidepressants. CYP3As are inducible by broad range of compounds such as antibiotics, polychlorinated biphenyls or organochloride pesticides, though species-dependent differences were determined. For instance rifampicin, which is amacrocyclic antibiotic, induces the expression of the human *CYP3A4* and rabbit *CYP3A6* to a high extent, but not the respective *Cyp3a* analogues in rat or mice (Goodwin et al., 2002) (Kliewer et al., 2002a) (Kliewer et al.,

2002b). Besides the induction of CYP3A4, there is a broad range of CYP3A4 inhibitors such as erythromycin (an antibiotic), ketoconazole, and itraconazole (antimycotics) or components of the grapefruitjuice (such as bergamottin) (He et al., 1998) (Gibbs et al., 1999). Therefore, the transcriptional regulation of CYP3A isoenzymes is the centre of interest especially in relation to drug-drug interactions.

II.2.1.3.2 CYP3A Induction by PXR Signalling Pathway

The mechanism of the transcriptional up regulation of *Cyp3a* (analogous for *CYP3A*) by the pregnane X receptor (PXR) is featured in Figure 6. PXR belongs to the group of orphan nuclear receptors and is predominantly expressed in liver and intestine in humans, rats, mice, and rabbits (Wang et al., 2003). In the absence of an inducer PXR is located in the cytoplasma associated with HSP90 (heat shock protein with 90 kDa) and CCRP (cytoplasmic CAR retention protein) forming a complex. Upon ligand binding, such as rifampicin, to the PXR, HSP90 and CCRP are released and PXR translocates into the nucleus. In the nucleus, PXR forms a heterodimer with the retinoid X receptor (RXR). The PXR-RXR heterodimer binds with the aid of cofactors (such as SRC-1 or TIF2/GRIP1) to core promoter elements (DR3 and ER6 motifs in the CYP3A gene promoter, species-dependent) within the xenobiotic responsive enhancer module (XREM) resulting in the upstream of *CYP3A/Cyp3a* isoforms (Timsit et al., 2006).

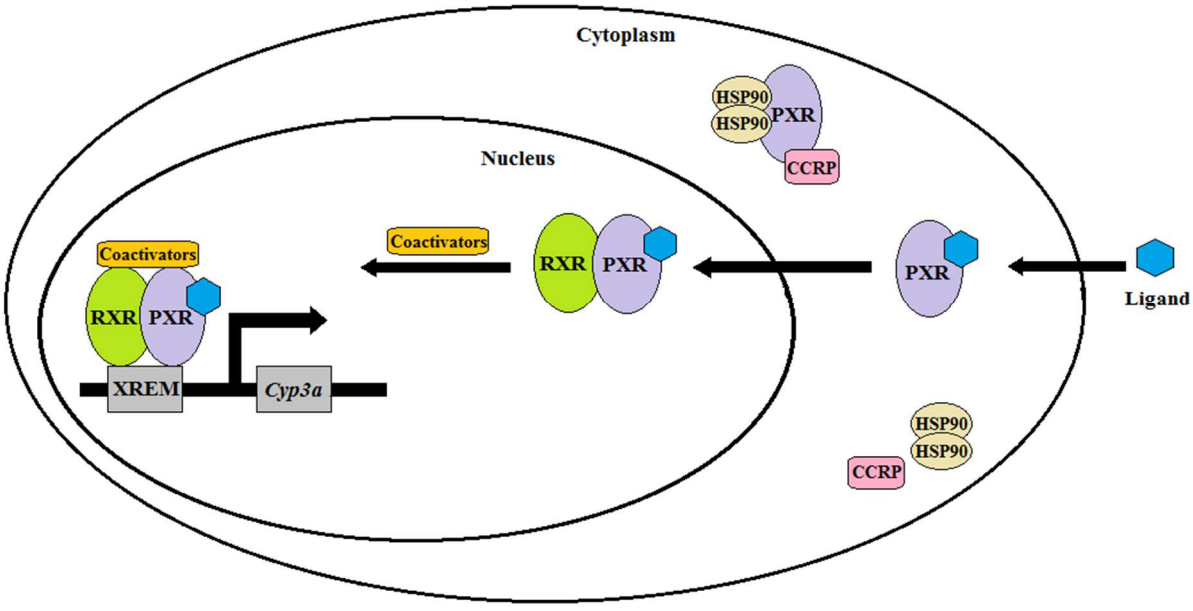

Figure 6. Molecular mechanism of activation of *Cyp3a* by PXR (according to Timsit et al., 2006).

The pregnane X receptor furthermore regulates the induction of genes involved in xenobiotic metabolism such as members of the cytochrome 2B subfamily and cytochromes 2C subfamily as well as sulfotransferases and glucoronosyl transferases. CYP2B and CYP2C isoenzymes are induced to a lesser extent than CYP3A isoenzymes by PXR. Hepatic genes associated

with the energy metabolism as well as genes involved in the bile acid homeostasis are also regulated by PXR (Ueda et al., 2001) (Goodwin et al., 2002) (Assem et al., 2004) (Konno et al., 2008) (Gao et al., 2010) (Fahmi et al., 2010).

II.3 Aryl hydrocarbon Receptor (AhR)

In 1976, Poland and Glover identified in the hepatic cytosol of C57BL/6J mice a high affinity binding site that reversibly binds radiolabelled TCDD (Poland et al., 1976). This protein was characterized and later named aryl hydrocarbon receptor due to its specific binding affinity to aryl hydrocarbons (Poland et al., 1982a).

The AhR is a member of the basic helix-loop-helix/Per-ARNT-Sim (bHLH/PAS) family of transcription factors which regulates ligand-dependently the expression of various genes (Denison et al., 2003). The AhR is expressed in many tissues. Highest levels were determined in lung, liver, thymus, and testes (Hahn et al., 1998). The scheme of the AhR protein, which outlines the different domains, is presented in Figure 7.

The N-terminal functional domains are responsible for DNA binding (DBD), ligand binding (LBD), and the dimerization with ARNT. The C-terminal domain of the AhR protein is in charge of transactivation. In the bHLH region the AhR maintains a nuclear localization signal (NLS) and a nuclear export signal (NES). The AhR forms a cytosolic multiprotein complex consisting of two molecules HSP90, p23, and XAP2 in the absence of ligands. It is suggested that due to binding of HSP90 the nuclear localization signal (NLS) is disguised and the AhR retains in the cytoplasma. The import of the ligand-AhR complex is inhibited by phosphorylation of the NLS by protein kinase C. The NR box consists of a LxxLL motif (x stands for any amino acid) which is additionally responsible for the cytosolic retention of the AhR by protein-protein interactions (Kawajiri et al., 2007) (Fujii-Kuriyama et al., 2010).

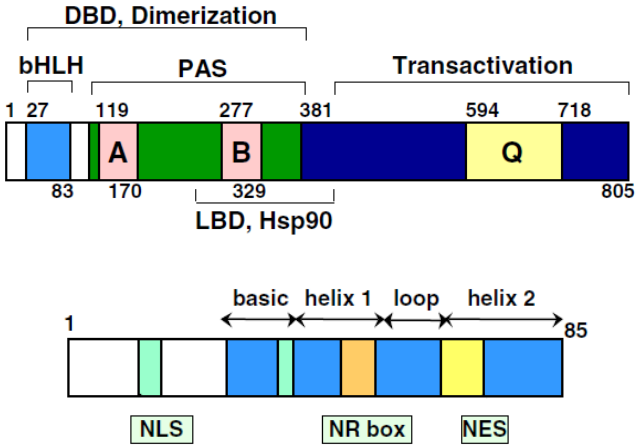

Figure 7. **Scheme of the functional domains (up) and the NH_2-terminal functional domains (down) of the AhR (Kawajiri et al., 2007)**
Annotations: A, B: weakly homologous repeated regions.
Q: glutamine-rich transcription activation region
DBD: DNA binding domain; LBD: ligand binding domain
NLS: nuclear localization signal, NES: nuclear export signal,
NR box: nuclear receptor box

II.3.1 AhR Signal Transduction

The AhR-mediated signalling pathway is featured in a previous chapter (II.2.1.1.2 CYP1 induction by AhR signalling pathway). Ligand binding ultimately leads to the transcriptional up or down regulation of AhR-responsive genes. Classic AhR target genes are involved in phase I and phase II of biotransformation processes including cytochromes P450 family 1, UDP glucuronosyl transferases (*UGT1A1, Ugt1a6/UGT1A6*), NAD(P)H: quinine oxido-reductase (*Nqo1/NQO1*), aldehyde dehydrogenase 3 family 1 (*Aldh3a1/ALDH3A1*), and glutathione S-transferase Ya (*Gsta1/GSTA1*) (Rowlands et al., 1997) (Nebert et al., 2000) (Schrenk et al., 1995). Besides those 'classic' AhR target genes involved in xenobiotic metabolism, the AhR regulates genes involved in cell cycle control and differentiation (Bock et al., 2006). A gene which negatively regulates the AhR activity is the aryl hydrocarbon receptor repressor. The AhRR is constitutively located in the nucleus where it forms a heterodimer with ARNT. The binding of the AhRR/ARNT heterodimer inhibits the transcriptional upstream of AhR-regulated genes. Furthermore, the AhR regulates the induction of the *Ahrr/AHRR* expression suggesting that the *Ahrr/AHRR* forms a negative feedback loop with the AhR (Evans et al., 2008) (Fujii-Kuriyama et al., 2010).

However, the transcriptional response due to ligand binding is species-, tissue-, and cell type-specific (Denison et al., 2003). Sun et al. developed a comparative computational approach in which the putative XREs of human, mouse, and rat were compared. Based on the analysis of XREs, there is striking evidence that the XREs are not well conserved across species, which could be the explanation for the species-dependent differences in gene expression (Sun et al., 2004). Recent microarray studies confirmed the earlier findings of Sun and co-workers. The analysis of the TCDD-altered gene expression in different species led to conclusion that the differential gene expression is not conserved between species which most likely contributes to

the species-specific responses and compound sensitivity (Dere et al., 2011) (Forgacs et al., 2013).

Despite the classical genomic mechanism of AhR signal transduction, the AhR interact in a variety of intracellular signalling pathways including several protein kinases (receptor tyrosine kinases, mitogen-activated protein kinases, c-Src kinases) and phosphatases (phosphodiesterase 2A) as well as the ligand/AhR interplay affects the calcium signalling pathways. Furthermore the crosstalk between the AhR and other ligand-activated transcription factors (among others estrogen receptor, glucocorticoid receptor, retinoic acid receptor, epidermal growth factor receptor) has been shown (Matthews et al., 2006) (Beischlag et al., 2008) (Haarmann-Stemmann et al., 2009) (Denison et al., 2011).

II.3.2 Physiological Role of the AhR

During the last two decades, the endogenous functions of the AhR in normal physiology and development were elucidated by the generation of mice with a mutation in the *Ahr* gene locus (Schmidt et al., 1996). Due to the knockout of the *Ahr* gene, mice do not express the AhR protein and classic AhR target genes (e.g. *Cyp1a1* or *Cyp1a2*) are not inducible by treatment with TCDD. *Ahr* knockout mice are resistent to the TCDD-mediated toxic effects which led to the conclusion that the AhR mediates most, if not all, biological and toxic effects of TCDD (Schmidt et al., 1996) (Denison et al., 2002) (Denison et al., 2003).

In the first few weeks after birth, *Ahr* knockout mice exhibited a slower growth rate and decreased body weights compared to *Ahr* wild-type mice (Schmidt et al., 1996) (Mimura et al., 2003). Furthermore, *Ahr* knockout mice display reduced liver weights compared to their wild-type littermates (Schmidt et al., 1996). The decreased liver weight is directly related to the reduction of hepatocyte size resulting from a portosystemic shunting in $Ahr^{-/-}$ mice. The portosystemic shunting is based on an open ductus venosus (Lahvis et al., 2000). In addition to the vascular defects in liver, several other abnormalities in the liver of *Ahr* knockout mice were detected such as fatty metamorphosis, portal fibrosis, and prolonged extramedullary hematopoesis (Schmidt et al., 1996) (Fernandez-Salguero et al., 1996). Liver fibrosis in *Ahr* knockout mice is most likely due to hepatic accumulation of retinoic acid as a result of the suppressed retinoic acid metabolism (Andreola et al., 2004).

Furthermore, the AhR seems to play a crucial role in the reproductive system. Female *Ahr* knockout mice exhibit infertility. This effect is most likely based on failures of follicular maturation and ovulation, probably due to insufficient synthesis of estradiol in the follicles of female knockout mice (Schmidt et al., 1996) (Mimura et al., 1997) (Baba et al., 2005).

There are indications that the AhR also plays a role in the immune system. *Ahr* knockout mice display reduced amounts of lymphocytes in the spleen compared to *Ahr* wildtype mice. This effect subsequently resulted in the decrease of splenic T and B cells. This disturbance in the peripheral immune system is probably the reason for premature deaths of newborns and older animals as a consequence of opportunistic bacterial infections.

Other clinical findings in aged *Ahr* knockout mice (eight months and older) included hypertrophy and fibrosis in the heart, hyperplasia and fibrosis in the skin, hyperplasia in the gastric pylorus, and extreme calcification in the uterus (Fernandez-Salguero et al., 1997) (Gonzalez et al., 1998).

As outlined above, the AhR plays an essential role in organ and cell physiology and homeostasis which supports the theory that the AhR is able to translocate into the nucleus due to endogenous signalling (Denison et al., 2003).

II.3.3 Types of AhR Ligands

A broad range of structurally diverse chemicals can bind to the AhR which leads in the following to its activation. Basically, ligands can be divided into two major categories, those that bind with 'high affinity' and those that bind only with 'low affinity' to the AhR. The majority of 'high affinity' ligands are aromatic, planar, and hydrophobic compounds such as halogenated aromatic hydrocarbons (polychlorinated dibenzo-*p*-dioxins, dibenzofurans, and dioxin-like biphenyls) and polycyclic aromatic hydrocarbons (benzo[a]pyrene, 3-methylcholanthrene) (Hankinson, 1995). Recently, a new group of AhR ligands and inducers was identified which differs in structure and physicochemical properties from the 'classical' AhR ligands. Compared to the 'high affinity' AhR ligand TCDD, the non-classical synthetic AhR ligands/agonists are rather weak CYP1A1 inducers and 'low affinity' AhR ligands. Members of the non-classical synthetic AhR ligands and inducers include thiabendazole (fungicide and parasiticide), omeprazole (agastric proton pump inhibitor), as well as the hepatoprotective agent YH439 (Upadhyay et al., 1980) (Quattrochi et al., 1993) (Lee et al., 1996) (Denison et al., 2002) (Denison et al., 2003) (Igaul-Adell et al., 2004) (Hong et al., 2005).

Humans and animals are mainly exposed to AhR ligands through their diet. Despite the synthetic AhR ligands, a great variety of natural AhR ligands has been identified in vegetables, fruits, teas, and herbs. The AhR signalling pathway can be activated and/or inhibited by those naturally occurring dietary substances. Natural AhR ligands include diverse dietary plant compounds such as indole-3-carbinol (I3C), curcumin, carotinoids, flavonoids, and polyphenols. Naturally occurring dietary compounds are weak AhR ligands, but can be converted into relatively potent AhR ligands. For example I3C is a natural AhR ligand which is found in vegetables of the *Brassica* genus such as cabbage, cauliflower, and Brussel sprouts. I3C itself is a weak AhR ligand compared to its generated acid condensation products identified after administration of I3C to male Sprague-Dawley rats by oral gavage in the acidic environment of the gastro intestinal tract. ICZ (indolo[3,2-b]carbazole) is the most potent AhR agonist of the I3C acid condensation products. Bjeldanes and co-workers demonstrated by the use of a competitive binding assay thatICZ binds with a much higheraffinity compared to I3C to the AhR. The K_d-value of ICZ is 1.9×10^{-9} M, I3C has a K_d-value of 2.5×10^{-5} M, and the K_d-value of TCDD is 7.1×10^{-12} M in Hepa1c1c7 cells (Bjeldanes et al., 1991) (Ciolino et al., 1998) (Denison et al., 2003) (Gouédard et al., 2004) (Jeuken et al., 2003).

As mentioned in the previous chapter, several studies in *Ahr* knockout mice indicate that the AhR is responsible for normal development, physiological function, and homeostasis, suggesting the existence of endogenous ligands which bind to the AhR. Furthermore, several *in vitro* and *in vivo* experiments demonstrated the presence of the activated AhR in the nucleus in absence of exogenous ligands which also supports this theory (Abbott et al., 1994) (Chang et al., 1998) (Singh et al., 1996) (Fernandez-Salguero et al., 1996) (Tijet et al., 2005) (Boutros et al., 2009).

Divers endogenous compounds which regulate the AhR activity have been identified such as indoles, tetrapyroles, or arachidonic acid metabolites. However, a single endogenous ligand with high affinity for the AhR that mediates its endogenous functions has not been identified up to the present day (Denison et al., 2002) (Denison et al., 2003) (Nguyen et al., 2008) (Denison et al., 2011).

The vast majority of AhR ligands are generated from tryptophan by different biological and physicochemical processes. For instance, photooxidation of tryptophan leads to the formation of endogenous AhR ligands such as FICZ (6-formylindolo[3,2-b]carbazole). FICZ possesses structural similarities to the indole-derived high affinity AhR ligand ICZ. Various other examples for the formation of tryptophan metabolites upon light exposure, which can bind to the AhR, activate it, and regulate the AhR-dependent gene expression, have been described (Rannug et al., 1987) (Rannug et al., 1995) (Denison et al., 2003) (Diani-Moore et al., 2006) (Haarmann-Stemmann et al., 2009). The tryptophan catabolites kynurenine and kynurenic acidwere also identified as endogenous ligands of the human and murine AhR (Denison et al., 2003) (DiNatale et al., 2010) (Opitz et al., 2011).

A large variety of endogenous AhR activators/ligands were identified, though their physiological role and contribution to the abnormalities of the *Ahr* knockout mice is still uncertain, which therefore trigger the need for further investigations.

III Research Problem and Objectives

Polychlorinated dioxins, furans, and biphenyls are widespread persistent environmental pollutants which accumulate in the feed and food chain (Poland et al., 1982a). Exposure to dioxin-like compounds results in a myriad of biochemical and toxic responses including dermal toxicity, immunotoxicity, hepatotoxicity and carcinogenicity as well as adverse effects on reproduction, development, and the endocrine system (Holsapple et al., 1991) (Birnbaum, 1994) (Schmidt et al., 1996) (Fernandez-Salguero et al., 1996) (Gonzalez et al., 1998) (Nebert et al., 2000) (Schrenk et al., 1995) (IARC, 1997) (Kerkvliet et al., 2002). Most, if not all, toxic and biological responses elicited by dioxin-like compounds in different species are mediated by the aryl hydrocarbon receptor. Since DLCs occur as complex mixtures in the human diet, the toxic equivalency (TEQ) concept was developed to assess human exposure and risk (NATO, 1988) (Ahlborg et al., 1991) (Denison et al., 2011). Current human TEQs have been mainly derived from *in vivo* animal experiments resulting in so called 'intake' toxic equivalency factors (TEFs). These 'intake' TEFs are commonly used to calculate human TEQs for blood and tissues, although only insufficient data is currently available to confirm if the use of 'intake' TEFs for calculation of the human risk is appropriate or not (van den Berg et al., 2006).

Therefore, the SYSTEQ project was initiated which primarily focused on the development, validation, and establishment of human systemic TEFs (relative effect potencies REPs) and TEQs as biomarkers for dioxin-like compounds. The potency of a compound relative to TCDD gained by a single *in vivo* or *in vitro* study is featured as REP value (van den Berg et al., 1998). Additionally, *in vitro* TEFs (REPs) from human and rodent experimental cellular models from different endpoints will be derived for a large group of PCDD/Fs and DL-PCBs which will be compared to the 'systemic' situation. The European Commission funded the project under the 7th framework programme. Further major objectives of the SYSTEQ project included the search for novel quantifiable biomarkers for AhR activation as well as the identification of differences between human and experimental species. Our research objectives within the SYSTEQ project were divided into several subprojects, as presented in the following passage.

In two mouse *in vivo* studies (mouse 3-day and 14-day study), the influence of selected dioxin-like compounds (TCDD, 1-PnCDD, 4-PnCDF, PCB 118, PCB 126, and PCB 156) as well as non dioxin-like PCB 153 on the hepatic xenobiotic metabolism should be determined after a single dose of each test compound. Hence, three cytochrome P450s involved in phase I in the xenobiotic metabolism were selected *Cyp1a1, Cyp2b10,* and *Cyp3a44*. Their respective hepatic mRNA expression was analyzed by quantitative real-time PCR. The induction of CYP1A, CYP2B, and CYP3A is associated with the activation of three different receptor-mediated signalling pathways, i.e. AhR, CAR, and PXR, respectively.

In order to find, establish, and implement novel biomarkers for AhR activation due to exposure to dioxin-like compounds, a microarray study was performed using liver samples from mouse 3-day study (TCDD as reference compound for DLCs and as negative control NDL-PCB 153). The alterations in hepatic gene expression by TCDD and NDL-PCB 153

should provide further information about AhR-dependent and AhR-independent mechanisms in mouse.

Further major objectives included *in vitro* experiments performed in human hepatocellular carcinoma cell line HepG2 and freshly isolated primary human hepatocytes. Primary human liver cells represent the closest *in vitro* model to the human liver (Hewitt et al., 2007). HepG2 cells were applied in the present work to characterize possible similarities and differences between tumour-derived immortalized cells and non-transformed cells because HepG2 cells are frequently used to assess biological responses of DL-compounds in *in vitro* studies (Lipp et al., 1992) (Zeiger et al., 2001) (Kim et al., 2009) (Dere et al., 2011). Since pronounced differences in TEFs, e.g. relative effect potencies (REPs), were determined in different animal species (Haws et al., 2006), the use of human *in vitro* models, especially primary human hepatocytes, should provide essential datasets which function as a basis for novel human *in vitro* TEFs.

As preliminary test method, a cytotocixity assay, i.e. the Alamar Blue assay, was performed with all experimentally applied substances in both human cell models to exclude cytotoxic effects of test compounds in the subsequent experimental approaches.

The induction of CYP1A1 is the most sensitive marker for exposure to dioxins and dioxin-like compounds (Vanden Heuvel et al., 1993) (Drahushuk et al., 1996) (Behnisch et al., 2002) and was used in the present work to assess the relative effect potencies and efficencies of the selected compounds. Therefore, the catalytic CYP1A1 activity was measured after exposure to TCDD, 1-PnCDD, 4-PnCDF, PCB 118, PCB 126, and PCB 156 as well as NDL-PCB 153 in both human cell models. These five DL-compounds are with about 90 % the major contributors to the total dioxin-like activity in the human diet (Liem et al., 2000). Despite the concentration-dependent changes in the catalytic CYP1A1 activity of the seven core congeners, *CYP1A1* and *CYP1B1* mRNA levels were additionally determined in HepG2 cells by RT-PCR. Concentration-dependent effects on the CYP1A1 catalytic activity were also determined for seven further DL-compounds (1,6-HxCDD, 1,4,6-HpCDD, TCDF, 1,4-HxCDF, 1,4,6-HxCDF, PCB 77, and PCB 105) by EROD assay as well as CYP1A1 protein levels were assessed after exposure to further PCDD/Fs congeners in HepG2 cells by Western blot analysis.

Gene expression alterations elicited by DL-compounds in both human liver models ought to be characterized in two performed microarray experiments. In the first experimental toxicogenomic approach, altered gene expression in primary human hepatocytes of selected DL-compounds (TCDD, 1-PnCDD, 4-PnCDF, and PCB 126) and NDL-PCB 153 ought to be analyzed, and if possible, affected metabolic processes and pathways ought to be characterized. The emphasis of this experiment was to outline commonly regulated genes by DLCs to identify novel quantifiable biomarkers for DL-compounds.

In the second performed microarray experiment, TCDD- and PCB 153-elicited gene expression alterations in HepG2 cells were determined and afterwards compared to the obtained findings for these two compounds in primary human hepatocytes. Additionally, the TCDD-altered gene expression data obtained from the microarray experiments (hHeps, HepG2, and mouse 3-day study) was used to select AhR target genes in search for novel quantifiable biomarkers for DL-compounds. Subsequently, the mRNA expression levels of

chosen AhR target genes were verified by the use of RT-PCR analysis. Based on these findings, the role of individual AhR target genes as novel quantifiable biomarkers ought to be critically discussed.

Another major research objective within the present work focused on the physiological role of the AhR and the AhR-mediated biological effects elicited by TCDD in the mouse liver. It has been postulated that the AhR mediates most, if not all, biological and toxic responses of TCDD and related compounds. Furthermore, various studies demonstrated that the AhR is responsible for normal development, physiological function, and homeostasis in absence of an exogenous ligand (Schmidt et al., 1996) (Mimura et al., 1997) (Fernandez-Salguero et al., 1996) (Denison et al., 2002) (Mimura et al., 2003). A research project was initiated which focused on the investigation of AhR-dependent and AhR-independent responses in the livers of *Ahr* knockout and *Ahr* wild-type mice.The project was funded by the 'Stiftung Rheinland-Pfalz für Innovation'.

In a first experimental approach, blood plasma metabolites of *Ahr* knockout and wild-type mice should be identified and genotype-specific differences in metabolite spectrum ought to be characterized. Hence, an extraction method for blood plasma metabolites was established and a HPLC-ESI-MS/MS program setup was developed and validated in the present work.
AhR-dependent and -independent effects of TCDD on livers of *Ahr* knockout and wild-type mice were assessed *in vivo* after administration of a single dose of TCDD.

The mouse liver was the target tissue and primary topic of interest in the subsequently performed experiments. TCDD and related compounds induce several xenobiotic metabolizing enzymes in the liver. Therefore, the hepatic mRNA expression levels of selected cytochrome P450s (*Cyp1a1, Cyp1a2, Cyp2b10,* and *Cyp3a44*) were determined by RT-PCR. Additionally, TCDD-induced changes in hepatic gene expression in *Ahr* knockout and wild-type mice were assessed by microarray analysis whereupon metabolic processes and pathways ought to be identified.

IV Results and Discussion

IV.1 *in vivo* Experiments Part I

IV.1.1 Mouse Studies I and II

The EU-project SYSTEQ aimed to develop, validate, and establish human systemic TEFs and TEQs as indicators of toxicity for dioxin-like compounds (DLCs). The best known AhR-regulated marker for dioxin exposure is the induction of the cytochrome isoenzymes, i.e. CYP1A1, 1A2, and 1B1. The *in vivo* studies presented within this work focused on the search and establishment of a novel quantifiable biomarker for DL-compounds as well as analyzing the AhR-dependent and AhR-independent effects due to DLC treatment.

The 3-day and 14-day mouse studies were performed within the framework of the European project SYSTEQ at the Department of Toxicology, Institute for Risk Assessment Sciences (IRAS) at Utrecht University, the Netherlands, under supervision of Prof. Dr. Martin van den Berg. The dioxin-like compounds analyzed in the mouse 3-day and 14-day study (TCDD, 1-PnCDD, 4-PnCDF, PCB 118, PCB 126, and PCB 156) contribute about 90 % to the dioxin-like activity in the human food chain (Liem et al., 2000). The non dioxin-like PCB 153 is used as negative control in the animal experiments. In both acute toxicity studies, mice received a single dose by gavage, only the post-treatment time varied. Blood and tissues were shipped to the different European project partners. In the present work the mouse liver is the centre of interest. Detailed information about the preparation of mouse livers is given in chapter six (VI Methods).

IV.1.1.1 Study I - Mouse 3-day Study

In the 3-day study, adult female C57BL/6 mice were exposed to seven selected compounds (TCDD, 1-PnCDD, 4-PnCDF, PCB 126, PCB 118, PCB 153, and PCB 156). The examined dose levels used in mouse study I are featured in the table below. Each dose group consisted of six female C57BL/6 mice. Total RNA was isolated using Qiagen RNeasy Mini Kit (Qiagen, Hilden) according to the manufacturer's instruction. The RNA concentration was spectrophotometrically determined at an absorption wavelength of 260 and 280 nm via NanoDrop (Peqlab, Erlangen). The RNA purity and integrity was verified using 2100 Bioanalyzer (Agilent Technologies, Waldbronn) and associated RNA 6000 Pico LabChip Kit (VI Methods). Subsequently isolated RNA was used for microarray analysis (TCDD or PCB 153-treated mice) or transcribed into cDNA to perform gene expression analysis by RT-PCR.

Table 3. Overview mouse study I - 3-day (dose levels).

Study	Treatment	Single dose (µg/kg bw)					TEF (WHO, 2005)
3-day	**TCDD**	0	0.5	2.5	10		1.0
	1-PnCDD	0	0.5	2.5	10		1.0
	4-PnCDF	0	5	25	100		0.3
	PCB 126	0	5	25	100		0.1
	PCB 118	0				150000	0.00003
	PCB 153	0				150000	-
	PCB 156	0				150000	0.00003

IV.1.1.1.1 Gene Expression Analysis by RT-PCR

The mRNA expression levels of genes, which play key roles in xenobiotic metabolism, were measured in the following RT-PCR experiments. Therefore, genes were selected for assessing the activation of different receptor-mediated signalling pathways (AhR, CAR, and PXR). The induction of *Cyp1a1* implicates that the respective test compound presumly has bound to the AhR and actives the AhR signalling pathway. *Cyp2b10* represents the murine analog to the human *CYP2B6* which is primarily CAR-regulated, whereas *Cyp3a44* was chosen to analyze the possible ligand binding to the PXR due to compound exposure. Complementary DNA (cDNA) was synthesized using iScript cDNA Synthesis Kit (BioRad). 1 µl of the transcribed cDNA was used to perform each RT-PCR. The *Cyp1a1*, *Cyp2b10*, and *Cyp3a44* mRNA expression was normalized using *36b4* as housekeeping gene and calculated relative to the expression in the corresponding vehicle control (0 µg/kg bw).

TCDD-treated animals revealed no change in gene expression of *Cyp2b10* and *Cyp3a44* as expected, whereas a dose-dependent increase of *Cyp1a1* expression was determined in the present study as shown in Figure 8. A statistically significant induction of *Cyp1a1* mRNA expression was measured starting from 2.5 µg/kg bw which resulted in a 1382.08 ± 378.28-fold induction. After the treatment of female C57BL/6 mice with 1-PnCDD in the chosen four dose levels, there was no statistically significant increase in gene expression, neither with *Cyp2b10* nor with *Cyp3a44*. A dose-dependent induction of *Cyp1a1* mRNA expression by 1-PnCDD was measured in mouse study I. A statistically highly significant induction of *Cyp1a1* was detected after treatment with 2.5 µg/kg bw (970.24 ± 443.08) and 10 µg/kg bw 1-PnCDD (1860.10 ± 750.21) as featured in Figure 8 on the right-hand side.

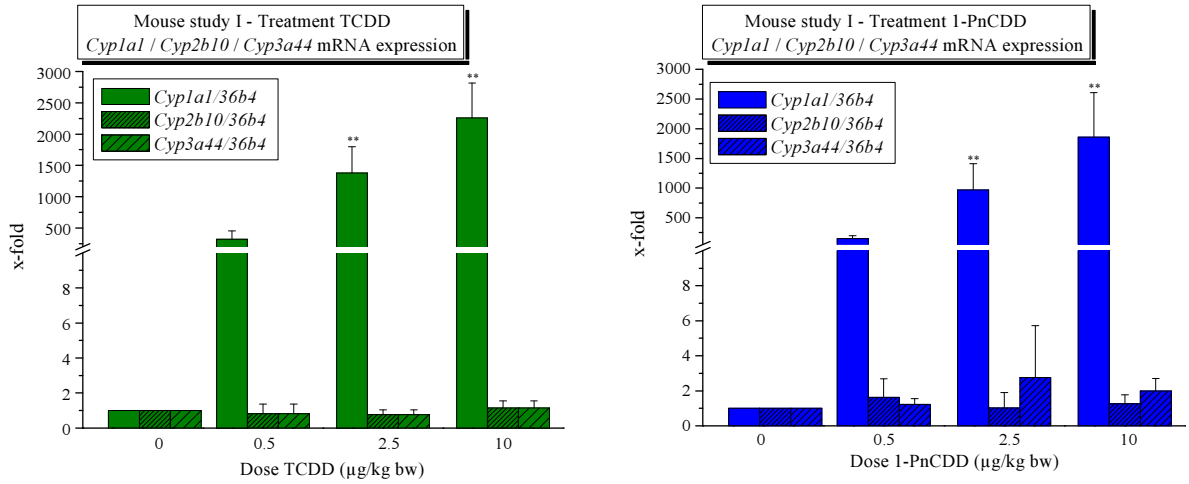

Figure 8. Real-time PCR ratios of female mice treated with TCDD (left) or 1-PnCDD (right) - mouse study I. *36b4* served as housekeeping gene, compound as one-time administered dose. Data represent means + SD of six different adult female mice, normalized to corresponding vehicle control. One-way analysis of variance (ANOVA) with Dunnett's post-test ,= p ≤0.01.**

A dose-dependent increase in *Cyp1a1* mRNA expression was also determined after treatment with 4-PnCDF (Figure 9) as shown before for TCDD and 1-PnCDD, however, accomplished with higher dose levels. A statistically highly significant *Cyp1a1* induction was achieved with a dosage of ≥ 25 µg/kg bw, while no alterations of the *Cyp2b10* and *Cyp3a44* mRNA gene expression were examined. Six female C57BL/6 mice were also exposed to PCB 126 in four dose level groups from 0-100 µg/kg bw (Figure 9). A dose-dependent increase in *Cyp1a1* mRNA was obtained for the DL-PCB resulting in a statistically highly significant induction after exposure to ≥ 25 PCB 126 µg/kg bw. Gene expression of the CAR-regulated *Cyp2b10* was not statistically significantly changed in the selected doses. A slight but statistically significant increase of *Cyp3a44* mRNA levels was determined after treatment with 25 µg PCB 126/kg bw which led to a fold-change of 3.14 ± 1.49. No dose-dependent increase was observed in mouse study I. However, the *Cyp3a44* fold induction of one animal was two times higher than that of the other five animals.

Figure 10 displays the results of the RT-PCR analysis of PCB 118, PCB 156, and PCB 153. Vehicle control animals were compared to animals which received a single dose of 150000 µg/kg bw of the respective test compound. Treatment with PCB 118 resulted in a high induction of *Cyp1a1* mRNA expression (fold-change 1539.50 ± 427.56), which was statistically extremely significant (p ≤ 0.001). *Cyp2b10* mRNA expression was also induced, but about seventy-times lower than the *Cyp1a1* mRNA levels (20.95 ± 4.80). The *Cyp3a44* mRNA levels were neither up nor down regulated by the selected dosage. As pictured in Figure 10, PCB 153, which belongs to the family of non dioxin-like biphenyls, led to the induction of *Cyp2b10* mRNA expression (67.06 ± 28.19). Hepatic *Cyp1a1* and *Cyp3a44* mRNA levels were not significantly altered after the treatment with 150000 µg/kg bw PCB 153. *Cyp1a1*, *Cyp2b10*, and *Cyp3a44* mRNA levels were all significantly induced in mouse liver samples after treatment with PCB 156 as shown in Figure 10. The *Cyp1a1* mRNA expression achieved the highest induction with 2599.23 ± 1065.00-fold over control, followed by *Cyp2b10* (88.91 ± 26.93-fold), and *Cyp3a44* (4.69 ± 4.27-fold).

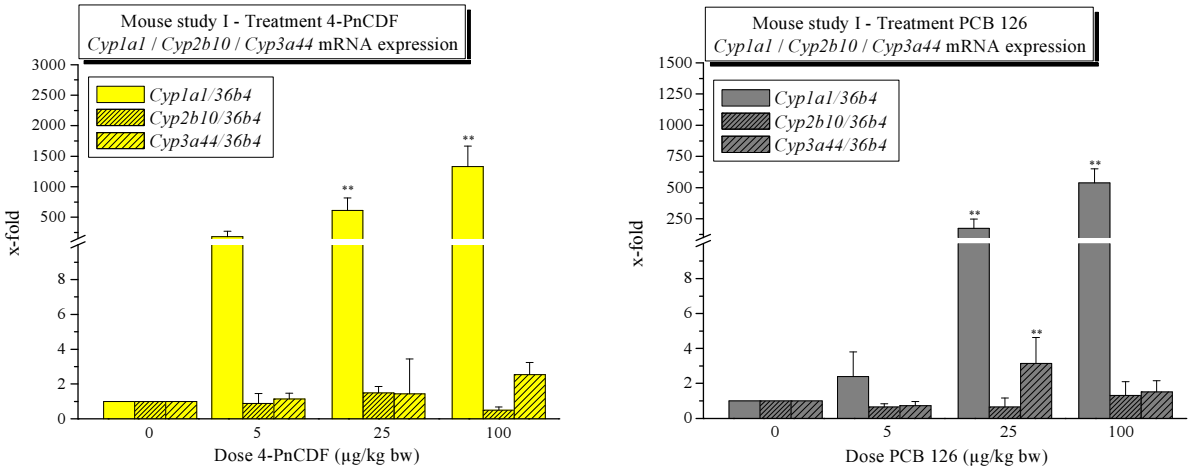

Figure 9. **Real-time PCR ratios of female mice treated with 4-PnCDF (left) or PCB 126 (right) - mouse study I. *36b4* served as housekeeping gene, compound as one-time administered dose. Data represent means + SD of six different adult female mice, normalized to corresponding vehicle control. One-way analysis of variance (ANOVA) with Dunnett's post-test ,**= p ≤0.01.**

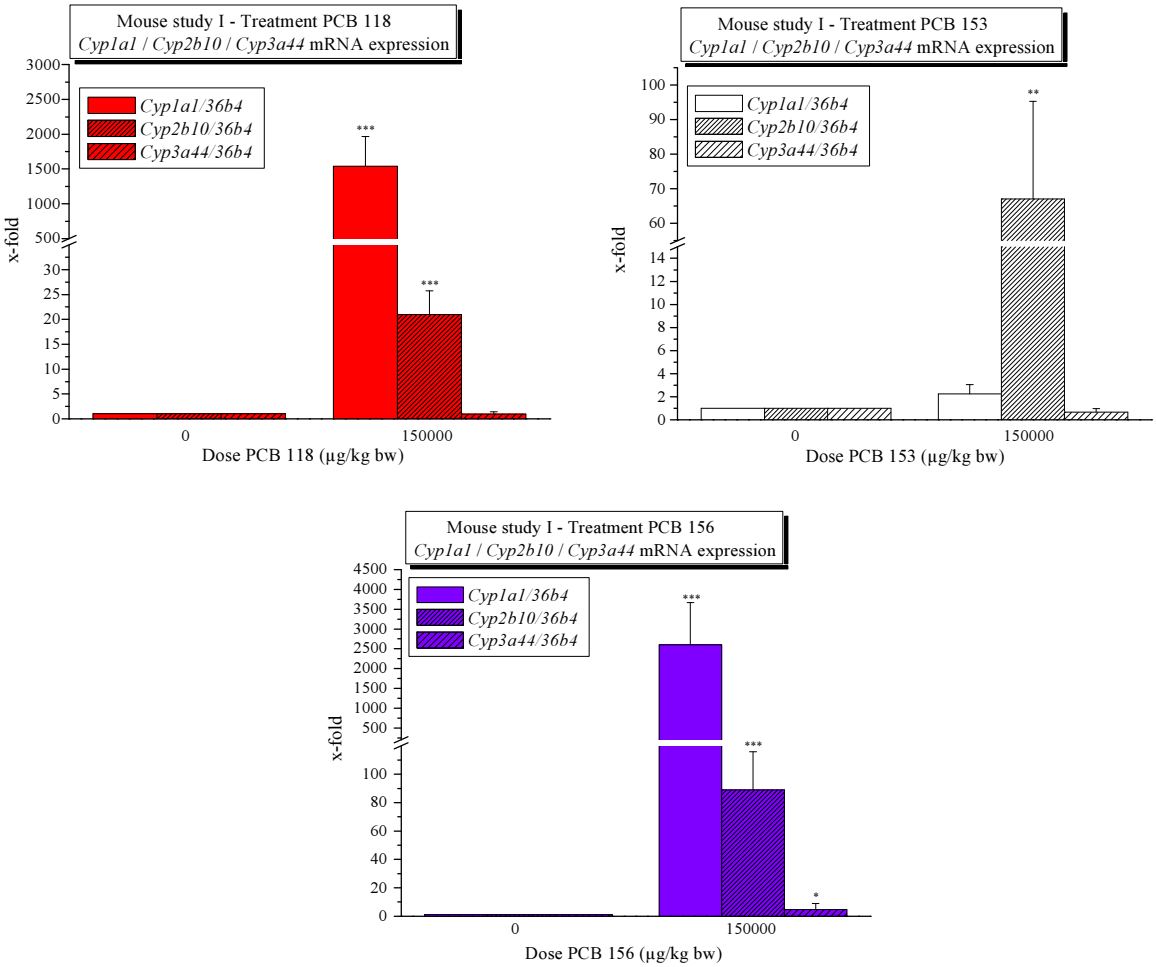

Figure 10. **Real-time PCR ratios of female mice treated with PCB 118 (up left), PCB 156 (up right), or PCB 153 (down middle) - mouse study I. *36b4* served as housekeeping gene, compound as one-time administered dose. Data represent means + SD of six different adult female mice, normalized to corresponding vehicle control. One-way analysis of variance (ANOVA) with Dunnett's post-test,*= p ≤0.05, **= p ≤0.01.**

In summary, the mouse 3-day acute toxicity study after single dose administration of the selected compounds revealed the dose-dependent AhR-mediated increase of *Cyp1a1* mRNA expression after treatment with TCDD, 1-PnCDD, 4-PnCDF, and PCB 126. Neither CAR, nor PXR were activated due to treatment with the four test compounds. In case of the polychlorinated biphenyls, the administered high dosages of PCB 118 and PCB156 led to the activation of AhR and CAR, though the *Cyp1a1* mRNA expression was 73-fold and 23-fold higher compared to the *Cyp2b10* mRNA expression. Furthermore, the hepatic *Cyp3a44* mRNA expression was also significantly increased in case of PCB 156 although the high standard deviation has to be taken into consideration. Treatment of female C57BL/6 mice with PCB 153 only resulted in the induction of *Cyp2b10* mRNA levels leading to the suggestion that only CAR was activated.

IV.1.1.1.2 Microarray Analysis - Mouse Study I

Microarray analysis is a powerful tool to examine a large number of genes simultaneously. Application of this new molecular biological technique could reveal further information about gene expression after exposure to dioxin-like compounds. In a 3-day study, six female C57BL/6 mice received a single dose of either TCDD (25 µg/kg bw) or non dioxin-like PCB 153 (150000 µg/kg bw) by gavage, whereas vehicle control animals were treated with corn oil.

Table 4. Overview dose levels mouse 3-day study for microarray analysis.

Study	Treatment	Single dose (µg/kg bw)		TEF (WHO, 2005)
3-day	**TCDD**	0	25	1.0
	PCB 153	0	150000	-

At day three animals were sacrificed by CO_2/O_2 asphyxiation, tissues including mouse liver was extracted surgically and immediately frozen in liquid nitrogen and stored at -80 °C until usage. Total RNA was isolated using Qiagen RNeasy Mini Kit (Qiagen, Hilden). RNA concentrations were determined via NanoDrop (Peqlab, Erlangen). RNA purities were verified by Agilent 2100 Bioanalyzer and associated RNA 6000 Pico LabChip kit (Agilent Technologies, Waldbronn). Afterwards, Agilent's Two-Color Microarray-based Expression Analysis according to Agilent's Low Input Quick Amp Labeling Kit was performed using cyanine 3- and cyanine 5-labelled targets to measure expression in experimental and control samples. Vehicle control samples and compound-treated samples were stained oppositionally. 100 ng per sample was selected as starting RNA concentration. Whole Mouse Genome Oligo Microarray 4x44K (Agilent Technologie, Waldbronn) was used to measure altered genes between control groups (treated with corn oil) and compound-treated mice. Further information about the experimental procedures and conditions as well as data processing and statistical analysis are presented in chapter six (VI Methods).

Further studies, not presented in this work, included microarray analysis of mouse liver samples after treatment with 1-PnCDD (25 µg/kg bw), 4-PnCDF (250 µg/kg bw), PCB 118 (150000 µg/kg bw), PCB 126 (250 µg/kg bw), and PCB 156 (150000 µg/kg bw). Microarray data derived from all seven core congeners was summarized in one single data file. Microarray results were filtered by selected cut-off values for the signal intensity A ≥ 7, the log2 fold-change ≥ 1 or ≤ -1, and the p-value ≤ 0.05.

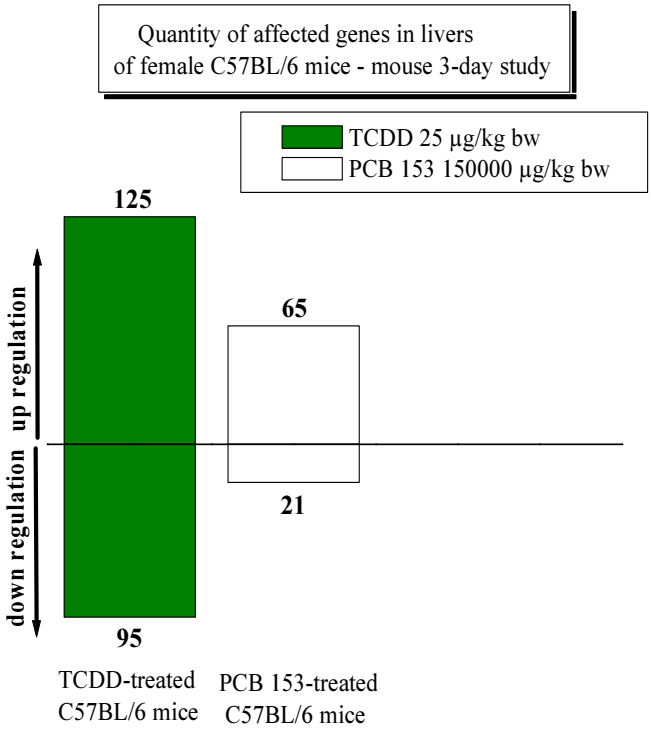

Figure 11. **Microarray results of mouse study I - 3-day study - mouse study I.**
Selected parameters: A ≥ 7, log2 fc ≥ 1 or ≤ -1, p-value ≤ 0.05.

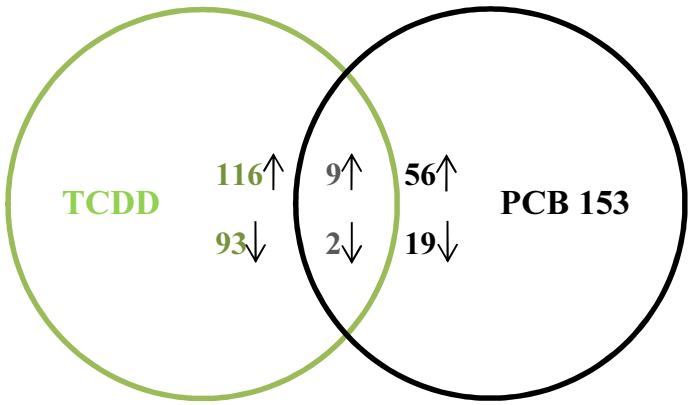

Figure 12. **Microarray results of mouse study I featured as Venn diagram.**
Up and down regulated genes in livers of female C57BL/6 mice after treatment with TCDD (25 µg/kg bw) or PCB 153 (150000 µg/kg bw).
Selected parameters: A ≥ 7, log2 fc ≥ 1 or ≤ -1, p-value ≤ 0.05.

IV.1.1.1.2.1 Microarray Results - TCDD Treatment

After treatment with TCDD (25 µg/kg bw) 125 unique genes were up and 95 genes down regulated in female mouse liver (Figure 11). A complete list of all significantly up and down regulated genes is attached to the present work (Tables 81 and 82).
An overview of the 10 highest up and down regulated genes is given in Table 5 below. The highest up regulated gene after TCDD treatment in livers of C57BL/6 mice was *Cyp1a1* by far. Induction of *Cyp1a1* is up to the present day the most sensitive marker for AhR activation upon dioxin treatment. Other established dioxin-inducible members of the *Cyp1* family, *Cyp1b1* and *Cyp1a2*, were additionally strongly induced in livers of female C57BL/6 mice (Table 5). The fragile histidine triad (*Fhit*) was also among the ten highest up regulated genes in livers of TCDD-treated female C57BL/6 mice. *FHIT* is a known tumour suppressor gene in humans (Schlott et al., 1999). The up regulation of the human *FHIT* gene was demonstrated in a previous performed microarray study in human liver cell line (HL1-1) after treatment with TCDD (10 nM) (Kim et al., 2009).

Tuba8 (tubulin alpha 8) was also among the ten highest up regulated genes. Alpha-tubulin and beta-tubulin form a heterodimer complex that assembles into microtubules which constitute one of the major components of the cytoskeleton in eukaryotic cells and are therefore involved in various essential processes including cell division, motility, and intracellular transport. The potential role of TUBA8 in the regulation of cell growth, proliferation, and cellular migration was demonstrated in an *in vitro* study in which Huh7 and HepG2 cells were stable transfected with the murine *Tuba8* gene (Kamino et al., 2011). The induction of *Tuba8* was also observed in TCDD-treated male C57BL/6 mice in a microarray study performed by Tijet and co-workers (Tijet et al., 2006). *Slc46a3* was also up regulated in female C57BL/6 mice. Slc46a3 encodes a protein which is involved in transmembrane transport.

Tiparp (TCDD-inducible poly(ADP-ribose) polymerase) was also among the ten highest up regulated genes upon TCDD-treatment. Ma and co-workers identified *Tiparp* as TCDD-inducible gene in the mouse hepatoma cell line Hepa1c1c7 (Ma et al., 2001). Diani-Moore et al. demonstrated in their study for the first time that an AhR target gene (*Tiparp*) directly mediates a TCDD-elicited toxic effect, in particular the suppression of hepatic gluconeogenesis (Diani-Moore et al., 2010). *Gsta1*, the glutathione S-transferase gene was also up regulated in mouse study I. *Gsta1* encodes an enzyme which belongs to the murine aromatic hydrocarbon gene battery (Nebert et al., 2000). Glutathione S-transferases play key roles in xenobiotic metabolism, precisely during phase II of drug metabolism, by conjugating xenobiotics (Boverhof et al., 2006) (Yeager et al., 2009). *Htatip2* was among the ten highest up regulated hepatic genes in TCDD-treated female C57BL/6 mice. *Htatip2* is a tumour suppressor gene which encodes a protein that promotes apoptosis and furthermore inhibits angiogenesis (Ito et al., 2003). Induction of *Htatip2* after TCDD treatment in an AhR-dependent manner in liver and kidney was demonstrated by Boutros and co-workers in mouse, but not in rat (Boutros et al., 2009). Furthermore, *Htatip2* was altered in livers of mice with a constitutively active AhR (Moennikes et al., 2004).

TCDD treatment led to the down regulation of 95 unique genes based on the chosen criteria (A ≥ 7, log2 fc ≤ -1, p-value ≤ 0.05). The highest down regulated gene was the Kruppel-like factor 10 (*Klf10*). Kruppel-like transcription factors are DNA-binding transcriptional regulators which play key roles in regulating biological processes such as cell growth, differentiation, and embryogenesis. *KLF10* is formerly known as *TIEG1* (transforming growth factor beta-inducible early gene 1) which received its name as a consequence to the primary response to TGF-β treatment in human osteoblasts (Subramaniam et al., 2005). The *Rgs16* (regulator of G-protein signalling 16) gene was also down regulated in livers of C57BL/6 mice. G protein-coupled receptor pathways control the glucose and fatty acid metabolism. Pashkov and co-workers demonstrated that RSG16 inhibits hepatic fatty acid oxidation in a carbohydrate response element-binding protein (ChREBP)-dependent manner (Pashkov et al., 2011). The peptidase inhibitor pseudogene (*Serpina4-PS1*) was also down regulated in the present microarray study although *Serpina6*, *Serpinb6a*, and *Serpinb6c* were up regulated in livers of TCDD-treated C57BL/6 mice. These findings suggest that the encoded proteins maintain different cellular functions.

The hepatic *Egfr* (epidermal growth factor receptor) gene expression was down regulated after exposure to TCDD compared to the respective vehicle control animals. EGFR protein is a transmembrane glycoprotein with a ligand-dependent intrinsic tyrosine kinase activity. The receptor and its downstream pathways play key roles in the regulation of normal cellular processes such as cell proliferation, differentiation, and migration. The *EGFR* expression rate is abnormally high in the majority of human epithelial cancers in which EGFR activation appears to be critical for tumour progession and pathogenesis. The interplay between TCDD and the EGFR-triggered signalling pathways has been described in various studies. TCDD does neither bind to the EGFR itself, nor changes it the binding affinity of EGF to its receptor. It was postulated that the decline in EGF-binding seems to be due to a reduced EGFR content on the cell membrane (Clark et al., 1992) (Sewall et al., 1995) (Haarmann-Stemmann et al., 2009). *Socs2* (suppressor of cytokine signalling 2) gene was also down regulated in livers of female C57BL/6 mice after treatment with TCDD. *Socs2* has been associated with the regulation of growth hormone signalling. *Socs2*-deficient mice feature gigantism which was postulated to be the result of the deregulated growth hormone signalling (Alexander et al., 2003) (Burns-Naas et al., 2006). TCDD-mediated mRNA induction of *Socs2* (about 3-fold) was also detected in the murine CH12.LX B cells, but not in the other tested AhR-responsive cells (Hepa1c1c7 and MCF-7). The slight induction of *Socs2* by TCDD seems to be a cell-type specific effect (Boverhof et al., 2006). Perhaps the suppression of *Socs2* in female C57BL/6 mice could be the result of the TCDD-mediated interference in growth factor signalling. Moreover, the suppression of *Socs2* could be the result of a female-mouse specific effect. *Csad* (cysteine sulfinic acid decarboxylase) was also among the ten highest down regulated genes. *Csad* encodes an enzyme which is involved in biosynthesis of taurine. Taurine is needed for fundamental biological processes such as the development of the brain and eye, reproduction as well as osmoregulation (Park et al., 2002). *Csad* was also among the down regulated genes in livers of TCDD-treated (100 µg/kg bw) male $Ahr^{+/+}$ mice after 72 h in a study performed by Yoon and co-workers (Yoon et al., 2006). *Bcl6* (B-cell leukemia/lymphoma 6) gene was also among the ten highest down regulated genes. The *Bcl6* gene encodes a protein which acts as transcriptional repressor and plays key roles in germinal

centre formation, T helper cell differentiation, and in the development of lymphomas (lymphomagenesis) (Pixeley et al., 2005).

125 were up and 95 down regulated in liver by TCDD treatment in the mouse study I. Considering all up and down regulated genes, mainly genes involved in xenobiotic, lipid, and glucose metabolism were altered in the performed microarray study. Various genes are linked to biotransformation processes (amongst others *Cyp1a1, 1a2, 1b1, Ugt1a6a, Ugt1a10, Sult5a1, Gsta1, Gsta2, Gstm2, Gstp1, and Gstp2*). *Nqo1* and *Nqo2* were both highly up regulated, but due to the cut-off value for the colour intensity of 7, *Nqo1* is not listed among all significantly up regulated genes (Table 81). In addition, several other genes which were linked to the AhR (*Tiparp, Cd36, Hsd17b2,* and *Ahrr*) were up regulated by TCDD treatment. *Aldh3a1* was not significantly up regulated by TCDD in the present study, although it belongs to the group of classic murine AhR target genes according to Nebert et al. (2000). Hence, it might be reasonably expected that this gene should be up regulated in the mouse liver by TCDD, too. Nevertheless, the lack of induction in the present study was also demonstrated in other *in vivo* studies (Vasiliou et al., 1993) (Alnouti et al., 2006). However, *Aldh3a1* was induced by TCDD in various mouse and other carcinoma cell lines and in rat *in vivo*. Alnouti et al. postulated that *Aldh3a1* was categorized to the murine AhR gene battery most likely due to the aforementioned findings.

Tuba8, Fmo3, and *Pcp4l1* were highly up regulated by TCDD as it was also demonstrated in a microarray study performed by Tijet and co-workers in which AhR-dependent and AhR-independent effects were outlined in livers of TCDD-treated male $Ahr^{+/+}$ and $Ahr^{-/-}$ mice. The constitutive expression of *Tuba8* was much lower in $Ahr^{+/+}$ mice than in $Ahr^{-/-}$ mice which led to the suggestion that the AhR suppresses *Tuba8* in absence of a ligand. Treatment of TCDD results in the rehabilitation of *Tuba8* mRNA levels in $Ahr^{+/+}$ mice. *Fmo3*, the flavin containing monooxygenase 3, belongs to the group of microsomal enzymes which convert highly lipophilic substrates into oxygenated metabolites with higher polarity thereby faciliating their excretion (Celius et al., 2008). The AhR dependency of *Fmo3* was proven in several studies (Tijet et al., 2006) (Celius et al., 2008).

Genes involved in lipid metabolism were also altered in the present study in a way that several were up and others down regulated by TCDD. Amongst the up regulated genes related to lipid metabolism were *Acot1* (acyl-CoA thioesterase 1), *Fabp4* (fatty acid-binding protein 4), *Lpin1* (lipin 1), *Mgll* (monoglyceride lipase), *Pla2g12a* (phospholipase A2, group XIIA), *Cd36* (CD36 antigen), and *Vldlr* (very low density lipoprotein receptor). The acetyl-Coenzyme A carboxylase alpha (*Acaca*), the ATP citrate lyase (*Acly*), the elongation of very long-chain fatty acids 2 (*Elovl2*) and 6 (*Elovl6*), fatty acid-binding protein 5 (*Fabp5*), and the fatty acid synthase (*Fasn*) were on the contrary down regulated in mouse livers.

Acot1 belongs to the class of Acyl-CoA thioesterases which play key roles in fatty acid metabolism. They hydrolyze acyl CoAs to the corresponding free fatty acid and CoASH and therefore control the intracellular levels of both (Hunt et al., 2006). Fatty acid-binding proteins play key roles in the intracellular fatty acid transport. *Fabp4* was up and *Fabp5* down regulated in the present study which hints at the tight metabolic regulation. FAPBs are associated with the metabolic syndrome and obesity (Maeda et al., 2003). Lipin1 dephosphorylates phosphatic acid in order to generate diacylglycerol which displays the

penultimate step in the triglyceride synthesis. Furthermore, Lipin1 also acts as coregulatory protein which is able to translocate to the nucleus and regulates the activity of the DNA-bound transcription factors (for example PPAR) (Mitra et al., 2012). *Mgll* and *Pla2g12a* belong to the class of lipolytic genes which encode proteins that hydrolyze hepatocellular triglyceride levels into free fatty acids and monoglycerides (Giller et al., 1992) (Angrish et al., 2012). CD36 and VLDLR are cell surface receptors involved in the uptake of lipoproteins. CD36 is addionally responsible for the transport of fatty acids and has a high affinity for the uptake of long-chain fatty acids (Febbraio et al., 1999) (Bonen et al., 2004) (Boverhof et al., 2006). However, VLDLR regulates the internalization and degradation of triglyceride-rich lipoproteins (Yagyu et al., 2002) (Boverhof et al., 2006).

The acetyl-Coenzyme A carboxylase alpha (ACACA) and the ATP citrate lyase (ACLY) play key roles in the synthesis of fatty acids. ACACA catalyzes the carboxylation of acetyl CoA to malonyl-CoA which represents the first and rate-limiting step in the *de novo* fatty acid biosynthesis (Colbert et al., 2010). The gene long-chain fatty acid synthase (*Fasn*) was also down regulated after treatment with TCDD which leads to the suggestion that the total increase of the hepatic lipid content is most likely not based on the *de novo* fatty acid synthesis (Mashima et al., 2009) (Forgacs et al., 2012) (Angrish et al., 2012). ELOVL2 has been shown to be involved in the elongation of C20 and C22 polyunsaturated fatty acids (PUFAs) to produce C24:4n-6 and C24:5n-3 PUFAs (Zadravec et al., 2011). ELOVL6 is involved in the elongation of stearate (C18) from palmitate (C16), as well as the elongation of vaccinate (C18:1n-7) from palmitoleate (C16:1n-7) (Matsuzaka et al., 2007).

The glucose-6-phosphatase (*G6pc*), the phosphoenolpyruvate carboxykinase 1 (*Pck1*), and the pyruvate kinase liver and red blood cells (*Pklr*) were among the down regulated genes in the present study. These genes play key roles in glycolysis (*Pklr*) and glyconeogenesis (*G6pc, Pck1*) (Berg et al., 2003). The disturbance of the glycolysis and glyconeogenesis by TCDD postulates a direct interference with the triglyceride synthesis.

These findings once more outline the role of TCDD in the dysregulation of the hepatic lipid metabolism. TCDD is known to cause extremely enlarged livers (hepatomegaly) as well as hepatocellular neoplasms, inflammation, necrosis, and steatosis. Several mouse *in vivo* studies demonstrated that the expression of genes involved in metabolism and transport of lipids is fatally altered by TCDD (Poland et al., 1982a) (Huff et al., 1991) (Boverhof et al., 2006) (Kopec et al., 2010a) (Kopec et al., 2010b) (Angrish et al., 2012).

Table 5. 10 highest up and down regulated genes in livers of TCDD-treated female C57BL/6 mice (Mouse study I - mouse 3-day study).
TCDD as one time administered dose (25 µg/kg bw).
Selected parameters for microarray analysis: cut-off values: A ≥ 7, log2 fc ≥ 1 or ≤ -1, p-value ≤ 0.05
Annotations: '*'calculated mean log2 fc-value from identical probes
'#'analysis revealed non-identical probes of this gene have different log2 fc values

Gene	Gene description	Probe name	Systematic name	Log2 fc
Up regulation				
Cyp1a1	Cytochromes P450 family 1, subunit a, polypeptide 1	A_51_P279693	NM_009992	9.48
Cyp1b1	Cytochromes P450 family 1, subunit b, polypeptide 1	A_51_P255456	NM_009994	5.17
Cyp1a2	Cytochromes P450 family 1, subunit a, polypeptide 2	A_52_P595871	NM_009993	3.99
Fhit	Fragile histidine triad gene	A_55_P2032714	NM_010210	3.58
Tuba8	Tubulin alpha 8	A_66_P119518	NM_017379	3.38
Slc46a3	Solute carrier family 46, member 3	A_51_P299805	NM_027872	3.10
Tiparp	TCDD-inducible poly(ADP-ribose) polymerase	A_55_P1985890	NM_178892	2.90
Gsta1	Glutathione S-transferase alpha 1 (Ya)	A_55_P2032946	NM_008181	2.82
Gm9933	Predicted gene ENSMUSG00000054044	A_55_P2004099	XM_001477458	2.72
Htatip2	HIV-1 tat interactive protein 2 homolog (human), transcript variant 1	A_52_P515036	NM_016865	2.68
Down regulation				
Klf10	Kruppel-like factor 10	A_55_P2022074	NM_013692	-2.85
Rgs16	Regulator of G-protein signalling 16	A_51_P249286	NM_011267	-2.60
Serpina4-ps1	Serine (or cysteine) peptidase inhibitor clade A, member 4, pseudogene 1 (cDNA clone IMAGE:5123840)	A_55_P1997003	BC031891	-2.57
Serpina4-ps1	Serine (or cysteine) peptidase inhibitor clade A, member 4, pseudogene 1, non coding RNA	A_55_P2004606	NR_002861	-2.49
Egfr$^{\#}$	Epidermal growth factor receptor, transcript variant 1	A_52_P106259	NM_207655	-2.18*
Socs2$^{\#}$	Suppressor of cytokine signalling 2, transcript variant 1	A_51_P107362	NM_007706	-2.07*
Csad	Cysteine sulfinic acid decarboxylase	A_51_P268529	NM_144942	-2.03
LOC100046261	Predicted: similar to myosin XV	A_55_P1954698	XM_001475897	-1.89
Bcl6	B-cell leukemia/lymphoma 6	A_52_P161495	NM_009744	-1.89
LOC676974	Predicted: similar to Glucose phosphate isomerase 1, transcript variant 2	A_55_P2073789	XM_001003154	-1.82

IV.1.1.1.2.2 Microarray Results - PCB 153 Treatment

In mouse liver samples, a total of 86 genes were identified as expressed above background in all six C57BL/6 mice treated with NDL-PCB 153, from which 65 genes were up and 21 genes down regulated based on the chosen criteria (A ≥ 7, log2 fc ≥ 1 or ≤ -1, p-value ≤ 0.05). The top ten of the highest up und down regulated genes is shown in Table 6. A list with all significantly up and down regulated genes is attached to the present work (Tables 83 and 84).

Gsta1 (glutathione S-transferase, alpha 1) was the highest up regulated gene in livers of C57BL/6 mice after treatment with PCB 153 (150000 µg/kg bw). Another member of the glutathione S-transferases, by name *Gsta2*, was also among the ten highest up regulated genes due to treatment with PCB 153. *Gsta1* belongs to the murine aromatic hydrocarbon gene battery (Nebert et al., 2000), but considering the fact that PCB 153 is a non dioxin-like PCB, the induction of *Gsta1* must be due to activation of a different receptor. NDL-PCB 153 leads to the activation of the constitutive androstane receptor (CAR). CAR is able to induce the expression of several detoxification genes (enzymes) linked to phase II of xenobiotic metabolism such as glutathione S-transferases (e.g. *Gsta1, Gsta2*) or UDP-glucoronosyl transferases (*Ugt1a1*) (Hernandez et al., 2009). *Cyp2b10* was also up regulated due to treatment with PCB 153. The up regulation of *Cyp2b10* expression is known to be primarily mediated by CAR. Earlier presented RT-PCR data confirmed these findings; *Cyp2b10* mRNA levels were significantly induced in livers of female C57BL/6 mice after treatment with PCB 153 (150000 µg/kg bw) (IV.1.2.1.1 Gene expression analysis RT-PCR) as well as *Cyp2b9* mRNA levels. The *Cyp3a44* gene was not significantly up regulated in livers of female C57BL/6 mice after exposure to PCB 153 which was confirmed by earlier presented RT-PCR results. The *Cyp3a44* gene expression is above all expressed in female mice and was demonstrated to be inducible by PXR ligands in a female mice-specific manner (Anakk et al., 2007). *Cyp3a11*, the major isoform of the *Cyp3a*'s in mice is slightly, but significantly up regulated (log2 fc value of 1.25). Whether this up regulation is based on the PXR activation or not has to be analyzed in further experiments (e.g. RT-PCR, Western blot) because CAR activators such as phenobarbital are also able to induce the *Cyp3a11* mRNA expression via cross-talk between CAR and PXR.

Cyp2c38 and *Cyp2c54* were also among the ten highest up regulated genes in the present study. Other members of the cytochromes 2c family were also significantly up regulated including *Cyp2c29, Cyp2c37,* and *Cyp2c39*. The mouse CYP2Cs play important roles in arachidonic acid (AA) and linoleic acid (LA) metabolism with different catalytic efficiencies and profiles. CYP2C54 primarly metabolizes AA to epoxyeicosatrienoic acids (EETs), and linoleic acid to epoxyoctadecenoic acids (EOAs). CYP2C29 mainly produces 14*R*, 15*S*-EET, and CYP2C37 primarily 8*S*,9*R*-EET, whereas CYP2C39 is responsible for the stereoselective formation of 8*R*,9*S*-EET (Wang et al., 2004). Umannova and co-workers demonstrated in a rat liver epithelial cell line (WB-F344) that NDL-PCB 153 extremely induced the release of arachidonic acid, but not DL-PCB 126. Arachidonic acid (AA) functions as second messenger and is involved in the modulation of cell survival and proliferation. Therefore, it has been suggested that the interference in the AA signalling pathways could possibly contribute to the

carcinogenic and toxic responses of non dioxin-like PCBs (Marks et al., 2000) (Umannova et al., 2008).

The *Orm3* (orosomucoid 3) gene was also up regulated in livers of female C57BL/6 mice by PCB 153 in the present study. *Orm3* encodes an acute phase protein. Acute phase proteins are a special class of proteins whose plasma concentrations increase or respectively decrease in response to inflammation, tissue injury, or bacterial infection (Carter et al., 1991) (Miura et al., 2009). The *Akr1b7* gene encodes the AKR1B7 protein. AKR1B7 belongs to the class of aldo-keto reductases which belong to the family of phase I metabolizing enzymes. They mediate the detoxification of harmful aldehydes and ketones generated for example from xenobiotics. The mouse *Akr1b7* is a shared transcriptional target gene of PXR and CAR in liver and intestine. The induction of the *Akr1b7* gene expression was demonstrated using a selective mCAR activator (TCPOBOP) (Liu et al., 2009) (Tolson et al., 2010). The *Ces6* gene was also among the ten highest up regulated genes in C57BL/6 mice after exposure to PCB 153. Carboxylesterase (CES) enzymes are predominantly involved in hydrolytic biotransformation processes in liver and intestine of mammals (Satoh et al., 1998). CES family members participate in biotransformation as well as hydrolysation of endogenous compounds such as short- and long-chain acyl-gylcerols and long chain acyl-CoA esters (Satoh et al., 1998) (Xu et al., 2009). Xu and co-workers demonstrated that *Ces6* is a CAR- and PXR-shared target gene in mice (Xu et al., 2009).

The number of down regulated genes was marginal. A total of 21 unique hepatic genes were down regulated in female C57BL/6 mice after treatment with PCB 153 (150000 µg/kg bw). Log2 fc values were only slightly, but statistically significantly down regulated (log2 fc values $\leq$ -1). The highest down regulated genes was *Tnni2* (troponin I, skeletal fast 2) with a log2 fc-value of -2.51. Troponin is a complex of three subunits, troponin I, troponin C, and troponin T which plays an important role in excitation-contraction coupling in the striated muscle. Troponin I is an actin-binding protein that is primarily responsible for the ability of troponin to inhibit the contractile interaction between myosin and actin-tropomyosin (Guenet et al., 1996). The tropomyosin 1 (*Tpm1*) gene itself was also among the ten highest down regulated genes in the present study due to treatment with PCB 153. Tropomyosin is an α-helical coiled-coil fibrous protein which is involved in the striated muscle contraction (Rajan et al., 2007). The *Neb* gene encodes the myofibrillar protein nebulin that is involved in the regulation of the actin filament assembly in the skeletal muscle (Schiaffino et al., 1996) (Gokhin et al., 2010). The gene *Eno3* encodes the protein β-enolase. The enzyme enolase (2-phospho-D-glycerate hydrolase) plays an important role in glycolysis by catalyzing the conversion of 2-phospho-D-glycerate to 2-phosphoenolpyruvate. Interestingly, the protein encoded by the *Eno3* gene is found in the skeletal muscle where it is appears to be involved in the muscle development and regeneration (Comi et al., 2001). The obtained data implicates that because of the exposure to the high dosage of PCB 153 (150000 µg/kg bw) possibly the muscle contraction in the liver could be an affected metabolic process.

Various genes which are involved in lipid metabolism were also among the 10 highest down regulated ones such as *Acot1* and *Cyp4a14*. *Acot1* encodes a cytosolic acyl-coenzyme A thioesterase I which hydrolyzes long-chain acyl-CoAs to free fatty acids and CoA and was identified as peroxisome proliferator-inducible enzyme in the rodent liver (Dongol et al.,

2007). The *Cyp4a14* gene was not the only gene of the cytochromes P450 family *4a* subfamily which was down regulated, *Cyp4a10* and *Cyp4a31* were also significantly down regulated after treatment with PCB 153 (Table 84). The members of the CYP4 family contribute to the ω-hydroxylation of fatty acids in liver and kidney (Hsu et al., 2007) (Hardwick et al., 2009). *Cyp4a10* and *Cyp4a14* are established PPARα-responsive genes. PPARα is a ligand-activated transcription factor that serves as a biological sensor for the intracellular fatty acid levels (Fisher et al., 2008) (Bumpus et al., 2011). The *Pdk4* (pyruvate dehydrogenase kinase, isoenzyme 4) gene encodes a protein which is also involved in energy delivering processes such as glucose metabolic processes or regulation of fatty acid biosynthetic process (Bowker-Kinley et al., 1999). *Cox7a1* was also among the ten highest down regulated genes in livers of PCB 153-treated C57BL/6 mice. The cytochrome c oxidase, which is located in the inner mitochondrial membrane, is involved in the mitochondrial electron transport within the respiratory chain. It has been therefore associated with the oxidation-reduction process (Hüttemann et al., 2001).

Summarizing the PCB 153-mediated hepatic effects in female C57BL/6 mice, 65 genes were up and 21 genes down regulated in mouse study I. However, the corresponding log2 fold change values of the regulated genes were not exceeding 3.6 or deceeding -2.5 implicating that the dosage of 150000 µg/kg bw PCB 153 had only a moderate impact on the alteration of the hepatic gene expression.
Genes involved in xenobiotic metabolism (*Cyp2b10, Cyp3a11, Aldh1a1, Akr1b7, Gsta1, Gsta2, Gstm4, Gstp1, Gstp2*) were up regulated due to treatment with the NDL-congener. Several cytochromes of the *Cyp2c* class (*Cyp2c29, Cyp2c37, Cyp2c38, Cyp2c38, Cyp2c39,* and *Cyp2c54*) which are involved in arachidonic acid metabolism were also up regulated suggesting the arachidonic acid signalling pathway was influenced in female mice by treatment with PCB 153. Umannova et al. suggested that the deregulation of the arachidonic acid signalling pathways could possibly contribute to the NDL-PCB-mediated carcinogenic and toxic effects (Umannova et al., 2008). Several genes associated with the lipid metabolism (*Acot1, Cyp4a10, Cyp4a14,* and *Pdk4*) were also down regulated in livers of female C57BL/6 mice after treatment with PCB 153.

Table 6. **10 highest up and down regulated genes in livers of PCB 153-treated female C57BL/6 mice (Mouse study I - mouse 3-day study).**
PCB 153 as one time administered dose (150000 µg/kg bw).
Selected parameters for microarray analysis: cutoff values: A ≥ 7, log2 fc ≥ 1 or ≤ -1, p-value ≤ 0.05
Annotations: '#'analysis revealed non-identical probes of this gene have different log2 fc-values

Gene name	Gene description	Probe name	Systematic name	Log2 fc
Up regulation				
Gsta1	Glutathione S-transferase alpha 1 (Ya)	A_55_P2032946	NM_008181	3.56
Cyp2c38	Cytochromes P450 family 2, subfamily c, member 38	A_55_P2116272	NM_010002	3.34
Gm10639[#]	Predicted gene 10639	A_55_P2102065	NM_001122660	2.69
Cyp2b10	Cytochromes P450 family 2, subfamily b, member 10	A_55_P2044653	NM_009999	2.51
Orm3	Orosomucoid 3	A_51_P311958	NM_013623	2.32
Akr1b7	Aldo-keto reductase family 1 member b7	A_51_P331288	NM_009731	2.32
Ces6	Carboxylesterase 6	A_55_P2293013	NM_133960	2.13
Gsta2	Glutathione S-transferase alpha 2 (Yc2)	A_55_P2170454	NM_008182	2.04
A_55_P2107528	Unknown	A_55_P2107528	A_55_P2107528	1.97
Cyp2c54[#]	Cytochromes P450 family 2, subfamily c, member 54	A_52_P154580	NM_206537	1.94
Down regulation				
Tnni2	Troponin I, skeletal fast 2	A_55_P2040893	NM_009405	-2.51
Acot1	Acyl-CoA thioesterase 1	A_55_P2038358	NM_012006	-1.95
Pdk4	Pyruvate dehydrogenase kinase, isoenzyme 4	A_51_P350453	NM_013743	-1.83
Cyp4a14	Cytochromes P450 family 4, subfamily a, polyeptide 14	A_51_P238576	NM_007822	-1.67
Tpm1	Tropomyosin 1 alpha	A_55_P2187043	NM_001164248	-1.56
Gm3734	Predicted: hypothetical protein LOC100046708	A_55_P2162970	XM_001476671	-1.49
Cox7a1	Cytochromes c oxidase subunit VIIa 1	A_51_P148612	NM_009944	-1.43
Neb	Nebulin	A_55_P2116973	NM_010889	-1.43
Eno3	Enolase 3 beta muscle, transcript variant 2	A_55_P1977533	NM_001136062	-1.37
ENSMUST00000113016	Gelsolin Precursor (Actin-depolymerizing factor)(ADF)(Brevin)	A_55_P2055638	ENSMUST00000113016	-1.29

IV.1.1.1.2.3 Comparison TCDD and PCB 153 Treatment

One major research topic within the present work was the identification, establishment, and implementation of novel biomarkers for the activation of the AhR due to treatment with dioxins and dioxin-like compounds. Several research approaches were used as described in detail in chapter VI.3.5 which finally led to 5 potential biomarker candidates. Within this chapter and the following chapters, the alterations on the mRNA expression of these target genes will be critically discussed to analyze if one or more of these target genes are suitable biomarkers for the activation of the AhR.

As expected, only a marginal overlap of in commonly altered gene expression occurred due to treatment with TCDD and NDL-PCB 153 (Table 7). Nine genes were in common up and two genes in common down regulated. After treatment of the C57BL/6 mice with the AhR ligand TCDD and the CAR activator PCB 153 several glutathione S-transferases (*Gsta1, Gsta2, Gstp1,* and *Gstp2*) were up regulated in liver. Considering the receptor-dependent inducibility, the induction of these four genes is in case of TCDD AhR-mediated and in case of PCB 153 CAR-mediated. *Cyp2c54* was also up regulated in liver due to both compound treatments. Though after treatment with PCB 153 additional cytochromes of the *Cyp2c* class were likewise up regulated (*Cyp2c29, Cyp2c37, Cyp2c38,* and *Cyp2c39*). In case of PCB 153 various genes of the *Cyp2c* class were up regulated, thus implicating the role of NDL-PCBs in the deregulation of the arachidonic acid signalling pathway (Umannova et al., 2008). *Ces2*, a carboxylesterase was significantly up regulated in livers of female C57BL/6 mice after treatment with TCDD and PCB 153. Carboxylesterases are enzymes which catalyze the hydrolysis of a diverse range of ester-containing endogenous and xenobiotic compounds. The murine *Ces2* was up regulated after activation of the AhR (TCDD) and CAR (PCB 153). This allows drawing the conclusion that the altered *Ces2* expression is not based on a strictly AhR- or CAR-mediated mechanism. However, the murine *Ces6* gene expression was only induced in liver upon treatment with PCB 153, but not after exposure to TCDD. Xu and co-workers demonstrated that *Ces6* is a CAR- and PXR-shared target gene in mice (Xu et al., 2009). *Ces6* is an obviously CAR-regulated target gene in the present study after treatment with PCB 153, but a clear nuclear receptor dependency could not be derived for the murine *Ces2*. The prominin 1 (*Prom1*) gene was also up regulated in livers of both compound-treated animals. The mammalian prominin gene family consists of two members the genes *Prom1* and *Prom2* which encode multispan transmembrane glycoproteins that are specifically sorted to microvilli and other plasma membrane protrusions. *Prom1* (alias *CD133*) was originally identified and cloned by Weigmann and co-workers as a protein selectively concentrated at the apical domain of neuroepithal progenitor cells and adult kidney proximal tubules. The human *PROM1* was first identified as surface antigen in hemotopotetic stem and progenitor cells (Zacchigna et al., 2009) (Katoh et al., 2007). The results gained within this study, however, indicate that the induction of *Prom1* does not depend on AhR or CAR activation.

Cox7a1 and *Cyp26b1* are the two genes which were in common down regulated in the female mouse liver after exposure to TCDD and PCB 153 respectively. CYP26 enzymes are likely responsible for metabolism of all-trans retinoic acid and furthermore contribute to the regulation of all-trans retinoic acid homeostasis and signalling. CYP26B1 is a hydroxylase

which forms 4-OH-retinoic acid and 18-OH-retinoic acid from all-trans retinoic acid (Topletz et al., 2012). TCDD treatment affects the retinoic homeostasis. Exposure to TCDD leads to growth retardation, abnormal immune function, and developmental defects reminiscent of vitamin A-deficient states postulate that dioxin-like compounds reduce all-trans retinoic acid signalling (Murphy et al., 2007) (Jacobs et al., 2011). However, *Cyp26b1* was also down regulated after exposure to PCB 153. The activation of the cytosolic CAR upon phentobarbital exposure leads after dissociation from different co-chaperone partners to the translocation of CAR into the nucleus where it forms a complex with the retinoid X receptor (RXR) (Kawamoto et al., 1999). RXR is also able to form a heterodimer with RAR (retinoic acid receptor) and can be actively involved in retinoic acid signalling pathways by regulating the retinoic acid-mediated gene transcription (Balmer et al., 2002). This poses a reasonable explanation why *Cyp26b1* levels were altered after exposure to a high dose of PCB 153.

Log2 fc values of selected genes after TCDD or PCB 153 treatment, identified by microarray analysis, are summarized in Table 8. Selected genes include the members of the murine aromatic hydrocarbongene battery (*Cyp1a1, Cyp1a2, Nqo1, Aldh3a1, Ugt1a6,* and *Gsta1*) (Nebert et al., 2000) as well as other cytochromes P450 genes (*Cyp2b10, Cyp3a11*, and *Cyp3a44*) and the additional selected target genes (*Aldh3a1, Tiparp, Hsd17b2, Cd36,* and *Ahrr*). All genes of the aromatic hydrocarbon gene battery were up regulated in C57BL/6 mice after treatment with TCDD except *Aldh3a1*. Several other mouse microarray studies, described in literature, failed to demonstrate the up regulation of *Aldh3a1* in the murine liver by TCDD treatment (Tijet et al., 2005) (Boutros et al., 2009). The induction of *Aldh3a1* mRNA in mouse hepatoma cell lines has been only demonstrated *in vitro,* but not *in vivo* after treatment of either C57BL/6J or DBA/2J mice with an extremely high dosage of 200 µg/kg bw TCDD (Vasiliou et al., 1993). The lack of *Aldh3a1* mRNA induction by TCDD (34 µg/kg bw administered as single dose) in the murine liver was also shown in the recent work of Alnouti and co-workers (Alnouti et al., 2006). This leads to the conclusion that the *Aldh3a1* gene is neither inducible by TCDD nor by PCB 153 in the mouse liver.

Treatment with PCB 153 led only to the induction of *Gsta1*, but no alteration in gene expression was observed for the other genes. As discussed above, the up regulation of *Gsta1* after exposure to PCB 153 is most likely CAR-mediated considering that the regulation of the non dioxin-like compound is based on an AhR-independent mechanism (Hernandez et al., 2009). *Cyp1b1* is an associated member of the murine AhR target gene battery. The strong induction of CYP1B1 after dioxin exposure in mouse und human liver was demonstrated in several studies. CYP2B10 on the other hand belongs to the P450 isoenzymes which featured a high induction upon treatment with NDL-congeners (Roos, 2011). In the present study the murine hepatic *Cyp2b10* expression was significantly up regulated due to treatment with PCB 153. The *Cyp3a44* gene was chosen in the present work to examine if the the nuclear receptor PXR has been activated after exposure to the seven core compounds. *Cyp3a44* is a female mouse-specific PXR-regulated gene (Bhadhprasit et al., 2007). No up regulation was determined after single dose exposure to PCB 153 (150000 µg/kg bw) in the present microarray study. However, *Cyp3a11* was slightly, but statistically signifiantly induced by treatment with PCB 153 in the microarray. Also no increase of the hepatic *Cyp3a44* mRNA

expression levels was measured after one-time exposure to 200000 µg/kg bw PCB 153 24 h after treatment in male and female C57BL/6 mice. Likewise, no increase of *Cyp3a44* mRNA levels was determined in mouse livers of both genders in a five days mouse study (2 doses of 200000 µg/kg bw PCB 153 on day 0 and 2). Only subchronic exposure to PCB 153 (ten doses of 200000 µg/kg bw PCB 153 during 28 days) led to a significant induction of the hepatic *Cyp3a44* mRNA expression (Roos, 2012).

The aim of the present microarray study was to determine AhR-dependent and AhR-independent effects on the hepatic mRNA gene expression in female C57BL/6 mice. Furthermore, the selected target genes (*Aldh3a1, Tiparp, CD36, Hsd17b2,* and *Ahrr*) in search for a novel quantifiable biomarker were all up regulated except *Aldh3a1* in livers of female mice after treatment with TCDD (25 µg/kg bw), but not after exposure to PCB 153 (150000 µg/kg bw). Due to different signalling pathways only a small overlap (9 up, 2 down) in altered gene expression occurred by single dose administration of TCDD (25 µg/kg bw) and PCB 153 (150000 µg/kg bw), respectively.

Table 7. In common up and down regulated genes after treatement with TCDD (25 µg/kg bw) and PCB 153 (150000 µg/kg bw) - mouse study I. Selected parameters for microarray analysis: cutoff values: A ≥ 7, log2 fc ≥ 1 or ≤ -1, p-value ≤ 0.05

Gene name	Gene description	Probe name	Systematic name	log2 fc TCDD	log2 fc PCB 153
In common up regulated genes					
Gsta1	Glutathione S-transferase alpha 1 (Ya)	A_55_P2032946	NM_008181	2.82	3.56
Gsta2	Glutathione S-transferase alpha 2 (Yc)	A_55_P2170454	NM_008182	1.30	2.04
Gstp1	Glutathione S-transferase pi 1	A_55_P2031668	NM_013541	1.86	1.05
Gstp2	Glutathione S-transferase pi 2	A_55_P2008704	NM_181796	1.56	1.01
Cyp2c54	Cytochromes P450, family 2, subfamily c, polypeptide 54	A_52_P154580	NM_206537	1.37	1.94
Ces2	Carboxylesterase 2	A_52_P318361	NM_145603	1.65	1.59
		A_55_P2124712	NM_145603	1.70	1.54
Prom1	Prominin 1, transcript variant 2	A_55_P2059931	NM_001163577	1.76	1.53
Gm10639	Predicted gene 10639	A_55_P2102065	NM_001122660	1.85	2.69
		A_55_P2069969	NM_001122660	1.04	1.76
BC015286	cDNA sequence BC015286	A_52_P627269	NM_198171	1.63	1.52
In common down regulated genes					
Cox7a1	Cytochromes c oxidase, subunit VIIa 1	A_51_P148612	NM_009944	-1.04	-1.43
Cyp26b1	Cytochromes P450 family 26, subfamily b, polypeptide 1	A_51_P501844	NM_175475	-1.54	-1.01

Table 8. **Comparison of selected genes in liver of female C57BL/6 mice treated with TCDD or PCB 153.**
The table features aspects such as gene name, probe name, systematic name, colour intensity value, and corresponding log2 fc values.
Selected parameters: log2 fc ≥ 1, p-value ≤ 0.05.
Annotations: '→' gene was not up regulated in microarray experiment.

Gene name	Probe name	Gene description	Colour intensity	Log2 fc TCDD	Log2 fc PCB 153
Cyp1a1	A_51_P279693	NM_009992	10.23	9.48	→
Cyp1a2	A_52_P595871	NM_009993	13.33	3.99	→
Cyp1b1	A_51_P255456	NM_009994	7.16	5.17	→
Cyp2b10	A_55_P2044653	NM_009999	13.31	→	2.51
Cyp3a11	A_55_P2121225	NM_007818	14.96	→	1.25
Cyp3a44	A_52_P366803	NM_177380	10.41	→	→
Nqo1	A_51_P424338	NM_008706	6.97	1.75	→
Gsta1 (Ya)	A_55_P2032946	NM_008181	9.36	2.82	3.56
Ugt1a6a	A_55_P2143765	NM_145079	8.42	1.60	→
Aldh3a1	A_55_P2065562	NM_007436	8.62	→	→
Tiparp	A_55_P1985890	NM_178892	7.10	2.90	→
Hsd17b2	A_51_P441914	NM_008290	11.34	1.41	→
Cd36	A_51_P375146	NM_007643	7.22	1.76	→
Ahrr	A_51_P254425	NM_009644	5.65	3.91	→

IV.1.1.2 Study II - Mouse 14-day Study

In this short-term 14-day acute toxicity study, groups of six adult female C57BL/6 mice received a single dose of each chosen compound or corn oil by gavage. An overview of examined dose levels is featured in Table 9. Each compound-treated group will be compared to its corresponding vehicle control group (0 µg/kg bw). Immediately after the sacrifice of the animals, blood and tissue samples were collected, instantly frozen in liquid nitrogen and stored at -80 °C until usage. In the present work the mouse liver represents the target tissue. Liver sample preparation and further isolation of RNA are described in chapter six (VI Methods) in detail. Concentration and purity of liver samples were spectrophotometrically determined by NanoDrop (Peqlab, Erlangen). Influence and effects of the administered compounds were measured by quantitative real-time PCR on mRNA level.

Table 9. Overview mouse study II - 14-day study (dose levels).

Study	Treatment	Single dose (µg/kg bw)				TEF (WHO, 2005)
14-day	**TCDD**	0	25			1.0
	1-PnCDD	0	25			1.0
	4-PnCDF	0		250		0.3
	PCB 126	0		250		0.1
	PCB 118	0			150000	0.00003
	PCB 153	0			150000	-
	PCB 156	0			150000	0.00003

IV.1.1.2.1 Gene Expression Analysis by RT-PCR

The mRNA expression levels of three genes which play key roles in xenobiotic metabolism were measured in the following RT-PCR experiments. Genes were accordingly selected to identify receptor-mediated specific effects after treatment with test compounds. Alterations in *Cyp1a1* gene expression reveal the affinity of the test compound to the AhR. *Cyp2b10* represents the murine analog to the human *CYP2B6* which is primarily CAR-regulated. Additionally, *Cyp3a44* was chosen to analyze the PXR-mediated effects in the female mouse liver due to compound exposure. Complementary DNA (cDNA) was synthesized using iScriptc DNA Synthesis Kit (BioRad). 1 µl of the transcribed cDNA was used to perform each RT-PCR. The *Cyp1a1, Cyp2b10,* and *Cyp3a44* mRNA expression was normalized using *36b4* as housekeeping gene and calculated relative to the expression in the corresponding vehicle control (0 µg/kg bw).

An extremely high *Cyp1a1* mRNA induction (5914.35 ± 1224.90) was measured after treatment with 25 µg/kg bw TCDD in the 14-day mouse study, whereas no alterations in the hepatic *Cyp2b10* mRNA expression were determined by RT-PCR. *Cyp3a44* was significantly down regulated resulting in a fold-change of 0.60 ± 0.29 compared to the corresponding vehicle control (Figure 13). The hepatic *Cyp1a1* mRNA expression was induced up to

5908.92 ± 1185.28 after treatment with 1-PnCDD. A small but statistically significant increase in *Cyp2b10* mRNA expression was measured after treatment with 1-PnCDD which led to an induction of 2.07 ± 0.94. However, *Cyp3a44* mRNA expression levels were not altered in livers of female C57BL/6 mice (Figure 13).

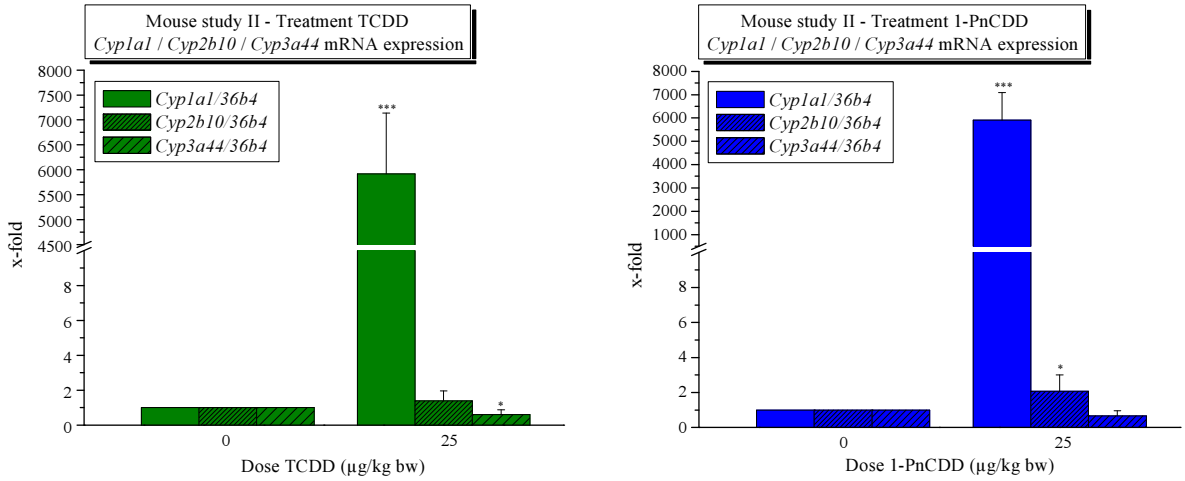

Figure 13. **Real-time PCR ratios of female mice treated with TCDD (left) or 1-PnCDD (right) - mouse study II. *36b4* served as housekeeping gene, compound as one-time administered dose. Data represent means + SD of six different adult female mice, normalized to corresponding vehicle control. One-tailed unpaired Student's t-test with Welch correction, *= p ≤ 0.05, ***= p ≤ 0.001.**

The results of the real-time PCR analysis after the treatment with 250 µg/kg bw 4-PnCDF revealed a high *Cyp1a1* mRNA induction resulting in a fold-change of 6063.98 ± 914.96 (Figure 14). In addition, *Cyp2b10* mRNA levels were also significantly increased resulting in a fold-change of 4.11 ± 1.10, whereas no alteration of *Cyp3a44* expression was measured by RT-PCR. A high, statistically significant *Cyp1a1* mRNA induction (5150.62 ± 1521.82) was furthermore measured after female C57BL/6 mice received a single dose of 250 µg/kg bw PCB 126 (Figure 14). In addition, a small but significant increase of the *Cyp2b10* mRNA expression (3.11 ± 1.35) was determined in mouse study II. *Cyp3a44* mRNA levels were not affected by treatment with PCB 126.

Treatment with PCB 118 led to the high *Cyp1a1* induction resulting in a fold-change of 782.48 ± 156.85 (Figure 15). Moreover, *Cyp2b10* mRNA levels (33.09 ± 5.39) were additionally significantly induced by PCB 118 in mouse study II. However, *Cyp3a44* mRNA levels were down regulated (0.33 ± 0.12) compared to the corresponding vehicle control.
After treatment with 15000 µg/kg bw PCB 153 no alterations of *Cyp1a1* and *Cyp3a44* mRNA expression levels were measured by RT-PCR, whereas *Cyp2b10* mRNA levels were significantly induced (25.09 ± 7.36-fold) (Figure 15).
Single-dose treatment with PCB 156 resulted in a high induction of the *Cyp1a1* (3443.01 ± 863.65) and *Cyp2b10* (90.56 ± 25.01) mRNA levels in the 14-day study, while the *Cyp3a44* mRNA gene expression was down regulated (0.45 ± 0.12).

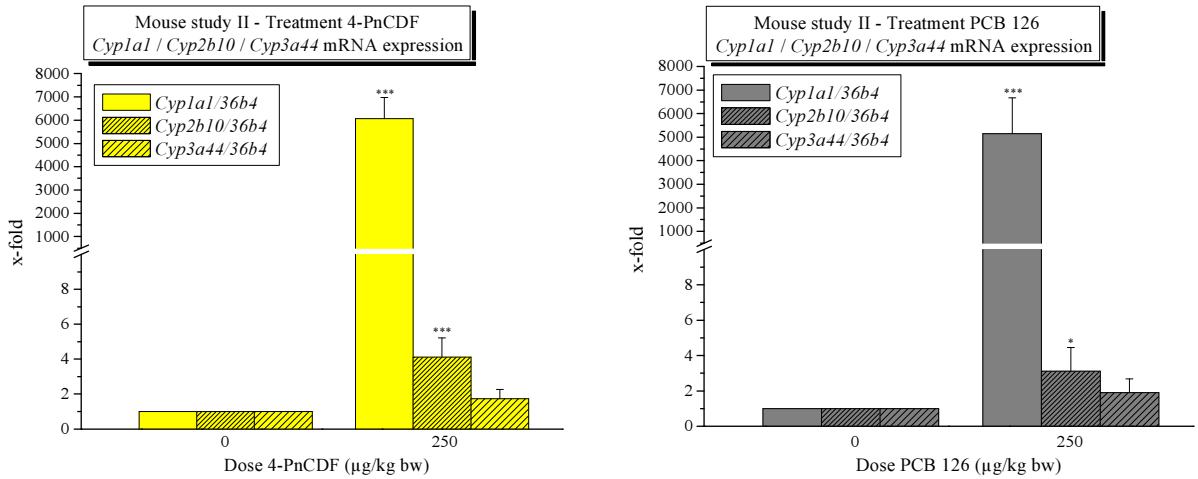

Figure 14. **Real-time PCR ratios of female mice treated with 4-PnCDF (left) or PCB 126 (right) - mouse study II. *36b4* served as housekeeping gene, compound as one-time administered dose. Data represent means + SD of six different adult female mice, normalized to corresponding vehicle control. One-tailed unpaired Student's t-test with Welch correction, *= p ≤ 0.05, ***= p ≤ 0.001.**

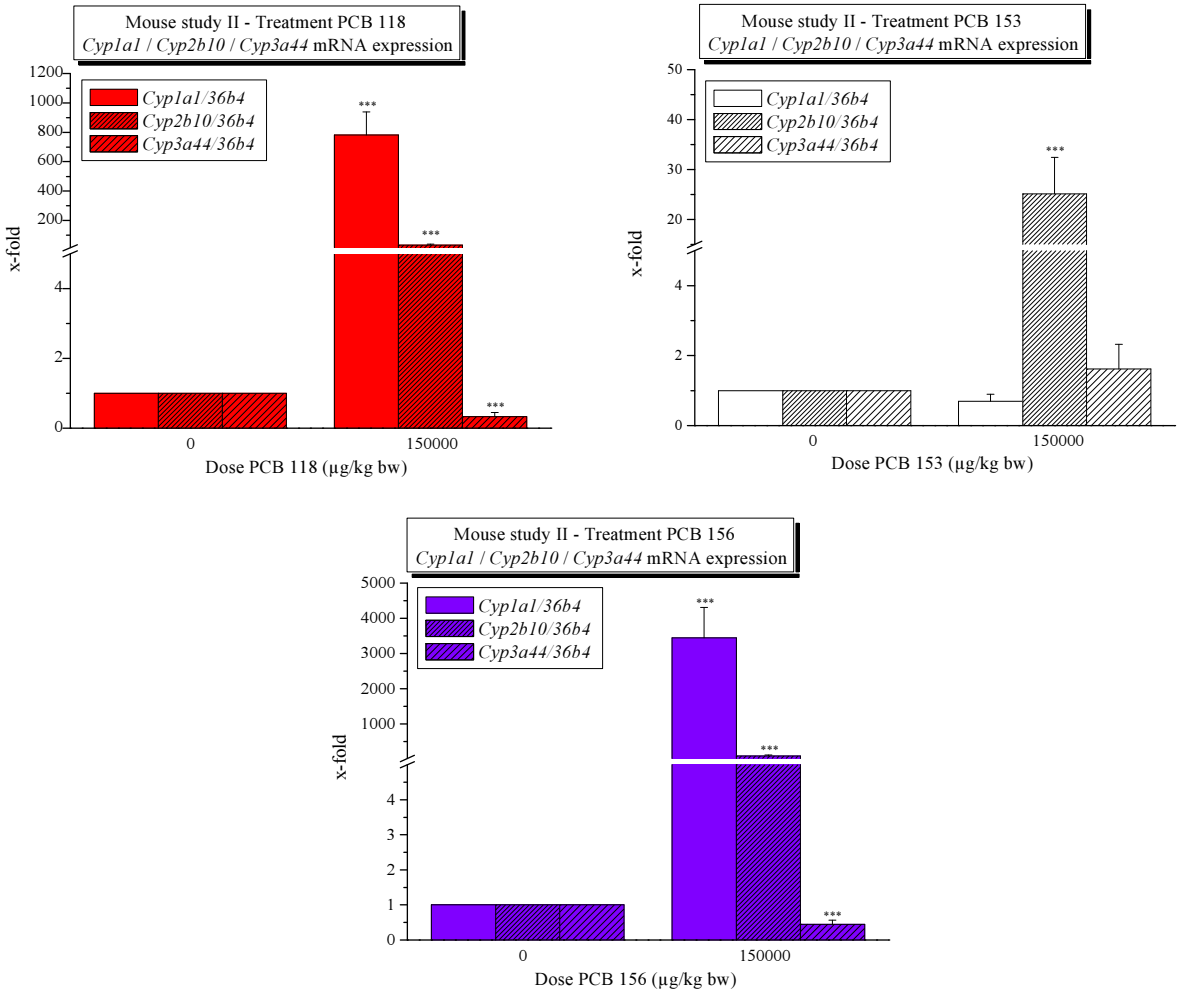

Figure 15. **Real-time PCR ratios of female mice treated with PCB 118 (up left), PCB 153 (up right right), or PCB 153 (down middle) - mouse study II. *36b4* served as housekeeping gene, compound as one-time administered dose. Data represent means + SD of six different adult female mice, normalized to corresponding vehicle control. One-tailed unpaired Student's t-test with Welch correction, ***= p ≤ 0.001.**

In summary, the mouse 14-day acute toxicity study confirmed the findings of the mouse 3-day studies, though distinct differences were observed. Fourteen days after single dose treatment with TCDD (25 µg/kg bw), only *Cyp1a1* mRNA levels were highly induced due to activation of the AhR. In addition to the detected high *Cyp1a1* expression levels, the statistically significant increase of the *Cyp2b10* mRNA levels after treatment with 1-PnCDD (25 µg/kg bw), 4-PnCDF (250 µg/kg bw), and PCB 126 (250 µg/kg bw) imply that exposure to dioxins and dioxin-like compounds in the chosen doses primarily led to the activation of the AhR, but the nuclear receptor CAR could be also activated fourteen days after single exposure. Fourteen days after the single dose administration of the DL-PCBs, PCB 118, and PCB 156 (150000 µg/kg bw) resulted in the activation of the AhR. The *Cyp1a1* mRNA response to PCB 156 was 4-times higher compared to PCB 118. Furthermore, the measured *Cyp2b10* mRNA induction draws to the conclusion that CAR was additionally activated by both dioxin-like PCBs. However, *Cyp3a44* mRNA levels were significantly down regulated by PCB 118 and 156 fourteen days after single dose treatment.

IV.1.1.3 Summary and Discussion *in vivo* Experiments Part I

In the present work, the influence of polychlorinated dibenzo-*p*-dioxins (TCDD, 1-PnCDD), dibenzofurans (4-PnCDF), polychlorinated dioxin-like biphenyls (PCB 118, 126, and 156) and the non dioxin-like biphenyl (PCB 153) on mRNA expression of selected genes associated with different xenobiotic signalling pathways (AhR, CAR, and PXR) were elucidated in both mouse studies (Table 10).

Table 10. Summary of in vivo experiments part I featuring gene expression changes in female mouse liver.
'↑' mRNA gene expression increased compared to vehicle control.
'↓' mRNA gene expression reduced compared to vehicle control.
'→' mRNA gene expression not significantly altered compared to vehicle control.

Compound	TCDD		1-PnCDD		4-PnCDF		PCB 118		PCB 126		PCB 153		PCB 156	
Study	3	14	3	14	3	14	3	14	3	14	3	14	3	14
Cyp1a1	↑↑	↑↑	↑↑	↑↑	↑↑	↑↑	↑↑	↑↑	↑↑	↑↑	→	→	↑↑	↑↑
Cyp2b10	→	→	→	↑	→	↑	↑	↑	→	↑	↑	↑	↑	↑
Cyp3a44	→	↓	→	→	→	→	→	↓	→	→	→	→	↑	↓

Single dose exposure toTCDD, 1-PnCDD, 4-PnCDF, and PCB 126 in both mouse studies led to the activation of the AhR, demonstrated by the examined high hepatic *Cyp1a1* mRNA expression. A weak activation of CAR could be additionally postulated in case of 1-PnCDD, 4-PnCDF, and PCB 126 in mouse 14-day study based on the slight increase of hepatic *Cyp2b10* mRNA expression. Treatment of mice with PCB 118 and PCB 156 led to the activation of the AhR and CAR in both studies. The induction of *Cyp1a1* mRNA was much more pronounced than the increase of the *Cyp2b10* mRNA expression. Hepatic *Cyp3a44* levels were slightly increased in the mouse 3-day study, but suppressed in mouse 14-day study, therefore no consistnent trend could be derived. PCB 153 belongs to the class of non

dioxin-like PCBs. PCB 153 treatment caused the induction of *Cyp2b10* mRNA levels in mouse liver, whereby no alterations in *Cyp1a1* and *Cyp3a44* mRNA levels were determined by RT-PCR. Based on these findings, single dose exposure of female mice to PCB 153 only led to the activation of CAR.

Furthermore, a microarray study was performed in search for novel quantifiable biomarkers for AhR activation by DLCs. The alterations in hepatic gene expression were determined three days after treatment with a single dose of either TCDD (25 µg/kg bw) or PCB 153 (150000 µg/kg bw) by gavage in livers of female C57BL/6 mice by microarray analysis.
A total of 125 unique genes were up and 95 down regulated by TCDD. Treatment with PCB 153 resulted in 65 up and 21 down regulated genes in mouse livers (identified by the selected cut-off values: A ≥7, log2 fc ≥ 1 or ≤ -1, and p-value ≤ 0.05). As expected, only a vanishingly small number of hepatic genes were regulated in common (9 up, 2 down) by both compounds.

TCDD treatment caused the high up regulation of genes associated with the xenobiotic metabolism such as *Cyp1a1, 1a2,* and *1b1*. But also other members of the AhR gene battery were highly up regulated (e.g. *Ugt1a6a* and *Gsta1*). In addition, various genes involved in lipid metabolism were also significantly altered by TCDD treatment in the present study. These results outline the role of TCDD in the dysregulation of the hepatic lipid metabolism which is primarily based on the AhR-mediated enhanced uptake of fatty acids and accumulation of triglycerides in the murine liver (Polandet al., 1982a) (Huff et al., 1991) (Boverhof et al., 2006) (Kopec et al., 2010a) (Kopec et al., 2010b) (Angrish et al., 2012).

PCB 153 had a weaker impact on the murine hepatic gene expression compared to TCDD. Single dose administration of 150000 µg/kg bw PCB 153 resulted in the up regulation of genes associated with xenobiotic metabolism such as *Cyp2b9*, *Cyp2b10, Cyp3a11, Aldh1a1, Akr1b7, Gsta1*, and *Gstp1*. *Cyp2b9* and *Cyp2b10* are markers for the activation of constitutive androstane receptor (CAR). The induction of the *Cyp2b10* mRNA expression was confirmed by RT-PCR analysis (Table 10) while the mRNA expression of *Cyp3a44* was not significantly induced. *Cyp3a44* is a female mouse-specific gene which is primarily and selectively regulated by PXR and not by CAR (Bhadhprasit et al., 2007) (Anakk et al., 2007). *Cyp3a11* was slightly up regulated in the performed microarray study. CYP3A11 is the main representative of the CYP3A isoenzyme class and commonly used as marker for PXR activation. Previous studies demonstrated the CAR-dependent regulation of *Cyp3a11*, e.g. by phenobarbital, a CAR inducer (Anakk et al., 2004) (Anakk et al., 2007). These findings strongly suggest that the up regulation of *Cyp3a11* is most likely mediated by the constitutive androstane receptor. The *Cyp3a44* mRNA expression was neither up regulated in the microarray study nor in RT-PCR analysis, implying that the PXR was not activated by PCB 153. Several cytochromes of the *Cyp2c* class (*Cyp2c29, Cyp2c37, Cyp2c38, Cyp2c38, Cyp2c39,* and *Cyp2c54*), which are involved in arachidonic acid metabolism, were also up regulated. The deregulation of the arachidonic acid signalling pathway by NDL-PCBs has been demonstrated in previously performed studies (Marks et al., 2000) (Umannova et al., 2008).
The implemented microarray study confirmed the role of TCDD as prototype for effects mediated by the aryl hydrocarbon receptor (AhR), whereas the effects caused by PCB 153, a NDL-PCB, are mainly faciliated by the constitutive androstane receptor (CAR).

IV.2 *in vivo* Experiments Part II

The aryl hydrocarbon receptor mediates most, if not all, biological and toxic effects of DLCs (Poland et al., 1982a). TCDD, as the most potent representative, was classified with a Toxic Equivalency Factor (TEF) of 1.0 (Ahlborg et al., 1991). The TCDD-mediated toxic mechanisms are expected to be clarified in the following animal experiment by elucidation of the role of the aryl hydrocarbon receptor. The assessment of the systemic exposure is the centre of interest by investigating the blood (metabolomics) as well as the gene expression (RT-PCR and microarray analysis) in livers of *Ahr* knockout and control mice. The research project was gratefully supported by the 'Stiftung Innovation Rheinland-Pfalz'.

Heterozygous C57BL/6 mice ($Ahr^{+/-}$) were obtained from Jackson Laboratory (Bar Habor, ME, USA). Breeding of *Ahr* knockout mice was started at the National Institute for Health and Welfare, Kupio, Finland, under supervision of Dr. Matti Viluksela and continued in our laboratory animal unit at the University Kaiserslautern. All animals were genotyped before different experimental approaches were carried out. Further information about the genetic background, breeding, and genotyping of transgenic mice is given in chapter six (VI Methods).

IV.2.1 Metabolomics

The terminus 'metabolomics' means the global analysis of metabolites in a biofluid or tissue. This innovative powerful technique aims to capture all small molecules generated in the process of metabolism. Metabolomics and the other 'omics approaches, including genomics, transcriptomics, and proteomics aspire to understand the biology of an organism and its response to exogenous or endogenous stimuli or respectively to genetic perturbance. Two different strategies in metabolomic analysis have emerged during the last decade, metabolic profiling and metabolic fingerprinting. Metabolic profiling focuses on the quantitative analysis of a group of metabolites related to a class of compounds or to a specific metabolic pathway. Metabolic fingerprinting, however, constitutes a global screening approach by comparing patterns or 'fingerprints'. The emphasis is not to identify each metabolite but to detect distinctions between, i.e. different genotypes (Fiehn, 2002) (Dettmer et al., 2007).

In the present work, possible differences between aryl hydrocarbon receptor-deficient mice ($Ahr^{-/-}$) and wild-type mice ($Ahr^{+/+}$) were investigated by analyzing mouse plasma of each genotype by HPLC-ESI-MS/MS. Both approaches were used in the present work with the emphasis being on the identification of differences in patterns of the mouse plasma. Additionally, a database consisting of mouse plasma metabolites has been initiated.
Adult female and male $Ahr^{+/+}$ and $Ahr^{-/-}$mice aged 4 - 9 month were narcotized and mouse blood was isolated from *vena cava caudalis*. Mouse plasma was segregated from whole blood, proteins were then extracted, and the protein-free mouse plasma extracts were evaporated to dryness and immediately measured or stored at -80 °C. Mouse plasma extracts were solved in water/methanol (95:5) immediately before HPLC-MS/MS analysis.

Detailed information about the isolation of mouse plasma and extraction steps is given in chapter six (VI Methods).

The following tables feature information about HPLC-specific parameters (Table 11) as well as mass spectrometer conditions applied to each identified substance (Table 12).

Table 11. Instrument specific parameters of HPLC (Perkin-Elmer).

Column	LiChroCart - LiChrosphere, Merck
Material	RP18, 250 mm x 4 mm, 5 µm
Flow rate	0.75 ml/min
Solvents	A: water (0.1 % HCOOH) B: methanol
Injection volume	30 µl
UV detection	260 nm

Time (min)	Solvent A (%)	Solvent B (%)
0.1	100	0
41	10	90
44	10	90
50	100	0
55	100	0

Table 12. Instrument specific parameters mass spectrometer (API 2000, AB Sciex).
DP: declustering potential; EP: entrance potential; CE: collision energy; CEP: cell entrance potential; CXP: cell exit potential; CUR: curtain gas; CAD: collisionally activated dissociation; IS: ionspray voltage; TEM: temperature; GS1: gas 1; GS2: gas 2.

Parameter (Quadrupole)	Values
DP (V)	20
EP (V)	200
CE (V)	15-25
CEP (V)	9.69
CXP (V)	15
Source/gas	**Values**
CUR (psi)	20
CAD	5
IS (V)	4200
TEM (°C)	400
GS1	20
GS2	20

The collision energy varied depending on the analyzed plasma metabolite resulting in the following CE values: tryptophan (CE: 25); phenylalanine: (CE: 15); tyrosine (CE: 15); valine (CE: 20); leucine (CE:15); methionine (CE:15); betaine (CE:15).

IV.2.1.1 Metabolic Profiling

First of all, the established HPLC-MS/MS method described in detail in the prior chapter was used to perform preliminary experiments using plasma samples of *Ahr* wild-type mice.
The identification of metabolites was not possible only with the aid of the total ion current (TIC) chromatogram (Figure 16 at top) due to the low metabolite concentrations in the mouse plasma. Nevertheless, the UV chromatogram (Figure 16 at bottom) revealed a number of peaks. Obviously, patterns of both *Ahr* wild-type mice were similar to each other, only the peak height varied. These differences in peak height can be explained by interindividual differences and variations of isolated blood volumes, but these effects cannot be attributed to a specific gender without doubt.

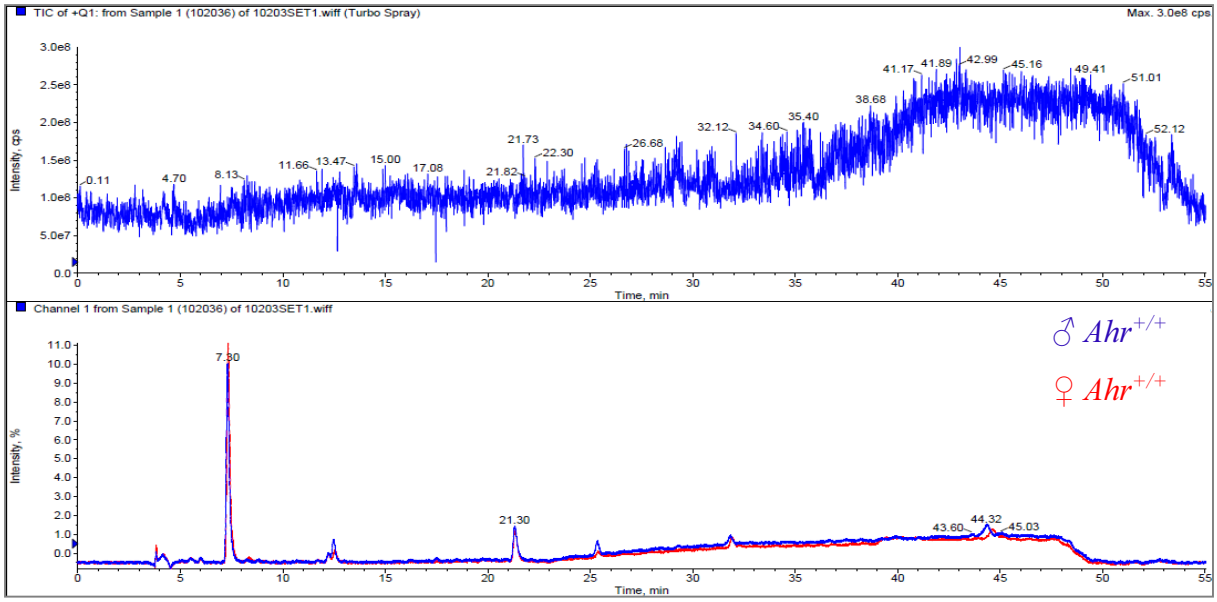

Figure 16. **Measurement of mouse plasma metabolites of two adult *Ahr*$^{+/+}$ mice by HPLC-MS/MS. At top total ion current (TIC) chromatogram, at bottom UV chromatogram (260 nm). Overlay of two different *Ahr* wild-type mice with different genders: male (blue), female (red).**

The analysis of the chromatographic fingerprints of *Ahr* knockout and wild-type mice was the major research objective with emphasis on the identification of differences and similarities between both genotypes. Several complications affected the research task. Unfortunately, the breeding of *Ahr* knockout mice was proven very difficult due to the infertility of *Ahr* knockout mice. Homozygous *Ahr*$^{-/-}$ mice and homozygous *Ahr*$^{+/+}$ mice were achieved by mating female and male heterozygous *Ahr*$^{+/-}$mice. A few hours after birth or within the first two to three weeks the majority of *Ahr* knockout mice died. These findings outline the physiological role of the aryl hydrocarbon receptor in normal development.

The following figure displays the comparison of UV chromatograms of plasma extracts obtained from *Ahr* knockout and wild-type mice. Comparing the four UV chromatograms at 260 nm by overlaying UV data from *Ahr* knockout mouse (green) and *Ahr* wild-type mice (red, grey, and blue) resulted in an interestingly large overlap of various peaks (black arrows in Figure 17). As indicated in Figure 16 before, the peak heights differ most likely due to the

maintained blood volume. Most differences in UV peak pattern were observed at an early stage (retention times four to ten minutes) where hydrophilic compounds were expected to be eluted due to the selected HPLC conditions.
With retention times between six to seven minutes two peaks were identified as *Ahr*$^{-/-}$-specific (green arrows). Furthermore, two additional peaks with retention times between eight to ten minutes were only visible in plasma extracts obtained from *Ahr*$^{-/-}$ mouse. Nevertheless, it was not possible to detect significant differences in peak patterns with increasing retention times until the end of the established program. In summary, by analyzing the metabolic profile of *Ahr* knockout and *Ahr* wild-type mice with the established HPLC-MS/MS set up, it was possible to detect differences in the peak pattern of both genotypes, suggesting putative hydrophilic metabolites which were rather *Ahr*$^{-/-}$-specific.

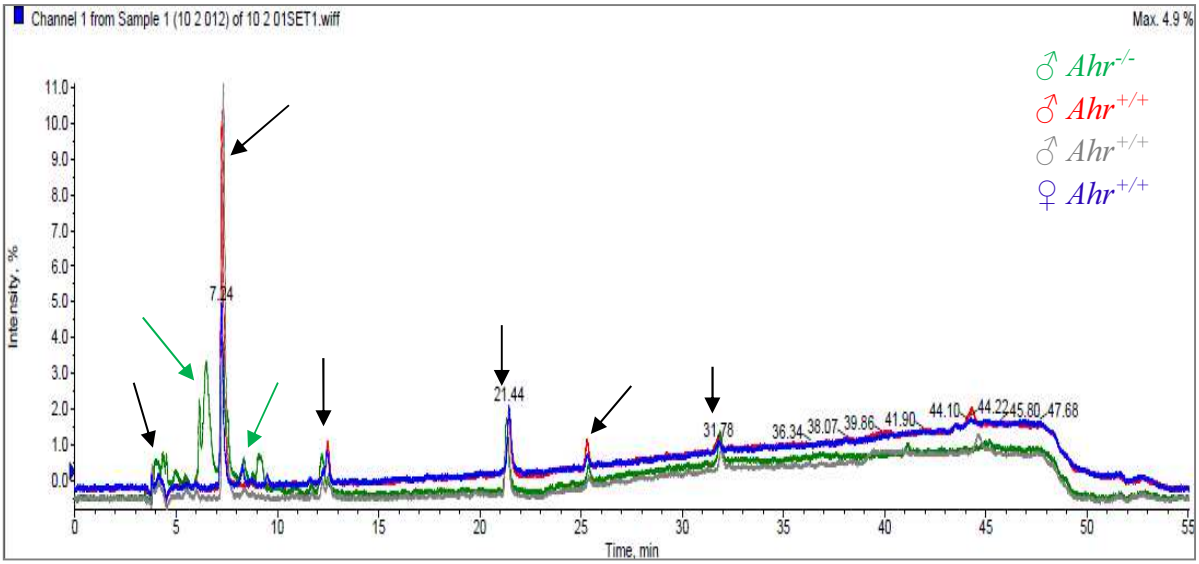

Figure 17. **Metabolic profiling approach - results from HPLC-MS/MS analysis.**
Overlay of UV chromatograms at 260 nm.
Comparing mouse plasma metabolites of 3 adult *Ahr*$^{+/+}$ mice to an adult *Ahr*$^{-/-}$ mouse.
Male *Ahr*$^{-/-}$ mouse (green); male *Ahr*$^{+/+}$ mice (red, grey); female *Ahr*$^{+/+}$ mouse (blue).

IV.2.1.2 Metabolic Fingerprinting

The last chapter dealt with the metabolic profiling leading to UV peaks which were *Ahr*$^{-/-}$-specific. In the following chapter the centre of interest lays on the identification of these peaks, e.g. by HPLC-MS/MS. As shown in Figure 17, the peak pattern of an *Ahr* knockout mouse looks similar to a wild-type mouse, but additional peaks were detected in the UV chromatogram of the *Ahr* knockout mouse.
Figure 18 displays the results of the metabolic analysis by HPLC-MS/MS of mouse plasma obtained from an adult male *Ahr* knockout mouse featuring the stratetic approach for plasma metabolite identification. Because of the low plasma metabolite concentrations, the identification of metabolites only with the aid of the total ion current (TIC) chromatogram was not possible (Figure 18, at top). Nevertheless, the UV chromatogram (second up) led to a number of peaks. Each peak in the UV chromatogram was analyzed by examination of the mass to charge ratios (m/z) underneath (third).

First, a peak of interest was picked. In this case, the selected peak in the UV chromatogram with the retention time of 21.33 min (Figure 18, second up). Afterwards, the background around the chosen peak (± 1 min) was subtracted (not shown) to eliminate mass to charge ratios which were not relevant for the selected peak. All mass to charge ratios with an intensity ≥ 1000 cps were selected separately and examined if their intensities significantly exceeded the background noise. Of all detected mass to charge ratios (between 50-500 amu) in Q1 (Figure 18, third), only an m/z value of 205.2 led to an explicit peak with a correlating retention time in the extracted ion chromatogram (XIC). Retention times always differ between the UV and MS detector due to the order of instruments. Summarizing all gained information, it's highly probable that the m/z value of 205.2 only represents one unique plasma metabolite. By comparing data from metabolomic databases (Human Metabolome Database (HMDB), METLIN (Metabolite and Tandem MS Database)) and further experimental analysis via product ion scan of the selected mass to charge ratio of 205.2 led to the conclusion that tryptophan (Trp) is the mouse plasma metabolite with the featured characteristics. Finally, tryptophan as pure substance was also measured with the same HPLC-MS/MS settings confirming that the mouse plasma metabolite was positively identified as tryptophan.

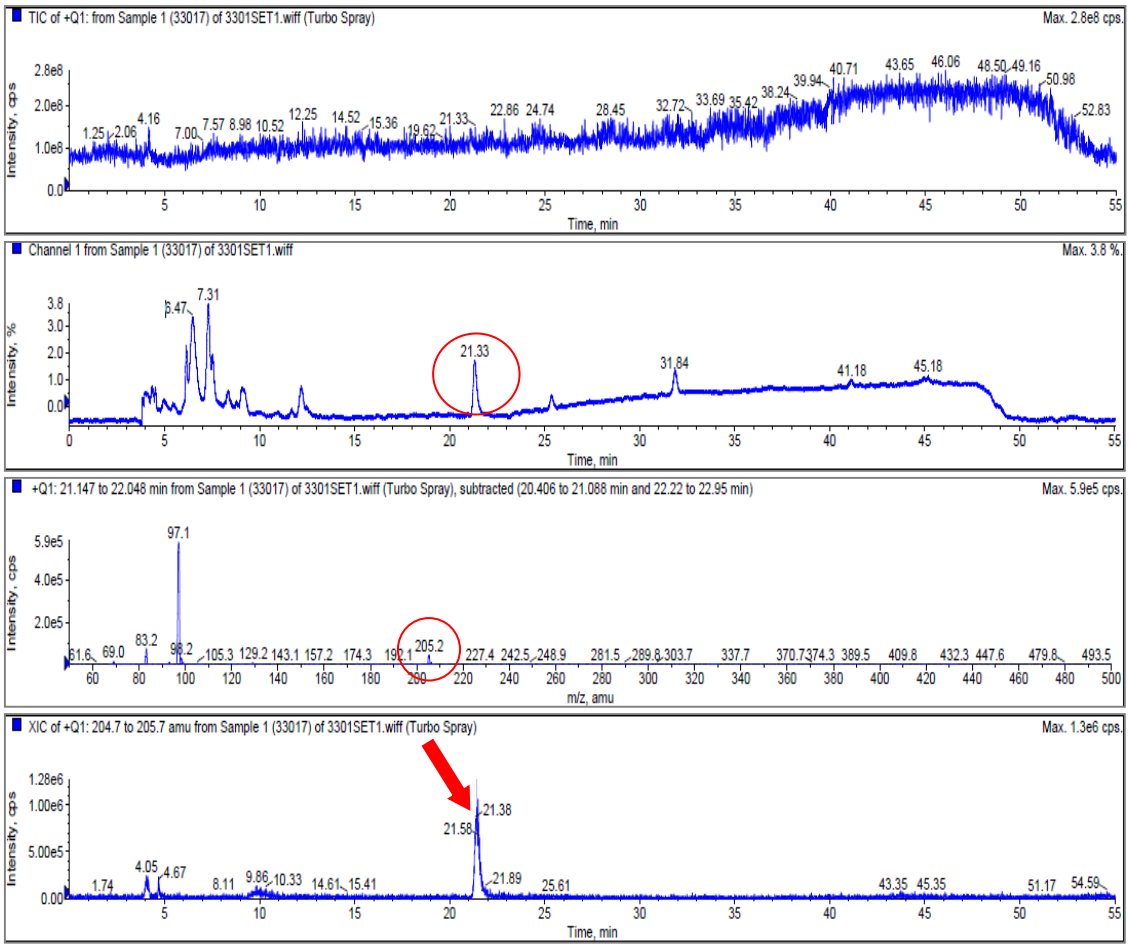

Figure 18. **Metabolic fingerprinting approach in mouse plasma samples. From top to bottom: total ion current (TIC) chromatogram, UV chromatogram (260 nm), Q1 mass scan of mass to charge ratios (m/z) of selected peak, extracted ion chromatogram (XIC) of selected peak with m/z 205.2.**

This strategy was used to identify further metabolites (Table 13). Though not all detected mouse metabolites were UV active. All peaks in the UV chromatogram at 260 nm were examined one by one with the chosen approach. In addition, tyrosine (Tyr), phenylalanine (Phe), valine (Va), leucine (Leu), methionine (Met), and betaine could be identified by this experimental approach. Extracted ion (XIC) chromatograms of mouse plasma metabolites are shown in Figure 19.

Table 13. **Overview identified mouse plasma metabolites.**

Metabolite	Molecular weight (g/mol)	UV absorbance at 260 nM	$[M+H]^+$
Tryptophan (Trp)	204.23	+	205.2
Phenylalanine (Phe)	165.19	-	166.2
Tyrosine (Tyr)	181.19	+	182.2
Valine (Va)	117.15	-	118.2
Leucine (Leu)	131.18	-	132.2
Methionine (Met)	149.21	-	150.2
Betaine	117.15	-	118.2

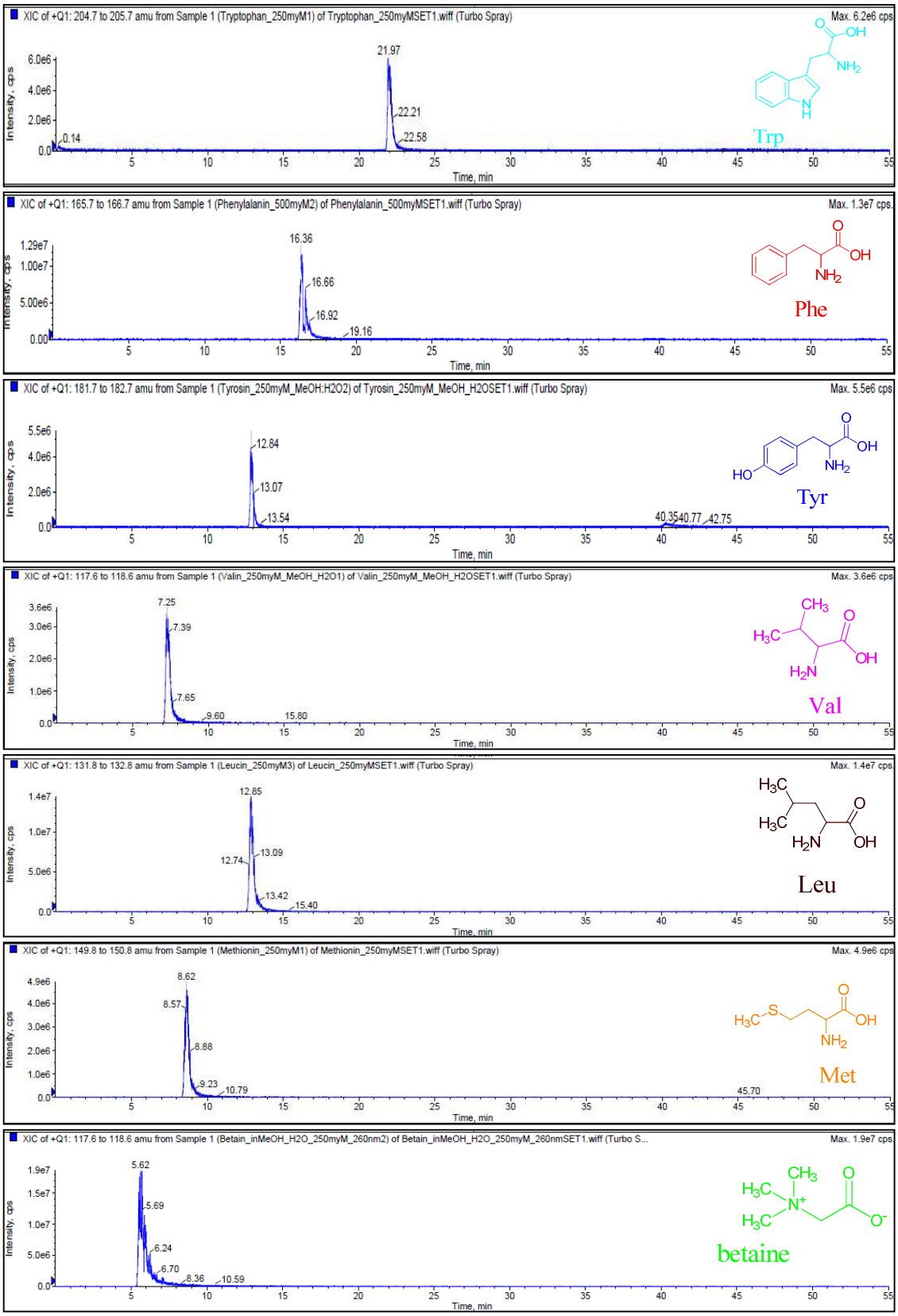

Figure 19. **Extracted ion (XIC) chromatograms of identified plasma metabolites in *Ahr*$^{+/+}$ and *Ahr*$^{-/-}$ mice. From top to bottom: tryptophan, phenylalanine, tyrosine, valine, leucine, methionine, and betaine.**

The identification of mouse plasma metabolites with priority on recognizing *Ahr* knockout-specific metabolites were the main objectives of the metabolic fingerprinting approach. Figure 20 below summarizes the obtained findings.

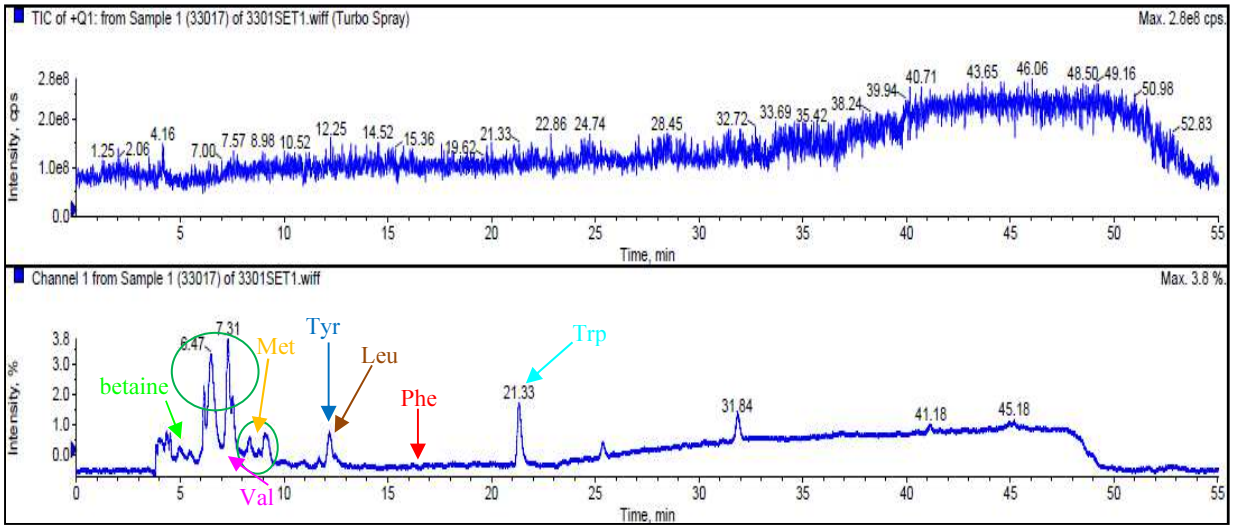

Figure 20. **Identification of plasma metabolites of an adult male *Ahr*$^{-/-}$ mouse. At top total ion current (TIC) chromatogram, at bottom UV chromatogram (260 nm). Identified metabolites included: betaine, valine (Val), methionine (Met), tyrosine (Tyr), leucine (Leu), phenylalanine (Phe), and tryptophan (Trp).**

The identification of seven mouse plasma metabolites in mice of both genotypes was achieved with the developed, optimized, and established HPLC-ESI-MS/MS program and settings. Betaine, Val, Met, Leu, Phe, Tyr, and Trp were successfully identified, thus only the last two were UV active at 260 nm. It was unfortunately not possible to detect the UV active *Ahr*$^{-/-}$-specific peaks (green marking). This leads to the suggestion that the metabolites disguised underneath these peaks likely compromise similar polarities. Another difficulty in the chosen approach was the low plasma metabolite concentrations. In the present work, plasma samples of each genotype were measured separately to achieve individual information from each animal. Another possible research approach would be the pooling of the samples, whereas individual information would get lost and a possible abnormality of one sample could lead to ambiguous conclusions.

IV.2.2 Mouse Study III - Transgenic Mouse Study

The transgenic mouse five days study was performed at the University Kaiserslautern. Four female mice of each genotype (*Ahr*$^{-/-}$ and *Ahr*$^{+/+}$) were either treated with a single dose of TCDD (25 µg/kg bw) or corn oil by gavage. The application volume was 2.5 ml/kg bw. Mice were anesthetized with an overdose of pentobarbital and liver samples were extracted surgically from animals 96 h after single dose treatment, cut into slices, and were snap frozen immediately in liquid nitrogen and stored at -80 °C. Further information about the animal experiment is given in chapter six (VI Methods).

IV.2.2.1 Relative Liver Weights

The relative liver weight was calculated as the ratio between the absolute liver weight and the related body weight of each animal. Figure 21 summarizes the results of the mouse five days study. Relative liver weights of *Ahr*$^{-/-}$ mice were significantly reduced compared to their *Ahr*$^{+/+}$ littermates. The decrease in liver weight is directly related to a reduction in hepatocyte size which is a result of the massive portosystemic shunting in *Ahr*$^{-/-}$ mice (Lahvis et al., 2000). A small, but not significant increase of the relative liver weights was determined comparing the *Ahr*$^{-/-}$ vehicle control animals (3.51 % ± 0.27 %) to the TCDD-treated *Ahr*$^{-/-}$ animals (4.27 % ± 1.17 %). The high standard deviations were due to interindividual differences between the four animals. A significant increase of the relative liver weight was measured between *Ahr*$^{+/+}$ vehicle control mice (4.41 % ± 0.24 %) and TCDD-treated *Ahr*$^{+/+}$ animals (6.52 % ± 0.29 %). In a toxicogenomic study performed by Boverhof et al (2006), the relative liver weights of male *Ahr*$^{+/+}$ were also significantly increased after treatment with TCDD (100 and 300 µg/kg bw), whereas lower TCDD-doses (0.001 - 10 µg/kg bw) had no impact on the murine liver weight.

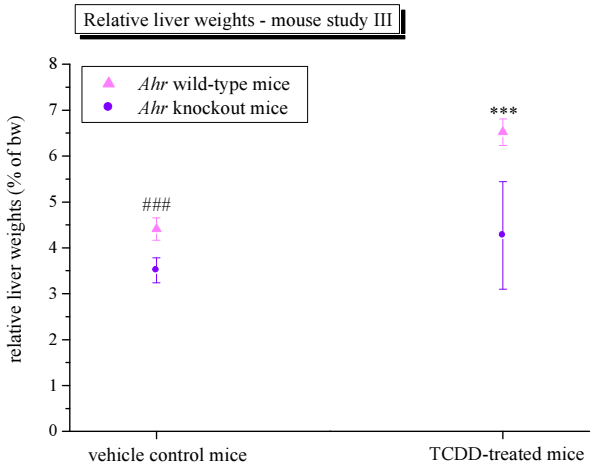

Figure 21. Relative liver weights of female *Ahr*$^{-/-}$ and *Ahr*$^{+/+}$ mice in mouse study III.
Absolute liver weights related to body weights, application volume 2.5 ml/kg bw.
TCDD as one time administered dose (25 µg/kg bw), vehicle control treated with corn oil
Data represent means ± SD of four different adult female mice. One-tailed unpaired Student's t-test, ###= p ≤ 0.001 (vehicle control *Ahr* knockout vs. vehicle control *Ahr* wild-type), ***= p ≤ 0.001 (comparing vehicle control vs. TCDD-treated animals).

IV.2.2.2 Gene Expression Analysis by RT-PCR

The effects of TCDD on mRNA gene expression of *Cyp1a1*, *Cyp1a2*, *Cyp2b10*, and *Cyp3a44* in the mouse study III are presented in Figures 22. Single dose administration of TCDD (25 µg/kg bw) led to an extensive induction of *Cyp1a1* mRNA levels in female $Ahr^{+/+}$animals, i.e. 5346.81 ± 1079.35-fold. In female $Ahr^{-/-}$ mice *Cyp1a1* mRNA levels were below *Cyp1a1* mRNA expression of related vehicle control animals resulting in a fold-change of 0.55 ± 0.23. *Cyp1a2* mRNA expression, as additional marker for AhR activation, was additionally examined. TCDD significantly induced the hepatic *Cyp1a2* expression in $Ahr^{+/+}$ animals (66.67 ± 27.78-fold) compared to control animals and $Ahr^{-/-}$ animals (0.26 ± 0.08-fold). The hepatic *Cyp2b10* mRNA levels in female $Ahr^{+/+}$ animals were also significantly enhanced by TCDD compared to control animals and resulted in a fold-change of 2.09 ± 0.30. TCDD had no influence on *Cyp2b10* levels in female $Ahr^{-/-}$ animals in this study compared to corresponding vehicle control animals. *Cyp3a44* mRNA levels were in TCDD-treated *Ahr* wild-type and in *Ahr* knockout mice below the *Cyp3a44* expression of the respective vehicle control group. The genes *Cyp2b10* and *Cyp3a44* encode proteins which function as hepatic xenobiotic metabolising enzymes. Their expression is not regulated through the AhR, but through different transcription factors CAR and PXR, respectively. The mRNA levels for *Cyp3a44* were suppressed about the same order of magnitude in both. *Cyp3a44* is a female mouse-specific gene which is primarily regulated by PXR (Sakuma et al., 2002). Considering the fact that *Cyp3a44* mRNA expression was down regulated in *Ahr* wild-type and knockout mice by TCDD, an AhR-independent mechanism could be responsible for this effect.

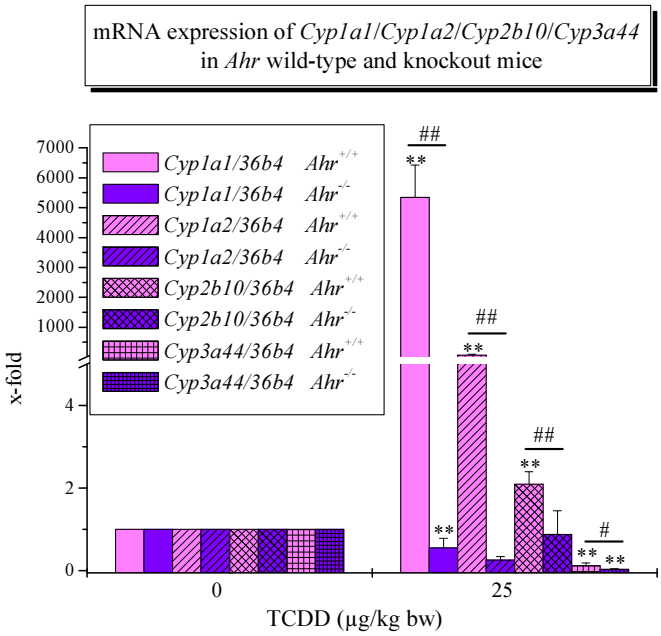

Figure 22. **Real-time PCR ratios of female $Ahr^{+/+}$ / $Ahr^{-/-}$ mice treated with TCDD - mouse study III. 36b4 served as housekeeping gene, TCDD as one-time administered dose (25 µg/kg bw). Data represent means + SD of four different adult female mice. Normalized to corresponding vehicle control. One-tailed unpaired Student's t-test with Welch correction, *= $p \leq 0.05$, **= $p \leq 0.01$ (comparing vehicle control vs. TCDD-treated animals), #= $p \leq 0.05$, ##= $p \leq 0.01$ (comparing TCDD-treated *Ahr* wild-type vs. TCDD-treated *Ahr* knockout animals).**

IV.2.2.3 Microarray Analysis - Mouse Study III

Results of the real-time PCR analysis revealed distinct differences between TCDD-treated *Ahr* knockout and wild-type mice (IV.2.2.2 Gene expression analysis by RT-PCR). Alterations in gene expression of the different genotypes after TCDD treatment were examined by applying microarray analysis of the female mouse liver. After sacrificing of the animals, tissues including mouse liver and kidney were isolated, cut into smaller pieces (30 mg), immediately snap frozen in liquid nitrogen, and stored at -80 °C until further usage. In the present work the female mouse liver was the centre of attention. As a result of this, the following microarray analysis was performed using samples of female mouse livers.

Whole Mouse Genome Oligo Microarray 4x44K (Agilent Technologies, Waldbronn) was used to measure altered genes between control groups (treated with corn oil) and compound-treated mice. Further information about the experimental procedures and conditions as well as data processing and statistical analysis are given in chapters six and seven (VI Methods and VII Materials) of the present work. Microarray data from liver and kidney of each genotype is summarized in one data file to extract all information from this microarray experiment. The microarray analysis of mouse livers is featured in the present chapter. Microarray results were filtered by cut-off values for the signal intensity $A \geq 7$, the log2 fold-change ≥ 1 or ≤ -1, and the p-value ≤ 0.05.

The mRNA alteration of a specific oligonucleotide sequence of a gene (probe) displays the possible up or down regulation of the respective gene. On the Agilent microarray slide sometimes different mRNA sequences (oligonucleotides) of the corresponding gene were spotted. In some cases those mRNA sequences differed in their respective up or down regulated mRNA expression which led to different log2 fold-changes. This phenomenon can be due to various reasons. On one hand, this can be attributed to the manufacturer's chosen nucleotide sequence which results in different binding affinities of the sample onto the slide. On the other hand, it could also depend on the RNA integrity of the samples. The last aformentioned suggestion can be excluded because the purity of the applied RNA was verified by Bioanalyzer before starting the experimental procedure as well as during the experiment by measuring the cRNA purity by nanodrop before hybridization. It both cases the applied samples were proven to be of good quality. Microarray analysis after exposure to an exogenous stimulus provides important and useful information about induced and suppressed metabolic pathways, but it requires further experimental gene analysis. Subsequent verification of gene expression levels, e.g. by RT-PCR, is necessary and fundamental.

In the present work fold-changes of a gene with identical probes and RefSeq accession numbers (NM_) were calculated as average values. No average fold-change values were calculated if non-identical probes of one gene were obtained by microarray analysis. Though the term gene is used to present the microarray results, it has to be considered that the alteration of mRNA expression of an oligonucleotide was measured within this microarray experiment.

IV.2.2.3.1 Microarray Results - Overview Mouse Study III

The large number of genes affected in livers of female wild-type and *Ahr* knockout mice by single dose treatment with TCDD (25 µg/kg bw) and subsequent sacrificing after 96 h were unexpected (Figure 23). 282 unique genes were up and 203 down regulated in TCDD-treated $Ahr^{+/+}$ mice. Treatment with TCDD led to 242 up and 234 down regulated genes in $Ahr^{-/-}$ mice. Interestingly, the number of altered genes in both mouse genotypes was within the same extent although the aryl hydrocarbon receptor was knocked out. The following chapters deal with the separate closer examination of genes affected in livers of female $Ahr^{+/+}$ and $Ahr^{-/-}$ mice first, before up and down regulated genes of both genotypes are compared to each other. First, an overview of the obtained results is featured in the presented heatmap below (Figure 24). Both heatmaps show how differently genes were altered in both genotypes. An up regulation is illustrated as intense, bright red (*Cyp1a1*) and the down regulation of a gene is pictured in the heatmap as a light, vibrant green (*Sult3a1*). The two featured heatmaps visualize the TCDD-mediated alterations in hepatic gene expression in livers of $Ahr^{+/+}$ and $Ahr^{-/-}$ mice which will be analyzed in the following chapters.

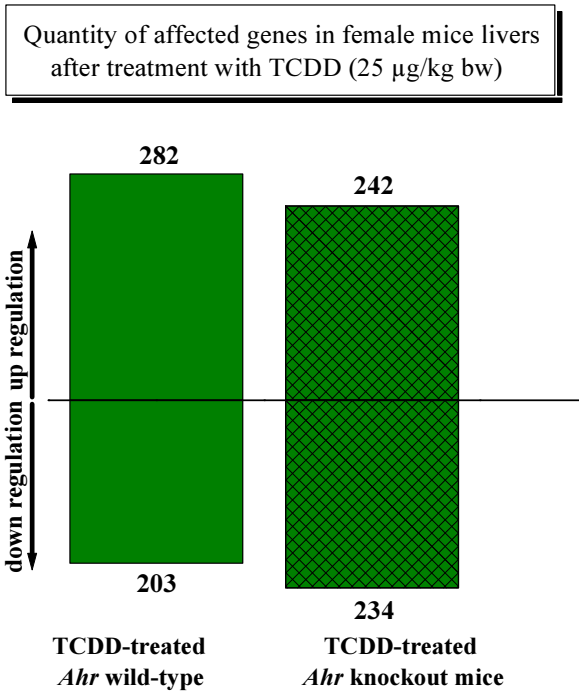

Figure 23. **Microarray results of mouse five days study - mouse study III. Quantity of affected genes in female mouse livers after treatment with TCDD (25 µg/kg bw) in *Ahr* wild-type (left-hand side) and *Ahr* knockout (right-hand side). Selected cut-off values: A ≥ 7, log2 fc ≥ 1 or ≤ -1, p-value ≤ 0.05**

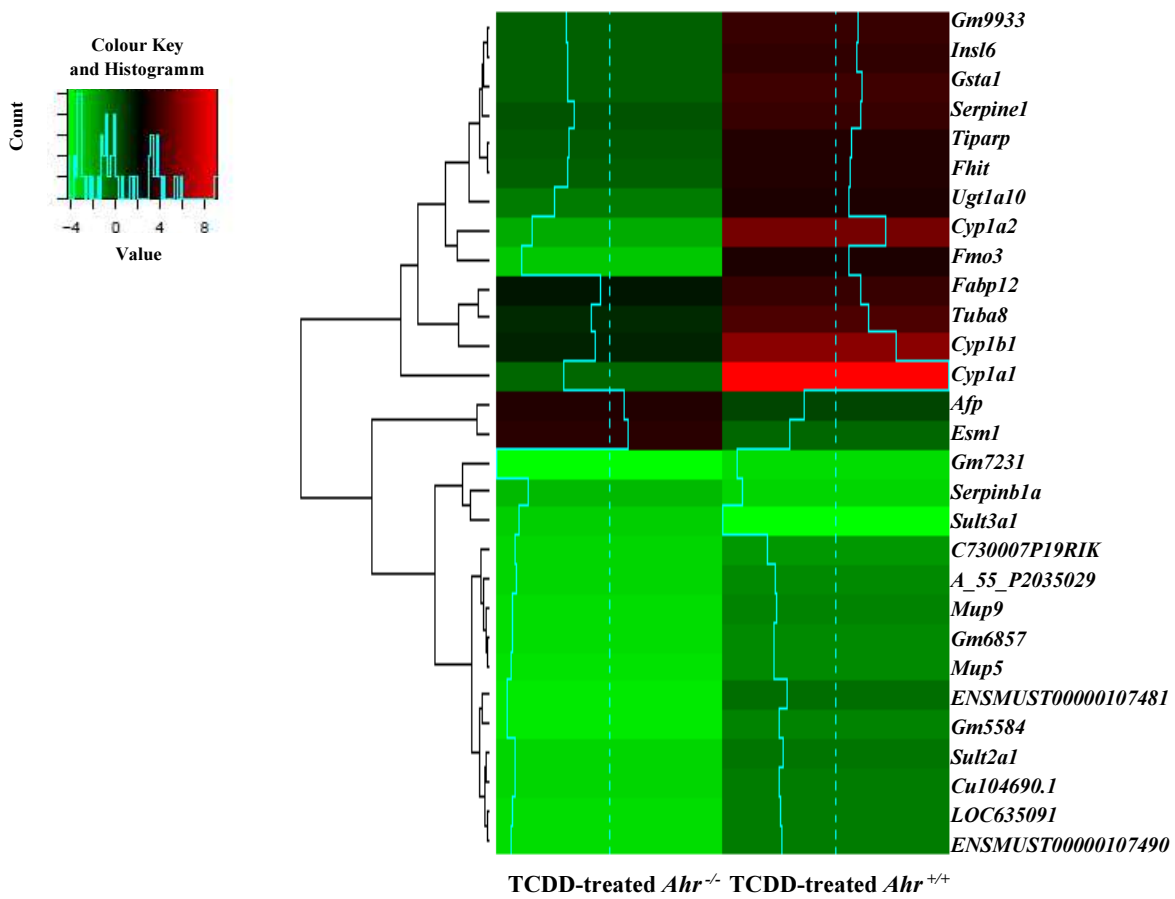

Figure 24. **Heatmaps obtained from microarray data - mouse study III.**
Two times Pearson correlation, cutoff-values: A ≥ 7, log2 fc ≥ 2 or ≤ -2, p-value ≤ 0.05.

IV.2.2.3.2 TCDD-treated *Ahr* Wild-type Mice

Due to the large amount of affected genes after treatment with TCDD, only a selection of the most relevant genes is described in detail in the following chapter. A list of all significantly up and down regulated genes is attached to the present work (Tables 85 and 86). TCDD treatment led to 282 unique up and 203 down regulated genes in livers of female $Ahr^{+/+}$ mice by applying selected cut-off values (Figure 23). From the 282 up regulated genes in female mice livers after exposure to TCDD (25 µg/kg bw) the majority of genes (about 70 %) were only slightly, but statistically significantly up regulated (log2 fc values between 1 - 2). Only 13 genes had log2 fc-values ≥ 3. The top ten of the highest up and down regulated are listed in the Table 14. The highest up regulated genes in female mouse liver were the best known markers for AhR activation upon dioxin-exposure namely *Cyp1a1*, *1b1*, and *1a2* with *Cyp1a1* being by far the highest up regulated gene in livers of *Ahr* wild-type mice treated with TCDD, followed by *Cyp1b1* and *Cyp1a2*.

Tuba8 (tubulin alpha 8) was also among the ten highest up regulated genes. Alpha-tubulin and β-tubulin form a heterodimer complex that assembles into microtubules which constitute one of the major components of the cytoskeleton in eukaryotic cells and are therefore involved in various essential processes including cell division, motility, and intracellular transport. The potential role of TUBA8 in the regulation of cell growth, proliferation, and cellular migration was demonstrated in an *in vitro* study in which Huh7 and HepG2 cells were stable transfected with the murine *Tuba8* (Kamino et al., 2011). The induction of *Tuba8* was also observed in TCDD-treated male *Ahr* wild-type mice in a study performed by Tijet and co-workers (Tijet et al., 2006). *Gsta1* (glutathione S-transferase alpha 1) belongs to the murine aromatic hydrocarbon gene battery (Nebert et al., 2000) and was also induced in livers of female *Ahr* wild-type mice. Other members of the family of glutathione S-transferases were likewise up regulated in livers of TCDD-treated wild-type mice including *Gsta2, Gstm1, Gstm2, Gstm3, Gstm4, Gstp1, Gstp2,* and *Gstt2*. Glutathione S-transferases play key roles within drug metabolism, more concretely, during phase II drug metabolism by conjugating xenobiotics (Boverhof et al., 2006) (Yeager et al., 2009). Consistently, UDP glucorosyltransferases which are also involved in biotransformation of xenobiotics (*Ugt1a6a, Ugt1a10,* and *Ugt2b35*) were up regulated in TCDD-treated wild-type mice.

Serpine1 (serine (or cysteine) peptidase inhibitor clade E, member 1) was also among the ten highest up regulated genes in livers of $Ahr^{+/+}$ mice. Three other members of this class of peptidase inhibitors were also significantly up regulated including *Serpina6, Serpinb6a*, and *Serpinb6c*. Likewise, insulin-like 6 (*Insl6*) was among the 10 highest up regulated genes. *Insl6* encodes a protein with several physiological functions (Burnicka-Turek et al., 2009) (Zeng et al., 2010). Insl6 mRNA levels were strikingly induced upon skeletal muscle injury. Zeng et al. demonstrated that insulin-like 6 is a myokine and that its overexpression resulted in the stimulated proliferation and reduced apoptosis in cultured myogenic cells. The knockdown of *Insl6* led to the reduced proliferation and increased apoptosis in mice (Zeng et al., 2010). *Tiparp* (TCDD-inducible poly (ADP-ribose) polymerase) and *Hsd17b2* (hydroxysteroid (17-beta) dehydrogenase) were also significantly up regulated in livers of *Ahr* wild-type mice. *Fhit*, the flavin histidine triade gene, was also among the top ten of significantly up regulated genes in wild-type mice. *FHIT* is a known tumour suppressor gene in humans (Schlott et al., 1999). The up regulation of the human *FHIT* by TCDD was furthermore demonstrated in a microarray study by the use of the human liver cell line HL1-1 (Kim et al., 2009).

From the 203 down regulated genes the majority of genes were slightly but statistically significantly suppressed ($-1 \leq \log2\ fc \geq -1$) in livers of TCDD-treated female *Ahr* wild-type mice. The highest down regulated gene in TCDD-treated *Ahr* wild-type mice was *Sult3a1* (sulfotransferase family 3a, member 1). Sulfotransferases belong to the phase II enzymes which are responsible to convert xenobiotics and their metabolites into hydrophilic products which afterwards can be excreted by the organism (Alnouti et al., 2006). In a previously published study it was demonstrated that *Sult3a1* mRNA levels after TCDD treatment were down regulated in livers of female $Ahr^{+/+}$ and $Ahr^{-/-}$ mice compared to the genotype-specific vehicle controls. However, hepatic Sult3a1 mRNA levels were not affected in livers of male mice of each genotype after TCDD-treatment. The constitutive hepatic levels of female $Ahr^{-/-}$ mice were already decreased compared to female $Ahr^{+/+}$ mice (Aleksunes et al., 2012).

In conclusion the down regulation of *Sult3a1* in the present mouse study is probably the result of a gender-specific effect.

As displayed in Table 14, in some cases genes, i.e. olionucleotides sequences are spotted on the microarray slide, but their biological functions are not fully determined. For instance at the time of the microarray design, *Gm7231* was annotated by Agilent Technologies as predicted gene. Analysis of the probe nucleotide sequence by using nucleotide BLAST software (National Center for Biotechnology Information) revealed that the *Gm7231*-assigned probe was specific for *Sult2a7* (sulfotransferase family 2a, dehydroepiandrosterone (DEHA)-preferring, member 7). Hydroxysteroid sulfotransferases such as SULT2A7 catalyze the sulfonation of xenobiotics, hydroxysteroids, and toxic hydrophobic bilde acids. Seven hepatic *Sult2a* (*Sult2a1-7*) genes are expressed in mouse. Their expression is regulated age- and sex-dependent. *Sult2a7* is expressed in the adult male and female liver, but not detected in the pre-pubertal mouse liver of either sex (Kocarek et al., 2008).

Serpinb1a (serine (or cysteine) peptidase inhibitor, clade B, member 1a) was also strongly suppressed in livers of TCDD-treated female wild-type mice. Other down regulated peptidase inhibitors were *Serpina3h*, *Serpina*7, and *Serpina11*. The mRNA down regulation of *Serpinb1a*, *Serpina3h*, *Serpina7*, and *Serpina11* is in harsh contrast to the strong induction of *Serpine1*, *Serpina6*, *Serpinb6a*, and *Serpinb6c*. This leads to the suggestion that the class of Serpin proteins have a broad range of biological functions which are tightly regulated by the different family members. The *Hao1* (hydroxyacid oxidase 1) gene was also among the group of the highest down regulated genes. In addition, the *Hao2* mRNA expression of this gene was also suppressed in livers of *Ahr* wild-type mice. Furthermore, the hepatic *Cyp3a44* gene was additionally down regulated in TCDD-treated female *Ahr* wild-type mice. CYP3A44, a member of the cytochrome P450 isoenzymes, is a female-specific xenobiotic metabolizing enzyme in the mouse liver. Regulation of *Cyp3a44* expression is mediated through the pregnane-X-receptor (PXR) (Anakk et al., 2004) (Bhadhprasit et al., 2007) (Roos, 2011).

Another gene down regulated in the mouse five days study was *Mup3* (major urinary protein 3). *Mup3* was not the only member of *Mup*s which was down regulated in mouse study III. The mRNA expression of *Mup9* and *Mup21* were also significantly down regulated compared to the vehicle controls. MUP is the major protein component of the mouse urine. Its expression is sex-dependent. Adult male mice secrete 5- to 20-times more MUPs than their female counterparts (Flower et al., 1996). Hakk and co-workers identified mouse MUP as TCDD carrier protein in which the highly lipophilic TCDD is at least partly eliminated by urine (Hakk et al., 2009) in *Cyp1a2*-deficient mice as well as in wild-type ones. *Csad* (cysteine sulfinic acid decarboxylase) was also among the ten highest down regulated genes. *Csad* encodes an enzyme which is involved in the biosynthesis of taurine. Taurine is needed for fundamental biological processes such as the development of brain and eye, reproduction, and the anti-inflammatory activity of leukocytes (Park et al., 2002). The suppression of *Csad* by TCDD in male $Ahr^{+/+}$ mice was demonstrated by Yoon and co-workers in a previous performed study (Yoon et al., 2006).

Due to the large amount of data the *Gene set enrichment analysis with* ***topGo*** was used to search for the key pathways which were affected in female mouse liver of $Ahr^{+/+}$ mice after treatment with TCDD. Different methods can be used to localize dependencies. In the following the method 'classic' was used to calculate the enrichment of each GO term independently based on a multiple t-test. Further information about data processing is given in chapter VI.3.7.2 Microarray data analysis and processing. Table 15 and 16 feature enriched GO terms and corresponding genes involved in up (Table 15) and down regulation (Table 16) in livers of *Ahr* wild-type mice after one-time treatment with TCDD (25 µg/kg bw). Affected pathways derived from up regulated genes included predominantly the response to a chemical stimulus (GO:0071466, GO:0009410, and GO:0042221), in particular xenobiotic metabolism (GO:0006805, GO:0071466, and GO:0042178) as well as various processes involved in small molecule metabolic processes (GO:0044281, GO:0042180, GO:0019752, GO:0043436, GO:0006082, and GO:0032787) and lipid metabolism (GO:0006629). The first position in the list of enriched GO terms based on data from up regulated genes was assigned to the glutathione metabolic process (GO:0006749) which is a metabolic branch of the sulphur compound metabolic process (GO:0006790). Furthermore, cellular metabolic processes involved in amino acid metabolisms were affected in TCDD-treated *Ahr* wild-type mice (GO:0006575 and GO:0006520), too.

Enriched GO terms based on data of down regulated genes in the present microarray study revealed suppressed metabolic branches. Predominantly processes within lipid metabolism (GO:0008610, GO:0044255, and GO:0006638) were down regulated such as triglyceride (GO:0019432 and GO:0006641), fatty acid (GO:0006631) and acylglycerol (GO:0006639) metabolic processes. Neutral lipid (e.g. triglyerides, fatty acids) metabolic processes include the chemical reaction and pathways involving neutral lipids which are only soluble in solvents of very low polarity. However, metabolic processes concerning small molecules (GO:0044281, GO:0044283, GO:000602, GO:0019752, GO:0043436, GO:0042180, GO:0044281, GO:0032787, GO:0016053, and GO:0046394) were also identified as enriched GO terms from the data of up regulated genes, whereas the genes associated with the different cellular processes differed from one another.

Table 14. **10 highest up and down regulated genes in livers of TCDD-treated *Ahr* wild-type mice (mouse study III - mouse five days study).**
TCDD as one time administered dose (25 µg/kg bw).
Selected parameters for microarray analysis: cut-off values: A ≥ 7, log2 fc ≥ 1 or ≤ -1, p-value ≤ 0.05
Annotations: '*'calculated mean log 2 fc-value from identical probes.
'#'analysis revealed non-identical probes of this gene have different log2 fc values.

Gene name	Gene description	Probe name	Systematic name	Log2 fc
Up regulation (top 10)				
Cyp1a1	Cytochrome P450 family 1, subunit a, polypeptide 1	A_51_P279693	NM_009992	9.11
Cyp1b1	Cytochrome P450 family 1, subunit b, polypeptide 1	A_51_P255456	NM_009994	6.00
Cyp1a2	Cytochrome P450 family 1, subunit a, polypeptide 2	A_52_P595871	NM_009993	5.38
Tuba8	Tubulin alpha 8	A_66_P119518	NM_017379	4.39
Gsta1	Glutathione S-transferase alpha 1 (Ya)	A_55_P2032946	NM_008181	3.98
Serpine1	Serine (or cysteine) peptidase inhibitor, clade E, member 1	A_55_P2119257	NM_008871	3.90
Gm9933	Predicted gene ENSMUSG00000054044	A_55_P2004099	XM_001477458	3.73
Insl6	Insulin-like 6	A_51_P459108	NM_013754	3.66
Tiparp[#]	TCDD-inducible poly(ADP-ribose) polymerase	A_55_P1985890	NM_178892	3.39
Fhit[#]	Fragile histidine triad gene	A_55_P2032714	NM_010210	3.30
Down regulation (top 10)				
Sult3a1	Sulfotransferase family 3A, member 1	A_55_P2129449	NM_020565	-4.36
Gm7231 (aka Sult2a7)	Predicted gene EG638251	A_52_P293682	XM_001477336	-3.44
Serpinb1a	Serine (or cysteine) peptidase inhibitor clade B, member 1a	A_55_P2006008	NM_025429	-3.19
Loc100047222	Similar to anti-glycoprotein-B of human Cytomegalovirus immunoglobulin Vl chain	A_52_P614207	XM_001477680	-2.97
ENSMUST00000103426	Immunoglobulin heavy chain C gene segment	A_51_P485421	ENSMUST00000103426	-2.93*
ENSMUST00000103401	Immunoglobulin Kappa light chain V gene segment	A_52_P502849	ENSMUST00000103401	-2.89
Hao1	Hydroxyacid oxidase 1	A_66_P105270	NM_010403	-2.86
Cyp3a44	Cytochrome P450 family 3, subunit a, polypeptide 44	A_52_P366803	NM_177380	-2.82
Mup3	Major urinary protein 3	A_55_P1971237	NM_001039544	-2.80
Csad	Cysteine sulfinic acid decarboxylase	A_51_P268529	NM_144942	-2.72

Table 15. Gene Ontology (GO) analysis using topGO of up regulated genes in *Ahr* wild-type mice (A-value ≥ 7, log2 fc ≥ 1, p ≤ 0.05).
Classical enrichment analysis by testing the over-representation of GO terms within the group of differentially expressed genes was performed using Fisher's exact test.
Annotations: '°' two unique probes of this gene were up regulated.
'>' three unique probes of this gene were up regulated.

	GO.ID	Term	Genes
1	GO:0006749	Glutathione metabolic process	*Gpx3, Gss, Gsta1, Gstm1, Gstm2>, Gstm3°, Gstp1°, Gstp2°, Gstt2*
2	GO:0042180	Cellular ketone metabolic process	*Acot1, Acot2, Acot3°, Acot4, Cbr1, Chdh, Cyb5, Cyp1A1, CYP1A2, CYP4a10>, Elovl5, Gss, Gsta1, Gstm1, Gstm2>, Gstm3°, Gstp1°, Gstp2°, Gstt2, Htatip2, Lpl°, Mgll°, Nags, Pdk2, Ppd4, Pkm2, Slc22a5, Slc35d1, Ucp3, Ugdh, Wdtc1*
3	GO:0019752	Carboxylic acid metabolic process	*Acot1, Acot2, Acot3°, Acot4, Cbr1, Chdh, Cyb5, Cyp1A1, CYP1A2, CYP4a10>, Elovl5, Gss, Gsta1, Gstm1, Gstm2>, Gstm3°, Gstp1°, Gstp2°, Gstt2, Htatip2, Lpl°, Mgll°, Nags, Pdk2, Ppd4, Pkm2, Slc22a5, Slc35d1, Ucp3, Ugdh, Wdtc1*
4	GO:0043436	Oxoacid metabolic process	*Acot1, Acot2, Acot3°, Acot4, Cbr1, Chdh, Cyb5, Cyp1A1, CYP1A2, CYP4a10>, Elovl5, Gss, Gsta1, Gstm1, Gstm2>, Gstm3°, Gstp1°, Gstp2°, Gstt2, Htatip2, Lpl°, Mgll°, Nags, Pdk2, Ppd4, Pkm2, Slc22a5, Slc35d1, Ucp3, Ugdh, Wdtc1*
5	GO:0006082	Organic acid metabolic process	*Acot1, Acot2, Acot3°, Acot4, Cbr1, Chdh, Cyb5, Cyp1A1, CYP1A2, CYP4a10>, Elovl5, Gss, Gsta1, Gstm1, Gstm2>, Gstm3°, Gstp1°, Gstp2°, Gstt2, Htatip2, Lpl°, Mgll°, Nags, Pdk2, Ppd4, Pkm2, Slc22a5, Slc35d1, Ucp3, Ugdh, Wdtc1*
6	GO:0006805	Xenobiotic metabolic process	*Cyp1a1, Gsta1, Gsta2, Gstm2>, Gstm4, Gstp1°, Gstp2°*
7	GO:0071466	Cellular response to xenobiotic stimulus	*Cyp1a1, Gsta1, Gsta2, Gstm2>, Gstm4, Gstp1°, Gstp2°*
8	GO:0006518	Peptide metabolic process	*Gpx3, Gss, Gsta1, Gstm1, Gstm2>, Gstm3°, Gstp1°, Gstp2°, Gstt2*
9	GO:0009410	Response to xenobiotic stimulus	*Cyp1a1, Gsta1, Gsta2, Gstm2>, Gstm4, Gstp1°, Gstp2°*
10	GO:0044281	Small molecule metabolic process	*6430573F11RIK, Acot1, Acot2, Acot3°, Acot4, Aldh1l1, Car2, Cat, Cbr1, Ccno, Chdh, Cyb5, Cyp1a2, Cyp1b1, Cyp4A10>, DCXR, Elovl5, ENSMUST00000106148, Entpd2, Entpd5, Fhit*, Gbp2, Gpx3, Gss, Gsta1, Gstm1, Gstm2>, Gstm3°, Gstp1°, Gstp2°, Gstt2, Htatip2, Lpl°, Mgll°, Nags, Pdk2, Pdk4, Pkm2, Pld6, Pmm1°, Retsat, Saa1, Slc22a5, Slc35d1, Srd5a3, Tgfb1, Tmem86b, Tpm1, Tuba8, Ucp3, Tubb4, Ugdh, Upp1, Vldlr, Wdr92, Wdtc1, Xdh*
11	GO:0042178	Xenobiotic catabolic process	*Cyp1a1, Gsta1, Gsta2, Gstm2>, Gstm4*
12	GO:0001676	Long-chain fatty acid metabolic process	*Acot1, Acot2, Acot3°, Acot4, Cyp4a10>, Elovl5, Mgll°*
13	GO:0006575	Cellular modified amino acid metabolic process	*Chdh, Gpx3, Gss, Gsta1, Gstm1, Gstm2>, Gstm3°, Gstp1°, Gstp2°*

14	GO:0006629	Lipid metabolic process	*Acot1, Acot2, Acot3°, Acot4, Cat, Cyb5, Cyp1a1, Cyp1a2, Cyp1b1, Cyp4a10>, Elovl5, ENSMUST00000109462, Hexa, Hsd17b2, Hsd17b6, Lpl°, Mgll°, Naga, Pla2g12a, Pla2g7°, Pld6, Retsat, Saa1, Serpina6, Srd5a3, Stard5, Tiparp°, Tmem86b, Ucp3, Vldlr, Wdtc1*
15	GO:0070887	Cellular response to chemical stimulus	*Cat, Ccl2, Ccl6, Cdh1, Col1a1, Col3a1, Col4a1, Csf2rb2, Cxcl10, Cyp1a1, ENSMUST00000105501, ENSMUST00000109462, Fcer1g, Fcgr3, Gbp2, Gpx3, Gsta1, Gsta2, Gstm2>, Gstm4, Gstp1°,Gstp2°, Hba-a2, Hmgb2, Il1r1, Jak3, Lcn2, Nfe2l2, Saa1, Serpine1, Vldlr, Wdtc1*
16	GO:0032787	Monocarboxylic acid metabolic process	*Acot1, Acot2, Acot3°, Acot4, Cyb5, Cyp1a1, Cyp1a2, Cyp4a10>, Elovl5, Lpl°, Mgll°, Pdk2, Pdk4, Pkm2, Slc35d1, Ucp3, Ugdh, Wdtc1*
17	GO:0006790	Sulfur compound metabolic process	*Gpx3, Gss, Gsta1, Gstm1, Gstm2>, Gstm3°, Gstp1°, Gstp2°, Gstt2*
18	GO:0042221	Response to chemical stimulus	*Acot2, Casp6, Cat, Ccl2, Ccl6, Ccnd3, CD14, Cdh1, Ces2°, Clec7a, Col1a1, Col3a1, Col4a1, Csf2rb2, Cxcl10, Cyp1a1, Cyp1a2, Cyp1b1, ENSMUST00000105501, ENSMUST00000109462, Ephx1, Fcer1g, Fcgr3, Gbp2, Gpx3, Gss, Gsta1, Gsta2, Gstm2>, Gstm4, Gstp1°, Gstp2°, Hba-a2, Hmgb2, Hsd17b2, Il1r1, Jak3, Lcn2, Nfe2l2, Nqo1, Sqq1, Selk, Serpine1, Slc22a5, Tgfb1, Txnip, Ucp2, Ucp3, Vldlr, Wdtc1, Xdh*
19	GO:0006520	Cellular amino acid metabolic process	*Chdh, Gpx3, Gss, Gsta1, Gstm1, Gstm2>, Gstm3°, Gstp1°, Gstp2°, Htatip2, Slc22a5*
20	GO:0071926	Endocannabinoid signalling pathway	*Abhd6°, Mgll°*

Table 16. Gene Ontology (GO) analysis using topGO of down regulated genes in *Ahr* wild-type mice (A-value ≥ 7, log2 fc ≤ -1, p ≤ 0.05).
Classical enrichment analysis by testing the over-representation of GO terms within the group of differentially expressed genes was performed using Fisher's exact test.
Annotations: '°' two unique probes of this gene were down regulated.
'tv' transcript variant.

	GO.ID	Term	Genes
1	GO:0006082	Organic acid metabolic process	*Acly°, Acnat2°, Acot11, Acsl3, Acss2, Afmid, Amdhd1, Avpr1a, Ccbl1, Cmah, Csad, Cyp4f14, Ddo, Dpys, Elovl2, Elovl6, Ensmust00000097698, Ensmust00000102901, Fasn, Ghr (tv 1), Ghr (tv 2), Gldc, Glud1, Got1, Hao1, Hao2, Me1°, Pah, Pdhb, Pecr, Pklr, Prkag2, Slc17a3, Slc37a4, Srebf1, Tars, Ugp2*
2	GO:0019752	Carboxylic acid metabolic process	*Acly°, Acnat2°, Acot11, Acsl3, Acss2, Afmid, Amdhd1, Avpr1a, Ccbl1, Cmah, Csad, Cyp4f14, Ddo, Dpys, Elovl2, Elovl6, Ensmust00000097698, Ensmust00000102901, Fasn, Ghr (tv 1), Ghr (tv 2), Gldc, Glud1, Got1, Hao1, Hao2, Me1°, Pah, Pdhb, Pecr, Pklr, Prkag2, Slc37a4, Srebf1, Tars, Ugp2*
3	GO:0043436	Oxoacid metabolic process	*Acly°, Acnat2°, Acot11, Acsl3, Acss2, Afmid, Amdhd1, Avpr1a, Ccbl1, Cmah, Csad, Cyp4f14, Ddo, Dpys, Elovl2, Elovl6, Ensmust00000097698, Ensmust00000102901, Fasn, Ghr (tv 1), Ghr (tv 2), Gldc, Glud1, Got1, Hao1, Hao2, Me1°, Pah, Pdhb, Pecr, Pklr, Prkag2, Slc37a4, Srebf1, Tars, Ugp2*
4	GO:0042180	Cellular ketone metabolic process	*Acly°, Acnat2°, Acot11, Acsl3, Acss2, Afmid, Amdhd1, Avpr1a, Ccbl1, Cmah, Csad, Cyp4f14, Ddo, Dpys, Elovl2, Elovl6, Ensmust00000097698, Ensmust00000102901, Fasn, Ghr (tv 1), Ghr (tv 2), Gldc, Glud1, Got1, Hao1, Hao2, Me1°, Pah, Pdhb, Pecr, Pklr, Prkag2, Slc37a4, Srebf1, Tars, Ugp2*
5	GO:0044281	Small molecule metabolic process	*Aadac, Acly°, Acnat2°, Acot11, Acsl3, Acss2, Afmid, Aldob, Amdhd1, Avpr1a, Car3, Ccbl1, Cmah, Csad, Cxcl13, Cyp4f14, Ddo, Dgat2, Dpys, Ebpl, Elovl2, Elovl6, Ensmust00000097698, Ensmust00000102901, Ensmust00000106328, Entpd8, Fasn, Fdps, Ghr (tv 1), Ghr (tv 2), Gldc, Glud1, Got1, Gpd2, Hao1, Hao2, Hmgcs1, Inmt, Khk, Me1°, Ntrk2, Pah, Pdhb, Pecr, Pklr, Prkag2, Pygl, Sc5d, Setdb2, Sgsm1, Slc17a3, Slc37a4, Sqle, Srebf1, Tars, Thrsp, Tk1, Ugp2*
6	GO:0032787	Monocarboxylic acid metabolic process	*Acly°, Acnat2°, Acot11, Acsl3, Acss2, Avpr1a, Ccbl1, Cyp4f14, Elovl2, Elovl6, ENSMUST00000097698, Fasn, Ghr (tv 1), Ghr (tv 2), Hao1, Hao2, Pdhb, Pecr, Pklr, Prkag2, Slc37a4, Srebf1, Ugp2*
f	GO:0006629	Lipid metabolic process	*Aadac, Acly°, Acnat2°,Acot11, Acsl3, Acss2, Avpr1a, Cyp4f14, Dgat2, Ebpl, Elovl2, Elovl6, ENSMUST00000080361, ENSMUST00000097698, ENSMUST00000102901, Fasn, Fdps, Ghr (tv 1), Ghr (tv 2), Hao1, Hao2, Hmgcs1, Mid1ip1, Pecr, Pla1a, Prkag2, Rdh11, Sc5d, Slc37a4, Sqle, Srd5a1, Srebf1, St6galnac6, Thrsp*

8	GO:0044283	Small molecule biosynthetic process	*Acly°, Acsl3, Acss2, Avpr1a, Ccbl1, Elovl2, Elovl6, ENSMUST00000097698, ENSMUST00000102901, Fasn, Fdps, Glud1, Got1, Gpd2, Pah, Pecr, Pklr, Prfag2, Pygl, Srebf1, Ugp2*
9	GO:0016053	Organic acid biosynthetic process	*Acly°, Acsl3, Acss2, Avpr1a, Ccbl1, Elovl2, Elovl6, ENSMUST00000097698, ENSMUST00000102901, Fasn, Glud1, Got1,Pah, Pecr, Pklr, Prkag2, Srebf1, Ugp2*
10	GO:0046394	Carboxylic acid biosynthetic process	*Acly°, Acsl3, Acss2, Avpr1a, Ccbl1, Elovl2, Elovl6, ENSMUST00000097698, ENSMUST00000102901, Fasn, Glud1, Got1,Pah, Pecr, Pklr, Prkag2, Srebf1, Ugp2*
11	GO:0019432	Triglyceride biosynthetic process	*Acly°, Acsl3, Dgat2, Elovl2, Elovl6, ENSMUST00000102901, Fasn, Srebf1, Thrsp*
12	GO:0046460	Neutral lipid biosynthetic process	*Acly°, Acsl3, Dgat2, Elovl2, Elovl6, ENSMUST00000102901, Fasn, Srebf1, Thrsp*
13	GO:0046463	Acylglycerol biosynthetic process	*Acly°, Acsl3, Dgat2, Elovl2, Elovl6,ENSMUST00000102901, Fasn, Srebf1, Thrsp*
14	GO:0046504	Glycerol ether biosynthetic process	*Acly°, Acsl3, Dgat2, Elovl2, Elovl6, ENSMUST00000102901, Fasn, Srebf1, Thrsp*
15	GO:0006641	Triglyceride metabolic process	*Aadac, Acly°, Acsl3, Dgat2, Elovl2, Elovl6, ENSMUST00000102901, Fasn, Slc37a4, Srebf1, Thrsp*
16	GO:0006631	Fatty acid metabolic process	*Acly°, Acnat2°, Acot11, Acsl3, Avpr1a, Cyp4f14, Elovl2, Elovl6, ENSMUST00000097698, Fasn, Ghr (tv 1), Ghr (tv2), Hao1, Hao2, Pecr, Prkag2, Srebf1*
17	GO:0006639	Acylglycerol metabolic process	*Aadac, Acly°, Acsl3, Dgat2, Elovl2, Elovl6, ENSMUST00000102901, Fasn, Slc37a4, Srebf1, Thrsp*
18	GO:0006638	Neutral lipid metabolic process	*Aadac, Acly°, Acsl3, Dgat2, Elovl2, Elovl6, ENSMUST00000102901, Fasn, Slc37a4, Srebf1, Thrsp*
19	GO:0008610	Lipid biosynthetic process	*Acly°, Acsl3, Acss2, Avpr1a, Dgat2, Elovl2, Elovl6, ENSMUST00000080361, ENSMUST00000097698, ENSMUST00000102901, Fasn, Fdps, Hmgcs1, Mid1ip1, Pecr, Prkag2, Sc5d, Srd5a1, Srebf1, St6galnac6, Thrsp*
20	GO:0044255	Cellular lipid metabolic process	*Aadac, Acly°, Acnat2°, Acot11, Acsl3, Avpr1a, Cyp4f14, Dgat2, Elovl2, Elovl6, ENSMUST00000097698, ENSMUST00000102901, Fasn, Fdps, Ghr (tv 1), Ghr (tv 2), Hao1, Hao2, Hmgcs1, Pecr, Prkag2, Slc37a4, Srebf1, St6galnac6, Thrsp*

IV.2.2.3.3 TCDD-treated *Ahr* Knockout Mice

Single dose treatment with TCDD (25 µg/kg bw) led to the up regulation of 242 and to down regulation of 234 unique genes in female *Ahr* knockout mice applying selected cut-off values. These findings were unexpected because the aryl hydrocarbon receptor was not present in the organism. This draws to the conclusion that the exogenous stimulus (TCDD) affected the hepatic gene expression in an AhR-independent manner. In the following, the TCDD-altered hepatic gene expression in female *Ahr* knockout mice is characterized and possible explanations are given for this phenomenon.
Because of the large amount of genes being up regulated in female mouse liver only the ten highest up and down regulated genes are listed below (Table 17). A list of all up and down regulated genes within the range of the selected parameters ($A \geq 7$, $\log2\ fc \geq 2$, and $p \leq 0.05$) is attached to the present work (Tables 87 and 88).

The highest up regulated gene in female mouse liver of $Ahr^{-/-}$ mice was the endothelial cell-specific molecule 1 (*Esm1*). *Esm1* encodes a dermatan sulphate proteoglycan which circulates in the blood in the healthy organism. Due to its circulating proteoglycan activity it can be rather fast present at sites of inflammation or tumour sites. Experimental evidence suggests its involvement in the modulation of major biological processes such as cell adhesion, inflammatory abnormalities, and tumour progression (Sarrazin et al., 2006). No correlation between TCDD treatment and the up regulation of *Esm1* gene has been described so far. The up regulation of Esm1 in the present study leads to the suggestion that TCDD, as exogenous stimulus, evoked an inflammatatory response in *Ahr* knockout mice which is AhR-independent. *Lysmd2* (LysM putative peptidoglycan-binding, domain containing 2) was also among the ten highest up regulated hepatic genes in TCDD-treated *Ahr* knockout mice. Its role and function in metabolism of rodents and humans has not been characterized up to the present day. The gene lipoprotein lipase (*Lpl*) encodes a protein that is a key enzyme in lipid metabolism which is responsible for storing fatty acids as triglycerides in the adipose tissue. The liver-specific *Lpl* overexpression has been associated with the development of fatty liver (Olson et al., 1998) (Hong et al., 2011).

Alpha fetoprotein (*Afp*) was additionally among the highest up regulated genes in livers of female *Ahr* knockout mice after exposure to TCDD. The *Afp* gene belongs to a multigenic family comprised of related genes encoding albumin, α-albumin, and vitamin D binding protein. Gabant et al. elucidated Afp's role in female fertility as they demonstrated that female *Afp*-deficient mice to be infertile in their performed study (Gabant et al., 2002). The leptin receptor (*Lepr*) gene encodes a protein which functions as 'adipostat' by passing information to the body about its status of energy storage in adipose tissues (Tartaglia et al., 1997). In addition, the calcium and integrin binding family member 3 (*Cib3*) was among the ten highest up regulated genes in female *Ahr* knockout mice. Integrins are heterdimeric adhesion receptors on the surface of platelets proteins which therefore play a fundamental role in homeostasis (Yamniuk et al., 2006) (DeNofrio et al., 2008). Consistently, another gene involved in cell-cell adhesion was also up regulated, namely cadherin 1 (*Cdh1*). *Cdh1* encodes the epithelial-cadherin protein (E-cadherin). Cadherins are calcium-dependent cell-cell adhesion molecules. Cadherins of the type E play important roles in salivary gland

morphogenesis (Shirayoshi et al., 1986) (Walker et al., 2008). Ras responsive element binding protein 1 (*Rreb1*, transcript variant 1) was furthermore up regulated in TCDD-treated *Ahr* knockout mice. RREB1 was identified as vascular estrogen-regulated transcription factor by Schnoes and co-workers (Schnoes et al., 2008). A gene involved in the cellular amino acid metabolism (asparagine synthetase, *Asns*) (Barbosa-Tessmann et al., 2000) was also among the highest up regulated genes in female TCDD-treated *Ahr*$^{-/-}$ mice.

234 unique genes were down regulated in livers of TCDD-treated *Ahr*$^{-/-}$ mice although only 14 genes obtained log2 fc values ≤ -3 compared to the corresponding corn-oil treated *Ahr*$^{-/-}$ mice using the selected parameters (A ≥ 7, log 2 fc ≤ -1, and p ≤ 0.05). On closer examination of 10 highest down regulated genes (Table 17), various genes were only predicted genes at the time of performing the microarray experiment. During analysis of the obtained microarray results the oligonucleotide sequences (probes) of those predicted genes (*Gm7231*, *Gm5584*, and *GM6957*) were blasted online using NCBI's Basic Local Alignment Search Tool (BLAST®, National Center for Biotechnology Information). Nucleotide BLAST software compares the inserted nucleotide sequences with species-specific database annotations. In case of the highest down regulated gene *Gm7231*, nucleotide blasting revealed that it is 100 % match with *Sult2a7* (sulfotransferase family 2a, dehydroepiandrosterone (DEHA)-preferring, member 7). Both nucleotide probes corresponding to *Gm5584* were down regulated. The nucleotide sequence of the probe A_52_P218833 was matching with the *Sult2a3* (sulfotransferase family 2a, dehydroepiandrosterone (DEHA)-preferring, member 3) and A_55_P2113587 was a 100 % match with *Sult2a4* (sulfotransferase family 2a, dehydro-epiandrosterone (DEHA)-preferring, member 4). Blasting of the nucleotide sequence of *Gm6957* (A_55_P2107223) led to 100 % match with *Sult2a6* (sulfotransferase family 2a, dehydroepiandrosterone (DEHA)-preferring, member 6). However, three other members (*Sult2a1*, *Sult2a5*, and *Sult2a3*) of the DEHA-preferring sulfotransferase genes led to a good correlation, too.

All of Agilent's annotated predicted genes discussed in the in the previous passage probably belong to the group of DEHA-preferring sulfotransferases. An additional member of this group, *Sult2a1*, was also among the highest down regulated genes in TCDD-treated *Ahr*$^{-/-}$ mice. Hydroxysteroid sulfotransferases catalyze the sulfonation of xenobiotics, hydroxysteriods, and toxic hydrophobic bile acids. Seven hepatic *Sult2a* (*Sult2a1-7*) enzymes are expressed in mice, but their mRNA expression is regulated age- and sex-dependent (Kocarek et al., 2008). The hepatic *Sult2a1* gene expression can be stimulated by PXR and CAR (Echchgadda et al., 2004). Therefore, it was unexpected that TCDD treatment led to the down regulation of those hydroxysteriod sulfotransferases in livers of *Ahr* knockout mice since both nuclear receptors are not involved in the dioxin-mediated biological responses. This allows drawing the conculsion that as a result of the *Ahr* knockdown, the signalling pathways of other nuclear receptors could additionally be affected but to verify this assumption further intensive research work is nessecary. *Sult2a1* is the predominant form of the hydroxysteroid sulfotransferases. No cellular effects and possible involvement in metabolism are described so far for the other isoforms as only the age- and sex-dependent expression in mouse liver has been demonstrated (Kocarek et al., 2008).

Among the other top ten of down regulated genes in liver of TCDD-treated *Ahr* knockout mice were the major urinary proteins and their precursor proteins (*Mup5*, *Mup9*, ENSMUST00000107481, and ENSMUST00000107490). Other *MUP* genes were also down regulated including *Mup2*, *Mup6*, and *Mup20*. MUPs belong to the lipocailin superfamily consisting of extracellular proteins such as retinol binding protein, β-lactoglobulin, and fatty acid binding protein, which bind small lipophilic molecules. MUP is the main protein component of the mouse urine. Its expression is sex-dependent. Adult male mice secrete 5- to 20-times more MUPs than females (Flower et al., 1996). Hakk and co-workers identified mouse MUP as TCDD carrier protein to which the highly lipophilic TCDD is bound and then is partly eliminated in the urine (Hakk et al., 2009).

In addition, *gene set enrichment analysis with* ***topGo*** was performed with the microarray data obtained from livers of TCDD-treated female *Ahr* knockout mice. Different methods can be used to localize dependencies. The method 'classic' was used to calculate the enrichment of each GO term independently, based on a multiple t-test. Additional information about the microarray data analysis and processing is given in chapter VI.3.7.2. Table 18 and 19 display the enriched GO terms and corresponding genes identified being up (Table 18) or down regulated (Table 19) in *Ahr* knockout mice after single dose treatment with TCDD (25 µg/kg bw).

TCDD treatment of *Ahr* knockout mice led to the up regulation of various cellular processes involved in the regulation of homeopoesis (GO:0002328, GO:0002244, GO:0030195, GO:1900047, GO:0032964,GO:0048821, and GO:0050819), cellular transport, and movements mechanisms (GO:0031340, GO:2000008, and GO:0006928). Genes involved in the regulation of prostaglandin biosynthesis (GO:0031392, GO:0031394) as well as the regulation of unsaturated fatty acid biosynthetic processes (GO:2001279, GO:2001280) were also enriched compared to the vehicle control animals. Furthermore, genes associated with the triglyceride biosynthetic process (GO:0019432) were additionally up regulated.
Gene ontology pathway profiling of the significantly down regulated genes in livers of TCDD-treated *Ahr* knockout mice resulted in diverse affected metabolic processes. Remarkably, TCDD treatment of *Ahr* knockout mice led to the enrichment of the metabolic processes involved in the response to a chemical stimulus (GO:0042221). Though, it must be taken into consideration that the respective genes which are responsible for the enrichment of those metabolic branches are down regulated in the present microarray study. The small molecule metabolic processes (GO:0006082, GO:0042180, GO:0019752, GO:0043436, and GO:0032787) were also down regulated in $Ahr^{-/-}$ mice as was the case for $Ahr^{+/+}$ mice. However, the genes which led to the down regulation of the mentioned metabolic processes overwhelmingly differed for both genotypes. Other down regulated cellular processes in livers of $Ahr^{-/-}$ mice included lipid metabolism (GO:0006629), regulation of hormone levels (GO:0010817, GO:0042445), secondary metabolic processes (GO:0019748), and processes involved in cellular oxidation-reduction (GO:0055114). Genes (*Pax2, Pax8*) involved in kidney processes (GO:0072017 and GO:0072025) were furthermore down regulated.

Upon closer examination of the enriched GO terms, only a small number of the 234 up regulated genes were associated with different metabolic processes. Besides the large amount of up and down regulated genes in liver of *Ahr* knockout mice, the overall gene inducibiliy resp. suppression was rather weak. Additionally, the majority of the significantly enriched pathways are associated with common metabolic processes drawing the conclusion that no specific pathway was affected by TCDD treatment in the female mouse liver of $Ahr^{-/-}$ mice, but rather the exogenous stimulus evoked a diverse AhR-independent response.

.

Table 17. 10 highest up and down regulated genes in livers of TCDD-treated *Ahr* knockout mice (mouse study III - mouse five days study).
TCDD as one time administered dose (25 µg/kg bw).
Selected parameters for microarray analysis: cutoff values: A ≥ 7, log 2 fc ≥ 1 or ≤ -1, p-value ≤ 0.05
Annotations: '*' calculated mean log 2 fc value from identical probes.
'#' analysis revealed non-identical probes of this gene have different values (colour intensity, p-value or log2 fc value).

Gene name	Gene description	Probe name	Systematic name	Log2 fc
Up regulation (top 10)				
Esm1	Endothelial cell-specific molecule 1	A_52_P257625	NM_023612	3.51
Lysmd2	LysM putative peptidoglycan-binding domain containing 2	A_51_P233160	NM_027309	3.09*
Lpl*	Lipoprotein lipase	A_51_P259296	NM_008509	2.86#
Afp	Alpha fetoprotein	A_51_P510891	NM_007423	1.07
Lepr	Leptin receptor, transcript variant 3	A_55_P2192662	NM_001122899	2.72
Cib3	Calcium and integrin binding family member 3	A_55_P2078494	NM_001080812	2.66
Rreb1	Ras responsive element binding protein 1, transcript variant 1	A_55_P1981714	NR_033218	2.64
Fabp5l2	Predicted gene EG622384	A_55_P2150976	XM_886827	2.44
Asns	Asparagine synthetase	A_55_P1959748	NM_012055	2.42
Cdh1	Cadherin 1	A_51_P137336	NM_009864	2.39*
Down regulation (top 10)				
Gm7231	Predicted gene EG638251	A_52_P293682	XM_001477336	-4.35
Gm5584	Predicted gene 5584	A_52_P218833	NM_001101586	-3.96
Gm5584	Predicted gene 5584	A_55_P1952507	NM_001101586	-3.46
ENSMUST00000107481	Major urinary protein 4 precursor (Mup 4) partial (69%) [TC1781567]	A_55_P2113587	ENSMUST00000107481	-3.71
Mup9	Major urinary protein 9	A_55_P1979904	NM_001126319	-3.56#
Mup5	Major urinary protein 5	A_52_P412506	NM_008649	-3.48
ENSMUST00000107490	uo03b07.y1 Sugano mouse liver mlia Mus musculus cDNA cloneIMAGE:2582293 5' similar to gb:M16358 Mouse major urinary protein IV (MOUSE)	A_55_P2033321	ENSMUST00000107490	-3.45
LOC635091	Similar to Predicted gene OTTMUSG00000007485	A_55_P2103703	XM_001475400	-3.39
Gm6957	Predicted gene 6957	A_55_P2107223	NM_001081325	-3.37
C730007P19Rik	RIKEN cDNA C730007P19 gene	A_55_P2172532	NM_009286	-3.23#
Sult2a1	Sulfotransferase family 2a dehydroepiandrosterone (DHEA)-preferring, member 1	A_55_P1952517	NM_001111296	-3.32

Table 18. Gene Ontology (GO) analysis using topGO of up regulated genes in *Ahr* knockout mice (A-value ≥ 7, log2 fc ≥ 1, p ≤ 0.05).
Classical enrichment analysis by testing the over-representation of GO terms within the group of differentially expressed genes was performed using Fisher's exact test.
Annotations: '°' two unique probes of this gene were up regulated

	GO.ID	Term	Genes
1	GO:0060693	Regulation of branching involved in salivary gland morphogenesis	*Cdh1, Fgfr1, Pdgfa*
2	GO:0031340	Positive regulation of vesicle fusion	*Anxa1, Pla2g4a*
3	GO:2000008	Regulation of protein localization to cell surface	*Dch1, Egf*
4	GO:0002328	Pro-B cell differentiation	*Prkdc, Xrcc4*
5	GO:0010890	Positive regulation of sequestering of triglyceride	*Lpl°*
6	GO:0002244	Hemopoietic progenitor cell differentiation	*Fst, Prkdc, Xrcc4*
7	GO:0030195	Negative regulation of blood coagulation	*F11, Pdgfa, Tspan8*
8	GO:1900047	Negative regulation of hemostasis	*F11, Pdgfa, Tspan8*
9	GO:0006928	Cellular component movement	*Abi2, Amot, Angpt2, Bbs4, Cckar,Ccl5, CD34, CD9, Cdhst3, Col1a1, Ctgf, Cyp1b1, Erbb4, F3, Fgfr1, Nck2, Pdgfa, Prkdc, Tlr2, Tuba1a1, Tuba8, Tubb6*
10	GO:0031392	Regulation of prostaglandin biosynthetic process	*Anxa1, Pla2g4a*
11	GO:0031394	Positive regulation of prostaglandin biosynthetic process	*Anxa1, Pla2g4a*
12	GO:2001279	Regulation of unsaturated fatty acid biosynthetic process	*Anxa1, Pla2g4a*
13	GO:2001280	Positive regulation of unsaturated fatty acid biosynthetic process	*Anxa1, Pla2g4a*
14	GO:0032964	Collagen biosynthetic process	*Col1a1, Col3a1, Ctgf*
15	GO:0019432	Triglyceride biosynthetic process	*Acsl4, Agpat9, Lpl°*
16	GO:0006303	Double-strand break repair via nonhomologous end joining	*Prkdc, Xrcc4*
17	GO:0046717	Acid secretion	*Anxa1, Cckar, Pla2g4a*
18	GO:0010740	Positive regulation of intracellular protein kinase cascade	*Ark2bp, C3, Ccl5, F3, Lepr, Nenf, Pdgfa, S100a4, Slc20a1, Ubd, Zdhhc13*
19	GO:0048821	Erythrocyte development	*Hba-a2, Hbb-b1, Hbb-b2*
20	GO:0050819	Negative regulation of coagulation	*F11, Pdgfa, Tspan8*

Table 19. Gene Ontology (GO) analysis using topGO of down regulated genes in *Ahr* knockout mice (A-value ≥ 7, log2 fc ≤ -1, p ≤ 0.05).
Classical enrichment analysis by testing the over-representation of GO terms within the group of differentially expressed genes was performed using Fisher's exact test.
Annotations: '°' two unique probes of this gene were down regulated

	GO.ID	Term	Genes
1	GO:0006082	Organic acid metabolic process	*Aacs, Acnat2, Acot3°, Acss2, Akr1d1, Aldh1a1, Cyp1a2, Fmo1, Ggt1, Glul, Gstm2, Hpgd, Lpin2, Me1°, Med1, Mgll, Pax8, Pdk1, Pklr, Rdh16, Sars2, Ucp3*
2	GO:0042180	Cellular ketone metabolic process	*Aacs, Acnat2, Acot3°, Acss2, Adra1b, Akr1d1, Aldh1a1, Cyp1a2, Foxo1, Ggt1, Glul, Gstm2, Hpgd,Lpin2, Me1°, Med1, Mgll, Pax8, Pdk1, Pklr, Rdh16, Sars2, Ucp3*
3	GO:0019752	Carboxylic acid metabolic process	*Aacs, Acnat2, Acot3°, Acss2, Adra1b, Akr1d1, Aldh1a1, Asna1, Ggt1, Glul, Gstm2, Hpgd,Lpin2, Me1°, Med1, Mgll, Pdk1, Pklr, Rdh16, Sars2, Ucp3*
4	GO:0043436	Oxoacid metabolic process	*Aacs, Acnat2, Acot3°, Acss2, Adra1b, Akr1d1, Aldh1a1, Asna1, Ggt1, Glul, Gstm2, Hpgd,Lpin2, Me1°, Med1, Mgll, Pdk1, Pklr, Rdh16, Sars2, Ucp3*
5	GO:0044281	Small molecule metabolic process	*Aacs, Acnat2, Acot3°, Acss2, Adra1b, Akr1d1, Aldh1a1, Asna1, Cyp1a2, Cyp2e1, Diras1, Fmo1, Foxo1, Ggt1, Glul, Gstm2, Hpgd, Inmt, Jun, Lpin2, Me1°, Med1, Mgll, Mogat1, Ncor1, Npr2, P2ry1, Pax8, Pdk1, Pklr, Ppp2r4, Rdh16, Sars2, Setmar, Slc9a3r1, Tbc1d20, Tmem86b, Tpm2°, Tubg2, Ucp3*
6	GO:0032787	Monocarboxylic acid metabolic process	*Aacs, Acnat2, Acot3°, Acss2, Akr1d1, Aldh1a1, Cyp1a2, Hpgd, Lpin2, Mgll, Pdk1, Pklr, Rdh16, Ucp3*
7	GO:0017144	Drug metabolic process	*Cyp1a2, Cyp2e1, Fmo3*
8	GO:0010817	Regulation of hormone levels	*Aacs, Akr1d1, Aldh1a1, Dio1°, Glul, Med1, P2ry1, Pax8, Rdh16, Slc22a1, Ugt2b1*
9	GO:0019748	Secondary metabolic process	*Cyp1a2, Dct°, Fmo1*
10	GO:0042445	Hormone metabolic process	*Akr1d1, Aldh1a1, Dio1°, Med1, Pax8, Rdh16, Ugt2b1*
11	GO:0006629	Lipid metabolic process	*Aacs, Acnat2, Acot3°, Acss2, Akr1d1, Aldh1a1, Cyp1a2, Cyp2e1, Hpgd, Inpp5e, Lpin2,Med1, Mgll, Mogat1, Pnpla1, Ptdss1, Rdh16, Sult2A1, Tmem86b, Ucp3, Ugt2b1*
12	GO:0055114	Oxidation-reduction process	*Adra1b, Akr1d1, Aldh1a1, Cyp1a2, Cyp2b13, Cyp2c37, Cyp2e1, Cyp3a44, Dhrs1, Dio1°, Duox1, Fmo1, Fmo3, Hpgd, Me1°, Prkaca, Rdh16, Sepw1, Vat1*
13	GO:0009719	Response to endogenous stimulus	*Aacs, Adra1b, Ar, Cfl1, Esrrg, Foxo1, Me1°, Pax8, Prkaca, Rorc°, Slc1a2°, Socs2*
14	GO:0042493	Response to drug	*Aacs, Aldh1a1, Cyp1a2, Fos, Jun, Slc1a2, Slc22a1*
15	GO:0032788	Saturated monocarboxylic acid metabolic process	*Acot3°*
16	GO:0032789	Unsaturated monocarboxylic acid metabolic process	*Acot3°*

17	GO:0042221	Response to chemical stimulus	*Aacs, Adra1b, Adh1a1, Ar, Asna1, Cfl1, Chac1,Cryaa, Cyp1a2, Cyp2e1, Duox1, ENSMUST00000062980, Esrrg, Fga, Fos, Foxo1, Glul, Gstm2, Jun, Lifr, Me1, Mup20, Pax8, Pklr, Prkaca, Prlr, Rorc°, Slc1a2°, Slc22a1, Socs2, Ucp3, Ugt2b1*
18	GO:0006721	Terpenoid metabolic process	*Aldh1a1, Cyp1a2, Cyp2e1, Rdh16*
19	GO:0072017	Distal tubule development	*Pax2, Pax8*
20	GO:0072025	Distal convoluted tubule development	*Pax2, Pax8*

IV.2.2.3.4 Comparison of Microarray Gene Expression Data

The pattern of regulated gene in the murine liver elicited by TCDD predominantly differed in each genotype, resulting only in a small overlap of affected genes with 15 genes in common up and 18 genes in common down regulated (Figure 25). The entire list of all in common up and down regulated genes is attached to the present work. As expected due to the knockdown of the AhR the number of genes being in common up or down regulated in *Ahr* wild-type and knockout mice is remarkably small and will be discussed in the following passage. In addition, several genes are selected including established members of the murine aromatic hydrocarbon gene battery (*Cyp1a1*, *Cyp1a2*, *Nqo1*, *Aldh3a1*, *Ugt1a6*, and *Gsta1*) for discussion in the following paragraph (Nebert et al., 2000).

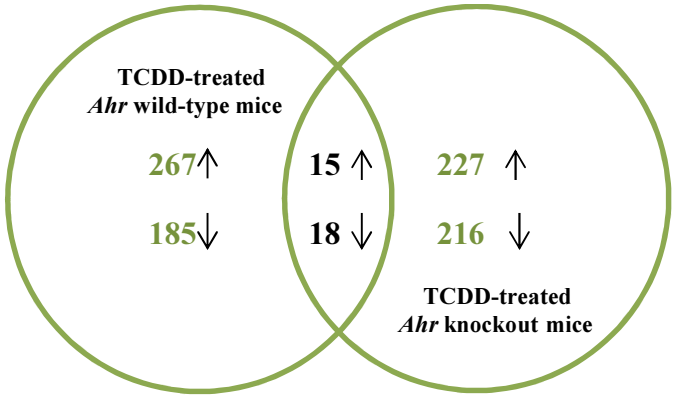

Figure 25. **Comparison of in common up and down regulated gene expression in livers of *Ahr* wild-type and knockout mice treated with TCDD.**
TCDD as one time administered dose (25 µg/kg bw).
Selected cut-off values: A ≥ 7, log2 fc ≥ 1 or ≤ -1, p-value ≤ 0.05.

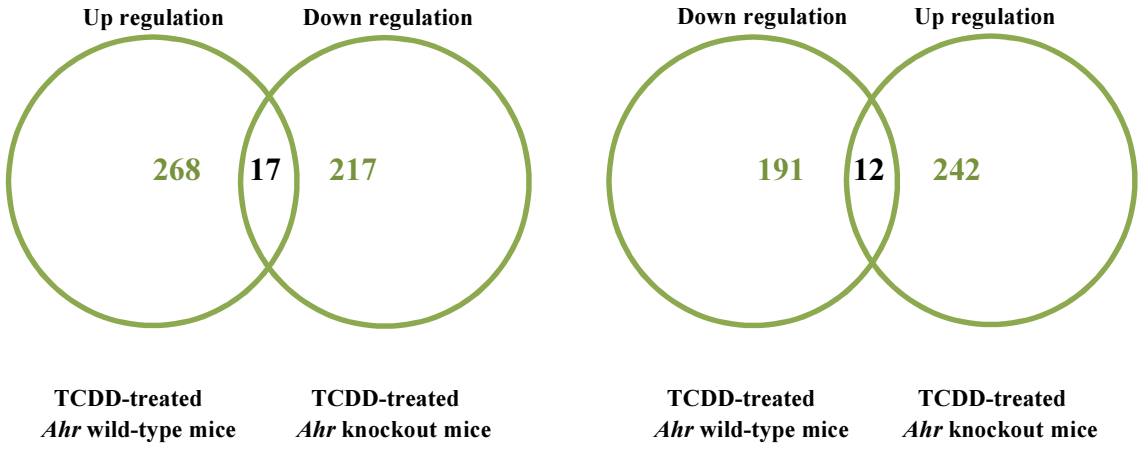

Figure 26. **Comparison of differently regulated gene expression in livers of wild-type and knockout mice after treatment with TCDD. TCDD as one time administered dose (25 µg/kg bw).**
Selected cut-off values: A ≥ 7, log2 fc ≥ 1 ≤ -1, p-value ≤ 0.05.

The induction of CYP1A1, CYP1A2, and CYP1B1 is an established marker for AhR activation by dioxin exposure in mouse (Shimada et al., 2002a). A high induction of *Cyp1a1* was obtained from TCDD-treated *Ahr* wild-type mice, whereas no significant increase or decrease was determined in livers of *Ahr* knockout mice as expected. Furthermore, the *Cyp1a2* gene was also highly up regulated in wild-type mice, whereas *Cyp1a2* was slightly, but statistically significantly down regulated in *Ahr* knockout mice. *Cyp1a2* belongs to the murine AhR gene battery and is known to be inducible by TCDD (Nebert et al., 2000) (Nebert et al., 2004). Tijet and co-workers demonstrated that male $Ahr^{+/+}$ mice featured a higher a *Cyp1a2* expression (about 4-fold) compared to $Ahr^{-/-}$ mice (Tijet et al., 2006). The lowered constitutive expression of the murine *Cyp1a2* gene in livers of $Ahr^{-/-}$ mice was demonstrated by Shimada et al., too (Shimada et al., 2002b). A high *Cyp1b1* mRNA expression was obtained from *Ahr* wild-type mice, thus the *Cyp1b1* gene was also slightly up regulated in *Ahr* knockout mice. It was observed in various studies that the TCDD-induced *Cyp1b1* induction is based on AhR activation. (Nebert et al., 2004) (Tijet et al., 2006) (Boutros et al., 2009). However, *Cyp1b1* is only constitutively expressed at very low levels in livers of wild-type and *Ahr* knockout mice (Shimada et al., 2002b). Bui and co-workers demonstrated that the hepatic *Cyp1b1* mRNA expression levels after treatment with TCDD (50 µg/kg bw) in *Ahr* knockout mice were also slightly higher compared to mRNA levels of *Cyp1a1* and *Cyp1a2* in livers of $Ahr^{-/-}$ mice (Bui et al., 2012). The slight, but significant up regulation of this gene could be mediated by a different receptor than the AhR, but this possibility has to be confirmed by further analysis. Of the four non *Cyp* P450 classic AhR-regulated genes *Nqo1*, *Gsta1*, and *Ugt1a6a* showed a solid induction in *Ahr* wild-type mice, but not in knockout mice, whereas no change in *Aldh3a1* gene expression was determined for both genotypes in the present microarray study. The AhR-mediated induction of *Aldh3a1* was demonstrated in various carcinoma cell lines and in rat, but the high dosage of TCDD (200 µg/kg bw) did not induce the hepatic *Aldh3a1* expression in mouse *in vivo*, only *in vitro* in several murine hepatoma cell lines (Vasiliou et al., 1993) (Alnouti et al., 2006) (Tijet et al., 2006). In order to find novel quantifiable biomarkers for dioxin exposure five target genes were selected (*Aldh3a1*, *Tiparp*, *Hsd17b2*, *Cd36*, and *Ahrr*); within those candidates *Tiparp*, *Hsd17b2*, and *Ahrr* were up regulated in the present mouse microarray study, but the obtained colour intensity for *Ahrr* were below the selected value of 7.

Table 20. Comparison of selected genes in *Ahr*$^{-/-}$ and *Ahr*$^{+/+}$ mice.
Table features aspects such as gene name, probe name, systematic name, and corresponding log2 fold-changes.
Annotations: '→' gene was not up regulated in microarray experiment.

Gene name	Probe name	Systematic name	Colour intensity	Log2 fc *Ahr*$^{+/+}$	Log2 fc *Ahr*$^{-/-}$
Cyp1a1	A_51_P279693	NM_009992	8.29	9.11	→
Cyp1a2	A_52_P595871	NM_009993	9.86	5.38	-2.19
Cyp1b1	A_51_P255456	NM_009994	9.46	6.00	1.51
Nqo1	A_51_P424338	NM_008706	10.40	1.79	→
Gsta1 (Ya)	A_55_P2032946	NM_008181	11.78	3.98	→
Ugt1a6a	A_55_P2143765	NM_145079	9.48	1.76	→
Ugt1a6a	A_55_P1962404	NM_145079	16.21	1.44	→
Aldh3a1	A_55_P2065562	NM_007436	6.47	→	→
Tiparp	A_55_P1985890	NM_178892	9.35	3.39	→
Tiparp	A_51_P514961	NM_178892	9.90	3.26	→
Hsd17b2	A_51_P441914	NM_008290	10.73	1.54	→
Cd36	A_51_P375146	NM_007643	10.98	→	→
Ahrr	A_55_P2128388	NM_009644	5.06	1.07	→
Ahrr	A_51_P254425	NM_009644	6.44	3.98	→

Table 21 features the differently regulated hepatic genes, i.e. which were up regulated in *Ahr* wild-type mice and down regulated in *Ahr* knockout mice. The most striking contrast in gene expression between both genotypes was gained for *Cyp1a2* which was already discussed in the previous part.

Fmo3, the flavin containing monooxygenase 3, belongs to the group of microsomal enzymes which convert highly lipophilic substrates into oxygenated metabolites with higher polarity to facilitate the excretion by the organism. The *Fmo3* gene was strongly induced in female *Ahr* wild-type mice and suppressed in female *Ahr* knockout mice. These findings suggest an AhR-dependent mechanism which was additionally postulated by Tijet and co-workers (Tijet et al., 2006). The published microarray study revealed the induction of *Fmo2* and *Fmo3* mRNA expression by TCDD in livers of male C57BL/6J mice (wild-type mice), but not in *Ahr* knockout mice (Tijet et al., 2006). The *Fmo2* mRNA expression was not affected by TCDD treatment in both genotypes leading to the conculsion that the up regulation of *Fmo2* is a male-mouse specific effect. It was demonstrated that the TCDD-induced *Fmo3* induction was a primary AhR-mediated response in 2008 (Celius et al., 2008). Furthermore, no significant *Fmo* induction by TCDD was determined in the rat liver (Moffat et al., 2010).

Gstm2, the glutathione S-transferase m2, was induced in *Ahr* wild-type mice and suppressed in *Ahr* knockout mice. Other members of the family of glutathione S-transferases were also up regulated in livers of TCDD-treated wild-type mice including *Gsta1*, *Gsta2*, *Gstm1*, *Gstm3*, *Gstm4*, *Gstp1*, *Gstp2*, and *Gstt2*. No alterations of mRNA levels were measured in *Ahr* knockout mice for these glutathione S-transferase genes. Glutathione S-transferases play key

roles within drug metabolism, more precisely during phase II of drug metabolism in which xenobiotics are conjugated with highly hydrophilic endogenous molecules (Boverhof et al., 2006) (Yeager et al., 2009).

Purkinje cell protein 4-like 1 (*Pcp4l1*) encodes a neuronal protein. No studies on its biochemical properties are performed up to the present day (Morgan et al., 2012). The strong induction of *Pcp4l1* was also determined in livers of male mice treated with TCDD (1000 µg/kg) (Tijet et al., 2006). *Ucp3* (mitochondrial uncoupling protein 3) gene encodes a protein which is involved in the regulation of the energy metabolism in muscle cells by dissipating the proton gradient in the inner mitochondrial membrane. It was postulated that a UCP3-mediated proton leak might help to limit oxidative damage (Krauss et al., 2005).

The genes *Mgll* (monoglyceride lipase), *Acot3* (acyl-CoA thioesterase 3), and *Acot 5* (acyl-CoA thioesterase 5) were all up regulated in *Ahr* wild-type mice and at the same time down regulated in *Ahr* knockout mice. *Mgll* encodes a lipolytic enzyme which is involved in various cellular processes within lipid metabolism such as arachidonic acid metabolic process. Acyl-CoA thioesterases (ACOTs) play key roles in fatty acid metabolism by catalyzing the hydrolysis of acyl-CoAs of different chain lengths to free fatty acids and CoASH (Hunt et al., 2006). *Tmem86b* encodes the transmembrane protein 86b which has been additionally linked to lipid metabolism. *Lhpp* and *Slc26a10* were also among the genotype-specific differently-expressed genes. *Lhpp* encodes an enzyme which is involved in phosphate metabolism and *Slc26a10* encodes a solute carrier which is involved in the transmembrane sulphate transport.

The expression of the immediate early response 3 gene (*Ier3*) is induced upon a diverse variety of stimuli (cytokines, growth hormones, and other types of stress). The encoded protein is involved in the cell cycle control and apoptosis (Arlt et al., 2011). Otherwise, ELMO3 protein plays a major role in the engulfment and removal of cells during the apoptosis (Gumienny et al., 2001). *Sunc1* (aka *Sun3*) encodes a protein which belongs to a protein family that is linked to infertility in mice of both genders. SUN1 is needed for telomere attachment to the nuclear envelope during meiosis. *Sun1*$^{-/-}$ mice of both genders are infertile due to massive apoptotic events in the gonads of *Sun1*-deficient mice (Ding et al., 2007). The *Lmnb2* gene encodes the proteinlamin B2 (*Lmb2*). B-type of lamins are major components of the nuclear lamina which are believed to be essential for cell proliferation and survival (Kim et al., 2011).

Table 21. Overview hepatic genes up regulated in *Ahr*$^{+/+}$ mice and down regulated by *Ahr*$^{-/-}$ mice. Table features aspects such as gene name, probe name, systematic name, and corresponding log2 fold-changes. Selected parameters: A ≥ 7, log2 fc ≥ 1 ≤ -1, p-value ≤ 0.05.

Gene name	Probe name	Systematic name	Log2 fc Ahr$^{+/+}$	Log 2 fc Ahr$^{-/-}$
Cyp1a2	A_52_P595871	NM_009993	5.38	-2.12
Fmo3	A_55_P2059586	NM_008030	3.16	-2.80
Fmo3	A_51_P269404	NM_008030	2.97	-2.38
Gstm2	A_55_P1966438	NM_008183	1.28	-1.25
Pcp4l1	A_55_P1983754	NM_025557	2.70	-2.11
Ucp3	A_66_P108247	NM_009464	2.80	-1.40
Mgll	A_55_P2063312	NM_001166250	1.32	-1.37
Acot3	A_55_P2069907	NM_134246	2.08	-1.60
Acot3	A_55_P2038347	NM_134246	1.47	-1.22
Acot5	A_55_P2038362	NM_145444	1.88	-1.16
Tmem86b	A_52_P183524	NM_023440	2.65	-1.14
Lhpp	A_66_P140507	NM_029609	1.18	-1.23
Slc26a10	A_52_P140881	NM_177615	1.01	-1.22
Ier3	A_51_P286488	NM_133662	1.63	-1.39
Elmo3	A_55_P2295933	NM_172760	1.05	-1.06
Sunc1	A_55_P2040860	NM_177576	1.66	-1.22
Lmnb2	A_55_P2219059	NM_010722	1.49	-1.50
ENSMUST00000063239	A_55_P2065249	ENSMUST00000063239	1.12	-1.33
Gm7120	A_55_P2183914	NM_001039244	1.32	-1.22

IV.2.3 Summary and Discussion *in vivo* Experiments Part II

The AhR is a ligand-activated transcription factor. The activation of the AhR by xenobiotics (e.g. dioxins) results in the transcriptional up regulation of the AhR-responsive genes, i.e. so called 'classic' AhR target genes (*Cyp1a1*, *Cyp1a2*, *Nqo1*, *Aldh3a1*, *Ugt1a6*, and *Gsta1*) (Nebert et al., 2000). The corresponding enzymes are involved in oxidative detoxification or activation of ligands. The activation of the AhR by endogenous ligands was postulated by various research groups during the last decades. The AhR possesses various enogenous functions, for instance in different systems such as the immune, cardiovascular, neural, and reproductive system as well as in different tissues such as in hepatocytes, skin cells, and adipocytes (Nebert et al., 2000) (Nebert et al., 2004).

The aim of the performed metabolomics study was to provide a basis for the establishment of an AhR metabolomics platform. Therefore, an HPLC-ESI-MS/MS method was developed and established to analyze the spectrum of mouse plasma metabolites in both *Ahr* genotypes. Several substances could be identified in blood plasma of *Ahr* wild-type and knockout mice, namely tryptophan, phenylalanine, leucine, thyrosin, valin, methionine, and betaine.

Amino acids play fundamental roles in metabolism, for instance they can be converted into metabolic intermediates which subsequently can be used to form glucose via gluconeogenesis (Berg et al., 2006). The suppression of gluconeogenesis represents a major characteristic of the TCDD-induced AhR-mediated hepatotoxicity in rodents (Viluksela et al., 1999) (Diani-Moore et al., 2010).

Furthermore, distinct differences could be detected by the use of the HPLC-UV-Vis-MS/MS between *Ahr* wild-type and knockout mice. The identification of these outstanding peaks was not possible, probably due to the low plasma metabolite concentrations and the rather limited number of animals. Nevertheless, the performed metabolomics experiments demonstrated that the mouse plasma metabolites of *Ahr* wild-type and knockout mice differ. Further analysis is necessary, in particular with regard to AhR-mediated alterations of plasma amino acid concentrations, since the impact on the circulating amino acid levels likely contribute to the TCDD-elicited hepatotoxic effects in rodents. Moreover, the use of whole blood instead of blood plasma could be another research approach which not only increases the analyze volume, but also could enhance the number of detectable metabolites.

The aim of mouse study III was to analyse AhR-dependent and -independent effects in female *Ahr* knockout and wild-type mice 96 h after single dose treatment with 25 µg/kg bw TCDD. In the present study the relative liver weights of $Ahr^{-/-}$control animals were significantly reduced compared to their $Ahr^{+/+}$ littermates. The decrease in the relative liver weight is directly related to the reduction in hepatocyte size which is a result of the massive portosystemic shunting in $Ahr^{-/-}$ mice (Lahvis et al., 2000). The relative liver weights of TCDD-treated $Ahr^{+/+}$ mice were significantly increased compared to the respective vehicle control animals, whereas the relative liver weights of $Ahr^{-/-}$ mice were not significantly changed by TCDD. Microarray analysis and the subsequently performed *Gene set enrichment analysis* of the TCDD-treated $Ahr^{+/+}$ mouse livers revealed that a large number of genes associated with the lipid metabolism were altered by TCDD. For example TCDD induced several Acyl-CoA thioesterases (*Acot 1*, *2*, *3*, and *4*) which hydrolyze acyl CoAs to free fatty acid and CoASH resulting in the regulation of the intracellular levels of both (Hunt et al., 2006). Other lipolytic genes up regulated by TCDD were *Lpl*, *Plas2g12*, *Plas2g7*, and *Mgll*. The lipoprotein lipase (LPL), the phospholipases (PLA2G12A and PLA2G7), and monoglyceride lipase (MGLL) hydrolyze the hepatocellular triglyceride stores into free fatty acids and monoglycerides (Giller et al., 1992) (Angrish et al., 2011). The very low density lipoprotein receptor (VLDLR) is a cell surface receptor involved in the uptake of lipoproteins by internalization and degradation of triglyceride-rich lipoproteins (Yagyu et al., 2002) (Boverhof et al., 2006). The *Elovl5* (fatty acid elongase 5) gene encodes a key enzyme which is involved in polyunsaturated fatty acid (PUFA) synthesis. ELOVL5 regulates the C20-22 PUFA content, different signalling pathways (Act and PP2A), and diverse transcriptional factors (SREBP-1, PPARα, FoxO1, and PGC1α) which control fatty acid synthesis and gluconeogenesis (Jump, 2011).

On the other hand, several genes involved in lipid metabolism were down regulated, e.g. *Acly*, *Fasn*, *Elovl2*, and *Elovl6*. ACLY (ATP citrate lyase) plays a key role in the synthesis of fatty acids. The TCDD-elicited down regulation of *Fasn* allows drawing the conclusion that the increase of the hepatic lipid content is not based on the *de novo* fatty acid synthesis (Forgacs et al., 2012) (Angrish et al., 2012). ELOVL2 has been shown to be involved in the elongation

of C20 and C22 polyunsaturated fatty acids (PUFAs) to produce C24:4n-6 and C24:5n-3 PUFAs (Zadravec et al., 2011). ELOVL6 is responsible for the elongation of stearate (C18) from palmitate (C16), as well as the elongation of vaccinate (C18:1n-7) from palmitoleate (C16:1n-7) (Matsuzaka et al., 2007).
The significantly increased liver weights together with the distinct alterations in mRNA expression of genes associated with lipid metabolism in female $Ahr^{+/+}$ mice suggest the development of a hepatic steatosis due to single dose treatment with 25 µg/kg bw TCDD. TCDD is known to cause extremely enlarged livers as well as other liver pathologies including hepatic steatosis. Additionally, recent microarray studies revealed numerous alterations in the expression of genes linked to lipid metabolism and transport in mouse livers predominantly involved in hepatic steatosis (Poland et al., 1982a) (Huff et al., 1991) (Boverhof et al., 2006) (Kopec et al., 2010a) (Kopec et al., 2010b) (Angruish et al., 2012).

Furthermore, various genes linked to the xenobiotic metabolism (*Cyp1a1*, *Cyp1a2*, *Nqo1*, *Ugt1a6a*, *Gsta1*, *Gsta2*, *Gstm2*, *Gstm4*, *Gstp1*, and *Gstp2*) were up regulated in female $Ahr^{+/+}$ mice, but not in $Ahr^{-/-}$ mice. *Cyp1a1* was by far the highest up regulated gene by TCDD in $Ahr^{+/+}$ mice, followed by *Cyp1b1* and *Cyp1a2*. Associated AhR-responsive genes such as *Tuba8*, *Fmo3*, and *Pcp4l1* (Tijet et al., 2006) were recently reported to be inducible by TCDD in $Ahr^{+/+}$ mice. From the group of selected target genes *Tiparp*, *Hsd17b2*, and *Ahrr* were also up regulated in $Ahr^{+/+}$ mice, although *Ahrr* had a diminished colour intensity value compared to the selected value.

Unexpectedly, one-time administration of TCDD resulted in the up and down regulation of a large number of hepatic genes in female $Ahr^{-/-}$ mice. The pattern of significantly up and down regulated genes in $Ahr^{-/-}$ mice distinctly differed from $Ahr^{+/+}$ mice. *Gene set enrichment analysis* was additionally carried out to identify significantly enriched functional categories (Gene Ontology terms) based on the significantly up and down regulated genes in $Ahr^{-/-}$ mice. Only a vanishingly small number of genes could be associated to diverse cellular processes such as homeopoesis, cellular transport and movement, or lipid metabolism implying that most, if not all, TCDD-mediated effects are AhR-dependent. Single dose treatment with TCDD led to alterations of a large amount of genes in absence of the AhR. These findings should be analyzed in further experimental approaches to determine if these altered AhR-independent genes contribute to the TCDD-mediated toxicity in mice and also in other species.

IV.3 *in vitro* Experiments

In the present work human liver cell models (primary human hepatocytes and HepG2 cells) were used to assess the effects mediated by dioxins and dioxin-like compounds. The liver represents the target tissue in which TCDD has been shown to elicit carcinogenic and tumour promoting effects in rodents (Knerr et. al, 2006). Humans are predominantly exposed to PnCDD/PnCDFs and PCBs through the food chain, but also as a consequence to their occupations or accidents (for example Sevenso, Italy 1976). Performing essential *in vitro* experiments by the use of primary human hepatocytes and the human hepatocellular carcinoma cell line (HepG2) provides important information which could lead to a better understanding of the risk after exposure to PnCDD/Fs and PCBs in humans. Furthermore, the challenging task was to identify, validate, and establish quantifiable novel biomarkers for dioxin exposure and AhR-dependent modes of action.

A set of seven core compounds, i.e. TCDD, 1-PnCDD, 4-PnCDF, PCB 126, PCB 118, PCB 153, and PCB 156 and additional congeners TCDF, 1,4-HxCDF, 1,4,6-HpCDF, 1,6-HxCDD, 1,4,6-HpCDD, PCB 77, and PCB 105 were selected for analysis in the present work (Table 22). All test compounds were dissolved in DMSO. Final DMSO concentrations in culture medium did not exceed 1 % for all experiments. Primary human hepatocytes (hHeps) as well as the immortalized human hepatocellular carcinoma cell line HepG2 were used in the present work to determine concentration-dependent effects on induction of AhR-regulated gene expression and enzyme activity. Effects of core congeners were examined in hHeps and HepG2, whereas effects of further congeners were only determined in HepG2 cells. Cells were treated over an incubation period of 24 h with selected test substances in all experiments. Afterwards cells were processed depending on the subsequent experimental procedure (VI Methods).

Table 22. Applied test compounds for *in vitro* experiments in order from high to low TEF values. Seven core congeners are indicated in bold.

Test compound	TEF (WHO, 2005)
TCDD	1.0
1-PnCDD	1.0
1,6-HxCDD	0.1
1,4,6-HpCDD	0.01
TCDF	0.1
4-PnCDF	0.3
1,4-HxCDF	0.1
1,4,6-HpCDF	0.01
PCB 77	0.001
PCB 105	0.00003
PCB 118	0.00003
PCB 126	0.1
PCB 153	-
PCB 156	0.00003

IV.3.1 Primary Human Hepatocytes

Primary human liver cells represent the closest *in vitro* model to the human liver as they express the complete spectrum of hepatic drug-metabolizing enzymes (Hewitt et al., 2007). The characterization of the responses elicited by dioxins, dioxin-like, and non dioxin-like compounds in primary human hepatocytes provide a basis for the establishment of human *in vitro* TEFs/TEQs. Furthermore, the comparison with results obtained from the immortalized human hepatocellular carcinoma cell line HepG2 will provide essential insight about similarities and differences between untransformed cells and immortalized tumour-derived cell lines. (Lipp et al., 1992) (Zeiger et al., 2001) (Kim et al., 2009) (Dere et al., 2011).

IV.3.1.1 Cytotoxicity Testing

The Alamar Blue assay was applied to measure cell viability after incubation with the test compounds for 24 h under standard conditions. Assay conditions and further information about the experimental procedure are given in chapter six (VI Methods). In order to examine if the chosen test compounds cause cytotoxic effects, the viability of primary human hepatocytes was determined after incubation with the selected compounds. The Alamar Blue assay was primarily performed to identify non-cytotoxic concentration levels that could be used for further experimental testing. Each experiment consisted of negative controls (DMSO 0.1 %, 0.5 %, or 1 % respectively and culture medium) as well as saponine (0.1 % in culture medium) as positive control.

The seven core congeners showed no significant effects on cell viability in primary human hepatocytes after incubation for 24 hours. The viability values of the compound-treated cellswere at the same levels as the corresponding solvent controls. Therefore, test compound concentrations could be applied to subsequent experimental testing.

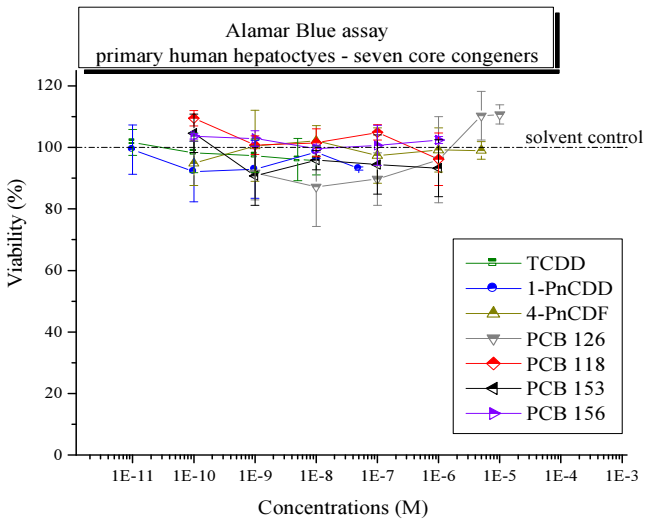

Figure 27. Cytotoxicity testing - Alamar Blue assay in hHeps after exposure to seven core congeners. Data represent means ± SD, n ≥ 3, results normalized to solvent control (DMSO 0.1 %, 0.5 % or 1 %).

IV.3.1.2 Ethoxyresorufin-O-deethylase (EROD) Activity

The catalytic activity of CYP1A1 in primary human hepatocytes was examined by measuring the ethoxyresorufin-O-deethylase (EROD) assay. The following figures display the results of the EROD assay after exposure to the seven core congeners. All experiments consisted of negative controls (DMSO 0.1, 0.5, or 1 % in cell culture medium) as well as one positive control for CYP1A1 induction (TCDD 10 nM). Findings are presented as box plot diagrams. Box plots, also known as box-and-whisker plots, are tools of descriptive statistics which display differences between populations, in the present work, between different donors.

Figure 28 features the results of the catalytic activity of CYP1A1 in EROD assay after exposure to TCDD (left) and 1-PnCDD (right). A concentration-dependent increase in EROD activity was measured as expected for both congeners until a full response was reached. Maximal induction in hHeps after treatment with TCDD (1000 nM) and 1-PnCDD (500 nM) led to an EROD activity of 7.58 ± 2.21 and 20.04 ± 5.80 pmol/min*mg protein. The efficiency varied donor- and compound-dependent as featured in the figures presented below.
Treatment of primary human hepatocytes with 4-PnCDF and PCB 126 also resulted in a concentration-dependent induction of CYP1A1 in EROD assay as presented in Figure 29. Maximal CYP1A1 induction was reached after hHeps were exposed to 1000 nM 4-PnCDF and 500 nM PCB 126 leading to an EROD activity of 20.35 ± 10.45 and 15.48 ± 5.76 pmol/min*mg protein, respectively. Large differences in CYP1A1 inducibility were observed after exposure of hHeps to high concentrations of 4-PnCDF and PCB 126. On one hand, this occurrence could be due to the overall higher response in EROD activity and on the other hand, this effect could be based on interindividual variability among donors.
PCB 118, PCB 156, and NDL-PCB 153 did not evoke any EROD induction in primary human hepatocytes as pictured in Figure 30 below.

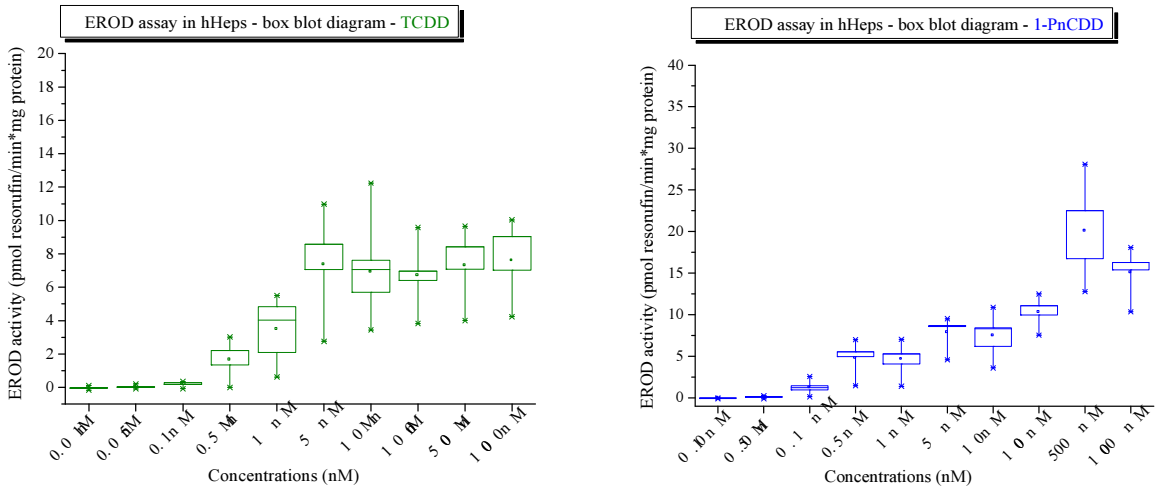

Figure 28. **EROD assay results visualized by box plot diagrams (n ≥ 4) - TCDD and 1-PnCDD. Left-hand side diagram visualizes results of EROD assay in hHeps after exposure to TCDD, right-hand side results of EROD assay after exposure to 1-PnCDD. EROD activity of the respective solvent control was considered as background level and subtracted from the data.**

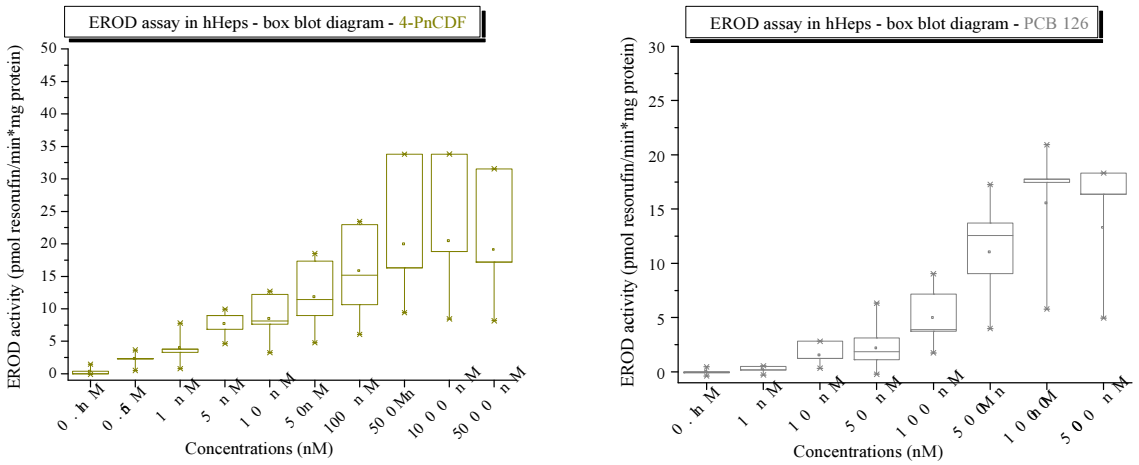

Figure 29. **EROD assay results visualized by box plot diagrams (n ≥ 4) - 4-PnCDF and PCB 126. Left-hand side diagram visualizes results of EROD assay in hHeps after exposure to 4-PnCDF, right-hand side results of EROD assay after exposure to PCB 126. EROD activity of the respective solvent control was considered as background level and subtracted from the data.**

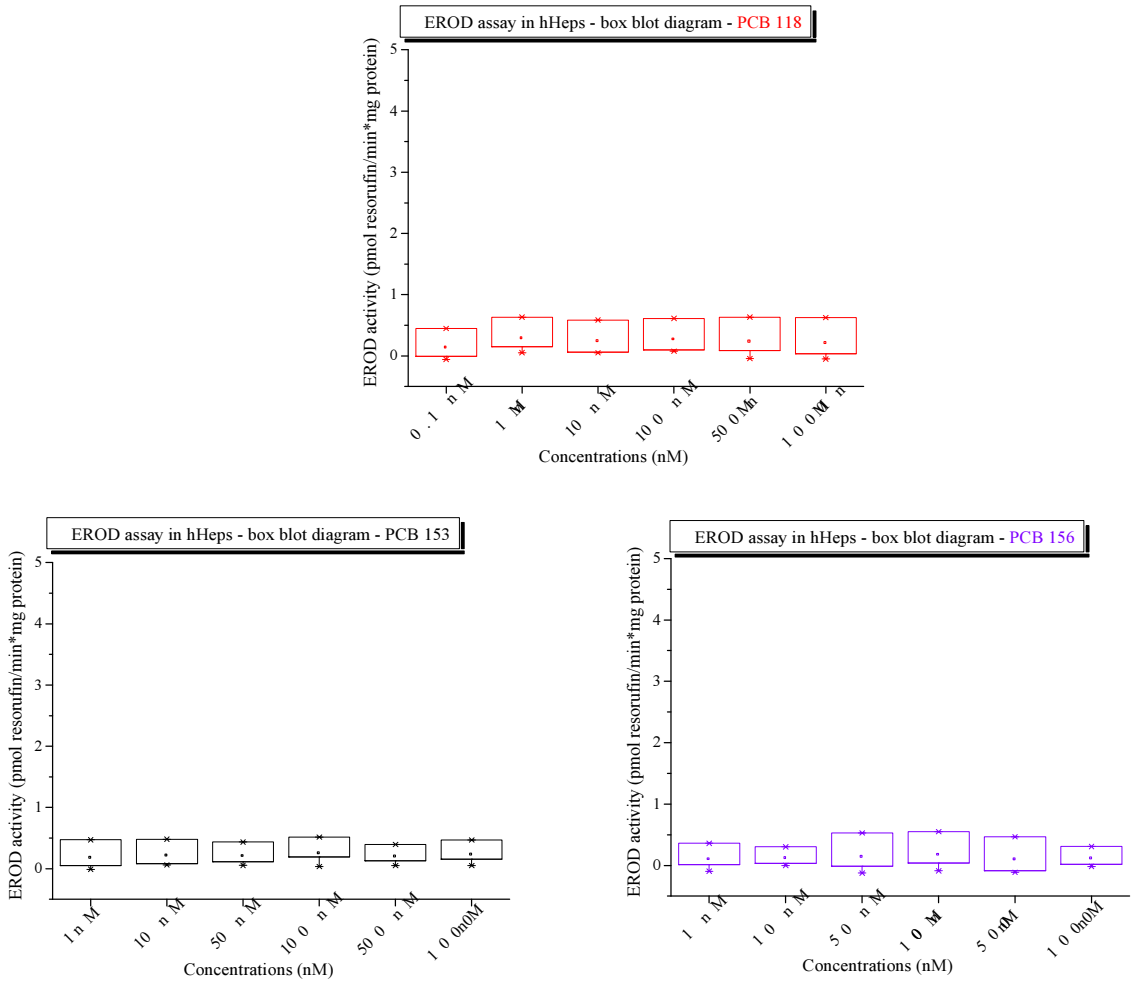

Figure 30. **EROD assay results visualized by box plot diagrams (n = 3) - PCB 118, 153, and 156. At top box: plot diagram visualizes results of EROD assay in hHeps after exposure to PCB 118. At bottom: left-hand side diagram reflect results of EROD assay in hHeps after exposure to PCB 153, right-hand side results of EROD assay after exposure to PCB 156. EROD activity of the respective solvent control was considered as background level and subtracted from the data.**

In Figure 31 the used compound concentrations are plotted in a logarithmic scale against gained EROD activities. EC_{50} values were derived by sigmoidal fitting using Origin software (Microcal Software, Northhampton, MA, USA). The respective solvent control was regarded as background level and subtracted from EROD activity data. The EC_{50} value represents the test compound concentration where 50 % of its maximal effect is obtained. For EC_{20} values, the upper limit of the TCDD-derived EROD activity in hHeps was set 100 % and the congener concentration needed to achieve 20 % of the maximal TCDD response was calculated as EC_{20}. Relative effect potencies (REPs) were obtained by dividing the EC_{50}/EC_{20} of the reference compound TCDD by the EC_{50}/EC_{20} of the test compound.

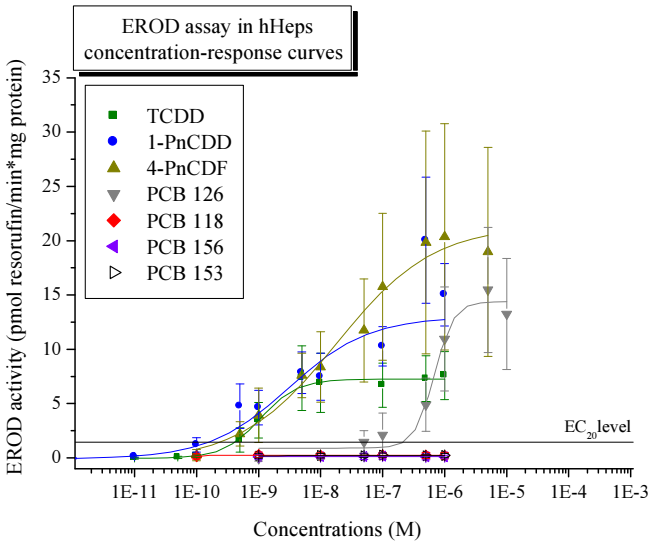

Figure 31. **EROD activity (pmol resorufin/min*mg protein) plotted in a logarithmic scale - hHeps. Primary human hepatocytes treated with either TCDD, 1-PnCDD, 4-PnCDF, PCB 118, PCB 126, PCB 153, or PCB 156 for 24 h. The respective solvent control was regarded as background level and subtracted from the corresponding EROD activity.**

Figure 31 displays the concentration-response curves for the seven core congeners and Table 23 the derived parameters from this data. The concentration-response curves of TCDD, 1-PnCDD, and 4-PnCDF featured similar curve shapes in the range of the respective EC_{50} values, whereas in the range of the TCDD-derived EC_{20} level distinct differences could be determined. The EROD activity obtained from 1-PnCDD and 4-PnCDF increased at low concentrations ($\leq 5 \times 10^{-10}$ M) but no increase was determined by TCDD in this concentration range. Furthermore, the TCDD-elicited EROD activity in hHeps reached its maximum before 1-PnCDD and 4-PnCDF reached their respective maxima. Moreover, 1-PnCDD and 4-PnCDF revealed both higher efficiencies. PCB 126 also reached a high efficiency, but by the use of high concentrations of this congener compared to TCDD.

EC_{50}/EC_{20} values and respective derived REP values are compiled and compared with WHO-TEFs (van den Berg et al., 2006) in Table 23. The dose-dependent induction of the EROD activity by TCDD resulted in an EC_{50} value of 1.06 ± 0.57 nM which is less sensitive compared to other published data from hHeps ($EC_{50\ TCDD}$ 0.15 nM Silkworth et al., 2005; $EC_{50\ TCDD}$ 0.24 nM Budinski et al., 2010). The human diversity in EROD response has to be

considered which is characterized by sensitivity and maximal response (Silkwort et al., 2005). Previously performed studies on primary human hepatocytes suggested that humans have similar sensitivities towards TCDD, but differ in their maximal response (Schrenk et al., 1995). Figure 31 displays the difference in EROD inducibility of different donors which illustrates the individual variability in maximal EROD response.

EC_{50} values of 1-PnCDD and 4-PnCDF were markably below the EC_{50} value of TCDD, the opposite was obtained for the EC_{20} levels. No EC values could be derived for PCB 118, 153, and 156 which was due to their lack of EROD activity in hHeps. The higher EC_{20} (and corresponding REP) values are probably based on the fact that 1-PnCDD and 4-PnCDF induced the EROD activity in hHeps at lower concentrations than TCDD and furthermore as a result of the higher CYP1A1 inducibilities of both congeners compared to TCDD. The developed EC_{20} calculation concept was used in the present work as an approach to assess the potency of weaker substances compared to TCDD since they might not reach the respective EC_{50} levels. This EC_{20} calculation method was based on a consensus between all SYSTEQ project partners to assess the potencies of weaker test compounds compared to TCDD.

REP values are additionally featured in Table 23. The relative effect potency (REP) describes the congener's potency in relation to the reference compound TCDD. REPs were obtained by dividing the EC value (EC_{50}/EC_{20}) of the reference compound TCDD by the EC value (EC_{50}/EC_{20}) of the test compound. REPs of TCDD are constantly 1.0, as the TEF concept is based on TCDD being the reference compound. It was not possible to derive any REPs for the PCBs (118, 153, and 156) because of the lack in EROD induction in hHeps. REPs derived from EC_{50} values of 1-PnCDD and 4-PnCDF were below the current WHO-TEF by 3-fold and 5-fold in particular. These results are in harsh contrast to REPs derived from EC_{20} values of 1-PnCDD and 4-PnCDF which were about 3-fold and 6-fold higher than the current WHO-TEF. REPs derived of PCB 126 in primary human hepatocytes were 63-fold and 53-fold below the current WHO-TEF, respectively. As described above, EC_{50} values are based on the obtained data from each compound itself, whereas EC_{20} values were calculated in relation to TCDD. REPs based on EC_{20} values are higher than the current WHO-TEF and most likely do not reflect the true potencies of both congeners. The developed concept for EC_{20} calculation is only applicable if test compounds have a similar or weaker activity than TCDD. It must be analyzed if a different calculation concept would be more suitable such as the separate calculation of EC_{20} values, as used for EC_{50} values, on the basis of the concentration-response data from each congener itself not in relation to TCDD.

Table 23. Derived parameters from EROD induction in primary human hepatocytes.

Congener	EC_{50} (nM)	REP (EC_{50})	EC_{20} (nM)	REP (EC_{20})	TEF (WHO, 2005)
TCDD	1.06 ± 0.57	1.0	0.420	1.0	1.0
1-PnCDD	3.07 ± 2.44	0.35	0.158	2.66	1.0
4-PnCDF	18.00 ± 8.59	0.059	0.242	1.74	0.3
PCB 118	-	-	-	-	0.00003
PCB 126	678.45 ± 90.36	0.0016	216.74	0.0019	0.1
PCB 153	-	-	-		-
PCB 156	-	-	-		0.00003

IV.3.1.3 Microarray Analysis

The induction of cytochrome P450 isoenzymes, i.e. CYP1A1, CYP1A2, and CYP1B1 is the best known indicator for AhR activation due to treatment with DLCs (Shimada et al., 2002). The development, validation, and establishment of novel quantifiable biomarkers for exposure to DLCs were the aspired targets of the following toxicogenomic study in primary human hepatocytes. Primary human hepatocytes were treated with TCDD, 1-PnCDD, 4-PnCDF, PCB 126, or NDL-PCB 153 for 24 h.

Donor and treatment information is summarized in Tables 24 and 25. After RNA isolation, the sample RNA concentration was determined via NanoDrop (Peqlab, Erlangen). RNA purity was additionally verified by Agilent 2100 Bioanalyzer and associated RNA 6000 Pico LabChip kit (Agilent Technolgies, Waldbronn).

In Figure 32 a representative electropherogram is featured. RNA integrity, i.e. the ratio between the 18S to 28S ribosomal subunits of all donors, was determined and the so called RINs (RNA Integrity Numbers) were obtained. All samples featured high-quality RNA (RIN $\geq$ 8.9). Afterwards, Agilent's Two-Color Microarray-based Expression Analysis according to Agilent's Low Input Quick Amp Labeling Kit was performed using cyanine 3- and cyanine 5-labelled targets to measure expression in experimental and control samples. Solvent control samples and compound-treated samples were stained oppositionally. 100 ng per sample was chosen as starting RNA concentration. Alterations in mRNA expression of the spotted oligonucleotides were measured using the Whole Human Genome Oligo Microarray 4x44K (Agilent Technologies, Waldbronn). Further information about the experimental procedures and conditions as well as data processing and statistical analysis are given in chapter six (VI Methods).

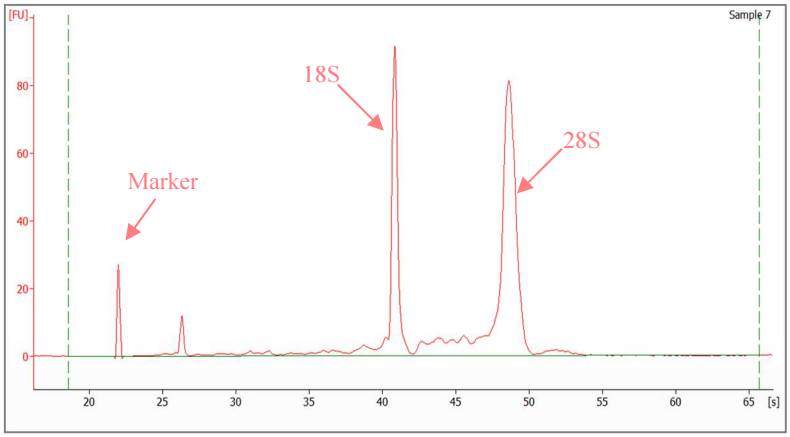

Figure 32. **Representative electropherogram analyzing RNA quality.**
RNA isolated from TCDD-treated (10 nM) primary human hepatocytes (Donor 2).
Obtained RIN value: 9.7.

Table 24. Background information about human donors - hHeps used for microarray and real-time PCR analysis.

Donor	Age (years)	Gender	Ethnicity	Viability (%)	HIV1/HBC/HCV[a]	Smoking	Alcohol	Diabetes	Heart Disease	Hypertension	Liver pathology
1	63	Female	Unknown	91	negative	no	no	no	no	no	Not available
2	48	Female	Caucasian	88	negative	yes	no	no	no	no	Adenocarcinoma from a rectosigmoid cancer
3	64	Male	Unknown	95	negative	no	no	no	no	yes	Left liver tumour
4	45	Female	Caucasian	94	negative	no	no	no	no	no	Hepatocellular carcinoma (HCC)
5	59	Male	Unknown	85	negative	no	yes	no	no	yes	Hepatic metastases
6	65	Male	Unknown	93	negative	yes	unknown	no	unknown	unknown	Hepatic metastases
7	61	Male	Unknown	82	negative	no	no	no	no	no	Liver metastases from carcinoma of the colon
8	60	Female	Unknown	86	negative	no	unknown	no	unknown	unknown	Hepatic metastases
9	73	Male	Caucasian	85	unknown	unknown	unknown	unknown	yes	yes	Not available
10	50	Male	Caucasian	88	negative	no	no	no	no	no	Liver metastases from carcinoma of the colon

[a]Human immunodeficiency virus 1/Hepatitis B virus/Hepatitis C virus

Primary human hepatocytes from donors 1-5 were exposed to TCDD as positive control, PCB 153 as negative control, and DMSO as solvent control (DMSO 0.1 % in culture medium) for 24 h. After these first experiments were carried out, further studies were realized by treatment of hHeps isolated from donors 6-10 with 1-PnCDD, 4-PnCDF, PCB 126, and DMSO (solvent control 0.1 % in culture medium). Based on current WHO-TEFs, treatment-concentrations were chosen, whereby for NDL-PCB 153 the highest stock solution was used for treatment.

Table 25. Microarray analysis of hHeps - test compound incubation concentrations.

Congener	Concentrations (nM)	TEF (WHO, 2005)
TCDD	10	1.0
1-PnCDD	10	1.0
4-PnCDF	30	0.3
PCB 126	100	0.1
PCB 153	1000	-

Microarray data of all compound treatments (TCDD, 1-PnCDD, 4-PnCDF, PCB 126, and PCB 153) is summarized in one data file. Results are filtered by cut-off values for the signal intensity A ≥ 7, the log2 fold-change ≥ 1 or ≤ -1, and the p-value ≤ 0.05.

Figure 33 displays the principle component analysis (PCA) based on the microarray data from all human donors and all treatments. The derived microarray data of donors concerning the respective treatment was highly homogenous, no outliners could be identified. Considering the results of the PCA, all performed microarray experiments were included in data analysis.

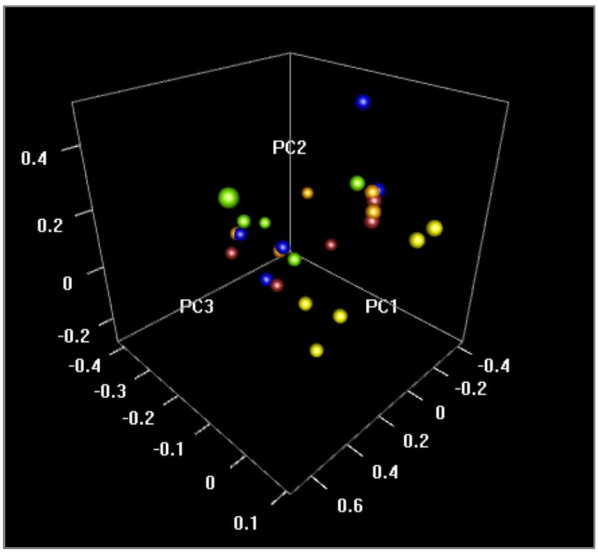

Figure 33. Principle component analysis of hHeps microarray results with emphasis on treatment. Blue: TCDD (10 nM), green: 1-PnCDD (10 nM), orange: 4-PnCDF (30 nM), brown: PCB 126 (100 nM), yellow: PCB 153 (1000 nM).

The quantity of affected genes in primary human hepatocytes is displayed in Figure 34. TCDD treatment resulted in the up regulation of 112 genes, whereas only 17 genes were down regulated. Treatment with 1-PnCDD affected a total of 96 genes, whereby 74 were up and 12 down regulated in hHeps. Moreover, 4-PnCDF treatment had impact on 95 (up) and 7 (down). On the other hand, PCB 126 treatment led to smaller numbers resulting in 26 unique up regulated genes and no significantly down regulated genes. Treatment with NDL-PCB 153 did not affect the mRNA gene expression in primary human hepatocytes within the range of the selected parameters.

The most extensive overlap (Figure 35) was detected between TCDD and 4-PnCDF treatment by sharing 71 up and 6 down regulated genes. With 62 in common up and 9 down regulated genes, TCDD and 1-PnCDD treatment resulted additionally in a large overlap. The very small numbers of genes affected by PCB 126 treatment were almost completely overlapping with those affected by TCDD leading to 25 in common up regulated genes by both compounds.

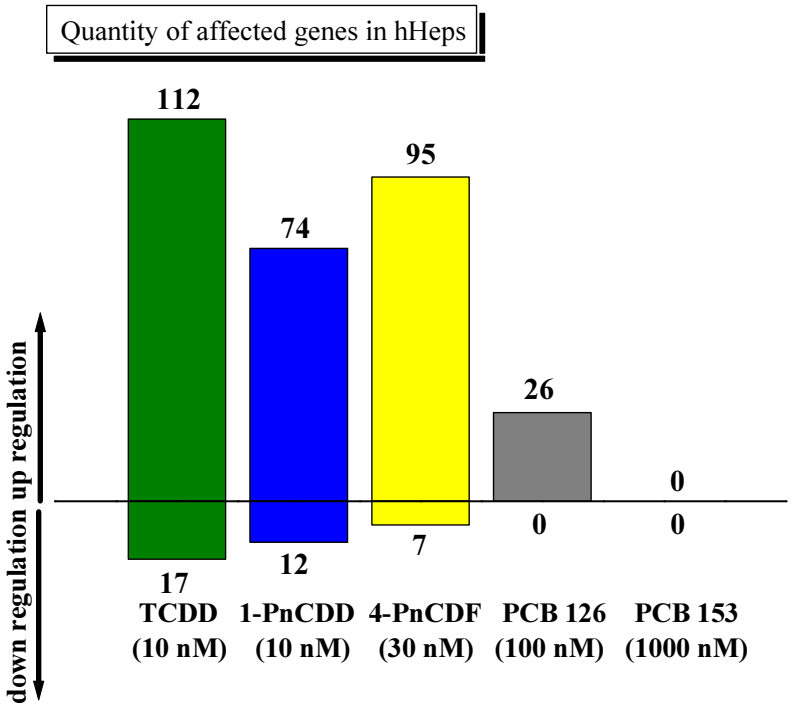

Figure 34. **Microarray results primary human hepatocytes - unique up and down regulated genes. Selected parameters: A ≥7, log2 fc ≥ 1 or ≤ -1, p-value ≤ 0.05.**

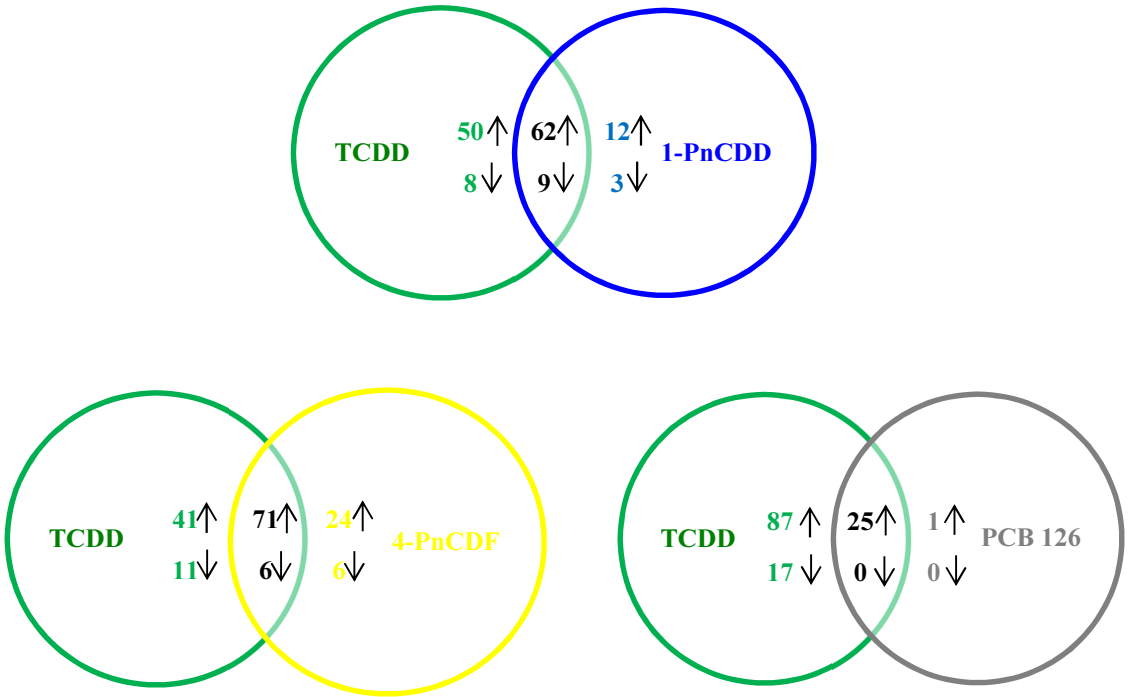

Figure 35. **Up and down regulated genes illustrated as Venn diagrams. Comparison between TCDD and 1-PnCDD, 4-PnCDF as well as PCB 126. Selected parameters: A ≥7, log2 fc ≥ 1 or ≤ -1, p-value ≤ 0.05.**

The obtained microarray data was extremely homogenous among DL-compounds (TCDD, 1-PnCDD, 4-PnCDF, and DL-PCB 126) as shown in the heatmaps (Figure 36) below. An intensive red colour (for example *CYP1B1* and *CYP1A1*) represents the strong up regulation of genes, whereas the fading of red towards black indicates that these genes were less induced, if at all.

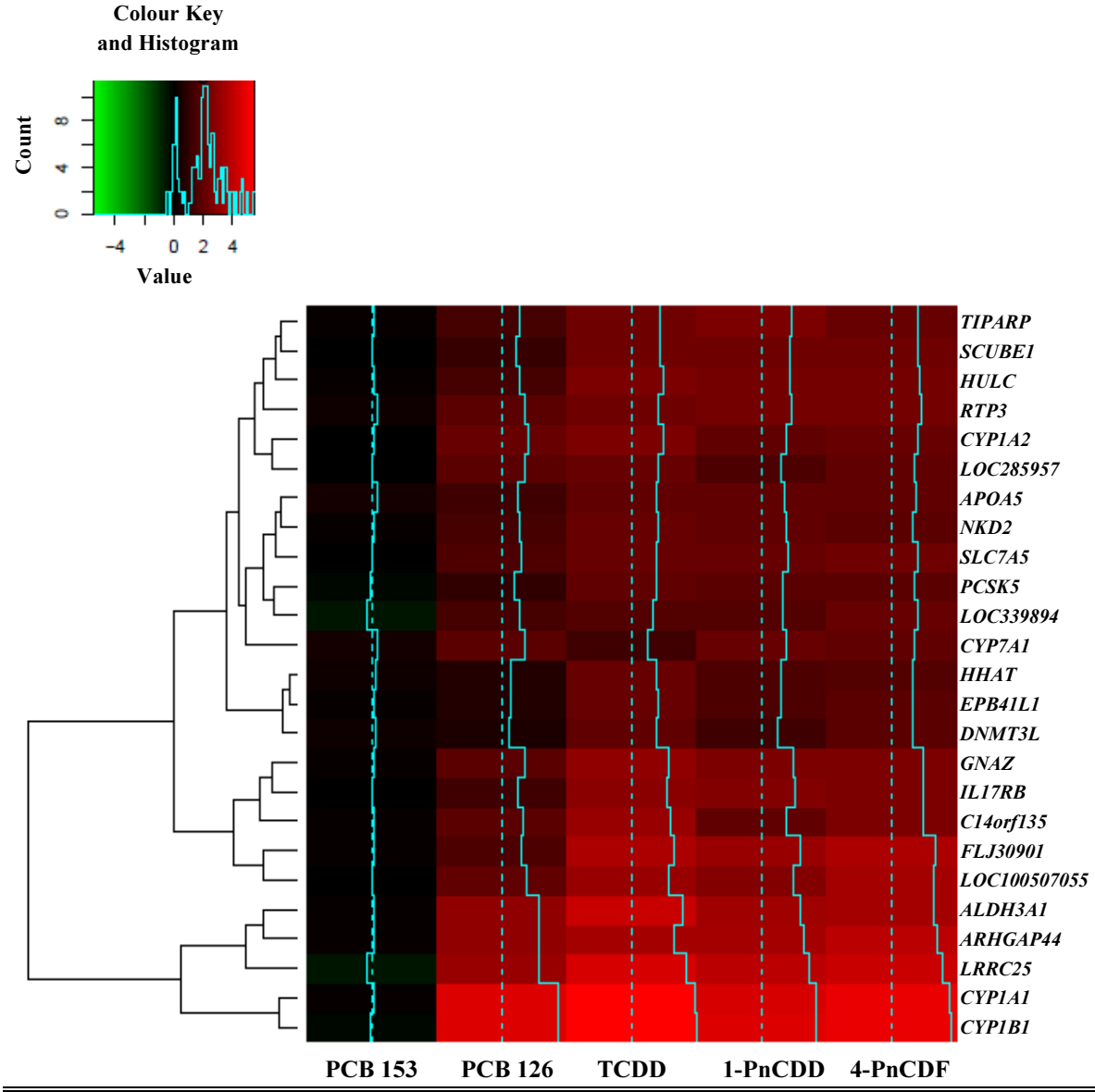

Figure 36. Heatmaps microarray analysis in hHeps.
Two times Pearson correlation, cut-off values: log2 fc ≥ 2, p-value ≤ 0.05.

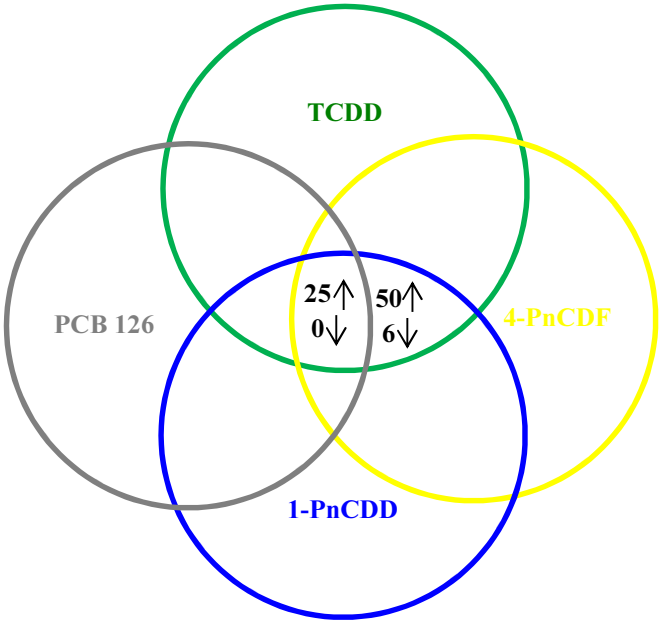

Figure 37. **In common up and down regulated genes in hHeps.**
Overlap between dioxin-like compounds featured as Venn diagram.
Selected parameters: A ≥ 7, log2 fc ≥ 1 or ≤ 1, p-value ≤ 0.05.

The aim of the present microarray experiment was to find quantifiable novel biomarkers for AhR activation due to dioxin exposure. Therefore, the following data analysis focuses on the in common up regulation of genes by dioxins and dioxin-like compounds to investigate the mechanisms of action and to assess the potentially dioxin-mediated toxicity in humans.

25 in common genes were up regulated by TCDD, 1-PnCDD, 4-PnCDF, and PCB 126 (Table 26). The entire list of the 25 in common up regulated genes is featured in Table 26 below. Comparing genes affected by TCDD, 1-PnCDD, and 4-PnCDF led to a large overlap of 50 up and 6 down regulated genes among the group of PnCDDs and PnCDFs. This outstanding gene overlap between DLCs was already elucidated in the presented heatmaps above.

The following passage deals with the closer examination of in common up regulated genes with emphasis on TCDD, 1-PnCDD, 4-PnCDF, and PCB 126. Among the highest up regulated genes are members of the cytochrome P450 superfamily *CYP1A1*, *1A2*, and *1B1* (featured in an intense red colour in the heatmaps in Figure 36). The induction of those CYP isoenzymes by dioxins and dioxin-like compounds is mediated by the AhR signalling pathway. Down to the present day, the induction of CYP1A1 is the best and most sensitive marker for AhR activation by dioxins. Other enzymes involved in xenobiotic metabolism are also highly up regulated such as *SLC7A5*, *TIPARP*, and *ALDH3A1*.
SLC5A7 is an amino acid transporter which is involved in the sodium-independent amino acid exchange of large neutral amino acids (Babuet al., 2003). *SLC5A7* was already identified as TCDD-responsive gene in HepG2 cells by Sarkar et al. (1999). Viluksela et al. demonstrated that circulating concentrations of amino acids were remarkebly increased by TCDD in L/E rats (Viluksela et al., 1999). *TIPARP* was additionally up regulated in hHeps after exposure to DLCs. *TIPARP* was described as novel TCDD-responsive gene by Ma et al.

in 2001. The AhR-mediated induction of TIPARP results in the suppression of the hepatic glucose production (Diani-Moore et al., 2010). Both transcript variants of the *ALDH3A1* gene were highly up regulated. Class 3 aldehyde dehydrogenases are normally not measurable in liver, but are highly inducible by xenobiotics such as TCDD and other members of the group of polycyclic aromatic hydrocarbons. Induction of *ALDH3A1* by TCDD is based on an AhR-dependent mechanism which was demonstrated in mouse *in vivo* (Nebert et al., 1987) (Boesch et al., 1996) (Sládek et al., 2002) (Vasiliou et al. 2004) (Bock et al., 2006).

Moreover, the *LRRC25* gene was significantly up regulated in hHeps. Several leucine rich repeat proteins with distinct cellular functions have been identified in various organisms including humans and rodents (mouse and rat). LRR proteins participate among others in signal transduction, cell adhesion, development, DNA repair, recombination, transcription as well as RNA processing (Kobe et al., 1995). Although LRRC proteins have various functions in different cellular components, they do have specific repetitive sequences in common and they all are involved in protein-protein interactions. *LRRC25* was identified as a novel AhR-regulated target gene which takes part in the PAH-induced immunotoxicity (Iwano et al., 2010).

Amphiregulin (AREG) plays a role in the epidermal growth factor signalling pathway. The epidermal growth factor receptor (EGFR) and its downstream signalling pathways are involved in diverse cellular processes such as cell proliferation, differentiation, and migration. Furthermore, EGFR activation is likely to be involved in tumour progression and pathogenesis. The interplay between TCDD and EGFR has been described intensively as a direct cross-talk of the AhR and EGFR signal transduction (Haarmann-Stemmann et al., 2009). Amphiregulin as endogenous ligand of the EGFR leads to its activation upon binding to the EGFR (Shoyab et al., 1989) (Haarmann-Stemmann et al., 2009). *TNFaiP2* encodes the tumour necrosis factor alpha-induced protein 2 which is regulated by TNFα, e.g. in endothelial cells. TNFaiP2 protein is likely to be involved in angiogenesis (Sarma et al., 1992). In 2010, Rivera and co-workers identified *Tnfaip2* as novel dioxin-inducible gene in the mouse Hepa-1 hepatoma cell line. High expression of *TNFAIP2* in haematopoietic and lymphoid tissue indicated that TNFAIP2 is probably involved in haematopoiesis/myelopoiesis (Rivera et al., 2007). Interestingly, it was demonstrated in mouse that TCDD also increased myelopoiesis (Choi et al., 2003).

UGCG, the UDP-glucose ceramide glycosyltransferase gene was also slightly up regulated in hHeps after exposure to DLCs. The UGCG enzyme is involved in glycosphingolipid biosynthesis in which it catalyzes the transfer of glucose from UDP-glucose to ceramide (Ichikawa et al., 1996). Glycosphingolipids are integral plasma membrane proteins which play substantial roles in various cellular processes such as cell recognition, proliferation, differentiation, and signal transduction (Paul et al., 1996) (Yamashita et al., 1999). Interleukin 17 receptor B (*IL17RB*) gene is involved in the cytokine-mediated signalling pathway. IL17RB specifically binds to IL17B and IL17E. *IL17RB* is only expressed in selected B cells, T cells, and myeloid cell lines whichleads to the suggestion that its dysregulation could lead to myeloid leukemia (Tian et al., 2000) (Shi et al., 2000) (Moseley et al., 2003).

The NKD2 protein is a negative regulator of the Wnt signalling pathway, in particular by binding to so called Dishevelled proteins (Dsh) during the canonical Wnt signalling pathway (Creyghton et al., 2005). *NDK2* encodes also a protein which is responsible for the transport of the transforming growth factor α to the basolateral plasma membrane (Li et al., 2004). The Wnt signalling pathway is involved in various cellular processes such as development, differentiation, and cellular homeostasis (Behari et al., 2010). Interactions between β-catenin (key regulator of the canonical Wnt signalling) and the AhR due to treatment with TCDD were shown in liver progenitor cells (Procházková et al., 2011).

The guanine nucleotide binding protein (G protein) alpha z polypeptidegene, in short *GNAZ*, was additionally up regulated in hHeps by all DLCs. Heterotrimeric G proteins are involved in G protein receptor signalling pathways. GNAZ only mediates signal transduction in pertussis toxin insensitive systems (Fong et al., 1988) (Matsuoka et al., 1990) (Casey et al., 1990). Recently the possible involvement of *GNAZ* in melanoma progression was described as a result of the detected high somatic mutation rates in this gene (Cardenas-Navia et al., 2010). The protein encoded by the exophilin 5 gene (*EXPH 5*) takes part in regulation of exocytosis and may act as rabphillin (Rab) effector protein. Rabphillin proteins function in processes involving vesicle trafficking (Kondo et al., 2006). A protein which can also be involved in cellular trafficking is Rho GTPase activating protein 44 (ARHGAP44). ARHGAP44 belongs to the GTPase superfamily which acts as molecular switches activated by extracellular stimuli. Active GTP-bound Rho proteins take part in diverse cellular processes which lead to the regulation of gene transcription as well as structural cell aspects (actin cytoskeleton re-arrangement) (Moon et al., 2003).

The *CDK5RAP2* gene was also up regulated. The CDK5RAP2 protein directly regulates CDK5 and CDK5R1 (isoform of CDK5) activities. Both are involved in the cell cycle process (Kraemer et al., 2011). Furthermore, Barrera et al. (2010) demonstrated in mice that CDK5RAP2 is required for the maintenance of centriole engagement and cohesion. Proprotein convertase subtilisin/kexin type 5 (PCKS5) is a member of the subtilisin/kexin-like proprotein convertase enzymes which are responsible for functional maturation of target proteins (Turpeinen et al., 2011). The lymphocyte-activation gene 3 (*LAG3*) is expressed in human activated T and NK cells (Triebel et al., 1989) and is involved in the cell surface signalling pathway. LAG3 negatively regulates T cell homeostasis (Workman et al., 2005).

RTP3 alias *TMEM7* encodes the transmembrane protein 7 which likely plays a role in hepatocarcinogenesis, i.e. human hepatocellular carcinomas (HCC). The induction of TMEM7 is linked to tumour suppression and invasion. Zhou and co-workers postulated that TMEM7 possess tumour suppressor activity which could be used in therapy of hepatocellular carcinoma (Zhou et al., 2007). Another gene involved in human liver pathogenesis, especially hepatocellular carcinoma, is *HULC* (Panzitt et al., 2007). HULC is the short form of 'highly up regulated in liver cancer'. The apolipoprotein A5 (*APOA5*) gene is involved in lipid metabolism by regulating triglyceride levels (Pennacchio et al., 2002). APOA5 was identified as liver-specific protein which is linked to early stages of liver regeneration in rat (van der Vliet et al., 2001) (Ress et al., 2011).

Table 26. List of in common up regulated genes by TCDD, 1-PnCDD, 4-PnCDF, and PCB 126 in hHeps. Selected parameters: A ≥ 7, log2 fc ≥ 1, p-value ≤ 0.05.

Gene Name	Gene Description	Systematic name	Probe name	Log2 fc TCDD	Log2 fc 1-PnCDD	Log2 fc 4-PnCDF	Log2 fc PCB 126
ALDH3A1	Aldehyde dehydrogenase 3 family, member 1A, transcript variant 1	NM_001135168	A_33_P3238433	4.20	3.11	3.41	2.81
ALDH3A1	Aldehyde dehydrogenase 3 family, member 1A, transcript variant 2	NM_000691	A_23_P207213	4.41	3.54	3.79	3.33
APOA5	Apolipoprotein A-V, transcript variant 1	NM_052968	A_23_P75630	2.01	2.00	2.08	1.31
AREG	Amphiregulin	NM_001657	A_23_P259071	1.65	1.70	1.69	1.77
		NM_001657	A_33_P3419190	1.20	1.58	1.63	1.64
ARHGAP44	Rho GTPase activating protein 44	NM_014859	A_23_P26854	3.53	3.57	3.93	3.09
CDK5RAP2	CDK5 regulatory subunit associated protein 2, transcript variant 1	NM_018249	A_23_P83110	1.64	1.66	1.88	1.28
		NM_018249	A_33_P3389060	1.44	1.35	1.68	1.16
C14orf135	cDNA FLJ38170 fis clone FCBBF1000024.	AK095489	A_33_P3397795	3.26	2.07	2.64	1.84
CYP1A1	Cytochrome P450, family 1, subfamiliy A, polypeptide 1	NM_000499	A_23_P163402	5.37	4.61	4.93	4.71
CYP1A2	Cytochrome P450, familiy 1, subfamiliy A, polypeptide 2	NM_000761	A_33_P3253747	2.63	2.06	2.23	2.19
CYP1B1	Cytochrome P450, familiy 1, subfamiliy B, polypeptide 1	NM_000104	A_33_P3290343	4.43	3.89	4.11	4.02
		NM_000104	A_23_P209625	6.59	5.46	5.96	5.45
EXPH5	Exophilin 5	NM_015065	A_23_P403335	1.57	1.66	1.54	1.13
GNAZ	Guanine nucleotide binding protein (G protein) alpha z polypeptide	NM_002073	A_23_P416581	3.11	2.72	2.61	1.91
HULC	Highly up-regulated in liver cancer (non-protein coding)	NR_004855	A_33_P3222762	2.71	2.44	2.45	1.50
IL17RB	Interleukin 17 receptor B	NM_018725	A_24_P157370	2.95	2.82	2.71	1.33
LAG3	Lymphocyte-activation gene 3	NM_002286	A_23_P116942	1.93	1.63	1.94	1.23
LOC285957	cDNA FLJ40207 fis clone TESTI2020946.	AK097526	A_33_P3734384	2.28	1.66	2.02	1.87
LOC100507055	Hypothetical LOC100507055	NM_001195520	A_32_P49867	3.17	2.73	3.52	2.11
LRRC25	Leucine rich repeat containing 25	NM_145256	A_23_P165136	4.58	4.03	4.32	3.19
NKD2	Naked cuticle homolog 2 (Drosophila)	NM_033120	A_23_P41804	2.24	2.02	1.84	1.41
PCSK5	Proprotein convertase subtilisin/kexin type 5 transcript variant 2	NM_006200	A_23_P257003	2.12	1.85	1.97	1.10
RTP3	Receptor (chemosensory) transporter protein 3	NM_031440	A_23_P57910	2.29	2.53	2.47	1.90
SLC7A5	Solute carrier family 7 (amino acid transporter light chain L system) member 5	NM_003486	A_24_P335620	2.14	2.20	2.28	1.65
TIPARP	TCDD-inducible poly(ADP-ribose) polymerase, transcript variant 2	NM_015508	A_23_P143845	2.31	2.61	2.19	1.45
TNFAIP2	Tumour necrosis factor alpha-induced protein 2	NM_006291	A_23_P421423	1.81	1.34	1.84	1.36
UGCG	UDP-glucose ceramide glucosyltransferase	NM_003358	A_23_P313389	1.26	1.15	1.31	1.07

One major research objective of the SYSTEQ project was the identification of novel quantifiable biomarkers for AhR activation by dioxins and dioxin-like compounds. Based on the experimental data gained from microarray experiments in hHeps, HepG2 cells, mouse 3-day study as well as a microarray experiment performed by a project partner from the Karolinska Institutet in *Ahr*$^{-/-}$ and *Ahr*$^{+/+}$ mice potential candidates were selected.
Data combination resulted in the selection of five target genes (*ALDH3A1*, *HSD17B2*, *CD36*, *TIPARP*, and *AHRR*). The following table (Table 27) summarizes the results of the microarray data derived from hHeps treated with different DLCs with regard to the chosen target genes. Additionally, the obtained log2 fc values of the established markers for AhR activation (cytochromes P450 *1A1*, *1A2*, and *1B1*) are featured. Cytochromes P450 *1A1*, *1A2*, *1B1*, both transcript variants of *ALDH3A1*, and *TIPARP* were all up regulated by TCDD, 1-PnCDD, 4-PnCDF, and PCB 126. However, *HSD17B2* was only up regulated in the present microarray study after exposure to PnCDD/Fs, but not after treatment with DL-PCB 126. Genes *CD36* and *AHRR* were not up regulated within the range of the selected parameters.
The mRNA levels of all eight genes were subsequently measured by RT-PCR. Further experimental analysis is necessary to verify if one of the genes could be chosen as quantifiable novel biomarker for AhR activation.

Table 27. AhR target genes in hHeps microarray experiments.
Table features aspects such as gene name, systematic name, and corresponding fold-change.
Selected parameters: A ≥ 7, log2 fc ≥ 1, p-value ≤ 0.05.
Annotations: (1) transcript variant 1; (2) transcript variant 2;
'*' log2 fc value calculated as mean from identical probes of the corresponding gene
'→' this gene was not up regulated in microarray experiments.

Gene name	Probe name	Systematic name	Log2 fc TCDD	Log2 fc 1-PnCDD	Log2 fc 4-PnCDF	Log2 fc PCB 126
CYP1A1	A_23_P163402	NM_000499	5.37	4.61	4.93	4.71
CYP1A2	A_33_P3253747	NM_000761	2.63	2.06	2.23	2.19
CYP1B1	A_23_P209625	NM_000104	6.59	5.46	5.96	5.45
CYP1B1	A_32_P3290343	NM_000104	4.43	3.89	4.11	4.02
ALDH3A1 (1)	A_33_P2328433	NM_001135168	4.12	3.11	3.41	2.81
ALDH3A1 (2)	A_23_P207213	NM_000691	4.41	3.54	3.79	3.33
HSD17B2	A_23_P118065	NM_002153	1.24*	1.05*	1.19*	→
CD36	A_23_P111583	NM_001001547	→	→	→	→
TIPARP	A_23_P143845	NM_015508	2.31	2.61	2.19	1.45
AHRR	A_23_P358709	NM_020731	→	→	→	→

In summary, the highest up regulated genes in primary human hepatocytes after treatment with dioxin-like compounds were primarily genes known to be dioxin-inducible, i.e. genes which are associated with the xenobiotic metabolism such as *CYP1A1*, *CYP1A2*, *CYP1B1*, *SLC5A7*, *ALDH3A1*, as well as genes mediating TCDD-induced toxicity (*TIPARP*). The *LRRC25* gene was highly induced in the present study. Moreover, an AhR-dependent mechanism was postulated by Iwano and co-workers (Iwano et al., 2010). Commonly up regulated genes by dioxins and dioxin-like compounds also included genes linked to diverse cellular processes such as cell cycle regulation (*CDK5RAP2*), cellular trafficking (*ARHGAP44*, *EXPH5*), and cell surface signalling (*LAG3*) as well as cell angiogenesis (*TNFAIP2*).

Furthermore, genes associated with lipid metabolism (*APOA5*, *UGCG*) were also up regulated as well as a gene involved in the cytokine-mediated signalling pathway (*IL17RB*). Indications for a receptor crosstalk could also be determined in the present microarray study (*AREG*, *NKD2*). For instance, AREG is involved in the epidermal growth factor signalling pathway. The up regulation of *AREG* by dioxins and dioxin-like compounds in hHeps could be due to direct interactions between the AhR and EGFR, since the interplay between TCDD and EGFR had been demonstrated in several studies (Haarmann-Stemmann et al., 2009).

IV.3.1.4 Gene Expression of Target Genes by RT-PCR

The genes aldehyde dehydrogenase 3A1 (*ALDH3A1*), hydrosteroid dehydrogenase 17 beta 2 (*HSD17B2*), *CD36* (thrombospondin receptor), *TIPARP* (TCDD-inducible poly(ADP-ribose) polymerase), and *AHRR* (aryl hydrocarbon receptor repressor) were selected as potential novel target genes for AhR activation based on the experimental data gained from three performed microarray experiments in the present work as well as a microarray experiment performed by a project partner from the Karolinska Institutet.

Therefore, RNA of hHeps (the same as applied in the microarray experiment) was transcribed into complementary DNA and subsequently mRNA gene expression of the chosen five genes were determined by RT-PCR. Additionally, the mRNA expression levels of the cytochromes P450 *1A1*, *1A2*, and *1B1* were examined by RT-PCR. Gene expression levels of *CYP1A1*, *1A2*, *1B1*, *ALDH3A1*, *HSD17B2*, *CD36*, *TIPARP*, and *AHRR* are presented in Figure 38.

After 24 h incubation, dioxins and dioxin-like compounds led to the extensive induction of *CYP1A1* mRNA gene expression resulting in a 1354.66 ± 771.74-fold, 3279.75 ± 1680.61-fold, 4409.15 ± 1690.89-fold, and 2336.97 ± 1401.35-fold increase for TCDD, 1-PnCDD, 4-PnCDF, and PCB 126 respectively.
CYP1A2 mRNA levels were also highly induced by treatment with dioxins and dioxin-like compounds leading to a 597.96 ± 398.00-fold, 464.29 ± 301.44-fold, 824.62 ± 713.43-fold, and 278.01 ± 168.07-fold expression after treatment with TCDD, 1-PnCDD, 4-PnCDF, and PCB 126. Similarly, mRNA gene expression levels were obtained for *CYP1B1* after incubation with TCDD (628.59 ± 277.90), 1-PnCDD (419.81 ± 242.07), 4-PnCDF (807.39 ±

513.02), and PCB 126 (274.5 ± 198.6). PCB 153-treated hHeps led to no significant alterations of the *CYP1A1*, *1A2*, and *1B1* mRNA expression.

ALDH3A1, a selected potential novel AhR target gene, was significantly increased after treatment with DLCs, leading to the highest induction (20.42 ± 12.99-fold) after incubation of hHeps with TCDD, followed by 4-PnCDF (8.44 ± 6.58-fold), 1-PnCDD (6.37 ± 4.41-fold), and PCB 126 (4.49 ± 2.70-fold).

HSD17B2 mRNA levels were only significantly induced in hHeps after treatment with TCDD (2.98 ± 1.20-fold) and 4-PnCDF (3.57 ± 1.78-fold). An increase of the *HSD17B2* mRNA expression was also determined after incubation with 1-PnCDD (1.96 ± 0.57-fold) and PCB 126 (1.81 ± 0.65-fold), although both were not statistically significant increased.

In a similar manner *TIPARP* mRNA levels were affected. This resulted in a significant increase after treatment with TCDD (3.01 ± 0.35-fold) and 4-PnCDF (2.45 ± 1.00-fold). *TIPARP* mRNA levels were only slightly and not statistically significantly increased by 1-PnCDD (2.13 ± 1.14-fold) and PCB 126 (1.39 ± 1.01-fold).

Likewise as earlier shown with the CYPs, mRNA levels of *ALDH3A1*, *TIPARP*, and *HSD17B2* were not significantly altered in hHeps after exposure to PCB 153. In hHeps *CD36* and *AHRR* mRNA levels were not affected by all compounds, as expected from the previously performed microarray experiment (IV.3.1.3 Microarray analysis).

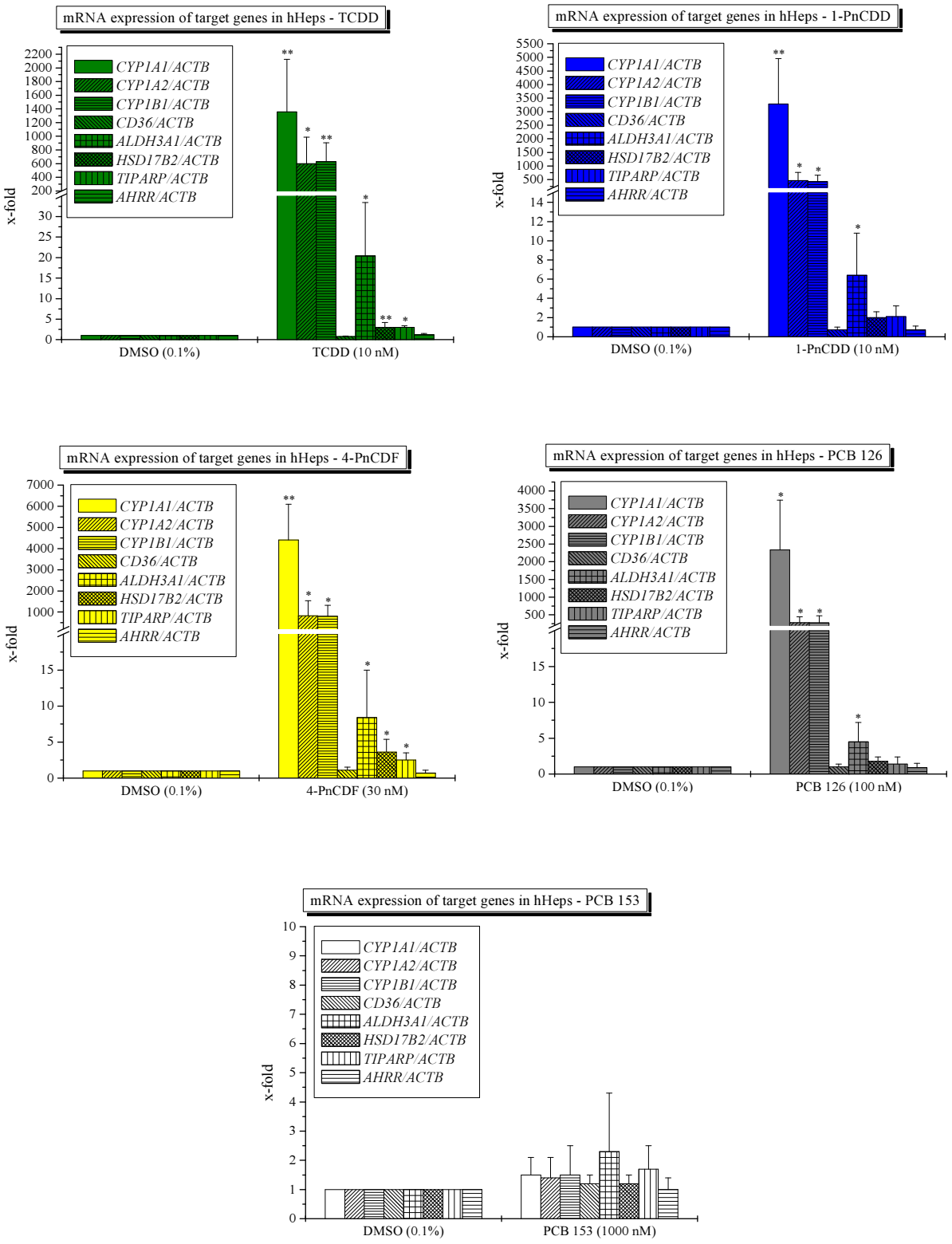

Figure 38. **Real-time PCR ratios of primary human hepatocytes treated with test compounds and solvent control. ß-actin (*ACTB*) served as housekeeping gene. Data represent means + SD of data from n = 5 different donors, normalized to solvent control. One-tailed unpaired Student's t-test,*=p ≤ 0.05, **= p ≤ 0.01 different from corresponding solvent control.**

IV.3.2 Human Hepatocellular Carcinoma Cell Line HepG2

IV.3.2.1 Cytotoxicity Testing

In order to examine whether the chosen test compound concentrations cause cytotoxic effects, the viability of the human hepatocellular carcinoma cell line HepG2 was tested after incubation with the selected compounds for 24 h under standard conditions. Primarily, the Alamar Blue assay was performed aiming to identify non-cytotoxic concentration levels that could be applied for subsequent experimental testing. Each experiment consisted of two negative controls (DMSO 0.1 % and medium) and saponine (0.1 %) as positive control. No cytotoxic effects were determined in HepG2 cells after incubation with the 14 test compounds (Figure 39). The viability of the compound-treated cells was in the same range as the solvent control (DMSO 0.1 %). Incubation with 50 nM PCB 126 led to a significant increase in cell viability, but this effect is the result of the small standard deviation. Hence, the chosen test compound concentrations could be applied to subsequent experimental testing.

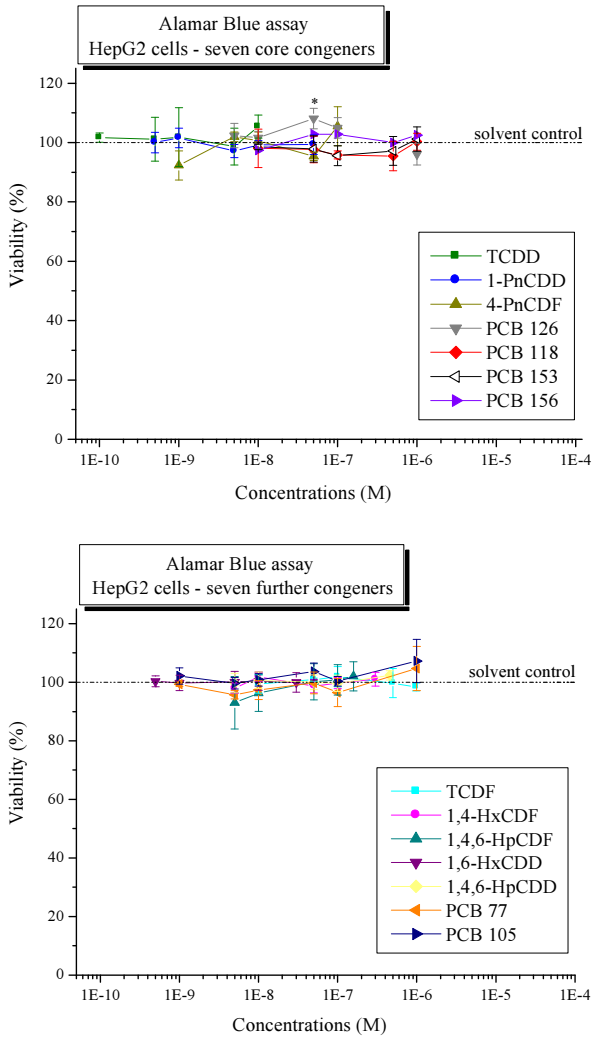

Figure 39. **Cytotoxicity testing - Alamar Blue assay results in HepG2 after exposure to seven core congeners (at top) and seven further compounds (at bottom).**
Data represent means ± SD of three independent experiments (n=3), results normalized to solvent control (DMSO 0.1 %). One-way analysis of variance (ANOVA) with Dunnett's post-test,*= $p \leq 0.05$

IV.3.2.2 Ethoxyresorufin-O-deethylase (EROD) Activity

The catalytic activity of CYP1A1 was determined subsequent to the incubation of HepG2 cells with seven core congeners and seven further congeners. All experiments consisted of one negative control (DMSO 0.1 % in culture medium) and one positive control for CYP1A1 induction (TCDD 10 nM). Figure 40 presents the results of the performed assay by plotting the used test compound concentrations in a logarithmic scale against obtained EROD activities, whereby EC_{50} values were derived by sigmoidal fitting using Origin software (Microcal Software, Northhampton, MA, USA). The respective solvent control was regarded as background level and subtracted from EROD activity data. For EC_{20} values, the upper limit of the TCDD-derived EROD induction in HepG2 was set 100 % and the test compound concentration needed to achieve 20 % of the maximal TCDD EROD response was calculated as EC_{20}. Relative effect potencies (REPs) were obtained by dividing the respective EC value (EC_{50}/EC_{20}) of the reference compound TCDD by the EC value (EC_{50}/EC_{20}) of the test compound.

In Figure 40 (left-hand side) a concentration-dependent increase in EROD activity was measured for TCDD, 1-PnCDD, 4-PnCDF, and PCB 126 in HepG2 cells. No increase in CYP1A1 activity was determined after treatment with PCB 118, PCB 156, and PCB 153. Concentration-response curves of 1-PnCDD, 4-PnCDF, and PCB 126 were similar to the TCDD curve with only their efficiencies differing. Maximal activity for TCDD-induced, 1-PnCDD-induced, 4-PnCDF-induced, and PCB 126-induced were 299.56 ± 51.90, 335.99 ± 71.46, 284.10 ± 31.63, and 120.17 ± 13.33 pmol resorufin/min*mg protein, respectively.

In Figure 40 (right-hand side) the results of the EROD assay after exposure to further congeners are featured. A concentration-dependent increase in EROD activity was obtained after exposure to DLCs, but not after HepG2 cells were exposed to PCB 77 and PCB 105. Maximal activity for 1,6-HxCDD-induced, 1,4,6-HpCDD-induced, TCDF-induced, 1,4-HxCDF-induced, and 1,4,6-HpCDF-induced EROD activity were 300.23 ± 15.51, 386.72 ± 49.34 , 241.04 ± 72.73, 255.54 ± 39.70, and 334.26 ± 38.89 pmol/min*mg protein.

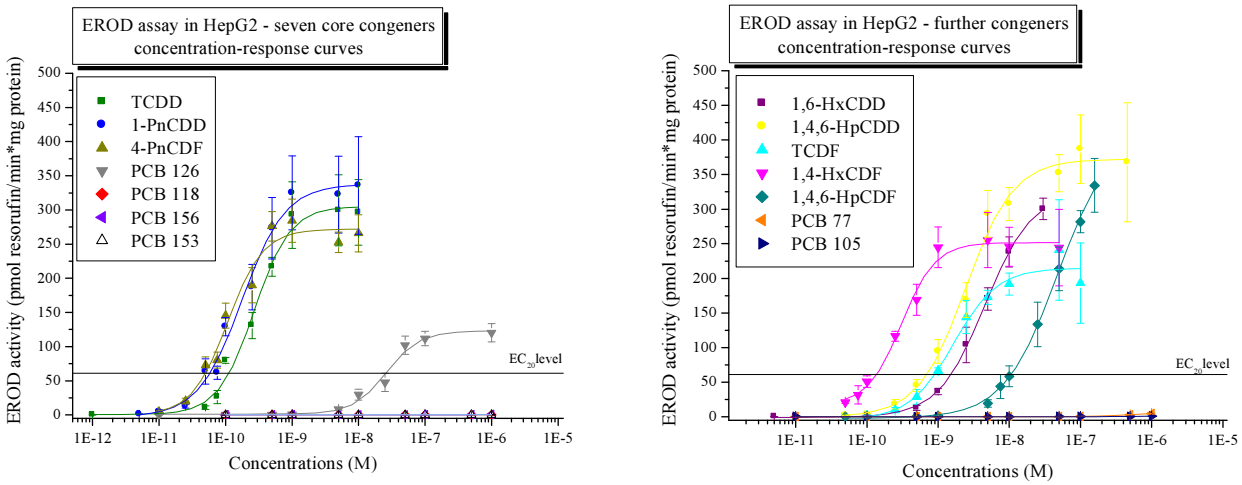

Figure 40. **EROD activity (pmol resorufin/mg protein*min) in HepG2 cells after 24 h exposure with core congeners (TCDD, 1-PnCDD, 4-PnCDF, PCB 118, PCB 126, PCB 153, or PCB 156) and further congeners (1,6-HxCDD, 1,4,6-HpCDD, TCDF, 1,4-HxCDF, 1,4,6-HpCDF, PCB 77 or PCB 105).**

Table 28. **Derived parameters from EROD induction in HepG2 cells.**

	EC_{50} (nM)	REP (EC_{50})	EC_{20} (nM)	REP (EC_{20})	TEF (WHO, 2005)
TCDD	0.269 ± 0.034	1.0	0.113	1.0	1.0
1-PnCDD	0.176 ± 0.023	1.53	0.058	1.92	1.0
4-PnCDF	0.107 ± 0.020	2.51	0.050	2.26	0.3
1,6-HxCDD	4.57 ± 0.12	0.059	1.53	0.074	0.1
1,4,6-HpCDD	2.45 ± 0.29	0.11	0.699	0.16	0.01
TCDF	1.64 ± 0.37	0.16	0.894	0.13	0.1
1,4-HxCDF	0.306 ± 0.041	0.88	0.137	0.82	0.1
1,4,6-HpCDF	47.55 ± 4.82	0.0057	10.73	0.011	0.01
PCB 77	-	-	-	-	0.0001
PCB 105	-	-	-	-	0.00003
PCB 118	-	-	-	-	0.00003
PCB 126	26.27 ± 3.62	0.010	25.75	0.0044	0.1
PCB 153	-	-	-	-	-
PCB 156	-	-	-	-	0.00003

Table 28 summarizes the results derived REPs from EROD assay in HepG2 cells. REPs gained from HepG2 cells confirmed to major parts the current WHO-TEFs. Nevertheless, several deviations were observed. In case of 4-PnCDF and 1,4-HxCDF, REP values were 8- and 9-fold higher than the current WHO-TEFs. REPs obtained from 1-PnCDD, 1,4-HxCDD, TCDF, and 1,4,6-HpCDF were within the same range as the corresponding WHO-TEFs. In HepG2 cells, REP values for PCB 126 were approximately 10- to 23-fold below the current TEF. It was not possible to derive any REPs for the other PCBs (77, 105, 118, 153, and 156) due to the lack of EROD induction in HepG2 cells.

IV.3.2.3 Protein Levels

In order to confirm the present findings from EROD assay, CYP1A1 protein levels were determined in the human hepatocellular carcinoma cell line HepG2 by Western blot. Therefore, microsomes were isolated from compound-exposed HepG2 cells. 25 µg protein of each sample was used in electrophoresis. CYP1A1 protein levels were determined in three independent experiments. Voltage-dependent anion-selective channel protein 1 (VDAC1) was used as loading control, TCDD (10 nM) as positive control for CYP1A1 induction, and DMSO (0.1 % in culture medium) as solvent control. Representative Western blots are featured in the following Figures.

In Figure 41 displays representative Western blots for CYP1A1 levels in HepG2 cells after exposure to the seven core congeners. Western Blot analysis of CYP1A1 protein levels after exposure to core congeners was performed by Angela Dörr as part of her diploma thesis (Dörr, 2010).

As expected, a concentration-dependent increase of CYP1A1 protein was determined after treatment of HepG2 cells with various concentrations of TCDD. The highest protein levels were obtained with 10 nM TCDD. Likewise, the CYP1A1 protein levels were increased in a concentration-dependent manner after HepG2 cells were treated with 1-PnCDD resulting in the highest protein levels of CYP1A1 after incubation with 5 nM 1-PnCDD for 24 h. A concentration-dependent increase of CYP1A1 protein levels was determined in HepG2 cells after exposure to 4-PnCDF, resulting in a maximal CYP1A1 expression after incubation with 1 nM. In case of PCB 126, only the two highest concentrations led to an increase of CYP1A1 protein levels. CYP1A1 protein levels were not affected by exposure of HepG2 cells to PCB 118, PCB 156, or PCB 153 (data not shown). As featured in these representative Western blots, some difficulties arose as the detection of CYP1A1 bands also evoked small bands for the respective solvent control or minor test compound concentrations. Unfortunately, several attempts to prevent this effect failed such as extending the blocking time, variation of antibody incubation time, or changing antibody diluter as well as cutting the membranes and subsequent separately detection of loading control and CYP1A1. However, the CYP1A1 lane was detected for DMSO in most cases, but this effect was considered to have no influence on the evaluation of the Western blot data.

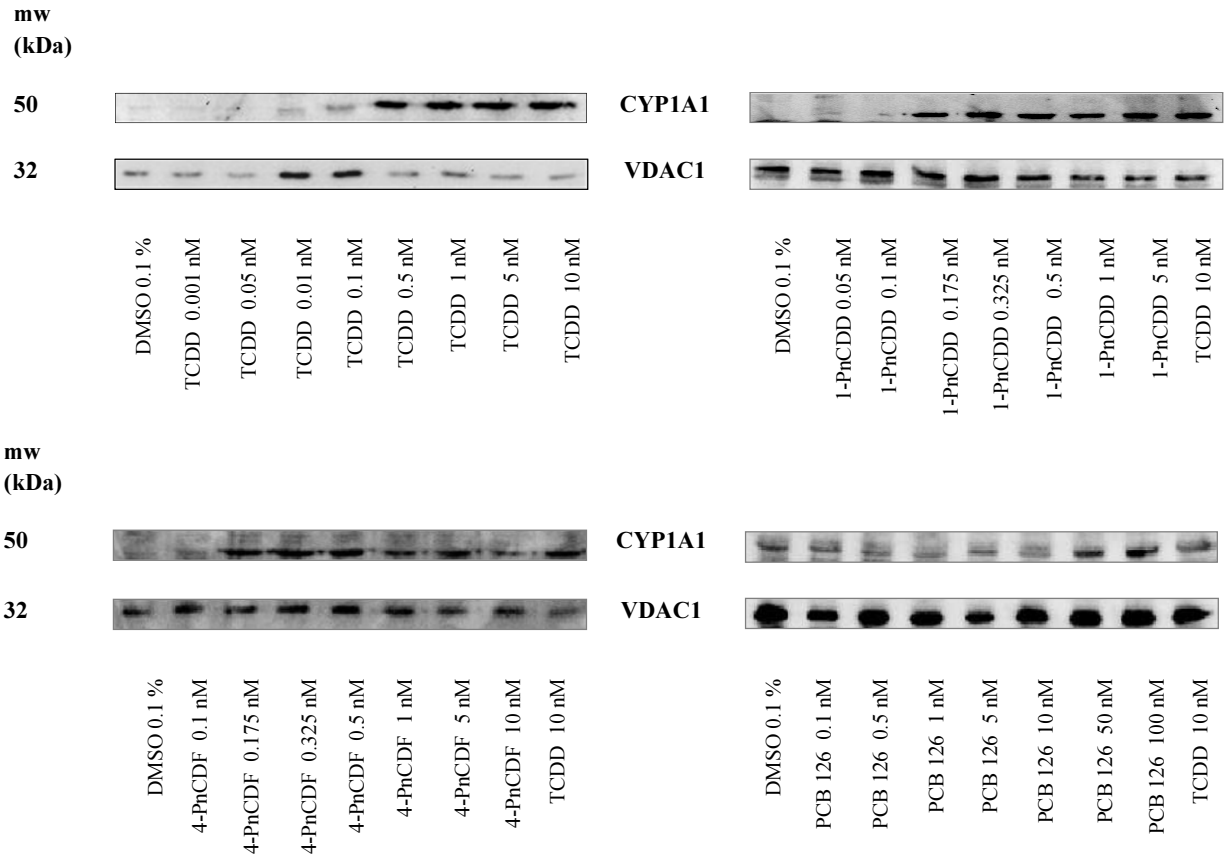

Figure 41. Representative Western blots of CYP1A1 proteins in HepG2 cells after treatment with core congeners. Isolated microsomes derived from HepG2 after treatment with TCDD, 1-PnCDD, 4-PnCDF, and PCB 126 for 24 h. VDAC1 applied as loading control.
Featured Western blots after exposure to 1-PnCDD, 4-PnCDF, and PCB 126 were performed by Angela Dörr within her diploma thesis (Dörr, 2010).

Western blot analysis of CYP1A1 protein levels in HepG2 after exposure to seven further congeners was additionally performed. Due to their inability to induce a distinct EROD activity, PCB 77 and 105 were excluded from this experiment. Figure 42 displays the results of CYP1A1 protein level determination after treatment with further congeners for 24 h. CYP1A1 protein levels were increased in a concentration-dependent manner after HepG2 cells were exposed to 1,6-HxCDD resulting in the highest CYP1A1 protein levels after incubation with 30 nM. This was also the case for 1,4,6-HpCDD. Exposure of HepG2 cells to this congener resulted in a concentration-dependent increase of CYP1A1 protein up to the highest applied concentration. PCDFs including TCDF, 1,4-HxCDF, and 1,4,6-HpCDF confirmed the findings retrieved from EROD assay, as a concentration-dependent increase of CYP1A1 protein levels was obtained in HepG2 cells, too.

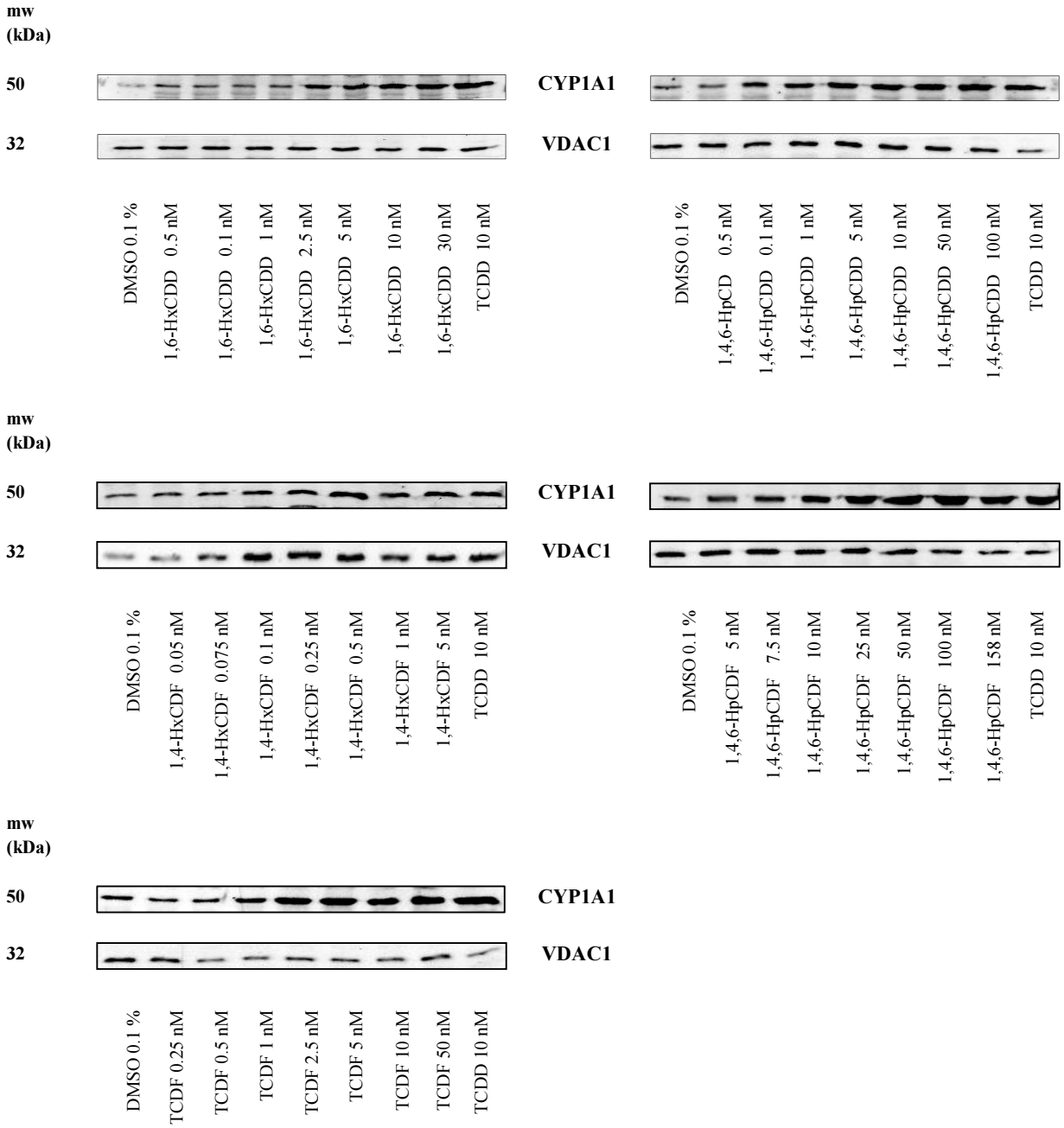

Figure 42. Representative Western blots of CYP1A1 proteins in HepG2 cells after exposure to further congeners. Isolated microsomes derived from HepG2 after treatment with 1,6-HxCDD, 1,4,6-HpCDD, 1,4-HxCDF, 1,4,6-HxCDF, and TCDF for 24 h.VDAC1 applied as loading control.

In summary, measurement of CYP1A1 protein levels after exposure to all 14 congeners confirmed the obtained findings from the EROD assay. A concentration-dependent increase of CYP1A1 protein levels was observed for TCDD, 1-PnCDD, 4-PnCDF, 1,6-HxCDD, 1,6-HpCDD, TCDF, 1,4-HxCDF, and 1,4,6-HpCDF. Treatment with PCB 126 for 24 h led only to an increase of CYP1A1 protein in the two highest applied concentrations. Incubation of HepG2 cells with PCB 118, 153, and 156 resulted in no increase of CYP1A1 protein levels.

IV.3.2.4 Gene Expression of Target Genes by RT-PCR

The mRNA expression of AhR target genes was determined in this experimental approach by RT-PCR. First, the isolated RNA from compound-treated HepG2 cells was transcribed into complementary DNA (cDNA). Then, 1 µl of cDNA was used to perform each RT-PCR experiment. Gene-specific expression, normalized using β-actin as housekeeping gene, was calculated relative to the expression of the corresponding solvent control (DMSO 0.1 %). Each experiment consisted of two controls including DMSO (0.1 % in culture medium) and TCDD (10 nM) exposed HepG2 cells.

The mRNA expression levels of the five potential AhR target genes (*ALDH3A1*, *HSD17B2*, *TIPARP*, *CD36*, and *AHRR*) and established AhR-dependent cytochromes P450 *1A1*, *1A2*, and *1B1* were determined in HepG2 cells by RT-PCR after 24 h exposure to various concentrations of TCDD. TCDD as prototype of PCDD/Fs was used in a concentration range of 0.0001 nM to 10 nM. Figure 43 displays the results of the RT-PCR analysis of these eight target genes.

CYP1A1 mRNA levels were induced in a concentration-dependent manner resulting in a 575.95 ± 38.47-fold expression after exposure to 10 nM TCDD. *CYP1A2* mRNA expression levels were not significantly altered compared to the corresponding solvent control. A concentration-dependent increase of the *CYP1B1* mRNA levels was additionally determined, resulting in the highest fold-change (63.77 ± 12.37-fold) after exposure to 5 nM TCDD. *ALDH3A1*, a selected novel AhR target gene, was significantly induced after exposure to the two highest applied TCDD concentrations (5 and 10 nM) leading to a 3.31 ± 0.96-fold and 4.34 ± 0.67-fold induction of *ALDH3A1* mRNA levels, respectively. *HSD17B2* mRNA levels were only significantly increased in HepG2 cells after treatment with 10 nM TCDD (2.37 ± 0.80-fold). However, *CD36*, *TIPARP*, and *AHRR* mRNA gene expression levels were not significantly altered compared to the corresponding solvent controls subsequent to TCDD treatment. Based on these results, relevant alterations of *HSD17B2*, *CD36*, *TIPARP*, and *AHRR* mRNA levels were not expected and hence, measurements were not carried out for the other core congeners.

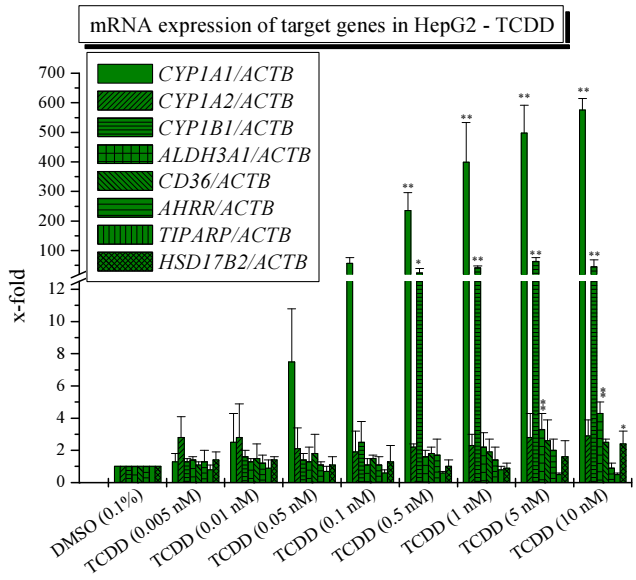

Figure 43. Real-time PCR ratios of HepG2 cells exposed to TCDD and DMSO 0.1%. β-actin (*ACTB*) served as housekeeping gene. Data represent means + SD of data from n = 3, normalized to solvent control. One-tailed unpaired Student's t-test,*= p ≤ 0.05, **= p ≤ 0.01 different from corresponding solvent control.

Exposure of HepG2 cells to 1-PnCDD, 4-PnCDF, and PCB 126 resulted in a concentration-dependent increase of *CYP1A1* mRNA expression leading to maximal a *CYP1A1* expression of 634.39 ± 71.64-fold, 1257.28 ± 381.06-fold, and 212.15 ± 40.88-fold induction for 1-PnCDD, 4-PnCDF, and PCB 126, respectively (Figure 44). Likewise, 1-PnCDD, 4-PnCDF, and PCB 126 significantly increased *CYP1B1* mRNA levels resulting in a 63.59 ± 23.67-fold, 181.27 ± 60.90-fold, and 31.44 ± 7.76-fold induction. A small, but statistically significant increase of *CYP1A2* mRNA expression was observed after HepG2 cells were exposed to 0.5 nM 1-PnCDD (3.41 ± 1.92). In addition, 4-PnCDF treatment resulted in a steady increase of CYP1A2 mRNA expression, which was proven to be statistically significant for the highest applied concentration (6.46 ± 2.40-fold) in HepG2 cells. After HepG2 cells were exposed to PCB 126, no alterations of CYP1A2 mRNA expression levels were determined by RT-PCR.

A constant increase of *ALDH3A1* mRNA levels was observed after exposure to 1-PnCDD, starting at 0.01 nM and reaching its maximum at 1 nM (5.09 ± 3.19-fold). This phenomenon was also observed with 4-PnCDF, whereby the steady increase started at 0.5 nM and stopped at 5 nM thus leading to the highest obtainable fold-change of 6.59 ± 1.86. *ALDH3A1* mRNA levels were not affected by PCB 126 in HepG2 cells. In HepG2 cells *CYP1A1*, *1A2*, *1B1*, and *ALDH3A1* mRNA levels were not significantly altered compared to the respective solvent controls after cells were exposed to PCB 118, 156, and 153 for 24 h.

Summarizing the obtained results, treatment with TCDD, 1-PnCDD, 4-PnCDF, and PCB 126 resulted in the concentration-dependent induction of *CYP1A1* and *CYP1B1.* The maximal fold induction of *CYP1A1* mRNA followed the relationship: 4-PnCDF > 1-PnCDD > TCDD > PCB 126. Similiar findings were obtained for the maximal CYP1B1 mRNA expression: 4-PnCDF > 1-PnCDD ≈ TCDD > PCB 126. The maximal *ALDH3A1* mRNA expression was 7-fold, 5-fold, and 4-fold higher compared to the respective solvent controls for 4-PnCDF, 1-PnCDD, and TCDD, respectively.

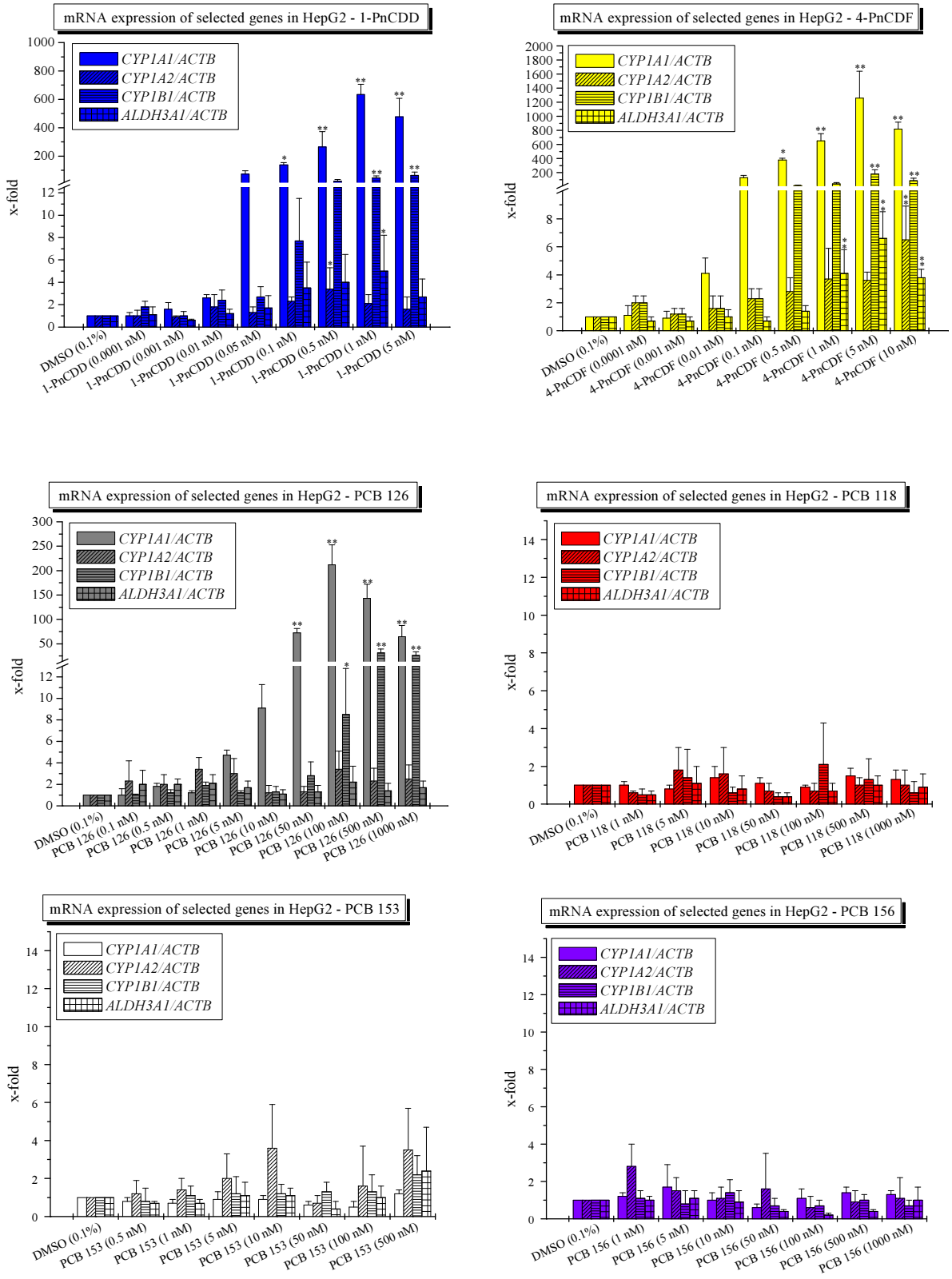

Figure 44. **Real-time PCR ratios of HepG2 cells treated with 1-PnCDD, 4-PnCDF, PCB 126, PCB 118, PCB 156, PCB 153, and DMSO 0.1 %.**
β-actin (*ACTB*) served as housekeeping gene. Data represent means + SD of data from n = 3, normalized to solvent control. One-tailed unpaired Student's t-test,*=p ≤ 0.05, **= p ≤ 0.01 different from corresponding solvent control.

Measurement of *CYP1A1* and *CYP1B1* mRNA levels led to the following concentration-response curves (Figure 45) and derived parameters (Table 29 and 30).
CYP1A1 curve slopes of TCDD and 1-PnCDD are similar to each other. A higher increase of *CYP1A1* mRNA expression was obtained for 1-PnCDD when using lower compound concentrations compared to TCDD. The *CYP1A1*-derived curve slope for 4-PnCDF is in the low concentration range similar to the TCDD-derived curve slope, but the three highest applied 4-PnCDF concentrations led to an extremely high *CYP1A1* mRNA expression. The higher efficiency of 4-PnCDF compared to TCDD at the high concentration range is visualized on the left-hand side of Figure 45, although the high standard deviations must be taken into consideration when comparing EC values. The derived concentration-response curve for PCB 126 is extremely flat compared to the other three potent congeners. Only the two highest applied PCB 126 concentrations barely surpassed the TCDD-derived EC_{20} level.
No concentration-response curves were obtained for PCB 118, 153, and 156 in HepG2 cells because of the very low, not statistically significant expression of *CYP1A1* mRNA compared to the respective solvent controls.

The concentration-response curves derived from *CYP1B1* mRNA expression is featured on the right-hand side of Figure 45. The *CYP1B1* curve slope of 1-PnCDD and 4-PnCDF closely resembles the TCDD curve slope, but a much higher *CYP1B1* mRNA response was determined by the use of the second highest applied 4-PnCDF concentration (5 nM). Sigmoidal fitting of the *CYP1B1* mRNA expression after incubation with various concentrations of 4-PnCDF resulted in the expected efficacy, but lead to a much higher efficiency compared to TCDD and 1-PnCDD in HepG2 cells. This phenomenon was also observed for the *CYP1A1* mRNA derived concentration-response curves. Likewise to *CYP1A1*, no *CYP1B1* concentration-response curves were gained after incubation with PCB 118, 153, and 156 because compound treatment of HepG2 cells did not lead to a significant increase of *CYP1B1* mRNA levels.

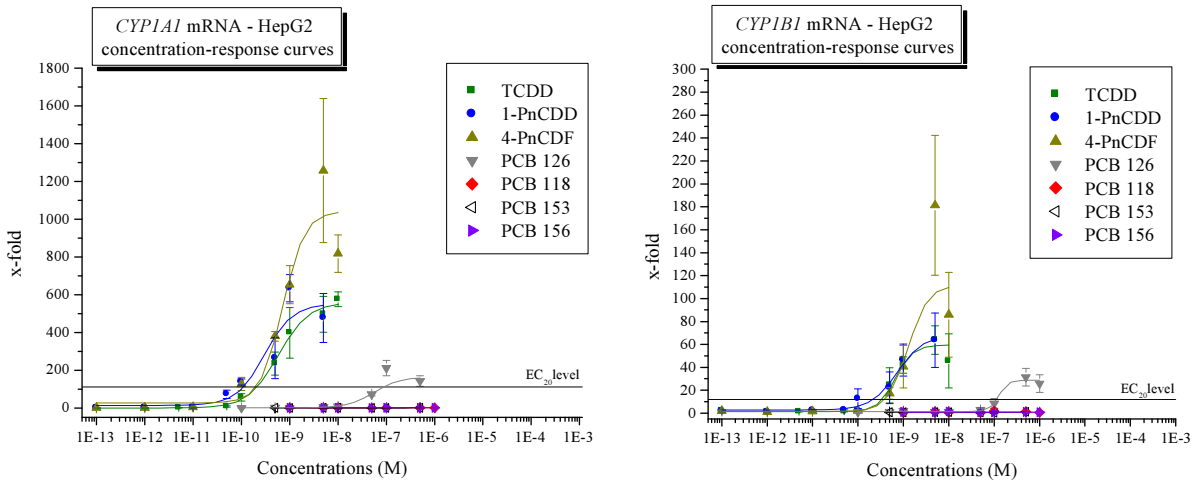

Figure 45. ***CYP1A1*** **(left) and** ***CYP1B1*** **(right) mRNA concentration-response curves in HepG2 cells.** ***CYP1A1/CYP1B1*** **gene expression (x-fold to DMSO 0.1 %) in HepG2 cells after 24 h exposure with core congeners (TCDD, 1-PnCDD, 4-PnCDF, PCB 118, PCB 126, PCB 153, or PCB 156). β-actin (*** ***ACTB*** **) served as housekeeping gene. Data represents means ± SD, n = 3, normalized to solvent control (DMSO 0.1 %).**

Sigmoidal fitting of *CYP1A1* and *1B1* mRNA data led to respective EC_{50} values. For EC_{20} values, the upper limit of the TCDD-derived *CYP1A1*/*CYP1B1* mRNA expression in HepG2 cells was set 100 % and test compound concentrations needed to achieve 20 % of the maximal *CYP1A1*/*CYP1B1* TCDD response were calculated as EC_{20}. In case of TCDD, EC_{50} and EC_{20} values derived from *CYP1A1* mRNA levels were consistently confirmed by *CYP1B1* mRNA data although EC_{50}/EC_{20} values tended to be higher than their *CYP1A1* counterparts.

CYP1B1-derived EC_{50} and EC_{20} values for 1-PnCDD, 4-PnCDF, and PCB 126 were about twice higher than their CYP1A1-derived counterparts. This effect could be based on *CYP1A1* being the more sensitive marker for AhR activation compared to *CYP1B1* which was confirmed by the extremely high *CYP1A1* mRNA levels in HepG2 cells.

Table 29. EC_{50}/EC_{20} values derived from sigmoidal fitting of *CYP1A1* and *1B1* mRNA data in HepG2 cells.

	***CYP1A1* mRNA**		***CYP1B1* mRNA**	
	EC_{50} ± SD (nM)	**EC_{20} (nM)**	**EC_{50} ± SD (nM)**	**EC_{20} (nM)**
TCDD	0.583 ± 0.064	0.213	0.671 ± 0.224	0.344
1-PnCDD	0.302 ± 0.208	0.111	0.718 ± 0.163	0.218
4-PnCDF	0.704 ± 0.244	0.204	1.27 ± 0.52	0.398
PCB 118	-	-	-	-
PCB 126	55.24 ± 14.64	88.10	126.51 ± 44.08	113.55
PCB 153	-	-	-	-
PCB 156	-	-	-	-

In Table 30 REPs are summarized regarding *CYP1A1* and *CYP1B1* mRNA data. REPs were obtained by dividing the EC value (EC_{50}/EC_{20}) of the reference compound TCDD by the EC value (EC_{50}/EC_{20}) of the test compound. Since the TEF concept is based on TCDD being the reference compound, REPs for treatment with TCDD are constantly set as 1.0. REPs gained from EC_{50} and EC_{20} values deviated from the current TEF.

In case of 1-PnCDD, REP values derived from *CYP1A1* mRNA data were twice higher than the 2005-TEFs. REPs based on *CYP1B1* mRNA data confirmed the current TEF. REPs for 4-PnCDF were 2- to 3-times higher than the current TEF. A different picture was obtained for PCB 126. Derived REPs were far below the TEF by approximately 9- to 42-fold.
It was not possible to derive any REPs for the PCBs 118, 153, and 156 based on the very low *CYP1A1*/*CYP1B1* mRNA expression levels in HepG2 cells.

Table 30. Relative effect potencies derived from EC_{50}/EC_{20} values of *CYP1A1* and *CYP1B1* mRNA expression levels in HepG2 cells.

	CYP1A1 mRNA		*CYP1B1* mRNA		TEF
	REP (EC_{50})	REP (EC_{20})	REP (EC_{50})	REP (EC_{20})	(WHO, 2005)
TCDD	1.0	1.0	1.0	1.0	1.0
1-PnCDD	1.93	1.92	0.93	1.58	1.0
4-PnCDF	0.83	1.04	0.53	0.87	0.3
PCB 118	-	-	-	-	0.00003
PCB 126	0.011	0.0024	0.0053	0.0030	0.1
PCB 153	-	-	-	-	-
PCB 156	-	-	-	-	0.00003

IV.3.3 Microarray HepG2 vs. hHeps

IV.3.3.1 Microarray Analysis

This microarray study aimed to analyze similarities and differences in gene expression after dioxin exposure of the immortalized human hepatocellular carcinoma cell line HepG2 and primary human hepatocytes. Primary human hepatocytes represent the closest model to the human liver by expressing the complete spectrum of hepatic drug-metabolizing enzymes (Hewitt et al., 2007). HepG2 cells are often used in *in vitro* studies in which the human liver is the major target tissue. In order to identify novel quantifiable biomarkers for dioxin exposure, gene expression analysis of both human cell models could contribute important information concerning this topic.

Therefore, HepG2 cells and primary human hepatocytes were exposed to TCDD (10 nM) and PCB 153 (1000 nM). PCB 153 belongs to the group of non dioxin-like PCBs and was used in this toxicogenomic study as negative control. Primary human hepatocytes were obtained from five different donors (Table 24) and five independent experiments (using HepG2 in five different passage numbers) were also performed for HepG2 cells. RNA purity and yield was verified by 2100 Bioanalyzer (Agilent Technologies, Waldbronn) and associated RNA 6000 Pico LabChip kit. All samples featured high-quality RNA and could be used for microarray anaylsis.

Afterwards Agilent's Two-Color Microarray-based Gene Expression Analysis was carried out using cyanine 3- and cyanine 5-labelled targets to measure expression in experimental and control samples, whereas solvent control samples and compound-treated samples were stained oppositionally. 100 ng per each sample was chosen as starting RNA concentration. Whole Human Genome Oligo Microarray 4x44K (Agilent Technologies, Waldbronn) was applied. Further information about the experimental procedures and conditions as well as data processing and statistical analysis is given in chapter six (VI Methods).

Microarray data from different human cell models were independently analyzed in two data files (hHeps and HepG2). Results in both cases were filtered by cut-off values for the signal intensity A ≥ 5, the log2 fc ≥ 1 or ≤ -1, and the p-value ≤ 0.05. The colour intensity was reduced from 7 to 5 in the present *in vitro* toxiconomic study. This adaptation had to be carried out due to the weaker colour intensity of the microarray slides from HepG2 cells. During the data analysis, it was noticed that *CYP1B1*, which also serves a marker for the activation of the AhR in human cell models, was missing in the list of up regulated genes. After evaluation of all possible reasons for this gene's absence, it was discovered that *CYP1B1* was missing as a result of the weaker colour intensity value of the respective oligonucleotide on the microarray slide. *CYP1B1* was highly up regulated by HepG2 (log2 fc value: 3.52), but only with a corresponding colour intensity value of 5.66. In addition, RT-PCR analysis confirmed that *CYP1B1* mRNA levels were strongly induced by TCDD treatment in HepG2 (IV.3.2.6 Gene expression of target genes by RT-PCR). For this purpose, the colour intensity was reduced to a value of 5 in the present microarray study.

Though in both *in vitro* models the same TCDD concentration (10 nM) was used for incubation, the number of affected genes (up and down regulated) in primary human hepatocytes was more than 3-times lower than in HepG2 cells. 247 unique genes were significantly up and 44 down regulated in HepG2, whereas TCDD exposure led to 72 up and only 8 down regulated genes in hHeps (Figure 46). Treatment with PCB 153 resulted in almost no altered gene expression compared to the respective controls in both cell models. Due to the large number of affected genes by TCDD treatment, only distinct characteristics are presented below, but the list of all up and down regulated genes in both human cell models is attached to the present work (Tables 96, 97, 98, 99).

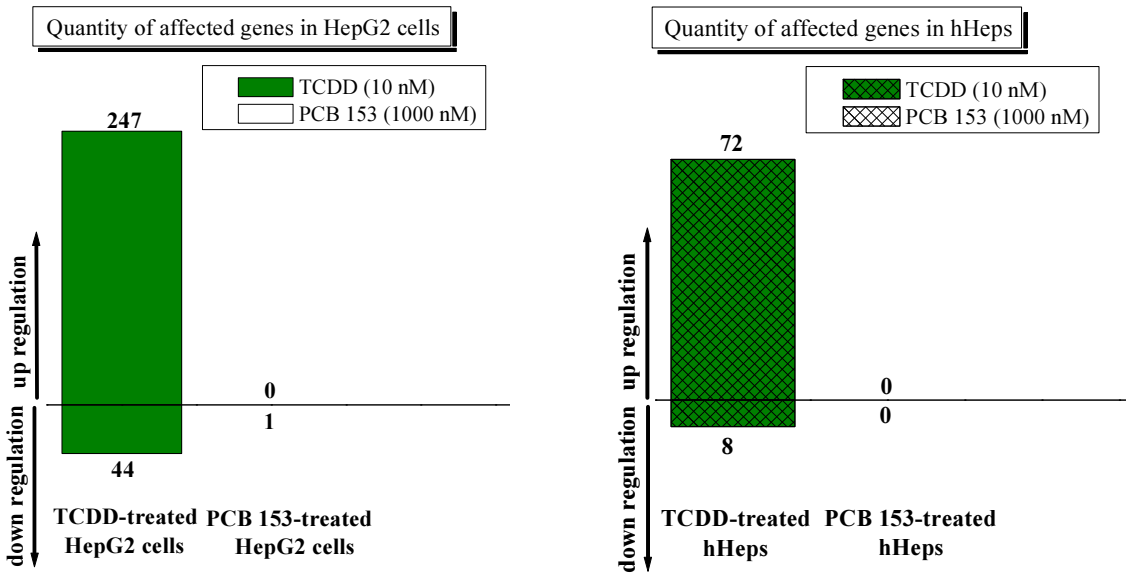

Figure 46. Microarray results HepG2 vs. hHeps.
Quantity of affected genes in HepG2 cells (left) and hHeps (right) after treatment with TCDD (10 nM) and PCB 153 (1000 nM).
Selected cut-off values: A ≥ 5, log2 fc ≥ 1 or ≤ -1, p-value ≤ 0.05

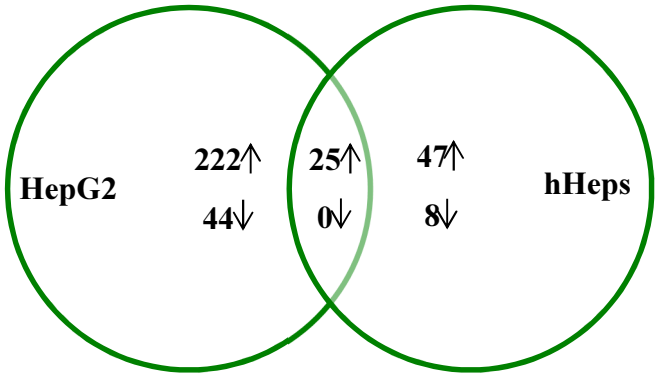

Figure 47. **Up and down regulated genes in HepG2 cells and hHeps after treatment with TCDD (10 nM) for24 h. Microarray results illustrated as Venn diagram.**
Selected cut-off values: A ≥ 5, log2 fc ≥ 1 or ≤ -1, and p-value ≤ 0.05.

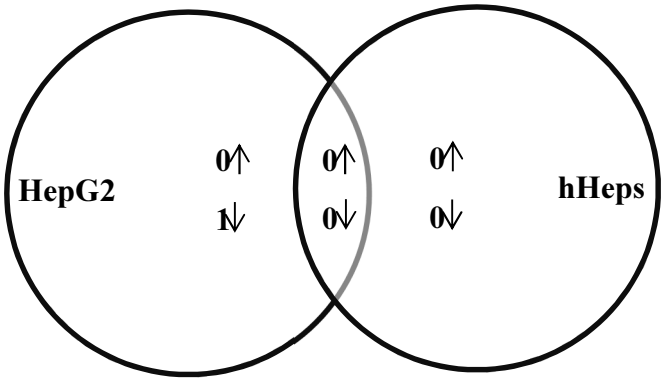

Figure 48. **Up and down regulated genes in HepG2 cells and hHeps after treatment with PCB 153 (1000 nM) for 24 h. Microarray results illustrated as Venn diagram.**
Selected cut-off values: A ≥ 5, log2 fc ≥ 1 or ≤ -1, and p-value ≤ 0.05.

When comparing both human liver cell models, there was an unexpectedly small overlap of genes being up or down regulated. In both cell types, only 25 genes were commonly up regulated by TCDD *in vitro* liver cell models, but none commonly down regulated. Table 31 features the list of in common up regulated genes by TCDD in HepG2 cells and hHeps in alphabetical order.

TCDD treatment of HepG2 cells for 24 h resulted in the up regulation of genes associated with xenobiotic metabolism. Established dioxin-inducible genes included genes associated with phase I (*CYP1A1*, *CYP1A2*, *CYP1B1*, *ALDH3A1*, *NQO1*) and phase II (*UGT1A6* and *GSTP1*) of xenobiotic metabolism (Nebert et al., 2000) (Bock et al., 2005a) (Bock et al., 2005b). Several solute carrier genes were also among the significantly up regulated genes such as *SLC2A8*, *SLC2A11*, *SLC5A7*, *SLC7A5*, *SLC16A6*, *SLC19A2*, *SLC25A30*, *SLC32A2*, and *SLC43A2*. Solute carriers are involved in diverse transport processes such as the sodium/glucose co-transport (*SLC5As*), the transport of amino acids (*SLC7As*), and glucose transport (*SLC2As*) (Babu et al., 2003) (Wright et al., 2004) (Verrey et al., 2004) (Schmidt et al., 2009). *SLC7A5* was already identified as TCDD-responsive gene in HepG2 cells by Sarkar et al. (1999).

NKAIN1 and *FMOD* were also among the ten highest up regulated genes involved in HepG2 cells (Table 31). NKAIN1 (Na^+/K^+ transporting ATPase interacting 1) belongs to the class of NKAINs which interact with the β-subunit of the Na^+/K^+ ATPase. The Na^+/K^+ ATPase is a plasma membrane enzyme which plays an important role in the maintenance of the electrochemical gradient across cellular membranes (Gorokhova et al., 2007). The *FMOD* (fibromodulin) gene encodes the fibromodulin protein. Fibromodulin is a small leucine-rich proteoglycan involved in extracellular matrix organization. Mormone and co-workers identified FMOD as an oxidative stress-sensitive proteoglycan which contributes to the pathogenesis of fibrosis in mice (Mormone et al., 2012). The involvement of the AhR in the regulation of hepatic fibrosis by modulation of the TGF-β-binding protein-1 (LTBP-1) was demonstrated by Corchero and co-workers (Corchero et al., 2004).

Another highly induced gene after exposure to TCDD in HepG2 cells was *WNT11* (wingless-type MMTV integration site family, member 11). *WNT6* was additionally up regulated, but to a lesser extent (log2 fc value: 2.66). WNT11 and WNT6 are members of the WNT protein family which play important roles in cell proliferation, differentiation, polarity, and migration. High expression levels of *WNT11* in HepG2 cells have been examined by Toyama and co-workers (Toyama et al., 2010). They discovered that the high *WNT11* mRNA levels were based on an inactiving β-catenin mutation. The high up regulation of *FMOD*, *NKAIN1*, and *WNT11* were consistent with the results from a recently published microarray study in which HepG2 cells were treated with TCDD, too (Dere et al., 2011).

Treatment of hHeps resulted in the up regulation of 72 unique genes leading to the suggestion that hHeps are less-sensitive in terms of differently regulated genes (Table 32). TCDD treatment of hHeps for 24 h resulted in the up regulation of established dioxin-inducible genes which are associated with xenobiotic metabolism such as *CYP1A1*, *CYP1A2*, *CYP1B1*, *ALDH3A1*, *ALDH3A2*, and *UGT1A6* (Nebert et al., 2000) (Bock et al., 2005a) (Bock et al., 2005b). Several solute carrier genes were also among the significantly up regulated genes such as *SLC7A5*, *SLC12A7*, and *SLC20A2*. As described before with HepG2 cells, the proteins encoded by *SLC*s are involved in diverse transport processes such as the transport of amino acids (*SLC7A5*), potassium/chloride (*SLC12A7*), and sodium/phosphate (*SLC20A2*) (Buba et al., 2003) (Collins et al., 2004) (Herbert et al., 2004).
ARHGAP44 was among the ten highest up regulated genes (Table 32). ARHGAP44 belongs to the GTPase superfamily which functions as molecular switches reacting to extracellular stimuli. Active GTP-bound Rho proteins take part in diverse cellular processes which lead to the regulation of gene transcription as well as structural cell aspects (actin cytoskeleton re-arrangement) (Moon et al., 2003). The guanine nucleotide binding protein (G protein), alpha z polypeptide gene, in short *GNAZ,* was up regulated, too. Heterotrimeric G proteins are involved in G protein receptor signalling pathways. GNAZ only mediates signal transduction in pertussis toxin insensitive systems (Fong et al., 1988) (Matsuoka et al., 1990)(Casey et al., 1990). Recently the possible involvement of GNAZ in melanoma progression was described causing high somatic mutation rates in this gene (Cardenas-Navia et al., 2010).

Table 31. Highest up regulated genes in HepG2 cells after treatment with TCDD (10 nM).
Selected cut-off values: A ≥ 5, log2 fc ≥ 1, p-value ≤ 0.05. Annotations: '*' Log2 fc value calculated as mean value from identical probes.

Gene name	Gene description	Probe name	Systematic name	Log2 fc
CYP1A1	Cytochrome P450 family 1, subfamily A, polypeptide 1	A_23_P163402	NM_000499	5.00
NKAIN1	Na^+/K^+ transporting ATPase interacting 1	A_23_P51376	NM_024522	4.88
LRRC25	Leucine rich repeat containing 25	A_23_P165136	NM_145256	4.88
WNT11	Wingless-type MMTV integration site family, member 1	A_24_P253003	NM_004626	4.54
SLC16A6	Solute carrier family 16 member 6 (monocarboxylic acid transporter 7)	A_23_P152791	NM_004694	4.40
FMOD	Fibromodulin	A_23_P114883	NM_002023	4.20*
LIM2	Lens intrinsic membrane protein 2	A_23_P130435	NM_030657	4.11
AHRR	Aryl hydrocarbon receptor repressor	A_23_P358709	NM_020731	3.99
CYP1B1	Cytochrome P450 family 1, subfamily B, polypeptide 1	A_23_P209625	NM_000104	3.52
SEC14L4	SEC14-like 4 (S. cerevisiae) transcript variant 1	A_23_P421032	NM_174977	3.47

Table 32. Highest up regulated genes in hHeps after treatment with TCDD (10 nM).
Selected cut-off values: A ≥ 5, log2 fc ≥ 1, p-value ≤ 0.05.

Gene name	Gene description	Probe name	Systematic name	Log2 fc
CYP1B1	Cytochrome P450 family 1, subfamily B, polypeptide 1	A_23_P209625	NM_000104	6.59
CYP1B1	Cytochrome P450 family 1, subfamily B, polypeptide 1	A_33_P3290343	NM_000104	4.43
CYP1A1	Cytochrome P450 family 1, subfamily 1, polypeptide 1	A_23_P163402	NM_000499	5.37
LRRC25	Leucine rich repeat containing 25	A_23_P165136	NM_145256	4.58
ALDH3A1	Aldehyde dehydrogenase 3 family A, member 1, transcript variant 2	A_23_P207213	NM_000691	4.41
ALDH3A1	Aldehyde dehydrogenase 3 family A, member 1, transcript variant 1	A_33_P3238433	NM_001135168	4.20
FLJ30901	cDNA FLJ30901 fis clone FEBRA2005778	A_33_P3480395	AK055463	3.60
ARHGAP44	Rho GTPase activating protein 44	A_23_P26854	NM_014859	3.53
C14orf135	cDNA FLJ38170 fis clone FCBBF1000024	A_33_P3397795	AK095489	3.26
LOC100507055	Hypothetical LOC100507055	A_32_P49867	NM_001195520	3.17
GNAZ	Guanine nucleotide binding protein (G protein) alpha z polypeptide	A_23_P416581	NM_002073	3.11

The small number of in common up regulated genes in both human liver cell models (Table 33) was unexpected because HepG2 cells are often used as *in vitro* model to investigate mechanisms of action of dioxins and dioxin-like compounds.

Cytochromes P450 *1A1*, *1A2*, *1B1* and *ALDH3A1*, being proven phase I xenobiotic metabolising enzymes, were up regulated in both human cell models. *UGT1A6*, a member of group of phase II metabolizing enzymes, was also among the group of 25 commonly up regulated genes. UGT1A6 is the main representative of the UGT1A family. Uridine diphosphate glucuronosyl transferases belong to the class of type I transmembrane proteins which are involved in biotransformation of exogenous and endogenous substrates. UGT1A6 catalyzes the conjugation of the substrate with glucuronic acid to enhance the substrate's water solubility and to improve its biliary and uric excretion (Bock et al., 2006). *HSD17B2* was furthermore up regulated in both human liver cell models. HSD17B2 plays an important role in estrogen metabolism by catalyzing the inactivation of estradiol to the less potent estrone (Plourde et al., 2008). Hayes and co-workers discovered the AhR-dependent TCDD-inducible up regulation of *Hsd17b2* in mice (Hayes et al., 2007). Another gene being commonly up regulated was *SLC7A5*. This gene encodes the LAT1 protein which is responsible for the sodium-independent amino acid exchange of large neutral amino acids (Babuet al., 2003) (Verrey et al., 2004). *SLC7A5* was already identified as TCDD-responsive gene in HepG2 cells by Sarkar et al. (Sarkar et al., 1999).

Genes linked to further signal transduction processes were up regulated after TCDD treatment, too. *LRRC25* was highly up regulated in HepG2 and hHeps by TCDD. A large number of leucine rich repeat containing proteins with distinguished functions in different cellular compartments have been identified in humans, rodents, plants, flies, and yeast so far. They all have specific repetitive sequences in common and are involved in protein-protein interactions. LRR proteins among others participate in signal transduction, DNA repair, recombination, transcription, or RNA processing (Kobe et al., 1995). *LRRC25* was identified as novel AhR-regulated target gene involved in PAH-induced immunotoxicity by Iwano and co-workers (Iwano et al., 2010). *SECTM1* encodes a transmembrane and secreted protein (type 1). SECTM1 is primarily expressed in epithelial cells and in peripheral blood cells (neutrophils and monocytes). The SECTM1 protein is involved in T cell proliferation as well as the secretion of various cytokines (TNFα, INFγ) due to its high affinity to the CD7 receptor (Huyten et al., 2011). The protein encoded by *MAFF* is a transcription factor without a transactivation domain. MAF proteins have been linked to gene regulation, differentiation, oncogenesis, and development in various organisms (Massrieh et al., 2006).

The gene *MBL2* was furthermore up regulated in both human liver models. The MBL2 protein belongs to the group of acute-phase proteins which are produced as a response to inflammation. MBL2 plays an important role in the innate immune system. Mannose-binding proteins not only function as pattern recognition molecules in the complement system by binding apoptotic cells but they additionally increase the engulfment of intact apoptotic cells and cell debris (Turner et al., 1998) (Ogden et al., 2001) (Stuart et al., 2005) (Herpers et al., 2009).

Moreover, further genes involved in cellular growth, differentiation, proliferation, cell cycle and apoptosis were up regulated in both cell types by TCDD. The anti-apoptotic gene Bcl-2 modifying factor (*BMF*) was also up regulated. Bcl-2 (B cell lymphoma 2) is the founding member of Bcl-2 family of proteins which regulate the programmed cell death (apoptosis) (Chao et al., 1998). The *CDK5RAP2* gene encodes the CDK5RAP2 protein which directly regulates CDK5 and CDK5R1 (isoform of CDK5) activities. Both are involved in the cell cycle process (Kraemer et al., 2011). Furthermore, Barrera et al. (2010) demonstrated in mouse model that CDK5RAP2 is required for the maintenance of centriole engagement and cohesion (Barrerra et al., 2010). TCDD additionally induced the up regulation of the myoferlin gene (*MYOF*). Myoferlin (MYOF) is a member of the ferlin family. Ferlin proteins are membrane-associated proteins which are associated with diverse in biological processes such as endothelial cell membrane regeneration and growth, growth factor receptor stability, as well as endocytosis (Demonbreun et al., 2010) (Eisenberg et al., 2011).

The protein encoded by the *PDLIM2* gene, is a member of the PDZ and LIM domain containing protein family, which are enganged in various cellular processes such as cytoskeletal organization, neuronal signalling, cell linage specification, organ development, and oncogenesis (Loughran et al., 2005) (te Vethuis et al., 2007). Furthermore, as a nuclear regulator of NF-κB, PDLIM2 determines the NF-κB activity. NF-κB is a transcription factor taking part in innate and adaptive immunity, inflammation, cellular stress responses, cell adhesion, proliferation as well as apoptosis (Tanaka et al., 2007) (Mankan et al., 2009). *GDF15* encodes the growth and differentiation factor (GDF15) protein which belongs to the transforming growth factor-β (TGF-β) superfamily. High levels of GDF15 were measured in the adult liver as a result of a liver injury (Hsiao et al., 2000). GDF15 is additionally involved in cardiac hypertrophy and programmed cell death (apoptosis) (Ago et al., 2006).

Proprotein convertase subtilisin/kexin type 5 is a member of the subtilisin/kexin-like proprotein convertase enzymes which are responsible for functional maturation of target proteins (Turpeinen et al., 2011). The *FBXO25* gene encodes the FBXO25 protein which is one of 68 human F-box proteins. It functions as one of four subunits of the ubiquitin protein ligase complex (SCF1-complex) and is involved in the detection of proteins which should be eliminated from the organism by the ubiquitin proteasome complex (Teixeira et al., 2010). *SERTAD2* was slightly, but significantly up regulated in HepG2 cells and hHeps. SERTA domain containing proteins take part in various cellular processes including the regulation of the transcription factor E2f1 during cell cycle progression, the p53-dependent stress response, and cancer pathogenesis (Hsu, et. al., 2001) (Cheong et al., 2009) (Fernandez-Marcos et al., 2010).

DNMT3L is a member of the group of DNA methyl transferases.Transcriptional repression by CpG methylation is an important step which plays a key role in various processes such as embryonic development, genomic imprinting, as well as X-chromosome inactivation. DNMT3L is not able to methylate the DNA in contrast to its other family members, but it stimulates the enzyme activity of the DNA cytosine methyltransferase 3α as well as it acts as a transcriptional repressor for the histone deacetylase HDAC1 (Deplus et al., 2002) (Xu et al., 2010).

The NKD2 protein is a negative regulator of the Wnt signalling pathway, in particular by binding to theso called Dishevelled proteins (Dsh) during the canonical Wnt signalling pathway (Creyghton et al., 2005) (Hu et al., 2009). *NDK2* furthermore encodes a protein which is responsible for the transport of the transforming growth factor α to the basolateral plasma membrane (Li et al., 2004). The Wnt signalling pathway is involved in various cellular processes such as development, differentiation, as well as the maintenance of the cellular homeostasis (Behari et al., 2010). Interactions between the β-catenin (key regulator of the canonical Wnt signalling) and the AhR subsequently to TCDD treatment were demonstrated in liver progenitor cells (Prochazkovaet al., 2011). The slight induction of this gene implies that TCDD treatment leads to a possible interplay between the AhR and Wnt signalling in both human liver cell models.

The suppressor of cytokine signalling 2 (*SOCS2*) was also up regulated in both hepatic cell models. Though, the HepG2 cells log2 fc value was 4-times higher than in hHeps where only a slight increase was observed. SOCS proteins are cytokine-inducible negative regulators of the cytokine receptor signalling by the JAK/STAT signalling pathway. SOCS2 plays an important role in growth hormone receptor signalling. Deregulation of growth hormone signalling was proven in *Socs2*-deficient mouse model in which *Socs2* knockout mice exhibited gigantism (Alexander et al., 2003) (Rico-Bautista et al., 2006) (Vesterlund et al., 2011). In 2004, an *in vitro* study performed in murine B cell lymphoma cells revealed that SOCS2 is not only induced by cytokines and growth hormones, but also by TCDD. Furthermore, the induction of SOCS2 was proven to be mediated by the activation of the AhR signalling pathway in the chosen *in vitro* model. Boverhof and co-workers demonstrated that SOCS2 is a negative regulator of cytokine signalling acting via a classic negative feedback loop (Boverhof et al., 2004). The TCDD-mediated transcriptional induction of *SOCS2* in hHeps and HepG2 could be based on the enhanced secretion of cytokines as a cellular response to the TCDD-induced inflammation in both human liver cell models.

The present toxicogenomic study in HepG2 cells and primary human hepatocytes elucidated the AhR-mediated effects of TCDD. TCDD treatment led to the up regulation of established AhR-responsive genes associated with xenobiotic metabolisms (*CYP1A1*, *1A2*, *1B1*, *ALDH3A1*, and *UGT1A6*). Other in both cell types commonly up regulated genes are associated with diverse biological processes such as cell cycle regulation (*CDKRAP2*), cellular growth and differentiation (*SERTAD2*, *PDLIM2*, *GDF15*), apoptosis (*BMF*) transcriptional regulation (*SERTAD2*, *DNMTL3*, *MAFF*), immune response (*SOCS2*, *MBL2*, *SECTM1*), and cellular transport (*SLC7A5*).

Table 33. In common up regulated genes in HepG2 cells and hHeps in alphabetical order.
Selected cut-off values: A ≥ 5, log2 fc ≥ 1, p-value ≤ 0.05. Explanations: '*' Log2 fc value calculated as mean value from identical probes.

Gene Name	Gene Description	Systematic Name	Probe Name	Log2 fc HepG2	Log2 fc hHeps
ALDH3A1	Aldehyde dehydrogenase 3 family, member 1A, transcript variant 2	NM_000691	A_23_P207213	3.47	4.41
ALDH3A1	Aldehyde dehydrogenase 3 family, member 1A, transcript variant 1	NM_001135168	A_33_P3238433	3.32	4.20
BMF	Bcl-2 modifying factor (BMF) transcript variant 1	NM_001003940	A_23_P379649	2.39	2.52
CDK5RAP2	CDK5 regulatory subunit associated protein 2 transcript variant 1	NM_018249	A_23_P83110	1.14	1.64
CYP1A1	Cytochrome P450, family 1, subfamiliy A, polypeptide 1	NM_000499	A_23_P163402	5.00	5.37
CYP1A2	Cytochrome P450, familiy 1, subfamiliy A, polypeptide 2	NM_000761	A_33_P3253747	1.83	2.62
CYP1B1	Cytochrome P450, familiy 1, subfamiliy B, polypeptide 1	NM_000104	A_23_P209625	3.52	6.59
DNMT3L	DNA (cytosine-5-)-methyltransferase 3-like transcript variant 1	NM_013369	A_23_P17673	1.46	2.08
FBXO25	F-box protein 25 (FBXO25) transcript variant 2	NM_183421	A_23_P94159	1.36	1.84
GDF15	Growth differentiation factor 15	NM_004864	A_23_P16523	1.39	1.38
HSD17B2	Hydroxysteroid (17-beta) dehydrogenase 2	NM_002153	A_23_P118065	1.84*	1.24*
LOC100507055	Hypothetical LOC100507055	NM_001195520	A_32_P49867	2.41	3.17
LOC286161	cDNA FLJ34353 fis clone FEBRA2011665	AK091672	A_33_P3841368	1.12	1.70
LRRC25	Leucine rich repeat containing 25	NM_145256	A_23_P165136	4.88	4.58
MAFF	v-maf musculoaponeurotic fibrosarcoma oncogene homolog F (avian), transcript variant 1	NM_012323	A_23_P103110	1.45*	1.39
MBL2	Mannose-binding lectin (protein C) 2 soluble	NM_000242	A_23_P35529	2.21	1.64
MYOF	Myoferlin, transcript variant 1	NM_013451	A_23_P354387	2.74	1.36
NKD2	Naked cuticle homolog 2 (Drosophila)	NM_033120	A_23_P41804	1.14	2.24
PCSK5	Proprotein convertase subtilisin/kexin type 5, transcript variant 2	NM_006200	A_23_P257003	1.82	2.12
PDLIM2	PDZ and LIM domain 2 (mystique), transcript variant 3	NM_198042	A_33_P3311371	1.61	1.01
SECTM1	Secreted and transmembrane 1	NM_003004	A_24_P48204	1.25	2.32
SERTAD2	SERTA domain containing 2	NM_014755	A_24_P294124	1.65	1.22
SLC7A5	Solute carrier family 7 (amino acid transporter light chain L system) member 5	NM_003486	A_24_P335620	1.50	2.14
SOCS2	Suppressor of cytokine signalling 2	NM_003877	A_23_P128215	3.02	1.10
UGT1A6	UDP glucuronosyltransferase 1 family, polypeptide A6	NM_001072	A_23_P60599	1.13	1.17

In order to find, establish, and implement novel quantifiable biomarkers for AhR activation due to exposure to DLCs, the gene expression of five potential AhR target genes as well as established markers for AhR activation (*CYP*s) are presented in Table 34. The table displays the obtained log2 fold-change values of the eight target genes from microarray analysis, whereby both transcript variants (transcript variants 1 and 2) of the aldehyde dehydrogenase (*ALDH3A1*) are indicated. Despite the induction of *CYP1A1*, *CYP1A2*, and *CYP1B1, ALDH3A1* and *HSD17B2* were the only genes among the group of potential novel target genes which were up regulated in both *in vitro* models. *CD36* and *AHRR* were only up regulated in HepG2 cells, but not in hHeps. *TIPARP*, on the other hand, was only up regulated in hHeps, but not in HepG2 cells. Gene expression of selected target genes obtained by the current microarray experiment had been verified using RT-PCR analysis which is presented in the following chapter.

Table 34. AhR target genes in hHeps and HepG2 identified by microarray.
Table features aspects such as gene name, systematic name, and corresponding fold-change.
Selected parameters: A ≥ 5, log2 fc ≥ 1, p-value ≤ 0.05.
Explanations: (1) transcript variant 1; (2) transcript variant 2;
'*' Log2 fc value calculated as mean value from identical probes.
'→' This gene was not up regulated in microarray experiment.

Gene name	Probe name	Systematic name	Log2 fc HepG2	Log2 fc hHeps
CYP1A1	A_23_P163402	NM_000499	5.00	5.37
CYP1A2	A_33_P3253747	NM_000761	1.82	2.63
CYP1B1	A_23_P209625	NM_000104	3.52	6.59
ALDH3A1 (1)	A_33_P3238433	NM_001135168	3.32	4.20
ALDH3A1 (2)	A_23_P207213	NM_000691	3.47	4.41
HSD17B2	A_23_P118065	NM_002153	1.89*	1.24*
CD36	A_23_P111583	NM_001001547	1.52	→
TIPARP	A_23_P143845	NM_015508	→	2.31
AHRR	A_23_P358709	NM_020731	3.99	→

IV.3.3.2 Gene Expression of Target Genes by RT-PCR

After performing microarray analysis in HepG2 and hHeps, the mRNA gene expression of the selected eight target genes was determined by RT-PCR. The isolated RNA from compound-treated HepG2 cells and primary human hepatocytes was first transcribed into complementary DNA (cDNA). 1 µl of cDNA was used to perform each RT-PCR experiment. The target gene expression was normalized to the selected housekeeping gene (β-actin (*ACTB*)) before the gene-specific expression was calculated relative to the expression of the corresponding solvent control (DMSO 0.1 %). The following two figures (Figure 49 and 50) summarize the results of the mRNA expression levels of the AhR-regulated cytochromes P450 *1A1*, *1A2*, and *1B1* as well as the selected potential biomarker genes *ALDH3A1*, *HSD17B2*, *CD36*, *TIPARP*, and *AHRR*.

Gene expression levels of all eight target genes were not affected compared to the respective solvent controls after 24 h exposure to NDL-PCB 153 in both human liver cell models as expected, taking into account the earlier presented microarray studies. *CYP1A1* mRNA expression was strongly induced after incubation with TCDD (10 nM) for 24 h in both cell models leading to a 1354.66 ± 771.74-fold and 679.34 ± 351.01-fold induction for hHeps and HepG2 cells, respectively. This was also the case for *CYP1B1*; here, *CYP1B1* mRNA levels in hHeps were about 6-times higher than in the human hepatocellular carcinoma cell line resulting in a 628.59 ± 277.90 and 97.37 ± 47.32 *CYP1B1* fold-induction. In contrast to these findings, the gene expression of *CYP1A2* was highly induced in primary human hepatocytes (597.86 ± 389.00), but not in HepG2 cells (2.04 ± 1.32).

ALDH3A1 was induced in both cell types (Figure 50). The *ALDH3A1* mRNA levels were about 4-times higher (20.42 ± 12.99-fold) in hHeps than in TCDD-treated HepG2 cells (4.78 ± 1.67-fold). *HSD17B2* mRNA expression was slightly, but statistically significantly induced after exposure to TCDD in hHeps (2.98 ± 1.20) and HepG2 cells (2.60 ± 0.53). *CD36* as another selected potential novel target gene was slightly induced in HepG2 cells (2.23 ± 0.78-fold), but not in primary human hepatocytes. Opposed to this, *TIPARP* mRNA levels were only enhanced in hHeps (3.01 ± 0.35-fold) compared to the solvent control, but not in HepG2 cells. Gene expression of the aryl hydrocarbon receptor repressor (*AHRR*) was neither induced in hHeps nor in HepG2 cells.

Among the potential novel target genes only *ALDH3A1* was induced to a higher extend after exposure to TCDD (10 nM) in both human liver cell models. The maximal mRNA induction in hHeps was 4-times higher than in HepG2 cells. But this experiment clearly shows that *ALDH3A1* does not by far reach the mRNA inducibility of *CYP1A1* as established biomarker for AhR activation. *CYP1A2* was strongly induced in primary human hepatocytes, but not in HepG2 cells. The human *CYP1A2* gene is only expressed in the adult liver (Xu et. al., 2000). The immortalized human hepatoma cell line HepG2 was derived from a liver tumour of a fifteen year old Caucasian Argentine male with a hepatocellular carcinoma suggesting that the lack of *CYP1A2* induction is an age-specific effect (Aden et al., 1979) (Knowles et al., 1980).

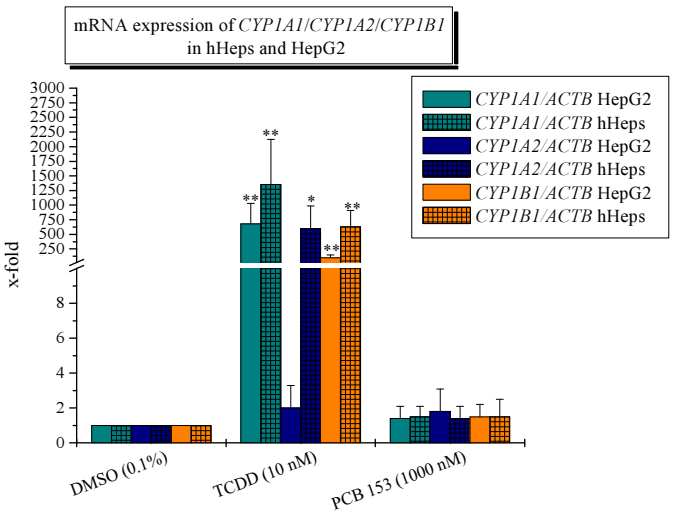

Figure 49. **Real-time PCR ratios of cytochromes P450s in HepG2 (plain-coloured bars) cells and hHeps (plaid bars) treated with TCDD (10 nM), PCB 153 (1000 nM), or DMSO (0.1 %). β-actin (*ACTB*) served as housekeeping gene. Data represent means + SD of data from n = 5 independent experiments or donors, normalized to solvent control. One-tailed unpaired Student's t-test,*= p ≤ 0.05, **= p ≤ 0.01 different from corresponding solvent control.**

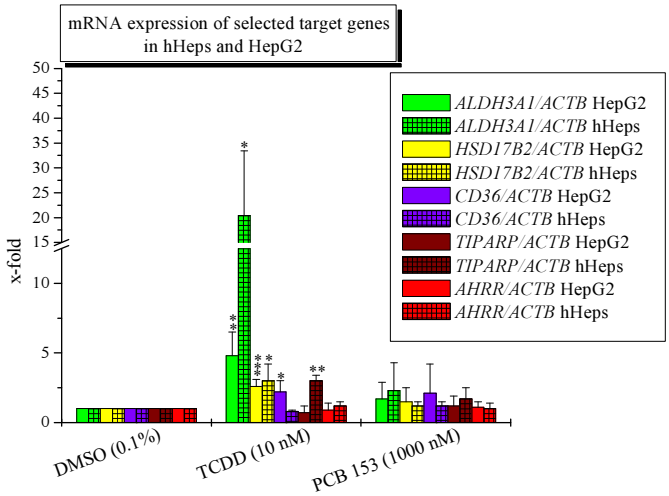

Figure 50. **Real-time PCR ratios of selected target genes in HepG2 (plain-coloured bars) cells and hHeps (plaid bars) exposed to TCDD (10 nM), PCB 153 (1000 nM), and DMSO (0.1 %). β-actin (*ACTB*) served as housekeeping gene. Data represent means + SD of data from n = 5 independent experiments or donors respectively, normalized to solvent control. One-tailed unpaired Student's t-test,*= p ≤ 0.05, **= p ≤ 0.01 different from corresponding solvent control.**

IV.3.4 Summary and Discussion *in vitro* Experiments

In the present work, human liver cell models (primary human hepatocytes and HepG2 cells) were used to assess the effects mediated by dioxins and dioxin-like compounds. The liver represents the target tissue in which TCDD has been shown to elicit carcinogenic and tumour promoting effects in rodents (Knerr et. al, 2006). Hepatotoxic effects mediated by TCDD include hepatomegaly, hepatocellular neoplasms, inflammation, necrosis, steatosis, as well as alterations in the expression of genes associated with lipid metabolism and transport in the murine liver (Poland et al., 1982a) (Huff et al., 1991) (Boverhof et al., 2006) (Kopec et al., 2010a) (Kopec et al., 2010b) (Angrish et al., 2011).

Humans are predominantly exposed to PnCDD/PnCDFs and PCBs via the food chain, but also as a consequence to their occupations or accidents. Hepatic responses elicited by TCDD in humans include alteration in hepatic enzyme levels, triglyceride levels as well as liver enlargement and liver cirrhosis (DeVito et al., 1995) (Pelclova et al., 2006).
Performing essential *in vitro* experiments by the use of primary human hepatocytes and the human hepatocellular carcinoma cell line (HepG2) provides important information which can lead to a better understanding of risks after exposure to PnCDD/Fs and DL-PCBs in humans. Furthermore, the challenging task was to identify, validate, and establish quantifiable novel biomarkers for dioxin exposure and AhR-dependent modes of action.

A set of seven core compounds including TCDD, 1-PnCDD, 4-PnCDF, PCB 126, PCB 118, PCB 153, and PCB 156 and additional further congeners, i.e. TCDF, 1,4-HxCDF, 1,4,6-HpCDF, 1,6-HxCDD, 1,4,6-HpCDD, PCB 77, and PCB 105 were selected in the present work. Primary human hepatocytes (hHeps) as well as the immortalized human hepatocellular carcinoma cell line HepG2 were used in the present work to determine concentration-dependent effects on induction of AhR-regulated gene expression and activity after 24 h treatment with test compounds. The effects of core congeners were examined in hHeps and HepG2 cells, whereas effects of further congeners were only determined in HepG2 cells.

IV.3.4.1 EROD Data HepG2 vs. hHeps

The catalytic activity of CYP1A1 in primary human hepatocytes and HepG2 cells was examined by measuring the Ethoxyresorufin-O-deethylase (EROD) activity. EC_{50}/EC_{20} values and respective REPs values are compiled and compared with WHO-TEFs (van den Berg et al., 2006) in Table 35 and 36. The EROD activities of the core congeners (TCDD, 1-PnCDD, 4-PnCDF, PCB 118, 126, 153, and 156) were determined in both human liver cell models, whereas the EROD activities of the seven further congeners were only measured in HepG2 cells.

Based these findings, primary human hepatocytes were in summary less sensitive towards TCDD, 1-PnCDD, 4-PnCDF, and PCB 126 compared to HepG2 cells. Silkworth et al. published a similar EROD-derived EC_{50} value for HepG2 (0.29 nM), but a much lower EC_{50} value for primary human hepatocytes (0.15 nM) (Silkworth et al., 2005). In a recently

published study the EROD-derived EC_{50} value of TCDD in hHeps was also lower than the obtained value in the present thesis (0.239 nM) (Budinski et al., 2010). The higher obtained EC_{50} value of TCDD in hHeps could be attributed to the human diversity in EROD response which is characterized by sensitivity as well as the maximal inducibility. Silkworth and co-workers demonstrated in their study that the EC_{50} values from four of the five donors were within a seven-fold range while the fifth donor was a poor responder to TCDD (Silkworth et al., 2005). In the same study the EROD activity of PCB 126 in hHeps was additionally determined. After 48 h of treatment a 6-fold higher EC_{50} value in HepG2 (150 nM) and a 15-fold lower EC_{50} value in hHeps (45 nM) was determined. The differences in EC_{50} values concerning hHeps could again be attributed to the donor individuality, e.g. interindividual response. Likewise, the difference in maximal response and sensitivity of human donors was also observed in case of 4-PnCDF. The EROD-derived EC_{50} value in hHeps was 32-fold higher compared to the previously published study (0.563 nM) (Budinsky et al., 2010).

Table 35. EC values derived from *in vitro* EROD assay.
Explanation: 'n.e.' not examined

	HepG2		Primary human hepatocytes	
	EC_{50} (nM)	**EC_{20} (nM)**	**EC_{50} (nM)**	**EC_{20} (nM)**
TCDD	0.269 ± 0.034	0.113	1.06 ± 0.57	0.420
1-PnCDD	0.176 ± 0.023	0.058	3.07 ± 2.44	0.158
4-PnCDF	0.107 ± 0.020	0.050	18.00 ± 8.59	0.242
1,6-HxCDD	4.57 ± 0.12	1.53	n.e.	n.e.
1,4,6-HpCDD	2.45 ± 0.29	0.699	n.e.	n.e.
TCDF	1.64 ± 0.37	0.894	n.e.	n.e.
1,4-HxCDF	0.306 ± 0.041	0.137	n.e.	n.e.
1,4,6-HpCDF	47.55 ± 4.82	10.73	n.e.	n.e.
PCB 77	-	-	n.e.	n.e.
PCB 105	-	-	n.e.	n.e.
PCB 118	-	-	-	-
PCB 126	26.27 ± 3.62	25.75	678.78 ± 90.36	216.74
PCB 153	-	-	-	-
PCB 156	-	-	-	-

Table 36. Relative effect potencies (REPs) derived from *in vitro* EROD assay. Comparison with WHO-TEFs. Explanation: 'n.e.' not examined

	HepG2		Primary human hepatocytes		TEF
	REP (EC_{50})	REP (EC_{20})	REP (EC_{50})	REP (EC_{20})	(WHO, 2005)
TCDD	1.0	1.0	1.0	1.0	1.0
1-PnCDD	1.53	1.92	0.35	2.66	1.0
4-PnCDF	2.51	2.26	0.059	1.73	0.3
1,6-HxCDD	0.059	0.074	n.e.	n.e.	0.1
1,4,6-HpCDD	0.11	0.16	n.e.	n.e.	0.01
TCDF	0.16	0.13	n.e.	n.e.	0.1
1,4-HxCDF	0.88	0.82	n.e.	n.e.	0.1
1,4,6-HpCDF	0.0057	0.011	n.e.	n.e.	0.01
PCB 77	-	-	n.e.	n.e.	0.0001
PCB 105	-	-	n.e.	n.e.	0.00003
PCB 118	-	-	-	-	0.00003
PCB 126	0.010	0.0044	0.0016	0.0019	0.1
PCB 153	-	-	-	-	-
PCB 156	-	-	-	-	0.00003

REPs derived from HepG2 cells mostly confirmed the current WHO-TEFs (Table 36). Nevertheless, several deviations were observed. In case of 4-PnCDF and 1,4-HxCDF, REP values were 8- and 9-fold higher than the current WHO-TEFs. REPs obtained for 1-PnCDD, 1,4-HxCDD, TCDF and 1,4,6-HpCDF were within the same range as the current WHO-TEFs. In HepG2 cells, REP values for PCB 126 were below the current TEF by 10- and 23-fold. It was not possible to derive any REPs for the PCBs (PCB 77, 105, 118, 153, and 156) due to the lacking EROD induction in HepG2 cells. REPs obtained from hHeps differed from the current WHO-TEF. No REPs could be derived for PCB 118, 153, and 156 due to the lack in EROD activities in hHeps. REPs derived for PCB 126 were 63-fold and 53-fold below the current WHO-TEF, respectively.

An inconsistent trend was obtained for 1-PnCDD and 4-PnCDF. REPs derived from EC_{50} values of 1-PnCDD and 4-PnCDF were below the current WHO-TEF, 3-fold and 5-fold in particular. However, REPs derived from EC_{20} values were higher than the current WHO-TEF, 3-fold and 6-fold, respectively. As described before, the EC_{50} is the effective concentration to achieve 50 % maximal response and therefore is only based on the respective test compound itself. On the other hand, the EC_{20} values were calculated in relation to TCDD. 1-PnCDD and 4-PnCDF both evoked higher EROD activities at low concentrations compared to TCDD as well as a higher maximal EROD response, e.g. inducibility. Based on this, the higher REPs derived from EC_{20} values can be explained.

For EC_{20} values, a different calculation concept was developed than vor EC_{50} values. This calculation method was elaborated to be able to compare the less potent DL-compounds, which might not reach the EC_{50} levels, with the most potent representative of the group of DLCs, TCDD.

This EC_{20} calculation method was based on a consensus between all SYSTEQ project partners to assess the potencies of weaker test. Hence, the separate calculation of EC_{20} values based on the data from each test compound itself should be taken into consideration as possible calculation approach.

As described in the previous passage, 1-PnCDD and 4-PnCDF exhibited higher EROD responses in terms of overall CYP1A1 inducibility as well as higher EROD activities for both congeners in the low concentration range compared to TCDD in hHeps. It should be further analyzed if this phenomenon is a donor-specific effect. Therefore, the number of experiments in primary human hepatocytes should be increased. The relative effect potencies derived from CYP1A1 EROD data of 1-PnCDD and 4-PnCDF also suggest the higher potencies of both congeners compared to TCDD in HepG2 cells. Nevertheless, it should be examined if these findings are based on a cell-type specific effect or not, e.g. by the use of a different human liver cell model such as the immortalized hepatocellular carcinoma cell line HepaRG. The current TEFs are predominantly based on *in vivo* animal studies. *In vivo* and *in vitro* studies used for TEF value calculations are among others based on different endpoints and timepoints providing explicable reasons for the detected differences (Haws et al., 2006) (van den Berg et al., 2006).

Further analysis of DLCs including experiments in hHeps by the use of additional donors, other human cell types (e.g. lymphocytes) as well as other transformed and untransformed human and rodent *in vitro* cell models is necessary to derive *in vitro* TEFs. The characterization of species- and cell type-specific responses provides essential knowledge for assessing the human risk towards DLCs.

IV.3.4.2 Comparison of CYP1A1 and CYP1B1 mRNA Expression with EROD Induction in HepG2 cells

EC_{50} and EC_{20} values derived from EROD assay and *CYP1A1*/*CYP1B1* mRNA are summarized in Table 37. When comparing EC values of CYP1A1 enzyme activity (EROD) with *CYP1A1* mRNA, the EROD assay was the more sensitive test method. Differences in EC values could be attributed to different experimental approaches. When comparing *CYP1A1* with *CYP1B1*, *CYP1A1* was the more sensitive biomarker for AhR activation due to treatment with dioxins and dioxin-like compounds. The maximal fold inductions of *CYP1A1* mRNA was about 10-fold higher compared to *CYP1B1* mRNA in HepG2 cells-treated with TCDD, 1-PnCDD, 4-PnCDF, or PCB 126.

REPs derived from EROD induction and *CYP1A1* mRNA were constantly higher for 1-PnCDD and 4-PnCDF than the current WHO-TEFs. REPs for 1-PnCDD were between 1.5 to 2-fold and REPs for 4-PnCDF were 3 to 8.5-fold higher compared to the established TEFs in 2005 (van den Berg et al., 2006). On the other side, REPs derived for PCB 126 were below the current TEF of 0.1 by several orders of magnitude.
As described in the previous chapter, it must be taken into account that the current TEFs are primarily based on REPs derived from *in vivo* animal studies when comparing REP values from the present study. Multiple endpoints, timepoints, tissues, and cell types were used for calculation of WHO-TEFs (2005), whereupon the deviations can be explained (Haws et al., 2006) (van den Berg et al., 2006). Furthermore, the obtained results should be compared to other *in vitro* data (human, rat, and mouse) to derive fundamental information about species-specific and cell type-specific effects. In summary, 1-PnCDD and 4-PnCDF seem to be more potent than TCDD in HepG2 cells, but further experimental approaches, for instance by the use of a different immortalized human hepatocarcinoma cell line (HepaRG), are required to confirm whether these findings are cell type-specific responses or not.

Table 37. **EC_{50} and EC_{20} values derived by EROD assay, *CYP1A1* and *CYP1B1* mRNA in HepG2 cells.**

		TCDD	1-PnCDD	4-PnCDF	PCB 118	PCB 126	PCB 153	PCB 156
EROD	**EC_{50} ± SD (nM)**	0.269 ± 0.034	0.176 ± 0.023	0.107 ± 0.020	-	26.27 ± 3.62	-	-
	EC_{20} (nM)	0.113	0.058	0.05	-	25.75	-	-
***CYP1A1* mRNA**	**EC_{50} ± SD (nM)**	0.583 ± 0.064	0.302 ± 0.208	0.704 ± 0.244	-	55.24 ± 14.64	-	-
	EC_{20} (nM)	0.213	0.111	0.204	-	88.10	-	-
***CYP1B1* mRNA**	**EC_{50} ± SD (nM)**	0.671 ± 0.224	0.718 ± 0.163	1.27 ± 0.52	-	126.51 ± 44.08	-	-
	EC_{20} (nM)	0.344	0.218	0.398	-	113.55	-	-

Table 38. **Relative effect potencies (REPs) derived from EROD assay, *CYP1A1* and *CYP1B1* mRNA in HepG2 cells. Comparison to WHO-TEFs (2005).**

		TCDD	1-PnCDD	4-PnCDF	PCB 118	PCB 126	PCB 153	PCB 156
EROD	**REP (EC_{50})**	1.0	1.53	2.51	-	0.010	-	-
	REP (EC_{20})	1.0	1.92	2.26	-	0.0044	-	-
***CYP1A1* mRNA**	**REP (EC_{50})**	1.0	1.93	0.83	-	0.011	-	-
	REP (EC_{20})	1.0	1.92	1.04	-	0.0024	-	-
***CYP1B1* mRNA**	**REP (EC_{50})**	1.0	0.93	0.53	-	0.0053	-	-
	REP (EC_{20})	1.0	1.58	0.87	-	0.0030	-	-
TEF (WHO, 2005)		1.0	1.0	0.3	0.00003	0.1	-	0.00003

IV.3.5 Microarray Studies *in vivo* vs. *in vitro* and mRNA Expression of Target Genes

Four microarray studies were performed in the present work. Two toxicogenomic studies focused on the AhR-dependent and AhR-independent effects in female mouse liver by the use of the AhR ligand TCDD and the CAR inducer PCB 153 (mouse study I - mouse 3-day study) in the first place and in the second place by using a transgenic mouse model in which the TCDD-altered hepatic gene expression was analyzed in *Ahr* wild-type and *Ahr* knockout mice. The TCDD-altered gene expression was additionally determined in the human hepatocarcinoma cell line HepG2 and primary human hepatocytes. HepG2 cells are often used in *in vitro* studies in which the human liver is the target tissue. Comparison of the TCDD-elicited alterations in gene expression provides essential information about similarities and differences in both human *in vitro* cell models. TCDD as the most potent congener of the class of dioxins and related compounds is often used *in vitro* models as reference for dioxin-mediated activation of the AhR. Little is known about other potent congeners (1-PnCDD, 4-PnCDF, and PCB 126) and their effect on gene expression, especially in hHeps. Therefore, the changes in gene expression patterns induced by TCDD, 1-PnCDD, 4-PnCDF, PCB 126, and PCB 153 were determined in primary human hepatocytes.

In both mouse microarray studies female C57BL/6 mice received a single dose of TCDD (25 µg/kg bw), only the post-treatment time varied (72 h vs. 96 h). The quantity of significantly altered hepatic genes ($A \geq 7$, $\log2\ fc \geq 1$, p-value ≤ 0.05) was approximately 2-times higher in mice with an enhanced exposure time (96 h) compared to mice sacrificed 72 h after single dose administration. This effect can most likely be attributed to the different exposure times, but the age of the animals could possibly have an effect on the alterations in gene expression, too. C57BL/6 mice exposed to TCDD in mouse study III were older (4-6 months) compared to the C57BL/6 mice of mouse study I (8 weeks). These factors must be taken into consideration when comparing the obtained results from both mouse microarray studies.

However, the highest up regulated genes in both microarray studies were associated with the xenobiotic metabolism as was the case in all performed microarray experiments, except in livers of *Ahr* knockout mice. In TCDD-treated C57BL/6 mice of mouse study I and TCDD-treated C57BL/6 (*Ahr* wild-type) mice of mouse study III, the altered hepatic gene expression was associated with the lipid and glucose metabolism. The profiling of differently regulated genes draws to the conclusion that TCDD induced the AhR-mediated increased uptake of fatty acids and the accumulation of triglycerides in the murine liver. These results confirmed the role of TCDD in the dysregulation of the hepatic lipid metabolism and suggesting the development of a hepatic steatosis. Nevertheless, further analysis is necessary to confirm this thesis and to elucidate the responsible mechanisms and pathways by measuring the mRNA expression of genes and corresponding enzyme activities, analyzing the serum enzyme levels (AST, ALT, and GGT), the microscopic examination of the liver (histopathology), as well as dose-response studies are required.

25 genes were commonly up regulated in primary human hepatocytes and HepG2 cells after treatment with TCDD. Microarray analysis of TCDD-altered genes revealed that hHeps were less sensitive in terms of differently regulated genes resulting in 72 up and 2 down in hHeps and 247 up and 44 down in HepG2 cells. In addition to genes associated with biotransformation of xenobiotics, in particular genes linked to phase I and II of xenobiotic metabolism, two lipolytic genes were among the group of 25. Additionally, the TCDD-induced altered gene expression included genes associated with diverse biological processes such as cell cycle regulation, cellular growth and differentiation, apoptosis, regulation of transcription, and immune response. These findings confirmed an earlier toxicogenomic study in HepG2 cells in which TCDD altered genes involved in cell cycle progression, differentiation, and apoptosis in presence of a ligand such as TCDD (Puga et al., 2002).

Figure 51 summarizes the commonly up regulated genes after TCDD treatment for the different microarray experiments using the selected parameters.

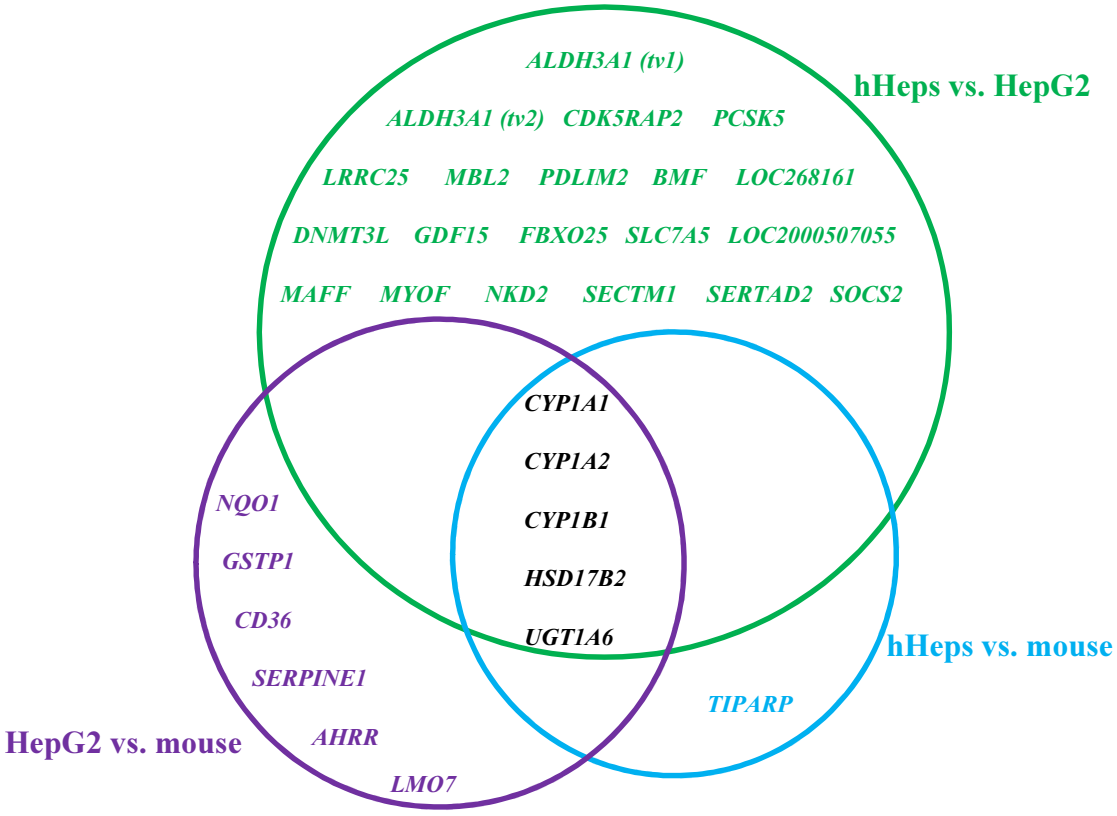

Figure 51. **In common up regulated genes by TCDD in different microarray studies.**
Featured gene names are quoted in the human gene nomenclature (HUGO Gene Nomenclature Committee (HGNC)).
Annotations: 'tv' = transcription variant.
Comparison between significantly up regulated genes in mouse 3-day study, in hHeps, and in HepG2 cells by TCDD. Selected parameters: A ≥ 5, log2 fc ≥ 1, p-value ≤ 0.05.

The most extensive overlap occurred between HepG2 and hHeps (25 genes) as expected because both have a human origin. Interestingly, the overlap of commonly up regulated genes in TCDD-treated HepG2 cells and TCDD-treated female mice was bigger (11 genes) as the overlap between TCDD-treated hHeps and TCDD-treated female mice (6 genes). *CYP1A1 (Cyp1a1), CYP1A2 (Cyp1a2), CYP1B1 (Cyp1b1), HSD17B2 (Hsd17b2),* and *UGT1A6 (Ugt1a6a)* were up regulated *in vivo* and *in vitro.*

CYP1A1 (Cyp1a1) was in almost all microarray experiments the highest up regulated gene as a consequence of TCDD treatment. Up to the present day, the induction of CYP1A1 is the best known biomarker for AhR activation due to dioxin exposure (Nebert et al., 2000) (Nebert et al., 2004) (Ma et al., 2007). The AhR-mediated inducibility of CYP1A1, CYP1A2, CYP1B1, and UGT1A6 was demonstrated in various studies (Bock et al., 2005a) (Hankinson, 1995) (Nebert et al., 2000) (Nebert et al., 2004).

Based on the microarray results of the mouse 3-day study (IV.1.1.1.2Microarray analysis - mouse study I), the microarray study performed in HepG2 cells and hHeps (IV.3.2.5 Microarray analysis HepG2 vs. hHeps), and a microarray study performed by the SYSTEQ project partner from the Karoliska Institutet, Sweden, potential target genes were selected in order to find novel quantifiable biomarkers for AhR activation. Including the results of all experimental models (mouse vs. human and *in vivo* vs. *in vitro*) five target genes (*ALDH3A1/Aldh3a1, HSD17B2/Hsd17b2, TIPARP/Tiparp, CD36/Cd36,* and *AHRR/Ahrr*) were selected in a consensus between all SYSTEQ project partners.

Aldh3a1 belongs to the 'classic' murine AhR gene battery (Nebert et al., 2000). Aldehyde dehydrogenases are involved in phase II of the xenobiotic metabolism of exogenous compounds. Aldehyde dehydrogenases catalyze the oxidation of aldehydes to the respective ketones and carboxylic acids (Nebert et al., 2000). ALDH3A1 predominantly detoxifies aromatic and medium-chain aliphatic aldehydes derived from lipid peroxidation (Vasiliou et al., 2000) (Muzio et al, 2012). *ALDH3A1* is expressed at low concentrations, if expressed at all, in normal liver, but high *ALDH3A1*/*Aldh3a1* expression levels were detected in hepatoma and other various cancer cells (Alnouti et al., 2008). About 50 % of patients with liver tumours exhibited high *ALDH3A1* expression levels. A direct correlation between the activity and amount of ALDH3A1 and cell proliferation has been demonstrated in various studies. The inhibition of ALDH3A1 activity could be used to reduce tumour cell proliferation. In normal cells the induction of *ALDH3A1* expression could possibly contribute to tissue regeneration (Muzio et al., 2012). The AhR-dependent TCDD-mediated induction of Aldh3a1 has been demonstrated, although some species and cell type-specific responses were determined (Vasiliou et al., 1992) (Nebert et al., 2000) (Alnouti et al., 2008). ALDH3A1 is strongly induced by TCDD in carcinoma cell lines, in rat (*in vivo* and *in vitro*), and in *in vitro* mouse models, but not in mouse *in vivo* (Vasiliou et al., 1993) (Alnouti et al., 2008). The TCDD-mediated induction of *ALDH3A1* mRNA expression has been demonstrated by several microarray experiments in transformed human cell lines as well as in primary human hepatocytes (Kim et al., 2009) (Vee et al., 2010) (Dere et al., 2011) (Black et al., 2012).

The hydroxysteroid (17-β) dehydrogenase 2 is a member of the short-chain dehydrogenases/reductases family. *HSD17B2* is expressed in various tissues including the human placenta, liver, kidney, endometrium, intestine, pancreas, colon, and prostate. It

catalyzes various reactions within the steroid metabolism, among others the conversion of 17β-estradiol to estrone, the reaction of testosterone to androstendione, as well as the oxidation of androstendiol to dehydroepiandrosterone (Casey et al., 1994) (Sun et al., 2011). Polymorphisms in the *HSD17B2* gene have been associated with diseases such as breast and prostate cancer (Plourde et al., 2008) (Sun et al., 2011). Recent studies identified novel functions of HSD17B2 in addition to its role in sex steroid metabolism. *Hsd17b2* knockout mice exhibited growth retardation, several abnormalities in placenta, kidney, and brain as well as a 70 % increased embryonic lethality (Rantakari et al., 2008). Transgenic mice expressing the human *HSD17B2* also featured growth retardation as well as delayed eye opening and disrupted spermatogenesis which resulted in the infertility of all male mice at the age of three months (Zhongyi et al., 2007). Implications that the phenotype-specific changes are not based on decreased estrogen and androgen levels, but rather are the result of the interference with the retinoic acid signalling, are given because the administration of a synthetic retinoid acid analog rescued the testis phenotype in the aforementioned study (Zhongyi et al., 2007) (Moeller et al., 2009). Hayes and co-workers described the AhR-dependent up regulation of *Hsd17b2* due to TCDD treatment in mice (Hayes et al., 2007). The toxicogenomic study performed by Fletcher et al. also demonstrated the TCDD-induced the up regulation of the *Hsd17b2* mRNA expression in rat liver (Fletcher et al., 2005).

The TCDD-inducible poly(ADP-ribose) polymerase, in short TIPARP (also known as PARP-7), belongs to the class of poly (ADP-ribose) polymerases (PARPs). Poly ADP-ribosylation is a posttranscriptional protein modification mechanism by which poly(ADP-ribose) polymerases catalyze the transfer of ADP-ribose from nicotinamid adenine dinucleotide (NAD^+) to protein acceptors. This reaction is essential for multiple cellular processes such as DNA repair, transcription, proliferation, and cell death (Schreiber et al., 2006) (MacPherson et al., 2013). *Tiparp* is constitutively expressed in various tissues such as heart, kidney, testis, liver, lung and brain (Ma et al., 2001). Ma and co-workers identified *Tiparp* as AhR-regulated TCDD-inducible gene (Ma et al., 2001) (Ma, 2002). TIPARP plays a fundamental role in the TCDD-mediated toxicity by suppression of the hepatic gluconeogenesis. TCDD induces the *TIPARP* expression, which subsequently results in the suppression of hepatic glucose metabolism, as demonstrated in chicken embryo hepatocytes (Diani-Moore et al., 2010). *TIPARP* siRNA led to an increase in glucose metabolism which was not significantly altered by TCDD compared to the control (Diani-Moore et al., 2010). A recently published study revealed that TIPARP exhibits rather mono(ADP-ribosyl)transferase activity than poly(ADP-ribosyl)polymerase activity. As aforementioned, the expression of *TIPARP* is mediated by the AhR and inducible by TCDD. It has now been postulated that TIPARP possibly functions as a repressor of the AhR signalling pathway in human cell lines and mouse embryonic fibrolasts derived from wildtype and *Tiparp*-deficient mice. TIPARP binds to the AhR/ARNT-complex which is bound to the XREs and thereby inhibits its transcription as well as the transcription of other AhR target genes (*Cyp1a1/CYP1A1*). Alternatively, it has been postulated that TIPARP itself binds to the DNA, which results in the dissociation of the AhR from the XREs and initiates the AhR proteosomal degradation process (MacPherson et al., 2013). The up regulation of *TIPARP* by TCDD in primary human hepatocytes has been demonstrated in recently published toxicogenomic studies (Dere et al., 2011) (Black et al., 2012) (Forgacs et al., 2013).

The aryl hydrocarbon receptor repressor (AhRR) is a member of the helix-loop-helix/Per-ARNT-Sim (bHLH/PAS) protein family. The aryl hydrocarbon receptor repressor is expressed in humans and animal tissues as well as in various cell lines. In humans, the *AHRR* is constitutively expressed in various organs such as testis, liver, kidney, colon, breast, adrenal glands, and other tissues. The highest expression levels were by far determined in testis. In the mouse, highest expression levels were measured in heart and brain, followed by testis, kidney, ovary, liver, spleen, lung, and thymus. The up regulation of the *AHRR/Ahrr* expression by various AhR agonists has been demonstrated *in vitro* in various human, mouse, and rat cancer cell lines and *in vivo* (rat and mouse) (Mimura et al., 1999) (Tsuchiya et al., 2003) (Bernshausen et al., 2006) (Fujii-Kuriyama et al., 2010). Mimura and co-workers identified *in vitro* employing mouse reporter gene studies that the AhRR is a negative regulator of the AhR signalling pathway (Mimura et al., 1999). They suggested that the negative feedback regulation of the AhR by the AhRR is either based on the competition for its heterodimerization partner ARNT or competitive binding of the AhRR/ARNT-complex to the XREs (Mimura et al., 1999). Evans et al. revealed that the AhRR-mediated repression of AhR signalling is not based on sequestration for ARNT and that binding of the AhRR/ARNT-complex to the XREs is not a prequisite, but contributes to the repression. They proposed that AhRR repression of AhR signalling is possibly the result of protein-protein interactions with promoter-bound transcription factors, e.g. by essential coactivators or by a direct interplay between the AhR and AhRR (Evans et al., 2008). The involvement of the *AHRR* as potential tumour suppressor gene in a variety of human cancers has been suggested (Zudaire et al., 2008).

CD36, also known as thrombospondin receptor, is a member of the class B type of scavenger receptor family. Cluster of differentiation 36 (CD36) is a transmembrane glycoprotein with a variety of functions and is therefore expressed by a broad range of cell types and tissues including adipocytes, heart muscle, vascular endothelium, erythrocytes, monocytes/macrophages, platelets, and various others (Febbraio et al., 1999) (Zhang et al., 2003) (Saxena et al., 2012). CD36 binds various divergent ligands including thrombospondin, collagen, oxidized low density lipoproteins (LPL), long-chain fatty acids, native lipoproteins, oxidized phospholipids, and apoptotic cells (Silverstein et al., 1992) (Febbraio et al., 1999) (Zhang et al., 2003) (Bonen et al., 2004) (He et al., 2011). Results derived from various *in vitro* and *in vivo* studies suggest that CD36 mediates atherosclerosis, type 2 diabetes, obesity, inflammation and oxidative stress in various cell types (Febbraio et al., 1999) (Bonen et al., 2004) (He et al., 2011) (Saxena et al., 2012). Its role in fatty liver diseases has been characterized and elucidated in recent studies. Fatty acid transports into the liver is facilated by CD36 and fatty acid binding proteins (FABPs). Significantly increased CD36 levels were determined in patients diagnosed with the non-alcoholic fatty liver disease (Greco et al., 2008). A direct involvement of CD36 in the development of the AhR-regulated hepatic steatosis by TCDD has been demonstrated by Lee and co-workers. Transgenic mice, expressing a constitutively active *Ahr*, exhibited a significant hepatic induction of CD36 indentified by microarray, RT-PCR, Northern and Western blot analysis compared to wild-type animals. Additionally, in livers of *Ahr* wild-type mice treated with TCDD (30 µg/kg bw; sacrificed seven days later), the induction of CD36 was also observed which was not seen for *Ahr* knockout mice. They identified the human and mouse *CD36/Cd36* gene promoters as

transcriptional targets for the aryl hydrocarbon receptor. To further elucidate the role of CD36 in the TCDD-induced hepatic steatosis, Lee and co-workers created mice lacking the *Cd36* gene. TCDD (30 µg/kg bw; sacrificed seven days later)-treated wild-type mice featured significantly increased hepatic triglyceride and reduced plasma triglyceride levels, whereas no statistical alterations in hepatic and plasma triglyceride concentrations were determined in TCDD- and corn oil-treated *Cd36* knockout mice (Lee et al., 2010). Lee and co-workers hence showed that *Cd36* is an AhR target gene which plays a key role in AhR-mediated hepatic steatosis in mice.

The performed microarray experiments elucidated that there are distinct differences between species (human vs. mouse) and between different cellular models (HepG2 vs. hHeps). Considering the fact that the numbers of differently regulated genes was the lowest in hHeps, primary human hepatocytes seem to be less sensitive towards TCDD. Nevertheless, to estimate the potential human risk a broad range of experimental testing (primary cells, human lymphocytes as well as target organ slices) is essential.

For the quantitative verification of the five selected target genes the mRNA expression of *ALDH3A1*, *HSD17B2*, *TIPARP*, *AHRR*, and *CD36* were determined by RT-PCR. Real-time PCR analysis is the most sensitive experimental method for mRNA quantification. A data summary is featured in Table 39 below. Some difficulties had to be solved when analyzing the microarray data from HepG2 cells. Therefore, the colour intensity value was reduced from 7 to 5. For instance *CYP1B1*, an established AhR-regulated gene whose induction represents a marker for AhR activation due to exposure to DLCs, was assigned a high log2 fold-change, but had a lower colour intensity value compared to the selected cut-off value ($A \geq 7$). Real-time PCR analysis revealed that the *CYP1B1* mRNA expression was in fact strongly induced. *AHRR* was additionally among the up regulated genes but its colour intensity was also reduced ($A = 5.63$). Real-time PCR analysis demonstrated that the *AHRR* mRNA expression levels were not significantly induced. These findings elucidate that it is important to verify after the selection of a target gene from microarray study, if the mRNA expression of the respective gene is in fact induced, eg. by RT-PCR. *CD36* was not up regulated in the performed microarray experiment in HepG2 cells, but a slight up regulation (2.2-fold) was determined by RT-PCR, the more sensitive mRNA quantification method.

Table 39. Regulation of five selected target genes in HepG2 cells and hHeps evaluated by microarray and RT-PCR analysis. Treatment TCDD (10 nM, 24 h).
Selected parameters microarray: $A \geq 5$, log2 fc ≥ 1, p-value ≤ 0.05.
Annotations: '↑' up regulation;
'↓' down regulation;
'→' neither up nor down regulation

Gene	HepG2		hHeps	
	Microarray	RT-PCR	Microarray	RT-PCR
ALDH3A1	↑	↑	↑	↑
HSD17B2	↑	↑	↑	↑
TIPARP	→	→	↑	↑
AHRR	↑	→	→	→
CD36	→	↑	→	→

Among the selected target genes only *ALDH3A1* was induced to a higher extend after exposure to TCDD in both human cell models. The induction of the *ALDH3A1*mRNA seems to be the most reliable marker for AhR activation after exposure to TCDD and related compounds in human liver models. A concentration-dependent increase of *ALDH3A1* mRNA expression was determined in HepG2 cells after treatment with various concentrations of TCDD leading to the highest *ALDH3A1* levels after application of the highest chosen concentration (10 nM). Higher TCDD concentrations should be subsequently analyzed and ALDH3A1 protein levels ought to be additionally determined, e.g. by Western blot analysis. Furthermore, the concentration-dependent expression and inducibility of *ALDH3A1* should be also analyzed in primary human hepatocytes using various concentrations of TCDD and other DLCs. Moreover, the functions and actions in which ALDH3A1 is possibly involved in TCDD-mediated biological and toxic responses should be further characterized.

HSD17B2 was also induced in both human liver models though the inducibility was very weak, but statistically significant in both experimental approaches. Although this gene is the only gene among the five selected novel AhR target genes which was induced in both human cell models as well as in mouse livers, it is not a suitable and reliable marker for exposure to DLCs due to its rather weak inducibility (2- to 3-fold). However, the biological functions and actions of HSD17B2 should be further elucidated since transgenic mice which ubiquitously expressed the human *HSD17B2* gene exhibited phenotypic changes such as growth retardation and disrupted spermatogenesis which are typical indications also for suppressed retinoic acid signalling (Zhongy et al. 2007). In which way HSD17B2 potentially contributes to the TCDD-induced AhR-mediated deregulation of the retinoic acid signalling is also subject to further research investigations (Abbott et al., 1989) (Fletcher et al., 2001) (Murphy et al., 2007) (Jacobs et al., 2011).

TIPARP was only induced in primary human hepatocytes and in mice, but not in HepG2 cells. Its inducibility was weak, but statistically significant by the applied concentration/dose in mouse livers and hHeps. The TCDD-mediated induction of *TIPARP* has been linked to TCDD-induced suppression of gluconeogenesis (Diani-Moore et al., 2010). For human risk assessment, it is essential to characterize and elucidate its functions and actions in the human organism because it has been recently characterized as negative regulator of AhR signalling in various human cell lines as well as in mouse embryonic fibroblasts (MacPherson et al., 2013).

Based on the gained knowledge from the performed microarray experiments, *Ahrr* and *Cd36* are predominantly involved in TCDD-mediated responses in mouse. CD36 contributes to the AhR-mediated TCDD-induced uptake of free fatty acids which leads to the formation of a hepatic steatosis in mouse. However, elevated CD36 levels have been examined in patients with non-alcoholic fatty liver disease which leads to the suggestion that CD36 is a key player in the uptake of free fatty acids also in the absence of TCDD. Additional research effort is required to confirm whether or not it contributes to the TCDD-mediated biological effects in humans.

The performed microarray studies provided fundamental information about species- and cell type-specific gene expression responses. Unfortunately, no suitable in common biomarker for both species could be established, but novel species-specific markers for AhR activation were identified as well as novel TCDD-inducible genes were successfully characterized.

V Conclusive Summary

Polychlorinated dibenzo-*p*-dioxins, dibenzofurans, and polychlorinated biphenyls are persistent environmental contaminants which occur as complex mixtures and bioaccumulate in the food and feed chain due to their high lipophilic properties. Dioxin-like compounds (DLCs) evoke a broad spectrum of biological and toxic responses in laboratory animals and in humans. Most, if not all, of these effects are mediated by the aryl hydrocarbon receptor. Although the exposure levels decreased noticeably over the last few decades in most European countries, sensitive population groups, such as newborns and infants or humans being occupationally or accidentally exposed to DLCs are subjected to much higher exposure levels than those the WHO established as tolerable daily intake.

The present work ought to examine the elicited biochemical responses of a selection of dioxin-like compounds in mouse (*in vivo*) and in human liver cell models (*in vitro*). Emphasis was given to the main contributors to the total toxic equivalents in human blood and tissues TCDD, 1-PnCDD, 4-PnCDF, PCB 118, PCB 126, and PCB 156 which likewise contribute about 90 % to the total dioxin-like activity in the human food chain. Therefore, various experimental test systems such as the EROD assay, RT-PCR, HPLC-MS/MS, or microarray were established, optimized, and adjusted to the specific experimental requirements.

The 3-day and 14-day mouse studies were performed within the framework of the SYSTEQ project in the Institute for Risk Assessment Sciences (IRAS) at Utrecht University, the Netherlands. Female C57BL/6 mice were treated with single doses of TCDD, 1-PnCDD, 4-PnCDF, PCB 118, PCB 126, PCB 156, or non dioxin-like PCB 153 by oral gavage. Oral gavage was used as route of administration since ingestion of food is the major route for human exposure to DLCs. The hepatic mRNA expression of three selected genes (*Cyp1a1*, *Cyp2b10*, and *Cyp3a44*) was determined in both mouse studies. The respective enzyme inductions are associated with the activation of different xenobiotic signalling pathways (AhR, CAR, and PXR). The seven tested congeners can be classified into three different categories based on the obtained findings; the ones which are 'pure' AhR ligands (TCDD, 1-PnCDD, 4-PnCDF, and PCB 126), or solely CAR inducers (PCB 153), and the ones which are AhR/CAR mixed-type inducers (PCB 118 and 156).

Moreover, a novel experimental approach, the microarray analysis, was employed in the present work which permitted the analysis of thousands of genes simultaneously in female mouse liver samples from mice treated with single doses of TCDD or PCB 153 (mouse study I). In summary, the gene regulation patterns differed fundamentally. Profiling of significantly altered genes led to the conclusion that changes in gene expression were associated with different signalling pathways, in fact by AhR and CAR. The established classic AhR-regulated target genes involved in xenobiotic metabolism were induced by TCDD in mouse livers. Furthermore, the alterations in expression of genes associated with lipid metabolism and transport implied that TCDD likely induced hepatic steatosis in female C57BL/6 mice. PCB 153 treatment on the contrary resulted in the up regulation of genes linked to arachidonic acid metabolism suggesting that the deregulation of the arachidonic acid signalling possibly

contributes to the biological responses of NDL-PBCs as indicated by previously performed studies.

The characterization of AhR-dependent and AhR-independent responses was a major research objective within the present work, since overwhelming experimental evidence led to the conclusion that the AhR mediates the biological and toxic effects of DLCs. For investigating the role of the AhR in mediating biological responses, several experimental approaches were carried out such as the analysis of blood plasma metabolites in *Ahr* knockout and wild-type mice. In order to determine genotype specifics and similarities, a metabolite extraction method and HPLC-MS/MS setup was developed and successfully established. Several plasma metabolites could be identified in both genotypes such as various amino acids, but also differences detected as additional peaks in the UV chromatograms, were determined. It was not possible to characterize these $Ahr^{-/-}$-specific peaks, most likely due to the similar polarity of these 'hidden' metabolites. However, the gained knowledge from the performed experiment was used as a starting point for novel research approaches in our working group such as the analysis of whole blood metabolites in *Ahr* knockout and wild-type mice extending the initiated metabolomics database.

An animal experiment was performed aiming to characterize AhR-dependent and AhR-independent effects in female *Ahr* knockout and wild-type mice, which received a single dose of TCDD or corn oil by gavage. Microarray analysis of the mouse livers revealed that although the *Ahr* gene was knocked out in $Ahr^{-/-}$ mice, the quantity of affected genes were in the same order of magnitude as for $Ahr^{+/+}$ mice, though the pattern of altered genes distinctly differed. Furthermore, only a vanishingly small number of altered genes could be linked to specific metabolic pathways in livers of female $Ahr^{-/-}$ mice. As opposed to this, a large number of genes in livers of female $Ahr^{+/+}$ could be associated to different metabolic signalling pathways such as xenobiotic metabolism including established and novel AhR target genes or genes linked to lipid transport and metabolism. Further findings, such as the significantly increased relative liver weights of TCDD-treated $Ahr^{+/+}$ mice supported the assumption, that TCDD induced the development of hepatic steatosis in female *Ahr* wild-type.

The performed *in vitro* experiments aimed to analyze the effects elicited by selected DLCs and PCB 153 in human liver cell models. The human hepatocellular carcinoma cell line HepG2 and freshly isolated primary human hepatocytes were used in the present work to identify similarities and differences between both human cell models. The biological responses were measured by EROD assay, Western blot, RT-PCR, or microarray analysis. The measured endpoints provided important knowledge about the congeners' potencies, the so called relative effect potencies (REPs), which were not evaluated in human liver cell models for most of the congeners so far.
In vitro REPs gained from both liver cell models widely confirmed the current TEFs (van den Berg et al., 2006), but some deviations occurred, e.g. in case of 1-PnCDD and 4-PnCDF, which are both attributed with high TEF values. These findings outline that a comprehensive analysis of DLCs in different human *in vitro* models is essential for assessing the 'complete' *in vitro* potencies.

A general comparison between both liver cell models revealed that primary human hepatocytes were less responsive than HepG2 cells. This was not only observed by the comparison of EC values derived from EROD assay, but also regarding microarray analysis in terms of differently regulated genes. The comparison of the significantly TCDD-altered genes in both human cell types revealed that only a considerably small number of genes (25 in total) was in common up regulated by both human liver cell models such as the established AhR-regulated highly inducible cytochrome P450s *1A1*, *1A2*, and *1B1* as well as other AhR target genes. Although the overlap was rather small, the TCDD-induced genes could be associated with the broad spectrum of dioxin-related biological responses on e.g. cell cycle regulation, cellular growth and differentiation, or apoptosis.

The gene expression pattern in primary human hepatocytes after treatment with selected DLCs (TCDD, 1-PnCDD, 4-PnCDF, and PCB 126) and PCB 153 was additionally characterized by microarray analysis. This was the first time that the alterations in gene expression by the four DLCs attributed with the highest TEF values were examined in a toxicogenomic approach in primary human hepatocytes together. The highest response in terms of significantly altered genes was determined for TCDD, followed by 4-PnCDF, 1-PnCDD, and PCB 126, whereas exposure to PCB 153 did not evoke any significant changes in gene expression. The pattern of significantly altered genes was very homogenous among the four congeners. Genes associated with well-established DLC-related biological responses as well as novel dioxin-inducible target genes were identified. An extensive overlap occurred resulting in 25 in common up regulated genes by all four DLCs. These 25 represent almost the complete set of significantly up regulated genes by the least responsive congener (i.e. PCB 126).
In conclusion, the results from the *in vitro* experiments in primary human hepatocytes provide fundamental insight into the congeners' potencies and caused alterations in gene expression patterns. The obtained findings implicate that although the extent of enzyme inducibilities varied, most likely based on the interindividual variabilities (e.g. gender, age, ethnicity, or health status), the gene expression patterns are coincidental. The microarray analysis is an essential tool in the field of toxicogenomics which enables the possibility to further elucidate the molecular mechanisms of the toxic effects induced by DLCs in humans.

The identification of novel quantifiable biomarkers for AhR activation by DLCs was a major research objective within the present work. For this purpose, the obtained results from several microarray experiments which dealt with the TCDD-induced alterations in gene expression were analyzed and compared. As a result, five genes were selected as potential biomarker candidates, i.e. the aldehyde dehydrogenase 3 family member A1 (*ALDH3A1*), the hydroxysteroid (17-beta) dehydrogenase 2 (*HSD17B2*), the TCDD-inducible poly(ADP-ribose) polymerase (*TIPARP*), the aryl hydrocarbon receptor repressor (*AHRR*), and cluster of differentiation 36 (*CD36*). Species-specific (mouse vs. human) as well as model-specific (*in vitro* vs. *in vivo* and transformed cells vs. untransformed cells) differences were identified. *ALDH3A1* turned out to be the most reliable and suitable marker for exposure to DLCs in both human liver cell models eliciting the highest mRNA inducibility among the five chosen candidates, whereas it was not up regulated in the mouse liver *in vivo*. *TIPARP/Tiparp* was identified as a good indicator for dioxin exposure in hHeps and in mouse livers, though the extent of mRNA inducibility was several times lower as for *ALDH3A1*. *Cd36* and *Ahrr* were

both characterized as dioxin-inducible target genes in mouse livers. Although *HSD17B2/Hsd17b2* was significantly induced by TCDD *in vitro* and *in vivo*, the up regulation was only weak suggesting that this gene is not suitable to use as a sensitive biomarker for exposure to DLCs. The molecular functions and actions in which way these species- and cell type-specific markers are involved in the dioxin-mediated biological and toxic responses should be further characterized *in vivo* and *in vitro*. The search for sensitive biomarkers for exposure to DLCs should be continued and extended, e.g. by analyzing tissue and blood samples obtained from epidemiological studies.

The present work provides essential knowledge about the biological responses and relative potencies of a variety of dioxins and dioxin-like compounds in human liver cell models and in mouse. Established as well as novel dioxin-related responses were demonstrated and elucidated in the performed experimental approaches contributing fundamental information for human risk assessment.

VI Methods

VI.1 *in vivo* Mouse Experiments

The 3-day and 14-day mouse studies were performed within the framework of the European project SYSTEQ in the *Department of Toxicology, Institute for Risk Assessment Sciences (IRAS)* at Utrecht University, the Netherlands.
Blood samples and different tissues were shipped to the different European project partners. We obtained snap frozen liver samples for further investigation. During a research stay as a part of this doctoral thesis at the IRAS, liver RNA was isolated and cDNA prepared from both mouse studies which was analyzed in the present work.
The breeding of *Ahr* knockout mice and subsequent animal experiment was performed at the University of Kaiserslautern.

VI.1.1 Mouse Study I (3-day Study)

Female adult C57BL/6 mice were exposed to four dose levels of seven selected compounds (core congeners) TCDD, 1-PnCDD, 4-PnCDF, PCBs 118, 126, 153, and 156. Each dose group consisted of six female mice. On day 0, animals were orally exposed by gavage at a dosing volume of 10 ml/kg body weight. Test compounds were beforehand dissolved in corn oil. Control animals were exposed to corn oil only (dosing 0 µg/kg bw). On day 3, animals were killed by CO_2/O_2 asphyxiation. Blood and tissues were collected from animals, snap frozen, and stored at -80 °C.

Table 40. Overview dose levels mouse 3-day study.

Study	Treatment	Single dose (µg/kg bw)						TEF (WHO, 2005)
3-day	**TCDD**	0	0.5	2.5	10	25	100	1.0
	1-PnCDD	0	0.5	2.5	10	25	100	1.0
	4-PnCDF	0	0.5	2.5	10	250	1000	0.3
	PCB 126	0	5	25	100	250	1000	0.1
	PCB 118	0	5000	15000	50000	150000	500000	0.00003
	PCB 153	0	5000	15000	50000	150000	500000	-
	PCB 156	0	5000	15000	50000	150000	500000	0.00003

Due to initial investigative sample analysis from the project partners in the laboratories at the IRAS, it was decided only to perform RT-PCR analysis with the blue-marked dose-levels (Table 40). This decision was based on the large amount of time needed for sample preparation and analysis and therefore it was decided to skip the second highest dose level of TCDD, 1-PnCDD, 4-PnCDF, and PCB 126 because no further relevant additional information was expected. The lack of response determined in livers of mice exposed to PCBs in the first

performed experiments at Utrecht University with the PCBs lead to the decision to analyze only two dose levels (0 and 150000 µg/kg bw).

VI.1.2 Mouse Study II (14-day Study)

Female adult C57BL/6 mice were exposed to a single dose of the seven selected compounds TCDD, 1-PnCDD, 4-PnCDF, PCBs 118, 126, 153, and 156 by oral gavage at a dosing of 10 ml/kg bw (Table 41). Test compounds were dissolved in corn oil. Control animals were exposed to corn oil only (dosing 0 µg/kg bw). On day 14, animals were euthanized by CO_2/O_2 asphyxiation. Blood and tissues were collected from animals, snap frozen, and stored at -80 °C.

Table 41. Overview dose levels mouse 14-day study.

Study	Treatment	Single dose (µg/kg bw)		TEF (WHO, 2005)
14-day	**TCDD**	0	25	1.0
	1-PnCDD	0	25	1.0
	4-PnCDF	0	250	0.3
	PCB 126	0	250	0.1
	PCB 118	0	150000	0.00003
	PCB 153	0	150000	-
	PCB 156	0	150000	0.00003

VI.1.3 *Ahr* Wild-type / Knockout Mouse Study

VI.1.3.1 Breeding of *Ahr* Knockout Mice

The transgenic AhR mice ($Ahr^{+/-}$) were obtained from Jackson Laboratory (Bar Habor, ME). Breeding of *Ahr*-deficient mice ($Ahr^{-/-}$) was started at the Finnish Public Health Institute (Kuopio, Finland) and continued at the University Kaiserslautern. The strain was developed using a construct that removed exon 2 of the *Ahr* gene. The original Ahr^{tm1Bra} mutation has been crossed 10 times to C57BL/6. A summary of strain details is shown in the following table (Table 42): Homozygous *Ahr* knockout mice and homozygous *Ahr* wild-type mice were achieved by mating female and male heterozygous *Ahr* mice ($Ahr^{+/-}$). Mating of homozygous *Ahr* knockout mice was not possible due to reduced fertility of this genotype (Schmidt et al., 1996) (Fernandez-Salguero et al., 1996) (Mimura et al., 1997).

All mice were kept in the laboratory animal unit of the University of Kaiserslautern. The room was air-conditioned and artificially illuminated from 7 a.m. to 7 p.m. each day. Animals were subjected to regular health surveys consisting of serological and bacteriological screening. All mice were individually identified by earmarking.

The genotype of the offspring was characterized by DNA gel electrophoresis of the PCR-amplified DNA isolated from mouse tail or ear snips.

Table 42. Summary of strain details of transgenic *Ahr* mice (Jackson Laboratory, Bar Habor, ME).

Strain Name	B6.129-*Ahr*^{tm1Bra}
Stock Number	002831
Type	JAX®GEMM®Strain - Targeted Mutation Congenic
TJL Mating System	Heterozygote x Heterozygote
Generation	N12
ES Cell Line	R1 (129)
Donor Strain	129X1 x 129S1 via R1 (+$^{Kitl\text{-}SlJ}$) ES cell line
Donating Investigator	Dr. Christopher Bradfield, McArdle Laboratory for Cancer Research
Backcross Generation	N12F10 (15-jan-2003)
Background Strain	C57BL/6

VI.1.3.2 Mouse Genotyping

VI.1.3.2.1 DNA Isolation

First, mice (about 3-4 weeks of age) were narcotized and small pieces of the ear or tail were cut off by animal keepers. These snips were stored in sterile microtubes (1.5 ml) at -20 °C until DNA isolation. DNA from mouse tail or ear snips was isolated using E. Z. N. A. Tissue DNA Kit (Omega Bio-Tek) according to the manufacturer's instructions with a few modifications (Figure 52).

Primarily, mouse snips were brought to room temperature, whereupon 180 µl of Buffer TL and 25 µl proteinase K solution (50 mg/ml ddH_2O) were added to each sample. Proteinase K serves in combination with the Buffer TL for tissue lysis and digestion. The tissue-lysis-buffer solution was thoroughly mixed by vortexing for 2 min. Tissue lysis was then carried out at 56 °C in a microtube-adapted thermomixer (Eppendorf, Hamburg) overnight. The following steps were performed at room temperature. The digested samples were centrifuged for 2 min at maximum speed to pellet insoluble tissue debris and hair. Afterwards, the supernatant was carefully transferred into another sterile microtube (1.5 ml) and 200 µl of Buffer BL and 200 µl of ethanol (100 %) were added and mixed thoroughly by vortexing. Both components provide the basis for DNA binding to the column. Intermediately, a HiBind® DNA Mini column was activated by adding 100 µl of Equilibration Buffer and following centrifugation for 1 min at 13000 x g. The entire sample was then transferred onto the column, which was afterwards centrifuged for 1 min at 10000 x g. The flow-through was discarded and 500 µl of Buffer HB was added to bind the DNA. The column was centrifuged once again for 1 min at 10000 x g. The bound DNA was washed with 700 µl of Wash Buffer and was subsequently centrifuged for 1 min at 10000 x g. The washing step was repeated using 400 µl of Wash Buffer before centrifugation for 3 min at 10000 x g. Care was taken to completely dry the

membrane of the column because any ethanol residue interferes in the DNA elution process. The DNA containing column was placed into a sterile 1.5 ml microtube and 100 µl of preheated (70 °C) Elution Buffer was added directly on the membrane of the column. After resting for 2 min at room temperature, the column was centrifuged for 1 min at 10000 x g. The elution step was repeated one more time, before measuring the DNA quality and concentration using NanoDrop (Peqlab, Erlangen). The isolated DNA was then stored at -80 °C or directly amplified in PCR.

Figure 52. **Illustrated protocol of the DNA isolation method (Omega Bio-Tek, 2013).**

VI.1.3.2.2 Amplification of Mouse DNA using PCR

Polymerase chain reaction was invented 1983 by Kary Mullis (Mullis et al., 1987) and is nowadays a commonly used, fast method to amplify specific DNA sequences selectively and exponentially. This powerful tool finds many applications in diagnostics, molecular biology, and forensic analysis (Holland et al., 1991). PCR can be divided into three steps. First the double-stranded DNA template is converted into single-stranded DNA at 95 °C (denaturation). High temperature leads to the disruption of hydrogen bonds between complementary bases resulting in two single strands. Afterwards, primers (oligonucleotides consisting of 15-30 bases with complementary DNA sequence to the targeted DNA) anneal

complementary to DNA strands at 53 °C (annealing). As a last step, the polymerase binds to the primer template and is then able to add desoxynucleotides (dNTPs) at 72 °C (elongation), whereupon a primer-containing DNA fragment is selectively replicated. In each elongation step the amount of target DNA is doubled resulting in an exponential amplification of the DNA sequence. The amplification product is afterwards detected by DNA agarose gel electrophoresis.

First, a PCR reaction mix was prepared on ice using PCR master mix (consisting of Taq polymerase 0.05 U/µl, 0.4 mM of each dNTP, reaction buffers, 4 mM $MgCl_2$, and nuclease-free water), primers (Table 44) and isolated DNA (from mouse tail or ear snips). Then, PCR tubes were tightly closed, carefully mixed on a vortexer and centrifuged. The PCR reaction mix was placed into a MyCyler (Bio-Rad, Munich) running the optimized and established PCR programme (Table 45). After completing the PCR, amplified DNA was stored at -20 °C.

Table 43. Components of PCR reaction mix for mouse genotyping.

Components	Volume (µl)	Purchased from
PCR Master Mix (2x)	12.5	Fermentas
Primer forward *Ahr* wild-type	1	Eurofins MWG Operon
Primer reversed *Ahr* wild-type	1	Eurofins MWG Operon
Primer forward *Ahr* knockout	1	Eurofins MWG Operon
Primer reversed *Ahr* knockout	1	Eurofins MWG Operon
DNA template	8.5	-

Table 44. Primer sequences for mouse genotyping.

Primer	5`- 3`
Ahr wild-type	GACACAGAGACCGGCTGAAC
	AGCATGTACCATCCAAACAGC
Ahr knockout	TGAATGAACTGCAGGACGAG
	AATATCACGGGTAGCCAACG

Table 45. PCR thermocycling conditions for mouse genotyping.

Cycle	Temperature	Time	Step
1 Cycle	95 °C	4 min	Denaturation
40 Cycles	95 °C	40 s	Denaturation
	53 °C	40 s	Annealing
	72 °C	40 s	Elongation
1 Cycle	72 °C	10 min	Elongation

VI.1.3.2.3 DNA Agarose Gel Electrophoresis

Different-sized DNA fragments were separated using DNA agarose gel electrophoresis. The 1.5 % agarose gel was prepared by melting 0.75 g of agarose dissolved in 50 ml of TAE buffer (1x; further information is featured in Table 46) in a microwave. After cooling down of the heated agarose solution (about 50 °C) 10 µl of ethidium bromide (10 mg/ml) was added. The ethidium bromide-containing agarose solution was carefully casted in a horizontal gel chamber. Bubbles were removed and a comb was inserted into the still liquid gel forming 10 sample pockets. After the hardening of the gel (30-40 min), the gel chamber was filled completely with TAE buffer (1x) and the comb was carefully removed. After adding 5 µl of 6x loading buffer (Fermentas) to the amplified DNA (25 µl), 15 µl of the DNA/loading buffer mix was pipetted into each sample pocket sparing one of the ten pockets in which 5 µl of DNA ladder was loaded. Gel electrophoresis was conducted for 75-90 min at 90 V. The negatively-charged DNA (due to the pH of TAE buffer) migrates through the agarose gel to the anode, whereby small DNA fragments move faster than larger ones. Ethidium bromide intercalates with the DNA and those fluorescent DNA-ethidium bromide products can be visualized using ultraviolet light. The separated DNA fragments were then detected by taking a picture with the Eagly Eye II (Stratagene). Sizes of DNA fragments were determined using the DNA ladder (Fermentas). The evaluation of the results was conducted by analyzing the DNA fragement size distribution pattern. If only one detected DNA fragment of 380 base pairs was detected the genotype of the respective mouse is homozygous *Ahr* wild-type ($Ahr^{+/+}$). One band at 500 base pairs implies the mouse genotype is homozygous *Ahr* knockout ($Ahr^{-/-}$). Two bands (380 and 500 base pairs) stand for heterozygous *Ahr* mice ($Ahr^{+/-}$).

Table 46. TAE (Tris-acetate-EDTA) buffers.

TAE buffer (50x)	Tris (2 M)	242.2 g
	EDTA (50 mM)	14.6 g
	Acetic Acid (1 M)	57.2 ml
	ddH_2O	up to 1 l
	pH: 8.3	
	Store at room temperature	
TAE buffer (1x)	TAE buffer (50x)	20 ml
	ddH_2O	up to 1 l
	Store at room temperature	

VI.1.3.3 Mouse Plasma Analysis

VI.1.3.3.1 Mouse Plasma Extraction

Ahr wild-type and *Ahr* knockout mice were kept in the animal laboratory of the University Kaiserslautern. Mice were given standard pelleted feed and tap water ad libitum during a 12h/12h day and night cycle. To analyze the plasma of untreated *Ahr* wild-type and knockout mice, animals were anesthetized by intraperitoneal application of 3 µl/1g bw pentobarbital solution (33 mg/ml ddH_2O). In complete absence from pain, the abdominal cavity was opened and the gastro-intestinal system was thrusted aside. Mouse blood was collected from *vena cava* using a syringe which was pre-flushed with heparin. The blood was transferred into a sterile 1.5 microtube and immediately centrifuged at 2000 x g at room temperature for 15 min.

Plasma extraction was carried out using the approach of Want et al. (2006) with a few modifications. First, cold (-20 °C) methanol (100 %) was added to the isolated plasma in a ratio of 2:1, whereupon the methanol-plasma mix was vortexed, and incubated on ice for 20 min. Afterwards, the mix was centrifuged at 13000 x g for ten minutes at 4 °C. The supernatant was transferred into sterile 1.5 microtube leaving the precipitated proteins left behind. The plasma extract was subsequently dried using a vacuum centrifuge Univapo 150 H. Until the plasma analysis by HPLC-MS/MS, the dried samples were stored at -20 °C.

VI.1.3.3.2 Plasma Analysis

VI.1.3.3.2.1 High Pressure Liquid Chromatography (HPLC)

High pressure liquid chromatography (HPLC) is a powerful tool to separate components of a matrix such as blood plasma or serum using two different phases such as a stationary and a mobile phase. The mobile phase carries a mixture of substances when passing the stationary phase. Due to interactions with the stationary phase the elution of some substances is delayed, because of their physical and chemical properties, while other compounds just weakly interact with the stationary phase and are not held back resulting in an earlier compound elution and signal detection. Mechanisms of compound separation include the equilibrium distribution of the analyte between both phases as well as adsorption and desorption at the stationary phase.
A distinction is made in HPLC methods between the different stationary phases, the normal phase (NP) and reversed phase (RP). In NP-HPLC a nonpolar, mobile phase passes through a polar, stationary phase. Typical materials of polar, stationary phases are anionic adsorbent agents such as silicagel or aluminium oxide, which possess hydroxyle groups on their surface. RP-HPLC, on the other hand, is based on the principle of a polar, mobile phase which is transported along a nonpolar, stationary phase. Silica, whose surface has been modified by alkyl dimethyl chlorsilane, is used as a stationary phase. Polar fluids like acetonitrile, methanol, or water are used as mobile phase (Cammann, 2001) (Meyer, 2002).

The setup of a HPLC system is featured in Figure 53. A solvent mixture, the mobile phase, was conveyed through one or more pumps after degassing in the storage vessel. The dissolved sample is injected into the system using a valve. Separation of analytes occurs on the chromatographic column, which can be thermalized by the use of a column oven. Separated sample components can then be detected using an appropriate detector (Cammann, 2001).

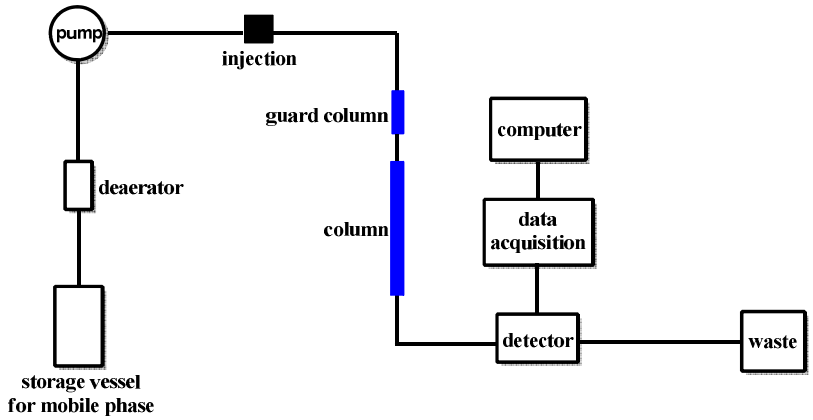

Figure 53. Scheme of a HPLC system (modified after Cammann, 2001).

One the one hand, the choice of the utilized detector is based on the special characteristics of the analytes of interest, and on the other hand, it is dependent onthe system's conditions (such as the selection of solvents, elution conditions, and transportation rate). Various detectors are established for HPLC systems such as evaporative light scattering detectors (ESLD), refractive index detectors (RID), UV-Vis detectors, fluorescence detectors, chemo-luminescence detectors, electrochemical detectors, or mass detectors (Cammann, 2001).

VI.1.3.3.2.2 UV Spectrometry

Ultraviolet/visual spectrometry is a physical method measuring light absorption by an analyte in the ultraviolet and visible range. UV/VIS absorption spectroscopy is based on the excitation of outer shell electrons by light in the ultraviolet and visible wavelength`s spectrum. Worldwide, absorption is the most frequently applied optical and analytical procedure to detect molecules in UV/VIS spectral range; however analytes must obtain at least one chromophoric group such as a carbonyl group or an aromatic ring. UV/VIS detectors possess high sensitivity, large linear range, and insensitivity against variations in temperature. They can be divided into different categories. A fixed wavelength detector only captures the sample absorption at one specific wavelength (depending on the specific applied filter, commonly 254 nm). A variable wavelength detector is an alternative to the first one mentioned. Using a variable wavelength detector has the advantage that the measured wavelength can be exactly applied to the sample´s absorption maximum. A diodearray detector (DAD) provides the opportunity to detect various wavelengths simultaneously by the use of many photodiodes (512 to 1024 diodes).

The diodearray detector offers the possibility of a high throughput screening and analysis of the applied matrix (Cammann, 2001) (Meyer et al., 2002).

VI.1.3.3.2.3 Mass Spectrometry

Mass spectrometry is a physical process that separates ions which are stable in the vacuum according to their respective mass to charge (m/z) ratio. Mass spectrometric analysis usually ensues under molecule fragmentation, or atomization and subsequent ionization of the sample (as gas, fluid, solid, and mixtures) which is then inserted into the vacuum of the mass spectrometer. Fragmentation of compounds depends on the chosen ionization method. Mass spectrometry is increasingly utilized in the field of qualitative and quantitative analysis of elements and molecules due to its speed, selectivity, and sensitivity. The identification of complex compound mixtures and the quantification in trace and ultra trace level is the focus of organic compound analysis. Commonly, organic compounds can be quantitatively detected until the range of 10^{-12} to 10^{-17} mol using mass spectrometry (Cammann, 2001).

The mass spectrometer is basically structured into an inlet system which transports the sample into the unit's vacuum, an ionization unit, a mass separation unit, and finally a detection unit. The sensitivity of a mass spectrometer depends on the amount of inserted analyte and the obtained ion yield. In MS analysis, the inserted substances must be transferred into free positively or negatively charged ions in order to be separated according to their mass to charge ratio by the applied electronic high voltage. Ion velocity is the result of the kinetic energy obtained from the ionization process and subsequent acceleration in the electrical field (Cammann, 2001).

VI.1.3.3.2.4 HPLC-ESI-MS/MS

Primarily, the HPLC eluate is transferred into an interface in which compound ionization takes place. Different ionization techniques are available, though the choice depends on the examined compound properties. In the present work, electrospray ionization (ESI) was used under atmospheric pressure before molecular ions can enter the mass unit in which mass separation and detection takes places using three linear arranged quadrupoles (triple quadrupoles) in high vaccum.

Electrospray ionization (ESI)

Electrospray ionization (ESI) belongs to the group of so called 'soft' ionization techniques. ESI is particularly suitable for already ionized compounds and compounds which can be easily protonated or deprotonated without fragmentation of large and sensitive molecules.

Molecular ions and quasi-molecular ions for example $[M+H]^+$, $[M+Na]^+$, or $[M-H]^-$ are generated using the ESI method. Those ions are formed by adding or subtracting a hydrogen or a sodium atom to the compound`s molecular mass/structure (Cammann, 2001). The ESI process is featured in the following figure:

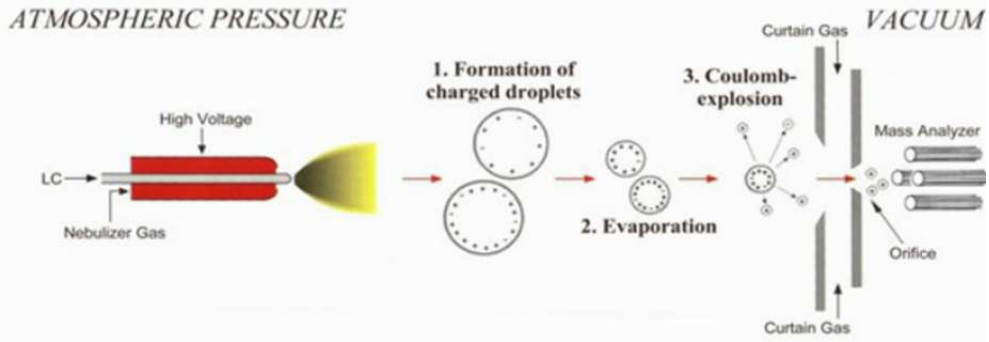

Figure 54. Analyte ionization using ESI (AB Sciex, 2010).

Elution solvent containing analytes are transported through a capillary biased by a high voltage into the ionizationunit (interface). Nitrogen acting as nebulizer gas is added simultaneously resulting in the formation of small charged droplets at the capillary tip. Due to the continuously evaporation of the solvent, the charge density increases on the droplet's surface. When the droplet`s charge compared to the surface exceeds the 'Raylight limit', the resulting Coulomb explosion leads to the formation of smaller charged daughter droplets. Those charged daughter droplets are then transferred through the orifice plate into the mass spectrometer in which mass separation and detection takes places in high vacuum (Cammann, 2001) (Fenn et al., 1989).

Tandem mass spectrometer

The most prevalent principle for mass separation is the quadrupole mass filter. The quadrupole filter consists of four parallel rod electrodes arranged in a concentrical manner, where each opposing rod pair is attached to a variable polarized direct current for given a DC voltage and RF frequency supply. Additionally, the system is superimposed by a high frequency voltage. Therefore, only ions with one m/z (mass filter) are able to reach the mass detector in stable helical trajectories by passing through electrodes.

The triple quadrupole consists of three linear arranged quadrupoles (Q1-Q3) as featured in Figure 55. In Q1 all ions are scanned according to their mass to charge (m/z) ratio. Q2 is defined as quadrupole although it is a collision cell. Due to the entering gas (N_2) and applied voltage, selected ions are fragmented. Afterwards, the mass to charge ratios of resulting fragment ions are determined in Q3.

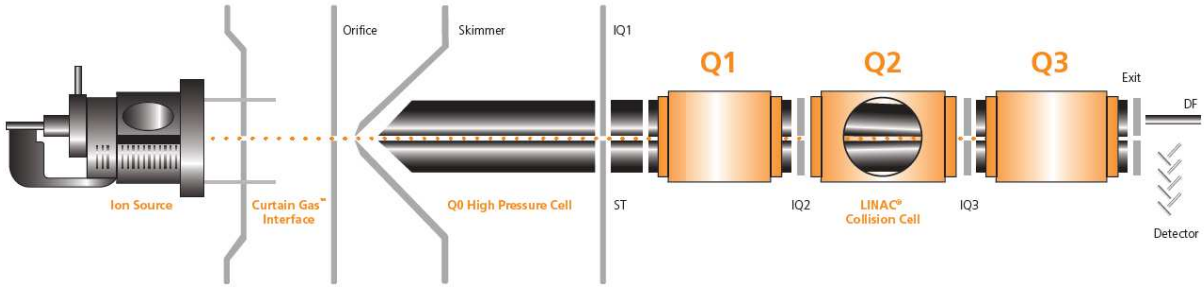

Figure 55. Scheme of a triple quadrupole mass analyzer (AB Sciex, 2010).

Different types of MS/MS experiments can be performed depending on the respective research objective. In the present work the method 'product ion scan' was used for identification of single components of the mouse plasma extract. The procedure is featured in the following figure:

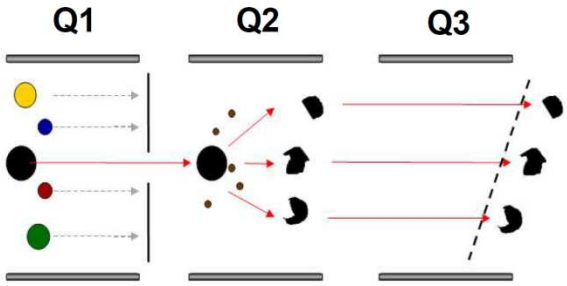

Figure 56. Scheme of product ion scan procedure (AB Sciex, 2008).

The precursor ion of interest can selectively pass through Q1 and is transferred into Q2. Precursor ions with the selected mass to charge ratios are fragmented in the collision cell and the generated fragment ions are detected in Q3 using a predefined m/z range (Cammann, 2001).

VI.1.3.4 Mouse Study III (5 days)

Four female mice of each genotype (*Ahr*$^{-/-}$ and *Ahr*$^{+/+}$ between 6 and 8 months old) received either a single dose of TCDD (25 µg/kg bw) or corn oil by gavage on the first day (day 1). The application volume was 2.5 ml/kg bw. All mice were housed separately in Makrolon cages throughout the experiment. On the 5th day, the mice were anesthetized by intraperitoneal application of 3 µl/1 g bw pentobarbital solution (33 mg/ml ddH_2O). In complete absence from pain, the abdominal cavity was opened and the gastro-intestinal system was thrusted aside. Mice livers were extracted surgically from animals, cut into slices, immediately snap frozen in liquid nitrogen and stored until use at -80 °C.

VI.2 *in vitro* Experiments

Cells were kept during cultivation respectively subcultivation and compound exposure in an incubator under standard conditions (37 °C, 5 % CO_2 and 97 % humidity) in a sterile atmosphere using disposable pipettes and autoclaved glass materials. All solutions which were in direct contact with cultured cells were prior tempered at 37 °C in a water bath. Both experimentally applied human liver cell models were exposed to test compounds for 24 h.

VI.2.1 Primary Human Hepatocytes

Freshly prepared primary human hepatocytes (hHeps) were purchased from LONZA (Verviers, Belgium). Cells were isolated from single donors and were plated on collagen-coated 6- and 96-well plates. Detailed donor information, if possible, including age, gender, ethnic background, and health status (smoking, alcohol, diabetes, heart disease, hypertension, liver pathology) was entailed in each delivery, whereas all donors were tested negative for HIV 1, HBV und HCV. Viabilities of hHeps were between 82-95 %.

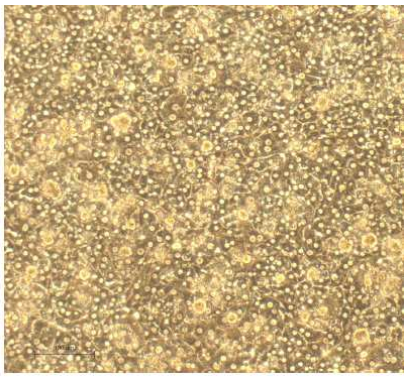

Figure 57. Primary human hepatocytes in culture (light microscope picture, 10x resolution).

VI.2.1.1 Handling of Primary Human Hepatocytes

Freshly prepared human hepatocytes (hHeps) were delivered within 48 h after isolation from donor livers. Cells were plated on collagen-coated multiwell plates filled with Hepatocytes Maintenance Medium (HMM™) representing the shipping medium. Primary human hepatocytes were cultivated using manufacturer's instruction. After arrival, the sealing cover was carefully peeled off from the multiwell plates and hHeps were stored for 2-3 h in an incubator under standard conditions. This procedure was necessary so that hHeps could recover from the shipping process. Afterwards, the shipping medium was replaced by 200 µl HCM™ BulletKit solution consisting of Hepatocyte Basal Medium (HBM™) and Hepatocyte Culture Medium SingleQuots® (containing various supplements and growth factors including ascorbic acid, BSA-FAF, transferrin, insulin, hEGF, hydrocortisone, GA-1000) and test compounds (Table 47).

Table 47. Primary human hepatocytes culture medium according to Lonza (Verviers, Belgium).

hHeps culture medium	Hepatocyte Culture medium (HCM™) BulletKit	Hepatocyte Basal Medium (HBM™)	Basal Medium w/o phenol red
		Hepatocyte Culture Medium (HCM™) SingleQuots®	Supplements and growth factors including ascorbic acid, BSA-FAF, transferrin, insulin, hEGF, hydrocortisone, GA-1000
	Store at 4 °C, 4 weeks		

VI.2.2 Human Hepatocellular Carcinoma Cell Line HepG2

HepG2 which were purchased from DSMZ, Heidelberg, is a permanent human hepatoma cell line which was derived from the liver tumour of a fifteen year old Caucasian Argentine male with hepatocellular carcinoma in 1975. HepG2 cells grow in an adherent manner with a doubling time of 50 - 60 hours. The epithelial-like cells accumulate mostly as monolayers and in small aggregates. Cells secrete various plasma proteins such as albumin, transferrin, plasminogen and β-lipoprotein (Aden et al., 1979) (Knowles et al., 1980).

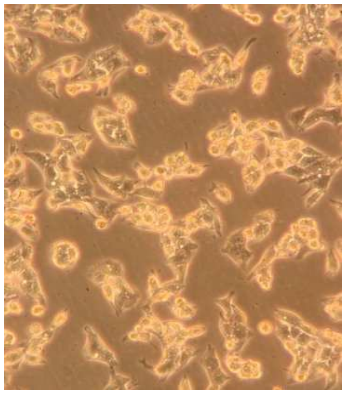

Figure 58. HepG2 cells in culture (light microscope picture, 10x resolution).

HepG2 cells were cultivated using the culture medium described in Table 48. Test compound incubation was carried out using the in Table 49 described incubation medium. The incubation medium consists of DMEM low glucose w/o phenol red, penicillin/streptomycine, and dexamethasone, but instead of FCS, DCC-FCS is used as growth stimulus. Dextran coated charcol-FCS is free of steroid hormones. DCC-FCS containing incubation medium is used to prevent any kind of interaction between steroids and the aryl hydrocarbon receptor because the AhR features similarities to the steroid receptor (Landers et al., 1991) (Schrenk et al., 1995).

Table 48. HepG2 cell culture medium for cultivation, e.g. subcultivation.

HepG2 culture medium	DMEM high glucose w/o phenol red	89 % (500 ml)
	Fetal calve serum (FCS)	10 % (56 ml)
	Penicillin/streptomycin	1 % (5.6 ml)
	Dexamethasone	10 nM (0.56 ml)
	Store at 4 °C, 4 weeks	

Table 49. HepG2 incubation medium for EROD, Western blot, Microarray, and RT-PCR.

HepG2 incubation medium	DMEM high glucose w/o phenol red	89 % (500 ml)
	Dextran coated charcoal-fetal calve serum (DCC-FCS)	10 % (56 ml)
	Penicillin/streptomycin	1 % (5.6 ml)
	Dexamethasone	10 nM (0.56 ml)
	Stored at 4 °C, 4 weeks	

VI.2.2.1 Thawing and Freezing of Cultured Cells

HepG2 cells were immediately stored at -84 °C in a biofreezer after arrival. Starting the cultivation was realized by thawing of the hepatoma cells. Therefore, cells (stored in a cryotube) were taken out of the biofreezer and instantly transferred on ice. Afterwards, cells were defrosted instantaneously in a water bath (37 °C) by carefully swaying the cryotube in the water. The thawed cell suspension is then transferred into a 15 ml tube containing 12 ml of HepG2 culture medium. Due to the high DMSO concentration in the freezing medium, these steps must be performed quickly. Otherwise cells may not attach and grow in the cell culture flask or die. Under standard conditions the high amount of DMSO (10 %) is cytotoxic to the hepatoma cells, but at -84 °C DMSO has protective effects by preventing crystallization and partial dehydration of cell plasma (Dumont et al., 2006) (Pegg et al., 2007). Subsequently, the cell-medium suspension mix was centrifuged at 500 x g for 5 min at room temperature. The supernatant was removed and the down-centrifuged HepG2 cells were resuspended in 1 ml culture medium by repeated pipetting. The cell solution is then transferred into a 25 cm^2 cell culture flask filled with 5 ml cell culture medium. Cells were cultivated in an incubator and the culture medium was changed after 24 h. After a complete monolayer was formed, cells were detached, counted, and splitted as described below. From this point on, cells were cultivated in 75 cm^2 cell culture flasks.

Performing *in vitro* experiments also included preparing a stock of cells with different passage numbers which were stored at -84 °C in the biofreezer. Therefore, HepG2 cells were frozen in a special freezing medium containing DMEM culture medium supplemented with 20 % FCS and 10 % DMSO (Table 50).
HepG2 cells, which built a complete monolayer in the 75 cm^2 flask, were detached by trypsination- Then cells were separated by up- and down-pipetting of the cell suspension,

transferred into an 15 ml tube, and centrifuged (500 x g, 5 min, room temperature). The supernatant was carefully removed and the residue was dissolved in 1 ml freezing medium and transferred into a cryo tube.

Table 50. HepG2 freezing medium.

HepG2 freezing medium	DMEM high glucose w/o phenol red	70 % (7 ml)
	Fetal calve serum (FCS)	20 % (2 ml)
	DMSO	10 % (1 ml)
	Store at 4 °C, 4 weeks	

Cryo tubes were first kept in a special freezing box filled with 4 °C-thermalized 100 % isopropanol and stored at -84 °C to permit cells to gently and steadily cool down about 1 °C/min. When cells were finally cooled down, they were stored in cryo boxes in the bio-freezer (-85 °C) until usage.

VI.2.2.2 Cultivation and Subcultivation of HepG2 Cells

HepG2 cells were cultivated under standard conditions in 75 cm^2 cell culture flasks with culture medium containing DMEM high glucose w/o phenol red, fetal calf serum, penicillin/streptomycin, and dexamethasone (Table 48). The culture medium was removed every two to three days to ensure that cells receive adequate nutrient supply. When a confluent cell layer was reached, cells had to be splitted. Otherwise cells would have stopped their growth due to contact inhibition which may result in the death of the whole culture as a worst case. Therefore, cells were partitioned into further cultures resulting in a continuous subcultivation. This process is called passaging, with each splitting step the passage number increases. HepG2 cells were subcultivated as long as cells showed normal growth behavior, and HepG2 cell-like appearance.

When confluency was reached the culture medium was carefully removed and the cell layer was rinsed out by adding 3 ml trypsin/EDTA to remove dead cells. Afterwards, 1 ml trypsin/EDTA was added and dispensed consistently over the entire cell layer. Cells were kept in the incubator up to ten minutes, i.e. until they easily detach from the flask surface. The reaction was stopped by adding 9 ml of culture medium. By multiple up- and down-pipetting of the cell suspension, cells were separated and counted to perform experiments or for further subcultivation.

VI.2.2.3 Cell Counting

Cell growth depends on the applied cell number at the beginning of each experiment. Therefore, cells were counted with the aid of the Neubauer counting chamber via hemocytometer by using trypan blue exclusion test. An example of the Neubauer chamber is presented in Figure 59 below.

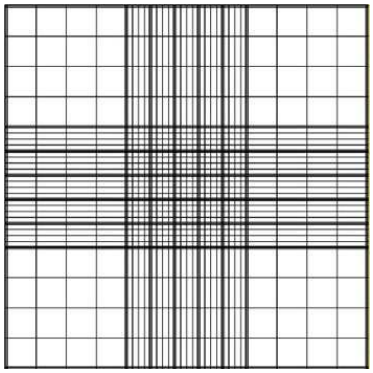

Figure 59. Neubauer counting chamber.

After trypsination and separation of cells, the cell suspension was dissolved at a ratio of 1:1 with trypan blue solution (0.4 %) and afterwards placed on the hemocytometer. Dead cells appear in the light microscope (10x resolution) blue, whereas viable cells are uncoloured. Four large squares consisting of 4x4 small squares were counted under the light microscope and the number of viable cells per ml was calculated as follows:

$$\text{Cell count}\left(\frac{\text{cells}}{\text{ml}}\right) = \sum\left(\frac{S_1 + S_2 + S_3 + S_4}{4}\right) \times \text{df} \times 10^4$$

with $S_{1\text{-}4}$ = cell count of a large square
df = dilution factor = 2
10^4 = hemocytometer-specific parameter of the Neubauer chamber

VI.2.3 Cell Seeding and Compound Treatment

HepG2 cells were seeded in culture medium at the appropriate cell density depending on the respective multiwell plate format so that human hepatoma cells achieved approximately 70 % of cell confluence before compound treatment. Information about cell density and well volume is outlined in the following table:

Table 51. Information about format, volume, and concentration of seeded cells related to cell type.

	Assay, Method	Format	Volume (ml/well)	Seeded cell concentration (cells/well)
HepG2	Alamar Blue assay EROD assay	24-well	1	8.5×10^4
	Preparation of microsomes	Ø 94 mm	7	4×10^6
	Extraction of RNA	6-well	2	1.5×10^6
hHeps	Alamar Blue assay EROD assay	96-well	0.2	5×10^4
	Extraction of RNA	6-well	2	1.8×10^6

24 h (HepG2) respectively 2-3 h upon arrival (hHeps) cell culture medium was removed and cells were incubated with test compounds over 24 h in the assay / cell type specific culture medium. All test compounds were dissolved in DMSO and added to the media so that the final solvent concentration never exceeded 1 % (v/v). Each performed experiment included positive as well as negative controls which are described for each method separately.

VI.2.4 Processing of Compound-treated Cultured Cells and Tissues

VI.2.4.1 Preparation of Microsomes from Cells

Microsomes are vesicle-like artifacts of the endoplasmatic reticulum which are obtained after homogenization of liver or liver cells and further differentiated centrifugation. The microsomal fraction contains various drug-metabolizing enzymes such as cytochromes P450 1A1, 1A2, and 1B1 (Berg et al., 2003).

Microsomes, as crude part of the endoplasmatic reticulum, were isolated and purified by homogenization of cultured HepG2 cells and subsequent differential centrifugation according to Sigma protocol for the endosplasmatic reticulum isolation (Sigma-Aldrich, 2005) with a few modifications. As described before, HepG2 cells were seeded on 95-diameter petri dishes, and after twenty-four hours of compound-treatment, preparation of microsomes started.

Cells were washed three times with 4 °C-thermalized NaCl solution (0.9 %); the subsequent steps were performed on ice. Primarily, 1 ml of ice-cold IEB buffer (1x), containing 0.1 % protease inhibitor cocktail (Sigma-Aldrich) was added to each petri dish. The protease inhibitor cocktail prevents the degradation of proteins in the prepared cell homogenate. Then, cells were manually scraped off the petri dishes and directly transferred into a sterile 1.5 ml microtube.

Afterwards, the cell suspension was homogenized using ultrasound (75 %, 3 s) and centrifuged (12000 x g, 15 min, 4 °C). 1 ml of each obtained supernatant was transferred into an ultracentrifugation microtube and centrifuged at 100000 x g for 60 min at 4 °C. The received pellet was resuspended in 75-100 µl NaPi-buffer (50 mM, pH: 7.6) and followed by homogenization using an ultrasonic probe (65 %, 2 s). 10 µl of each isolated microsome sample was transferred into another microtube to determine the protein concentrations with the aid of the BSA^{TM} assay. The remaining dissolved microsomes were stored at -80 °C until further use.

Table 52. Solutions used during microsome preparation.

NaCl solution (0.9 %)	NaCl	9 g
	dd H_2O	up to 1 l
	Store at room temperature	
PBS	NaCl(137 mM)	8.006 g
(phosphate buffered saline)	KCl (2.7 mM)	0.201 g
calcium and magnesium free	NaH_2PO_4 (6.5 mM)	0.923 g
	H_2PO_4 (1.5 mM)	0.204 g
	dd H_2O	up to 1 l
	pH: 7.4	
	Store at room temperature	
Isotonic extraction buffer 5x	HEPES (5 mM)	1.2 g
(IEB 5x)	Saccharose (1.25 M)	42.8 g
	EGTA (5 mM)	0.19 g
	KCl (125 mM)	0.93 g
	dd H_2O	up to 100 ml
	pH: 7.8	
	Sterile-filtered with an 0.45 µm filter	
	Store at 4 °C	
Isotonic extraction buffer 1x	5x IEB	2 ml
(IEB 1x)	dd H_2O	8 ml
	Protease inhibitor cocktail (0.1 %)	10 µl
	Preparation immediately before usein a sterile atmosphere	
	Store on ice	

NaPi-buffer (50 mM)	$Na_2HPO_4*H_2O$	7.52 g
	NaH_2PO_4	1.07 g
	dd H_2O	up to 1 l
	pH: 7.6	
	Store at 4 °C	

VI.2.4.2 Extraction of Total RNA from Cells

Total RNA was isolated from cells with the RNeasy Mini Kit from Qiagen according to the manufacturer's instructions (RNeasy Mini Handbook, 2010). This technique is based on the binding properties of RNA to a silica-based membrane in combination with the speed of microspin technology (Figure 60). Using this method, all RNA molecules longer than 200 nucleotides are purified. The procedure conveys the purification of mRNA. Most RNAs < 200 nucleotides (e.g. 5.8S rRNA, 5S rRNA, and tRNA) do not bind to the silica-based membrane and thus are excluded of the extraction process. Ribonucleases (RNases) are very stable and active enzymes which can destroy RNA within minutes. Therefore a few precautions have to be considered. Before starting the isolation, all benches, pipettes, and surfaces have to be cleaned with RNase Away solution.

Cells were seeded in 6-well plates, incubated with test compounds for 24 h and afterwards washed three times with PBS and stored at -80 °C until RNA extraction.

All subsequent steps were performed at room temperature. Primarily, cells were lysed and homogenized by a highly denaturating lyses buffer containing guanidine-thiocyanate. Therefore, 350 µl of buffer RLT (containing 1 % (v/v) β-mercaptoethanol) was added to each well. After a short incubation (2 min), cells were harvested with a cell scraper and then directly transferred into a 1.5 ml microtube. Then, cells were vortexed for 2 min to enhance the disruption and homogenization process and afterwards centrifuged for 2 min at maximum speed. This step prevents insoluble cell components from blocking the column during RNA elution. The supernatant was transferred into a 1.5 ml microtube filled with 350 µl ethanol (70 %), and mixed well by repeated up- and down-pipetting. The entire sample (700 µl) was then transferred into an RNeasy spin column, and centrifuged for 15 s at 8000 x g. During this step total RNA was bound to the membrane. Subsequently, three washing steps were carried out as the purification procedure. 700 µl of Buffer RW1 was added to the column which was then centrifuged for 15 s at 8000 x g. After that, 500 µl of Buffer RPE was added and the spin column was centrifuged 15 s at 8000 x g. The previous washing step was repeated once again and followed by the sample centrifugation at 8000 x g for 2 min. To ensure that no ethanol is carried over during RNA elution, the column was transferred into a new 2 ml collection tube and centrifuged for 1 min at maximum speed. This step was necessary because a carryover of the ethanol-containing Buffer RPE would decrease the RNA amount. Finally, the dried column was placed in a 1.5 ml microtube and 30 µl RNase-free water (supplied in the RNeasy Mini Kit) was added directly to the spin column membrane and the column was centrifuged for 1 min at 8000 x g. The eluted RNA was kept on ice until RNA yield and purification were determined. RNA samples were then stored at -80 °C until further usage.

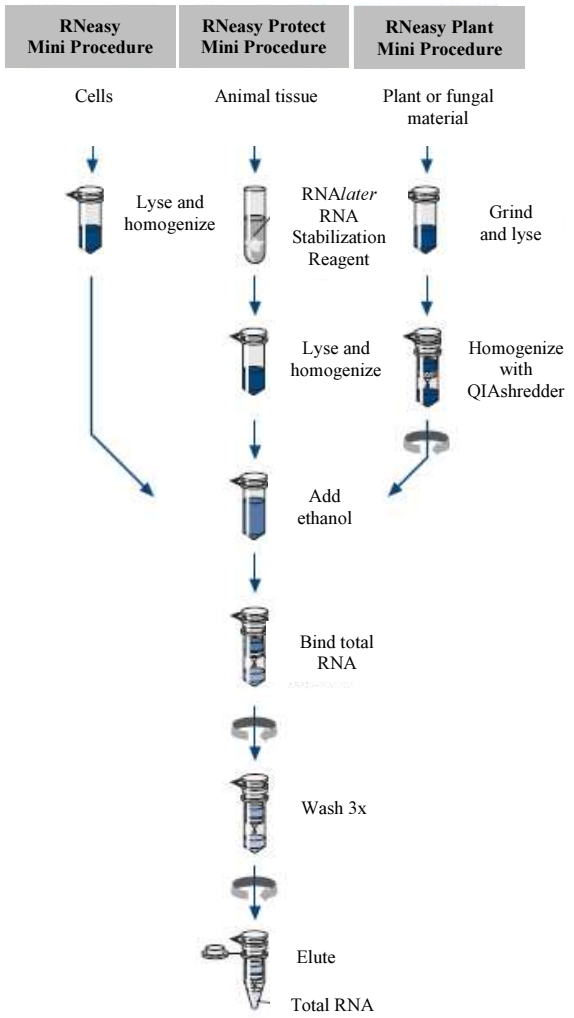

Figure 60. RNA extraction and purification using RNeasy technology (Qiagen, 2010).

VI.2.4.3 Extraction of Total RNA from Liver Tissue

Total RNA was isolated from liver tissue with Qiagen´s RNeasy Mini Kit according to the manufacturer`s instructions (RNeasy Mini Handbook, 2010). Tissue sample preparation from mouse study I and II was carried out in the laboratory units of the *Institute for Risk assessment Sciences (IRAS)*, at Utrecht University, whereas RNA isolation from liver of mouse study III was performed at the University Kaiserslautern. Tissue disruption and homogenization methods differed and are therefore described separately.

Before starting the isolation, all benches, pipettes and surfaces were cleaned with RNase Away solution (Thermo Fisher Scientific). Sterile, disposable RNase-free plasticware including special RNase-free microtubes and pipette tips were used during RNA extraction. Glass ware, mortar and pestle, as well as stainless steel beads, spatulas and scissors were thoroughly cleaned and flushed with RNase Away solution before they were autoclaved and dried.

Disruption and homogenization using TissueLyser

Frozen liver samples (mouse study I and II) were transferred on a 95 mm petri dish which was placed on ice. A small piece of each liver was cut off (30 mg) using a sterile scalpel and directly placed into a 2 ml microcentrifuge tube containing one stainless steel bead, 600 µl of Buffer RTL, and 6 µl of β-mercaptoethanol. Samples were then placed in the TissueLyser adapter and inserted in the TissueLyser. The tissue was disrupted and homogenized for 2 min at 20-30 Hz. Then the adapter set was dissembled, and the rack was rotated before operating the TissueLyser for another 2 min at 20-30 Hz. This procedure is necessary to achieve a complete disruption and homogenization of the mouse liver tissue (TissueLyser Handbook, Qiagen, 2010).

Disruption using mortar and pestle followed by homogenization by vortexing

The frozen liver samples (samples for microarray analysis from mouse study I and mouse study III) were directly placed in a liquid nitrogen containing mortar. A small piece was cut off (30 mg) and grinded thoroughly by pestle. Then, the tissue powder was decanted in a 2 ml microcentrifuge tube containing 600 µl of Buffer RLT and 6 µl of β-mercaptoethanol. The sample was afterwards mixed thoroughly by vortexing each sample for at least 2 min at room temperature.

Purification of Total RNA

The disrupted and homogenized samples were centrifuged for 3 min at maximum speed at room temperature. The supernatant was carefully transferred into another sterile 1.5 ml microtube containing 600 µl of ethanol (70 %). Insoluble material would interfere in the following steps and could block the column. The lysate-ethanol-mixture was mixed by repeated up- and down-pipetting, before 700 µl of the mix was transferred into an RNeasy spin column. The spin column was then centrifuged for 15 s at 8000 x g to bind the RNA. This step was repeated with the remaining lysate-ethanol-mix (500 µl) to bind the complete extracted RNA from the liver tissue to the column. The flow-through was discarded after each centrifugation. The membrane-bound RNA was washed in three subsequent steps.
First, 700 µl of Buffer RW1 was added to the column which was centrifuged for 15 s at 8000 x g. After that, 500 µl of Buffer RPE was added and the spin column was centrifuged 15 s at 8000 x g. The previous washing step was repeated once again by adding 500 µl of Buffer RPE to the spin column and centrifugation at 8000 x g for 2 min. To ensure that no ethanol would be carried over during RNA elution, the column was transferred into a new 2 ml collection tube and centrifuged for 1 min at maximum speed.
The last step is crucial because a carryover of the ethanol-containing Buffer RPE would have decreased the RNA amount. Finally, the dried column was placed in a 1.5 ml microtube and 30 µl of RNase-free water (supplied in the RNeasy® Mini Kit) was added directly to the spin column membrane and the column was centrifuged for 1 min at 8000 x g. The eluted RNA was kept on ice and stored at -80 °C until further usage.

VI.2.4.4 Quantification and Determination of RNA/DNA Quality

VI.2.4.4.1 Spectrophotometer

RNA concentration and quality was determined spectrophotometrically at an absorbance wavelength of 260 and 280 nm. Pure RNA has a 260/280 ratio between 1.9 and 2.1. A ratio of smaller than 1.8 indicates that the RNA is contaminated with proteins. (Berg et al., 2003) (RNeasy Mini Handbook, 2010). RNA samples were quantified with the NanoDrop 1000 spectrophotometer (Peqlab), whereas 1.5 µl of the samples were applied for quantification. A 260/280 ratio in the range of 1.8-2.3 was considered acceptable and used for further experimental research.

VI.2.4.4.2 Bioanalyzer

Purity of RNA was determined using the Agilent 2100 bioanalyzer and associated RNA 6000 Pico LabChip kit. Figure 61 summarizes the procedure for determination of RNA purity and yield.
First, RNA isolated from mouse liver was separated by gel electrophoresis on a microfabricated chip and afterwards examined using laser induced fluorescence detection. The bioanalyzer software generates the electropherogram and gel-like image as well as the ribosomal ratio (ratio of the 18S to 28S ribosomal subunits) as featured in Figure 62. A new approach of Agilent Technologies for the RNA quality assessment is the RNA Integrity Number (RIN). The RIN software algorithm was developed to standardize the RNA integrity interpretation, which before was only based on subjective visual evaluation in combination with the ribosomal ratio. The whole electropheric trace is embedded in the RIN software algorithm. Classification is based on a numbering system from 1 to 10, whereas RNA with a RIN of 1 is considered the most degraded sample and a RIN of 10 reflects the most intact RNA (Agilent Technologies, 2004).
Bioanalyzer analysis was performed using the Agilent RNA 6000 Pico LabChip kit according to the RNA 6000 Pico Kit Guide. Total RNA was adapted to a concentration of 1 ng/µl with ddH_2O. Analysis of RNA integrity was carried out using 2100 Expert Software Version B.02.02.

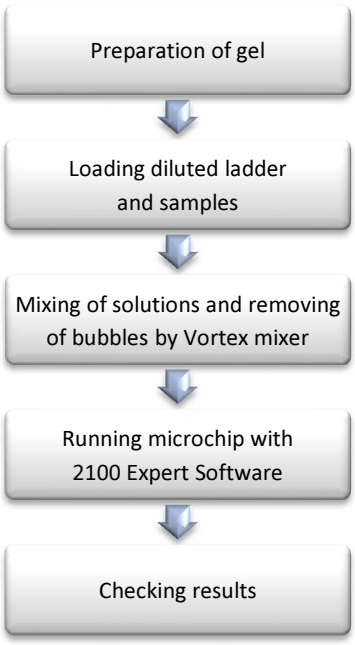

Figure 61. **Bioanalyzer procedure according to RNA 6000 Pico Kit Guide (Agilent Technologies, 2008).**

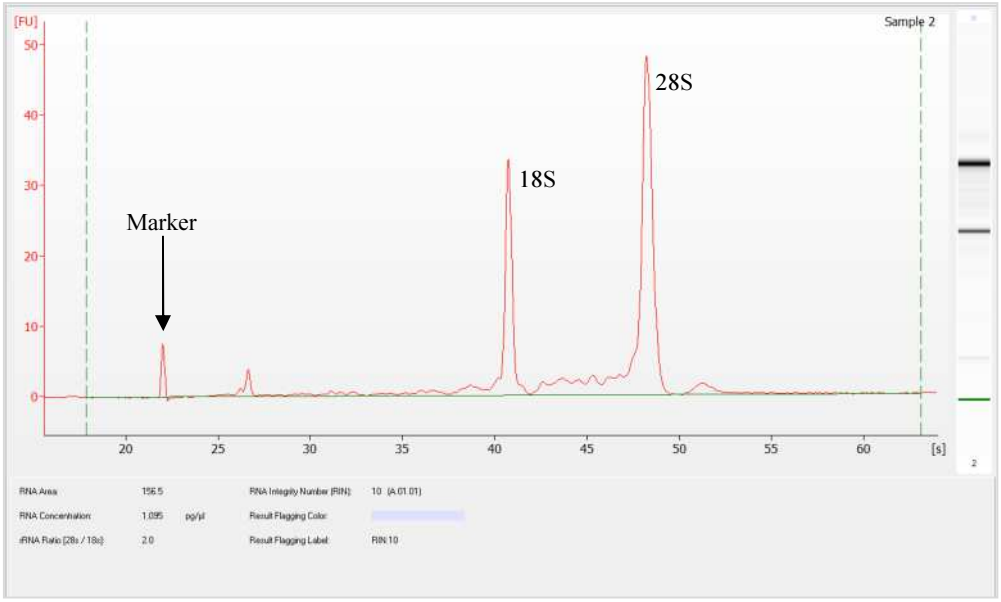

Figure 62. **Representative electropherogram and gel-like image (RNA from hHeps, RIN: 10). Information including RNA concentration, ribosomal ratio and RIN.**

VI.3 Biochemical Assays

VI.3.1 Alamar Blue Assay

The Alamar Blue assay, also referred as resazurin reduction assay, is a sensitive, simple, and fast test method to determine cytotoxicity and cell proliferation *in vitro* based on metabolic cell activity.

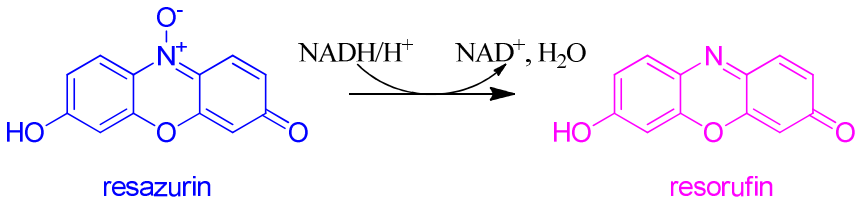

Figure 63. Reduction of resazurin (blue) to resorufin (pink) by usage of NADH.

Oxidized, blue, non-fluorescent resazurin is reduced to the pink-fluorescent resorufin (Figure 63) by cell activity or mitochondrial enzymes (De Fries et al., 1995). Resorufin fluorescence was measured at 544 nm excitation and 590 nm emission using Fluoroscan Ascent microplate reader (Labsystems).
It is proven that there is a direct correlation between the reduction of resazurin in the growth media and the cell proliferation of living cells. It has not been verified, if the reaction takes place intracellularly using mitochondrial enzyme activity, at the surface of the plasma membrane, or as a chemical reaction in the cell culture medium extracellularly (O´Brien et al., 2000).

Resazurin working solution was prepared immediately before use and protected from light (Table 53). The incubation medium of compound-treated HepG2 and hHeps was removed after 24 h and cells were washed with 1 ml/well (HepG2) or 200 µl/well (hHeps) of prewarmed PBS. Afterwards, 1 ml/well (HepG2) or 200 µl/well (hHeps) of resazurin working solution was added and cells were kept in an incubator for another 60 min (HepG2) or 90 min (hHeps) under standard conditions. Finally, fluorescence was measured at 544 nm excitation and 590 nm emission using Fluorescent Ascent plate reader.

Saponine (0.1 %) served as positive control. Different concentrations of DMSO (0.1-1 %) were used as respective solvent controls as well as a blank (non-cell containing well). The blank value was subtracted from all fluorescence intensities. The mean of two (HepG2) or four (hHeps) replicates was related to the mean value of the corresponding solvent control. Viability of cells was calculated as the percentage of viable cells compared to control cells (DMSO 0.1-1 %):

$$\text{Viability (\%)} = \frac{MV_{T\text{-}B}}{MV_{C\text{-}B}} \times 100$$

with: $MV_{T\text{-}B}$: measured value of compound-treated cells minus blank value
$MV_{C\text{-}B}$: measured value of solvent control-treated cells minus blank value

Table 53. Solutions used for Alamar Blue assay.

PBS (phosphate buffered saline) calcium and magnesium free	NaCl (137 mM) KCl (2.7 mM) NaH_2PO_4 (6.5 mM) H_2PO_4 (1.5 mM) dd H_2O pH: 7.4 Store at room temperature	8.006 g 0.201 g 0.923 g 0.204 g up to 1 l
Resazurin stock solution (440 mM)	Resazurin DMF Store at 4 °C for 1 week and exclude from light	110.5 mg 1 ml
NaCl/Pi-buffer	KH_2PO_4 (1.1 mM) NaCl (154 mM) Na_2HPO_4 (3.7 mM) ddH_2O Store at 4 °C up to 4 weeks	0.144 g 9.0 g 0.528 g up to 1 l
Resazurin-NaCl/Pi solution (440 µM)	Resazurin stock solution NaCL/Pi-buffer Store at 4 °C for 4 weeks and exclude from light	0.1 ml 999.9 ml
Resazurin working solution HepG2 cells	Resazurin-NaPi solution DMEM w/o phenol red Preparation immediately before use and exclude from light	1: 10 (v/v)
Resazurin working solution hHeps	Resazurin-NaPi solution HMC™ medium Preparation immediately before use and exclude from light	1: 10 (v/v)

VI.3.2 Ethoxyresorufin-O-deethylase (EROD) Assay

The ethoxyresorufin-O-deethylase (EROD) assay is a well established and widely used test method to determine cytochromes P450 1A1 enzyme activity in liver tissue and cells. Induction of CYP1A1 is the best known biomarker for AhR activation and provides important information about toxicity mediated by environmental pollutants like PCDDs, PCDFs, and DL-PCBs. The EROD assay includes the oxidative deethylation of 7-ethoxyresorufin to the pink- fluorescent resorufin. This dealkylation reaction (Figure 64) is catalyzed by CYP1A1 whereby the fluorescence intensity is direct proportional to the CYP1A1 concentration (Behnisch et al., 2001) (Petrulis et al., 2001) (Behnisch et al., 2002) (van Duursen et al., 2005). Each experiment included a positive control for CYP1A1 induction (TCDD, 10 nM) as well as solvent controls (DMSO 0.1-1 %).

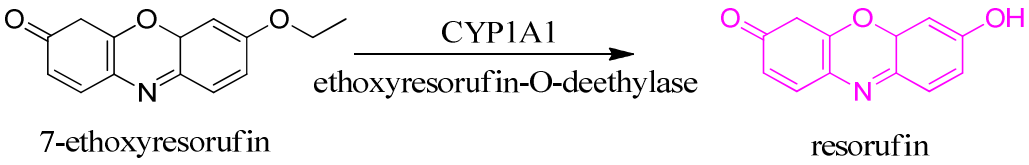

Figure 64. Dealkylation of 7-ethoxyresorufin to the pink-fluorescent resorufin.

In the present work the EROD activity was performed and measured according to van Duursen et al. (2005) with modifications. After a period of 24 h of compound incubation, cells were washed twice with 1 ml/well (HepG2) or 200 µl/well (hHeps) prewarmed PBS. Then, 1 ml/well (HepG2) or 200 µl/well (hHeps) of freshly prepared EROD medium was added to the cells and multiwell plates were directly inserted in the thermalized (37 °C) Fluorescent Ascent plate reader. Fluorescence was measured at an excitation wavelength of 544 nm and emission wavelength of 590 nm every 90 s for 30 min. Afterwards, cells were washed with 2 ml/well or 400 µl/well (hHeps) prewarmed PBS and frozen (-80 °C) over night.

A calibration curve of resorufin was used to quantify the activity. A pipetting layout is presented in Table 55, with DMEM high glucose w/o phenol red being used for HepG2 cells and HCM^{TM} medium for primary human hepatocytes. After a period of 10 min at 37 °C in the Fluorescent Ascent plate reader (Labsystems, Dreieich), fluorescence was measured (excitation: 544 nm, emission: 590 nm).

With the aid of the resorufin calibration curve the resorufin content per well per min was determined but only the linear section of the obtained line was used for calculation. Including the protein content of the corresponding well leads to the specific EROD activity expressed as pmol resorufin/mg protein* min.

Table 54. Solutions used in EROD assay.

PBS	NaCl(137 mM)	8.006 g
(phosphate buffered saline)	KCl (2.7 mM)	0.201 g
calcium and magnesium free	NaH_2PO_4 (6.5 mM)	0.923 g
	H_2PO_4 (1.5 mM)	0.204 g
	dd H_2O	up to 1 l
	pH: 7.4	
	Store at room temperature	
7-ethoxyresorufin(1 mM)	7-ethoxyresorufin	5 mg
	DMSO	20.73 ml
	Store at -20 °C and exclude from light	
Resorufin stock solution (10 mM)	Resorufin sodium salt	23.5 mg
	DMSO	10 ml
	Store at room temperature and exclude from light	
Resorufin working solution (10 nM)	Resorufin stock solution	0.1 ml
	DMSO	9.9 ml
	Preparation immediately before use and exclude from light	
Magnesium chloride solution (1 M)	$MgCl_2$	9.521 g
	ddH_20	100 ml
	Store at room temperature	
NaOH (0.2 M)	NaOH	0.8 g
	ddH_20	100 ml
	Store at room temperature	
Dicumarol (10 mM)	Dicumarol	33.36 mg
	NaOH (0.2 M)	10 ml
	Store at 4 °C	
EROD medium	DMEM high glucose w/o	25 ml
HepG2	phenol red	125 µl
	$MgCl_2$ (1M)	25 µl
	Dicumarol (10 mM)	125 µl
	7-ethoxyresorufin (1 mM)	
EROD medium	HCM™ medium	20 ml
hHeps	$MgCl_2$ (1M)	100 µl
	Dicumarol (10 mM)	16 µl
	7-ethoxyresorufin (1 mM)	100 µl

Table 55. Layout of resorufin calibration curve.

Vial	Medium (µl)	Resorufin working solution/vials	Resorufin concentration (nM)
1	9900	100 µlresorufin working solution	1000
2	3000	3000 µl Vial 1	500
3	3000	1000 µl Vial 1	250
4	2400	600 µl Vial 2	100
5	2484	216 µl Vial 1	75
6	4000	1000 µl Vial 3	50
7	2400	600 µl Vial 4	20
8	2400	600 µl Vial 6	10
9	2000	0	0

VI.3.3 Bicinchoninic Acid (BCA) Assay

The BCA™ assay is a rapid and sensitive test method for quantification of the total protein content. The underlying reaction is based on two steps: the reduction of Cu^{2+} to Cu^{+} by protein in an alkaline medium (biuret reaction) and afterwards the sensitive and selective colourimetric detection of the cuprous cation (Cu^{+}) by binding to bicinchoninic acid as pictured below:

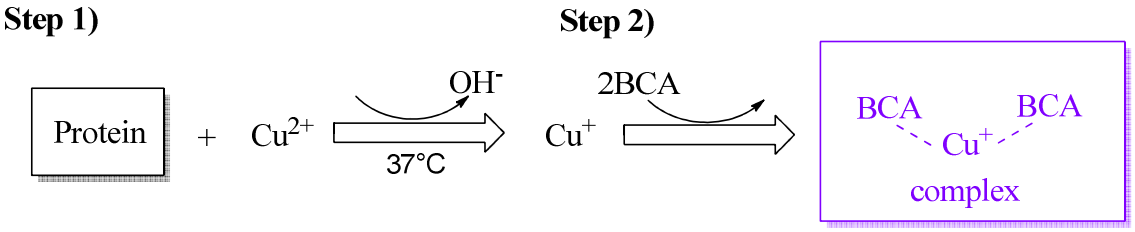

Figure 65. Scheme of the BCA reaction (Pierce).

The purple-coloured reaction product is formed by the chelation of two molecules of BCA with one cuprous ion. This purple complex exhibits a strong absorbance at 562 nm that is nearly linear with increasing protein concentrations over a large concentration range (20-20000 µg/ml) (Pierce, 2010).

The BCA assay was used to quantify the total protein content after performing EROD assay respectively measuring the protein concentration in microsomes. After measuring the EROD activity, HepG2 cells and hHeps were frozen over night in multiwell plates at -80 °C. Cells were cracked by thawing three times for 15 min at room temperature and freezing (-80 °C) for at least 3 h in between. Depending on the used multiwell format, different volumes were applied as described in Table 56.

First of all, the cracked cells in each well were solved in a corresponding amount of double-distilled water (Table 56). Afterwards the BCA working solution was freshly prepared by mixing 50 parts of Reagent A with 1 part of Reagent B and the respective volume of the working solution was added to each well. Then, the plates were carefully shaken to enhance the mixing process and kept in a humidified chamber at 37 °C for 30 min. Subsequently, fluorescence was measured at a wavelength of 562 nm using the MWGt plate reader (BioTek Instruments Inc.).

The experimental procedure for microsomes was similar, first microsomes were defrozen on ice. Afterwards, microsomes were diluted with double-distilled water 1:10 whereby 50 µl of the diluted microsomes were transferred into a 48-well plate and mixed with the freshly prepared BSA working solution (Reagent A:Reagent B, 50:1). The subsequent steps were performed as described above.

A BSA calibration curve was used to quantify the protein content; the pipetting layout is presented in Table 57. Known BSA concentrations were measured and the BSA concentrations were fitted against the obtained sample fluorescence at 562 nm.

Table 56. Information about format-related volumes in BCA assay.

Format	ddH_2O (µl)	Volume BCA working reagent (µl)
24-well	75	600
48-well	50	400
96-well	25	200

Table 57. Preparation of diluted BSA standards for BSA calibration curve.

Vial	Volume ddH_2O (µl)	Volume and source of BSA	BSA concentration (µg/ml)
A	0	300 µl BSA stock solution	2000
B	125	375 µl BSA stock solution	1500
C	325	325 µl BSA stock solution	1000
D	175	175 µl Vial B	750
E	325	325 µl Vial C	500
F	325	325 µl Vial E	250
G	325	325 µl Vial F	125
H	400	325 µl Vial G	25
I	400	0	0

VI.3.4 SDS Polyacrylamide Gel Electrophoresis (SDS-PAGE)

The principle of the sodium dodecyl sulfate polyacrylamide gel electrophoresis (SDS-PAGE) is the separation of charged particles, in the present work, proteins in a homogenous electrical field. Adding SDS (an anionic detergent) to the samples and subsequent heating up to 95 °C leads to the masking of the protein self charge, thus the protein migration is directly proportional to the molecular weight and no longer depends on the charge distribution. Furthermore, the secondary and tertiary protein structure is ruptured by disconnecting the hydrogen bridges. The β-mercaptoethanol, as another component of the loading buffer (Laemmli buffer), leads to the reductive splitting of disulfide bonds in proteins.

Proteins are separated depending on their specific molecular weight using a discontinuous electrophoresis. Denatured samples are loaded onto a polyacrylamide gel (consisting of a stacking and resolving gel) and are separated by applying a suitable voltage. Discontinuities in pore sizes and pH values enhance the sharpness of bands compared to a continuous electrophoresis. The stacking gel (pH: 6.8) with a large pore size, is placed onto the separation gel, the so called resolving gel (pH: 8.8) with smaller pores. In the stacking gel all proteins migrate at the same migration speed and build a sharp stacking line. Migration into the small pore-sized resolving gel leads to a sieving effect which results in a solely weight-dependent separation of proteins because small proteins migrate faster than larger molecules through the gel. A protein marker is added to each electrophoresis to monitor electrophoretic separation and identify protein bands (Lottspeich et al., 1998) (Cammann, 2001).

Microsomes were diluted with double-destilled water each 15 µl sample containing 25 µg protein. 3 µl loading buffer (Laemmli 6x, Table 58) was added to the diluted samples. Samples were vortexed and centrifuged at room temperature for 5 min at maximum speed and subsequently denatured for 5 min at 95 °C. Afterwards, samples were cooled down on ice and centrifuged for 5 min at room temperature.

First, the resolving gel solution (Table 59) was prepared and quickly casted between to glass plates in a gel caster. The surface of the resolving gel was coated with 2-propanol (70 %) to obtain a bubble-free, smooth gel surface. After 30 min, the resolving gel was polymerized and 2-propanol was carefully removed using filtering paper. Then, the stacking gel solution was mixed, and quickly casted on top of the polymerized resolving gel. A comb was inserted into the soluble stacking gel solution to create 10 sample pockets. After another 30 min the resolving gel was polymerized and always two gels were placed into a vertical electrophoresis chamber (Mini Protean IV Apparatus, Bio-Rad) which subsequently was completely filled with electrophoresis buffer (1x). Afterwards, the comb was carefully removed and the denatured protein samples (18 µl) were loaded into the pockets. A defined protein marker (Precision Plus Kaleidoscope Protein Standard, Bio-Rad) was also loaded into one lane per gel (5 µl). At first, a constant voltage of 80 V was applied. After protein samples reached the resolving gel (about 15 min), the voltage was increased to 120 V. Once the dye front reached the end of the resolving gel, the electrophoresis was stopped (approximately after another 90 min).

Table 58. Laemmli loading buffer for SDS-PAGE (6x).

Laemmli (loading buffer 6x)	Tris/HCl (0.5 M; pH 6.8)	50 ml
	SDS	1.244 g
	Glycerine	40 ml
	Bromophenol blue	0.16 g
	β-mercaptoethanol	5.0 ml
	ddH_2O	up to 100 ml
	Store at -20 C	

Table 59. Solutions and combustion of resolving and stacking gel for SDS-PAGE.

Tris/HCl (1.5 M)	Tris	18.2 g
	ddH_2O	up to 100 ml
	Adjust to pH: 8.8	
	Store at room temperature	
Tris/HCl (0.5 M)	Tris	6.1 g
	ddH_2O	up to 100 ml
	Adjust to pH: 6.8	
	Store at room temperature	
Resolving gel (10 %)	Acrylamide (30 % solution)	1.64 ml
	ddH_2O	2.0 ml
	Tris/HCl (1.5 M, pH: 8.8)	1.23 ml
	SDS (10 %)	50 µl
	APS (10 %)	50 µl
	TEMED	4 µl
Stacking gel (4 %)	Acrylamide (30 % solution)	0.25 ml
	ddH_2O	1.2 ml
	Tris/HCl (0.5 M, pH: 6.8)	0.5 ml
	SDS (10 %)	20 µl
	APS (10 %)	20 µl
	TEMED	4 µl

Table 60. Electrophoresis buffer for SDS-PAGE.

Electrophoresis buffer (10x)	Glycine (2 M)	720 g
	Tris (250 M)	150 g
	SDS (20 % solution)	250 ml
	ddH_2O	up to 5 l
	Adjust to pH 8.4	
	Store at room temperature	
Electrophoresis buffer (1x)	Electrophoresis buffer (10x)	250 ml
	ddH_2O	up to 2.5 l
	Store at room temperature	

VI.3.5 Western Blot and Immunoblot

Western blot was performed subsequent to protein separation using SDS-PAGE. Separated proteins are transferred from a gel to a membrane (polyvinylidene fluoride (PVDF)) in an electrical field. After proteins are bound to a membrane, they can be detected by using protein-specific monoclonal or polyclonal antibodies. Separated proteins are transferred from the polyacrylamide gel to the polyvinylidene fluoride membrane by a vertically positioned electrical field. Proteins stick to the PVDF membrane due to hydrophobic interactions and can be identified by binding of specific antibodies. The primary antibody binds directly to the examined protein, whereby unbound primary antibody is removed by several washing steps. Afterwards, the membrane is exposed to another antibody which is directed against the primary antibody. The secondary antibody used in the present work is linked to an enzyme (horseradish peroxidase) which catalyzes a chemoluminescent reaction finally visualizing the protein bands.The horseradish peroxidase-linked secondary antibody catalizes the oxidation of luminol in the presence of H_2O_2. The formed reaction product is in an excited state falling back to the ground state by emitting light (Figure 66). Phenolic compounds, such as *p*-coumaric acid, are able to enhance the light emission (Lottspeich et al., 1998) (Towbin et al., 1979).

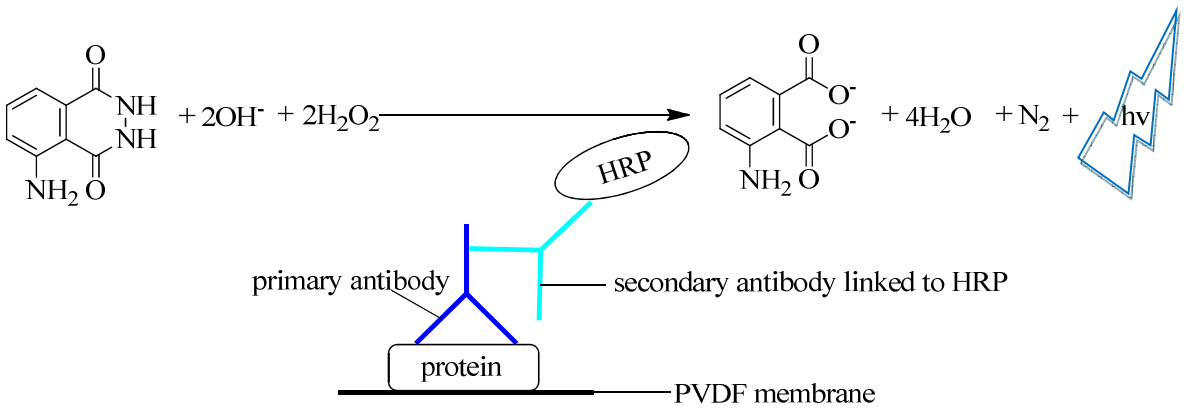

Figure 66. Chemoluminscent reaction.

First, separated proteins were transferred from the polyacrylamide gel to the PVDF membrane using a semi-dry transfer system (Hoefer). The PVDF membrane (6.5 x 8 cm) was immersed a few seconds in methanol (100 %), then, washed in ddH_2O and afterwards equilibrated for at least 10 min in anode buffer I. All polyacrylamide gels were equilibrated for 10 min in cathode buffer before starting the following procedure.

First, the anode of the semi-dry blot was moisturized with anode buffer I. A Whatman filter paper (7.5 x 9 cm) soaked with anode buffer I was placed on the anode followed by two Whatman filter papers soaked with anode buffer II. The equilibrated PVDF membrane was positioned on top of this filter paper stack. Carefully, the polyacrylamide gel was placed on the PVDF membrane. Three Whatman filter papers soaked with cathode buffer were put on top of the gel. Finally, the cathode was placed on the 'sandwich' (Figure 67). A weight of 5 kg was positioned on the semi-dry apparatus. Blotting was performed using constant amperage of 0.8 mA/cm^2 (45 mA per membrane) for 75 min.

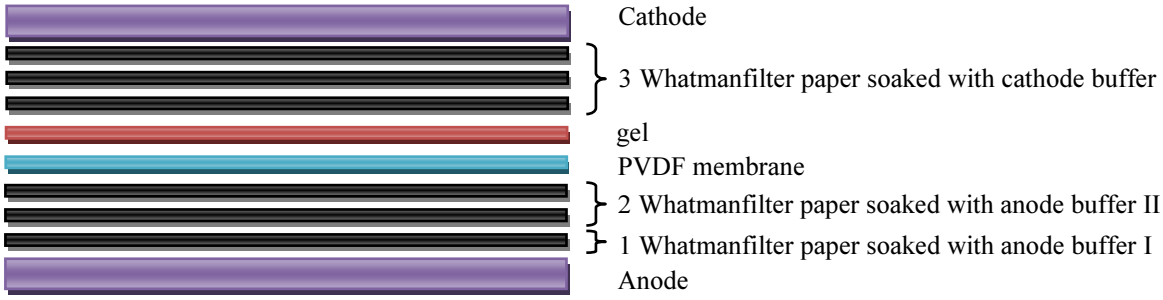

Figure 67. Schematic illustration of semi-dry blot apparatus.

Table 61. Blotting buffers.

Anode buffer I	Tris (300 mM)	36.3 g
	Methanol	100 ml
	ddH_2O	up to 1 l
	Adjust to pH: 10.4	
	Store at room temperature	
Anode buffer II	Tris (25 mM)	3 g
	Methanol	100 ml
	ddH_2O	Up to 1 l
	Adjust to pH: 10.4	
	Store at room temperature	
Cathode buffer	Glycine	3 g
	Tris	3 g
	Methanol	200 ml
	SDS (20 % solution)	250 µl
	ddH_2O	up to 1 l
	Adjust to pH: 9.4	
	Store at room temperature	

After transferring the separated proteins to the PVDF membrane, the membrane was incubated with blocking buffer (Table 62) on a shaker for 1 h at room temperature to block unspecific binding sites. Then, the membrane was transferred into a 50 ml tube and washed three times for 5 min with TBS-T (tris buffered saline; Table 62) and subsequently incubated with the respective primary antibody (Table 63) for 1 h at room temperature, respectively at 4 °C over night, on a rotating mixer. After three washing steps with TBS-T for 5 min, the membrane was finally incubated with the horseradish peroxidase (HPR)-labelled secondary antibody (Table 63) for 1 h at room temperature on a rotating mixer. Afterwards, the membrane was washed twice with TBS-T and once with TBS (Table 62). The membrane was stored in TBS until chemoluminescence detection was carried out.

Table 62. Solutions used for immunoblot.

TBS (20x)	NaCl (2.6 M)	304 g
	Tris/HCl (0.4 M)	97 g
	ddH_2O	up to 1 l
	Adjust to pH: 7.4	
	Store at room temperature	
TBS-T (1x)	TBS (1x)	2 l
	Tween-20	6 ml
	Store at room temperature	
Blocking buffer	TBS-T (1x)	100 ml
	Skimmed milk powder (0.5 %)	5 g
	Prepare immediately before use	

Table 63. List of primary and secondary antibodies including experimental conditions.

Primary antibody	Dilution with TBS-T	Incubation period	Purchased from	Secondary antibody	Dilution with TBS-T	Incubation period	Purchased from
Rabbit anti-CYP1A1	1:1000	1 h	Abcam	Goat anti-rabbit IgG-HRP	1:2000	1 h	Santa Cruz Biotechnology
Rabbit anti-VDAC1	1:1000	Over night	Cell Signaling Technology	Goat anti-rabbit IgG-HRP	1:2000	1 h	Santa Cruz Biotechnology

Detection of chemoluminescence by enzyme substrate reaction was realized as described in the following steps. Therefore, the membrane was incubated with the chemoluminescence detection solution consisting of solution A (9 ml, Table 64), solution B (1 ml, Table 64), and 100 µl of the H_2O_2-Tris/HCL solution (Table 64) for 1 min in a darkened box. As described in Figure 66, luminol is oxidized by the horseradish peroxidase in alkaline environment. The formed reaction product 3-aminophtalate returns from an excited state to the ground state by emitting light. This light was detected with the aid of the LumiImager and LumiAnalyst 3.1 software (Roche Diagnostics).

Table 64. Solutions used for chemoluminescence detection.

Tris/HCl (0.1 %)	Tris	2.428 g
	ddH_2O	up to 200 ml
	Adjust to pH: 8.6	
	Store at room temperature	
Solution A	Luminol	50 mg
	Tris/HCl (0.1 M)	200 ml
	Store in a darkened container at 4 °C	
Solution B	*p*-coumaric acid	22 mg
	DMSO	20 ml
	Store in a darkened container at room temperature	
H_2O_2-Tris/HCL-(0.1 %) solution	H_2O_2 (30 %)	50 µl
	Tris/HCL (0.1 M)	1000 µl
	Preparation immediately before use in a darkened microreaction tube	

VI.3.6 Real-Time Polymerase Chain Reaction

VI.3.6.1 Reverse Transcription

Reverse transcription marks the first step within real-time PCR analysis. During this reaction, the isolated RNA (from cells or tissue) is transcribed into complementary DNA (cDNA) using the enzyme reverse transcriptase. The synthesized cDNA can then be applied in quantitative RT-PCR experiments.

In the present work the iScript™ cDNA Synthesis Kit (Bio-Rad) was used to transcribe RNA into cDNA using MMLV-derived reverse transcriptase. MMLV reverse transcriptase is isolated from the moloney murine leukemia virus and transcribes RNA into cDNA using a unique blend of oligo(dT) and random hexamer primers (Berg et al., 2003) (Bio-Rad).

Reverse transcription was carried out using the iScript™ cDNA Synthesis Kit according to the manufacturer's instructions (Bio-Rad). A master mix consisting of 5x iScript reaction mix, reverse transcriptase, and nuclease-free water was prepared and added to the RNA template (Figure 65). Then the template-iScript solution was carefully mixed, centrifuged and placed into the MyCycler (Bio-Rad). The reaction protocol is featured below (Table 66). Afterwards, the cDNA was stored at -20 °C.

Table 65. Components for reverse transcription reaction.

Components	Volume per reaction (µl)
5x iScript reaction mix	4
iScript reverse transcriptase	1
Nuclease-free water	14
RNA template (1 µg/µl)	1

Table 66. Thermocycling conditions according to manufacturer's instructions.

Temperature	Duration time (min)
25 °C	5
42 °C	30
85 °C	5
4 °C	Hold

IV.3.6.2 Quantitative Real-Time PCR

Quantitative real-time PCR (RT-PCR) is a technique which enables both amplification and quantification of a targeted DNA simultaneously. The reaction progress is monitored in 'real time' compared to a conventional PCR in which the reaction product is verified at its end, e.g. using an agarose gel electrophoresis.
In the present work, the amplified targeted DNA was quantified using the fluorescence dye SYBR®Green. SYBR®Green is a cyanine dye which binds to the double-stranded DNA, thus the fluorescence of the formed SYBR Green-DNA complex can be measured at 490 nm. So the number of amplified DNA increases with the increasing fluorescence which is directly proportional to amplified DNA amount (Tichopad et al., 2003) (Bio-Rad, 2006).

Amplification can be divided into three different stages. In the first phase, no significant increase of fluorescence can be detected despite product amplification (linear background stage). In the linear log phase (second stage), the fluorescence rises in a logarithmic manner until reaching the third phase (plateau stage) in which no increase of fluorescence is registered. Substrates are depleted and the activity of the Taq polymerase decreases due to the heat load throughout the PCR. The early linear log phase is used for quantification of the amplified product measuring the C_t-value (threshold cycle). The C_t-value represents the cycle at which the fluorescence rises above the background for the first time. In the present work this value is used for quantification of the amplified product as described below (Holland et al., 1991) (Pfaffl et al., 2001) (Tichopad et al., 2003) (Pfaffl et al., 2004).

First, 1 µl of the transcribed cDNA (IV.3.6.1 Reverse transcription) was transferred into a PCR tube placed on ice. The RT-PCR master mix containing 12.5 µl of ABsolute™ QPCR SYBR® Green Fluorescein Mix (Thermo Fisher Scientific), 2 µl of the primer mix (forward and reverse primer of targeted gene) and 9.5 µl of RNase-free water was added to the cDNA template (Table 67). All PCR tubes were covered with optic lids, spinned down, and were put into the iCycler (Bio-Rad) using the optimized thermocycling programme (Table 68).

Table 67. Components for real-time PCR.

Components	Volume (µl)
ABsolute™ QPCR SYBR® Green Fluorescein Mix	12.5
Primer forward	1
Primer reversed	1
RNase-free water	9.5
cDNA template	1

Table 68. Thermocycling conditions for RT-PCR.
Annotations: T_A: primer specific annealing temperature

		Temperature (°C)	Time	Process
Cycle 1	1x	95	15 min	Activation of Taq polymerase
Cycle 2	40x	95	20 s	Denaturation
		T_A	30 s	Primer specific annealing
		72	30 s	Product amplification
Cycle 3	1x	95	1 min	Final denaturation
Cycle 4	1x	T_A	1 min	Starting melting curve
Cycle 5	80x	T_A + 0.5	10 s	

A list of the used primers is featured in Table 69 below. All primers were purchased from Eurofins MWG Operon and were dissolved in nuclease-free water according to manufacturer's instruction. The primers *CYP1A1*, *CYP1A2*, *CYP1B1*, *ALDH3A1*, *CD36*, and *TIPARP* were validated by our project partner in Utrecht, whereas *HSD17B2* and *AHRR* were validated in our laboratory. All mouse primer were already validated and used in our laboratory (Roos, 2011).

Table 69. Overview of primer information featuring species, gene of interest, systematic gene name, primer sequence, length and annealing temperature (T_A).
Annotations: a) Andersson et al., 2011; b) Chuang et al., 2009; c) Ooi et al., 2011; d) Su et al., 2007 e) designed by the use of Primer BLAST (Basic Local Alignment Search Tool) of the NCBI database; f) Roos, 2011; g) Dörr, 2010

Gene	Systematic name	5`- 3`	Length	T_A (°C)	Reference
human					
CYP1A1	NM_000499	CAGAAGATGGTCAAGGAGCA	20	60	a)
		GACATTGGCGTTCTCATCC	19		
CYP1A2	NM_000761	CCCAGAATGCCCTCAACA	18	60	c)
		CCACTGACACCACCACCTGAT	21		
CYP1B1	NM_000104	CGGCCACTATCACTGACATC	20	60	a)
		CTCGAGTCTGCACATCAGGA	20		
ALDH3A1	NM_001135168	GCAAGCAAGTAAGGGAGCGGA	21	60	e)
		ACCCGAGTCCTAAGCCGAACTG	22		
HSD17B2	NM_002153	CTGAGGAATTGCGAAGAACC	20	60	e)
		AAGAAGCTCCCCATCAGTTG	20		
TIPARP	NM_001184717	GCGCACAAGTCTTCGTCTTCCTCC	24	60	e)
		AAAAATCCTCCCGAGGAGCGTCCAA	25		
AHRR	NM_020731	CTTCATCTGCCGTGTGCGCT	20	57	e)
		ATGAGTGGCTCGGGACAGCAGA	22		
CD36	NM_001127444	AGATGCAGCCTCATTTCCAC	20	60	b)
		CGTCGGATTCAAATACAGCA	20		
ACTB	NM_001101	CGTGCGTGACATTAAGGAGAA	21	55.7	g)
		CAATGCCAAGGCAGGAAGG	19		

mouse					
Cyp1a1	NM_009992	ACTTCATTCCTGTCCTCCGTTACC	24	52	f)
		GCCCTTCTCAAATGTCCTGTAGTG	24		
Cyp1a2	NM_009993	CCGAGGAGAAGATTGTCAACATTG	24	52	f)
		GCCAACCACCGTGTCCAG	18		
Cyp2b10	NM_009999	AGTGTGGAGGAGCGGATTCAGG	22	60	f)
		AACAGCTCCAGCAGGCGCAA	20		
Cyp3a44	NM_177380	ACAGAGAGTCACACATACATCTGGAGG	27	58	f)
		TGTGTACGGGTCCCATATCGGTAGAG	26		
36b4	NM_007475	GCCACCTGGAGAACAACC	18	58	f)
		GCCAACAGCATATCCCGAATC	21		

Calculation of mRNA expression

Calculations were carried out using the comparative delta delta C_T ($\Delta\Delta C_T$) method according to Pfaffl (2001). First, the relative expression level of a target gene is compared to a reference gene (housekeeping gene, *36b4*, or *ACTB*) resulting in the ΔC_T value. Then, the ΔC_T value of the control was subtracted from ΔC_T value of compound-treatment leading to the x-fold mRNA induction of the target gene:

$$\Delta C_T = C_T \text{ (target gene)} - C_T \text{ (housekeeping gene)}$$
$$\Delta\Delta C_T = \Delta C_T \text{ (treatment)} - \Delta C_T \text{ (control)}$$
$$\text{x-fold induction} = 2^{-\Delta\Delta C_T}$$

The value of 2 is derived based on an optimal primer efficiency of 100 %, which means that with each cycle the amplified product is doubled. All primers were either already validated in our laboratory, in a laboratory of our project partner, published in literature or online available at the NCBI platform. Primer requirements included that they may only synthesize one specific product and have a complementary RNA sequence to the target sequence which is distinguished by exon bridges. Furthermore, the formed product should not be longer than 200 base pairs. The respective primer annealing temperature was determined using a temperature gradient. Primers efficiency was assigned based on a serial dilution of cDNA. Only primers with an efficiency of approximately 100 % were applied in RT-PCR.

VI.3.7 Microarray

Microarray technology is a powerful tool to examine large numbers of genes simultaneously. Microarrays were developed during the mid-nineties of the last century by down screening of large-sized hybridization and other interaction techniques (Müller et al., 2004) (Shena et al., 1995). The term is composed of two words 'micro' and 'array'. Micro means something 'extremely small'. However, only a few definitions are given for the noun array but the following is the most appropriate one: array - 'a large group or collection of things, usually arranged so that you can see them all' (Dictionary of Contemporary English, 1995). Implying a large number of molecules for example oligonucleotides are placed on an extremely small surface. Throughout the years, various improvements have been carried out resulting in a standardized, user friendly, and fast screening method within the field of Genomics. There are different types of microarrays available on the market depending on starting material (DNA or RNA) and requested endpoint.

VI.3.7.1 Microarray Procedure

In the present work, gene expression analysis was performed according to the Agilent's Two-Color Microarray-based Gene Expression Analysis using Whole Human (or Mouse) Genome Oligo Microarray Kit 4 x 44K (Agilent Technologies).

The chosen microarray experiment is based on a two-colour labelling reaction using the two different fluorophores cyanine 3 (Cy3) and cyanine 5 (Cy5) with an emission wavelength of 570 nm (green part of light spectrum) and 670 nm (red part of the light spectrum) (Ernst et al., 1989) (Tang et al., 2007). Compound-treated samples and control samples were labelled oppositionally. At least four independent experiments were performed within the mouse studies and five within the *in vitro* cell studies. Additionally, a dye-swap was carried out meaning compound-treated samples and control samples were labelled differently in each independent experiment. For example TCDD-treated hHeps were labelled with Cy3 in the first experiment and labelled with Cy5 in the second experiment. The dye change in each experiment was performed to reduce possible errors due to the dye colour. Figure 68 features the individual steps and procedures within the microarray experiment.

First, by the use of Agilent's Low Input Quick Amp Labeling Kit, the isolated RNA (100 ng per sample) was transcribed into cDNA before cRNA was synthesized, dye-labelled, and amplified. Afterwards, the synthesized cRNA was purified using RNeasy Mini Kit (Qiagen) and prepared for hybridization (Gene Expression Hybridization Kit, Agilent Technology). Hybridization was carried out for 17 h at 65 °C in a rotating hybridization chamber. Then, microarray slides were washed using Agilent's Gene Expression Wash Buffer Kit and dried. Afterwards slides were scanned by Agilent B Microarray scanner and data was extracted using Agilent Feature Extraction Software (version 9.5.1).

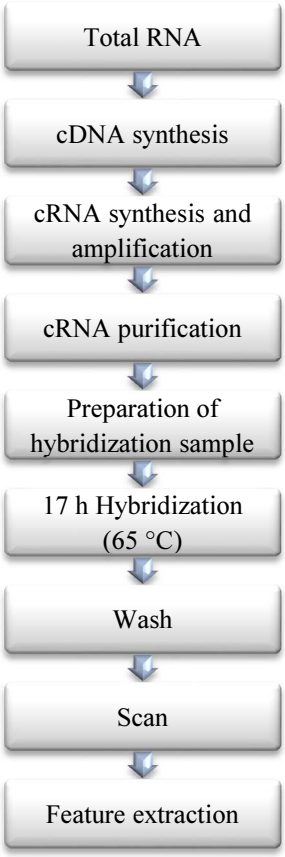

Figure 68. Workflow for sample preparation and array processing (Agilent Technologies, 2010).

Step 1: Preparing Spike-Ins

Initially, RNA Spike-In solutions were prepared according to user's manual. The used oligonucleotides microarrays contain positive controls which were designed to hybridize with the Spike-Ins. Positive controls (*in vitro* synthesized polyadenylated transcripts derived from the Adenovirus E1A transkriptome) are used to monitor the workflow from sample amplification and labelling to microarray processing. This procedure provides important information about the system`s linearity, sensitivity, and accuracy which can later be used to normalize the target probes. Both Spike-In solutions (Spike A Mix labelled with Cy3; Spike B Mix labelled with Cy5) were prepared as described below.

Table 70. Dilutions of Spike A and Spike B Mix.

Starting amount of RNA Total RNA (ng)	**Serial dilution** First	Second	Third	**Spike-In mix volume used in labelling reaction (µl)**
100	1:20	1:40	1:32	2

The following description of the applied experimental procedure pertains for both Spike-In mixes. The first dilution was created by mixing the stock solution (Spike A / Spike B Mix) and transferring 2 µl in a 1.5 ml microtube containing 38 µl of provided Dilution Buffer. Then, the first dilution was mixed thoroughly and spinned down. Afterwards, the second dilution was prepared pipetting 2 µl of the first dilution into another 1.5 ml microtube containing 75 µl of Dilution Buffer. The second dilution was mixed by vortexing and spinned down. Then, the third and final dilution was carried out using 2 µl of second dilution and 62 µl of Dilution Buffer in another 1.5 ml microtube. The third dilution was thoroughly vortexted and centrifuged.

Step 2: Preparing labelling reaction

All samples were diluted with nuclease-free water so that the starting amount of RNA for each sample was 100 ng in 1.5 µl. These 1.5 µl were transferred into a 1.5 ml microtube and 2 µl of Spike A mix (cyanine 3-labelled) or respectively Spike B mix (cyanine 5-labelled) was added. The T7 Promotor Primer Mix was prepared (Table 71) and 1.8 µl were additionally transferred into the tube. Denaturation of primer and template was carried out by incubating the reaction mix at 65 °C in a thermomixer (Eppendorf) for 10 min. The reaction mix was placed on ice and incubated for 5 min. Then, samples were centrifuged at 10 000 rpm for 30 s at 4 °C and again placed on ice. Subsequently, 4.7 µl of the cDNA Master Mix (Table 72) was added to each reaction solution mix and thoroughly mixed by repeated up- and down-pipetting. Thereafter, samples were incubated at 40 °C in a thermomixer for 2 h. During this step, RNA samples were transcribed into cDNA which is equipped with a T7 RNA polymerase promoter sequence.

Table 71. T7 Promoter Primer Mix.

Component	Volume (µl) per reaction
T7 Promoter Primer	0.8
Nuclease-free water	1.0
Total volume	**1.8**

Table 72. cDNA Master Mix.

Component	Volume (µl) per reaction
First Strand Buffer (5X)	2.0
DDT (0.1 M)	1.0
dNTP mix (10 mM)	0.5
AffinityScript RNase Block Mix	1.2
Total volume	**4.7**

Then, samples were immediately incubated at 70 °C in a thermomixer (Eppendorf) for 15 min to inactivate the AffinityScript enzymes. After that, samples were placed on ice for 5 min and briefly centrifuged (30 s, 10000 rpm, 4 °C) to spin down any contents from the walls and lid of the tube. The Transcription Master Mix was prepared (Table 73) and 6 µl was added to each sample. The sample reaction mixture was blended by up- and down-pipetting and incubated for another 2 h at 40 °C in a thermomixer (Eppendorf).

Table 73. Transcription Master Mix.

Component	Volume (µl) per reaction
Nuclease-free water	0.75
Transcription Buffer (5X)	3.2
DTT (0.1 M)	0.6
NTP mix	1.0
T7 Polymerase Blend	0.21
Cyanine 3-CTP or cyanine 5-CTP	0.24
Total volume	**6.0**

Figure 69 summarizes the amplified cRNA procedure. With the aid of the T7 RNA polymerase cDNA is transcribed into cRNA which is subsequently amplified. Furthermore, the T7 RNA polymerase also incorporates cyanine 3- or cyanine 5-labelled CTP. In the following, cRNA samples were placed on ice for 5 min and were briefly centrifuged before starting purification procedure.

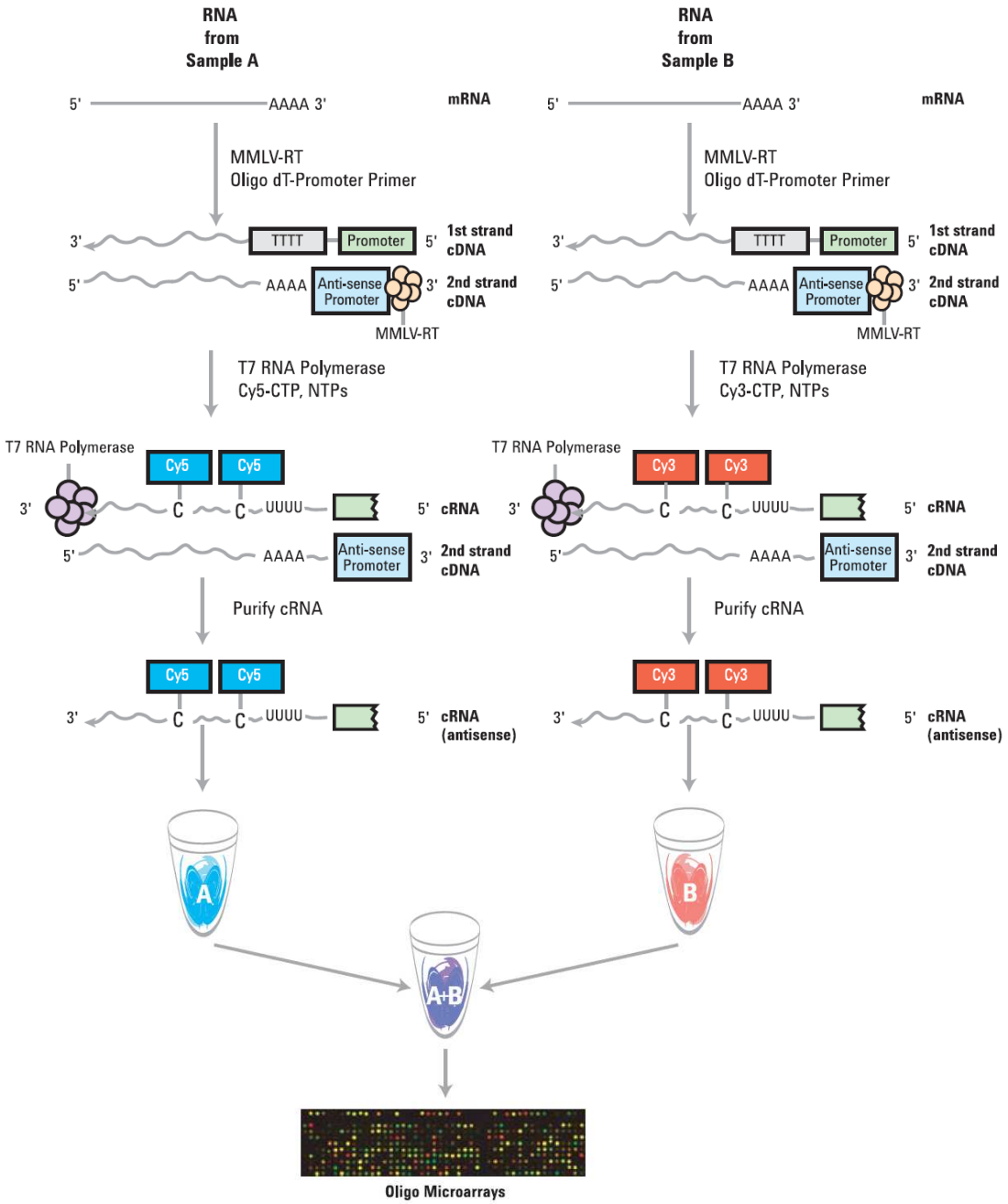

Figure 69. Generated and amplified cRNA procedure (Agilent Technologies, 2010).

Step 3: Purification of labelled/amplified cRNA

The purification step was carried out using the RNeasy Mini Kit (Qiagen). 84 µl of nuclease-free water and 350 µl of Buffer RLT were added to each cRNA sample and mixed well by pipetting. Following this, 250 µl of ethanol (100 %) were added and mixed thoroughly by repeated up- and down-pipetting. The entire cRNA-ethanol sample (700 µl) was then transferred into an RNeasy Mini column which was then centrifuged at 4 °C for 30 s at 13000 rpm. The generated and amplified cRNA was bound to the membrane during this step. Subsequently, the bound cRNA was washed using 500 µl of Buffer RPE and centrifuged at 4 °C for 30 s at 13000 rpm.

This step was repeated once again, but the centrifugation time was enhanced to 1 min to remove any remaining traces of Buffer RPE. The column was then transferred into another 1.5 ml tube and 30 µl of nuclease-free water were directly added onto the filter membrane. After a delay of 1 min, purified cRNA was eluted by centrifugation (4 °C, 30 s, 13000 rpm). Upon elution, the cleaned cRNA was placed on ice.

Step 4: Quantification of cRNA

Purified cRNA was quantified by NanoDrop 1000 using the Microarray measurements which records:

- Cyanine 3 or cyanine 5 dye concentrations (pmol/µl)
- RNA absorbance (260 nm/280 nm)
- cRNA concentration (ng/µl)

The yield of cRNA was calculated as follows:

$$\frac{(\text{concentration of cRNA}) \times 30\ \mu\text{l (elution volume)}}{1000} = \mu\text{g of cRNA}$$

The **specific activity** was determined using the subsequent equation:

$$\frac{\text{concentration of Cy3 or Cy5}}{\text{concentration of cRNA}} \times 1000 = \text{pmol Cy3 or Cy5 per } \mu\text{g cRNA}$$

The yield should be > 0.825 µg and the specific activity > 6 pmol Cy3 or Cy5 per µg cRNA. These values depend on the chosen microarray format (4-pack) and are recommended to proceed to the hybridization step (Agilent Technologies, 2010).

Step 5: Preparation for hybridization

Hybridization of the fluorescence-labelled purified cRNA was performed using Agilent`s Gene Expression Hybridization Kit (Agilent Technolgies, 2010).

First, the lyophilized 10x Blocking Agent was dissolved in 500 µl nuclease-free water, vortexted, and incubated for 5 min at 37 °C in a thermomixer (Eppendorf). Afterwards, any material adhering was driven down by centrifugation for 10 s.

In the present work, the 4 x 44K microarray format was chosen. The fragmentation mix was prepared according to Table 74. As described before, compound-treated samples and respective control samples were labelled with cyanine fluorophores complementary and were at this point of the experiment combined and together hybridized. The unified samples were incubated at 60 °C for exactly 30 min in a thermomixer (Eppendorf) to fragmentate RNA.

Afterwards, samples were immediately placed on ice for 1 min before 55 µl of 2x GEx Hybridization Buffer HI-RPM were added. The hybridization mix was carefully mixed by up- and down-pipetting avoiding the formation of bubbles. Then, the mix was centrifuged for 1 min at room temperature at 13000 rpm and samples were immediately loaded onto the array.

Table 74. Fragmentation mix for 4-pack microarray format.

Component	Volume/Mass
Cyanine 3-labelled, linearly amplified cRNA	825 µg
Cyanine 5-labelled, linearlyamplified cRNA	825 µg
Blocking Agent (10x)	11 µl
Nuclease-free water	Bring volume to 52.8
Fragmentation Buffer (25x)	2.2 µl
Total volume	**55 µl**

A hybridization gasket slide was inserted into the chamber base with the label reading 'Agilent' facing up. The hybridization sample was slowly dispensed onto the middle of the gasket well. This procedure was repeated for the other three wells noting the position of each sample on the gasket slide. Then, the microarray slide was slowly and gently placed on the gasket slide, so that the numeric barcode side was facing up. The chamber cover is placed onto the chamber base containing the 'sandwiched' slides. The clamp assembly was carefully slipped onto the chamber base and the cover resting at the centre of both and was finally tightened. The assembled chamber was rotated to check if the hybridization samples coat the entire surface of the array. Afterwards, the chambers were placed in rotisserie in a hybridization oven preheated at 65 °C and rotated at 10 rpm. Hybridization was carried out for 17 h.

Step 6: Microarray slide wash

After 17 h, the chamber was dissembled and the slide sandwich was carefully submerged into a slide-staining dish containing Wash Buffer 1. The sandwich was pried open from the barcode end using tweezers. The microarray slide is then placed into a slide-staining dish containing Wash Buffer 1 at room temperature for 1 min. Then, the slide was transferred in a slide-staining dish containing preheated (37 °C) Wash Buffer 2 at room temperature for another minute. Slowly the microarray slide was removed from the rack to avoid droplets on the slide. Slides were immediately put into a slide holder facing Agilent barcode up and were directly inserted in the scanner carousel. This procedure was repeated for each microarray slide.

Step 7: Scanning and feature extraction

The microarray slides were immediately scanned after the washing procedure using the Agilent B Microarray scanner (Agilent Technologies). After completing the scan process, the user obtains the microarray image scan which was is used for data evaluation. Data was extracted using Agilent Feature Extraction Software (version 9.5.1). Information from probe features was extracted from microarray scan data.

VI.3.7.2 Microarray Data Analysis and Processing

Agilent Technologies Scanner System (Scanner Model G2505B) with Agilent Scan Control Software Version A.7.0.1 was used for microarray scanning. Preliminary processing of data was made using the Agilent Feature Extraction Software (9.5.1.1, Agilent Technologies). Data normalisation and statistical analyses were performed using Bioconductor (Gentleman 2004) R (version 2.15.1) package limma (version 3.12.3) (Smyth et al., 2004). Raw signals were background corrected by subtracting local spot background. Two normalization methods were applied: first within arrays using the global loess method and second between the arrays using the Aquantile method. Differential expression was assessed using empirical Bayes moderated t-tests carried out in limma (Smyth et al., 2005) on the dataset. Cut-off criteria for further functional analysis were log2 fold change (lfc) ≥ 2, p-values ≤ 0.05 corrected by false discovery rate (FDR) using the Benjamini-Hochberg method (Benjamini et al., 1995) and an A-mean value ≥ 7 (in case of hHeps vs. HepG2 cells A ≥ 5). The clipped list was subjected to Gene Ontology (GO) analysis using the TopGO (version 2.8.0) package in R (Alexa et al., 2006). Classical enrichment analysis by testing the over-representation of GO terms within the group of differentially expressed genes was performed using Fisher's exact test.

VI.4 Statistical Analysis

In the present work statistical analysis of the obtained data was performed using GraphPad InStat 3.0 software (GraphPad Software, San Diego, CA, USA). Results are presented as means ± standard deviation (SD) from at least three independent experiments. One-way ANOVA (analysis of variance) with Dunnett`s post test was used when the difference between the control and various concentration of a test compound was determined (concentration-dependent measurements). The difference between the control and treatment (one test compound concentration) or between different compound treatments was determined using the one-tailed unpaired Student`s t-test with Welch correction. Significant effects are assigned in the present work with asterisks: * = $p \leq 0.05$, ** = $p \leq 0.01$, *** = $p \leq 0.001$.

Concentration-response curves from at least three independent experiments were obtained using Origin 6.0 Microcal software (OriginLab, Northampton, MA, USA). Plotting the used concentrations in a logarithmic scale against the assay-specific parameters (EROD: EROD activity; RT-PCR: x-fold), EC_{50} values were subsequently derived by sigmoidal fitting. For EC_{20} values the upper limit of the respective TCDD-derived induction was set 100 % and the test compound concentrations required to achieve 20 % of the TCDD response were defined as EC_{20}.

VII Materials

VII.1 Test Compounds

Test compounds used in *in vivo* mouse studies I and II and *in vitro* experiments are summarized in Tables 75 and 76. The purities of PCB 118, 153, and 156 were analyzed. Subsequently, PCB 118 and 156 were purified at the Department of Chemistry at Umeå University, Sweden. The final TEQ contributions of impurities after purification were 6.6 ng TEQ/g, 0.41 ng TEQ/g, and 36 ng TEQ/g for PCB 118, PCB 153, and PCB 156, respectively. These impurity values were considered to have no influence on the final outcome of the results (van Ede et al., 2013). The seven selected core congeners applied in mouse *in vivo* studies I and II were dissolved in corn oil and administered by oral gavage. All other compounds had a purity > 99 % except for 1,4,6-HpCDD (98.7 %). Compounds used in *in vitro* studies were dissolved in DMSO (dried, obtained from Sigma-Aldrich, Stockholm, Sweden). Prepared compound stock solutions were diluted with DMSO depending on compound, cell model, and assay-specific concentration range.

Table 75. List of compounds applied in *in vivo* studies (mouse study I and II).
Annotations: a) Wellington Laboratories Inc. (Guelph, Ontario, Canada)
b) Cerilliant Corp. (Round Rock, TX, USA)

Compound	Chlorination position and degree	Type of congener	Purchased from
TCDD	2,3,7,8-TetraCDD	PCDD	a)
1-PnCDD	1,2,3,7,8-PentaCDD	PCDD	a)
4-PnCDF	2,3,4,7,8-PentaCDF	PCDF	a)
PCB 118	2,3',4,4',5-PentaCB	Dioxin-like PCB	b)
PCB 126	3,3',4,4',5-PentaCB	Dioxin-like PCB	a)
PCB 153	2,2',4,4',5,5'-HexaCB	Non dioxin-like PCB	b)
PCB 156	2,3,3',4,4',5-HexaCB	Dioxin-like PCB	b)

TCDD used in the transgenic mouse study (mouse study III) was purchased from AccuStandard (New Haven, CT, USA) dissolved in corn oil and administered by oral gavage.

Table 76. List of compounds applied in *in vitro* studies.
Annotations: a) Wellington Laboratories Inc. (Guelph, Ontario, Canada)
b) Cerilliant Corp. (Round Rock, TX, USA)
c) Larodan Fine Chemicals (Malmö, Sweden)

Compound	Chlorination position and degree	Type of congener	Purchased from
TCDD	2,3,7,8-TetraCDD	PCDD	a)
1-PnCDD	1,2,3,7,8-PentaCDD	PCDD	a)
1,6-HxCDD	1,2,3,6,7,8-HexaCDD	PCDD	a)
1,4,6-HpCDD	1,2,3,4,6,7,8-HeptaCDD	PCDD	a)
TCDF	2,3,7,8-TetraPCDF	PCDF	a)
4-PnCDF	2,3,4,7,8-PentaCDF	PCDF	a)
1,4-HxCDF	1,2,3,4,7,8-HexaCDF	PCDF	a)
1,4,6-HpCDF	1,2,3,4,6,7,8-HeptaCDF	PCDF	a)
PCB 77	3,3',4,4'-TetraCB	Dioxin-like PCB	c)
PCB 105	2,3,3',4,4'-PentaCB	Dioxin-like PCB	c)
PCB 118	2,3',4,4',5-PentaCB	Dioxin-like PCB	b)
PCB 126	3,3',4,4',5-PentaCB	Dioxin-like PCB	a)
PCB 153	2,2',4,4',5,5'-HexaCB	Non dioxin-like PCB	b)
PCB 156	2,3,3',4,4',5-HexaCB	Dioxin-like PCB	b)

VII.2 Chemicals, Cell Cultures, Kits, Consumables, and Equipment

VII.2.1 Cell Cultures

The human hepatocellular carcinoma cell line HepG2 was purchased from DSMZ (Deutsche Sammlung von Mikroorganismen and Zellkulturen GmbH), Heidelberg, Germany.

Primary human hepatocytes as well as culture media and supplements were purchased from Lonza, Verviers, Belgium.

VII.2.2 Chemicals

All chemicals applied in the present work are summarized in the following list:

Table 77. List of chemicals/reagents in alphabetical order.

Chemical	Manufacturer, Purchaser
Accutase	PAA Laboratories GmbH, Coelbe, Germany
Acetonitrile (HPLC grade)	Merck, Darmstadt, Germany
Acrylamide-Mix (rotiphorese 30)	Roth, Karlsruhe, Germany
APS	Merck, Darmstadt, Germany
Bromophenol blue	Merck, Darmstadt, Germany
Copper sulphate	Merck, Darmstadt, Germany
DCC/FCS	PAA Laboratories GmbH, Coelbe, Germany
Dexamethasone	Sigma-Aldrich, Schnelldorf, Germany
Dicumarol	Sigma-Aldrich, Schnelldorf, Germany
DMSO	Fluka, Neu-Ulm, Germany
Disodium carbonate	Merck, Darmstadt, Germany
Disodium EDTA	Roth, Karlsruhe, Germany
Disodium hydrogen phosphate	Merck, Darmstadt, Germany
DMEM low glucose w/o phenol red	PAA Laboratories GmbH, Coelbe, Germany
DMF	Merck, Darmstadt, Germany
EDTA	Merck, Darmstadt, Germany
EGTA	Sigma-Aldrich, Schnelldorf, Germany
Ethanol p.a.	Merck, Darmstadt, Germany
Ethidium bromide solution (10 mg/ml)	Sigma-Adrich, Schnelldorf, Germany
Ethoxyresorufin	Sigma-Aldrich, Schnelldorf, Germany
FCS Gold Standard	PAA Laboratories GmbH, Coelbe, Germany
Glucose	Merck, Darmstadt, Germany
Glycine	Sigma-Aldrich, Schnelldorf, Germany
Heparin	Serva, Heidelberg, Germany
HEPES	Roth, Karlsruhe, Germany

Hydrogen peroxide solution (30 %)	Applichem, Darmstadt, Germany
Isopropanol	Merck, Darmstadt, Germany
Luminol	Sigma-Aldrich, Schnelldorf, Germany
Magnesium chloride	Merck, Darmstadt, Germany
Magnesium sulphate	Merck, Darmstadt, Germany
Mercaptoethanol	Merck, Darmstadt, Germany
Methanol (HLPC-grade)	Merck, Darmstadt, Germany
p-coumaric acid	Sigma-Aldrich, Schnelldorf, Germany
Penicilin/Streptomycin	PAA Laboratories GmbH, Coelbe, Germany
Pentobarbital	Sigma-Aldrich, Schnelldorf, Germany
Potassium chloride	Merck, Darmstadt, Germany
Potassium dihydrogen phosphate	Merck, Darmstadt, Germany
Potassium hydrogen phosphate	Merck, Darmstadt, Germany
Potassium phosphate	Merck, Darmstadt, Germany
Primer	MWG-Biotech AG, Ebersberg, Germany
Resorufin sodium salt	Sigma-Aldrich, Schnelldorf, Germany
Saponine	Sigma-Adrich, Schnelldorf, Germany
SDS	Merck, Darmstadt, Germany
Skimmed milk powder	Spinnrad GmbH, Gelsenkirchen, Germany
Sucrose	Merck, Darmstadt, Germany
Sodium chloride	Merck, Darmstadt, Germany
Sodium hydrogen phospate	Merck, Darmstadt, Germany
Sodium hydroxide	Merck, Darmstadt, Germany
TEMED	Serva, Heidelberg, Germany
Tris	Roth, Karlsruhe, Germany
Trypsin/EDTA(1:250)-solution	PAA Laboratories GmbH, Coelbe, Germany
Tween 20	Sigma-Aldrich, Schnelldorf, Germany

VII.2.3 Kits

All used kits in the present work are summarized in the following list:

Table 78. List of kits in alphabetical order.

Kit	Manufacturer, distributor
E. Z. N. A.® Tissue DNA Kit (Omega Bio-Tek)	VWR International GmbH, Darmstadt,Germany
RNeasy® Mini Kit	Bio-Rad Laboratories GmbH, Munich, Germany
BCA™ Protein Assay Kit (Pierce)	Thermo Fisher Scientific, Karlsruhe, Germany
iScript cDNA synthesis Kit	Bio-Rad Laboratories GmbH, Munich, Germany
ABsolute QPCR SYBR Green Fluorescein Mix	Thermo Fisher Scientific, Karlsruhe, Germany
Low Input Quick Amp Labeling Kit, Two-Color	Agilent Technologies, Waldbronn, Germany
RNA Spike-In Kit	Agilent Technologies, Waldbronn, Germany
Gene Expression Hybridization Kit	Agilent Technologies, Waldbronn, Germany
Gene Expression Wash Buffer Kit	Agilent Technologies, Waldbronn, Germany

VII.2.4 Consumables

All consumables utilized in the present work are summarized in the following list:

Table 79. List of consumables in alphabetical order.

Consumables	Manufacturer, distributor
Combitips (5 ml, 10 ml, 25 ml, Eppendorf Biopur)	VWR International GmbH, Darmstadt,Germany
Filter (0.2 & 0.45 µm PTFE)	Roth, Karlsruhe, Germany
Mikro reaction tubes (1.5 ml & 2 ml, PP)	Greiner Bio-one GmbH, Frickenhausen, Germany
Multiwell plates (6, 24 & 96 well, PP)	Greiner Bio-one GmbH, Frickenhausen, Germany
Pasteur pipettes (glass)	Roth, Karlsruhe, Germany
Petri dishes (94mm & 60mm)	Greiner Bio-one GmbH, Frickenhausen, Germany
Pipette tips (various sizes)	Greiner Bio-one GmbH, Frickenhausen, Germany
PCR tips (with filter; various sizes)	Peqlab Biotechnology GmbH, Erlangen, Germany
Needles single-use Sterican (26 G x 1)	B|Braun, Melsungen, Germany
Sample tubes (15ml, 50ml, PP)	Greiner Bio-one GmbH, Frickenhausen, Germany
Syringes Omnifix®-F (1 ml)	B|Braun, Melsungen, Germany
Cell culture flasks (250 ml, PP)	Greiner Bio-one GmbH, Frickenhausen, Germany

VII.2.5 Equipment

The following table summarizes the equipment used in the present work:

Table 80. List of applied equipment in alphabetical order.

Equipment	Manufacturer, distributor
Autoklaves	
Varioklav Typ 500	H&P Labortechnik, Munich, Germany
UNOLD, Electro	UNOLD, Hockenheim, Germany
Bioanalyzer	Agilent Technologies, Waldbronn, Germany
Biofreezer MDF-U6086S	Sanyo E&E Europe BV, AZ Etten Leur, NL
Camera (EOS 300 Canon)	Canon, Krefeld, Germany
Centrifuges	
Megafuge 1.0 R	Heraeus, Hanau, Germany
Microfuge R	Beckman Coulter, Krefeld, Germany
Rotina 35	Hettich GmbH & Co. KG, Tuttlingen, Germany
Sigma 1-13	Sigma Laboratory centrifuges GmbH, Osterode, Germany
Sigma 1 L-12	Sigma Laboratory centrifuges GmbH, Osterode, Germany
Ultracentrifuge Optima TL	Beckman Coulter, Krefeld, Germany
Cleanbenchs	
BSB 4A	Gelaire Flow Laboratories, Meckenheim, Germany
Hera Safe	Hereus, Hanau, Germany

Eagle Eye II Cabinet	Stratagene, Amsterdam, NL
Electrophoresis chamber Mini Protean III Apparatus	Bio-Rad Laboratories GmbH, Munich, Germany
Electrophoresis power supply Bio-Rad Power Pac 300	Bio-Rad Laboratories GmbH, Munich, Germany
Glassware (beakers, graduated pipettes & measuring cylinders, screw top bottles)	VWR International GmbH, Darmstadt, Germany
Hand tally counter	Roth, Karlsruhe, Germany
HPLC-ESI-MS/MS	
Massenspektrometer API 2000	AB Sciex, Darmstadt, Germany
PerkinElmer Series 2000	PerkinElmer, Rodgau, Germany
PerkinElmer Ultraviolet detector 785 A	PerkinElmer, Rodgau, Germany
HPLC column	
LiChrospher® 100 RP-18 (125mm x 4mm, 5 µm), Merck	VWR International GmbH, Darmstadt, Germany
HPLC guard column	
LiChrospher® 100 RP-18 (5 µm) LiChroCART® 4-4, Merck	VWR International GmbH, Darmstadt, Germany
HPLC cartridge holder	
manu-Cart® NT, Merck	VWR International GmbH, Darmstadt, Germany
Homogenizer ultrasonic needle	B|Braun, Melsungen, Germany
Incubators	
BBD6220 Heraeus	Heraeus, Hanau, Germany
Cytosperm	Heraeus, Hanau, Germany
Light microscopes	
Axiovert 25	Zeiss, Jena, Germany
Axioskop	Zeiss, Jena, Germany
Zeiss IM	Zeiss, Jena, Germany
Leica DM IRB	Leica, Bonn, Germany
Lumi Imager	Roche, Mannheim, Germany
Luminometer Lumat LB 9507	Berthold, Bad Wildbad, Germany
Magnetic stirrer MR 3001	Heidolph Elektro, Kelheim, Germany
Microarray scanner B G2505	Agilent Technologies, Waldbronn, Germany
Multipette ® (Research plus, Eppendorf)	VWR International GmbH, Darmstadt, Germany
NanoDrop®(ND-1000 Spectrophotometer)	Peqlab, Erlangen, Germany
Neubauer Counting Chamber	Roth, Karlsruhe, Germany
pH meter	Eutech Instruments Europe B.V. AG Nijkerk, NL
Pipettes	
Eppendorf Research	VWR International GmbH, Darmstadt, Germany
Pipetman Gilson	VWR International GmbH, Darmstadt, Germany
Pipetus® accu-jet pro	Brand GmbH & Co KG, Wertheim, Germany
Plate readers	
Fluoroskan Ascent FL	Labsystems, Dreieich, Germany
MWGt Sirius HT Injector	BioTek Instruments Inc., Winooski, VT, USA

Refrigerators and freezer combinations	Liebherr, Karlsruhe, Germany Phillips, Herrsching, Germany
Scales	
Sartorius BP 210 S	Sartorius AG, Goettingen, Germany
Sartorius CP64-OCE	Sartorius AG, Goettingen, Germany
Sartorius CPA 2245	Sartorius AG, Goettingen, Germany
OHAUS Precision Standard	OHAUS, Bradford, MA, USA
Semi-dry blotter TE 77	Hoever Inc., San Francisco, CA, USA
Shaker PMS-1000	Grant-bio Ltd., Cambridgeshire, UK
Thermomixer comfort	Eppendorf AG, Hamburg, Germany
Thermal cyclers	
MyCycler™	Bio-Rad Laboratories GmbH, Munich, Germany
iCycler™	Bio-Rad Laboratories GmbH, Munich, Germany
Ultrasonic probe Sonoplus	Bandelin electronics GmbH & Co. KG, Berlin, Germany
Vortex Relax 2000	Heidolph, Frankfurt/Main, Germany
Water baths	
GFL 1083	GFL, Burgwedel, Germany
Julabo 13	Julabo, Seelbach, Germany

VIII References

Abbott B. D., Birnbaum L. S. (1989). Cellular alterations and enhanced induction of cleft palate after coadministration of retinoic acid and TCDD. *Toxicology and Applied Pharmacology*, 99(2):287-301.

Abbott B. D., Perdew G. H., Birnbaum L. S. (1994). Ah receptor in embryonic mouse palate and effects of TCDD on receptor expression. *Toxicology and Applied Pharmacology*, 126(1):16-25.

Aden D. P., Fogel A., Plotkin S., Damjanov I., Knowles B. B. (1979). Controlled synthesis of HBsAg in a differentiated human liver carcinoma-derived cell line. *Nature*, 282(5739):615-616.

Ago T., Sadoshima J. (2006). GDF15, a cardioprotective TGF-β superfamily protein. *Circulation Research*, 98(3):294-297.

Ahlborg U. G., Becking G. C., Birnbaum L. S., Brouwer A., Derks H. J. G. M., Feeley M., Color G. Hanberg A., Larsen J. C., Liem A. K. D., Safe S. H., Schlatter C., Waern F., Younes M., Yrjäneikki E. (1994). Toxic equivalency factors for dioxin-like PCBs - Report on a WHO-ECEH and IPCS consultation. *Chemosphere*, 28(6):1049-1067.

Alcock R. E., Behnisch P. A., Jones K. C., Hagenmaier H. (1998). Dioxin-like PCBs in the environment - human exposure and the significance of sources. *Chemosphere*, 37(8):1457-1472.

Aleksunes L. M., Klaassen C. D. (2012). Coordinated regulation of hepatic phase I and II drug-metabolizing genes and transporters using AhR-, CAR-, PXR-, PPARα-, and Nrf2-null mice. *Drug Metabolism and Disposition*, 40(7):1366-1379.

Alexa A., Rahnenfuhrer J., Lengauer T. (2006). Improved scoring of functional groups from gene expression data by decorrelating GO graph structure. *Bioinformatics*, 22(13):1600-1607.

Alexander W. S., Hilton D. J., (2003). The role of suppressors of cytokine signaling (SOCS) proteins in regulation of the immune response. *Annual Review of Immunology*, 22:503-529.

Alnouti Y., Klaassen C. D. (2006). Tissue distribution and ontogeny of sulfotransferase enzymes in mice. *Toxicological Sciences*, 93(2):242-255.

Alnouti Y., Klaassen C. D. (2008). Tissue distribution, ontogeny, and regulation of aldehyde dehydrogenase (Aldh) enzymes mRNA by prototypical microsomal enzyme inducers in mice. *Toxicologocial Sciences*, 101(1):51-64.

Anakk S., Kalsotra A., Kikuta Y., Huang W., Zhang J., Staudinger J. L., Moore D. D., Strobel H. W. (2004). CAR/PXR provide directives for *Cyp3a41* gene regulation differently from *Cyp3a11*. *Pharmacogenomics Journal*, 4(2):1-11.

Anakk S., Huang W., Staudinger J. L., Tan K., Cole T. J., Moore D. D., Strobel H. W. (2007). Gender dictates the nuclear receptor-mediated regulation of the CYP3A44. *Drug Metabolism and Disposition*, 35(1):36-42.

Andersson H., Garscha U., Brittebo E. (2011). Effects of PCB126 and 17β-oestradiol on endothelium-derived vasoactive factors in human endothelial cells. *Toxicology,* 285(1-2):46-56.

Andreola F., Hayhurst G. P., Luo G., Ferguson S. S., Gonzalez F. J., Goldstein J. A., De Luca L. M. (2004). Mouse liver CYP2C39 is a novel retinoic acid 4-hydroxylase. Its down-regulation offers a molecular basis for liver retinoid accumulation and fibrosis in aryl hydrocarbon receptor-null mice. *Journal of Biological Chemistry*, 279(5):3434-3438.

Angrish M. M., Jones A. D., Harkema J. R., Zacharewski T. R. (2011). Aryl hydrocarbon receptor-mediated induction of stearoyl-CoA desaturase 1 alters hepatic fatty acid composition in TCDD-elicited steatosis. *Toxicological Science*s, 124(2):299-310.

Angrish M. M., Mets B. D., Jones A. D., Zacharewski T. R. (2012). Dietary fat is a lipid source in 2,3,7,8-tetrachlorodibenzo-*p*-dioxin (TCDD)-elicited hepatic steatosis in C57BL/6 mice. *Toxicological Sciences*, 128(2):377-386.

Angrish M. M., Dominici C. Y., Zacharewski T. R. (2013). TCDD-elicited effects on liver, serum, and adipose lipid composition in C57BL/6 mice. *Toxicological Sciences*, 131(1):108-115.

Arlt A., Schäfer H. (2011). Role of the immediate early response 3 (IER3) gene in cellular stress response, inflammation and tumourigenesis. *European Journal of Cell Biology*, 90(6-7):545-552.

Assem M., Schuetz E G., Leggas M., Sun D., Yasunda K., Reid G., Zelcer N., Adachi M., Strom S., Evans R. M., Moore D. D., Borst P., Schuetz J. D. (2004). Interactions between hepatic *Mrp4* and *Sult2a* as revealed by the constitutive androstane receptor and *Mrp4* knockout mice, *Journal of Biological Chemistry*, 279(21):22250-22257.

ATSDR. (1998). Toxicological profile for chlorinated dibenzo-*p*-dioxins. Agency for Toxic Substances and Disease Registry. Division of Toxicology/Toxicology Information Branch, Atlanta.

Baars A. J., Bakker M. I., Baumann R. A., Boon P. E., Freijer J. I., Hoogenboom L. A. P., Hoogerbrugge R., van Klaveren J. D., Liem A. K. D., Traag W. A., de Vries J. (2004). Dioxins, dioxin-like PCBs and non-dioxin-like PCBs in foodstuffs: occurrence and dietary intake in the Netherlands. *Toxicological Letters*, 151(1):51-61.

Baba T., Mimura J., Nakamura N., Harada N., Yamamoto M., Morohashi K.-I., Fujii-Kuriyama Y. (2005). Intrinsic function of the aryl hydrocarbon (dioxin) receptor as a key factor in female reproduction. *Molecular and Cellular Biology*, 25(22):10040-10051.

Babu E., Kanai T., Chairoungdua A., Kim D. K., Iribe Y., Tangtrongsup S., Jutabha P., Li Y., Ahmed N., Sakamoto S., Anzai N., Endou H. (2003). Identification of a novel system L amino acid transporter structurally distinct from heterodimeric amino acid transporters. *Journal of Biological Chemistry*, 278(44):43838-43845.

Balmer J. E. Blomhoff R. (2002). Gene expression regulation by retinoic acid. *Journal of Lipid Research*, 43(11):1773-1808.

Barbosa-Tessmann I. P., Chen C., Zhong C., Siu F., Schuster S. M., Nick H. S., Kilberg M. S. (2000). Activation of the human asparagine synthetase gene by the amino acid response and the endoplasmic reticulum stress response pathways occurs by common genomic elements. *Journal of Biological Chemistry*, 275(35):26976-26085.

Barrera J. A., Kao L.-R., Hammer R. E., Seemann J., Fuchs J. L., Megraw T. L. (2010). CDK5RAP2 regulates centriole engagement and cohesion in mice. *Developmental Cell*, 18(6):913-926.

Behari J. (2010). The Wnt/β-catenin signaling pathway in liver biology and disease. *Expert Review on Gastroenterolgy and Hepatology*, 4(6):745-756.

Beebe L. E:, Fornwald L. W., Diwan B. A., Anver M. R., Anderson L. M. (1995a). Promotion of *N*-nitrosodimethylamine-initiated hepatocellular tumors and hepatoblastomas by 2,3,7,8-tetrachlorodibenzo-*p*-dioxin or Aroclor 1254 in C57BL/6, DBA/2, and B6D2F1 mice. *Cancer Research*, 55(21):4875-4880.

Beebe L. E:, Anver M. R., Riggs C. W., Fornwald L. W., Anderson L. M. (1995b). Promotion of *N*-nitrosodiethylamine-initiated mouse lung tumors followed by expsoure to 2,3,7,8-tetrachlorodibenzo-*p*-dioxin. *Carcinogenesis*, 16(6):1345-1349.

Behnisch P. A., Hosoe K.., Sakai S. (2001). Bioanalytical screening methods for dioxins and dioxin-like compounds - a review of bioassay/biomarker technology. *Environment International*, 27(5):413-439.

Behnisch P. A., Hosoe K., Brouwer A., and Sakai S. (2002). Screening of Dioxin-Like toxic equivalents for various matrices with wildtype and rekombinant rat hepatoma H4IIE cells. *Toxicological Sciences*, 69(1):125-130.

Beischlag T. V., Morales J. L., Hollingshead B. D., Perdew G. H. (2008). The aryl hydrocarbon receptor complex and the control of gene expression. *Critical Reviews in Eukaryotic Gene Expression*, 18(3):207-250.

Benjamini Y., Hochberg Y. (1995). Controlling the fals discovery rate - a practical and powerful approach to multiple testing. *Journal of the Royal Statistical Society Series B*, 57(1):289-300.

Berg J. M., Tymoczko J. L., Stryer L. (2003). Biochemie. *Spectrum Lehrbuch,* 5. Auflage.

Bernshausen T., Jux B., Esser C., Abel J., Fritsche E. (2006). Tissue distribution and function of the aryl hydrocarbon repressor (AhRR) in C57BL/6 and aryl hydrocarbon receptor deficient mice. *Archives of Toxicology*, 80(4):206-211.

Bhadhprasit W., Sakuma T., Hatakeyama, Fuwa M., Kitajima K., Nemoto N. (2007). Involvement of glucocorticoid receptor and pregnane X receptor in the regulation of mouse CYP3A44 female-predominant expression by glucocorticoid hormone. *Drug Metabolism and Disposition*, 25(10):1880-1885.

Birnbaum L. S. (1986). Distribution and excretion of 2,3,7,8-tetrachlorodibenzo-p-dioxin in congenic strains of mice which differ at the Ah locus. *Drug Metabolism and Disposition*, 14(1):34-40.

Birnbaum L. S. (1994). The mechanism of dioxin toxicity: relationship to risk assessment. *Environmental Health Perspectives*, 102(Suppl 9):157-167.

Bjeldanes L. F., Kim J.-Y., Grose K. R., Bartholomew J. C., Bradfield C. A. (1991). Aromatic hydrocarbon responsiveness-receptor agonists generated from indole-3-carbinol in vitro and in vivo: comparisons with 2,3,7,8-tetrachlorodibenzo-p-dioxin. *Proceedings of the National Academy of Sciences*, 88(21):9543-9547.

Black M. B., Budinsky R. A., Dombkoswki A., Cukovic D., LeCluyse E. L., Ferguson S. S., Russel S. T., Rowlands J. C. (2012). Cross-species comparisons of transcriptomic alterations in human and rat primary hepatocytes exposed to 2,3,7,8-tetrachlorodibenzo-*p*-dioxin. *Toxicological Sciences*, 127(1):199-215.

Boesch J. S., Lee C., Lindahl R. G. (1996). Constitutive expression of class 3 aldehyde dehydrogenase in cultured rat corneal epithelium. *Journal of Biological Chemistry*, 271(9):5150-5157.

Bock K. W., Köhle C. (2005a). Ah receptor- and TCDD-mediated liver tumor promotion: clonal selection and expansion of cells evading growth arrest and apoptosis. *Biochemical Pharmacology*, 69(10):1403-1408.

Bock K. W., Köhle C. (2005b). UDP-glucuronosyltransferase 1A6: structural, functional, and regulatory aspects. *Methods Enzymology*, 400:57-75.

Bock K. W., Köhle C. (2006). Ah Receptor: dioxin-mediated toxic responses as hints to deregulated physiologic functions. *Biochemical Pharmacology*, 72(4):393-404.

Bonen A., Campbell S. E., Benton C. R., Chabowski A., Coort S. L., Han X. X., Koonen D. P., Glatz J. F., Luiken J. J., (2004). Regulation of fatty acid transport by fatty acid translocase/CD36. *Proceedings of the Nutrition Society*. 63(2):245-249.

Boutros P. C., Bielefeld K. A., Pohjanvirta R., Harper P. A. (2009). Dioxin-dependent and dioxin-independent gene batteries: comparison of liver and kidney in Ahr-null mice. *Toxicological Sciences*, 112(1):245-256.

Boverhof D. R., Tarn E., Harney A. S., Crawford R. B., Kaminski N. E., Zacharewski T. R. (2004). 2,3,7,8-Tetrachlorodibenzo-*p*-dioxin induces suppressor of cytokine signaling 2 in murine B cells. *Molecular Pharmacology*, 66(6):1662-1670.

Boverhof D. R., Burgoon L. D., Tashiro C., Sharratt B., Chittim B., Harkema J. R., Mendrick D. L., Zachareweski T. R. (2006). Comparative toxicogenomic analysis of hepatotoxic effects of TCDD in Sprague Dawley rats and C57BL/6 mice. *Toxicological Sciences*, 94(2):398-416.

Bowker-Kinley M., Popov K. M. (1999). Evidence that pyruvate dehydrogenase kinase belongs to the ATPase/kinase superfamily. *Biochemical Journal*, 344(Pt 1):47-53.

Budinsky R. A., LeCluyse E. L., Ferguson S. S., Rowlands J. C., Simon T. (2010). Human and rat primary hepatocyte CYP1A1 and 1A2 induction with 2,3,7,8-Tetracholordibenzo-*p*-dioxin, 2,3,7,8-Tetrachlorodibenzofuran, and 2,3,7,8-Pentachlorodibenzofuran. *Toxicological Sciences*, 118(1):224-235.

Bui P., Solaimani P., Wu X., Hankinson O. (2012). 2,3,7,8-Tetracholordibezo-*p*-dioxin treatment alters eicosanoid levels in several organs of the mouse in an aryl hydrocarbon receptor-dependent fashion. *Toxicological and Applied Pharmacology*, 259(2):143-151.

Bumpus N. N., Johnson E. F. (2011). 5-Aminoimidazole-4-carboxyamide-ribonucleoside (AICAR)-stimulated hepatic expression of Cyp4a10, Cyp1a14, and Cyp4a31, and other peroxisome proliferator-activated receptor α-responsive mouse genes is AICAR 5α-monophosphate-dependent and AMP-activated protein kinase-independent. *Journal of Pharmacology and Experimental Therapeutics*, 339(3):886-895.

Bundesinstitut für Risikobewertung (BfR). (2011). Frauenmilch: Dioxingehalte sinken kontinuierlich. Information Nr. 011/2011.

Burnicka-Turek O., Shirneshan K., Paprotta I., Grzmil P., Meinhardt A., Engel W., Adham I. M. (2009). Inactivation of insulin-like factor 6 disrupts the progression of spermatogenesis at late meiotic prophase. *Endocrinology* 150(9):4348-4357.

Burns-Naas L. A., Dearmann R. J., Germolec D. R., Kaminski N. E., Kimber I., Ladics G. S., Luebke R. W., Pfau J. C., Pruett S. B. (2006). "Omics" technologies and the immune system (a), (b). *Toxicology Mechanisms and Methods*, 16(2-3):101-119.

Calvert G. M., Hornung R. W., Sweeney M. H., Fingerhut M. A., Halperin W. E. (1992). Hepatic and gastrointestinal effects in an occupational cohort exposed to 2,3,7,8-Tetrachlorodibenzo-*p*-dioxin. *Journal of the American Medical Association*, 267(16):2209-2214.

Cammann K. (2001). Instrumentelle Analytische Chemie. *Springer Akademischer Verlag*, 1. Auflage.

Caramaschi F., del Corno G., Favaretti C., Giambelluca S. E., Montesarchio E., Fara G. M. (1981). Chloracne following environmental contamination by TCDD in Seveso, Italy. *International Journal of Epidemiology*, 10(2):135-143.

Cardenas-Navia L. I., Cruz P., Lin J. C., NIS Comparative Sequencing Program, Rosenberg S. A., Samuels Y. (2010). Novel somatic mutations in heterotrimeric G proteins in melanoma. *Cancer Biology and Therapy*, 10(1):33-37.

Carter K. C., Post D. K., Papaconstantinou J. (1991). Differential expression of the mouse α_1-acid glycoprotein genes (AGP-1 and AGP-2) during inflammation and aging. *Biochimica and Biophysika Acta*, 1089(2):197-205.

Casey P. J., Fong H. K. W., Simon M. I., Gilman A. G. (1990). G_z, a guanine nucleotide-binding protein with unique biochemical properties. *Journal of Biological Chemistry*, 265(4):2383-2390.

Casey M. L., MacDonald P. C., Andersson S. (1994). 17β-Hydroxysteroid dehydrogenase type 2: chromosomal assignment and progestin regulation of gene expression in human endometrium. *Journal of Clinical Investigations*, 94(5):2135-2141.

Celius T., Roblin S., Harper P.A., Matthews J., Boutros P.C., Pohjanvirta R., Okey A. B. (2008). Aryl hydrocarbon receptor-dependent inductions of flavin-containing monooxygenase mRNAs in mouse liver. *Drug Metabolism and Disposition*, 36(12):2499-2505.

Chang C.-Y., Puga A. (1998). Constitutive activation of the aromatic hydrocarbon receptor. *Molecular and Cellular Biology*, 18(1):525-535.

Chao D. T., Korsmeyer S. J. (1998). BCL-2 familiy: regulators of cell death. *Annual Review of Immunology*, 16:395-419.

Cheng Y., Maher J., Dieter M. Z., Klaassen C. D. (2005). Regulation of mouse organic anion-transporting polypeptides (OATPS) in liver by protoypical microsomal enzyme inducers that activate distinct transcription factor pathways. *Drug Metabolism and Disposition*, 33(9): 1276-1282.

Cheong J. K., Gunaratnam L., Zang Z. J., Yang C. M., Sun X., Nasr S. L., Sim K. G., Peh B. K., Rashid S. B. A., Bonventre J. V., Salto-Tellez M., Hsu S. I. (2009). TRIP-Br2 promotes oncogenesis in nude mice and frequently overexpressed in multiple human tumors. *Journal of Translational Medicine*, 7-8:1-15.

Choi J. Y., Oughton J. A., Kerkvliet N. I (2003). Functional alterations in CD11b(+)Gr-1(+) cells in mice injected with allogeneic tumor cells and treated with 2,3,7,8-tetrachlorodibenzo-*p*-dioxin. *International Immunopharmacology* 3(4):553-570.

Chuang P. C., Wu M. H., Shoji Y., Tsai S. J. (2009). Downregulation of CD36 results in reduced phagocytic ability of peritoneal macrophages of women with endometriosis. *Journal of Pathology*, 219(2):232-241.

Ciolino H. P., Daschner P. J., Wang T. T. Y., Yeh G. C. (1998). Effects of curcumin on the aryl hydrocarbon receptor and cytochrome P450 1A1 in MCF-7 human breast carcinoma cells. *Biochemical Pharmacology*, 56(2):197-206.

Clark G., Tritscher A., Bell D., Lucier G. (1992). Integrated approach for evaluating species and interindividual differences in responsiveness to dioxins and structural analogs. *Environmental Health Perspectives*, 98:125-132.

Colbert C. L., Kim C.-W., Moon Y.-A., Henry L., Palnitkar M., McKean W. B., Fitzgerald K., Deisendorfer J., Horton J. D., Kwon H. J. (2010). Crystal structure of spot 14, a modulator of fatty acid synthesis. *Proceedings of the National Academy of Scienes*, 107 (44):18820-18825.

Collins J. F., Bai L., Ghishan F. K. (2004). The SLC20 family of proteins: dual functions as sodium-phosphate cotransporters and viral receptors. *Pflugers Archives - European Journal of Physiology*, 447(5):647-652.

Comi G. P., Fortunanto F., Lucchiari S., Bordoni A., Prelle A., Jann S., Keller A., Ciscato P., Galbiati S., Chiveri L., Torrente Y., Scarlato G., Bresolin N. (2001). Beta-enolase deficiency, a new metabolic myopathy of distal glycolysis. *Annals of Neurology*, 50(2):202-207.

Connor K. T., Aylward L. L. (2006). Human response to dioxin: aryl hydrocarbon receptor (AhR) molecular structure, function, and dose-response data for enzyme induction indicate an impaired human AhR. *Journal of Toxicology and Environmental Health*, Part B, 9(2):147-171.

Corchero J., Martin-Partido G., Dallas S. L., Fernandez-Salguero P. H. (2004). Liver portal fibrosis in dioxin receptor-null mice that overexpress the latent transforming growth factor-β-binding protein-1. *International Journal of Experimental Pathology*, 85:295-302.

Cornell D. W. (2005). Basic Concepts of Environmental Chemistry, C*RC Press*, Second Edition, Boca Raton, USA.

Creyghton M. P., Roel G., Eichhorn P. J. A., Hijmans E. M., Maurer I., Destrée O., Bernards R. (2005). PR72, a novel regulator of Wnt signaling required for Naked cuticle function. *Genes and Development*, 19(3):376-386.

Crow K. D. (1978). Chloracne- an up to date assessment. *Annals of Occupational Hygiene*, 21(3):297-298.

Crow K. D. (1981). Chloracne and its potential clinical implications. *Clinical and Experimental Dermatology*, 6(3):243-257.

Danielson P. B. (2002). The cytochrome P450 superfamily: biochemistry, evolution and drug metabolism in humans. *Current Drug Metabolism*, 3(6):561-597.

De Fries R., Mistuhashi M. (1995). Quantification of mitogen induced human lymphocyte proliferation: comparison of alamarBlue assay to 2H-thymidine incorporation assay. *Journal of Clinical Laboratory Analysis*, 9(2):89-95.

Della Porta G., Dragani T. A., Sozzi G. (1987). Carcinogenic effects of infantile and long-term 2,3,7,8-tetrachlorodibenzo-*p*-dioxin treatment in the mouse. *Tumori*, 73(2):99-107.

Demonbreun A. R., Posey A. D., Heretis K., Swaggart K. A., Earley J. U., Pytel P., McNally E. M. (2010). Myoferlin is required for insulin-like grwoth factor response and muscle growth. *FASEB Journal*, 24(4):1284-1295.

De Montello P. R., (2010). Hydrocarbon hydroxylation by cytochrome P450 enzymes. *Chemical Reviews*, 110(2):932-948.

Denison M. S., Pandini A., Nagy S. R., Baldwin E. P., Bonati L. (2002). Ligand binding and activation of the Ah receptor. *Chemico-Biological Interactions*, 141(1-2):3-24.

Denison M. S., Nagy S. R. (2003). Activation of the aryl hydrocarbon receptor by structurally diverse exogenous and endogenous chemicals. *Annual Review on Pharmacology and Toxicology*, 2003, 43:309-334.

Denison M. S., Soshilov A. A., He G., DeGroot D. E., Zhao B. (2011). Exactly the same but different: promiscuity and diversity in the molecular mechanisms of action of the aryl hydrocarbon (dioxin) receptor. *Toxicological Sciences*, 124(1):1-22.

DeNofrio J. C., Yuang W., Temple B. R., Gentry H. R., Parise L. V. (2008). Characterization of calcium- and integrin-binding protein 1 (CIB1) knockout platelets: potential compensation by CIB family members. *Thrombosis and Haemostasis*, 100(5):847-856.

Deplus R., Brenner C., Burgers W. A., Putmans P., Kouzarides T., Launoit Y., Fuks F. (2002). Dnmt3L is a transcriptional repressor that recruits histone deactylase. *Nucleic Acid Research*, 30(17):3831-3838.

Dere E., Lee A. W., Burgoon L. D., Zacharewski T. R. (2011). Differences in TCDD-elicited gene expression profiles in human HepG2, mouse Hepa1c1c7 and rat H4IIE hepatoma cells. *BMC Genomics*, 12(193):1-14.

Dettmer K., Aranov P. A., Hammock B. D. (2007). Mass spectrometry-based metabolomics. *Mass Spectrometry Reviews*, 26(1):51-78.

Diani-Moore S., Labitzke E., Brown R., Garvin A., Wong L., Rifkind A. B. (2006). Sunlight generates multiple tryptophan photoproducts eliciting high efficacy CYP1A Induction in chicken hepatocytes and *in vivo*. *Toxicological Sciences*, 90(1):96-110.

Diani-Moore S., Ram P., Li X., Mondal P., Youn D. Y., Sauve A. A., Rifkind A. B. (2010). Identification of the aryl hydrocarbon receptor target gene TIPARP as a mediator supression of hepatic gluconeogenesis by 2,3,7,8-Tetrachlorodibenzo-*p*-dioxin and of nicotinamide as a corrective agent for this effect. *Journal of Biological Chemistry*, 285(50):38801-38810.

Diliberto J. J., Burgin D. E., Birnbaum L. (1999). Effects of CYP1A2 on disposition of 2,3,7,8-tetrachlorodibenzo-p-dioxin, 2,3,4,7,8-pentachlorodibenzofuran, 2,2',4,4',5,5'-hexa chlorobiphenyl in CYP1A2 knockout and parental (C57BL/6N) and 129/Sv) strains of mice. *Toxicology and Applied Pharmacology,* 159(1):52-64.

DiNatale B. C., Murray I. A., Schroeder J. C., Flaveny C. A., Lahoti T. S., Laurenzana E. M., Omiecinski C. J., Perdew G. H. (2010). Kynurenic acid is a potent endogenous aryl hydrocarbon receptor ligand that synergistically induces interleukin-6 in the presence of inflammatory signaling. *Toxicological Sciences*, 115(1):89-97.

Ding X., Kaminsky L.S. (2003). Human extrahepatic cytochromes P450: function in xenobiotic metabolism and tissue-selective chemical toxicity in the respiratory and gastrointestinal tracts. *Annual Review of Pharmacology and Toxicology*, 43:149-173.

Ding X., Xu R., Yu J., Xu T., Zhuang Y., Han M. (2007). SUN1 is required for telomere attachment to nuclear envelope and gametogenesis in mice. *Developmental Cell*, 12(6):863-872.

Dongol B., Shah Y., Kim I., Gonzalez F. J., Hunt M. C. (2007). The acyl-CoA thioesterase I is regulated by PPARα and HNF4α via a distal response element in the promoter. *Journal of Lipid Research*, 48(8):1781-1791.

Dörr A. (2010). Beeinflussung der Ah-Rezeptorabhängigen CYP1A Aktivität durch dioxinartige Verbindungen in der humanen Hepatomzelllinie HepG2. Diplomarbeit, TU Kaiserslautern.

Drahushuk A. T., McGarrigle B. P., Tai H.-L., Kitareewan S., Goldstein J. A., Olson J. R. (1996). Validation of precision-cut liver slices in dynamic organ culture as an *in vitro* model for studying CYP1A1 and CYP1A2 induction. *Toxicological and Applied Pharmacology*, 140(2):393-403.

Dumont F., Marechal P.-A., Gervais P. (2006). Involvement of two specific causes of cell mortality in freeze-thaw cycles with freezing to -196 °C. *Applied and Environmental Microbiology*, 72(2):1330-1335.

Egeland G. M., Sweeney M. H., Fingerhut M. A., Wille K. K., Schnorr T. M., Halperin W. E. (1994). Total serum testosterone and gonadotropins in workers exposed to dioxins. *American Journal of Epidemiology*, 139(3):272-281.

European Food Safety Authority (EFSA). (2010). Results of monitoring of dioxins levels in food and feed. *EFSA Journal*, 8(3):1385.

European Food Safety Authority (EFSA) (2012). Update of the monitoring of levels of dioxins and PCBs in food and feed. *EFSA Journal*, 10(7):2832.

Echchgadda I., Song C. S., Oh T.-S., Cho S.-C., Rivera O. J., Chatterjee B. (2004). Gene regulation of the senescence marker protein DHEA-sulfotransferase by xenobiotic-activated nuclear pregnane X receptor (PXR). *Mechanisms of Ageing and Development*, 125(10-11):733-745.

Eisenberg M. C., Kim Y., Li R., Ackerman W. E., Kniss D. A., Friedman A. (2011). Mechanistic modeling of the effects of myoferlin on tumor cell invasion. *Proceedings of the National Academy of Sciences*, 108(50):20078-20083.

Ernst L. A., Gupta R. K. G., Mujumdar R. B. M., Waggoner A. S. (1989). Cyanine dye labeling reagents for sulfhydryl groups. *Cytometry*, 10 (1):3-10.

Evans B. R., Karchner S. I., Allan L. L., Pollenz R. S., Tanguay R. L., Jenny M. J., Sherr D. H., Hahn M. E. (2008). Repression of aryl hydrocarbon receptor (AHR) signaling by AHR repressor: role of DNA binding and competition for AHR nuclear translocator. *Molecular Pharmacology*, 73(2):387-398.

Fahmi O. A., Kish M., Boldt S., Obach R. S. (2010). Cytochrome P450 3A4 mRNA is a more reliable marker than CYP3A4 activity for detecting pregnane X receptor-activated induction of drug-metabolizing enzymes. *Drug Metabolism and Disposition*, 38(9):1605-1610.

Fattore E., Fanelli R., Turrini A., di Domenico A. (2006). Current dietary exposure to polychlorodibenzo-*p*-dioxins, polychlorodibenzofurans, and dioxin-like polychlorobiphenyls in Italy. *Molecular Nutrition Food Research*, 50(10):915-921.

Febbraio M., Abumrad N. A:, Hajjar D. P., Sharma D. P., Cheng. K., Pearce S. F. A., Silverstein R. L. (1999). A null mutation in murine CD36 reveals an important role in fatty acid and lipoprotein metabolism. *Journal of Biological Chemistry*. 274(27):19055-19062.

Fenn J. B., Mann M., Meng C. K., Wong S. F., Whitehouse C. M. (1989). Electrospray ionization for mass spectrometry of large biomolecules. *Science*, 246(4926):64-71.

Fernandez-Salguero P. M., Hilbert D. M., Rudikoff S., Ward J. M., Gonzalez F. J. (1996). Aryl-hydrocarbon receptor-deficient mice are resistant to 2,3,7,8-tetrachlorodibenzo-*p*-dioxin-induced toxicity. *Toxicology and Applied Pharmacology*, 140(1):173-179.

Fiedler H., Lau C., Schulz S., Wagner C., Hutzinger O., von der Wreck T., (1995). Stoffbericht Polychlorierte Biphenyle, Landesanstalt für Umweltschutz Baden-Württemberg, 16/95.

Fiedler H. (2003). The handbook of environmental chemistry, Volume 3, part O. Persistent organic pollutants - dioxins and furans. Springer Verlag, Heidelberg.

Fiehn O. (2002). Metabolomics - link between genotypes and phenotypes. *Plant Molecular Biology*, 48(1-2):155-171.

Fisher C. D., Jackson J. P., Lickteig A. J., Augustine L. M., Cherrington N. J. (2008). Drug metabolizing enzyme induction pathways in experimental non-alcoholic steatohepatitis. *Archives of Toxicology*, 82(12):959-964.

Flesch-Janys D., Berger J., Gurn P., Manz A., Nagel S., Waltsgott H., Dwyer J. H. (1995). Exposure to polychlorinated dioxins and furans (PCDD/F) and mortality in a cohort of workers from a herbicide-producing plant in Hamburg, Federal Republic of Germany. *American Journal of Epidemiology*, 142(11):1165-1175.

Fletcher N., Hanberg A., Hakansson H. (2001). Hepatic vitamin A depletion is a sensitive marker for 2,3,7,8-Tetrachlorodibenzo-*p*-dioxin (TCDD) exposure in four rodent species. *Toxicological Sciences*, 62(1):166-175.

Fletcher N., Wahlström D., Lundberg R., Nilsson C. B., Nilsson K. C., Stockling K., Hellmond H., Hakansson H. (2005). 2,3,7,8-Tetrachlorodibenzo-*p*-dioxin (TCDD) alters the mRNA expression of critical genes associated with cholesterol metabolism, bile acid biosynthesis, and bile transport in rat liver: A microarray study. *Toxicology and Applied Pharmacology*, 207(1):1-24.

Flower D. R. (1996). The lipocalin protein family: structure and function. *Biochemical Journal*, 318(Pt 1):1-14.

Fong H. K. W., Yoshimoto K. K., Eversole-Cire P., Simon M. I. (1988). Identification of a GTP-binding protein a subunit that lacks an apparent ADP-ribosylation site for pertussis toxin. *Proceedings of the National Academy of Sciences*, 85(9):3066-3070.

Focant J.-F., Eppe G., Pirard C., Massart A.-C., Andre J.-E., De Pauw E. (2002). Levels and congener distributions of PCDDs, PCDFs and non-ortho PCBs in Belgian foodstuffs - assessment of dietary intake. *Chemosphere*, 48(2):167-179.

Focant J.-F., Frery N., Bidondo M.-L., Eppe G., Scholl G., Saoudi A., Oleko A., Vandentorren S. (2013). Levels of polychlorinated dibenzo-*p*-dioxins, polychlorinated dibenzofurans and polychlorinated biphenyls in human milk from different regions of France. *Science of the Total Environment*, 452-453:155-162.

Forgacs A. L., Kent M. N., Makley M. K., Mets B., DelRaso N., Jahns G. L., Burgoon L. D., Zacharewski T. R., Reo N. V. (2012). Comparative metabolomic and genomic analyses of TCDD-elicted metabolic disruption in mouse and rat liver. *Toxicological Sciences*, 125(1):41-55.

Forgacs A. L., Dere E., Angrish M. M., Zacharewski T. Z. (2013). Comparative analysis of temporal and dose-dependent TCDD-elicited gene expression in human, mouse, and rat primary hepatocytes. *Toxicological Scienes*, 133(1):54-66.

Forth W., Henschler D., Rummel W., Förstermann U., Starke E. (2001). Allgemeine und spezielle Pharmakologie und Toxikologie. *Urban und Fischer*, 8. Auflage, München.

Fujii-Kuriyama Y., Kawajiri K. (2010). Molecular mechanisms of the physiological functions of the aryl hydrocarbon (dioxin) receptor, a multifunctional regulator that senses and responds

to environmental stimuli. *Proceedings of the Japan Academy*, *Series B*, *Physical and Biological Sciences,* 86(1):40-53.

Gabant P., Forrester L., Nichols J., Van Reeth T., De Mees C., Pajack B., Watt A., Smitz J., Alexandre H., Szirper C., Szirper J. (2002). Alpha-fetoprotein, the major fetal serum protein, is not essential for embryonic development but is required for female fertility. *Proceedings of the National Academy of Scienes*, 99(20):12865-12870.

Gao J., Xie W. (2010). Pregnane X receptor and constitutive androstane receptor at the crossroads of drug metabolism and energy metabolism. *Drug Metabolism and Disposition*, 38(12):2091-2095.

Gentleman R., Carey V., Bates D., Bolstad B., Dettling M. (2004). Bioconductor: open software development for computational biology and bioinformatics. *Genome Biology*, 5:R80.

Gene Ontology Consortium (2004). The Gene Ontology (GO) database and informatics resource. *Nucleic Acids Research*, 32:D258-D261.

Gibbs M. A., Thummel K. E., Shen D. D., Kunze K. L. (1999). Inhibition of cytochrome P-450 3A (CYP3A) in human intestinal and liver microsomes: comparison of K_I values and impact of CYP3A5 expression. *Drug Metabolism and Disposition*, 27(2):180-187.

Giesy J. P., Kannan K. (1998). Dioxin-like and non-dioxin-like toxic effects of polychlorinated biphenyls (PCBs): implications for risk assessment. *Critical Reviews in Toxicology*, 28(6):511-569.

Giller T., Buchwald P., Blum-Kaelin D., Hunziker W. (1992). Two novel human pancreatic lipase related proteins, hPLRP1 and hPLRP2. Differences in colipase dependence and in lipase activity. *Journal of Biological Chemistry*, 267(13):16509-16516.

Gokhin D. S., Lewis R. A., McKeown C. R., Nowak R. B., Kim N. E., Littlefield R. S., Lieber R. L., Fowler V. M. (2010). Tropomodulin isoforms regulate thin filament pointed-end capping and skeletal muscle physiology. *Journal of Cell Biology*, 189(1):95-109.

Gonzalez F. J., Fernando-Salguero P. (1998). The aryl hydrocarbon receptor: studies using the AHR-null mice. *Drug Metabolism and Disposition*, 26(12):1194-1198.

Goodwin B., Redinbo M. R., Kliewer S. A. (2002). Regulation of CYP3A gene transcription by the pregnane X receptor. *Annual Review of Pharmacology and Toxicology*, 42:1-13.

Gorokhova S., Bibert S., Geering K., Heintz N. (2007). A novel familiy of transmembrane proteins interacting with beta subunit of the Na,K-ATPase. *Human Molecular Genetics*, 16(20):2394-2410.

Gouédard C., Barouki R., Morel Y. (2004). Dietary polyphenols increase paraoxonase 1 gene expression by an aryl hydrocarbon receptor-dependent mechanism. *Molecular and Cellular Biology*, 24(12):5209-5222.

Greco D., Kotronen A., Westerbacka J., Puig O., Arkkila P., Kiviluoto T., Laitinen S., Kolak M., Fisher R. M., Hamsten A., Auvinen P., Yki-Järvinen H. (2008). Gene expression in human NAFLD. *American Journal of Physiology - Gastrointestinal and Liver Physiology*, 294(5):G1218-G1287.

Guengerich F. P. (2010). 4.04 - Cytochrome P450 enzymes. *Comprehensive Toxicology*, (4):47-76.

Guenet J.-L., Chazottes-Simon D., Gravel M., Hastings K. E. M., Schiaffino S. (1996). Cardiac and skeletal muscle troponin I isoforms are encoded by a dispersed gene family on mouse chromosomes 1 and 7. *Mammalian Genome*, 7(1):13-15.

Gumienny T. L., Brugnera E., Tosello-Trampont A.-C., Kinchen J. M., Haney L. B., Nishiwaki K., Walk S. F., Nemergut M. E., Macara I. G., Francis R., Schedl T., Qin Y., Van Aelst L., Hengartner M. O., Ravichandran K. S. (2001). CED-12/ELMO, a novel member of the Crkll/Dock180/Rac pathway, is required for phagocytosis and cell migration. *Cell Press*, 107(1):27-41.

Haarmann-Stemmann T., Bothe H., Abel J. (2009). Growth factors, cytokines and their receptors as downstream targets of arylhydrocarbon receptor (AhR) signaling pathways. *Biochemical Pharmacology*, 77(4):508-520.

Hahn M. E. (1998). The aryl hydrocarbon receptor: a comparative perspective. *Comparative Biochemistry and Physiology Part C*, 121(1-3):23-53.

Hakk H., Diliberto J. J., Birnbaum L. S. (2009). The effect of dose on 2,3,7,8-TCDD tissue distribution, metabolism and elimination in CYP1A2 (-/-) knockout and C57/BL6N parental strains of mice. *Toxicology and Applied Pharmacology*, 241(1):119-126.

Hankinson O. (1995). The aryl hydrocarbon receptor complex. *Annual Review of Pharmacology and Toxicology*, 35:307-340.

Hardwick J. P., Osei-Hyiaman D., Wiland H., Abdelmegeed M. A., Song B.-J. (2009). PAR/RXR regulation of fatty acid metabolism and fatty acid ω-hydroxylase (CYP4) isozymes: implications for prevention of lipotoxicity in fatty liver disease. *PPAR Research*, 952734:1-20.

Haws L. C., Su S. H., Harris M., DeVito M. J., Walker N. J., Farland W. H., Finley B., Birnbaum L. S. (2006). Development of a refined database of mammalian relative potency estimates for dioxin-like compounds. *Toxicological Sciences*, 89(1):4-30.

Hayes K. R., Zastrow G. M., Nukaya M., Pande K., Glover E., Maufort J. P., Liss A. L., Liu Y., Moran S. M., Vollrath A. L., Bradfield C. A. (2007). Hepatic transcriptional networks induced by exposure to 2,3,7,8-tetrachlorodibenzo-*p*-dioxin. *Chemical Research in Toxicology*, 20(11):1573-1581.

He K., Iyer K. R., Hayes R. N., Sinz M. W., Woolf T. F., Hollenberg P. F. (1998). Inactivation of cytochrome P450 3A4 by bergamottin, component of grapefruit juice. *Chemical Research in Toxicology*, 11(4):252-259.

He J., Lee J. H., Febbraio M., Xie W. (2011). The emerging roles of fatty acid translocase/CD36 and the aryl hydrocarbon receptor in fatty acid liver disease. *Experimental Biology and Medicine*, 236(10):1116-1121.

Hemming H., Bager Y., Flodström S., Nordgren I., Kronevi T., Ahlborg U. G., Wärngard L. (1995). Liver tumour promoting activity of 3,4,5,3',4'-pentachlorobiphenyl and its interaction

with 2,3,7,8-tetrachlorodibenzo-*p*-dioxin. *European Journal of Pharmacology*, 292(3-4):241-249.

Henriksen G. L., Ketchum N. S., Michalek J. E., Swaby J. A. (1997). Serum dioxin and diabetes mellitus in veterans of Operation Ranch Hand. *Epidemiology*, 8(3):252-258.

Herbert S. C., Mount D. B., Gamba G. (2004). Molecular physiology of cation-coupled Cl^- -cotransport: the SLC12 family. *Pflugers Archives - European Journal of Physiology*, 447(5):580-593.

Hernandez J. P., Mota L. C., Baldwin W. S. (2009). Activation of CAR and PXR by dietary, environmental and occupational chemicals alters drug metabolism, intermediary metabolism, and cell proliferation. *Current Pharmacogenomics and Personalized Medicine*, 7(2):81-105.

Herpers B. L., Endeman H., de Jongh B. A. W., Grutters J. C., Biesma D. H., van Velzen-Blad H. (2009). Acute-phase responsiveness of mannose-binding lectin in community-acquired pneumonia is highly dependent upon MBL2 genotypes. *Clinical and Experimental Immunology*, 156(3):488-494.

Hewitt N. J., Gómez Lechón M. J., Houston J. B., Hallifax D., Brown H. S., Maurel P., Kenna J. G., Gustavsson L., Lohmann C., Skonberg C., Guillouzo A., Tuschl G., Li A. P., LeCluyse E., Groothuis G. M., Hengstler J. G. (2007). Primary hepatoctyes: current understanding of the regulation of metabolic enzymes and transporter proteins, and pharmaceutical practice for the use of hepatocytes in metabolism, enzyme induction, transporter clearance, and hepatotoxicity studies. *Drug Metabolism Reviews*, 39(1):159-234.

Holland P. M., Abramson R. D., Watson R., Gelfland D. H. (1991). Detection od specific polyermase chain reaction product by utilizing the 5`-> 3`exonuclease activity of Thermus aquaticus DNA polymerase. *Proceedings of the National Academy of Scienes*, 88(16):7276-7280.

Holsapple M. P., Morris D. L., Wood S. C., Snyder N. K. (1991). 2,3,7,8-tetrachlorodibenzo-*p*-dioxin-induced changes in immunocompetence: possible mechanisms. *Annual Review of Pharmacology and Toxicology*, 31:73-100.

Hong S.-S., Li H., Choi M.-K., Chung S.-J., Shim C.-K. (2005). Effect of a new hepatoprotective agent, YH-439, on the hepatobiliary transport of organic cations (OCs): Selective inhibition of sinusoidal OCs uptake without influencing glucose uptake and canalicular OCs excretion. *Archives of Pharmacal Research*, 28(3):330-334.

Hong L., Cui W., Klaassen C. D. (2011). Nrf2 protects against 2,3,7,8-tetrachlorodibenzo-*p*-dioxin (TCDD)-induced oxidative injury and steatohepatitis. *Toxicology and Applied Pharmacology*, 256(2):122-135.

Honkakoski P., Moore R., Gynther J., Negishi M. (1996). Characterization of phenobarbital-inducible mouse *Cyp2b10* gene transcription in primary hepatocytes. *Journal of Biological Chemistry*, 271(16):9746-9753.

Honkakoski P., Negishi M. (2000). Regulation of cytochrome P450 (CYP) genes by nuclear receptors. *Biochemical Journal*, 347(Pt 2):321-337.

Hsiao E. C., Koniaris L. G., Zimmers-Koniaris T., Sebald S. M., Huynh T. V., Lee S.-J. (2000). Characterization of growth-differentation factor 15, a transforming growth factor beta superfamily member induced following liver injury. *Molecular and Cellular Biology*, 20(10):3742-3751.

Hsu S. I.-H., Yang S. M., Sim K. G., Hentschel D., O´Leary E., Bonventre J. B. (2001). TRIP-Br: a novel family of PHD zinc finger- and bromodomain-interacting proteins that regulate the transcriptional activity of E2F-1/DP-1. *EMBEO Journal*, 20(9):2273-2285.

Hsu M.-H., Savas U., Griffin K. J., Johnson E. F. (2007). Human cytochrome P450 family 4 enzymes: function, genetic variation and regulation. *Drug Metabolism Reviews*, 39(2-3):515-538.

Huff J., Cirvello J., Haseman J., Bucher J. (1991). Chemicals associated with site-specific neoplasia in 1394 long-term carcinogenesis experiments in laboratory rodents. *Environmental Health Perspective*s, 93:247-270.

Huisman M., Koopman-Esseboom C., Fidler V., Hadders-Algra M., van der Paauw C. G., Tuinstra L.-G., Weisglas-Kuperus N., Sauer P.J., Touwen B. C., Boersma E. R. (1995). Perinatal exposure to polychlorinated biphenyls and dioxins and its effect on neonatal neurological developement. *Early Human Development*, 41(2):111-127.

Hunt M. C., Rautanen A., Westin M. A. K., Svensson L. T., Alexson S. E. H. (2006). Analysis of the mouse and human acyl-CoA thioesterase (ACOT) gene clusters shows that convergent, functional evolution results in a reduced number of human peroxisomal ACOTs. *FASEB Journa*l, 20(11):1855-1864.

Hüttemann M., Kadenbach B., Grossman L. I. (2001). Mammalian subunit IV isoforms of cytochrome c oxidase. *Gene*, 267(1):111-123.

Huyten T., Göttmann W., Bade-Döring C., Paine A., Blascyk R. (2011). The T/NK cell co-stimulatory molecule *SECTM1* is an IFN "early response gene" that is negatively regulated by LPS in Human monocytic cells. *Biochimica and Biophysica Acta*, 1810(12):1294-1301.

Ichikawa S., Sakiyama K., Suzuki G., Hiadari K. I.-P. J., Hirabayashi Y. (1996). Expression cloning of a cDNA for human ceramide glucosyltransferase that catalyzes the first glycosylation step of glycosphingolipid synthesis. *Proceedings of the National Academy of Sciences*, 93(10):4638-4643.

Ideo G., Bellati G., Bellobuono A., Moccarelli P., Marocchi A., Brambilla P. (1982). Increased urinary D-glucaric acid excretion by children living in an area polluted with tetrachlorodibenzoparadioxin (TCDD). *Clinical Chimica Acta*, 120(3):273-283.

Igual-Adell R., Oltra-Alcaraz C., Soler-Company E., Sánchez-Sánchez P., Matogo-Oyana J., Rodríguez-Calabuig D. (2004). Efficacy and safety of ivermectin and thiabendazole in the treatment of strongyloidiasis. *Expert Opinion on Pharmacotherapy*, 5(12): 2615-2619.

IARC. (1987). International Agency for Research on Cancer (IARC) Monographs on the evaluation of carcinogenic risks to humans. Overall evaluations of carcinogenicity: an updating of IARC Monographs volumes 1 to 42. Supplement 7:1-440.

IARC. (1997). International Agency for Research on Cancer (IARC) Monographs on the evaluation of carcinogenic risks to humans. Polychlorinated dibenzo-para-dioxins and polychlorinated dibenzofurans, 69:1-631.

IARC. (2012). International Agency for Research on Cancer (IARC) Monographs on the evaluation of carcinogenic risks to humans. Chemical agents and related occuptations: a review of human carcinogens. 2,3,7,8-Tetrachloro-*para*-dibenzodioxin, 2,3,4,7,8-Pentachlorodibenzofuran, and 3,3',4,4',5-Pentachlorobiphenyl, 100F:339-378.

Ito M., Jiang C., Krumm K., Zhang X., Pecha J., Zhao J., Guo Y., Roeder R. G., Xiao H. (2003). TIP30 deficiency increases susceptibility to tumorigenesis. *Cancer Research*, 63(24): 8763-8767.

Iwano S., Ichikawa M., Takizawa S., Hashimoto H., Miyamoto Y. (2010). Identification of AhR-regulated genes involved in PAH-induced immunotoxicity using a highly-sensitive DNA chip, 3D-Gene Human Immunity and Metabolic Syndrome 9k. *Toxicology In Vitro*, 24(1):85-91.

Jacobs H., Dennefeld C., Féret B., Viluksela M., Hakansson H., Mark M., Ghyselinck N. B. (2011). Retinoic acid drives aryl hydrocarbon receptor expression and is instrumental to dioxin-induced toxicity during palate development. *Environmental Health Perspectives*, 119(11):1590-1595.

Jeuken A., Keser B. J. G., Khan E., Brouwer A., Koeman J., Denison M. S. (2003). Activation of the Ah receptor by extracts of dietary herbal supplements, vegetables, and fruits. *Journal of Agricultural and Food Chemistry*, 51(18):5478-5487.

Jirasek L., Kalensky J., Kubec K.,Pazderova J., Lukas E. (1976). [Chloracne, porphyria cutanea tarda and other poisonings due to the herbicides.] *Hautarzt*, 27(7):328-333.

Jones K. C., de Voogt P. (1999). Persitent organic pollutants (POPs): state of the science. *Environmental Pollution*, 100(1-3):209-221.

Jump D. B. (2011). Fatty acid regulation of hepatic lipid metabolism. Current Opinion in *Clinical Nutrition and Metabolic Care*, 14(2):115-120.

Kamino H., Moore R., Negishi M. (2011). The role of a novel CAR-induced gene, TUBA8, in hepatocellular carcinoma cell lines. *Cancer Genetics*, 204(7):382-391.

Katoh Y., Katoh M. (2007). Comparative genomics on PROM1 gene encoding stem cell marker CD133. *International Journal of Molecular Medicine,* 19(6):967-970.

Kawajiri K., Fujii-Kuriyama Y. (2007). Cytochrome P450 gene regulation and physiological fundtion mediated by the aryl hydrocarbon receptor. *Archives of Biochemistry and Biophysics*, 464(2):207-212.

Kawamoto T., Sueyoshi T., Zelko I., Moore R., Washburn K., Negishi M. (1999). Phenobarbital-responsive nuclear translocation of the receptor CAR in induction of the CYP2B gene. *Molecular and Cellular Biology*, 19(9):6318-6322.

Kerkvliet N. I. (2002). Recent advances in understanding the mechanisms of TCDD immunotoxicity. *International Immunopharmacology*, 2(2-3):277-291.

Kim S., Dere E., Burgoon L. D., Chang C.-C., Zacharewski T. R. (2009). Comparative analysis of AhR-mediated TCDD-elicited gene expression in human liver adult stem cells. *Toxicological Sciences*, 2009, 112(1):229-244.

Kim Y., Sharov A. A., McDole K., Cheng M., Hao H., Fan C.-M., Gaiano N., Ko M. S. H., Zheng Y. (2011). Mouse B-type lamins are required for proper organogenesis but not by embryonic stem cells. *Science*, 334(6063):1706-1710.

Kiviranta H., Ovaskainen M.-L., Vartiainen T. (2004). Market basket study on dietary intake of PCDD/Fs, PCBs, and PBDEs in Finland. *Environmental International*, 30(7):923-932.

Kliewer S. A., Willson T. M. (2002a). Regulation of xenobiotic and bile acid metabolism by the nuclear pregnane X receptor. *Journal of Lipid Research*, 43(3):359-364.

Kliewer S. A., Goodwin B., Willson T. M. (2002b). The nuclear pregnane X receptor: a key regulator of xenobiotic metabolism. *Endocrine Reviews*, 23(5):687-702.

Knerr S., Schrenk D. (2006). Carcinogenicity of 2,3,7,8-tetrachlorodibenzo-*p*-dioxin in experimental models. *Molecular Nutrition Food Research*, 50(10):897-907.

Knowles B. B., Howe C. C., Aden D. P. (1980). Human hepatocellular carcinoma cell lines secrete the major plasma proteins and hepatitis surface antigen. *Science*, 209(4455):497-499.

Kobe B., Deisenhofer J. (1995). Proteins with leucine-rich repeats. *Current Opinion in Structural Biology*, 5(3):409-416.

Kocarek T. A., Duanmu Z., Fang H.-L., Runge-Morris M. (2008). Age- and sex-dependent expression of multiple murine hepatic hydroxysteroid sulfotransferases (SULT2A) genes. *Biochemical Pharmacology*, 76(8):1036-1046.

Kondo H., Shirakawa R., Higashi T., Kawato M., Fukuda M., Kita T., Horiuchi H. (2006). Constitutive GDP/GTP exchange and secretion-dependent GTP hydrolysis activity for Rab27 in platelets. *Journal of Biological Chemistry*, 281(39):28657-28665.

Konno Y., Negishi M., Kodama S. (2008). The roles of nuclear receptors CAR and PXR in hepatic energy metabolism. *Drug Metabolism and Pharmacokinetics*, 23(1):8-13.

Kopec A. K., Burgoon L. D., Ibrahim-Aibo D., Mets B. D., Tashiro C. Potter D., Sharratt B., Harkema J. E., Zacharewski T. R. (2010a). PCB153-elicited hepatic responses in the immature, ovariomectomized C57/BL/6 mice: comparative toxicogenomic effects of dioxins and non-dioxin-like ligands. *Toxicology and Applied Pharmacology*, 243(3):359-371.

Kopec A. K., Burgoon L. D., Ibrahim-Aibo D., Burg A. R., Lee A. E., Tashiro C., Potter D., Sharratt B., Harkema J. R., Rowlands J. C., Budinsky R. A., Zacharewski T. R. (2010b). Automated dose-response analysis and comparative toxicogenomic evaluation of the hepatic effects elicited by TCDD, TCDF, and PCB126 in C57BL/6 mice. *Toxicological Sciences,* 118(1):286-297.

Kopf P. G., Scott J. A., Agbor L. N., Boberg J. R., Elased K. M., Huwe J. K., Walker M. K. (2010). Cytochrome P4501A1 is required for vascular dysfunction and hypertension induced by 2,3,7,8-Tetrachlorodibenzo-*p*-dioxin. *Toxicological Sciences*, 177(2):537-546.

Kraemer N., Issa L., Hauck S. C. R., Mani S., Ninnemann Ö., Kaindl A. M. (2011). What´s the hype about CDK5RAP2? *Cellular and Molecular Life Sciences*, 68(10):1719-1736.

Kraus S., Zhang C.-Y., Lowell B. B. (2005). The mitochondrial uncoupling-protein homologues. *Nature Reviews Molecular Cell Biology*, 6(3):248-261.

Lahvis G. P., Lindell S. L., Thomas R. S., McCuskey R. S., Murphy C., Glover E., Bentz M., Southard J., Bradfield C. A. (2000). Portosystemic shunting and persistent fetal vascular structures in aryl hydrocarbon receptor-deficient mice. *Proceedings of the National Academy of Sciences*, 97(19):10442-10447.

Landers J. P., Bunce N. J. (1991). The Ah receptor and the mechanism of dioxin toxicity. *Biochemical Sciences*, 276(Pt 2):273-287.

Lee I. J., Jeong K. S., Roberts B. J., Kallarakal A. T., Fernandez-Salguero P., Gonzalez, F. J., Song B. J. (1996). Transcriptional induction of a cytochrome P4501A1 gene by a thiazolium compound, YH439. *Molecular Pharmacology*, 49(6):980-988.

Lee J. H., Wada T., Febbraio M., He J., Matsubara T., Lee T. M., Gonzalez F. J., Xie W. (2010). A novel role for the dioxin receptor in fatty acid metabolism and hepatic steatosis. *Gastroenterology*, 139(2):653-663.

Li C., Franklin J. L., Graves-Deal R., Jerome W. G., Cao Z., Coffey R. J. (2004). Myristoylated Naked2 escorts transforming growth factor alpha to the basolateral plasma membrane of polarized epithelial cells. *Proceedings of the National Academy of Sciences*, 101(15):5571-5576.

Liem A.-K. D., Fürst P., Rappe C. (2000). Exposure of populations to dioxins and related compounds. *Food Additives and Contaminants*, 17(4):241-259.

Lipp H.-P., Schrenk D., Wiesmüller T., Hagenmaier H., Bock K. W. (1992). Assessment of biological activities of mixtures of polychlorinated dibenzo-*p*-dioxins (PCDDs) and their constituents in human HepG2 cells. *Archives of Toxicology*, 66(3):220-223.

Liu M.-J., Takahashi Y., Wada T., He J., Gao J., Tian Y., Li S., Xie W. (2009). The aldo-keto reductase Akr1b7 gene is a common transcriptional target of xenobiotic receptors pregnane X receptor and constitutive androstane receptor. *Molecular Pharmacology*, 76(3):604-611.

Lohmann R., Jones K. C. (1998). Dioxins and furans in air and deposition: a review of levels, behaviour and processes. *The Science of the Total Environment*, 219(1):53-81.

Loughran G., Healy N. C., Kiely P. A., Huigsloot M., Kedersha N. L., O´Connor R. (2005). Mystique is a new insulin-like growth factor-I-regulated PDZ-LIM domain protein that promotes cell attachment and migration and suppresses anchorage-independent growth. *Molecular Biology of the Cell*, 16(4):1811-1822.

Lottspeich F., Zorbas H. (1998). Bioanalytik. *Spektrum Akademischer Verlag*. 1. Auflage.

Ma Q., Baldwin K. T., Renzelli, A. J., McDaniel A., Dong L. (2001). TCDD-inducible poly(ADP-ribose) polymerase: a novel response to 2,3,7,8-Tetrachlorodibenzo-*p*-dioxin. *Biochemical and Biophysical Research Communications*, 289 (2):499-506.

Ma Q. (2002). Induction and superinductin of 2,3,7,8-tetrachlorodibenzo-*p*-dioxin-inducible poly(ADP-ribose) polymerase: role of the aryl hydrocarbon receptor/aryl hydrocarbon receptor nuclear translocator transcription activation domains and a labile transcription repressor. *Archives of Biochemistry and Biophysics*, 404:309-316.

Ma Q., Lu A. Y. H. (2007). CYP1A induction and human risk assessment: an evolving tale of in vitro and in vivo studies. *Drug Metabolism and Disposition*, 35(7):1009-1016.

Mackay D., Shiu W. Y., Ma K.-C., Lee S. C. (2006). Handbook of Physical-Chemical Properties and Environmental Fate for Organic Chemicals: Halogenated Hydrocarbons: Volume 2, *CRC Press*, Edition 2, Boca Raton, USA.

MacPherson L., Tamblyn L., Rajendra S., Bralha F., McPherson J. P., Mattews J. (2013). 2,3,7,8-Tetrachlorodibenzo-*p*-dioxin poly(ADP-ribose) polymerase (TiPARP, ARTD14) is a mono-ADP-ribosyltransferase and repressor of aryl hydrocarbon receptor transactivation. *Nucleic Acids Research*, 41(3):1604-1621.

Maeda K., Uysal K. T., Makowski L., Görgün C. Z., Atsumi G., Parker R. A., Brüning J., Vogel Hertzel A., Bernlohr D. A., Hotamisligil G. S. (2003). Role of fatty acid binding protein mal1 in obesity and insulin resistance. *Diabetes*, 52(2):300-307.

Malisch R. Rolaf van Leeuwen F. X. (2003). Results of the WHO-coordinated exposure study on the levels of PCBs, PCDDs and PCDFs in human milk. *Organohalogen Compounds*, 64:140-143.

Mankan A. K., Lawless M. W., Gray S. G., Kelleher D., McManus R. (2009). Nf-kβ regulation: the nuclear response. *Journal of Cellular and Molecular Medicine*, 13(4):631-643.

Marks F., Müller-Decker K., Fürstenberger G. (2000). A causal relationship between unscheduled eicosanoid signaling and tumor development: cancer chemoprevention by inhibitors of arachidonic acid metabolism. *Toxicology*, 153(1-3):11-26.

Marquardt H., Schäfer S. G. (2004). Lehrbuch der Toxikologie. *Wissenschaftliche Verlagsgesellschaft*, 2. Auflage.

Martin L., Klaassen D. (2010). Differential effects of polychlorinated biphenyl congeners on serum thyroid hormone levels in rats. *Toxicological Sciences*, 117(1):36-44.

Mathar W. (2003). Tägliche Aufnahme von Dioxin und dioxinähnlichen PCB eines Erwachsenen in Deutschland über die Nahrung. Bundesinstitut für Risikobewertung (BfR).

Mashima T., Seimiya H., Tsuruo T. (2009). De novo fatty acid synthesis and related pathways as molecular targets for cancer therapy. *British Journal of Cancer*, 100(9):1369-1372.

Massrieh W., Derjunga A., Doualla-Bell F., Ku C.-Y., Sanborn B. M., Blank V. (2006). Regulation of MAFF transcription factor by proinflammatory cytokines in myyometrial cells. *Biology of Reproduction*, 74:699-705.

Matsuoka M., Itoh H., Kaziro Y. (1990). Characterization of the human gene $G_x\alpha$ pertussis toxin-insensitive regulatory GTP-bingin protein. *Journal of Biological Chemistry*, 265(22):13215-13220.

Matsuzaka T., Shimano H., Yahagi N., Kato T., Atsumi A., Yamamoto T., Inoue N., Ishikawa M., Okada S., Ishigaki N., Iwasaki H., Iwasaki Y., Karasawa T., Kumadaki S., Mastui T., Sekiya M., Ohashi K., Hasty A. H., Nakagawa Y., Takahashi A., Suzuki H., Yatoh S., Sone H., Toyoshima H., Osuga J.-I. Yamada N. (2007). Crucial role of a long-chain fatty acid elongase, Elovl6, in obesity-induced insluin resistance. *Nature Medicine*, 13(10):1193-1202.

Matthews J., Gustafsson J.-A. (2006). Estrogen receptor and aryl hydrocarbon receptor signaling pathways. *Nuclear Receptor Signaling*, 4:1-4.

McFarland V. A., Clarke J. U. (1989). Environmental occurrence, abundance, and potential toxicity of polychlorinated biphenyl congeners: considerations for a congener-specific analysis. *Environmental Health Perspectives*, 81:225-239.

Meyer V. R. (2002). Praxis der Hochleistungsflüssigkeitschromatographie. *Otto Salle Verlag*, 8. Auflage.

Milbrath M. O., Wenger Y., Chang C.-W., Emond C., Garabrant D., Gillespie W. B., Jolliet O. (2009). Apparent half-lives of dioxins, furans, and polychlorinated biphenyls as a function of age, body fat, smoking status, and breast-feeding. *Environmental Health* Perspectives, 117(3):417-425.

Mimura J., Yamashita K., Nakamura K., Morita M., Takagi T. N., Nakao K., Ema M., Sogawa K., Yasuda M., Kastuki M., Fuji-Kuriyama Y. (1997). Loss of teratogenic response to 2,3,7,8-tetrachlorodibenzo-*p*-dioxin (TCDD) in mice lacking the Ah (dioxin) receptor. *Genes to Cells*, 2(10):645-654.

Mimura J., Erna M., Sogawa K., Fujii-Kuriyama Y. (1999). Identification of a novel mechanism of regulation of Ah (dioxin) receptor function. *Genes and Development*, 13(1):20-25.

Mimura J., Fujii-Kuriyama Y. (2003). Functional role of AhR in the expression of toxic effects by TCDD. *Biochimica et Biophysica Acta*, 1619(3):263-268.

Mitra M. S., Chen Z., Ren H., Harris T. E., Chambers K. T., Hall A. M., Nadra K., Klein S., Chrast R., Su X., Morris A. J., Finck B. N. (2012). Mice with an adipocyte-specific lipin 1 separation-of-function allele reveal unexpected roles for phosphatidic acid in metabolic regulation. *Proceedings of the National Academy of Sciences*, 110(2):642-647.

Miura K., Rikihisa Y. (2009). Liver transcriptome profiles associated with strain-specific *Ehrlichia chaffeensis*-induced hepatitits in SCID mice. *Infection and Immunity*, 77(1):245-254.

Mocarelli P., Brambilla P., Gerthoux P. M., Patterson D. G. Jr., Needham L. L. (1996). Change in sex ratio with exposure to dioxin. *Lancet*, 348(9024):409.

Mocarelli P., Gerthoux P. M., Patterson D. G. Jr., Milani S., Limonata G., Bertona M., Signorini S., Tramacere P., Colombo L., Crespi C., Brambilla P., Sarto C., Carreri V., Sampson E. J., Turner W. E., Needham L. L. (2008). Dioxin exposure, from infancy through puberty, produces endocrine disruption and affects human semen quality. *Environmental Health Perspectives*, 116(1):70-77.

Moeller G., Adamski J. (2009). Integrated view on 17beta-hydroxysteroid dehydrogenases. *Molecular and Cellular Endocrinology*, 301(1-2):7-19.

Moennikes O., Loeppen S., Buchmann A., Andersson P., Ittrich C., Poellinger L., Schwarz M. (2004). A constitutively active dioxin/aryl hydrocarbon receptor promotes hepatocarcinogenesis in mice. *Cancer Research*, 64 (14):4707-4710.

Moffat I. D., Boutros P. C., Chen H., Okey A. B. Pohjanvirta R. (2010). Aryl hydrocarbon receptor (AHR)-regulated transcriptomic changes in rats sensitive or resistent to major dioxin toxicities. *BMC Genomics*, 11:263.

Moon S. Y., Zheng Y. (2003). Rho GTPase-activating proteins in cell regulation. *Trends in Cell Biology*, 13(1):13-22.

Morgan M. A. J., Morgan J. I. (2012). Pcp4l1 contains an auto-inhibitory element that prevents its IQ motif from binding to calmodulin. *Journal of Neurochemistry*, 121(6):843-851.

Mormone E., Lu Y., Ge X., Fiel M. I., Nieto N. (2012). Fibromodulin, an oxidative stress-sensitive proteoglycan, regulates the fibrogenic response to liver injury in mice. *Gastroenterology*, 142(3):612-621.

Moseley T. A., Haudenschild D. R., Rose L., Reddi A. H. (2003). Interleukin-17 family and IL-17 receptors. *Cytokine and Growth Factor Reviews*, 14(2):155-174.

Moses M., Lilis R., Crow K. D., Thornton J., Fischbein A., Anderson H. A., Selikoff I. J. (1984). Health status of workers with past exposure to 2,3,7,8-tetrachlorodibenzo-*p*-dioxin in the manufacture of 2,4,5-trichlorophenoxyacetic acid: comparison of findings with and without chloracne. *American Journal of Industrial Medicine*, 5(3):161-182.

Müller H.-J., Röder T. (2004). *Der Experimentator Microarrays. Spektrum Akademischer Verlag*, 1. Auflage.

Mullis K. B., Faloona F. A. (1987). Specific synthesis of DNA in vitro via polymerase-catalyzed chain reaction. *Methods Enzymology*, 155:335-350.

Murphy K. A., Quadro L., White L. A. (2007). The intersection between the aryl hydrocarbon receptor (AHR)- and retinoid acid-signaling pathways. *Vitamins and Hormones*, 74:33-66.

Murray G. I., Barnes T. S., Sewell H. F., Ewen S. W. B., Melvin W. T., Burke M. D. (1988). The immunicytochemical localisation and distribution of the cytochrome P-450 in normal human hepatic and extrahepatic tissues with monoclonal antibody to human cytochrome P-450. *British Journal of Clinical Pharmacology*, 25(4):465-475.

Muzio G., Maggiora A., Paiuzzi E., Oraldi M., Canuto R. A. (2012). Aldehyde dehydrogenases and cell proliferation. *Free Radical Biology & Medicine*, 52:735-742.

NATO (North Atlantic Treaty Organization) (1988). Pilot study on international information exchange on dioxins and related compounds: emissions of dioxins and related compounds from combustion and incineration sources (Report No. 172). *North Atlantic Treaty Organization*.

Nebert D. W. (1987). P450 genes: structure, evolution, and regulation. *Annual Review of Biochemistry*, 56:945-993.

Nebert D. W., Nelson D. R., Feyereisen R. (1989). Evolution of the cytochrome P450 genes. *Xenobiotica*, 19(10):1149-1160.

Nebert D. W., Roe A. L., Dieter M. Z., Solis W. A., Yang Y., Dalton T. P. (2000). Role of the aromatic hydrocarbon receptor and [Ah] gene battery in the oxidative stress response, cell cycle control, and apoptosis. *Biochemical Pharmacology*, 59(1):65-85.

Nebert W. N., Russel D. W. (2002). Clinical importance of the cytochromes P450. *Lancet*, 360(9340):1155-1162.

Nelson D. R., Zeldin D. C., Hoffman S. M. G., Maltais L. J., Wain H. M., Nebert D. W. (2004). Comparison of cytochrome P450 (*CYP*) genes from the mouse and human genomes, including nomenclature recommendations for genes, pseudogenes and alternative-splice variants. *Pharmacogenetics*, 14(1):1-18.

Nguyen L. P., Bradfield C. A. (2008). The search for endogenous activators of the aryl hydrocarbon receptor. *Chemical Research in Toxicology*, 21(1):102-116.

Niittynen M., Tuomisto J. T., Auriola S., Pohjanvirta R., Syrjälä P., Simanainen U., Viluksela M., Tuomisto J. (2002). 2,3,7,8-tetrachlorodibenzo-*p*-dioxin (TCDD)-induced accumulation of biliverdin and hepatic peliosis in rats. *Toxicological Sciences*, 71(1):112-123.

NTP. (1982). Technical report on the carcinogenesis bioassay of 2,3,7,8-Tetrachloro-*p*-dioxin in Osborne-Mendel rats and B6C3F1 mice (gavage study). NTP-80-31. NIH Publication No. 82-1765.

NTP. (2006a). Technical report on the toxicology and carcinogenesis. Studies of 3,3',4,4',5-Pentachlorobiphenyl (PCB 126) in female Harlan Sprague-Dawley rats (gavage studies). NTP TR 520. NIH Publication No. 06-4454.

NTP. (2006b). Technical report on the toxicology and carcinogenesis. Studies of 2,3,7,8-Tetrachloro-*p*-dioxin (TCDD) in female Harlan Sprague-Dawley rats (gavage studies). NTP TR 521. NIH Publication No. 06-4468.

NTP. (2006c). Technical report on the toxicology and carcinogenesis. Studies of 2,3,4,7,8-Pentachlorogibenzofuran (PeCDF) in female Harlan Sprague-Dawley rats (gavage studies). NTP TR 525. NIH Publication No. 06-4461.

NTP. (2006d). Technical report on the toxicology and carcinogenesis. Studies of 2,2',4,4',5,5'-Hexachlorobiphenyl (PCB 153) in female Harlan Sprague-Dawley rats (gavage studies). NTP TR 529. NIH Publication No. 06-4465.

NTP. (2010). Technical report on the toxicology and carcinogenesis. Studies of 2,3',4,4',5-Pentachlorobiphenyl (PCB 118) in female Harlan Sprague-Dawley rats (gavage studies). NTP TR 559. NIH Publication No. 11-5900.

O'Brien J., Wilson I., Ortan T., Pognan F. (2000). Investigation of the Alamar Blue (resazurin) fluorescent dye for the assessment of the mammalian cell cytotoxicity. *European Journal of Biochemistry*, 267(17):5421-5426.

Ogden C. A., de Cathelineau A., Hoffmann P. R., Bratton D., Ghebrehiwet B., Fadok V. A., Henson P. M. (2001). C1q and mannose binding lectin engagement of cell surface calrecticulin and CD91 initiates macropinocytosis and uptake of apoptotic cells. *Journal of Experimental Medicine*, 194(6):781-795.

OME (Ontario Ministry of the Environment).(1985). Scientific criteria document for standard development (Report No. 4-84). Polychlorinated dibenzo-p-dioxins (PCDDs) and polychlorinated dibenzofurans (PCDFs). *Ontario Ministry of the Environment*, Canada.

Omiecinski C. J., Vanden Heuvel J. P., Perdew G. H., Peters J. M. (2011). Xenobiotic metabolism, disposition, and regulation by receptors: from biochemical phenomenon to predictors of major toxicities. *Toxicological Sciences*, 120(S1):S49-75.

Ooi J. P., Kuroyanagi M., Sulaiman S F., Muhammad T. S., Tan M. L. (2011). Andrographolide and 14-deoxy-11, 12-didehydroandrographolide inhibit cytochrome P450s in HepG2 hepatoma cells. *Life Science*, 88(9-10):447-454.

Opitz C. A., Litzenburger U. M., Sahm F., Ott M., Tritschler I., Trump S., Schumacher T., Jestaedt L., Schrenk D., Weller M., Jugold M., Guillemin G. J., Miller C. L., Lutz C., Radlwimmer B., Lehmann I., von Deimling A., Wick W., Platten M. (2011). An endogenous tumour-promoting ligand of the human aryl hydrocarbon receptor. *Nature*, 478(7368):197-203.

Ott M. G., Zober A., Germann C. (1994). Laboratory results for selected target organs in 138 individuals occupationally exposed to TCDD. *Chemosphere*, 29(9-11):2423-2437.

Panzitt K., Tschernatsch M. M. O., Guelly C., Moustafa T., Stradner M., Strohmaier H. M., Buck C. R., Denk H., Schroeder R., Trauner M., Zatloukal K. (2007). Characterization of HULC, a novel gene with striking up-regulation in hepatocellular carcinoma, as noncoding RNA. *Gastroenterology*, 132(1):330-342.

Park J.-Y. K., Shigenaga M. K., Ames B. N. (1996). Induction of cytochrome P4501A1 by 2,3,7,8-tetrachlorodibenzo-p-dioxin or indolo(3,2b)carbazole is associated with DNA damage. *Proceedings of the National Academy of Sciences*, 93(6):2322-2327.

Park E., Park S. Y., Wang C., Xu J., LaFauci G., Schuller-Levis G. (2002). Cloning of murine cysteine sulfic acid decarboxylase and ist mRNA expression in murine tissues. *Biochimica et Biophysica Acta*, 1547(3):403-406.

Paul P., Kamisaka Y., Marks F. L., Pagano R. E. (1996). Purification and characterization of UDP-glucose: ceramide glucosyltransferase from rat liver golgi membranes. *Journal of Biological Chemistry*, 271(4):2287-2293.

Pashkov V., Huang J., Parameswara V. K., Kedzierski W., Kurrasch D. M., Tall G. G., Esser V., Gerard R. D., Uyeda K., Towle H. C., Wilkle T. M. (2011). Regulator of G protein signaling (RGS16) inhibits hepatic fatty acid oxidation in a carbohydrate response element-binding protein (ChREBP)-dependent manner. *Journal of Biological Chemistry*, 286(17):15116-15125.

Pegg D. E. (2007). Principles of cryopreservation. *Methods in Molecular Biology*, 368: 39-57.

Peirera M. d. S. (2004). Polychlorinated dibenzo-*p*-dioxins (PCDD), dibenzofurans (PCDFs) and polychlorinated biphenyls (PCB): main sources, envioronmental behaviour and risk to man and biota. *Quimica Nova,* 27(6):934-943.

Pelclova D., Urban P., Prreiss J., Lukas E., Fenclova Z., Navratil T., Dubska Z., Senholdova Z. (2006). Adverse health effects in humans exposed to 2,3,7,8-tetrachlorodibenzo-*p*-dioxin (TCDD). *Reviews on Environmental Health*, 21(2):119-138.

Pennacchio L. A., Olivier M., Hubacek J. A., Krauss R. M., Rubin E. M., Cohen J. C. (2002). *Human Molecular Genetics*, 11(24):3031-3038.

Petrulis J. R., Guosheng C., Benn S., LaMarre J., Bunce N. J. (2001). Application of the ethoxyresorufin-O-deethylase (EROD) assay to mixtures of halogenated aromatic compounds." *Ernvironmental Toxicology*, 16(2):177-184.

Pfaffl W. M. (2001). A new mathematical model for relative quantification in real-time RT-PCR. *Nucleic Acids Research*, 29(9):2002-2007.

Pfaffl M. W. (2004). Quantification strategies in real-time PCR. *A-Z of quantitative PCR* Chapter 3:87-112.

Pirkle J. L., Wolfe W. M., Patterson D. G. Jr., Needham L. L., Michalek J. E., Miner J. C. (1989). Estimates of the half-life of 2,3,7,8-tetrachlorodibenzo-*p*-dioxin in Vietnam veterans of Operation Ranch Hand. *Journal of Toxicology and Environmental Health*, 27(2):165–171.

Pixeley F. J., Xiong Y., Yu R. Y.-L., Sahai E. A., Stanely E. R., Ye B. H. (2005). BCL6 suppresses RhoA activity to alter macrophage morphology and motility. *Journal of Cell Science*, 118(Pt 9):1873-1883.

Plourde M., Manhes C., Leblanc G., Durocher F., Dumont M., Sinilnikova O., INHERIT BRCAs, and Simard J. (2008). Mutation analysis and characterization of HSD17B2 sequence variants in breast cancer cases from French Canadian families with high risk of breast and ovarian cancer. *Journal of Molecular Endocrinology*, 40(4):161-172.

Poland A., Glover E., Kende A. (1976). Stereospecific, high affinity binding of 2,3,7,8-Tetrachlorodibenzo-p-dioxin by hepatic cytosol. *Journal of Biological Chemistry*, 251(16):4936-4946.

Poland A., Knutson J. C. (1982a). 2,3,7,8-Tetrachlorodibenzo-p-dioxin and related halogenated aromatic hydrocarbons: examination of the mechanism of toxicity. *Annual Review of Pharmacology and Toxicology*. 22:517-554.

Poland A., Palen D., Glover E. (1982b). Tumour promotion by TCDD in skin of HRS/J hairless mice. *Nature*, 300(5889):271-273.

Prochazkova J., Kabatkova M., Bryja V., Umannova L., Bernatik O., Kozubik A., Machala M., Vondracek J. (2011). The Interplay of the aryl hydrocarbon receptor and β-catenin alters both AhR-dependent transcription and Wnt/β-catenin signaling in liver progenitors. *Toxicological Sciences*, 122(2):349-360.

Quattrochi L. C., Tukey R. H. (1993). Nuclear uptake of the Ah (dioxin) receptor in response to omeprazole: transcriptional activation of the human CYP1A1 gene. *Molecular Pharmacology*, 43(4):504-508.

Rajan S., Ahmed R. P.H., Jagatheesan G., Petrashevskaya N., Biovin G. P., Urboniene D., Arteaga G. M., Wolska B. M., Solaro R. J., Liggett S. B., Wieczorek D. F. (2007). Dilated cardiomyopathy mutant tropomyosin mice develop cardiac dysfunction with significantly decreased fractional shortening and myofilament calcium sensitivity. *Cardiac Research*, 101(2):205-214.

Rannug A., Rannug U., Rosenkranz H. S., Winqvist L., Westerholm R., Agurell E., Grafström A.-K. (1987). Certain photooxidized derivatives of tryptophan bind with very high affinity to the ah receptor and are likely to be endogenous signal substances. *Journal of Biological Chemistry*, 262(32):15422-15427.

Rannug U., Rannug A., Sjöberg U., Li H., Westerholm R., Bergman J. (1995). Structure elucidation of two tryptophan-derived, high affinity Ah receptor ligands. *Chemical Biology*, 2(12):841-845.

Renaud H. J., Cui J. Y., Khan M., Klaassen C. D. (2011). Tissue distribution and gender-divergent expression of 78 cytochrome P450 mRNAs in mice. Toxicological Sciences, 124(2):261-277.

Rantakari P., Strauss L., Kiviranta R., Lagerbohm H., Paviala J., Holopainen I., Vainio S., Pakarinen P., Poutanen M. (2008). Placenta defects and embryonic lethality resulting from disruption of mouse hydroxysteroid (17-β) dehydrogenase 2 gene. *Molecular Endocrinology*, 22(3):665-675.

Ress C., Moschen A. R., Sausgruber N., Tschoner A., Graziadei I., WEiss H., Schgoer W., Ebenbichler C. F., Konrad R. J., Patsch J. R., Tilg H., Kaser S. (2011). The role of apolipoprotein A5 in non-alcoholic fatty liver disease. *International Journal of Gastroenterology and Hepatology*, 60(7):985-991.

Reggiani G. (1980). Acute human exposure to TCDD in Seveso, Italy. *Journal of Toxicology and Environmental Health*, 6(1):27-43.

Rico-Bautista E., Flores-Morales A., Fernandez-Perez L. (2006). Suppressor of cytokine signaling (SOCS) 2, a protein with multiple functions. *Cytokine and Growth Factor Reviews*, 17(6):431-439.

Rivera S. P., Saarikoski S. T., Sun W., Hankinson O. (2007). Identification of novel dioxin-responsive genes by representational difference analysis. *Xenobiotica*, 37(3):271-279.

Roos R. (2011). Einfluss hochreiner, nicht dioxin-artiger polychlorierter Biphenyle auf ausgewählte fremdstoffmetabolisierende Enzyme der Leber im Nager und in Zellkulturmodellen. Dissertation, TU Kaiserslautern, D386.

Rose J. Q., Ramsey J. C., Wentzler T. H., Hummel R. A., Gehring P. J. (1976). The fate of 2,3,7,8-tetrachlorodibenzo-*p*-dioxin following single and repeated oral doses to the rat. *Toxicology and Applied Pharmacology*, 36(2):209-226.

Rowlands J. G., Gustafsson J.-A. (1997). Aryl hydrocarbon receptor-mediated signal transduction. *Critical Reviews in Toxicology*, 27(2):109-134.

Sakuma T., Endo Y., Mashino M., Kuroiwa M., Ohara A., Jarunkamjorn K., Nemoto N. (2002). Regulation of the expression of two female-predominant CYP3A mRNAs (CYP3A41

and CYP3A44) in mouse liver by sex and growth hormones. *Archives of Biochemstry and Biophysics*, 404:234-242.

Sarkar D., Kambe F., Hirata A., Iseki A., Ohmori S., Seo H. (1999). Expression of E16/CD98LC/hLAT1 is responsive to 2,3,7,8-tetrachlorodibenzo-*p*-dioxin. *FEBS Letters*, 462(2):430-434.

Sarma V., Wolf F. W., Marks R. M., Shows T. B., Dixit V. M. (1992). Cloning of a novel tumor necrosis factor-alphainducible primary response gene that is differentially expressed in development and capillary tube-like formation in vitro. *Journal of Immunology*, 148(10):3302–3312.

Sarrazin S., Adam E., Lyon M., Depontieu F., Motte V., Landolfi C., Lortat-Jacobb H., Bechard D., Lassalle P., Delehedde M. (2006). Endocan or endothelial cell specific molecule-1 (ESM-1): a potential novel endothelial cell marker and a new target for cancer therapy. *Biochimica et Biophysica Acta*, 1765(1):25-37.

Saxena M., Vats P., Agrawal K., Banerjee M. (2012). Expression of macrophage scavenger receptor CD36 in humans - its implication in type 2 diabetes mellitus. *Annals of Biological Research*, 3(6):3015-3021.

Satoh T., Hosokawa M. (1998). The mammalian carboxylesterases: from molecules to functions. Annual Review of Pharmacology and Toxicology, 38:257-288.

Schecter A., Cramer P., Boggess K., Stanely J., Päpke O., Olson J., Silver A., Schmitz M. (2001). Intake of dioxins and related compounds from food in the U. S. population, Journal of *Toxicology and Environmental Health, Part A: Current Issues*, 63(1):1-18.

Schiaffino S., Reggiani C. (1996). Molecular diversity of myofibrillar proteins: gene regulation and functional significance. *Pharmacological Reviews*, 76(6):371-417.

Schlott T., Ahrens K., Ruschenburg I., Reimer S., Hartmann H., Droese M. (1999). Different gene expression of MDM2, GAGE-1, Ð2 and FHIT in hepatocellular carcinoma and focal nodular hyperplasia, *British Journal of Cance*r, 80(1-2):73-78.

Schmidt J. V., Huei-Ting Su G., Reddy J. K., Simon M. C., Bradfield C. A. (1996). Characterization of a murine Ahr null allele: involvement of the Ah receptor in hepatic growth and development. *Proceedings of the National Academy of Sciences*, 93(13):6731-6736.

Schmidt S., Joost H.-G., Schürmann A. (2009). GLUT8, the enigmatic intracellular hexose transporter. *American Journal of Physiology - Endocrinology and Metabolism*, 296(4):E614-E618.

Schrenk D., Stüven T., Gohl G., Viebahn R., Bock K. W. (1995). Induction of CYP1A and glutathione S-transferase activities by 2,3,7,8-tetrachlorodibenzo-p-dioxin in human hepatocyte cultures. *Carcinogenesis*, 16(4):943-946.

Schreiber V., Dantzer F., Arne J.-C., de Murcia G. (2006). Poly(ADP-ribose): novel functions for an old molecule. *Nature Reviews Molecular Cell Biology*, 7(7):517-528.

Sewall C. H., Bell D. A., Clark G. C., Tritscher A. M., Tully D. B., Vanden Heuvel J., Lucier G. W. (1995). Induced gene transcription: implications for biomarkers. *Clinical Chemistry*, 41(12 Pt 2):1829-1834.

Shen E. S., Gutman S. I., Olson J. R. (1991). Comparison of 2,3,7,8-tetrachlorodibenzo-*p*-dioxin-hepatotoxicity in C57BL/6J and DBA/2J mice. *Journal of Toxicology and Environmental Health: Current Issues*, 32(4):367-381.

Shena M., Shalon D., Davis R. W., Brown P. O. (1995). Quantitative monitoring of gene expression patterns with a complementary DNA microarray. *Science*, 270(5235):467-470.

Shi Y., Ullrich S. J., Zhang J., Connolly K., Grzegorzewski K. J., Barber M. C., Wang W., Wathen K., Hodge V., Fisher C. L., Olsen H., Ruben S. M., Knyazev I., Cho Y. H., Kao V., Wilkinson K. A., Carrell J. A., Ebner R. (2000). A novel cytokine receptor-ligand pair - identification, molecular characterization, and *in vivo* immunomodulatory activity. *Journal of Biological Chemistry*, 275(25):19167-19176.

Shimada T., Inoue K., Suzuki Y., Kawai T., Azuma E., Nakajima T., Shindo M., Kurose K., Sugie A., Yamagishi Y., Fuji-Kuriyama Y., Hashimoto M. (2002a). Arylhydrocarbon receptor-dependent induction of liver and lung cytochromes P450 1A1, 1A2, and 1B1 by polycyclic aromatic hydrocarbons and polychlorinated biphenyls in genetically engineered C57BL/6J mice. *Carcinogenesis*, 23(7):1199-1207.

Shimada T., Sugie A., Shindo M., Nakajima T., Hashimoto M., Inoue K. (2002b). Tissue-specific induction of cytochromes P450 1A1 and 1B1 by polycyclic aromatic hydrocarbons and polychlorinated biphenyls in engineered C57BL/6J mice of arylhydrocarbon receptor gene. *Toxicology and Applied Pharmacology*, 187(1):1-10.

Shoyab M., Plowman G. D., McDonald V. L., Bradeley J. G., Todaro G. J. (1989). Structure and function of human amphiregulin: a member of the epidermal growth factor family. *Science*, 243(4894 Pt 1):1074-1076.

Singh S. S., Hord N. G., Perdew G. H. (1996). Characterization of the activated form of the aryl hydrocarbon receptor in the nucleus of the HeLa cells in the absence of exogenous ligand. *Archives of Biochemistry and Biophysics*, 329(1):47-55.

Silkworth J. B., Koganti A., Illouz K., Possolo A., Zhao M., Hamilton S. B. (2005) Comparison of TCDD and PCB CYP1A induction sesitivities in fresh hepatocytes from human donors, Sprague-Dawley rats, and Rhesus Monkeys and HepG2 cells. *Toxicological Sciences*, 87(2):508-519.

Silverstein R. L., Baired M., Lo S. K., Yesner L.M. (1992). Sense and antisense cDNA transfection of CD36 (glycoprotein IV) in melanoma cells. *Journal of Biological Chemistry*, 267(23):16607-16612.

Sladek N. E. (2003). Human aldehyde dehydrogenases: potential pathology, pharmacological, and toxicological impact. *Journal of Biochemical Molecular Toxicology*, 17(1):7-23.

Smith A. G., Clothier B., Robinson S., Scullion M. J., Carthew P., Edwards R., Luo J., Lim C. K., Toledano M. (1998). Interaction between iron metabolism and 2,3,7,8-tetrachlorodibenzo-

p-dioxin in mice with variants of the *Ahr* gene: a hepatic oxidative mechanism. *Molecular Pharmacology*, 53(1):52-61.

Smyth G. K. (2004). Linear models and empirical bayes methods for assessing differential expression in microarray experiments. *Statistical Applications in Genetics and Molecular Biology*, 3 (1), Article 3.

Smyth G. K. (2005). Limma: linear models for microarray data. *Bioinformatics and Computational Biology Solutions using R and Bioconductor (Gentleman R., Carey V., Dudoit S., Irizarry R. and Huber W. (eds))*, pages 397-420.

Sorg O., Zennegg M., Schmid P., Fedosyuk R., Valikhanovskyi R., Galde O., Kniazevych V., Saurat J.-H. (2009). 2,3,7,8-tetrachlorodibenzo-*p*-dioxin (TCDD) poisoning in Victor Yushchenko: identification and measurement of TCDD metabolites. *Lancet*, 374(9696):1179-1185.

Stockinger B. (2009). Beyond toxicity: aryl hydrocarbon receptor-mediated functions in the immune system. *Journal of Biology*, 8(7):61.1-61.3.

Stuart L. M., Takahashi K., Shi L., Savill J., Ezekowitz R. A. B. (2005). Mannose-binding lectin-deficient mice display defective apoptotic cell cleareance but no autoimmune phenotype. *Journal of Immunology*, 174(6):3220-3226.

Su E. J., Cheng Y. H., Chatterton R. T., Lin Z. H., Yin P., Reierstad S., Innes J., Bulun S. E. (2007). Regulation of 17-beta hydroxysteroid dehydrogenase type 2 in human placental endothelial cells. *Biological of Reproduction*, 77(3):517-525.

Subramaniam M., Gorny G., Johnson S. A., Monroe D. G., Evans G. L., Fraser D. G., Rickard D. J., Rasmussen K., van Deursen J. M. A., Turner R. T., Oursler M. J., Spelsberg T. C. (2005). TIEG1 null mouse-derived osteoblasts are defective in mineralization and in support of osteoclast differentiation in vitro. *Molecular and Cellular Biology*, 25(3):1191-1199.

Sun Y. V., Boverhof D. R., Burgoon L. D., Fielden M. R., Zacharewski T. R. (2004). Comparative analysis of dioxin response elements in human, mouse and rat genomic sequences. *Nucleic Acids Research*, 32(15):4512-4523.

Sun T., Oh W. K., Jacobus S., Regan M., Pomerantz M., Freedman M. L., Lee G. S., Kantoff P. W. (2011). The impact on common genetic variations in genes of the sex hormone metabolic pathways on steroid hormone levels and prostate cancer aggressiveness. *Cancer Prevention Research*, 4(12):2044-2050.

Suskind R. R., Hertzberg V. S. (1984). Human health effects of 2,4,5-T and its toxic contaminants. *Journal of the American Medical Association*, 251(18):2372-2780.

Swales K., Negishi M. (2004). CAR, driving into the future. *Molecular Endocrinology*, 18(7):1589-1598.

Tanaka J., Yonemoto J., Zaha H., Kiyama R., Sone H. (2007). Estrogen-responsive genes newly found to be modified by TCDD exposure in human cell lines and mouse systems. *Molecular and Cellular Endocrinology*, 272(1-2):38-49.

Tang T., Francois N., Glatigny A., Agier N., Mucchielli M.-H., Aggerbeck L., Delacroix H. (2007). Expression ratio evaluation in two-color microarray experiments is significantly improved by correting image misalignment. *Bioinformatics*, 23(20):2686-2691.

The British National Corpus (1995). Longman Dictionary of Contemporary English. *Langenscheidt Longman GmbH*.

Tard A., Gallotti S., Leblanc J.-C., Volatier J.-L. (2007). Dioxin, furans and dioxin-like PCBs: occurrence in food and dietary intake in France. *Food Additives and Contaminants*, 24(9):1007-1017.

Tartaglia L. A. (1997). The leptin receptor. *Journal of Biological Chemistry*, 272(10):6093-6096.

te Velthuis A. J. W., Bagowski C. P. (2007). PDZ and LIM domain-encoding genes: molecular interactions and their role in development. *The Scientific World Journal*, 7:1470-1492.

Telliez A., Furman C., Pommery N., Henichart J. P. (2006). Mechanisms leading to COX-2 expression and COX-2 induced tumorigenesis: topical therapeutic strategies targeting COX-2 expression and activity. *Anti-Cancer Agents Medical Chemistry*, 6(3):187-208.

Teixeira F. R., Yokoo S., Gartner C. G., Manfiolli A. O., Baqui M. M. A., Assmann E. M., Maragno A. L. G. C., Yu H., de Lanerolle P., Kobarg J., Gygi S. P., Gomes M. D. (2010). Identification of FBXO25-interacting proteins using an integrated proteomics approach. *Proteomics*, 10(15):2746-2757.

Tian E., Sawyer J. R., Largaespada D. A., Jenkins N. A., Copeland N. G., Shaughnessy J. D. Jr. (2000). Evi27 encodes a novel membrane protein with homology to the IL17 receptor. *Oncogene*, 19(17):2098-2109.

Tichopad A., Dilger M., Schwarz G., Pfaffl M. W. (2003). Standardized determination of real-time PCR effeciency from a single reaction set-up. *Nucleic Acids Research*, 31(20):6688.

Timsit Y. E., Negishi M. (2007). CAR and PXR: the xenobiotic-sensing receptors. *Steroids*, 72(3):231-246.

Tijet N., Boutros P. C., Moffat I. D., Okey A. B., Tuomista J., Pohjanvirta R. (2006). Aryl hydrocarbon receptor regulates distinct dioxin-dependent and dioxin-independent gene batteries. *Molecular Pharmacology*, 69(1):140-153.

Tolson A. H., Wang H. (2010). Regulation of drug-metabolizing enzymes by xenobiotic receptors: PXR and CAR. Advances Drug Delivery Review, 62(13):1238-1249.

Topletz A. R., Thatcher J. E., Zelter A, Lutz J. D., Tay S., Nelson W. L., Isoherranen N. (2012). Comparison of the function and expression of CYP26A1 and CYP26B1, two retinoid acid hydroxylases. *Biochemical Pharmacology*, 83(1):149-163.

Toth K., Somfai-Relle S., Sugar J., Bence J. (1979). Carcinogenicity testing of herbicide 2,4,5-trichlorophenoxyethanol containing dioxin and of pure dioxin in Swiss mice. *Nature*, 278(5704):548–549.

Towbin H., Staehlint T., Gordon J. (1979). Electrophoretic transfer of proteins from polyacrylamide gels to nitrocellulose sheets: procedure and some applications (ribosomal proteins/radioimmunoassay/fluorescent antibody assay/peroxidase conjugated antibody /autoradiography). *Proceedings of the National Academy of Sciences*, 76(9):4350-4354.

Toyama T., Lee H. C., Koga H., Wands J. R., Kim M. (2010). Noncanonical Wnt11 inhibits hepatocellular carcinoma cell proliferation and migration. *Molecular Cancer Research*, 8(2):254-265.

Triebel F., Jitsukawa S., Baixeras E., Roman-Roman S., Genevee C., Viegas-Pequignot E., Hercend T. (1990). LAG-3, a novel lymphocyte activation gene closely related to CD4. *Journal of Experimental Medicine*, 171(5):1393-1405.

Tsuchiya Y., Nakajima M., Itoh S., Iwanari M., Yokoi T. (2003). Expression of aryl hydrocarbon receptor repressor in normal human tissues and inducibility by polycyclic aromatic hydrocarbons in human tumor-derived cell lines. *Toxicological Sciences*, 72(2):253-259.

Tsutsumi T., Yanagi T., Nakamura M., Kono Y., Uchibe H., Iida T., Hori T., Nakagawa R., Tobiishi K., Matsuda R., Sasaki K., Toyoda M. (2001). Update of daily intake of PCDDs, PCDFs, and dioxin-like PCBs from food in Japan. *Chemosphere*, 45(8):1129-1137.

Turner M. W. (1998). Mannose-binding lectin (MBL) in health and disease. *Immunobiology*, 199(2):327-339.

Turpeinen H., Kukkarainen S., Pulkkinen K., Kauppilla T., Ojala K., Hytönen V. P., Pesu M. (2011). Identification of proprotein convertase substrates using genome-wide expression correlation analysis. *BMC Genomics*, 12:618.

Ueda A., Hamadeh H. K., Webb H. K., Yamamoto Y., Sueyoshi T., Afshari C. A., Lehmann J. M., Negishi M. (2002). Diverse roles of the nuclear receptor CAR in regulating hepatic genes in response to phenobarbital. *Molecular Pharmacology*, 61(1):1-6.

Ulaszewska M. M., Zuccato E., Davoli E. (2011). PCDD/Fs and dioxin-like PCBs in human milk and estimation of infants' daily intake: a review. *Chemosphere*, 83(6):774-782.

Umannova L., Neca J., Andrysik Z., Vondracek J., Upham B. L., Trosko J. E., Hofmanova J., Kozubik A., Machala M. (2008). Non-dioxin-like polychlorinated biphenyls induce a release of arachidonic acid in liver epithelial cells: a partial role of the cyosolic phospholipase A2 and extracellular signal-regulated kinases 1/2 signalling. *Toxicology*, 247(1):55-60.

USAF. 1991. Air Force health study: An epidemiological investigation of health effects in Air Force personnel following exposure to herbicides. Chapters 1-5, 18, 19. U.S. Air Force, Brooks Air Force Base, Texas, USA.

Upadhyay M. P., West E. P., and Sharma A. P. (1980). Keratitis due to Aspergillus flavus successfully treated with thiabendazole. *British Journal of Ophthalmology*, 64(1):30-32.

van Birgelen A. P. J. M., van der Kolk J., Fase K. M., Bol I., Poiger H., van den Berg M., Brouwer A. (1994). Toxic potency of 2,3,3',4,4',5-hexachlorobiphenyl relative to and in combination with 2,3,7,8-tetrachlorodibenzo-p-dioxin in a subchronic feeding study in the rat. *Toxicology and Applied Pharmacology*, 126(2):202-213.

van den Berg M., de Jong J., Poiger H., Olson J. R. (1994). The toxicokinetics and metabolism of polychlorinated dibenzo-p-dioxins (PCDDs) and dibenzofurans (PCDFs) and their relevance for toxicity. *Critical Reviews in Toxicology*, 24(1):1-74.

van den Berg M., Birnbaum L., Bosveld A. T. C., Brunström B., Cook P., Feeley M., Giesy J. P., Hanberg A., Hasegawa R., Kennedy S. W., Kubiak T., Larsen J. C., van Leeuwen R. F. X., Liem D. A. K., Nolt C., Peterson R. E., Peollinger L., Safe S., Schrenk D., Tillit D., Tysklind M., Younes M., Waern F., Zacharewski T. (1998). Toxic equivalency factors (TEFs) for PCBs, PCDDs, PCDFs for humans and wildlife. *Environmental Health Perspectives*, 106(12): 775-792.

van den Berg M., Birnbaum L. S., Denison M., De Vito M., Farland W., Feeley M., Fiedler H., Hakansson H., Hanberg A., Haws M., Safe S., Schrenk D., Tohyma C., Trischer A., Tuomisto J., Tysklind M., Walker N. and Peterson R. E. (2006). The 2005 World Health Organization reevaluation of human and mammalian toxic equivalency factors for dioxins and dioxin-like compounds. *Toxicological Sciences*, 93(2):223-241.

van Duursen M. B. M, Sanderson J. T., van den Berg M. (2005). Cytochrome P450 1A1 and 1B1 in human blood lymphocytes are not suitable as biomarkers of exposure to dioxin-like compounds: polymorphisms and interindividual variation in expression and inducibility. *Toxicological Sciences*, 85(1):703-712.

Vanden Heuvel J. P., Clark G. C., Thompson C. L., McCoy Z., Miller C. R., Lucier G. W., Bell D. A. (1993). CYP1A1 mRNA levels as a human exposure biomarker: use of quantitative polymerase chain reaction to measure CYP1A1 expression in human peripheral blood lymphocytes. *Carcinogenesis*, 14(10):2003-2006.

van der Vliet H. N., Sammels M. G., Leegwater A. C. J., Levels J. H. M., Reitsma P. H., Boers W., Chamuleau R. A. F. M. (2001). Apolipoprotein A-V: a novel apolipoprotein associated with an early phase of liver regeneration. *Journal of Biological Chemistry*, 276(48):44513-44520.

van Ede K. I., Andersson P. L., Gaisch K. P. J., van den Berg M., van Duursen M. B. M. (2013). Comparison of intake and systemic relative effeect potencies of dioxin-like compounds in female mice after a single oral dose. *Environmental Health Perspectives,* 121(7): 847-853.

van Leeuwen F. X. R., Feeley M., Schrenk D., Larsen J. C., Farland W., Younes M. (2000). Dioxins: WHO´s tolerable daily intake (TDI) revisited. *Chemosphere*, 40(9-11):1095-1101.

van Leeuwen F. X. R., Malisch R. (2002) Results of the third round of the WHO-coordinated exposure study on the levels of PCBs, PCDDs and PCDFs in human milk. *Organohalogen Compounds*, 56:311-316.

Vasiliou V., Reuter S. F., Kozak C. A., Nebert D. W. (1993). Mouse dioxin-inducible cytosolic aldehyde dehydrogenase-3: AHD4 cDNA sequence, genetic mapping, and differences in mRNA levels. *Pharmacogenetics*, 3(6):281-290.

Vasiliou V., Pappa A., Estey T. (2004). Role of the human aldehyde dehydrogenase in endobiotic and xenobiotic metabolism. *Drug Metabolism Reviews*, 36(2):279-299.

Verrey F., Closs E. I., Wagner C. A., Palacin M., Endou H., Kanai Y. (2004). CATs and HATs: the SLC7 family of amino acid transporters. *Pflugers Archives - European Journal of Physiology*, 447(5):532-542.

Vesterlund M., Zadjali F., Persson T., Nielson M. L., Kessler B. M., Norstedt G., Flores-Morales A. (2011). The SOCS2 ubiquitin ligase complex regulates growth hormone receptor levels. *PLOS ONE*, 6(9):e25358.

Viluskela M., Unkila M., Pohjanvirta R., Tuomista J. T., Stahl B. U., Rozman K. K., Tuomista J. (1999). Effects of 2,3,7,8-tetrachlorodibenzo-*p*-dioxin (TCDD) on liver phosphoenolpyruvate carboxykinase (PEPCK) activity, glucose homeostasis and plasma amino acid concentrations in the most TCDD-susceptible and the most TCDD-resistant rat strains. *Archives of Toxicology*, 73(6):323-336.

Waern F., Flodström S., Busk L., Kronevi T., Nordgren I., Ahlborg U. G. (1991). Relative liver tumour promoting activity and toxicity of some polychlorinated dibenzo-*p*-dioxin- and dibenzofuran-congeners in female Sprague-Dawley rats. *Pharmacology and Toxicology*, 69(6):450-458.

Wang H., Negishi M. (2003). Transcriptional regulation of cytochrome P450 2B genes by nuclear receptors. *Current Drug Metabolism,* 4(6):515-525.

Wang H., Zhao Y., Bradbury A., Graves J. P., Foley J., Blaisdell J. A., Goldstein J. A., Zeldin D. C. (2004). Cloning, expression, and characterization of three new mouse cytochrome P450 enzymes and partial characterization of their fatty acid oxidation activities. *Molecular Pharmacology*, 65(5):1148-1158.

Want E. J., O`Maille G., Smith C. A., Brandon T. R., Uriboonthai W., Qin C., Trauger S. A., Siuzdak G. (2006). Solvent-dependent metabolite distribution, clustering, and protein extraction for serum profiling with mass spectrometry. *Analytical Chemistry*, 78(3):743-752.

Welfad F. C., Devlin B. H., Williams R. S. (1990). Functional heterogeneity of mammalian TATA-box sequences revealed by interaction with a cell-specific enhancer. *Nature*, 344(6263):260-262.

Wolfe W. H., Michalek J. E., Miner J. C., Pirkle J. L., Patterson D. G. Jr., Needham L. L. (1994). Determination of TCDD half-life in veterans of Operation Ranch Hand. *Journal of Toxicology and Environmental Health*, 41(4):481-488.

World Health Organization (WHO) Consultation. (1998). Assessment of the health risk of dioxins: re-evalution of the tolerable daily intake (TDI).

Workman C. J., Vignali D. A. (2005). Negative regulation of T cell homeostasis by lymphocyte activation gene-3 (CD223). *Journal of Immunology*, 174(2):688-695.

Wright E. M., Turk E. (2004). The sodium/glucose cotransport family SLC5. *Pflugers Archives - European Journal of Physiology*, 447(5):510-518.

Wyde M. E., Braen A. P., Hejtmancik M., Johnson J. D., Toft J. D., Blake J. C., Cooper S. D., Mahler J., Vallant M., Bucher J. R., Walker N. J. (2004). Oral and dermal exposure to 2,3,7,8-tetrachlorodibenzo-*p*-dioxin (TCDD) induces cutaneous papillomas and squamous cell

carcinomas in female hemizygous Tg.AC transgenic mice. *Toxicological Sciences*, 82(1):34-45.

Xu L., Li A. P., Kaminski D. L., Ruh M. F. (2000). 2,3,7,8 Tetrachlorodibenzo-*p*-dioxin induction of cytochrome P4501A in cultured rat and human hepatocytes. C*hemico-Biological Interactions*, 124(3):173-189.

Xu C., Wang X., Staudinger J. L. (2009). Regulation of tissue-specific carboxylesterase expression by pregnane X receptor and constitutive androstane receptor. *Drug Metabolism and Disposition*, 37(7):1539-1547.

Xu F., Mao C., Ding Y., Rui C., Wu L., Shi A., Zhang H., Zhang L., Xu Z. (2010). Molecular and enzymatic profiles of mammalian DNA methyltransferases: structures and targets for drugs. *Current Medicinal Chemistry*, 17(33):4052-4071.

Yagyi H., Lutz E. P., Kako Y., Marks S., Hu Y., Choi S. Y., Bensadoun A., Goldberg I. J. (2002). Very low density lipoprotein (VLDL) receptor-deficient mice have reduced lipoprotein lipase activity. *Journal of Biological Chemistry*, 277(12):10037-10043.

Yamashita T., Wada R., Sasaki T., Deng C., Bierfreund U., Sandhoff K., Proia R. L. (1999). A vital role for glycosphingolipid synthesis during development and differentiation. *Proceedings of the National Academy of Sciences*, 96(16):9142-9147.

Yamniuk A. P., Vogel H. J. (2006). Insights into the structure and function of calcium and integrin-binding proteins. *Calcium Binding Proteins*, 1(3):150-155.

Yeager R. L., Reisman S. A., Aleksunes L. M., Klaassen C. D. (2009). Introducing the "TCDD-inducible AhR-Nrf2 gene battery". *Toxicological Sciences*, 111(2):238-246.

Yoon C.Y., Park M., Kim B. H., Park J. Y., Park M. S., Jeong Y. K., Kwon H., Jung H. K., Kang H., Lee Y. S., Lee B. J. (2006). Gene expression profile of 2,3,7,8-Tetrachlorodibenzo-*p*-dioxin in the liver of wild-type (AhR+/+) and aryl hydrocarbon receptor-deficient (AhR-/-) mice. *Journal of Veterinary Medical Science*, 68(7):663-668.

Zadravec D., Tvrdik P., Guillou H., Haslam R., Kobayashi T., Napier J. A., Capecchi M. R., Jacobsson A. (2011). ELOVL2 controls the level of n-6 28:5 and 30:5 fatty acids in testis, a prerequisite for male fertility and sperm maturation in mice. *Journal of Lipid Research*, 52 (2):245-255.

Zacchinga S., Oh H., Wilsch-Bräuninger M., Missol-Kolka E., Jaszai J., Jansen S., Tanimoto N., Tonagel F., Seelinger M., Huttner W. B., Corbeil D., Dewerchin M., Vinckier S., Moons L., Carmeliet P. (2009). Loss of cholesterol-binding protein prominin-1/CD133 causes disk dysmorphogenesis and photoreceptor degeneration. *Journal of Neuroscience*, 29(7):2297-2308.

Zadravec D., Tvrdik P., Guillou H., Haslam R., Kobayashi T., Napier J. A., Capecchi M. R., Jocbsson A. (2011). ELOVL2 controls the level of n-6 28:5 and 30:5 fatty acids in testis, a prequesite for male fertility and sperm maturation in mice. *Journal of Lipid Research*, 52(2):245-255.

Zhang X., Fitzsimmons R. L., Cleland L. G., Ey P. L., Zannettino A. C. W., Farmer E.-A., Sincock P., Mayrhofer G. (2003). CD36/Fatty acid translocase in rats: distribution, isolation

from hepatocytes, and comparison with the scavenger receptor SR-B1. *Laboratory Investigations*, 83(3):317-332.

Zeiger M., Haag R., Höckel J., Schrenk D., Schmitz H.-J. (2001). Inducing effects of dioxin-like polychlorinated biphenyls on CYP1A in the human hepatoblastoma cell line HepG2, the rat hepatoma cell line H4IIE, and rat primary hepatocytes: comparison of relative potencies. *Toxicological Sciences*, 63(1):65-73.

Zeng L., Akasaki Y., Ouchi N., Izumiya Y., Walsh K. (2010). Insulin-like 6 is induced by muscle injury and functions as a regenerative factor. *Journal of Biological Chemistry*, 285(46):36060-36069.

Zhongy S., Rantakari P., Lamminen T., Toppari J., Poutanen M. (2007). Transgenic male mice expressing human hydroxysteroid dehydrogenase 2 indicate a role of enzyme independent of its action on sex steroids. *Endocrinology*, 148(8):3827-3836.

Zhou X., Popescu N. C., Klein G., Imreh S. (2007). The transmembrane protein *TMEM7* is an IFN-α responsive gene that suppresses cell proliferation and is down-regulated in human hepatocellular carcinoma. *Cancer Genetics and Cytogenetics*, 177(1):6-15.

Zhongyi S., Rantakari P., Lamminen T., Toppari J., Poutanen M. (2007). Transgenic male mice expressing human hydroxysteroid dehydrogenase 2 indicate a role for the enzyme independent of its actions on sex steroids. *Endocrinology*, 148(8):3827-3826.

Zober A., Ott M. G., Messerer P. (1994). Morbidity follow up study of BASF employees exposed to 2,3,7,8-tetrachlorodibenzo-*p*-dioxin (TCDD) after a 1953 chemical reactor incident. *Occupational and Environmental Medicine*, 51(7):479-486.

Zudaire E., Cuesta N., Murty V., Woodson K., Adams L., Gonzalez N., Martinez A., Narayan G., Kirsch I., Franklin W., Hirsch F., Birrer M., Cuttitta F. (2008). The aryl hydrocarbon receptor repressor is a putative tumor suppressor gene in multiple human cancers. *Journal of Clinical Investigations*, 118(2):640-650.

IX Appendices

IX.1 Supplemental Data Microarrays

Following tables display the significantly up and down regulated genes identified by microarray analysis as a result of compound treatment. Each table features the gene name, systematic name, and the official gene description. Furthermore, the specific probe name, corresponding colour intensity value (A-value), logarithmic fold-change (log2 fc value), and the p-value are additionally featured for each significantly altered gene.

Table 81. All significantly up regulated genes in livers of female C57BL/6 mice by TCDD (25 µg/kg bw) identified by microarray analysis - mouse 3-day study. Selected parameters: A-value ≥ 7, log2 fc ≥ 1, p-value ≤ 0.05.

A	Log2 fc	p-value	Probe name	Gene name	Systematic name	Gene description
10.23	9.478	0	A_51_P279693	*Cyp1a1*	NM_009992	ref|Mus musculus cytochrome P450 family 1 subfamily a polypeptide 1 transcript variant 1 mRNA
7.16	5.169	0	A_51_P255456	*Cyp1b1*	NM_009994	ref|Mus musculus cytochrome P450 family 1 subfamily b polypeptide 1 mRNA
13.33	3.985	0	A_52_P595871	*Cyp1a2*	NM_009993	ref|Mus musculus cytochrome P450 family 1 subfamily a polypeptide 2 mRNA
7.97	3.582	0	A_55_P2032714	*Fhit*	NM_010210	ref|Mus musculus fragile histidine triad gene mRNA
9.92	3.379	0	A_66_P119518	*Tuba8*	NM_017379	ref|Mus musculus tubulin alpha 8 mRNA
11.31	3.103	0	A_51_P299805	*Slc46a3*	NM_027872	ref|Mus musculus solute carrier family 46 member 3 mRNA
7.10	2.903	0	A_55_P1985890	*Tiparp*	NM_178892	ref|Mus musculus TCDD-inducible poly(ADP-ribose) polymerase mRNA
9.36	2.819	0	A_55_P2032946	*Gsta1*	NM_008181	ref|Mus musculus glutathione S-transferase alpha 1 (Ya) mRNA
9.22	2.722	0	A_55_P2004099	*Gm9933*	XM_001477458	ref|PREDICTED: Mus musculus predicted gene ENSMUSG00000054044 mRNA
8.86	2.678	0	A_52_P515036	*Htatip2*	NM_016865	ref|Mus musculus HIV-1 tat interactive protein 2 homolog (human) transcript variant 1 mRNA
10.50	2.518	0	A_55_P1983754	*Pcp4l1*	NM_025557	ref|Mus musculus Purkinje cell protein 4-like 1 mRNA
9.26	2.386	0	A_55_P1972720	*Pmm1*	NM_013872	ref|Mus musculus phosphomannomutase 1 mRNA
8.41	2.153	0	A_52_P183524	*Tmem86b*	NM_023440	ref|Mus musculus transmembrane protein 86B mRNA
7.94	2.123	0	A_51_P357561	*Fbxw9*	NM_026791	ref|Mus musculus F-box and WD-40 domain protein 9 mRNA
7.17	1.978	3.00E-05	A_51_P378622	*0610012H03Rik*	NM_028747	ref|Mus musculus RIKEN cDNA 0610012H03 gene transcript variant 1 mRNA
11.29	1.931	0	A_55_P2178036	*Serpina6*	NM_007618	ref|Mus musculus serine (or cysteine) peptidase inhibitor clade A member 6 mRNA
11.84	1.857	0	A_55_P2031668	*Gstp1*	NM_013541	ref|Mus musculus glutathione S-transferase pi 1 mRNA
10.80	1.853	1.00E-05	A_55_P2102065	*Gm10639*	NM_001122660	ref|Mus musculus predicted gene 10639 mRNA
8.56	1.762	0	A_55_P2059931	*Prom1*	NM_001163577	ref|Mus musculus prominin 1 transcript variant 2 mRNA
7.22	1.758	0.00048	A_51_P375146	*Cd36*	NM_007643	ref|Mus musculus CD36 antigen transcript variant 2 mRNA
7.17	1.702	0	A_51_P480073	*Chad*	NM_007689	ref|Mus musculus chondroadherin mRNA
9.85	1.696	0	A_55_P2124712	*Ces2*	NM_145603	ref|Mus musculus carboxylesterase 2 mRNA
9.68	1.694	0.00083	A_55_P1989248	*Gm6168*	XM_885022	ref|PREDICTED: Mus musculus predicted gene EG620627 mRNA
8.13	1.653	0	A_55_P2063312	*Mgll*	NM_001166250	ref|Mus musculus monoglyceride lipase transcript variant 4 mRNA
7.80	1.652	1.00E-05	A_51_P511176	*Triap1*	NM_026933	ref|Mus musculus TP53 regulated inhibitor of apoptosis 1 mRNA
8.99	1.650	0	A_52_P318361	*Ces2*	NM_145603	ref|Mus musculus carboxylesterase 2 mRNA
9.38	1.630	0	A_52_P627269	*BC015286*	NM_198171	ref|Mus musculus cDNA sequence BC015286 mRNA
7.71	1.621	0	A_55_P1984675	*Abhd6*	NM_025341	ref|Mus musculus abhydrolase domain containing 6 mRNA

9.59	1.602	0	A_51_P411271	*Nfe2l2*	NM_010902	ref|Mus musculus nuclear factor erythroid derived 2 like 2 mRNA
8.41	1.597	0	A_55_P2143765	*Ugt1a6a*	NM_145079	ref|Mus musculus UDP glucuronosyltransferase 1 family polypeptide A6A mRNA
8.13	1.584	0	A_55_P2178800	*Ugt1a10*	NM_201641	ref|Mus musculus UDP glycosyltransferase 1 family polypeptide A10 mRNA
9.22	1.565	0	A_51_P471458	*Sult5a1*	NM_020564	ref|Mus musculus sulfotransferase family 5A member 1 mRNA
12.91	1.559	0	A_55_P2008704	*Gstp2*	NM_181796	ref|Mus musculus glutathione S-transferase pi 2 mRNA
9.18	1.528	0	A_55_P2066727	*Serpinb6a*	NM_001164118	ref|Mus musculus serine (or cysteine) peptidase inhibitor clade B member 6a transcript variant 3 mRNA
9.48	1.520	0	A_52_P327156	*0610008F07Rik*	NR_027970	ref|Mus musculus RIKEN cDNA 0610008F07 gene non-coding RNA
7.62	1.502	0	A_55_P2013038	*Serpinb6c*	NM_148942	ref|Mus musculus serine (or cysteine) peptidase inhibitor clade B member 6c mRNA
10.43	1.499	0	A_51_P181319	*Dcxr*	NM_026428	ref|Mus musculus dicarbonyl L-xylulose reductase mRNA
8.74	1.497	0.00084	A_51_P326685	*Lrtm1*	NM_176920	ref|Mus musculus leucine-rich repeats and transmembrane domains 1 mRNA
12.41	1.481	2.00E-05	A_51_P269404	*Fmo3*	NM_008030	ref|Mus musculus flavin containing monooxygenase 3 mRNA
8.78	1.452	0	A_55_P1966438	*Gstm2*	NM_008183	ref|Mus musculus glutathione S-transferase mu 2 mRNA
14.49	1.441	0	A_55_P1961014	*Selenbp1*	NM_009150	ref|Mus musculus selenium binding protein 1 mRNA
9.34	1.43	0	A_51_P418526	*Sfxn1*	NM_027324	ref|Mus musculus sideroflexin 1 mRNA
7.97	1.423	5.00E-05	A_55_P2060107	*Pkm2*	NM_011099	ref|Mus musculus pyruvate kinase muscle mRNA
11.34	1.414	0	A_51_P441914	*Hsd17b2*	NM_008290	ref|Mus musculus hydroxysteroid (17-beta) dehydrogenase 2 mRNA
9.71	1.407	0	A_55_P2077628	*ENSMUST00000106148*	ENSMUST00000106148	ens|L-xylulose reductase (XR)(EC 1.1.1.10)(Dicarbonyl/L-xylulose reductase) [Source:UniProtKB/Swiss-Prot;Acc:Q91X52]
8.68	1.394	0	A_51_P163578	*Ugt2b35*	NM_172881	ref|Mus musculus UDP glucuronosyltransferase 2 family polypeptide B35 mRNA
11.23	1.391	0	A_55_P2006236	*Ugdh*	NM_009466	ref|Mus musculus UDP-glucose dehydrogenase mRNA
8.87	1.391	0	A_55_P2047768	*Serpinb6c*	NM_148942	ref|Mus musculus serine (or cysteine) peptidase inhibitor clade B member 6c mRNA
8.48	1.382	3.00E-05	A_55_P2030524	*Vldlr*	NM_013703	ref|Mus musculus very low density lipoprotein receptor transcript variant 1 mRNA
7.60	1.374	0	A_55_P2108151	*ENSMUST00000023934*	ENSMUST00000023934	ens|Hemoglobin subunit beta-1 (Hemoglobin beta-1 chain)(Beta-1-globin)(Hemoglobin beta-major chain) [Source:UniProtKB/Swiss-Prot;Acc:P02088]
10.70	1.371	0.00145	A_55_P2038358	*Acot1*	NM_012006	ref|Mus musculus acyl-CoA thioesterase 1 mRNA
9.32	1.366	0	A_52_P154580	*Cyp2c54*	NM_206537	ref|Mus musculus cytochrome P450 family 2 subfamily c polypeptide 54 mRNA
12.65	1.362	0	A_51_P374464	*Gstp1*	NM_013541	ref|Mus musculus glutathione S-transferase pi 1 mRNA
8.64	1.328	0	A_55_P1971093	*NAP096516-001*	NAP096516-001	Unknown
10.18	1.316	0	A_51_P329441	*Bsg*	NM_009768	ref|Mus musculus basigin (Bsg) transcript variant 1 mRNA
8.92	1.309	0.00027	A_55_P2059323	*Gm13315*	NR_028497	ref|Mus musculus predicted gene 13315 non-coding RNA
11.10	1.297	0.00034	A_55_P2170454	*Gsta2*	NM_008182	ref|Mus musculus glutathione S-transferase alpha 2 (Yc2) mRNA
7.90	1.290	1.00E-05	A_51_P316951	*Wipf3*	NM_001167860	ref|Mus musculus WAS/WASL interacting protein family member 3 transcript variant 1 mRNA

8.20	1.286	0	A_55_P2055742	*9530008L14Rik*	NM_001145875	ref|Mus musculus RIKEN cDNA 9530008L14 gene transcript variant 2 mRNA
7.63	1.282	0	A_55_P2095035	*Gm1833*	XM_129965	ref|PREDICTED: Mus musculus gene model 1833 (NCBI) mRNA
7.89	1.273	1.00E-05	A_55_P2037689	*A_55_P2037689*	A_55_P2037689	Unknown
9.62	1.264	0	A_51_P468329	*Psmb7*	NM_011187	ref|Mus musculus proteasome (prosome macropain) subunit beta type 7 mRNA
10.75	1.259	0	A_52_P282905	*Gm5158*	NM_001081372	ref|Mus musculus predicted gene 5158 mRNA
9.51	1.247	0	A_51_P458778	*Hpgd*	NM_008278	ref|Mus musculus hydroxyprostaglandin dehydrogenase 15 (NAD) mRNA
11.37	1.244	2.00E-05	A_55_P1959923	*Cth*	NM_145953	ref|Mus musculus cystathionase (cystathionine gamma-lyase) mRNA
7.53	1.244	0	A_55_P2114498	*Gm8801*	NR_028278	ref|Mus musculus predicted gene 8801 non-coding RNA
9.47	1.241	0	A_55_P1995447	*A_55_P1995447*	A_55_P1995447	Unknown
7.60	1.235	0.00039	A_55_P2012439	*Tnfrsf19*	NM_013869	ref|Mus musculus tumor necrosis factor receptor superfamily member 19 transcript variant 1 mRNA
7.59	1.229	0	A_51_P406557	*AI464131*	NM_001085515	ref|Mus musculus expressed sequence AI464131 mRNA
11.98	1.229	0	A_51_P255682	*Mfge8*	NM_008594	ref|Mus musculus milk fat globule-EGF factor 8 protein transcript variant 1 mRNA
7.97	1.211	1.00E-05	A_55_P2029366	*Abhd6*	NM_025341	ref|Mus musculus abhydrolase domain containing 6 mRNA
8.30	1.209	1.00E-05	A_55_P2035424	*Hpgd*	NM_008278	ref|Mus musculus hydroxyprostaglandin dehydrogenase 15 (NAD) mRNA
9.26	1.207	1.00E-05	A_55_P2118810	*A_55_P2118810*	A_55_P2118810	Unknown
7.62	1.206	0	A_55_P2051796	*Gm128*	NM_001024841	ref|Mus musculus predicted gene 128 mRNA
8.74	1.198	0	A_51_P459350	*Dstn*	NM_019771	ref|Mus musculus destrin mRNA
9.06	1.197	0	A_52_P87964	*Pla2g12a*	NM_183423	ref|Mus musculus phospholipase A2 group XIIA transcript variant 2 mRNA
15.43	1.187	0	A_55_P1957038	*Gstp2*	NM_181796	ref|Mus musculus glutathione S-transferase pi 2 mRNA
9.45	1.183	0	A_51_P312121	*Xdh*	NM_011723	ref|Mus musculus xanthine dehydrogenase mRNA
9.46	1.181	0.00012	A_55_P2168781	*A_55_P2168781*	A_55_P2168781	Unknown
7.98	1.178	0.00064	A_51_P391727	*Slc3a1*	NM_009205	ref|Mus musculus solute carrier family 3 member 1 mRNA
7.16	1.176	0.00751	A_66_P128931	*LOC100047937*	XM_001479188	ref|PREDICTED: Mus musculus similar to Aldehyde dehydrogenase 1 family member L1 mRNA
10.44	1.165	0	A_55_P2141878	*Ldha*	NM_001136069	ref|Mus musculus lactate dehydrogenase A transcript variant 2 mRNA
11.37	1.156	6.00E-05	A_65_P03442	*Pgk1*	NM_008828	ref|Mus musculus phosphoglycerate kinase 1 mRNA
11.34	1.153	0	A_51_P502872	*2200002D01Rik*	NM_028179	ref|Mus musculus RIKEN cDNA 2200002D01 gene mRNA
7.12	1.150	0.00019	A_51_P297105	*Ucp2*	NM_011671	ref|Mus musculus uncoupling protein 2 (mitochondrial proton carrier) nuclear gene encoding mitochondrial protein mRNA
8.32	1.146	0.00122	A_51_P419637	*Dclk3*	NM_172928	ref|Mus musculus doublecortin-like kinase 3 mRNA
7.82	1.139	0.00078	A_55_P2078955	*Aqp8*	NM_007474	ref|Mus musculus aquaporin 8 transcript variant 1 mRNA
7.55	1.138	0.00076	A_55_P2055232	*Sdf4*	NM_011341	ref|Mus musculus stromal cell derived factor 4 mRNA

7.45	1.136	0.00109	A_51_P246653	*Clec7a*	NM_020008	ref|Mus musculus C-type lectin domain family 7 member a mRNA
10.12	1.135	0.00047	A_55_P2013273	*A_55_P2013273*	A_55_P2013273	Unknown
10.18	1.134	0.00013	A_55_P2059586	*Fmo3*	NM_008030	ref|Mus musculus flavin containing monooxygenase 3 mRNA
9.06	1.130	0	A_52_P487436	*Nags*	NM_145829	ref|Mus musculus N-acetylglutamate synthase transcript variant 1 mRNA
11.01	1.127	2.00E-05	A_66_P111747	*NAP096647-001*	NAP096647-001	tc|MUSXPGK phosphoglycerate kinase {Mus musculus} (exp=0; wgp=1; cg=0) partial (43%) [TC1657415]
7.47	1.115	0.00289	A_51_P201904	*Ndufb5*	NM_025316	ref|Mus musculus NADH dehydrogenase (ubiquinone) 1 beta subcomplex 5 nuclear gene encoding mitochondrial protein mRNA
10.90	1.113	0.00922	A_52_P318673	*Saa1*	NM_009117	ref|Mus musculus serum amyloid A 1 mRNA
9.07	1.111	3.00E-05	A_51_P295312	*Gabarap*	NM_019749	ref|Mus musculus gamma-aminobutyric acid receptor associated protein mRNA
15.57	1.105	0	A_66_P125722	*Cyb5*	NM_025797	ref|Mus musculus cytochrome b-5 mRNA
7.43	1.104	0	A_55_P2110512	*Lmo7*	NM_201529	ref|Mus musculus LIM domain only 7 mRNA
9.44	1.103	0.00033	A_55_P2051159	*Upp2*	NM_029692	ref|Mus musculus uridine phosphorylase 2 mRNA
8.36	1.094	5.00E-05	A_51_P215922	*Casp6*	NM_009811	ref|Mus musculus caspase 6 mRNA
7.56	1.093	0.00067	A_51_P455647	*Car2*	NM_009801	ref|Mus musculus carbonic anhydrase 2 mRNA
8.23	1.092	0	A_51_P519189	*Eif3i*	NM_018799	ref|Mus musculus eukaryotic translation initiation factor 3 subunit I mRNA
11.88	1.088	0.0083	A_55_P2172532	*C730007P19Rik*	NM_009286	ref|Mus musculus RIKEN cDNA C730007P19 gene mRNA
8.03	1.088	0	A_55_P1971962	*Tmem176b*	NM_023056	ref|Mus musculus transmembrane protein 176B transcript variant 1 mRNA
8.12	1.080	0.00158	A_51_P336833	*Fabp4*	NM_024406	ref|Mus musculus fatty acid binding protein 4 adipocyte mRNA
7.10	1.080	0	A_52_P44030	*Exoc3*	NM_177333	ref|Mus musculus exocyst complex component 3 mRNA
7.40	1.074	0.0014	A_66_P108247	*Ucp3*	NM_009464	ref|Mus musculus uncoupling protein 3 (mitochondrial proton carrier) nuclear gene encoding mitochondrial protein mRNA
7.46	1.072	0.00026	A_51_P519385	*Sacm1l*	NM_030692	ref|Mus musculus SAC1 (suppressor of actin mutations 1 homolog)-like (S. cerevisiae) mRNA
8.55	1.069	1.00E-05	A_51_P386503	*Abhd15*	NM_026185	ref|Mus musculus abhydrolase domain containing 15 mRNA
11.55	1.066	0	A_52_P151320	*Tnfaip8l1*	NM_025566	ref|Mus musculus tumor necrosis factor alpha-induced protein 8-like 1 mRNA
9.51	1.065	0	A_51_P142896	*Cd59a*	NM_007652	ref|Mus musculus CD59a antigen transcript variant 2 mRNA
8.30	1.059	9.00E-05	A_51_P142515	*Antxr2*	NM_133738	ref|Mus musculus anthrax toxin receptor 2 mRNA
11.11	1.057	7.00E-05	A_51_P431737	*Cth*	NM_145953	ref|Mus musculus cystathionase (cystathionine gamma-lyase) mRNA
7.12	1.052	7.00E-04	A_55_P2128181	*A_55_P2128181*	A_55_P2128181	Unknown
8.94	1.050	0	A_55_P2110513	*Lmo7*	NM_201529	ref|Mus musculus LIM domain only 7 mRNA
9.11	1.048	6.00E-05	A_55_P2038540	*Hbb-b2*	NM_016956	ref|Mus musculus hemoglobin beta adult minor chain mRNA
7.45	1.045	3.00E-05	A_55_P2005859	*Fn3k*	NM_022014	ref|Mus musculus fructosamine 3 kinase transcript variant 1 mRNA
9.90	1.044	0.00021	A_55_P2185840	*Nnmt*	NM_010924	ref|Mus musculus nicotinamide N-methyltransferase mRNA

10.20	1.043	0	A_55_P2077635	*A_55_P2077635*	A_55_P2077635	Unknown
8.09	1.040	0.00762	A_51_P307168	*Ddah1*	NM_026993	ref|Mus musculus dimethylarginine dimethylaminohydrolase 1 mRNA
7.40	1.039	0.00742	A_55_P2083481	*Lpin1*	NM_001130412	ref|Mus musculus lipin 1 transcript variant 3 mRNA
14.14	1.039	0	A_51_P133562	*Serpina6*	NM_007618	ref|Mus musculus serine (or cysteine) peptidase inhibitor clade A member 6 mRNA
8.83	1.036	0.0035	A_55_P2069969	*Gm10639*	NM_001122660	ref|Mus musculus predicted gene 10639 mRNA
10.72	1.034	0	A_55_P2138097	*Gm9294*	NM_001081036	ref|Mus musculus predicted gene 9294 mRNA
7.16	1.034	5.00E-04	A_55_P2157225	*Nqo2*	NM_020282	ref|Mus musculus NAD(P)H dehydrogenase quinone 2 transcript variant 1 mRNA
9.91	1.028	0.00012	A_55_P2068812	*AK203298*	AK203298	gb|Mus musculus cDNA clone:Y1G0144G24 strand:minus reference:ENSEMBL:Mouse-Transcript-ENST:ENSMUST00000061523 based on BLAT search
9.20	1.027	0	A_51_P293901	*Dhrs1*	NM_026819	ref|Mus musculus dehydrogenase/reductase (SDR family) member 1 mRNA
8.19	1.023	0.00108	A_51_P120461	*Mina*	NM_025910	ref|Mus musculus myc induced nuclear antigen mRNA
14.50	1.020	0.00029	A_55_P1966690	*Cyp2e1*	NM_021282	ref|Mus musculus cytochrome P450 family 2 subfamily e polypeptide 1 mRNA
11.53	1.019	1.00E-04	A_52_P404341	*Tdo2*	NM_019911	ref|Mus musculus tryptophan 23-dioxygenase mRNA
7.90	1.014	1.00E-05	A_51_P271503	*Il1r1*	NM_008362	ref|Mus musculus interleukin 1 receptor type I transcript variant 1 mRNA
8.06	1.013	0	A_52_P148678	*ENSMUST00000109462*	ENSMUST00000109462	ens|1-phosphatidylinositol-45-bisphosphate phosphodiesterase gamma-1 (EC 3.1.4.11)(Phosphoinositide phospholipase C)(Phospholipase C-gamma-1)(PLC-gamma-1)(PLC-II)(PLC-148) [Source:UniProtKB/Swiss-Prot;Acc:Q62077]
9.56	1.003	0.00389	A_52_P579252	*Gm9644*	XR_005114	gb|PREDICTED: Mus musculus similar to Ribosomal protein L3 misc RNA
7.10	1.002	0.00881	A_51_P487547	*Ccdc91*	NM_025911	ref|Mus musculus coiled-coil domain containing 91 mRNA
10.58	1.002	1.00E-05	A_55_P2131027	*Gm3699*	XM_001477613	ref|PREDICTED: Mus musculus hypothetical protein LOC100042155 mRNA
8.21	1.000	3.00E-05	A_55_P2048368	*Fggy*	NM_029347	ref|Mus musculus FGGY carbohydrate kinase domain containing transcript variant 2 mRNA

Table 82. All significantly down regulated genes livers of female C57BL/6 mice by TCDD (25 µg/kg bw) identified by microarray analysis – mouse 3-day study. Selected parameters: A-value ≥ 7, log2 fc ≤ -1, p-value ≤ 0.05.

A	Log2 fc	p-value	Probe name	Gene name	Systematic name	Gene description
8.11	-2.846	0	A_55_P2022074	*Klf10*	NM_013692	ref|Mus musculus Kruppel-like factor 10 mRNA
8.35	-2.601	5.00E-05	A_51_P249286	*Rgs16*	NM_011267	ref|Mus musculus regulator of G-protein signaling 16 mRNA
9.43	-2.573	0	A_55_P1997003	*Serpina4-ps1*	BC031891	gb|Mus musculus serine (or cysteine) peptidase inhibitor clade A member 4 pseudogene 1 mRNA (cDNA clone IMAGE:5123840)
9.98	-2.488	1.00E-05	A_55_P2004606	*Serpina4-ps1*	NR_002861	ref|Mus musculus serine (or cysteine) peptidase inhibitor clade A member 4 pseudogene 1 non-coding RNA
11.37	-2.276	0	A_52_P106259	*Egfr*	NM_207655	ref|Mus musculus epidermal growth factor receptor transcript variant 1 mRNA
11.51	-2.183	0	A_52_P106259	*Egfr*	NM_207655	ref|Mus musculus epidermal growth factor receptor transcript variant 1 mRNA
11.24	-2.18	0	A_52_P106259	*Egfr*	NM_207655	ref|Mus musculus epidermal growth factor receptor transcript variant 1 mRNA
11.40	-2.176	0	A_52_P106259	*Egfr*	NM_207655	ref|Mus musculus epidermal growth factor receptor transcript variant 1 mRNA
11.34	-2.173	0	A_52_P106259	*Egfr*	NM_207655	ref|Mus musculus epidermal growth factor receptor transcript variant 1 mRNA
11.24	-2.169	0	A_52_P106259	*Egfr*	NM_207655	ref|Mus musculus epidermal growth factor receptor transcript variant 1 mRNA
11.41	-2.158	0	A_52_P106259	*Egfr*	NM_207655	ref|Mus musculus epidermal growth factor receptor transcript variant 1 mRNA
11.36	-2.157	0	A_52_P106259	*Egfr*	NM_207655	ref|Mus musculus epidermal growth factor receptor transcript variant 1 mRNA
11.42	-2.150	0	A_52_P106259	*Egfr*	NM_207655	ref|Mus musculus epidermal growth factor receptor transcript variant 1 mRNA
11.31	-2.141	0	A_52_P106259	*Egfr*	NM_207655	ref|Mus musculus epidermal growth factor receptor transcript variant 1 mRNA
8.94	-2.125	2.00E-05	A_51_P107362	*Socs2*	NM_007706	ref|Mus musculus suppressor of cytokine signaling 2 transcript variant 1 mRNA
8.94	-2.106	3.00E-05	A_51_P107362	*Socs2*	NM_007706	ref|Mus musculus suppressor of cytokine signaling 2 transcript variant 1 mRNA
8.74	-2.103	4.00E-05	A_51_P107362	*Socs2*	NM_007706	ref|Mus musculus suppressor of cytokine signaling 2 transcript variant 1 mRNA
8.67	-2.090	2.00E-05	A_51_P107362	*Socs2*	NM_007706	ref|Mus musculus suppressor of cytokine signaling 2 transcript variant 1 mRNA
8.58	-2.072	3.00E-05	A_51_P107362	*Socs2*	NM_007706	ref|Mus musculus suppressor of cytokine signaling 2 transcript variant 1 mRNA
8.68	-2.059	3.00E-05	A_51_P107362	*Socs2*	NM_007706	ref|Mus musculus suppressor of cytokine signaling 2 transcript variant 1 mRNA
8.77	-2.048	3.00E-05	A_51_P107362	*Socs2*	NM_007706	ref|Mus musculus suppressor of cytokine signaling 2 transcript variant 1 mRNA
8.66	-2.038	2.00E-05	A_51_P107362	*Socs2*	NM_007706	ref|Mus musculus suppressor of cytokine signaling 2 transcript variant 1 mRNA
10.36	-2.025	0	A_51_P268529	*Csad*	NM_144942	ref|Mus musculus cysteine sulfinic acid decarboxylase mRNA
8.67	-2.013	9.00E-05	A_51_P107362	*Socs2*	NM_007706	ref|Mus musculus suppressor of cytokine signaling 2 transcript variant 1 mRNA
8.89	-2.003	6.00E-05	A_51_P107362	*Socs2*	NM_007706	ref|Mus musculus suppressor of cytokine signaling 2 transcript variant 1 mRNA
8.48	-1.890	0	A_55_P1954698	*LOC100046261*	XM_001475897	ref|PREDICTED: Mus musculus similar to myosin XV mRNA
8.72	-1.886	0.00031	A_52_P161495	*Bcl6*	NM_009744	ref|Mus musculus B-cell leukemia/lymphoma 6 mRNA

7.59	-1.832	9.00E-05	A_55_P1992838	*Socs2*	NM_007706	ref|Mus musculus suppressor of cytokine signaling 2 transcript variant 1 mRNA
7.86	-1.821	0	A_55_P2073789	*LOC676974*	XM_001003154	ref|PREDICTED: Mus musculus similar to Glucose phosphate isomerase 1 transcript variant 2 mRNA
9.99	-1.806	0	A_51_P463440	*Elovl6*	NM_130450	ref|Mus musculus ELOVL family member 6 elongation of long chain fatty acids (yeast) mRNA
8.65	-1.752	0	A_51_P272553	*Bhlhe40*	NM_011498	ref|Mus musculus basic helix-loop-helix family member e40 mRNA
7.55	-1.734	0	A_55_P1978502	*H2-Q1*	NM_010390	ref|Mus musculus histocompatibility 2 Q region locus 1 mRNA
10.80	-1.694	0	A_66_P102260	*Irs2*	NM_001081212	ref|Mus musculus insulin receptor substrate 2 mRNA
10.86	-1.689	0	A_51_P122246	*Creld2*	NM_029720	ref|Mus musculus cysteine-rich with EGF-like domains 2 mRNA
10.87	-1.676	0	A_51_P122246	*Creld2*	NM_029720	ref|Mus musculus cysteine-rich with EGF-like domains 2 mRNA
7.05	-1.675	2.00E-05	A_55_P1954393	*Susd4*	NM_144796	ref|Mus musculus sushi domain containing 4 mRNA
14.31	-1.669	0.00022	A_52_P21486	*Hamp2*	NM_183257	ref|Mus musculus hepcidin antimicrobial peptide 2) mRNA
10.97	-1.656	0	A_51_P122246	*Creld2*	NM_029720	ref|Mus musculus cysteine-rich with EGF-like domains 2 mRNA
10.47	-1.654	0	A_51_P122246	*Creld2*	NM_029720	ref|Mus musculus cysteine-rich with EGF-like domains 2 mRNA
11.54	-1.649	9.00E-05	A_55_P2150976	*Fabp5l2*	XM_886827	ref|PREDICTED: Mus musculus predicted gene EG622384mRNA
10.50	-1.648	0	A_51_P122246	*Creld2*	NM_029720	ref|Mus musculus cysteine-rich with EGF-like domains 2 mRNA
7.41	-1.645	0.00232	A_66_P122699	*Cux2*	ENSMUST00000111752	ens|Homeobox protein cut-like 2 (Cut-like 2)(Homeobox protein Cux-2) [Source:UniProtKB/Swiss-Prot;Acc:P70298]
10.61	-1.635	0	A_51_P122246	*Creld2*	NM_029720	ref|Mus musculus cysteine-rich with EGF-like domains 2 mRNA
10.67	-1.629	0	A_51_P122246	*Creld2*	NM_029720	ref|Mus musculus cysteine-rich with EGF-like domains 2 mRNA
10.57	-1.627	0	A_51_P122246	*Creld2*	NM_029720	ref|Mus musculus cysteine-rich with EGF-like domains 2 mRNA
10.51	-1.604	0	A_51_P122246	*Creld2*	NM_029720	ref|Mus musculus cysteine-rich with EGF-like domains 2 mRNA
10.92	-1.594	0	A_51_P122246	*Creld2*	NM_029720	ref|Mus musculus cysteine-rich with EGF-like domains 2 mRNA
7.11	-1.560	0	A_66_P118430	*Slc17a2*	ENSMUST00000006786	ens|Sodium-dependent phosphate transport protein 3 (Sodium/phosphate cotransporter 3)(Na(+)/PI cotransporter 3)(Solute carrier family 17 member 2) [Source:UniProtKB/Swiss-Prot;Acc:Q5SZA1]
7.20	-1.557	0	A_51_P256384	*Atp2b2*	NM_009723	ref|Mus musculus ATPase Ca^{2+}transporting plasma membrane 2 transcript variant 1 mRNA
12.54	-1.555	0	A_66_P135391	*Igfbp2*	NM_008342	ref|Mus musculus insulin-like growth factor binding protein 2 mRNA
7.66	-1.545	1.00E-04	A_55_P1992834	*Socs2*	NM_007706	ref|Mus musculus suppressor of cytokine signaling 2 transcript variant 1 mRNA
8.34	-1.538	9.00E-05	A_51_P501844	*Cyp26b1*	NM_175475	ref|Mus musculus cytochrome P450 family 26 subfamily b polypeptide 1 mRNA
10.25	-1.531	0.00018	A_55_P2122841	*NAP114472-1*	NAP114472-1	Unknown
11.07	-1.525	0.00016	A_55_P1953387	*Fabp5*	NM_010634	ref|Mus musculus fatty acid binding protein 5 epidermal mRNA
12.39	-1.508	0	A_55_P2056729	*Igfbp2*	NM_008342	ref|Mus musculus insulin-like growth factor binding protein 2 mRNA
10.08	-1.502	0	A_55_P2118866	*Cmah*	NM_001111110	ref|Mus musculus cytidine monophospho-N-acetylneuraminic acid hydroxylase transcript variant 2 mRNA
12.03	-1.481	0	A_55_P2015734	*Synv1*	NM_028769	ref|Mus musculus synovial apoptosis inhibitor 1 synoviolin transcript variant 1 mRNA

10.43	-1.461	4.00E-05	A_55_P2032081	*Dbp*	NM_016974	ref|Mus musculus D site albumin promoter binding protein mRNA
7.42	-1.439	0	A_55_P2081273	*Gabbr2*	NM_001081141	ref|Mus musculus gamma-aminobutyric acid (GABA) B receptor 2 mRNA
15.10	-1.432	0	A_51_P431329	*Car3*	NM_007606	ref|Mus musculus carbonic anhydrase 3 mRNA
9.97	-1.429	1.00E-05	A_55_P2032079	*Dbp*	NM_016974	ref|Mus musculus D site albumin promoter binding protein mRNA
12.39	-1.425	0.00058	A_51_P462385	*G6pc*	NM_008061	ref|Mus musculus glucose-6-phosphatase catalytic mRNA
7.89	-1.423	0.00064	A_55_P2082914	*Acly*	NM_134037	ref|Mus musculus ATP citrate lyase mRNA
8.52	-1.405	0	A_55_P2003513	*Hsph1*	NM_013559	ref|Mus musculus heat shock 105kDa/110kDa protein 1 mRNA
9.08	-1.390	0	A_66_P111562	*Ccnd1*	NM_007631	ref|Mus musculus cyclin D1 mRNA
7.49	-1.387	0	A_55_P2211164	*5330406M23Rik*	AK017236	gb|Mus musculus adult male pituitary gland cDNA RIKEN full-length enriched library clone:5330406M23 product:unclassifiable full insert sequence
15.00	-1.387	0	A_51_P408082	*Apoa1*	NM_009692	ref|Mus musculus apolipoprotein A-I mRNA
13.41	-1.378	0	A_55_P2422650	*5031425E22Rik*	AK017143	gb|Mus musculus 11 days pregnant adult female ovary and uterus cDNA RIKEN full-length enriched library clone: 5031425E22 product:unclassifiable full insert sequence
11.83	-1.374	0	A_55_P2153517	*Enho*	NM_027147	ref|Mus musculus energy homeostasis associated mRNA
7.21	-1.369	0.00103	A_52_P140005	*Nipal1*	NM_001081205	ref|Mus musculus NIPA-like domain containing 1 mRNA
13.29	-1.368	8.00E-05	A_66_P121110	*Pck1*	NM_011044	ref|Mus musculus phosphoenolpyruvate carboxykinase 1 cytosolic mRNA
7.72	-1.367	0	A_52_P68702	*Frmd4b*	NM_145148	ref|Mus musculus FERM domain containing 4B mRNA
14.98	-1.363	0	A_51_P408082	*Apoa1*	NM_009692	ref|Mus musculus apolipoprotein A-I mRNA
7.35	-1.361	0.00029	A_52_P627816	*Tgm1*	NM_019984	ref|Mus musculus transglutaminase 1 K polypeptide transcript variant 2 mRNA
15.15	-1.353	0	A_51_P408082	*Apoa1*	NM_009692	ref|Mus musculus apolipoprotein A-I mRNA
14.80	-1.350	0	A_51_P408082	*Apoa1*	NM_009692	ref|Mus musculus apolipoprotein A-I mRNA
14.83	-1.348	1.00E-05	A_51_P408082	*Apoa1*	NM_009692	ref|Mus musculus apolipoprotein A-I mRNA
14.69	-1.348	0	A_51_P408082	*Apoa1*	NM_009692	ref|Mus musculus apolipoprotein A-I mRNA
15.15	-1.345	0	A_51_P408082	*Apoa1*	NM_009692	ref|Mus musculus apolipoprotein A-I mRNA
14.98	-1.336	1.00E-05	A_51_P408082	*Apoa1*	NM_009692	ref|Mus musculus apolipoprotein A-I mRNA
14.72	-1.336	0	A_51_P408082	*Apoa1*	NM_009692	ref|Mus musculus apolipoprotein A-I mRNA
12.13	-1.335	0	A_55_P2062737	*Elovl2*	NM_019423	ref|Mus musculus elongation of very long chain fatty acids (FEN1/Elo2 SUR4/Elo3 yeast)-like 2 mRNA
14.84	-1.328	1.00E-05	A_51_P408082	*Apoa1*	NM_009692	ref|Mus musculus apolipoprotein A-I mRNA
11.55	-1.328	0	A_55_P2015753	*Enho*	NM_027147	ref|Mus musculus energy homeostasis associated mRNA
11.96	-1.313	0.00115	A_55_P2025954	*Acly*	NM_134037	ref|Mus musculus ATP citrate lyase mRNA
9.30	-1.309	5.00E-05	A_55_P2258261	*1810008I18Rik*	AK050412	gb|Mus musculus adult male liver tumor cDNA RIKEN full-length enriched library clone:C730046D02 product: unclassifiable full insert sequence

10.86	-1.306	0	A_55_P2129449	*Sult3a1*	NM_020565	ref|Mus musculus sulfotransferase family 3A member 1 mRNA
7.25	-1.305	0	A_66_P133450	*Dnajb9*	NM_013760	ref|Mus musculus DnaJ (Hsp40) homolog subfamily B member 9 mRNA
11.12	-1.295	0	A_55_P2048518	*Zfpm1*	NM_009569	ref|Mus musculus zinc finger protein multitype 1 mRNA
8.11	-1.284	0	A_55_P1960117	*1190002N15Rik*	NM_001033145	ref|Mus musculus RIKEN cDNA 1190002N15 gene mRNA
11.86	-1.280	0	A_55_P2025343	*Mup21*	NM_001009550	ref|Mus musculus major urinary protein 21 mRNA
10.81	-1.276	0	A_55_P2165091	*Acnat2*	NM_145368	ref|Mus musculus acyl-coenzyme A amino acid N-acyltransferase 2 mRNA
11.66	-1.273	2.00E-05	A_52_P662244	*AI132487*	NM_001012310	ref|Mus musculus expressed sequence AI132487 mRNA
7.61	-1.239	0.0022	A_55_P2078494	*Cib3*	NM_001080812	ref|Mus musculus calcium and integrin binding family member 3 mRNA
8.55	-1.237	0.00323	A_52_P100252	*Fasn*	NM_007988	ref|Mus musculus fatty acid synthase mRNA
9.84	-1.233	0	A_55_P2075263	*Acnat2*	NM_145368	ref|Mus musculus acyl-coenzyme A amino acid N-acyltransferase 2 mRNA
11.19	-1.229	0	A_55_P1994887	*Zfpm1*	NM_009569	ref|Mus musculus zinc finger protein multitype 1 mRNA
9.28	-1.214	0	A_55_P2143896	*Slc17a2*	NM_144836	ref|Mus musculus solute carrier family 17 (sodium phosphate) member 2 mRNA
8.16	-1.207	9.00E-05	A_55_P2057528	*Arl4d*	NM_025404	ref|Mus musculus ADP-ribosylation factor-like 4D mRNA
7.07	-1.205	0.00026	A_66_P124179	*Atp6v0d2*	NM_175406	ref|Mus musculus ATPase H^+ transporting lysosomal V0 subunit D2 mRNA
16.38	-1.195	0	A_55_P2048607	*Hp*	NM_017370	ref|Mus musculus haptoglobin mRNA
8.37	-1.177	0	A_55_P2159934	*Rnf186*	NM_025786	ref|Mus musculus ring finger protein 186 mRNA
9.66	-1.165	0	A_52_P70854	*Tob2*	NM_020507	ref|Mus musculus transducer of ERBB2 2 mRNA
8.22	-1.154	0	A_55_P1971054	*Paqr9*	NM_198414	ref|Mus musculus progestin and adipoQ receptor family member IX mRNA
7.25	-1.151	6.00E-05	A_51_P176042	*Pklr*	NM_013631	ref|Mus musculus pyruvate kinase liver and red blood cell nuclear gene encoding mitochondrial protein transcript variant 1 mRNA
9.30	-1.150	0	A_66_P121636	*Ablim3*	NM_198649	ref|Mus musculus actin binding LIM protein family member 3 transcript variant 1 mRNA
9.48	-1.136	0	A_55_P2009988	*Trib3*	NM_175093	ref|Mus musculus tribbles homolog 3 (Drosophila) mRNA
8.88	-1.135	0.00263	A_66_P124164	*ENSMUST00000099683*	ENSMUST00000099683	Unknown
10.21	-1.125	0	A_51_P215540	*Rnf4*	NM_011278	ref|Mus musculus ring finger protein 4 mRNA
9.23	-1.113	3.00E-05	A_55_P2067563	*Etnk2*	XM_001471861	ref|PREDICTED: Mus musculus hypothetical protein LOC100044148 mRNA
9.34	-1.108	0	A_55_P1956863	*Egfr*	NM_007912	ref|Mus musculus epidermal growth factor receptor transcript variant 2 mRNA
7.44	-1.107	0	A_55_P2076984	*Farp1*	NM_134082	ref|Mus musculus FERM RhoGEF (Arhgef) and pleckstrin domain protein 1 (chondrocyte-derived) mRNA
10.55	-1.103	0.00011	A_55_P2068289	*Slc17a2*	NM_144836	ref|Mus musculus solute carrier family 17 (sodium phosphate) member 2 mRNA
11.59	-1.103	0.00013	A_55_P2009042	*Gm4635*	XM_001481023	ref|PREDICTED: Mus musculus hypothetical protein LOC100043770 mRNA
8.77	-1.092	0.00375	A_55_P2138100	*ENSMUST00000099050*	ENSMUST00000099050	Unknown
11.39	-1.089	4.00E-05	A_55_P2019058	*Acaca*	NM_133360	ref|Mus musculus acetyl-Coenzyme A carboxylase alpha mRNA
13.64	-1.077	0	A_55_P2076772	*Hspa5*	NM_022310	ref|Mus musculus heat shock protein 5 transcript variant 2 mRNA

7.54	-1.073	0.00471	A_55_P2165554	*ENSMUST00000099046*	ENSMUST00000099046	Unknown
9.90	-1.071	0	A_51_P296036	*Nrbp2*	NM_144847	ref|Mus musculus nuclear receptor binding protein 2 mRNA
11.56	-1.068	0	A_51_P295192	*Nfkbia*	NM_010907	ref|Mus musculus nuclear factor of kappa light polypeptide gene enhancer in B-cells inhibitor alpha mRNA
7.52	-1.066	0	A_55_P2092864	*Emp2*	NM_007929	ref|Mus musculus epithelial membrane protein 2 mRNA
10.35	-1.064	0	A_66_P139387	*Prlr*	NM_011169	ref|Mus musculus prolactin receptor mRNA
10.97	-1.062	0	A_55_P1977314	*Ulk1*	NM_009469	ref|Mus musculus Unc-51 like kinase 1 (C. elegans) mRNA
14.93	-1.060	0	A_51_P205385	*Uox*	NM_009474	ref|Mus musculus urate oxidase mRNA
7.12	-1.058	0.00042	A_55_P2118630	*Lasp1*	NM_010688	ref|Mus musculus LIM and SH3 protein 1 mRNA
9.33	-1.055	0	A_55_P1976978	*Zfp707*	NM_001081065	ref|Mus musculus zinc finger protein 707 mRNA
7.95	-1.048	0	A_66_P136632	*1500003O03Rik*	NM_019769	ref|Mus musculus RIKEN cDNA 1500003O03 gene mRNA
9.39	-1.045	3.00E-05	A_51_P152845	*Trim24*	NM_145076	ref|Mus musculus tripartite motif-containing 24 mRNA
10.59	-1.035	0.00041	A_55_P2041723	*Mid1ip1*	NM_001166635	ref|Mus musculus Mid1 interacting protein 1 (gastrulation specific G12-like (zebrafish)) transcript variant 1 mRNA
8.78	-1.035	0.00977	A_51_P148612	*Cox7a1*	NM_009944	ref|Mus musculus cytochrome c oxidase subunit VIIa 1 mRNA
9.15	-1.035	0	A_66_P101519	*Abcc9*	NM_021041	ref|Mus musculus ATP-binding cassette sub-family C (CFTR/MRP) member 9 transcript variant 2 mRNA
7.21	-1.031	0.0073	A_55_P1978636	*ENSMUST00000099035*	ENSMUST00000099035	tc|Q4YHF0_PLABE (Q4YHF0) Pb-fam-2 protein (Fragment) partial (7%) [TC1642683]
9.03	-1.028	7.00E-05	A_55_P2014457	*LOC638627*	XM_914710	ref|PREDICTED: Mus musculus similar to EF-hand Ca2+ binding protein p22 mRNA
11.32	-1.024	0	A_55_P1992555	*Gys2*	NM_145572	ref|Mus musculus glycogen synthase 2 mRNA
14.26	-1.018	0.00332	A_52_P669922	*Hamp*	NM_032541	ref|Mus musculus hepcidin antimicrobial peptide mRNA
11.25	-1.013	2.00E-05	A_55_P2084706	*Acaca*	BC023946	gb|Mus musculus acetyl-Coenzyme A carboxylase alpha mRNA (cDNA clone IMAGE:5151139) with apparent retained intron
7.05	-1.013	0	A_55_P2124523	*Gm13620*	XM_988366	ref|PREDICTED: Mus musculus hypothetical LOC667106 mRNA
8.52	-1.009	0.00085	A_55_P1960735	*Gdf15*	NM_011819	ref|Mus musculus growth differentiation factor 15 mRNA
9.22	-1.006	0.00015	A_51_P418168	*Manf*	NM_029103	ref|Mus musculus mesencephalic astrocyte-derived neurotrophic factor mRNA
8.54	-1.002	0.00026	A_51_P280446	*Sdf2l1*	NM_022324	ref|Mus musculus stromal cell-derived factor 2-like 1 mRNA
8.41	-1.001	0.00867	A_55_P2138104	*ENSMUST00000099050*	ENSMUST00000099050	Unknown

Table 83. All significantly up regulated genes in livers of female C57BL/6 mice by PCB 153 (150000 µg/kg bw) identified by microarray analysis - mouse 3-day study. Selected parameters: A-value ≥ 7, log2 fc ≥ 1, p-value ≤ 0.05.

A	Log2 fc	p-value	Probe name	Gene name	Systematic name	Gene description
9.36	3.556	0	A_55_P2032946	*Gsta1*	NM_008181	ref|Mus musculus glutathione S-transferase alpha 1 (Ya) mRNA
12.00	3.336	0	A_55_P2116272	*Cyp2c38*	NM_010002	ref|Mus musculus cytochrome P450 family 2 subfamily c polypeptide 38 mRNA
10.80	2.690	0	A_55_P2102065	*Gm10639*	NM_001122660	ref|Mus musculus predicted gene 10639 mRNA
13.31	2.514	0	A_55_P2044653	*Cyp2b10*	NM_009999	ref|Mus musculus cytochrome P450 family 2 subfamily b polypeptide 10 transcript variant 2 mRNA
9.12	2.321	0	A_51_P311958	*Orm3*	NM_013623	ref|Mus musculus orosomucoid 3 mRNA
7.27	2.317	0	A_51_P331288	*Akr1b7*	NM_009731	ref|Mus musculus aldo-keto reductase family 1 member B7 mRNA
14.39	2.134	0	A_55_P2293013	*Ces6*	NM_133960	ref|Mus musculus carboxylesterase 6 mRNA
11.10	2.043	0	A_55_P2170454	*Gsta2*	NM_008182	ref|Mus musculus glutathione S-transferase alpha 2 (Yc2) mRNA
12.98	1.965	0	A_55_P2107528	*A_55_P2107528*	A_55_P2107528	Unknown
9.32	1.914	0	A_52_P154580	*Cyp2c54*	NM_206537	ref|Mus musculus cytochrome P450 family 2 subfamily c polypeptide 54 mRNA
13.80	1.884	0	A_55_P2005213	*Ces2*	NM_145603	ref|Mus musculus carboxylesterase 2 mRNA
12.76	1.846	0	A_55_P2102060	*Gstm3*	NM_010359	ref|Mus musculus glutathione S-transferase mu 3 mRNA
13.12	1.774	0.00021	A_51_P246317	*Mt2*	NM_008630	ref|Mus musculus metallothionein 2 mRNA
13.67	1.772	0	A_55_P1993419	*Cyp2c54*	NM_206537	ref|Mus musculus cytochrome P450 family 2 subfamily c polypeptide 54 mRNA
8.83	1.762	1.00E-05	A_55_P2069969	*Gm10639*	NM_001122660	ref|Mus musculus predicted gene 10639 mRNA
8.35	1.759	0	A_51_P421876	*Irf7*	NM_016850	ref|Mus musculus interferon regulatory factor 7 mRNA
7.87	1.722	7.00E-05	A_55_P1998471	*S100a9*	NM_009114	ref|Mus musculus S100 calcium binding protein A9 (calgranulin B) mRNA
7.65	1.712	0	A_66_P128537	*Isg15*	NM_015783	ref|Mus musculus ISG15 ubiquitin-like modifier mRNA
7.12	1.688	0	A_51_P327751	*Ifit1*	NM_008331	ref|Mus musculus interferon-induced protein with tetratricopeptide repeats 1 mRNA
14.11	1.665	0	A_55_P2020477	*Cyp2c50*	NM_134144	ref|Mus musculus cytochrome P450 family 2 subfamily c polypeptide 50 transcript variant 1 mRNA
7.02	1.659	5.00E-05	A_51_P487690	*Ifi44*	NM_133871	ref|Mus musculus interferon-induced protein 44 mRNA
8.99	1.591	0	A_52_P318361	*Ces2*	NM_145603	ref|Mus musculus carboxylesterase 2 mRNA
11.58	1.588	0	A_55_P2103698	*Isg15*	NM_015783	ref|Mus musculus ISG15 ubiquitin-like modifier mRNA
7.27	1.587	0	A_52_P382149	*Cyp26a1*	NM_007811	ref|Mus musculus cytochrome P450 family 26 subfamily a polypeptide 1 mRNA
12.58	1.582	0	A_55_P2065231	*Gstm3*	NM_010359	ref|Mus musculus glutathione S-transferase mu 3 mRNA
10.75	1.580	0	A_55_P2071906	*ENSMUST00000108392*	ENSMUST00000108392	ens|Cytochrome P-450b (phenobarbital-inducible) Fragment [Source:UniProtKB/TrEMBL;Acc:Q61461]
13.03	1.549	0	A_51_P498882	*Cyp2c37*	NM_010001	ref|Mus musculus cytochrome P450 family 2. subfamily c polypeptide 37 mRNA
10.64	1.546	0	A_55_P1964483	*Cyp2c37*	NM_010001	ref|Mus musculus cytochrome P450 family 2. subfamily c polypeptide 37 mRNA

9.85	1.539	0	A_55_P2124712	*Ces2*	NM_145603	ref|Mus musculus carboxylesterase 2 mRNA
8.56	1.526	0	A_55_P2059931	*Prom1*	NM_001163577	ref|Mus musculus prominin 1 transcript variant 2 mRNA
9.38	1.521	0	A_52_P627269	*BC015286*	NM_198171	ref|Mus musculus cDNA sequence BC015286 mRNA
15.09	1.517	0	A_55_P2062190	*Gstm1*	NM_010358	ref|Mus musculus glutathione S-transferase mu 1 mRNA
11.27	1.497	0.00037	A_55_P1999902	*ENSMUST00000107229*	ENSMUST00000107229	ens|Phosphatidylinositol-4-phosphate 5-kinase type-1 alpha (EC 2.7.1.68) (Phosphatidylinositol-4-phosphate 5-kinase type I alpha)(PtdIns(4)P-5-kinase alpha)(PIP5KIalpha)(Phosphatidylinositol-4-phosphate 5-kinase type I beta)(PI4P5KIbeta)(68 kDa type I phos
10.98	1.495	0	A_65_P02177	*Gstm4*	NM_026764	ref|Mus musculus glutathione S-transferase mu 4 transcript variant 1 mRNA
14.77	1.469	0	A_51_P103706	*Cyp2c29*	NM_007815	ref|Mus musculus cytochrome P450 family 2 subfamily c polypeptide 29 mRNA
14.59	1.466	0	A_51_P103706	*Cyp2c29*	NM_007815	ref|Mus musculus cytochrome P450 family 2 subfamily c polypeptide 29 mRNA
8.74	1.441	6.00E-05	A_55_P2085779	*Ifi27l2b*	NM_145449	ref|Mus musculus interferon alpha-inducible protein 27 like 2B mRNA
14.48	1.44	0	A_51_P103706	*Cyp2c29*	NM_007815	ref|Mus musculus cytochrome P450 family 2 subfamily c polypeptide 29 mRNA
14.77	1.437	0	A_51_P103706	*Cyp2c29*	NM_007815	ref|Mus musculus cytochrome P450 family 2 subfamily c polypeptide 29 mRNA
7.02	1.427	0	A_66_P139683	*Zbp1*	NM_021394	ref|Mus musculus Z-DNA binding protein 1 transcript variant 1 mRNA
14.57	1.424	0	A_51_P103706	*Cyp2c29*	NM_007815	ref|Mus musculus cytochrome P450 family 2 subfamily c polypeptide 29 mRNA
14.55	1.423	0	A_51_P103706	*Cyp2c29*	NM_007815	ref|Mus musculus cytochrome P450 family 2 subfamily c polypeptide 29 mRNA
7.74	1.419	0.00012	A_55_P2198983	*4930415C11Rik*	AI606402	gb|mr62b05.y1 Stratagene mouse testis (#937308) Mus musculus cDNA clone IMAGE:602001 5' similar to gb:J03952 Mouse glutathione transferase GT8.7 mRNA complete cds (MOUSE)
11.38	1.409	0	A_51_P304109	*Cyp2c39*	NM_010003	ref|Mus musculus cytochrome P450 family 2 subfamily c polypeptide 39 mRNA
14.79	1.406	0	A_51_P103706	*Cyp2c29*	NM_007815	ref|Mus musculus cytochrome P450 family 2 subfamily c polypeptide 29 mRNA
14.63	1.404	0	A_51_P103706	*Cyp2c29*	NM_007815	ref|Mus musculus cytochrome P450 family 2 subfamily c polypeptide 29 mRNA
12.82	1.401	0	A_55_P1966432	*Gstm1*	NM_010358	ref|Mus musculus glutathione S-transferase mu 1 mRNA
14.68	1.400	0	A_51_P103706	*Cyp2c29*	NM_007815	ref|Mus musculus cytochrome P450 family 2 subfamily c polypeptide 29 mRNA
7.43	1.395	0	A_51_P387123	*Oasl2*	NM_011854	ref|Mus musculus 2'-5' oligoadenylate synthetase-like 2 mRNA
8.51	1.392	0.00032	A_51_P265495	*Ly6a*	NM_010738	ref|Mus musculus lymphocyte antigen 6 complex locus A mRNA
14.8	1.388	0	A_51_P103706	*Cyp2c29*	NM_007815	ref|Mus musculus cytochrome P450 family 2 subfamily c polypeptide 29 mRNA
9.07	1.387	0	A_55_P2472435	*Gbp3*	NM_018734	ref|Mus musculus guanylate binding protein 3 mRNA
8.13	1.374	0	A_55_P2140042	*Krt31*	NM_010659	ref|Mus musculus keratin 31 mRNA
8.02	1.339	0	A_66_P101942	*Gm9706*	AK019325	gb|Mus musculus adult male hippocampus cDNA RIKEN full-length enriched library clone:2900034J12 product:interferon-stimulated protein (15 kDa) full insert sequence.
9.83	1.283	0	A_55_P1998943	*Oas1a*	NM_145211	ref|Mus musculus 2'-5' oligoadenylate synthetase 1A mRNA
7.22	1.266	0.00336	A_51_P343517	*Ly6d*	NM_010742	ref|Mus musculus lymphocyte antigen 6 complex locus D mRNA
14.96	1.252	0	A_55_P2121225	*Cyp3a11*	NM_007818	ref|Mus musculus cytochrome P450 family 3 subfamily a polypeptide 11 mRNA

8.33	1.217	0	A_51_P154842	*Oas1f*	NM_145153	ref|Mus musculus 2'-5' oligoadenylate synthetase 1F mRNA
7.24	1.216	0.00303	A_55_P2052385	*Mpa2l*	NM_194336	ref|Mus musculus macrophage activation 2 like mRNA
7.64	1.208	0.00038	A_55_P2039044	*Cyp3a59*	NM_001105160	ref|Mus musculus cytochrome P450 subfamily 3A polypeptide 59 mRNA
8.33	1.153	0	A_55_P1966833	*Xaf1*	NM_001037713	ref|Mus musculus XIAP associated factor 1 mRNA
7.03	1.148	0.00025	A_51_P219505	*Slc41a2*	NM_177388	ref|Mus musculus solute carrier family 41 member 2 mRNA
8.52	1.146	2.00E-04	A_55_P1960735	*Gdf15*	NM_011819	ref|Mus musculus growth differentiation factor 15 mRNA
8.84	1.139	0	A_51_P359570	*Ifit3*	NM_010501	ref|Mus musculus interferon-induced protein with tetratricopeptide repeats 3 mRNA
9.45	1.138	0	A_55_P2114953	*Usp18*	NM_011909	ref|Mus musculus ubiquitin specific peptidase 18 mRNA
11.96	1.129	0	A_51_P377856	*Gstt3*	NM_133994	ref|Mus musculus glutathione S-transferase theta 3 mRNA
10.23	1.124	0	A_52_P82765	*ENSMUST00000065861*	ENSMUST00000065861	ens|Testosterone 16a-hydroxylase type c Fragment [Source:UniProtKB/TrEMBL;Acc:Q61460]
8.54	1.122	2.00E-05	A_55_P1994042	*Zbp1*	NM_001139519	ref|Mus musculus Z-DNA binding protein 1 transcript variant 2 mRNA
11.20	1.118	0.00065	A_52_P90363	*Ifi27l2a*	NM_029803	ref|Mus musculus interferon alpha-inducible protein 27 like 2A mRNA
10.01	1.117	3.00E-05	A_55_P2070869	*Lcn2*	NM_008491	ref|Mus musculus lipocalin 2 mRNA
8.94	1.112	0.00041	A_51_P304170	*Rtp4*	NM_023386	ref|Mus musculus receptor transporter protein 4 mRNA
8.23	1.103	2.00E-05	A_55_P1962305	*Plac8*	NM_139198	ref|Mus musculus placenta-specific 8 mRNA
13.59	1.097	7.00E-05	A_51_P334942	*Aldh1a1*	NM_013467	ref|Mus musculus aldehyde dehydrogenase family 1 subfamily A1 mRNA
7.18	1.075	0.00412	A_51_P389885	*Spic*	NM_011461	ref|Mus musculus Spi-C transcription factor (Spi-1/PU.1 related) mRNA
10.68	1.069	0.00532	A_55_P2062246	*Tgtp2*	NM_001145164	ref|Mus musculus T-cell specific GTPase 2 mRNA
7.61	1.059	0.00785	A_55_P2078494	*Cib3*	NM_001080812	ref|Mus musculus calcium and integrin binding family member 3 mRNA
9.02	1.059	0	A_52_P267391	*Trim12*	NM_023835	ref|Mus musculus tripartite motif-containing 12 mRNA
9.58	1.058	1.00E-05	A_55_P2086433	*Oasl1*	NM_145209	ref|Mus musculus 2'-5' oligoadenylate synthetase-like 1 mRNA
11.37	1.056	0	A_55_P2158547	*Cyp2c54*	NM_206537	ref|Mus musculus cytochrome P450 family 2 subfamily c polypeptide 54 mRNA
7.99	1.050	0	A_55_P1998942	*Oas1a*	NM_145211	ref|Mus musculus 2'-5' oligoadenylate synthetase 1A mRNA
11.84	1.049	1.00E-05	A_55_P2031668	*Gstp1*	NM_013541	ref|Mus musculus glutathione S-transferase pi 1 mRNA
9.57	1.019	4.00E-05	A_52_P256914	*Cyp2b9*	NM_010000	ref|Mus musculus cytochrome P450 family 2 subfamily b polypeptide 9 mRNA
12.91	1.006	4.00E-05	A_55_P2008704	*Gstp2*	NM_181796	ref|Mus musculus glutathione S-transferase pi 2 mRNA
12.33	1.001	0.00034	A_51_P205779	*Cd5l*	NM_009690	ref|Mus musculus CD5 antigen-like mRNA

Table 84. All significantly down regulated genes in livers of female C57BL/6 mice by PCB 153 (150000 µg/kg bw) identified by microarray analysis - mouse 3-day study. Selected parameters: A-value ≥ 7, log2 fc ≤ -1, p-value ≤ 0.05.

A	Log2 fc	p-value	Probe name	Gene name	Systematic name	Gene description
7.91	-2.514	0.00259	A_55_P2040893	*Tnni2*	NM_009405	ref|Mus musculus troponin I skeletal fast 2 mRNA
10.70	-1.954	2.00E-05	A_55_P2038358	*Acot1*	NM_012006	ref|Mus musculus acyl-CoA thioesterase 1 mRNA
7.47	-1.832	3.00E-05	A_51_P350453	*Pdk4*	NM_013743	ref|Mus musculus pyruvate dehydrogenase kinase isoenzyme 4 mRNA
12.9	-1.666	5.00E-05	A_51_P238576	*Cyp4a14*	NM_007822	ref|Mus musculus cytochrome P450 family 4 subfamily a polypeptide 14 mRNA
7.09	-1.559	0.00714	A_55_P2187043	*Tpm1*	NM_001164248	ref|Mus musculus tropomyosin 1 alpha transcript variant 1 mRNA
9.34	-1.489	5.00E-05	A_55_P2162970	*Gm3734*	XM_001476671	ref|PREDICTED: Mus musculus hypothetical protein LOC100046708 mRNA
8.78	-1.432	0.00057	A_51_P148612	*Cox7a1*	NM_009944	ref|Mus musculus cytochrome c oxidase subunit VIIa 1 mRNA
7.74	-1.431	0.00038	A_55_P2116973	*Neb*	NM_010889	ref|Mus musculus nebulin mRNA
8.42	-1.368	0.00801	A_55_P1977533	*Eno3*	NM_001136062	ref|Mus musculus enolase 3 beta muscle transcript variant 2 mRNA
8.92	-1.291	0.00035	A_55_P2055638	*ENSMUST00000113016*	ENSMUST00000113016	ens|Gelsolin Precursor (Actin-depolymerizing factor)(ADF)(Brevin) [Source:UniProtKB/Swiss-Prot;Acc:P13020]
9.71	-1.291	0.00027	A_55_P2013948	*Gsn*	NM_146120	ref|Mus musculus gelsolin mRNA
8.58	-1.247	0.00221	A_55_P2024625	*Ccl21a*	NM_011124	ref|Mus musculus chemokine (C-C motif) ligand 21A mRNA
7.06	-1.222	0.00147	A_55_P2037141	*Jsrp1*	NM_028001	ref|Mus musculus junctional sarcoplasmic reticulum protein 1 mRNA
12.64	-1.214	0.00037	A_51_P254895	*Cyp4a10*	NM_010011	ref|Mus musculus cytochrome P450 family 4 subfamily a polypeptide 10 mRNA
12.75	-1.191	0.00054	A_55_P2011111	*Cyp4a10*	NM_010011	ref|Mus musculus cytochrome P450 family 4 subfamily a polypeptide 10 mRNA
12.27	-1.152	8.00E-04	A_55_P2050628	*Cyp4a31*	NM_201640	ref|Mus musculus cytochrome P450 family 4 subfamily a polypeptide 31 mRNA
8.44	-1.131	0.00346	A_55_P2038362	*Acot5*	NM_145444	ref|Mus musculus acyl-CoA thioesterase 5 mRNA
7.06	-1.125	0.00077	A_55_P2183433	*Rab30*	NM_029494	ref|Mus musculus RAB30 member RAS oncogene family mRNA
8.76	-1.109	0.00722	A_51_P497100	*Lgals4*	NM_010706	ref|Mus musculus lectin galactose binding soluble 4 mRNA
8.66	-1.097	0.00572	A_55_P2063256	*Lgals4*	NM_010706	ref|Mus musculus lectin galactose binding soluble 4 mRNA
7.95	-1.038	0.00282	A_55_P2024033	*Cyp4a31*	NM_201640	ref|Mus musculus cytochrome P450 family 4 subfamily a polypeptide 31 mRNA
7.00	-1.019	0.00158	A_55_P2022211	*Plxdc2*	NM_026162	ref|Mus musculus plexin domain containing 2 mRNA
8.34	-1.011	0.0065	A_51_P501844	*Cyp26b1*	NM_175475	ref|Mus musculus cytochrome P450 family 26 subfamily b polypeptide 1 mRNA
12.41	-1.001	0.00207	A_51_P269404	*Fmo3*	NM_008030	ref|Mus musculus flavin containing monooxygenase 3 mRNA

Table 85. All significantly up regulated genes in livers of female *Ahr* wild-type mice by TCDD (25 µg/kg bw) identified by microarray analysis - mouse 5 days study. Selected parameters: A-value ≥ 7, log2 fc ≥ 1, p-value ≤ 0.05.

A	Log2 fc	p-value	Probe name	Gene name	Systemtatic name	Gene description
8.29	9.106	0	A_51_P279693	*Cyp1a1*	NM_009992	ref|Mus musculus cytochrome P450 family 1 subfamily a polypeptide 1 transcript variant 1 mRNA
9.46	5.995	0	A_51_P255456	*Cyp1b1*	NM_009994	ref|Mus musculus cytochrome P450 family 1 subfamily b polypeptide 1 mRNA
9.86	5.375	0	A_52_P595871	*Cyp1a2*	NM_009993	ref|Mus musculus cytochrome P450 family 1 subfamily a polypeptide 2 mRNA
8.83	4.386	0	A_66_P119518	*Tuba8*	NM_017379	ref|Mus musculus tubulin alpha 8 mRNA
11.78	3.983	0	A_55_P2032946	*Gsta1*	NM_008181	ref|Mus musculus glutathione S-transferase alpha 1 (Ya) mRNA
8.14	3.895	0	A_55_P2119257	*Serpine1*	NM_008871	ref|Mus musculus serine (or cysteine) peptidase inhibitor clade E member 1 mRNA
8.43	3.728	0	A_55_P2004099	*Gm9933*	XM_001477458	ref|PREDICTED: Mus musculus predicted gene ENSMUSG00000054044 mRNA
8.63	3.657	0	A_51_P459108	*Insl6*	NM_013754	ref|Mus musculus insulin-like 6 mRNA
9.35	3.389	0	A_55_P1985890	*Tiparp*	NM_178892	ref|Mus musculus TCDD-inducible poly(ADP-ribose) polymerase mRNA
9.59	3.300	0	A_55_P2032714	*Fhit*	NM_010210	ref|Mus musculus fragile histidine triad gene mRNA
9.90	3.263	0	A_51_P514961	*Tiparp*	NM_178892	ref|Mus musculus TCDD-inducible poly(ADP-ribose) polymerase mRNA
9.16	3.179	0	A_51_P508959	*Prr15*	NM_030024	ref|Mus musculus proline rich 15 mRNA
10.22	3.172	0	A_55_P2178800	*Ugt1a10*	NM_201641	ref|Mus musculus UDP glycosyltransferase 1 family polypeptide A10 mRNA
9.02	3.156	0	A_55_P2059586	*Fmo3*	NM_008030	ref|Mus musculus flavin containing monooxygenase 3 mRNA
10.55	2.965	0	A_51_P269404	*Fmo3*	NM_008030	ref|Mus musculus flavin containing monooxygenase 3 mRNA
10.21	2.797	0	A_66_P108247	*Ucp3*	NM_009464	ref|Mus musculus uncoupling protein 3 (mitochondrial proton carrier) nuclear gene encoding mitochondrial protein mRNA
12.65	2.720	0	A_55_P2031668	*Gstp1*	NM_013541	ref|Mus musculus glutathione S-transferase pi 1 mRNA
10.33	2.700	0	A_55_P1983754	*Pcp4l1*	NM_025557	ref|Mus musculus Purkinje cell protein 4-like 1 mRNA
8.41	2.689	0	A_51_P471458	*Sult5a1*	NM_020564	ref|Mus musculus sulfotransferase family 5A member 1 mRNA
10.07	2.651	0.00129	A_55_P1994807	*Saa2*	NM_011314	ref|Mus musculus serum amyloid A 2 mRNA
10.48	2.651	0	A_51_P297105	*Ucp2*	NM_011671	ref|Mus musculus uncoupling protein 2 (mitochondrial proton carrier) nuclear gene encoding mitochondrial protein mRNA
9.23	2.648	0	A_52_P183524	*Tmem86b*	NM_023440	ref|Mus musculus transmembrane protein 86B mRNA
13.99	2.638	0	A_55_P2008704	*Gstp2*	NM_181796	ref|Mus musculus glutathione S-transferase pi 2 mRNA
8.07	2.611	0	A_55_P1972719	*Pmm1*	NM_013872	ref|Mus musculus phosphomannomutase 1 mRNA
14.51	2.599	0	A_55_P2102065	*Gm10639*	NM_001122660	ref|Mus musculus predicted gene 10639 mRNA
10.22	2.593	4.00E-05	A_51_P343350	*Amn*	NM_033603	ref|Mus musculus amnionless mRNA
13.45	2.505	0	A_51_P374464	*Gstp1*	NM_013541	ref|Mus musculus glutathione S-transferase pi 1 mRNA

10.22	2.504	1.00E-05	A_55_P2070869	*Lcn2*	NM_008491	ref|Mus musculus lipocalin 2 mRNA
11.40	2.497	0	A_51_P502872	*2200002D01Rik*	NM_028179	ref|Mus musculus RIKEN cDNA 2200002D01 gene mRNA
11.42	2.418	0	A_55_P1972720	*Pmm1*	NM_013872	ref|Mus musculus phosphomannomutase 1 mRNA
10.35	2.417	1.00E-05	A_52_P318673	*Saa1*	NM_009117	ref|Mus musculus serum amyloid A 1 mRNA
11.76	2.409	0	A_55_P2059931	*Prom1*	NM_001163577	ref|Mus musculus prominin 1 transcript variant 2 mRNA
11.58	2.366	0	A_51_P299805	*Slc46a3*	NM_027872	ref|Mus musculus solute carrier family 46 member 3 mRNA
8.15	2.338	3.00E-05	A_52_P608322	*Maff*	NM_010755	ref|Mus musculus v-maf musculoaponeurotic fibrosarcoma oncogene family protein F (avian) mRNA
11.61	2.315	0	A_55_P2060107	*Pkm2*	NM_011099	ref|Mus musculus pyruvate kinase muscle mRNA
8.57	2.310	0	A_51_P363947	*Cdkn1a*	NM_007669	ref|Mus musculus cyclin-dependent kinase inhibitor 1A (P21) transcript variant 1 mRNA
12.07	2.280	0	A_52_P627269	*BC015286*	NM_198171	ref|Mus musculus cDNA sequence BC015286 mRNA
10.43	2.269	0	A_55_P1962771	*Cyfip2*	NM_133769	ref|Mus musculus cytoplasmic FMR1 interacting protein 2 mRNA
15.19	2.249	2.00E-05	A_55_P1957038	*Gstp2*	NM_181796	ref|Mus musculus glutathione S-transferase pi 2 mRNA
10.57	2.219	0	A_52_P515036	*Htatip2*	NM_016865	ref|Mus musculus HIV-1 tat interactive protein 2 homolog (human) transcript variant 1 mRNA
9.42	2.216	0	A_55_P2080151	*Hspa2*	NM_008301	ref|Mus musculus heat shock protein 2 transcript variant 1 mRNA
12.62	2.215	0	A_55_P2124712	*Ces2*	NM_145603	ref|Mus musculus carboxylesterase 2 mRNA
13.44	2.156	0	A_51_P255682	*Mfge8*	NM_008594	ref|Mus musculus milk fat globule-EGF factor 8 protein transcript variant 1 mRNA
13.67	2.155	0	A_55_P2038358	*Acot1*	NM_012006	ref|Mus musculus acyl-CoA thioesterase 1 mRNA
10.26	2.138	0	A_55_P2157627	*NAP000319-003*	NAP000319-003	Unknown
8.55	2.129	0	A_51_P363947	*Cdkn1a*	NM_007669	ref|Mus musculus cyclin-dependent kinase inhibitor 1A (P21) transcript variant 1 mRNA
11.6	2.127	1.00E-05	A_52_P318361	*Ces2*	NM_145603	ref|Mus musculus carboxylesterase 2 mRNA
11.67	2.092	0	A_55_P2047768	*Serpinb6c*	NM_148942	ref|Mus musculus serine (or cysteine) peptidase inhibitor clade B member 6c mRNA
8.42	2.091	0	A_51_P363947	*Cdkn1a*	NM_007669	ref|Mus musculus cyclin-dependent kinase inhibitor 1A (P21) transcript variant 1 mRNA
12.45	2.088	0	A_55_P2068812	*AK203298*	AK203298	gb|Mus musculus cDNA clone:Y1G0144G24 strand:minus reference:ENSEMBL:Mouse-Transcript-ENST: ENSMUST00000061523 based on BLAT search.
8.22	2.077	1.00E-05	A_55_P2118520	*Col1a1*	NM_007742	ref|Mus musculus collagen type I alpha 1 mRNA
9.60	2.075	0	A_55_P2069907	*Acot3*	NM_134246	ref|Mus musculus acyl-CoA thioesterase 3 mRNA
8.45	2.054	2.00E-05	A_51_P363947	*Cdkn1a*	NM_007669	ref|Mus musculus cyclin-dependent kinase inhibitor 1A (P21) transcript variant 1 mRNA
8.21	2.048	0	A_51_P363947	*Cdkn1a*	NM_007669	ref|Mus musculus cyclin-dependent kinase inhibitor 1A (P21) transcript variant 1 mRNA
8.60	2.043	2.00E-05	A_51_P363947	*Cdkn1a*	NM_007669	ref|Mus musculus cyclin-dependent kinase inhibitor 1A (P21) transcript variant 1 mRNA
10.17	1.986	0	A_52_P87964	*Pla2g12a*	NM_183423	ref|Mus musculus phospholipase A2 group XIIA transcript variant 2 mRNA
12.26	1.985	0	A_51_P455647	*Car2*	NM_009801	ref|Mus musculus carbonic anhydrase 2 mRNA
8.66	1.967	1.00E-05	A_51_P363947	*Cdkn1a*	NM_007669	ref|Mus musculus cyclin-dependent kinase inhibitor 1A (P21) transcript variant 1 mRNA

12.24	1.964	0	A_55_P2066727	*Serpinb6a*	NM_001164118	ref|Mus musculus serine (or cysteine) peptidase inhibitor clade B member 6a transcript variant 3 mRNA
9.56	1.941	0	A_55_P1984675	*Abhd6*	NM_025341	ref|Mus musculus abhydrolase domain containing 6 mRNA
9.70	1.939	0	A_55_P2157307	*NAP113386-1*	NAP113386-1	Unknown
9.57	1.926	0	A_51_P357561	*Fbxw9*	NM_026791	ref|Mus musculus F-box and WD-40 domain protein 9 mRNA
9.23	1.913	0	A_55_P2095035	*Gm1833*	XM_129965	ref|PREDICTED: Mus musculus gene model 1833 (NCBI) mRNA
8.37	1.899	4.00E-05	A_51_P363947	*Cdkn1a*	NM_007669	ref|Mus musculus cyclin-dependent kinase inhibitor 1A (P21) transcript variant 1 mRNA
10.30	1.897	0	A_55_P2013038	*Serpinb6c*	NM_148942	ref|Mus musculus serine (or cysteine) peptidase inhibitor clade B member 6c mRNA
9.37	1.887	0	A_51_P316951	*Wipf3*	NM_001167860	ref|Mus musculus WAS/WASL interacting protein family member 3 transcript variant 1 mRNA
9.01	1.885	0	A_51_P271503	*Il1r1*	NM_008362	ref|Mus musculus interleukin 1 receptor type I transcript variant 1 mRNA [NM_008362]
9.59	1.879	1.00E-05	A_55_P2038362	*Acot5*	NM_145444	ref|Mus musculus acyl-CoA thioesterase 5 (mRNA
9.04	1.872	6.00E-05	A_52_P590154	*Hsd17b6*	NM_013786	ref|Mus musculus hydroxysteroid (17-beta) dehydrogenase 6mRNA
8.49	1.871	1.00E-05	A_51_P363947	*Cdkn1a*	NM_007669	ref|Mus musculus cyclin-dependent kinase inhibitor 1A (P21) transcript variant 1 mRNA
9.77	1.869	0	A_55_P2029366	*Abhd6*	NM_025341	ref|Mus musculus abhydrolase domain containing 6 mRNA
10.38	1.868	1.00E-04	A_55_P2178036	*Serpina6*	NM_007618	ref|Mus musculus serine (or cysteine) peptidase inhibitor clade A member 6 mRNA
7.67	1.867	0	A_51_P286737	*Ccl2*	NM_011333	ref|Mus musculus chemokine (C-C motif) ligand 2 mRNA
10.05	1.867	0	A_55_P2141884	*Tagln2*	NM_178598	ref|Mus musculus transgelin 2 mRNA
8.57	1.857	0	A_51_P363947	*Cdkn1a*	NM_007669	ref|Mus musculus cyclin-dependent kinase inhibitor 1A (P21) transcript variant 1 mRNA
8.32	1.817	0.00014	A_52_P525183	*Acot2*	NM_134188	ref|Mus musculus acyl-CoA thioesterase 2 nuclear gene encoding mitochondrial protein mRNA
12.37	1.815	0	A_55_P2077628	*ENSMUST00000106148*	ENSMUST00000106148	ens|L-xylulose reductase (XR)(EC 1.1.1.10)(Dicarbonyl/L-xylulose reductase) [Source:UniProtKB/Swiss-Prot;Acc: Q91X52]
7.95	1.810	7.00E-05	A_55_P1985433	*Nrg1*	NM_178591	ref|Mus musculus neuregulin 1 (Nrg1) mRNA
7.53	1.806	3.00E-05	A_51_P286737	*Ccl2*	NM_011333	ref|Mus musculus chemokine (C-C motif) ligand 2 mRNA
10.40	1.791	3.00E-05	A_51_P424338	*Nqo1*	NM_008706	ref|Mus musculus NAD(P)H dehydrogenase quinone 1 mRNA
8.96	1.779	1.00E-05	A_52_P1197913	*Gadd45b*	NM_008655	ref|Mus musculus growth arrest and DNA-damage-inducible 45 beta mRNA
10.88	1.776	7.00E-05	A_55_P2051596	*Gm4499*	XM_001479558	ref|PREDICTED: Mus musculus similar to pol protein mRNA
8.01	1.773	0	A_51_P209736	*Atoh8*	NM_153778	ref|Mus musculus atonal homolog 8 (Drosophila) mRNA
7.09	1.771	9.00E-05	A_65_P01247	*Hjurp*	NM_198652	ref|Mus musculus Holliday junction recognition protein mRNA
9.48	1.757	2.00E-05	A_55_P2143765	*Ugt1a6a*	NM_145079	ref|Mus musculus UDP glucuronosyltransferase 1 family polypeptide A6A mRNA
7.51	1.738	2.00E-05	A_51_P286737	*Ccl2*	NM_011333	ref|Mus musculus chemokine (C-C motif) ligand 2 mRNA
7.60	1.723	0	A_51_P291501	*Ccno*	NM_001081062	ref|Mus musculus cyclin O mRNA
9.00	1.716	0.00059	A_52_P675395	*Cxcr7*	NM_007722	ref|Mus musculus chemokine (C-X-C motif) receptor 7 mRNA
7.62	1.713	1.00E-05	A_51_P286737	*Ccl2*	NM_011333	ref|Mus musculus chemokine (C-C motif) ligand 2 mRNA

14.07	1.712	0	A_55_P1973352	*XM_001476722*	XM_001476722	ref|PREDICTED: Mus musculus hypothetical protein LOC100041156 mRNA
11.70	1.710	9.00E-05	A_55_P1998811	*Gm3430*	XM_001476688	ref|PREDICTED: Mus musculus similar to pol protein mRNA
13.76	1.706	4.00E-04	A_51_P315904	*Gadd45g*	NM_011817	ref|Mus musculus growth arrest and DNA-damage-inducible 45 gamma mRNA
7.20	1.697	0	A_51_P286737	*Ccl2*	NM_011333	ref|Mus musculus chemokine (C-C motif) ligand 2 mRNA
11.64	1.692	0	A_55_P2171116	*Lgals3*	NM_001145953	ref|Mus musculus lectin galactose binding soluble 3 transcript variant 1 mRNA
12.75	1.690	4.00E-05	A_51_P265495	*Ly6a*	NM_010738	ref|Mus musculus lymphocyte antigen 6 complex locus A mRNA
8.91	1.682	1.00E-05	A_55_P2164075	*LOC100048172*	XM_001479672	ref|PREDICTED: Mus musculus hypothetical protein LOC100048172 mRNA
11.69	1.676	0.00079	A_55_P2108151	*ENSMUST00000023934*	ENSMUST00000023934	ens|Hemoglobin subunit beta-1 (Hemoglobin beta-1 chain)(Beta-1-globin)(Hemoglobin beta-major chain) [Source:UniProtKB/Swiss-Prot;Acc:P02088]
8.32	1.657	0	A_55_P2040860	*Sunc1*	NM_177576	ref|Mus musculus Sad1 and UNC84 domain containing 1 mRNA
9.60	1.649	2.00E-05	A_51_P450278	*2010003K11Rik*	NM_027237	ref|Mus musculus RIKEN cDNA 2010003K11 gene mRNA
7.52	1.648	5.00E-05	A_51_P286737	*Ccl2*	NM_011333	ref|Mus musculus chemokine (C-C motif) ligand 2 mRNA
8.01	1.642	2.00E-05	A_51_P163578	*Ugt2b35*	NM_172881	ref|Mus musculus UDP glucuronosyltransferase 2 family polypeptide B35 mRNA
13.29	1.640	1.00E-05	A_51_P181319	*Dcxr*	NM_026428	ref|Mus musculus dicarbonyl L-xylulose reductase mRNA
11.04	1.636	1.00E-05	A_51_P509669	*Uap1l1*	NM_001033293	ref|Mus musculus UDP-N-acteylglucosamine pyrophosphorylase 1-like 1 mRNA
7.55	1.635	0.00017	A_51_P286737	*Ccl2*	NM_011333	ref|Mus musculus chemokine (C-C motif) ligand 2 mRNA
13.43	1.629	1.00E-04	A_51_P329441	*Bsg*	NM_009768	ref|Mus musculus basigin transcript variant 1 mRNA
8.67	1.628	1.00E-05	A_51_P286488	*Ier3*	NM_133662	ref|Mus musculus immediate early response 3 mRNA
7.91	1.590	0.00117	A_55_P2334424	*D630024D03Rik*	AK158188	gb|Mus musculus adult inner ear cDNA RIKEN full-length enriched library clone:F930039G01 product: unclassifiable full insert sequence
9.90	1.584	5.00E-05	A_51_P124254	*Col4a1*	NM_009931	ref|Mus musculus collagen type IV alpha 1 mRNA
12.06	1.570	0	A_51_P411271	*Nfe2l2*	NM_010902	ref|Mus musculus nuclear factor erythroid derived 2 like 2 mRNA
10.98	1.567	0	A_51_P378622	*0610012H03Rik*	NM_028747	ref|Mus musculus RIKEN cDNA 0610012H03 gene transcript variant 1 mRNA
15.63	1.559	2.00E-05	A_55_P1961014	*Selenbp1*	NM_009150	ref|Mus musculus selenium binding protein 1 mRNA
10.73	1.544	0	A_51_P441914	*Hsd17b2*	NM_008290	ref|Mus musculus hydroxysteroid (17-beta) dehydrogenase 2mRNA
7.67	1.543	6.00E-05	A_51_P286737	*Ccl2*	NM_011333	ref|Mus musculus chemokine (C-C motif) ligand 2mRNA
7.14	1.526	4.00E-05	A_55_P1985304	*Krtap5-3*	NM_023860	ref|Mus musculus keratin associated protein 5-3 mRNA
9.85	1.518	4.00E-05	A_51_P124254	*Col4a1*	NM_009931	ref|Mus musculus collagen type IV alpha 1 mRNA
7.53	1.518	0.00047	A_51_P286737	*Ccl2*	NM_011333	ref|Mus musculus chemokine (C-C motif) ligand 2 mRNA
10.60	1.515	5.00E-05	A_51_P419637	*Dclk3*	NM_172928	ref|Mus musculus doublecortin-like kinase 3 mRNA
12.45	1.512	0	A_55_P1952399	*Cyp4a31*	NM_201640	ref|Mus musculus cytochrome P450 family 4 subfamily a polypeptide 31 mRNA
9.97	1.509	0	A_55_P2110512	*Lmo7*	NM_201529	ref|Mus musculus LIM domain only 7 mRNA

11.31	1.507	3.00E-05	A_55_P2024033	*Cyp4a31*	NM_201640	ref|Mus musculus cytochrome P450 family 4 subfamily a polypeptide 31 mRNA
9.84	1.505	4.00E-05	A_51_P287198	*Krt23*	NM_033373	ref|Mus musculus keratin 23 mRNA
9.78	1.504	0.00078	A_51_P515605	*Col3a1*	NM_009930	ref|Mus musculus collagen type III alpha 1 mRNA
12.76	1.495	1.00E-05	A_55_P2065231	*Gstm3*	NM_010359	ref|Mus musculus glutathione S-transferase mu 3 mRNA
10.27	1.491	0	A_55_P2219059	*Lmnb2*	NM_010722	ref|Mus musculus lamin B2 mRNA
8.71	1.486	2.00E-05	A_55_P2140941	*Tinagl1*	NM_023476	ref|Mus musculus tubulointerstitial nephritis antigen-like 1 transcript variant 1 mRNA
14.47	1.483	0.00014	A_55_P1966432	*Gstm1*	NM_010358	ref|Mus musculus glutathione S-transferase mu 1 mRNA
8.64	1.482	5.00E-05	A_52_P487436	*Nags*	NM_145829	ref|Mus musculus N-acetylglutamate synthase transcript variant 1 mRNA
8.04	1.474	0.00038	A_52_P402786	*Prom1*	NM_008935	ref|Mus musculus prominin 1 transcript variant 1 mRNA
11.33	1.467	0	A_55_P2038347	*Acot3*	NM_134246	ref|Mus musculus acyl-CoA thioesterase 3 mRNA
7.30	1.463	1.00E-04	A_55_P1967196	*Lamb3*	NM_008484	ref|Mus musculus laminin beta 3 mRNA
8.92	1.463	4.00E-05	A_51_P387123	*Oasl2*	NM_011854	ref|Mus musculus 2'-5' oligoadenylate synthetase-like 2 mRNA
7.24	1.462	0.00035	A_55_P2051796	*Gm128*	NM_001024841	ref|Mus musculus predicted gene 128 mRNA
8.98	1.459	1.00E-04	A_55_P2037121	*Tmem106a*	NM_144830	ref|Mus musculus transmembrane protein 106A mRNA
13.24	1.456	0	A_55_P2006236	*Ugdh*	NM_009466	ref|Mus musculus UDP-glucose dehydrogenase mRNA
8.63	1.455	1.00E-05	A_55_P1988368	*Upp1*	NM_009477	ref|Mus musculus uridine phosphorylase 1 transcript variant 1 mRNA
8.82	1.442	0.00044	A_52_P2710	*Cml5*	NM_023493	ref|Mus musculus camello-like 5 mRNA
7.90	1.441	0.00015	A_52_P552665	*Fzd7*	NM_008057	ref|Mus musculus frizzled homolog 7 (Drosophila) mRNA
9.32	1.439	0.00011	A_51_P124254	*Col4a1*	NM_009931	ref|Mus musculus collagen type IV alpha 1 mRNA
7.71	1.437	3.00E-05	A_51_P286737	*Ccl2*	NM_011333	ref|Mus musculus chemokine (C-C motif) ligand 2 mRNA
9.46	1.436	0.00017	A_51_P124254	*Col4a1*	NM_009931	ref|Mus musculus collagen type IV alpha 1 mRNA
16.21	1.435	1.00E-05	A_55_P1962404	*Ugt1a6a*	NM_145079	ref|Mus musculus UDP glucuronosyltransferase 1 family polypeptide A6A mRNA
7.68	1.412	0.00012	A_51_P390715	*Tgfb1*	NM_011577	ref|Mus musculus transforming growth factor beta 1 mRNA
9.06	1.403	0.00024	A_66_P121583	*Gm7120*	NM_001039244	ref|Mus musculus predicted gene 7120 mRNA
11.33	1.398	0	A_51_P215922	*Casp6*	NM_009811	ref|Mus musculus caspase 6 mRNA
10.21	1.392	1.00E-04	A_52_P151320	*Tnfaip8l1*	NM_025566	ref|Mus musculus tumor necrosis factor alpha-induced protein 8-like 1 mRNA
9.83	1.386	0.00029	A_51_P124254	*Col4a1*	NM_009931	ref|Mus musculus collagen type IV alpha 1 mRNA
10.24	1.385	2.00E-05	A_55_P2107785	*Gm13105*	XM_001475876	ref|PREDICTED: Mus musculus similar to pol protein mRNA
8.18	1.384	1.00E-05	A_52_P452166	*Grpel2*	NM_021296	ref|Mus musculus GrpE-like 2 mitochondrial nuclear gene encoding mitochondrial protein mRNA
10.75	1.384	6.00E-05	A_55_P2110513	*Lmo7*	NM_201529	ref|Mus musculus LIM domain only 7 mRNA
9.59	1.381	4.00E-05	A_51_P137336	*Cdh1*	NM_009864	ref|Mus musculus cadherin 1 mRNA
9.90	1.381	0.00011	A_51_P124254	*Col4a1*	NM_009931	ref|Mus musculus collagen type IV alpha 1 mRNA

7.60	1.380	4.00E-05	A_55_P1967350	*Ugt2b35*	NM_172881	ref|Mus musculus UDP glucuronosyltransferase 2 family polypeptide B35 mRNA
11.29	1.380	6.00E-05	A_55_P2114318	*Gm4080*	XM_001478955	ref|PREDICTED: Mus musculus similar to pol protein mRNA
13.81	1.374	2.00E-05	A_55_P2092030	*Cyp4a10*	NM_010011	ref|Mus musculus cytochrome P450 family 4 subfamily a polypeptide 10 mRNA
8.67	1.368	3.00E-05	A_51_P392967	*Zmynd10*	NM_053253	ref|Mus musculus zinc finger MYND domain containing 10 mRNA
7.95	1.364	0.00016	A_52_P78373	*Sorbs3*	NM_011366	ref|Mus musculus sorbin and SH3 domain containing 3 mRNA
8.23	1.360	3.00E-05	A_52_P322941	*Gm11992*	NM_001037928	ref|Mus musculus predicted gene 11992 mRNA
7.90	1.359	0.00057	A_51_P146560	*Msln*	NM_018857	ref|Mus musculus mesothelin mRNA
8.21	1.358	3.00E-05	A_55_P2130627	*2210404O07Rik*	NM_001099917	ref|Mus musculus RIKEN cDNA 2210404O07 gene mRNA
9.41	1.351	1.00E-04	A_51_P124254	*Col4a1*	NM_009931	ref|Mus musculus collagen type IV alpha 1 mRNA
10.01	1.347	4.00E-05	A_51_P491350	*Col4a2*	NM_009932	ref|Mus musculus collagen type IV alpha 2 mRNA
10.82	1.346	3.00E-05	A_51_P165060	*Slc22a5*	NM_011396	ref|Mus musculus solute carrier family 22 (organic cation transporter) member 5 mRNA
9.66	1.341	0.00043	A_51_P124254	*Col4a1*	NM_009931	ref|Mus musculus collagen type IV alpha 1 mRNA
9.51	1.340	8.00E-05	A_51_P124254	*Col4a1*	NM_009931	ref|Mus musculus collagen type IV alpha 1 mRNA
9.21	1.330	1.00E-05	A_55_P2114953	*Usp18*	NM_011909	ref|Mus musculus ubiquitin specific peptidase 18 mRNA
7.97	1.325	0.0016	A_51_P390715	*Tgfb1*	NM_011577	ref|Mus musculus transforming growth factor beta 1 mRNA
9.46	1.322	0.00096	A_51_P371750	*Marco*	NM_010766	ref|Mus musculus macrophage receptor with collagenous structure mRNA
11.08	1.318	1.00E-05	A_55_P2063312	*Mgll*	NM_001166250	ref|Mus musculus monoglyceride lipase transcript variant 4 mRNA
8.33	1.317	3.00E-04	A_55_P2183914	*Gm7120*	NM_001039244	ref|Mus musculus predicted gene 7120 mRNA
7.84	1.303	0.00074	A_51_P390715	*Tgfb1*	NM_011577	ref|Mus musculus transforming growth factor beta 1 mRNA
9.76	1.299	3.00E-05	A_51_P137336	*Cdh1*	NM_009864	ref|Mus musculus cadherin 1 mRNA
11.99	1.297	1.00E-05	A_55_P1971962	*Tmem176b*	NM_023056	ref|Mus musculus transmembrane protein 176B transcript variant 1 mRNA
7.42	1.295	0.00131	A_52_P354373	*1190002F15Rik*	XM_001481164	ref|PREDICTED: Mus musculus RIKEN cDNA 1190002F15 gene mRNA
8.72	1.292	5.00E-05	A_52_P44030	*Exoc3*	NM_177333	ref|Mus musculus exocyst complex component 3 mRNA
8.35	1.29	0.00059	A_51_P322273	*Ptp4a3*	NM_008975	ref|Mus musculus protein tyrosine phosphatase 4a3 transcript variant 2 mRNA
7.58	1.286	0.00018	A_51_P155755	*Pld6*	NM_183139	ref|Mus musculus phospholipase D family member 6 mRNA
10.40	1.282	0.00029	A_55_P1966438	*Gstm2*	NM_008183	ref|Mus musculus glutathione S-transferase mu 2 mRNA
14.04	1.281	2.00E-05	A_51_P319070	*Retsat*	NM_026159	ref|Mus musculus retinol saturase (all trans retinol 1314 reductase) mRNA
9.45	1.279	0.00019	A_55_P2016462	*Cxcl10*	NM_021274	ref|Mus musculus chemokine (C-X-C motif) ligand 10 mRNA
9.36	1.279	6.00E-04	A_55_P2142527	*Gm13770*	XM_884324	ref|PREDICTED: Mus musculus similar to CGI-140 protein mRNA
8.14	1.278	0.00011	A_51_P320304	*Plod1*	NM_011122	ref|Mus musculus procollagen-lysine 2-oxoglutarate 5-dioxygenase 1 mRNA
11.54	1.275	1.00E-05	A_55_P1954718	*Cyb561*	NM_007805	ref|Mus musculus cytochrome b-561 mRNA
10.94	1.275	0.00016	A_55_P2007495	*Gm2034*	XM_001472204	ref|PREDICTED: Mus musculus similar to pol protein mRNA

7.81	1.268	0.00071	A_52_P283524	*Rcan3*	NM_022980	ref|Mus musculus regulator of calcineurin 3 mRNA
9.67	1.266	0.00101	A_51_P341108	*Spint1*	NM_016907	ref|Mus musculus serine protease inhibitor Kunitz type 1 mRNA
8.46	1.266	1.00E-05	A_51_P478952	*N4bp2l1*	NM_133898	ref|Mus musculus NEDD4 binding protein 2-like 1 mRNA
11.63	1.265	7.00E-05	A_55_P2009861	*Gm2015*	XM_001472138	ref|PREDICTED: Mus musculus similar to pol protein mRNA
9.97	1.260	0	A_55_P1994939	*Hmgb2*	NM_008252	ref|Mus musculus high mobility group box 2 mRNA
7.28	1.260	0.00032	A_55_P2106241	*4930432K21Rik*	NM_029045	ref|Mus musculus RIKEN cDNA 4930432K21 gene transcript variant 1 mRNA
7.96	1.260	0.00107	A_51_P347862	*Actn1*	NM_134156	ref|Mus musculus actinin alpha 1 mRNA
10.10	1.256	7.00E-05	A_55_P2102060	*Gstm3*	NM_010359	ref|Mus musculus glutathione S-transferase mu 3 mRNA
11.89	1.255	0.0014	A_51_P259296	*Lpl*	NM_008509	ref|Mus musculus lipoprotein lipase mRNA
12.20	1.251	0.00033	A_51_P346938	*Lrg1*	NM_029796	ref|Mus musculus leucine-rich alpha-2-glycoprotein 1 mRNA
13.21	1.250	2.00E-05	A_55_P1987620	*Cyp4a32*	NM_001100181	ref|Mus musculus cytochrome P450 family 4 subfamily a polypeptide 32 mRNA
8.77	1.247	0.00051	A_55_P2018417	*Osbpl3*	NM_001163645	ref|Mus musculus oxysterol binding protein-like 3 transcript variant 2 mRNA
8.52	1.246	2.00E-05	A_51_P172853	*Cd14*	NM_009841	ref|Mus musculus CD14 antigen mRNA
13.38	1.245	0.00016	A_55_P2071952	*Wdr92*	NM_178909	ref|Mus musculus WD repeat domain 92 mRNA
12.95	1.244	8.00E-05	A_52_P515094	*Tmem176a*	NM_025326	ref|Mus musculus transmembrane protein 176A transcript variant 1 mRNA
9.05	1.238	2.00E-05	A_66_P134090	*Grpel2*	NM_021296	ref|Mus musculus GrpE-like 2 mitochondrial nuclear gene encoding mitochondrial protein mRNA
8.15	1.237	1.00E-05	A_51_P401343	*Cldn14*	NM_019500	ref|Mus musculus claudin 14 transcript variant 1 mRNA
10.24	1.236	2.00E-04	A_51_P350453	*Pdk4*	NM_013743	ref|Mus musculus pyruvate dehydrogenase kinase isoenzyme 4 mRNA
11.56	1.23	0.00012	A_55_P2011436	*Gm11223*	XM_001474074	ref|PREDICTED: Mus musculus similar to Pr22 transcript variant 1 mRNA
11.72	1.229	1.00E-05	A_55_P2072908	*A_55_P2072908*	A_55_P2072908	Unknown
7.81	1.229	8.00E-04	A_55_P2005700	*Gm10651*	XM_001479811	ref|PREDICTED: Mus musculus similar to Josephin domain containing 1 mRNA
13.41	1.228	0.00055	A_51_P447545	*Igfbp1*	NM_008341	ref|Mus musculus insulin-like growth factor binding protein 1 mRNA
9.92	1.227	0.00059	A_51_P203955	*Gbp2*	NM_010260	ref|Mus musculus guanylate binding protein 2 mRNA
16.38	1.222	1.00E-05	A_66_P125722	*Cyb5*	NM_025797	ref|Mus musculus cytochrome b-5 mRNA
7.93	1.22	0.00166	A_51_P390715	*Tgfb1*	NM_011577	ref|Mus musculus transforming growth factor beta 1 mRNA
8.32	1.219	6.00E-05	A_51_P315795	*Tubb4*	NM_009451	ref|Mus musculus tubulin beta 4 mRNA
8.14	1.213	0.00012	A_52_P409731	*Scamp5*	NM_020270	ref|Mus musculus secretory carrier membrane protein 5 mRNA
7.91	1.212	0.00056	A_51_P390715	*Tgfb1*	NM_011577	ref|Mus musculus transforming growth factor beta 1 mRNA
12.43	1.206	4.00E-05	A_51_P189746	*Pim3*	NM_145478	ref|Mus musculus proviral integration site 3 mRNA
10.04	1.202	7.00E-05	A_55_P2162815	*ENSMUST00000059018*	ENSMUST00000059018	ens|Putative uncharacterized protein [Source:UniProtKB/TrEMBL;Acc:Q9D1L2]
9.24	1.200	0.00017	A_55_P2120545	*Wdtc1*	NM_199306	ref|Mus musculus WD and tetratricopeptide repeats 1 mRNA
9.84	1.199	1.00E-05	A_55_P1974645	*Entpd2*	NM_009849	ref|Mus musculus ectonucleoside triphosphate diphosphohydrolase 2 mRNA

7.22	1.196	0.00051	A_66_P114784	*Pla2g7*	NM_013737	ref|Mus musculus phospholipase A2 group VII (platelet-activating factor acetylhydrolase plasma) mRNA
10.28	1.196	0.00014	A_55_P2058117	*Slc35d1*	NM_177732	ref|Mus musculus solute carrier family 35 (UDP-glucuronic acid/UDP-N-acetylgalactosamine dual transporter) member D1 mRNA
9.33	1.195	0.00102	A_55_P2007496	*Gm2045*	XM_001472254	ref|PREDICTED: Mus musculus similar to pol protein mRNA
11.11	1.194	0.00014	A_52_P681391	*G0s2*	NM_008059	ref|Mus musculus G0/G1 switch gene 2 mRNA
10.42	1.192	0.00011	A_51_P312121	*Xdh*	NM_011723	ref|Mus musculus xanthine dehydrogenase mRNA
7.55	1.192	0.00011	A_52_P121491	*Msrb3*	NM_177092	ref|Mus musculus methionine sulfoxide reductase B3 mRNA
12.81	1.187	0.00017	A_51_P292008	*Gpx3*	NM_008161	ref|Mus musculus glutathione peroxidase 3 transcript variant 2 mRNA
17.03	1.186	0.00063	A_51_P311540	*Cox6a1*	NM_007748	ref|Mus musculus cytochrome c oxidase subunit VI a polypeptide 1 nuclear gene encoding mitochondrial protein mRNA
15.02	1.186	3.00E-05	A_55_P2170454	*Gsta2*	NM_008182	ref|Mus musculus glutathione S-transferase alpha 2 (Yc2) mRNA
15.17	1.186	6.00E-05	A_55_P2050628	*Cyp4a31*	NM_201640	ref|Mus musculus cytochrome P450 family 4 subfamily a polypeptide 31 mRNA
10.78	1.184	2.00E-05	A_55_P2043862	*Stmn1*	NM_019641	ref|Mus musculus stathmin 1 mRNA
12.30	1.184	0.00011	A_65_P02177	*Gstm4*	NM_026764	ref|Mus musculus glutathione S-transferase mu 4 transcript variant 1 mRNA
8.06	1.184	0.00024	A_66_P140507	*Lhpp*	NM_029609	ref|Mus musculus phospholysine phosphohistidine inorganic pyrophosphate phosphatase mRNA
7.88	1.182	0.00156	A_55_P1996941	*Ube2c*	NM_026785	ref|Mus musculus ubiquitin-conjugating enzyme E2C (Ube2c) mRNA [NM_026785]
7.52	1.178	0.00031	A_55_P2178798	*LOC100048662*	XM_001480833	ref|PREDICTED: Mus musculus similar to UDP glycosyltransferase 1 family polypeptide A13 mRNA
8.13	1.177	0.00095	A_52_P447944	*Epcam*	NM_008532	ref|Mus musculus epithelial cell adhesion molecule mRNA
11.40	1.171	1.00E-04	A_51_P238448	*Ccnd3*	NM_007632	ref|Mus musculus cyclin D3 transcript variant 1 mRNA
10.82	1.171	0.00031	A_66_P128963	*Cyp2d9*	NM_010006	ref|Mus musculus cytochrome P450 family 2 subfamily d polypeptide 9 mRNA
9.08	1.170	7.00E-05	A_52_P111031	*Pcdh17*	NM_001013753	ref|Mus musculus protocadherin 17 mRNA
9.84	1.169	0.00059	A_51_P124254	*Col4a1*	NM_009931	ref|Mus musculus collagen type IV alpha 1 mRNA
11.83	1.169	0	A_51_P282667	*Hexa*	NM_010421	ref|Mus musculus hexosaminidase A mRNA
7.89	1.169	0.00033	A_55_P1967168	*Lrp4*	NM_172668	ref|Mus musculus low density lipoprotein receptor-related protein 4 transcript variant 1 mRNA
12.17	1.165	2.00E-05	A_52_P358860	*Gss*	NM_008180	ref|Mus musculus glutathione synthetase mRNA
9.67	1.164	0.00041	A_55_P2016623	*Gm5068*	XM_204772	ref|PREDICTED: Mus musculus predicted gene EG277089 mRNA
10.06	1.163	0.00019	A_55_P2006255	*Txnip*	NM_001009935	ref|Mus musculus thioredoxin interacting protein transcript variant 1 mRNA
15.33	1.163	0.00011	A_51_P254895	*Cyp4a10*	NM_010011	ref|Mus musculus cytochrome P450 family 4 subfamily a polypeptide 10 mRNA
7.76	1.162	0.00059	A_51_P146753	*Csf2rb2*	NM_007781	ref|Mus musculus colony stimulating factor 2 receptor beta 2 low-affinity (granulocyte-macrophage) mRNA
12.00	1.160	6.00E-05	A_55_P2036240	*Gm3804*	XM_001478041	ref|PREDICTED: Mus musculus similar to pol protein mRNA
12.83	1.159	0.00014	A_51_P191611	*Cat*	NM_009804	ref|Mus musculus catalase mRNA
9.58	1.154	0.00027	A_66_P111021	*Nlrp6*	NM_001081389	ref|Mus musculus NLR family pyrin domain containing 6 mRNA

10.39	1.152	0.00053	A_55_P2024046	*Slc16a5*	NM_001080934	ref|Mus musculus solute carrier family 16 (monocarboxylic acid transporters) member 5 mRNA
11.04	1.150	5.00E-05	A_52_P295533	*Slc25a28*	NM_145156	ref|Mus musculus solute carrier family 25 member 28 mRNA
8.58	1.148	3.00E-04	A_55_P2164957	*Slc9a3r2*	NM_023055	ref|Mus musculus solute carrier family 9 (sodium/hydrogen exchanger) member 3 regulator 2 transcript variant A mRNA
15.88	1.142	0.00036	A_55_P1983733	*Aldh1l1*	NM_027406	ref|Mus musculus aldehyde dehydrogenase 1 family member L1 mRNA
7.98	1.139	0.00046	A_51_P418116	*Tmem119*	NM_146162	ref|Mus musculus transmembrane protein 119 mRNA
9.68	1.138	1.00E-05	A_51_P137336	*Cdh1*	NM_009864	ref|Mus musculus cadherin 1 mRNA
8.48	1.136	0.00028	A_66_P116888	*Arid1a*	NM_001080819	ref|Mus musculus AT rich interactive domain 1A (SWI-like) mRNA
8.26	1.133	0.00117	A_51_P114634	*Amz1*	NM_173405	ref|Mus musculus archaelysin family metallopeptidase 1 mRNA
8.18	1.13	0.00011	A_51_P126437	*Enc1*	NM_007930	ref|Mus musculus ectodermal-neural cortex 1 mRNA
7.76	1.128	0.00171	A_52_P452787	*Pdcd6ip*	NM_011052	ref|Mus musculus programmed cell death 6 interacting protein transcript variant 3 mRNA
9.76	1.127	3.00E-05	A_51_P137336	*Cdh1*	NM_009864	ref|Mus musculus cadherin 1 mRNA
7.84	1.126	0.00115	A_51_P390715	*Tgfb1*	NM_011577	ref|Mus musculus transforming growth factor beta 1 mRNA
10.22	1.123	4.00E-04	A_51_P351860	*C1qb*	NM_009777	ref|Mus musculus complement component 1 q subcomponent beta polypeptide mRNA
8.88	1.123	2.00E-05	A_52_P408757	*Fcgr3*	NM_010188	ref|Mus musculus Fc receptor IgG low affinity III mRNA
7.05	1.117	0.00151	A_55_P2065249	*ENSMUST00000063239*	ENSMUST00000063239	ens|Putative uncharacterized protein [Source:UniProtKB/TrEMBL;Acc:Q9D605]
7.86	1.117	0.00024	A_55_P2096599	*Tsc22d4*	NM_023910	ref|Mus musculus TSC22 domain family member 4 mRNA
8.25	1.115	0.00011	A_51_P117130	*Naga*	NM_008669	ref|Mus musculus N-acetyl galactosaminidase alpha mRNA
7.33	1.115	8.00E-05	A_51_P116447	*Xpo6*	NM_028816	ref|Mus musculus exportin 6 mRNA
8.30	1.112	0.00017	A_51_P126437	*Enc1*	NM_007930	ref|Mus musculus ectodermal-neural cortex 1 mRNA
13.53	1.112	4.00E-05	A_51_P405606	*Ndrg1*	NM_008681	ref|Mus musculus N-myc downstream regulated gene 1 mRNA
9.16	1.107	0.0018	A_52_P282905	*Gm5158*	NM_001081372	ref|Mus musculus predicted gene 5158 mRNA
10.90	1.103	0.00033	A_55_P1993940	*Sh3bgrl3*	NM_080559	ref|Mus musculus SH3 domain binding glutamic acid-rich protein-like 3 mRNA
13.11	1.101	2.00E-05	A_55_P2068988	*Gm5678*	XM_487442	ref|PREDICTED: Mus musculus predicted gene EG435489 mRNA
8.47	1.100	0.00053	A_51_P126437	*Enc1*	NM_007930	ref|Mus musculus ectodermal-neural cortex 1 mRNA
9.18	1.094	0.00012	A_55_P2070657	*2310044H10Rik*	NM_197991	ref|Mus musculus RIKEN cDNA 2310044H10 gene mRNA
10.09	1.093	5.00E-05	A_66_P119884	*Wdr91*	NM_001013366	ref|Mus musculus WD repeat domain 91 mRNA
10.45	1.093	0.00018	A_55_P2065991	*S100a11*	NM_016740	ref|Mus musculus S100 calcium binding protein A11 (calgizzarin) mRNA
7.79	1.092	5.00E-05	A_55_P2058783	*2310016C08Rik*	NM_023516	ref|Mus musculus RIKEN cDNA 2310016C08 gene mRNA
11.65	1.091	0.00041	A_55_P2068663	*Stmn1*	NM_019641	ref|Mus musculus stathmin 1 mRNA
7.96	1.090	0.00165	A_55_P2010912	*Jak3*	NM_010589	ref|Mus musculus Janus kinase 3 mRNA
10.91	1.089	0.00024	A_55_P2002577	*Ephx1*	NM_010145	ref|Mus musculus epoxide hydrolase 1 microsomal mRNA

8.89	1.089	6.00E-05	A_51_P407774	*Slc22a21*	NM_019723	ref|Mus musculus solute carrier family 22 (organic cation transporter) member 21 mRNA
9.74	1.085	0.00017	A_51_P244492	*Nbl1*	NM_008675	ref|Mus musculus neuroblastoma suppression of tumorigenicity 1 mRNA
15.52	1.085	6.00E-05	A_55_P2011111	*Cyp4a10*	NM_010011	ref|Mus musculus cytochrome P450 family 4 subfamily a polypeptide 10 (Cyp4a10) mRNA
16.62	1.082	0.00061	A_55_P1962299	*Hba-a2*	NM_001083955	ref|Mus musculus hemoglobin alpha adult chain 2 mRNA
8.49	1.081	1.00E-05	A_51_P168203	*Aig1*	NM_025446	ref|Mus musculus androgen-induced 1 mRNA
13.67	1.077	0	A_55_P2128821	*Selk*	NM_019979	ref|Mus musculus selenoprotein K mRNA
13.34	1.076	1.00E-05	A_51_P284486	*Gstm2*	NM_008183	ref|Mus musculus glutathione S-transferase mu 2 mRNA
8.57	1.075	0.00011	A_55_P2077783	*Tubb2a-ps2*	NR_003964	ref|Mus musculus tubulin beta 2a pseudogene 2 non-coding RNA
8.28	1.074	0.0012	A_51_P117130	*Naga*	NM_008669	ref|Mus musculus N-acetyl galactosaminidase alpha mRNA
8.85	1.074	0.00015	A_55_P2055875	*Josd2*	NM_025368	ref|Mus musculus Josephin domain containing 2 mRNA
13.97	1.072	0.00035	A_55_P1999648	*Plin2*	NM_007408	ref|Mus musculus perilipin 2 mRNA
13.53	1.072	1.00E-05	A_51_P350048	*Gstt2*	NM_010361	ref|Mus musculus glutathione S-transferase theta 2 mRNA
12.04	1.072	0.00029	A_55_P2090505	*Gm4382*	XM_001480011	ref|PREDICTED: Mus musculus similar to pol protein mRNA
10.03	1.071	0.00092	A_55_P2145833	*ENSMUST00000108472*	ENSMUST00000108472	ens|Myotonin-protein kinase (EC 2.7.11.1)(Myotonic dystrophy protein kinase)(MDPK)(DM-kinase)(DMK)(DMPK)(MT-PK) [Source:UniProtKB/Swiss-Prot;Acc:P54265]
7.41	1.071	0.00012	A_51_P100573	*Map3k3*	NM_011947	ref|Mus musculus mitogen-activated protein kinase kinase kinase 3 mRNA
9.64	1.068	0.00011	A_52_P188678	*Pvrl2*	NM_001159724	ref|Mus musculus poliovirus receptor-related 2 transcript variant 2 mRNA
8.25	1.065	2.00E-05	A_51_P352594	*St5*	NM_001001326	ref|Mus musculus suppression of tumorigenicity 5 transcript variant 1 mRNA
9.99	1.061	0.00011	A_55_P2011551	*Anapc5*	AK168135	gb|Mus musculus CRL-1722 L5178Y-R cDNA RIKEN full-length enriched library clone:I730060B02 product: anaphase-promoting complex subunit 5 full insert sequence.
8.04	1.061	0.00043	A_55_P2174836	*Vldlr*	NM_013703	ref|Mus musculus very low density lipoprotein receptor transcript variant 1 mRNA
9.97	1.060	3.00E-05	A_51_P251587	*Psmd9*	NM_026000	ref|Mus musculus proteasome (prosome macropain) 26S subunit non-ATPase 9 mRNA
9.60	1.059	0.00037	A_51_P460954	*Ccl6*	NM_009139	ref|Mus musculus chemokine (C-C motif) ligand 6 mRNA
12.83	1.059	5.00E-05	A_55_P2105843	*Gm2371*	XM_001472740	ref|PREDICTED: Mus musculus similar to pol protein mRNA
9.37	1.057	0.00014	A_51_P384754	*Ldb1*	NM_010697	ref|Mus musculus LIM domain binding 1 transcript variant 3 mRNA
12.31	1.057	0.00054	A_55_P2179413	*Lgals3bp*	NM_011150	ref|Mus musculus lectin galactoside-binding soluble 3 binding protein mRNA
10.65	1.054	3.00E-05	A_55_P2140031	*Fam129b*	NM_146119	ref|Mus musculus family with sequence similarity 129 member B mRNA
9.50	1.053	0.00085	A_55_P1954643	*Gm2708*	XM_001474512	ref|PREDICTED: Mus musculus hypothetical protein LOC100040315 mRNA
7.78	1.051	0.00087	A_55_P2295933	*Elmo3*	NM_172760	ref|Mus musculus engulfment and cell motility 3 ced-12 homolog (C. elegans) mRNA
9.87	1.050	0.00076	A_55_P2110978	*Atp6ap1*	NM_018794	ref|Mus musculus ATPase H^+ transporting lysosomal accessory protein 1 mRNA
9.74	1.048	0	A_52_P148678	*ENSMUST00000109462*	ENSMUST00000109462	ens|1-phosphatidylinositol-45-bisphosphate phosphodiesterase gamma-1 (EC 3.1.4.11)(Phosphoinositide phospholipase C)(Phospholipase C-gamma-1)(PLC-gamma-1)(PLC-II)(PLC-148) [Source:UniProtKB/Swiss-Prot;Acc:Q62077]

7.76	1.047	0.00133	A_55_P1974421	*Itga3*	NM_013565	ref|Mus musculus integrin alpha 3 mRNA
7.07	1.045	0.00062	A_51_P362013	*Rexo1*	NM_025852	ref|Mus musculus REX1 RNA exonuclease 1 homolog (S. cerevisiae) transcript variant 1 mRNA
7.52	1.045	0.00076	A_51_P118223	*Gm1943*	NR_002928	ref|Mus musculus predicted gene 1943 non-coding RNA
12.97	1.044	0.00034	A_55_P2156625	*A_55_P2156625*	A_55_P2156625	Unknown
9.21	1.044	0.00015	A_55_P1968193	*Fhit*	NM_010210	ref|Mus musculus fragile histidine triad gene mRNA
10.44	1.043	0.00051	A_51_P405476	*Fcer1g*	NM_010185	ref|Mus musculus Fc receptor IgE high affinity I gamma polypeptide mRNA
12.61	1.041	0.00016	A_51_P505493	*Elovl5*	NM_134255	ref|Mus musculus ELOVL family member 5 elongation of long chain fatty acids (yeast) mRNA
8.15	1.039	0.00015	A_52_P46310	*Dcaf7*	NM_027946	ref|Mus musculus DDB1 and CUL4 associated factor 7 mRNA
7.97	1.039	0.00103	A_51_P446825	*6430573F11Rik*	NM_176952	ref|Mus musculus RIKEN cDNA 6430573F11 gene mRNA
13.40	1.038	3.00E-04	A_51_P472901	*Slc3a2*	NM_008577	ref|Mus musculus solute carrier family 3 (activators of dibasic and neutral amino acid transport) member 2 transcript variant 2 mRNA
7.35	1.038	8.00E-05	A_55_P2035286	*Uhrf1*	NM_010931	ref|Mus musculus ubiquitin-like containing PHD and RING finger domains 1 transcript variant 1 mRNA
7.50	1.038	0.0016	A_51_P279639	*Col6a2*	NM_146007	ref|Mus musculus collagen type VI alpha 2 mRNA
10.95	1.036	3.00E-05	A_52_P215170	*Acot4*	NM_134247	ref|Mus musculus acyl-CoA thioesterase 4 mRNA
10.79	1.035	0.00147	A_51_P426276	*Pdk2*	AF267660	gb|Mus musculus pyruvate dehydrogenase kinase 2 mRNA complete cds
13.29	1.034	0.00012	A_55_P2063316	*Mgll*	NM_001166251	ref|Mus musculus monoglyceride lipase transcript variant 1 mRNA
9.37	1.034	0.00012	A_55_P2043892	*Srd5a3*	NM_020611	ref|Mus musculus steroid 5 alpha-reductase 3 (mRNA
9.04	1.033	7.00E-05	A_66_P119034	*Pla2g7*	NM_013737	ref|Mus musculus phospholipase A2 group VII (platelet-activating factor acetylhydrolase plasma) mRNA
9.89	1.032	0.00045	A_55_P2128181	*A_55_P2128181*	A_55_P2128181	Unknown
8.57	1.030	0.00146	A_52_P680038	*Cdk16*	NM_011049	ref|Mus musculus cyclin-dependent kinase 16 mRNA
11.52	1.029	9.00E-05	A_51_P450527	*Tagln*	NM_011526	ref|Mus musculus transgelin mRNA
10.55	1.027	0.00133	A_51_P220993	*Pfn1*	NM_011072	ref|Mus musculus profilin 1 mRNA
7.46	1.027	0.00142	A_55_P2104617	*Kctd5*	NM_027008	ref|Mus musculus potassium channel tetramerisation domain containing 5 mRNA
8.35	1.027	0.00174	A_55_P2183433	*Rab30*	NM_029494	ref|Mus musculus RAB30 member RAS oncogene family mRNA
9.23	1.027	3.00E-05	A_52_P432570	*Chdh*	NM_175343	ref|Mus musculus choline dehydrogenase transcript variant 2 mRNA
9.03	1.026	3.00E-05	A_52_P602091	*Csf1r*	NM_001037859	ref|Mus musculus colony stimulating factor 1 receptor mRNA
8.63	1.024	0.00086	A_55_P2128646	*Gmnn*	NM_020567	ref|Mus musculus geminin mRNA
9.12	1.021	0.00149	A_51_P246653	*Clec7a*	NM_020008	ref|Mus musculus C-type lectin domain family 7 member a mRNA
13.09	1.020	0.00012	A_55_P2134004	*Gstm2*	NM_008183	ref|Mus musculus glutathione S-transferase mu 2 mRNA
8.70	1.019	0.00012	A_52_P153189	*Arl2bp*	NM_024269	ref|Mus musculus ADP-ribosylation factor-like 2 binding protein transcript variant 2 mRNA
9.83	1.019	0.00048	A_51_P455906	*Pold4*	NM_027196	ref|Mus musculus polymerase (DNA-directed) delta 4 mRNA
10.40	1.017	7.00E-05	A_52_P320193	*Clec2h*	NM_053165	ref|Mus musculus C-type lectin domain family 2 member h mRNA

8.34	1.015	0.00054	A_51_P126437	*Enc1*	NM_007930	ref|Mus musculus ectodermal-neural cortex 1 mRNA
10.56	1.015	0.00019	A_52_P481182	*Stard5*	NM_023377	ref|Mus musculus StAR-related lipid transfer (START) domain containing 5 mRNA
9.45	1.014	0.00028	A_55_P2129309	*ENSMUST00000105501*	ENSMUST00000105501	ens|forkhead box O3 [Source:RefSeq peptide;Acc:NP_062714]
14.35	1.010	0.00021	A_66_P108152	*Cbr1*	NM_007620	ref|Mus musculus carbonyl reductase 1 mRNA
7.82	1.010	0.00017	A_51_P126437	*Enc1*	NM_007930	ref|Mus musculus ectodermal-neural cortex 1 mRNA
10.48	1.010	0.00108	A_52_P257812	*Lpl*	NM_008509	ref|Mus musculus lipoprotein lipase mRNA
11.87	1.007	0.00031	A_55_P1998656	*Entpd5*	NM_001026214	ref|Mus musculus ectonucleoside triphosphate diphosphohydrolase 5 transcript variant 2 mRNA [
9.56	1.007	0.00107	A_52_P418489	*Tinagl1*	NM_023476	ref|Mus musculus tubulointerstitial nephritis antigen-like 1 transcript variant 1 mRNA
9.45	1.006	1.00E-05	A_55_P2032192	*Tpm1*	NM_001164249	ref|Mus musculus tropomyosin 1 alpha transcript variant 2 mRNA
8.74	1.006	0.00021	A_51_P254646	*Jdp2*	NM_030887	ref|Mus musculus Jun dimerization protein 2 mRNA
7.52	1.006	0.0014	A_52_P140881	*Slc26a10*	NM_177615	ref|Mus musculus solute carrier family 26 member 10 mRNA
8.14	1.005	0.00041	A_51_P439085	*2310016C08Rik*	NM_023516	ref|Mus musculus RIKEN cDNA 2310016C08 gene mRNA
9.79	1.000	1.00E-04	A_52_P577384	*Il18bp*	NM_010531	ref|Mus musculus interleukin 18 binding protein mRNA

Table 86. All significantly down regulated genes in livers of female *Ahr* wild-type mice by TCDD (25 µg/kg bw) identified by microarray analysis - mouse 5 days study. Selected parameters: A-value ≥ 7, log2 fc ≥ 1, p-value ≤ 0.05.

A	Log2 fc	p-value	Probe name	Gene name	Systematic name	Gene description
7.24	-4.356	0	A_55_P2129449	*Sult3a1*	NM_020565	ref|Mus musculus sulfotransferase family 3A member 1 mRNA
7.70	-3.437	1.00E-05	A_52_P293682	*Gm7231*	XM_001477336	ref|PREDICTED: Mus musculus predicted gene EG638251 mRNA
10.45	-3.185	0	A_55_P2006008	*Serpinb1a*	NM_025429	ref|Mus musculus serine (or cysteine) peptidase inhibitor clade B member 1a mRNA
7.58	-2.970	0	A_52_P614207	*LOC100047222*	XM_001477680	ref|PREDICTED: Mus musculus similar to anti-glycoprotein-B of human Cytomegalovirus immunoglobulin Vl chain mRNA
8.70	-2.965	0.00143	A_51_P485421	*ENSMUST00000103426*	ENSMUST00000103426	ens|Immunoglobulin heavy chain C gene segment [Source:IMGT/GENE-DB;Acc:IGHM]
8.46	-2.960	0.00185	A_51_P485421	*ENSMUST00000103426*	ENSMUST00000103426	ens|Immunoglobulin heavy chain C gene segment [Source:IMGT/GENE-DB;Acc:IGHM]
8.60	-2.943	0.00129	A_51_P485421	*ENSMUST00000103426*	ENSMUST00000103426	ens|Immunoglobulin heavy chain C gene segment [Source:IMGT/GENE-DB;Acc:IGHM]
8.25	-2.930	0.00152	A_51_P485421	*ENSMUST00000103426*	ENSMUST00000103426	ens|Immunoglobulin heavy chain C gene segment [Source:IMGT/GENE-DB;Acc:IGHM]
8.59	-2.929	0.00084	A_51_P485421	*ENSMUST00000103426*	ENSMUST00000103426	ens|Immunoglobulin heavy chain C gene segment [Source:IMGT/GENE-DB;Acc:IGHM]
8.70	-2.922	0.001	A_51_P485421	*ENSMUST00000103426*	ENSMUST00000103426	ens|Immunoglobulin heavy chain C gene segment [Source:IMGT/GENE-DB;Acc:IGHM]

8.66	-2.915	0.00138	A_51_P485421	*ENSMUST00000103426*	ENSMUST00000103426	ens|Immunoglobulin heavy chain C gene segment [Source:IMGT/GENE-DB;Acc:IGHM]
8.70	-2.914	0.00112	A_51_P485421	*ENSMUST00000103426*	ENSMUST00000103426	ens|Immunoglobulin heavy chain C gene segment [Source:IMGT/GENE-DB;Acc:IGHM]
8.57	-2.906	0.00097	A_51_P485421	*ENSMUST00000103426*	ENSMUST00000103426	ens|Immunoglobulin heavy chain C gene segment [Source:IMGT/GENE-DB;Acc:IGHM]
8.71	-2.906	0.00076	A_51_P485421	*ENSMUST00000103426*	ENSMUST00000103426	ens|Immunoglobulin heavy chain C gene segment [Source:IMGT/GENE-DB;Acc:IGHM]
7.21	-2.890	0	A_52_P502849	*ENSMUST00000103401*	ENSMUST00000103401	ens|Immunoglobulin Kappa light chain V gene segment [Source:IMGT/GENE-DB;Acc:IGKV3-4]
8.83	-2.857	0	A_66_P105270	*Hao1*	NM_010403	ref|Mus musculus hydroxyacid oxidase 1 liver mRNA
7.10	-2.822	6.00E-05	A_52_P366803	*Cyp3a44*	NM_177380	ref|Mus musculus cytochrome P450 family 3 subfamily a polypeptide 44 mRNA
10.88	-2.796	0.00014	A_55_P1971237	*Mup3*	NM_001039544	ref|Mus musculus major urinary protein 3 (Mup3) mRNA
12.64	-2.715	0	A_51_P268529	*Csad*	NM_144942	ref|Mus musculus cysteine sulfinic acid decarboxylase mRNA
9.63	-2.590	0	A_51_P217498	*Slc2a4*	NM_009204	ref|Mus musculus solute carrier family 2 (facilitated glucose transporter) member 4 mRNA
8.82	-2.585	0	A_52_P100252	*Fasn*	NM_007988	ref|Mus musculus fatty acid synthase mRNA
8.01	-2.532	0.00058	A_55_P2038183	*Insc*	NM_173767	ref|Mus musculus inscuteable homolog (Drosophila) mRNA
11.07	-2.528	0.00104	A_51_P108226	*1100001G20Rik*	NM_183249	ref|Mus musculus RIKEN cDNA 1100001G20 gene mRNA
8.30	-2.492	4.00E-05	A_52_P73552	*A1bg*	NM_001081067	ref|Mus musculus alpha-1-B glycoprotein mRNA
7.11	-2.481	0	A_66_P134171	*ENSMUST00000103384*	ENSMUST00000103384	ens|Immunoglobulin Kappa light chain V gene segment [Source:IMGT/GENE-DB;Acc:IGKV8-24]
11.19	-2.479	6.00E-04	A_51_P108226	*1100001G20Rik*	NM_183249	ref|Mus musculus RIKEN cDNA 1100001G20 gene mRNA
11.03	-2.460	0	A_55_P2165091	*Acnat2*	NM_145368	ref|Mus musculus acyl-coenzyme A amino acid N-acyltransferase 2 mRNA
11.18	-2.458	0.00091	A_51_P108226	*1100001G20Rik*	NM_183249	ref|Mus musculus RIKEN cDNA 1100001G20 gene mRNA
11.00	-2.454	0.00153	A_51_P108226	*1100001G20Rik*	NM_183249	ref|Mus musculus RIKEN cDNA 1100001G20 gene mRNA
10.59	-2.450	4.00E-05	A_51_P108226	*1100001G20Rik*	NM_183249	ref|Mus musculus RIKEN cDNA 1100001G20 gene mRNA
11.11	-2.442	0.00134	A_51_P108226	*1100001G20Rik*	NM_183249	ref|Mus musculus RIKEN cDNA 1100001G20 gene mRNA
10.82	-2.434	0.00026	A_51_P108226	*1100001G20Rik*	NM_183249	ref|Mus musculus RIKEN cDNA 1100001G20 gene mRNA
10.95	-2.432	0.00042	A_51_P108226	*1100001G20Rik*	NM_183249	ref|Mus musculus RIKEN cDNA 1100001G20 gene mRNA
9.62	-2.412	0	A_51_P217498	*Slc2a4*	NM_009204	ref|Mus musculus solute carrier family 2 (facilitated glucose transporter) member 4 mRNA
10.54	-2.392	0.0019	A_51_P108226	*1100001G20Rik*	NM_183249	ref|Mus musculus RIKEN cDNA 1100001G20 gene mRNA
9.64	-2.385	0	A_51_P217498	*Slc2a4*	NM_009204	ref|Mus musculus solute carrier family 2 (facilitated glucose transporter) member 4 mRNA
9.48	-2.357	0	A_51_P217498	*Slc2a4*	NM_009204	ref|Mus musculus solute carrier family 2 (facilitated glucose transporter) member 4 mRNA
10.77	-2.353	0.00013	A_51_P108226	*1100001G20Rik*	NM_183249	ref|Mus musculus RIKEN cDNA 1100001G20 gene mRNA
12.20	-2.318	0	A_55_P2041723	*Mid1ip1*	NM_001166635	ref|Mus musculus Mid1 interacting protein 1 (gastrulation specific G12-like (zebrafish)) transcript variant 1 mRNA
9.97	-2.310	0	A_55_P2022074	*Klf10*	NM_013692	ref|Mus musculus Kruppel-like factor 10 mRNA
9.91	-2.287	1.00E-05	A_55_P2025343	*Mup21*	NM_001009550	ref|Mus musculus major urinary protein 21 mRNA
10.52	-2.274	0	A_51_P440743	*Celsr1*	NM_009886	ref|Mus musculus cadherin EGF LAG seven-pass G-type receptor 1 (flamingo homolog Drosophila) mRNA

9.60	-2.260	0	A_51_P217498	*Slc2a4*	NM_009204	ref|Mus musculus solute carrier family 2 (facilitated glucose transporter) member 4 mRNA
9.14	-2.259	1.00E-05	A_51_P217498	*Slc2a4*	NM_009204	ref|Mus musculus solute carrier family 2 (facilitated glucose transporter) member 4 mRNA
10.77	-2.164	0	A_51_P189733	*2810007J24Rik*	NM_175250	ref|Mus musculus RIKEN cDNA 2810007J24 gene mRNA
13.71	-2.163	0	A_55_P2025954	*Acly*	NM_134037	ref|Mus musculus ATP citrate lyase mRNA
13.87	-2.153	0.00055	A_51_P431329	*Car3*	NM_007606	ref|Mus musculus carbonic anhydrase 3 mRNA
12.01	-2.152	0	A_51_P463440	*Elovl6*	NM_130450	ref|Mus musculus ELOVL family member 6 elongation of long chain fatty acids (yeast) mRNA
9.26	-2.151	0	A_51_P217498	*Slc2a4*	NM_009204	ref|Mus musculus solute carrier family 2 (facilitated glucose transporter) member 4 mRNA
10.43	-2.147	1.00E-05	A_55_P2075263	*Acnat2*	NM_145368	ref|Mus musculus acyl-coenzyme A amino acid N-acyltransferase 2 mRNA
11.08	-2.058	0	A_52_P614777	*Sucnr1*	NM_032400	ref|Mus musculus succinate receptor 1 mRNA
7.40	-2.026	0.00067	A_51_P513776	*LOC640979*	XM_918237	ref|PREDICTED: Mus musculus similar to E225 mRNA
7.84	-1.987	0	A_55_P2258261	*1810008I18Rik*	AK050412	gb|Mus musculus adult male liver tumor cDNA RIKEN full-length enriched library clone:C730046D02 product:unclassifiable
7.20	-1.910	1.00E-05	A_51_P162955	*Serpina7*	NM_177920	ref|Mus musculus serine (or cysteine) peptidase inhibitor clade A (alpha-1 antiproteinase antitrypsin) member 7 mRNA
14.91	-1.906	0	A_55_P1965931	*Cml1*	NM_023160	ref|Mus musculus camello-like 1 mRNA
9.17	-1.882	3.00E-05	A_51_P217498	*Slc2a4*	NM_009204	ref|Mus musculus solute carrier family 2 (facilitated glucose transporter) member 4 mRNA
9.35	-1.836	0	A_52_P164136	*Arrdc3*	NM_001042591	ref|Mus musculus arrestin domain containing 3 mRNA
7.35	-1.822	0.00012	A_51_P269792	*Rad51l1*	NM_009014	ref|Mus musculus RAD51-like 1 (S. cerevisiae) mRNA
9.76	-1.816	0.00023	A_51_P249286	*Rgs16*	NM_011267	ref|Mus musculus regulator of G-protein signaling 16 mRNA
8.10	-1.816	0	A_55_P2165324	*Acsl3*	NM_028817	ref|Mus musculus acyl-CoA synthetase long-chain family member 3 transcript variant 1 mRNA
7.72	-1.802	3.00E-05	A_55_P1952156	*Gm9622*	XM_001487821	ref|PREDICTED: Mus musculus hypothetical LOC674389 mRNA
10.62	-1.784	0	A_55_P2053266	*St6galnac6*	NM_016973	ref|Mus musculus ST6 (alpha-N-acetyl-neuraminyl-23-beta-galactosyl-1 3)-N-acetylgalactosaminide alpha-26-sialyltransferase 6 transcript variant 1 mRNA
8.99	-1.780	1.00E-05	A_51_P217498	*Slc2a4*	NM_009204	ref|Mus musculus solute carrier family 2 (facilitated glucose transporter) member 4 mRNA
7.42	-1.777	0.00149	A_55_P2003911	*ENSMUST00000103391*	ENSMUST00000103391	ens|Immunoglobulin Kappa light chain V gene segment [Source:IMGT/GENE-DB;Acc:IGKV6-17]
8.73	-1.761	0	A_51_P161946	*E130012A19Rik*	NM_175332	ref|Mus musculus RIKEN cDNA E130012A19 gene mRNA
8.62	-1.757	0.00012	A_55_P2006792	*Ntrk2*	NM_001025074	ref|Mus musculus neurotrophic tyrosine kinase receptor type 2 transcript variant 1 mRNA
9.04	-1.755	3.00E-05	A_55_P2096043	*Acot11*	NM_025590	ref|Mus musculus acyl-CoA thioesterase 11 mRNA
7.54	-1.712	0	A_52_P89335	*Tmie*	NM_146260	ref|Mus musculus transmembrane inner ear mRNA
12.35	-1.700	1.00E-05	A_55_P2062737	*Elovl2*	NM_019423	ref|Mus musculus elongation of very long chain fatty acids (FEN1/Elo2 SUR4/Elo3 yeast)-like 2 mRNA
10.22	-1.687	0.00032	A_55_P2115442	*Clec2d*	NM_053109	ref|Mus musculus C-type lectin domain family 2 member d mRNA
7.13	-1.684	0	A_51_P452153	*2010001M09Rik*	NM_027222	ref|Mus musculus RIKEN cDNA 2010001M09 gene mRNA
8.08	-1.679	0	A_55_P2394308	*Fst*	NM_008046	ref|Mus musculus follistatin mRNA

10.23	-1.650	0.00024	A_55_P2172532	*C730007P19Rik*	NM_009286	ref|Mus musculus RIKEN cDNA C730007P19 gene mRNA
14.93	-1.631	0	A_55_P2186961	*Nat8b*	XM_485799	ref|PREDICTED: Mus musculus predicted gene EG434057 mRNA
7.00	-1.623	0	A_51_P452153	*2010001M09Rik*	NM_027222	ref|Mus musculus RIKEN cDNA 2010001M09 gene mRNA
11.48	-1.611	0	A_51_P114722	*Hao2*	NM_019545	ref|Mus musculus hydroxyacid oxidase 2 mRNA
8.48	-1.609	3.00E-04	A_51_P483576	*ENSMUST00000103743*	ENSMUST00000103743	ens|Immunoglobulin Lambda light chain C gene segment [Source:IMGT/GENE-DB;Acc:IGLC3]
7.94	-1.605	1.00E-05	A_51_P176042	*Pklr*	NM_013631	ref|Mus musculus pyruvate kinase liver and red blood cell nuclear gene encoding mitochondrial protein transcript variant 1 mRNA
11.15	-1.605	0.00081	A_51_P134142	*Cyp2c70*	NM_145499	ref|Mus musculus cytochrome P450 family 2 subfamily c polypeptide 70 mRNA
7.24	-1.602	2.00E-05	A_51_P452153	*2010001M09Rik*	NM_027222	ref|Mus musculus RIKEN cDNA 2010001M09 gene mRNA
12.54	-1.599	0	A_51_P114722	*Hao2*	NM_019545	ref|Mus musculus hydroxyacid oxidase 2 mRNA
10.52	-1.598	0	A_55_P2015753	*Enho*	NM_027147	ref|Mus musculus energy homeostasis associated mRNA
10.49	-1.596	1.00E-05	A_55_P2048518	*Zfpm1*	NM_009569	ref|Mus musculus zinc finger protein multitype 1 mRNA
10.18	-1.590	0.00019	A_55_P2057528	*Arl4d*	NM_025404	ref|Mus musculus ADP-ribosylation factor-like 4D mRNA
10.08	-1.587	0	A_55_P2143923	*Slc13a2*	NM_022411	ref|Mus musculus solute carrier family 13 (sodium-dependent dicarboxylate transporter) member 2 mRNA
11.34	-1.585	1.00E-05	A_55_P2027102	*Rgs3*	NM_134257	ref|Mus musculus regulator of G-protein signaling 3 transcript variant 2 mRNA
12.49	-1.583	0	A_51_P114722	*Hao2*	NM_019545	ref|Mus musculus hydroxyacid oxidase 2 mRNA
12.48	-1.580	0	A_51_P114722	*Hao2*	NM_019545	ref|Mus musculus hydroxyacid oxidase 2 mRNA
10.12	-1.572	6.00E-05	A_55_P2020612	*Arl4d*	NM_025404	ref|Mus musculus ADP-ribosylation factor-like 4D mRNA
12.45	-1.571	0	A_51_P114722	*Hao2*	NM_019545	ref|Mus musculus hydroxyacid oxidase 2 mRNA
8.99	-1.568	0	A_55_P2002557	*Srebf1*	NM_011480	ref|Mus musculus sterol regulatory element binding transcription factor 1 mRNA
12.39	-1.567	0	A_51_P114722	*Hao2*	NM_019545	ref|Mus musculus hydroxyacid oxidase 2 mRNA
7.14	-1.560	2.00E-05	A_51_P452153	*2010001M09Rik*	NM_027222	ref|Mus musculus RIKEN cDNA 2010001M09 gene mRNA
12.38	-1.558	0	A_51_P114722	*Hao2*	NM_019545	ref|Mus musculus hydroxyacid oxidase 2 mRNA
12.49	-1.558	0	A_51_P114722	*Hao2*	NM_019545	ref|Mus musculus hydroxyacid oxidase 2 mRNA
7.54	-1.555	0	A_55_P1982186	*Sgsm1*	NM_172718	ref|Mus musculus small G protein signaling modulator 1 transcript variant 1 mRNA
8.24	-1.553	1.00E-05	A_51_P516085	*Dntt*	NM_009345	ref|Mus musculus deoxynucleotidyltransferase terminal transcript variant 1 mRNA
8.80	-1.550	3.00E-05	A_55_P2143896	*Slc17a2*	NM_144836	ref|Mus musculus solute carrier family 17 (sodium phosphate) member 2 mRNA
12.43	-1.544	0	A_51_P114722	*Hao2*	NM_019545	ref|Mus musculus hydroxyacid oxidase 2 mRNA
12.36	-1.544	0	A_51_P114722	*Hao2*	NM_019545	ref|Mus musculus hydroxyacid oxidase 2 mRNA
9.30	-1.541	1.00E-05	A_55_P1963134	*Gm6135*	XM_895691	ref|PREDICTED: Mus musculus predicted gene EG620205 mRNA
7.25	-1.531	0	A_51_P452153	*2010001M09Rik*	NM_027222	ref|Mus musculus RIKEN cDNA 2010001M09 gene mRNA
7.03	-1.519	4.00E-05	A_51_P452153	*2010001M09Rik*	NM_027222	ref|Mus musculus RIKEN cDNA 2010001M09 gene mRNA

7.49	-1.518	0.00036	A_55_P2039044	*Cyp3a59*	NM_001105160	ref|Mus musculus cytochrome P450 subfamily 3A polypeptide 59 mRNA
10.06	-1.511	0.00013	A_51_P112308	*1810011O10Rik*	NM_026931	ref|Mus musculus RIKEN cDNA 1810011O10 gene mRNA
9.57	-1.507	5.00E-05	A_51_P112308	*1810011O10Rik*	NM_026931	ref|Mus musculus RIKEN cDNA 1810011O10 gene mRNA
10.93	-1.506	0	A_55_P2153517	*Enho*	NM_027147	ref|Mus musculus energy homeostasis associated mRNA
8.82	-1.500	5.00E-05	A_51_P217498	*Slc2a4*	NM_009204	ref|Mus musculus solute carrier family 2 (facilitated glucose transporter) member 4 mRNA
10.67	-1.498	1.00E-05	A_55_P1994887	*Zfpm1*	NM_009569	ref|Mus musculus zinc finger protein multitype 1 mRNA
13.08	-1.495	3.00E-05	A_55_P2003483	*Gldc*	NM_138595	ref|Mus musculus glycine decarboxylase mRNA
14.32	-1.491	3.00E-05	A_55_P1958434	*Got1*	NM_010324	ref|Mus musculus glutamate oxaloacetate transaminase 1 soluble mRNA
9.63	-1.491	0	A_55_P2055423	*Nat8b*	XM_485799	ref|PREDICTED: Mus musculus predicted gene EG434057 mRNA
13.31	-1.488	0.00036	A_55_P2018666	*Thrsp*	NM_009381	ref|Mus musculus thyroid hormone responsive SPOT14 homolog (Rattus) mRNA
9.80	-1.487	0	A_51_P161830	*Enpep*	NM_007934	ref|Mus musculus glutamyl aminopeptidase mRNA
9.36	-1.482	0.00086	A_51_P134812	*Chac1*	NM_026929	ref|Mus musculus ChaC cation transport regulator-like 1 (E. coli) mRNA
7.88	-1.477	4.00E-05	A_51_P257885	*Mmd2*	NM_175217	ref|Mus musculus monocyte to macrophage differentiation-associated 2 mRNA
9.94	-1.473	7.00E-05	A_51_P112308	*1810011O10Rik*	NM_026931	ref|Mus musculus RIKEN cDNA 1810011O10 gene mRNA
9.88	-1.469	3.00E-05	A_51_P112308	*1810011O10Rik*	NM_026931	ref|Mus musculus RIKEN cDNA 1810011O10 gene mRNA
12.25	-1.463	1.00E-05	A_55_P2422650	*5031425E22Rik*	AK017143	gb|Mus musculus 11 days pregnant adult female ovary and uterus cDNA RIKEN full-length enriched library clone:5031425E22 product:unclassifiable full insert sequence
9.73	-1.456	4.00E-05	A_51_P112308	*1810011O10Rik*	NM_026931	ref|Mus musculus RIKEN cDNA 1810011O10 gene mRNA
7.16	-1.455	6.00E-05	A_51_P452153	*2010001M09Rik*	NM_027222	ref|Mus musculus RIKEN cDNA 2010001M09 gene mRNA
7.25	-1.449	0.00014	A_55_P2251974	*A930038B10Rik*	AK044736	gb|Mus musculus adult retina cDNA RIKEN full-length enriched library clone:A930038B10 product:hypothetical protein full insert sequence
9.62	-1.447	0.00021	A_51_P112308	*1810011O10Rik*	NM_026931	ref|Mus musculus RIKEN cDNA 1810011O10 gene mRNA
9.94	-1.443	0.00023	A_51_P112308	*1810011O10Rik*	NM_026931	ref|Mus musculus RIKEN cDNA 1810011O10 gene mRNA
10.56	-1.442	2.00E-05	A_51_P386648	*Glod5*	NM_027227	ref|Mus musculus glyoxalase domain containing 5 mRNA
7.47	-1.440	0.00059	A_55_P1978502	*H2-Q1*	NM_010390	ref|Mus musculus histocompatibility 2 Q region locus 1 mRNA
9.85	-1.438	2.00E-04	A_51_P112308	*1810011O10Rik*	NM_026931	ref|Mus musculus RIKEN cDNA 1810011O10 gene mRNA
10.65	-1.436	8.00E-05	A_55_P2068289	*Slc17a2*	NM_144836	ref|Mus musculus solute carrier family 17 (sodium phosphate) member 2 mRNA
10.06	-1.435	0.00066	A_55_P2005005	*Cdk5rap1*	NM_025876	ref|Mus musculus CDK5 regulatory subunit associated protein 1 mRNA
8.96	-1.434	0	A_55_P2053459	*Timd2*	NM_001161355	ref|Mus musculus T-cell immunoglobulin and mucin domain containing 2 transcript variant 1 mRNA
11.03	-1.433	0.00176	A_55_P2107182	*Gm6484*	NM_001080940	ref|Mus musculus predicted gene 6484 mRNA
9.39	-1.421	2.00E-05	A_51_P400016	*ENSMUST00000114964*	ENSMUST00000114964	ens|Kalirin (EC 2.7.11.1)(Protein Duo)(Serine/threonine kinase with Dbl- and pleckstrin homology domain) [Source:UniProtKB/Swiss-Prot;Acc:A2CG49]
9.32	-1.413	5.00E-05	A_51_P112308	*1810011O10Rik*	NM_026931	ref|Mus musculus RIKEN cDNA 1810011O10 gene mRNA

10.68	-1.408	0.00013	A_55_P2180086	*Lrrc28*	NM_175124	ref|Mus musculus leucine rich repeat containing 28 transcript variant 1 mRNA
12.08	-1.404	0	A_51_P336622	*Dexi*	NM_021428	ref|Mus musculus dexamethasone-induced transcript mRNA
14.09	-1.404	0	A_52_P86693	*Ifi27l1*	NM_026790	ref|Mus musculus interferon alpha-inducible protein 27 like 1 transcript variant 1
11.12	-1.379	0.00014	A_51_P382764	*ENSMUST00000080361*	ENSMUST00000080361	ens|aldo-keto reductase family 1 member C20 [Source:RefSeq peptide;Acc:NP_473421]
8.39	-1.377	3.00E-05	A_51_P315042	*Avpr1a*	NM_016847	ref|Mus musculus arginine vasopressin receptor 1A mRNA
12.91	-1.377	1.00E-05	A_51_P452779	*Pygl*	NM_133198	ref|Mus musculus liver glycogen phosphorylase mRNA
7.03	-1.371	6.00E-05	A_55_P2293414	*1700001C19Rik*	NM_029296	ref|Mus musculus RIKEN cDNA 1700001C19 gene mRNA
11.50	-1.363	0	A_51_P353895	*Sult1c2*	NM_026935	ref|Mus musculus sulfotransferase family cytosolic 1C member 2 mRNA
8.18	-1.358	0.00029	A_55_P2148071	*LOC673748*	XM_001481151	ref|PREDICTED: Mus musculus similar to cytochrome P450 CYP3A mRNA
12.59	-1.349	3.00E-05	A_55_P2168267	*NAP002856-002*	NAP002856-002	Unknown
9.33	-1.347	5.00E-05	A_51_P342481	*Gpd2*	NM_010274	ref|Mus musculus glycerol phosphate dehydrogenase 2 mitochondrial nuclear gene encoding mitochondrial protein transcript variant 2 mRNA
8.57	-1.337	0.00035	A_55_P2092730	*Wdfy1*	NM_001111279	ref|Mus musculus WD repeat and FYVE domain containing 1 transcript variant 1 mRNA
13.78	-1.337	1.00E-05	A_51_P337195	*Pipox*	NM_008952	ref|Mus musculus pipecolic acid oxidase mRNA
9.92	-1.327	8.00E-05	A_51_P112308	*1810011O10Rik*	NM_026931	ref|Mus musculus RIKEN cDNA 1810011O10 gene mRNA
13.07	-1.325	1.00E-05	A_55_P2026761	*NAP111402-1*	NAP111402-1	Unknown
11.12	-1.318	1.00E-05	A_51_P452768	*Cyp4f14*	NM_022434	ref|Mus musculus cytochrome P450 family 4 subfamily f polypeptide 14 mRNA
9.77	-1.316	2.00E-05	A_55_P2010191	*Serpina11*	BC024087	gb|Mus musculus serine (or cysteine) peptidase inhibitor clade A (alpha-1 antiproteinase antitrypsin) member 11 mRNA (cDNA clone MGC:37881 IMAGE:5101271)
15.12	-1.304	2.00E-05	A_51_P186547	*Pah*	NM_008777	ref|Mus musculus phenylalanine hydroxylase mRNA
14.79	-1.304	4.00E-05	A_51_P401987	*Tmem37*	NM_019432	ref|Mus musculus transmembrane protein 37 mRNA
12.31	-1.298	0	A_55_P2173702	*Ebpl*	NM_026598	ref|Mus musculus emopamil binding protein-like mRNA
10.31	-1.294	6.00E-05	A_55_P2042319	*Cyp2d40*	NM_023623	ref|Mus musculus cytochrome P450 family 2 subfamily d polypeptide 40 mRNA
7.57	-1.293	0.0016	A_52_P402127	*Mup9*	NM_001126319	ref|Mus musculus major urinary protein 9 mRNA
15.28	-1.293	0	A_51_P291749	*Pecr*	NM_023523	ref|Mus musculus peroxisomal trans-2-enoyl-CoA reductase mRNA
10.47	-1.291	0	A_52_P93910	*Nrp2*	NM_001077403	ref|Mus musculus neuropilin 2 transcript variant 1 mRNA]
9.02	-1.287	0.00018	A_55_P2118866	*Cmah*	NM_001111110	ref|Mus musculus cytidine monophospho-N-acetylneuraminic acid hydroxylase transcript variant 2 mRNA
9.76	-1.286	6.00E-05	A_55_P2139087	*Gm5631*	NM_001013820	ref|Mus musculus predicted gene 5631 mRNA
8.58	-1.282	0.00021	A_52_P218833	*Gm5584*	NM_001101534	ref|Mus musculus predicted gene 5584 mRNA
8.46	-1.275	1.00E-05	A_52_P306357	*Prok1*	ENSMUST00000049852	ens|prokineticin 1 [Source:RefSeq peptide;Acc:NP_001037847]
7.83	-1.274	9.00E-05	A_55_P1952628	*Dpys*	NM_022722	ref|Mus musculus dihydropyrimidinase transcript variant 1 mRNA
11.17	-1.274	6.00E-05	A_51_P296036	*Nrbp2*	NM_144847	ref|Mus musculus nuclear receptor binding protein 2 mRNA

9.62	-1.272	1.00E-05	A_51_P155196	*Abtb2*	NM_178890	ref|Mus musculus ankyrin repeat and BTB (POZ) domain containing 2 mRNA
12.84	-1.269	2.00E-05	A_55_P2046411	*A_55_P2046411*	A_55_P2046411	Unknown
11.72	-1.267	6.00E-05	A_51_P308048	*Cmtm8*	NM_027294	ref|Mus musculus CKLF-like MARVEL transmembrane domain containing 8 mRNA
9.60	-1.259	1.00E-05	A_51_P196862	*Amdhd1*	NM_027908	ref|Mus musculus amidohydrolase domain containing 1 mRNA
10.83	-1.257	0.00016	A_51_P420415	*Srd5a1*	NM_175283	ref|Mus musculus steroid 5 alpha-reductase 1 mRNA
7.52	-1.244	0.00013	A_55_P2169124	*ENSMUST00000120540*	ENSMUST00000120540	ens|integral membrane transport protein UST1R [Source:RefSeq peptide;Acc:NP_795976]
9.28	-1.237	0.00086	A_51_P248122	*Bbc3*	NM_133234	ref|Mus musculus BCL2 binding component 3 mRNA
13.37	-1.235	1.00E-05	A_55_P1966804	*Fdps*	NM_134469	ref|Mus musculus farnesyl diphosphate synthetase mRNA
8.73	-1.233	0	A_55_P2162404	*LOC100047327*	XM_001477908	ref|PREDICTED: Mus musculus hypothetical protein LOC100047327 mRNA
8.06	-1.227	0.00011	A_55_P2000022	*Ccdc151*	NM_001163787	ref|Mus musculus coiled-coil domain containing 151 transcript variant 1 mRNA
15.15	-1.226	1.00E-05	A_51_P253547	*Ctsl*	NM_009984	ref|Mus musculus cathepsin L mRNA
15.22	-1.223	3.00E-05	A_51_P394115	*Aadac*	NM_023383	ref|Mus musculus arylacetamide deacetylase (esterase) mRNA
7.90	-1.218	1.00E-04	A_55_P2043627	*Fam89a*	NM_001081120	ref|Mus musculus family with sequence similarity 89 member A mRNA
9.42	-1.217	2.00E-05	A_55_P2169417	*BC021767*	XM_619932	ref|PREDICTED: Mus musculus cDNA sequence BC021767 mRNA
10.36	-1.214	2.00E-05	A_55_P2014284	*Serpina11*	NM_199314	ref|Mus musculus serine (or cysteine) peptidase inhibitor clade A (alpha-1 antiproteinase antitrypsin) member 11 transcript variant 1 mRNA
8.34	-1.212	0.00029	A_55_P2134236	*Foxa2*	NM_010446	ref|Mus musculus forkhead box A2 mRNA
12.82	-1.209	0.00013	A_51_P249360	*Suox*	NM_173733	ref|Mus musculus sulfite oxidase nuclear gene encoding mitochondrial protein mRNA
9.83	-1.208	1.00E-05	A_55_P2097508	*Mcc*	NM_001085373	ref|Mus musculus mutated in colorectal cancers transcript variant 1 mRNA
13.05	-1.207	3.00E-05	A_52_P1029978	*Lasp1*	NM_010688	ref|Mus musculus LIM and SH3 protein 1 mRNA
11.96	-1.205	1.00E-05	A_55_P2144285	*Nnt*	NM_008710	ref|Mus musculus nicotinamide nucleotide transhydrogenase nuclear gene encoding mitochondrial protein transcript variant 1 mRNA
11.10	-1.203	5.00E-05	A_55_P2006703	*Bmp1*	NM_009755	ref|Mus musculus bone morphogenetic protein 1 mRNA
11.44	-1.196	0.0013	A_51_P418168	*Manf*	NM_029103	ref|Mus musculus mesencephalic astrocyte-derived neurotrophic factor mRNA
13.74	-1.195	2.00E-05	A_51_P499854	*Ghr*	NM_010284	ref|Mus musculus growth hormone receptor transcript variant 1 mRNA
9.80	-1.189	0.00032	A_55_P2024625	*Ccl21a*	NM_011124	ref|Mus musculus chemokine (C-C motif) ligand 21A mRNA
8.73	-1.187	0.00026	A_52_P641282	*Pdilt*	NM_027943	ref|Mus musculus protein disulfide isomerase-like testis expressed mRNA
9.96	-1.186	0.00011	A_52_P64687	*Camk2n1*	NM_025451	ref|Mus musculus calcium/calmodulin-dependent protein kinase II inhibitor 1 mRNA
13.77	-1.185	0.00026	A_55_P2009952	*Me1*	NM_008615	ref|Mus musculus malic enzyme 1 NADP(+)-dependent cytosolic mRNA
16.65	-1.183	2.00E-05	A_51_P337269	*Aldob*	NM_144903	ref|Mus musculus aldolase B fructose-bisphosphate mRNA
8.30	-1.181	9.00E-05	A_55_P2139587	*NAP092820-001*	NAP092820-001	Unknown
9.62	-1.180	1.00E-05	A_51_P204845	*ENSMUST00000111451*	ENSMUST00000111451	ens|CUG-BP- and ETR-3-like factor 1 (CELF-1)(Bruno-like protein 2)(RNA-binding protein BRUNOL-2)(CUG triplet repeat RNA-binding protein 1)(CUG-BP1)(Deadenylation factor CUG-BP)(Deadenylation factor EDEN-

						BP)(50 kDa nuclear polyadenylated RNA-binding protein
13.86	-1.178	0.00013	A_55_P2017418	*Cfh*	NM_009888	ref|Mus musculus complement component factor h mRNA
7.37	-1.175	0.00081	A_66_P118430	*Slc17a2*	ENSMUST00000006786	ens|Sodium-dependent phosphate transport protein 3 (Sodium/phosphate cotransporter 3)(Na(+)/PI cotransporter 3)(Solute carrier family 17 member 2) [Source:UniProtKB/Swiss-Prot;Acc:Q5SZA1]
13.64	-1.165	6.00E-05	A_55_P1970810	*ENSMUST00000102901*	ENSMUST00000102901	ens|1-acyl-sn-glycerol-3-phosphate acyltransferase beta (EC 2.3.1.51)(1-acylglycerol-3-phosphate O-acyltransferase 2)(1-AGP acyltransferase 2)(1-AGPAT 2)(Lysophosphatidic acid acyltransferase beta)(LPAAT-beta) [Source:UniProtKB/Swiss-Prot;Acc:Q8K3K7]
9.21	-1.163	0.00166	A_51_P111462	*Arl15*	NM_172595	ref|Mus musculus ADP-ribosylation factor-like 15 mRNA
11.60	-1.161	1.00E-05	A_52_P161297	*Tcea3*	NM_011542	ref|Mus musculus transcription elongation factor A (SII) 3 mRNA
12.70	-1.160	1.00E-05	A_55_P2045802	*Nelf*	NM_001039386	ref|Mus musculus nasal embryonic LHRH factor transcript variant 1 mRNA
9.15	-1.159	4.00E-05	A_52_P84275	*Derl2*	NM_033562	ref|Mus musculus Der1-like domain family member 2 mRNA
9.91	-1.157	0.00016	A_55_P1954356	*Ttc23*	NM_025905	ref|Mus musculus tetratricopeptide repeat domain 23 transcript variant 1 mRNA
8.32	-1.157	0.00162	A_55_P1954393	*Susd4*	NM_144796	ref|Mus musculus sushi domain containing 4 mRNA
10.75	-1.157	2.00E-05	A_51_P329949	*Fam13a*	NM_153574	ref|Mus musculus family with sequence similarity 13 member A mRNA
10.84	-1.156	0.00051	A_51_P514405	*Slc2a5*	NM_019741	ref|Mus musculus solute carrier family 2 (facilitated glucose transporter) member 5 mRNA
8.42	-1.154	0.00038	A_51_P354165	*Apcs*	NM_011318	ref|Mus musculus serum amyloid P-component mRNA
9.96	-1.148	1.00E-05	A_55_P2056496	*Tk1*	NM_009387	ref|Mus musculus thymidine kinase 1 mRNA
12.11	-1.147	0.00012	A_55_P2154709	*Pter*	NM_008961	ref|Mus musculus phosphotriesterase related mRNA
13.04	-1.146	1.00E-05	A_55_P2059352	*Col18a1*	NM_001109991	ref|Mus musculus collagen type XVIII alpha 1 transcript variant 1 mRNA
7.11	-1.145	9.00E-05	A_55_P2126192	*Lgr5*	NM_010195	ref|Mus musculus leucine rich repeat containing G protein coupled receptor 5 mRNA
9.97	-1.145	1.00E-05	A_51_P354077	*Svil*	NM_153153	ref|Mus musculus supervillin transcript variant 1 mRNA
11.79	-1.143	2.00E-05	A_51_P479052	*Tars*	NM_033074	ref|Mus musculus threonyl-tRNA synthetase mRNA
9.85	-1.142	0.00028	A_51_P111462	*Arl15*	NM_172595	ref|Mus musculus ADP-ribosylation factor-like 15 mRNA
7.21	-1.141	8.00E-05	A_51_P378789	*Cxcl13*	NM_018866	ref|Mus musculus chemokine (C-X-C motif) ligand 13 mRNA
11.30	-1.132	3.00E-05	A_55_P2180445	*Gm2742*	XM_001474578	ref|PREDICTED: Mus musculus similar to Ubtf protein mRNA
10.96	-1.130	2.00E-05	A_52_P219904	*Afmid*	NM_027827	ref|Mus musculus arylformamidase mRNA
8.73	-1.128	5.00E-05	A_52_P12001	*Erp44*	NM_029572	ref|Mus musculus endoplasmic reticulum protein 44 mRNA
7.04	-1.125	0.00037	A_55_P2082914	*Acly*	NM_134037	ref|Mus musculus ATP citrate lyase mRNA
8.84	-1.123	2.00E-05	A_66_P105046	*Il18*	NM_008360	ref|Mus musculus interleukin 18 mRNA
13.33	-1.117	0.00171	A_55_P2171413	*Me1*	NM_008615	ref|Mus musculus malic enzyme 1 NADP(+)-dependent cytosolic mRNA
9.90	-1.117	1.00E-05	A_55_P1981992	*LOC637149*	XM_912753	ref|PREDICTED: Mus musculus similar to doublecortin domain containing 2 mRNA
8.52	-1.116	0.00136	A_55_P2298319	*C730029A08Rik*	AK083183	gb|Mus musculus adult male hippocampus cDNA RIKEN full-length enriched library clone:C630024D06 product:unclassifiable full insert sequence

11.82	-1.116	1.00E-05	A_55_P2126950	*Zfp467*	NM_001085417	ref|Mus musculus zinc finger protein 467 transcript variant 4 mRNA
9.74	-1.115	0.00089	A_51_P111462	*Arl15*	NM_172595	ref|Mus musculus ADP-ribosylation factor-like 15 mRNA
9.14	-1.114	4.00E-05	A_55_P2024290	*Fam149a*	NM_153535	ref|Mus musculus family with sequence similarity 149 member A mRNA
13.29	-1.113	0	A_66_P115996	*Ccbl1*	NM_172404	ref|Mus musculus cysteine conjugate-beta lyase 1 mRNA
8.48	-1.109	0.00084	A_55_P2003638	*Stxbp6*	NM_144552	ref|Mus musculus syntaxin binding protein 6 (amisyn) mRNA
8.06	-1.109	5.00E-05	A_55_P2106844	*Gm7475*	XM_001476912	ref|PREDICTED: Mus musculus predicted gene EG665070 mRNA
11.1	-1.102	0.00051	A_55_P2013296	*Prkag2*	NM_145401	ref|Mus musculus protein kinase AMP-activated gamma 2 non-catalytic subunit transcript variant 1 mRNA
12.29	-1.096	0.00048	A_55_P1965114	*Spsb3*	NM_001163750	ref|Mus musculus splA/ryanodine receptor domain and SOCS box containing 3 transcript variant 1 mRNA
13.21	-1.094	2.00E-05	A_55_P1969776	*Pdhb*	NM_024221	ref|Mus musculus pyruvate dehydrogenase (lipoamide) beta mRNA
10.76	-1.090	0	A_52_P539161	*Rdh11*	NM_021557	ref|Mus musculus retinol dehydrogenase 11 mRNA
8.23	-1.078	0.00051	A_55_P2142222	*Serpina3h*	NM_001034870	ref|Mus musculus serine (or cysteine) peptidase inhibitor clade A member 3H mRNA
8.98	-1.078	9.00E-05	A_51_P437240	*Emp2*	NM_007929	ref|Mus musculus epithelial membrane protein 2 mRNA
9.28	-1.077	0.00114	A_51_P111462	*Arl15*	NM_172595	ref|Mus musculus ADP-ribosylation factor-like 15 mRNA
9.62	-1.076	0.00032	A_66_P121636	*Ablim3*	NM_198649	ref|Mus musculus actin binding LIM protein family member 3 transcript variant 1 mRNA
15.00	-1.074	1.00E-04	A_55_P2032966	*Hmgcs1*	NM_145942	ref|Mus musculus 3-hydroxy-3-methylglutaryl-Coenzyme A synthase 1 mRNA
11.93	-1.071	2.00E-05	A_51_P175424	*Car14*	NM_011797	ref|Mus musculus carbonic anhydrase 14 mRNA
16.30	-1.070	2.00E-05	A_52_P72434	*Khk*	NM_008439	ref|Mus musculus ketohexokinase mRNA
10.37	-1.070	3.00E-05	A_55_P2002757	*Blnk*	NM_008528	ref|Mus musculus B-cell linker mRNA
11.78	-1.070	0.00109	A_55_P1975185	*Sqle*	NM_009270	ref|Mus musculus squalene epoxidase mRNA
11.23	-1.070	3.00E-05	A_51_P381618	*Pla1a*	NM_134102	ref|Mus musculus phospholipase A1 member A mRNA
8.19	-1.065	0.00028	A_55_P2056493	*ENSMUST00000106328*	ENSMUST00000106328	ens|Thymidine kinase cytosolic (EC 2.7.1.21) [Source:UniProtKB/Swiss-Prot;Acc:P04184]
13.34	-1.062	1.00E-05	A_55_P1988789	*Acss2*	NM_019811	ref|Mus musculus acyl-CoA synthetase short-chain family member 2 mRNA
14.30	-1.061	0.00052	A_51_P385598	*Slc37a4*	NM_008063	ref|Mus musculus solute carrier family 37 (glucose-6-phosphate transporter) member 4 mRNA
9.59	-1.061	0.0013	A_51_P111462	*Arl15*	NM_172595	ref|Mus musculus ADP-ribosylation factor-like 15 mRNA
12.80	-1.059	6.00E-05	A_51_P418056	*Sc5d*	NM_172769	ref|Mus musculus sterol-C5-desaturase (fungal ERG3 delta-5-desaturase) homolog (S. cerevisae) mRNA
7.00	-1.056	0.00088	A_52_P559566	*ENSMUST00000103527*	ENSMUST00000103527	ens|Immunoglobulin heavy chain V gene segment [Source:IMGT/GENE-DB;Acc:IGHV1-56]
9.54	-1.048	0.00142	A_51_P111462	*Arl15*	NM_172595	ref|Mus musculus ADP-ribosylation factor-like 15 mRNA
9.22	-1.046	4.00E-05	A_55_P2113723	*ENSMUST00000097698*	ENSMUST00000097698	ens|Peroxisomal trans-2-enoyl-CoA reductase (EC 1.3.1.38) [Source:UniProtKB/Swiss-Prot;Acc:Q99MZ7]
14.85	-1.041	0.00016	A_51_P162162	*Inmt*	NM_009349	ref|Mus musculus indolethylamine N-methyltransferase mRNA
13.58	-1.038	3.00E-05	A_55_P2059412	*Ghr*	NM_001048178	ref|Mus musculus growth hormone receptor transcript variant 2 mRNA
8.58	-1.037	0.00021	A_55_P2045622	*Setdb2*	NM_001081024	ref|Mus musculus SET domain bifurcated 2 mRNA
11.02	-1.032	2.00E-05	A_55_P1989215	*Entpd8*	NM_028093	ref|Mus musculus ectonucleoside triphosphate diphosphohydrolase 8 mRNA

15.58	-1.029	1.00E-04	A_52_P592909	*Dgat2*	NM_026384	ref|Mus musculus diacylglycerol O-acyltransferase 2 mRNA
10.22	-1.027	0	A_55_P2008926	*Slc17a3*	NM_134069	ref|Mus musculus solute carrier family 17 (sodium phosphate) member 3 transcript variant 1 mRNA
12.45	-1.019	6.00E-05	A_51_P122246	*Creld2*	NM_029720	ref|Mus musculus cysteine-rich with EGF-like domains 2 mRNA
13.68	-1.018	1.00E-05	A_51_P498831	*Derl2*	NM_033562	ref|Mus musculus Der1-like domain family member 2 mRNA
10.88	-1.016	5.00E-05	A_66_P116326	*ENSMUST00000108435*	ENSMUST00000108435	ens|TLC domain-containing protein 2 [Source:UniProtKB/Swiss-Prot;Acc:Q8VC26]
12.94	-1.015	0	A_55_P2021049	*Ugp2*	NM_139297	ref|Mus musculus UDP-glucose pyrophosphorylase 2 mRNA
15.15	-1.012	3.00E-05	A_55_P2108171	*Glud1*	NM_008133	ref|Mus musculus glutamate dehydrogenase 1 nuclear gene encoding mitochondrial protein mRNA
13.95	-1.012	0.00034	A_55_P2032079	*Dbp*	NM_016974	ref|Mus musculus D site albumin promoter binding protein mRNA
11.56	-1.010	0.00161	A_51_P391616	*Agxt2l1*	NM_027907	ref|Mus musculus alanine-glyoxylate aminotransferase 2-like 1 transcript variant 1 mRNA
9.71	-1.010	0.00021	A_55_P2009042	*Gm4635*	XM_001481023	ref|PREDICTED: Mus musculus hypothetical protein LOC100043770 mRNA
10.96	-1.009	5.00E-05	A_51_P272553	*Bhlhe40*	NM_011498	ref|Mus musculus basic helix-loop-helix family member e40 mRNA
8.39	-1.005	0.00045	A_66_P124179	*Atp6v0d2*	NM_175406	ref|Mus musculus ATPase H+ transporting lysosomal V0 subunit D2 mRNA
13.61	-1.004	6.00E-05	A_55_P1987730	*5730469M10Rik*	NM_027464	ref|Mus musculus RIKEN cDNA 5730469M10 gene mRNA
9.71	-1.003	8.00E-05	A_66_P123155	*Ddo*	NM_027442	ref|Mus musculus D-aspartate oxidase mRNA
7.62	-1.002	3.00E-05	A_66_P136834	*Usp7*	NM_001003918	ref|Mus musculus ubiquitin specific peptidase 7 mRNA

Table 87. All significantly up regulated genes in livers of female *Ahr* knockout mice by TCDD (25 µg/kg bw) identified by microarray analysis - mouse 5 days study. Selected parameters: A-value ≥ 7, log2 fc ≥ 1, p-value ≤ 0.05.

A	Log2 fc	p-value	Probe name	Gene name	Systematic name	Gene description
10.15	3.513	0	A_52_P257625	*Esm1*	NM_023612	ref|Mus musculus endothelial cell-specific molecule 1 mRNA
7.45	3.384	0	A_51_P510891	*Afp*	NM_007423	ref|Mus musculus alpha fetoprotein mRNA
7.42	3.371	0	A_51_P510891	*Afp*	NM_007423	ref|Mus musculus alpha fetoprotein mRNA
7.43	3.360	0	A_51_P510891	*Afp*	NM_007423	ref|Mus musculus alpha fetoprotein mRNA
7.16	3.346	0	A_51_P510891	*Afp*	NM_007423	ref|Mus musculus alpha fetoprotein mRNA
7.44	3.337	0	A_51_P510891	*Afp*	NM_007423	ref|Mus musculus alpha fetoprotein mRNA
7.45	3.220	0	A_51_P510891	*Afp*	NM_007423	ref|Mus musculus alpha fetoprotein mRNA
7.14	3.176	0	A_51_P510891	*Afp*	NM_007423	ref|Mus musculus alpha fetoprotein mRNA
7.44	3.037	0	A_51_P510891	*Afp*	NM_007423	ref|Mus musculus alpha fetoprotein mRNA
7.47	2.860	0	A_51_P233160	*Lysmd2*	NM_027309	ref|Mus musculus LysM putative peptidoglycan-binding domain containing 2 mRNA
11.89	2.805	0	A_51_P259296	*Lpl*	NM_008509	ref|Mus musculus lipoprotein lipase mRNA
7.05	2.721	0	A_51_P510891	*Afp*	NM_007423	ref|Mus musculus alpha fetoprotein mRNA
7.22	2.716	1.00E-05	A_55_P2192662	*Lepr*	NM_001122899	ref|Mus musculus leptin receptor transcript variant 3 mRNA
7.18	2.659	0	A_55_P2078494	*Cib3*	NM_001080812	ref|Mus musculus calcium and integrin binding family member 3 mRNA
10.01	2.638	0.00112	A_55_P1981714	*Rreb1*	NR_033218	ref|Mus musculus ras responsive element binding protein 1 transcript variant 1 non-coding RNA
9.79	2.517	0	A_51_P137336	*Cdh1*	NM_009864	ref|Mus musculus cadherin 1 mRNA
9.33	2.486	1.00E-05	A_51_P137336	*Cdh1*	NM_009864	ref|Mus musculus cadherin 1 mRNA
12.20	2.435	0	A_55_P2150976	*Fabp5l2*	XM_886827	ref|PREDICTED: Mus musculus predicted gene EG622384 mRNA
9.80	2.430	0	A_51_P137336	*Cdh1*	NM_009864	ref|Mus musculus cadherin 1 mRNA
8.39	2.421	0	A_55_P1959748	*Asns*	NM_012055	ref|Mus musculus asparagine synthetase mRNA
9.76	2.416	0	A_51_P137336	*Cdh1*	NM_009864	ref|Mus musculus cadherin 1 mRNA
9.59	2.415	0	A_51_P137336	*Cdh1*	NM_009864	ref|Mus musculus cadherin 1 mRNA
9.68	2.398	0	A_51_P137336	*Cdh1*	NM_009864	ref|Mus musculus cadherin 1 mRNA
7.65	2.386	0.00156	A_51_P487690	*Ifi44*	NM_133871	ref|Mus musculus interferon-induced protein 44 mRNA
9.70	2.382	0	A_51_P137336	*Cdh1*	NM_009864	ref|Mus musculus cadherin 1 mRNA
9.66	2.313	0	A_51_P137336	*Cdh1*	NM_009864	ref|Mus musculus cadherin 1 mRNA
9.76	2.307	0	A_51_P137336	*Cdh1*	NM_009864	ref|Mus musculus cadherin 1 mRNA
11.70	2.307	0	A_51_P372550	*Cgref1*	NM_026770	ref|Mus musculus cell growth regulator with EF hand domain 1 transcript variant 1 mRNA

9.45	2.283	0	A_51_P137336	*Cdh1*	NM_009864	ref|Mus musculus cadherin 1 mRNA
7.60	2.282	3.00E-05	A_55_P2087805	*Hsd3b1*	NM_008293	ref|Mus musculus hydroxy-delta-5-steroid dehydrogenase 3 beta- and steroid delta-isomerase 1 mRNA
9.20	2.203	1.00E-05	A_51_P331288	*Akr1b7*	NM_009731	ref|Mus musculus aldo-keto reductase family 1 member B7 mRNA
9.97	2.181	2.00E-05	A_55_P2043122	*Arsg*	NM_028710	ref|Mus musculus arylsulfatase G transcript variant 1 mRNA
11.37	2.160	9.00E-05	A_55_P2067707	*Mep1a*	NM_008585	ref|Mus musculus meprin 1 alpha mRNA
7.40	2.141	0	A_52_P167278	*Mthfd1l*	NM_172308	ref|Mus musculus methylenetetrahydrofolate dehydrogenase (NADP+ dependent) 1-like nuclear gene encoding mitochondrial protein transcript variant 2 mRNA
8.67	2.053	0	A_55_P2077048	*Itih5*	NM_172471	ref|Mus musculus inter-alpha (globulin) inhibitor H5mRNA
10.68	2.011	2.00E-05	A_52_P21550	*Gcnt1*	NM_173442	ref|Mus musculus glucosaminyl (N-acetyl) transferase 1 core 2 transcript variant 1 mRNA
8.48	1.978	1.00E-05	A_52_P577388	*Epdr1*	NM_134065	ref|Mus musculus ependymin related protein 1 (zebrafish) mRNA
8.08	1.942	0	A_55_P2394308	*Fst*	NM_008046	ref|Mus musculus follistatin mRNA
12.27	1.940	1.00E-04	A_51_P336833	*Fabp4*	NM_024406	ref|Mus musculus fatty acid binding protein 4 adipocyte mRNA
7.41	1.909	0.00161	A_51_P510891	*Afp*	NM_007423	ref|Mus musculus alpha fetoprotein mRNA
11.42	1.888	2.00E-05	A_55_P2122841	*NAP114472-1*	NAP114472-1	Unknown
9.22	1.883	0.00094	A_52_P472324	*Slpi*	NM_011414	ref|Mus musculus secretory leukocyte peptidase inhibitor mRNA
7.79	1.872	3.00E-05	A_55_P1956488	*Epb4.9*	NM_013514	ref|Mus musculus erythrocyte protein band 4.9 mRNA
10.66	1.846	2.00E-05	A_55_P2387665	*9130221J18Rik*	AK033690	gb|Mus musculus adult male cecum cDNA RIKEN full-length enriched library clone:9130221J18 product:unclassifiable full insert sequence
12.09	1.836	5.00E-05	A_51_P157042	*Ctgf*	NM_010217	ref|Mus musculus connective tissue growth factor mRNA
8.93	1.826	4.00E-05	A_52_P566681	*Gpm6a*	NM_153581	ref|Mus musculus glycoprotein m6a mRNA
10.56	1.808	9.00E-05	A_51_P243755	*Slc10a2*	NM_011388	ref|Mus musculus solute carrier family 10 member 2 mRNA
7.48	1.799	0	A_55_P2116689	*1700024P16Rik*	NM_001162980	ref|Mus musculus RIKEN cDNA 1700024P16 gene mRNA
7.88	1.794	0	A_66_P110161	*Eppk1*	BC026387	gb|Mus musculus epiplakin 1 mRNA (cDNA clone IMAGE:4188338) partial cds
7.92	1.793	0.00067	A_55_P2023912	*A_55_P2023912*	A_55_P2023912	Unknown
7.81	1.791	1.00E-05	A_51_P477682	*Prss12*	NM_008939	ref|Mus musculus protease serine 12 neurotrypsin (motopsin) mRNA
7.22	1.785	0.00051	A_55_P1962937	*Trem2*	NM_031254	ref|Mus musculus triggering receptor expressed on myeloid cells 2 mRNA
12.40	1.768	4.00E-05	A_55_P1953387	*Fabp5*	NM_010634	ref|Mus musculus fatty acid binding protein 5 epidermal mRNA
8.62	1.763	0	A_55_P2112185	*Nhsl1*	NM_173390	ref|Mus musculus NHS-like 1 transcript variant 1 mRNA
7.91	1.761	1.00E-05	A_55_P1967538	*Hunk*	NM_015755	ref|Mus musculus hormonally upregulated Neu-associated kinase mRNA
7.88	1.755	1.00E-05	A_55_P2063508	*Gm4131*	XM_001479179	ref|PREDICTED: Mus musculus similar to hCG28707 mRNA
8.41	1.727	3.00E-05	A_51_P309920	*Itga8*	NM_001001309	ref|Mus musculus integrin alpha 8 mRNA
13.41	1.724	3.00E-05	A_51_P447545	*Igfbp1*	NM_008341	ref|Mus musculus insulin-like growth factor binding protein 1 mRNA

10.34	1.713	0	A_55_P2057777	*Fgfr1*	NM_010206	ref|Mus musculus fibroblast growth factor receptor 1 transcript variant 1 mRNA
7.27	1.712	3.00E-05	A_51_P108581	*Adrbk2*	NM_177078	ref|Mus musculus adrenergic receptor kinase beta 2 transcript variant 1 mRNA
11.96	1.671	0	A_51_P365516	*Spink3*	NM_009258	ref|Mus musculus serine peptidase inhibitor Kazal type 3 mRNA
8.03	1.659	1.00E-05	A_55_P2169356	*Gm1966*	XM_001000891	ref|PREDICTED: Mus musculus gene model 1966 (NCBI) transcript variant 1 mRNA
7.01	1.659	0	A_55_P2127179	*Gm379*	XM_142052	ref|PREDICTED: Mus musculus gene model 379 (NCBI) mRNA
9.78	1.642	4.00E-04	A_51_P515605	*Col3a1*	NM_009930	ref|Mus musculus collagen type III alpha 1 mRNA
11.06	1.623	2.00E-05	A_51_P204247	*C8a*	NM_146148	ref|Mus musculus complement component 8 alpha polypeptide mRNA
8.84	1.622	0	A_51_P420547	*Clic5*	NM_172621	ref|Mus musculus chloride intracellular channel 5 mRNA
7.28	1.619	0.00092	A_66_P118772	*Tmem136*	NM_001034863	ref|Mus musculus transmembrane protein 136 mRNA
11.67	1.617	0	A_55_P2059010	*Rbp1*	NM_011254	ref|Mus musculus retinol binding protein 1 cellular mRNA
9.03	1.602	1.00E-05	A_55_P1996973	*Gvin1*	NM_029000	ref|Mus musculus GTPase very large interferon inducible 1 transcript variant A mRNA
8.22	1.596	0.00014	A_55_P2118520	*Col1a1*	NM_007742	ref|Mus musculus collagen type I alpha 1 mRNA
9.28	1.587	2.00E-05	A_52_P585652	*Fndc3b*	NM_173182	ref|Mus musculus fibronectin type III domain containing 3B mRNA
8.73	1.585	0.00057	A_55_P1978681	*Tspan8*	NM_146010	ref|Mus musculus tetraspanin 8 transcript variant 1 mRNA
8.04	1.585	4.00E-05	A_51_P295237	*Lrp11*	NM_172784	ref|Mus musculus low density lipoprotein receptor-related protein 11 mRNA
11.13	1.582	0	A_51_P320852	*Cd9*	NM_007657	ref|Mus musculus CD9 antigen mRNA
9.36	1.574	0.00016	A_55_P2052290	*Psat1*	NM_177420	ref|Mus musculus phosphoserine aminotransferase 1 mRNA
11.23	1.554	1.00E-05	A_55_P2005984	*Wfdc15b*	NM_138685	ref|Mus musculus WAP four-disulfide core domain 15B transcript variant 1 mRNA
7.13	1.549	0	A_51_P108581	*Adrbk2*	NM_177078	ref|Mus musculus adrenergic receptor kinase beta 2 transcript variant 1 mRNA
9.07	1.547	2.00E-05	A_52_P679105	*Prss23*	NM_029614	ref|Mus musculus protease serine 23 mRNA
8.24	1.537	1.00E-05	A_51_P516085	*Dntt*	NM_009345	ref|Mus musculus deoxynucleotidyltransferase terminal transcript variant 1 mRNA
7.86	1.537	8.00E-05	A_52_P456750	*Aph1b*	NM_177583	ref|Mus musculus anterior pharynx defective 1b homolog (C. elegans) mRNA
8.85	1.528	3.00E-05	A_52_P312102	*Sema3g*	ENSMUST00000090180	ens|Semaphorin-3G Precursor [Source:UniProtKB/Swiss-Prot;Acc:Q4LFA9]
8.77	1.527	1.00E-04	A_55_P2018417	*Osbpl3*	NM_001163645	ref|Mus musculus oxysterol binding protein-like 3 transcript variant 2 mRNA
7.07	1.515	0.00024	A_55_P2157093	*Bcl2l14*	NM_025778	ref|Mus musculus BCL2-like 14 (apoptosis facilitator) mRNA
9.46	1.507	0	A_51_P255456	*Cyp1b1*	NM_009994	ref|Mus musculus cytochrome P450 family 1 subfamily b polypeptide 1 mRNA
8.50	1.488	0	A_52_P18765	*Hsbp1l1*	NM_001136181	ref|Mus musculus heat shock factor binding protein 1-like 1 mRNA
8.35	1.476	8.00E-05	A_51_P201982	*Angpt2*	NM_007426	ref|Mus musculus angiopoietin 2 mRNA
7.90	1.475	3.00E-04	A_51_P146560	*Msln*	NM_018857	ref|Mus musculus mesothelin mRNA
7.21	1.470	0.00116	A_52_P381484	*Spon2*	NM_133903	ref|Mus musculus spondin 2 extracellular matrix protein mRNA
7.15	1.466	8.00E-05	A_55_P1984881	*1700024P16Rik*	NM_001162980	ref|Mus musculus RIKEN cDNA 1700024P16 gene mRNA
7.93	1.465	0.00014	A_55_P2019684	*Bspry*	NM_138653	ref|Mus musculus B-box and SPRY domain containing mRNA

10.45	1.463	2.00E-04	A_55_P1980125	*Sfrs3*	NM_013663	ref|Mus musculus splicing factor arginine/serine-rich 3 (SRp20) mRNA
7.23	1.459	0.00016	A_51_P108581	*Adrbk2*	NM_177078	ref|Mus musculus adrenergic receptor kinase beta 2 transcript variant 1 mRNA
8.69	1.455	0.00072	A_55_P2168823	*NAP111644-1*	NAP111644-1	Unknown
8.82	1.445	3.00E-05	A_55_P1987645	*Unc13b*	NM_001081413	ref|Mus musculus unc-13 homolog B (C. elegans) mRNA
7.06	1.442	0.00017	A_51_P108581	*Adrbk2*	NM_177078	ref|Mus musculus adrenergic receptor kinase beta 2 transcript variant 1 mRNA
9.23	1.431	0.00012	A_55_P2117741	*Nck2*	NM_010879	ref|Mus musculus non-catalytic region of tyrosine kinase adaptor protein 2 mRNA
9.75	1.426	3.00E-05	A_55_P2092826	*Anxa1*	NM_010730	ref|Mus musculus annexin A1 mRNA
8.84	1.425	7.00E-05	A_52_P670026	*Rsad2*	NM_021384	ref|Mus musculus radical S-adenosyl methionine domain containing 2 mRNA
10.40	1.420	0	A_52_P320193	*Clec2h*	NM_053165	ref|Mus musculus C-type lectin domain family 2 member h mRNA
10.46	1.410	0.00057	A_55_P2002903	*Smoc2*	NM_022315	ref|Mus musculus SPARC related modular calcium binding 2 mRNA
7.04	1.404	0.00039	A_51_P108581	*Adrbk2*	NM_177078	ref|Mus musculus adrenergic receptor kinase beta 2 transcript variant 1 mRNA
11.54	1.402	0	A_55_P1954718	*Cyb561*	NM_007805	ref|Mus musculus cytochrome b-561 mRNA
8.61	1.398	2.00E-05	A_55_P2110351	*Eppk1*	NM_144848	ref|Mus musculus epiplakin 1 mRNA
9.60	1.393	9.00E-05	A_51_P450278	*2010003K11Rik*	NM_027237	ref|Mus musculus RIKEN cDNA 2010003K11 gene mRNA
7.18	1.387	0.00011	A_55_P1969650	*Rasgrp1*	NM_011246	ref|Mus musculus RAS guanyl releasing protein 1 mRNA
11.92	1.386	5.00E-05	A_66_P129048	*2610002J02Rik*	NM_001033134	ref|Mus musculus RIKEN cDNA 2610002J02 gene mRNA
8.24	1.371	0.00054	A_55_P2094060	*Gzma*	NM_010370	ref|Mus musculus granzyme A mRNA
7.47	1.370	0.00085	A_55_P1978502	*H2-Q1*	NM_010390	ref|Mus musculus histocompatibility 2 Q region locus 1 mRNA
8.37	1.364	8.00E-05	A_55_P2047330	*LOC554292*	NM_001024672	ref|Mus musculus UbiE-YGHL1 fusion protein mRNA
7.57	1.352	2.00E-04	A_55_P2073377	*Mki67*	NM_001081117	ref|Mus musculus antigen identified by monoclonal antibody Ki 67 mRNA
7.68	1.352	0.00022	A_55_P1982291	*Clca1*	NM_009899	ref|Mus musculus chloride channel calcium activated 1 mRNA
9.18	1.345	0.00021	A_55_P2055537	*Slc16a6*	NM_001029842	ref|Mus musculus solute carrier family 16 (monocarboxylic acid transporters) member 6 transcript variant 1 mRNA
9.46	1.344	0.00085	A_51_P371750	*Marco*	NM_010766	ref|Mus musculus macrophage receptor with collagenous structure mRNA
8.04	1.324	4.00E-05	A_52_P228236	*Tfrc*	NM_011638	ref|Mus musculus transferrin receptor mRNA
8.02	1.322	0.00038	A_51_P253803	*Mki67*	NM_001081117	ref|Mus musculus antigen identified by monoclonal antibody Ki 67 mRNA
7.51	1.321	2.00E-05	A_52_P281033	*Socs5*	NM_019654	ref|Mus musculus suppressor of cytokine signaling 5 mRNA
9.40	1.318	0.00074	A_52_P499907	*Kcnj1*	NM_019659	ref|Mus musculus potassium inwardly-rectifying channel subfamily J member 1 transcript variant 2 mRNA
8.16	1.316	1.00E-05	A_55_P1958165	*Ms4a7*	NM_001025610	ref|Mus musculus membrane-spanning 4-domains subfamily A member 7 transcript variant 2 mRNA
11.03	1.314	1.00E-05	A_55_P1968433	*Agpat9*	NM_172715	ref|Mus musculus 1-acylglycerol-3-phosphate O-acyltransferase 9 transcript variant 1 mRNA
10.06	1.304	0.00011	A_55_P2013586	*Prss8*	NM_133351	ref|Mus musculus protease serine 8 (prostasin) mRNA
11.32	1.298	0.00022	A_55_P2115582	*Slc20a1*	NM_015747	ref|Mus musculus solute carrier family 20 member 1 transcript variant 1 mRNA
10.13	1.298	0	A_55_P1998943	*Oas1a*	NM_145211	ref|Mus musculus 2'-5' oligoadenylate synthetase 1A mRNA

7.86	1.298	0.00097	A_55_P2085779	*Ifi27l2b*	NM_145449	ref|Mus musculus interferon alpha-inducible protein 27 like 2B mRNA
10.10	1.297	0.00011	A_51_P204740	*Cd34*	NM_133654	ref|Mus musculus CD34 antigen transcript variant 2 mRNA
8.89	1.295	0	A_51_P114878	*Ikbkap*	NM_026079	ref|Mus musculus inhibitor of kappa light polypeptide enhancer in B-cells kinase complex-associated protein mRNA
11.11	1.288	1.00E-05	A_52_P561936	*1110002B05Rik*	NM_134054	ref|Mus musculus RIKEN cDNA 1110002B05 gene mRNA
7.65	1.285	3.00E-05	A_55_P2178578	*Tmprss4*	NM_145403	ref|Mus musculus transmembrane protease serine 4 mRNA
7.09	1.284	0.00012	A_55_P2119917	*Ikzf4*	NM_011772	ref|Mus musculus IKAROS family zinc finger 4 mRNA
7.44	1.280	3.00E-05	A_51_P128463	*Grrp1*	NM_001099296	ref|Mus musculus glycine/arginine rich protein 1 mRNA
8.83	1.279	1.00E-05	A_66_P119518	*Tuba8*	NM_017379	ref|Mus musculus tubulin alpha 8 mRNA
8.71	1.278	0.00015	A_51_P114878	*Ikbkap*	NM_026079	ref|Mus musculus inhibitor of kappa light polypeptide enhancer in B-cells kinase complex-associated protein mRNA
9.28	1.278	0.00032	A_51_P502119	*F11*	NM_028066	ref|Mus musculus coagulation factor XI mRNA
9.04	1.275	1.00E-05	A_51_P519555	*Gnb1l*	NM_023120	ref|Mus musculus guanine nucleotide binding protein (G protein) beta polypeptide 1-like transcript variant 2 mRNA
9.31	1.269	0.00011	A_52_P142191	*Aph1b*	NM_177583	ref|Mus musculus anterior pharynx defective 1b homolog (C. elegans) mRNA
9.94	1.268	2.00E-05	A_52_P341449	*Pgm3*	NM_028352	ref|Mus musculus phosphoglucomutase 3 transcript variant 1 mRNA
12.64	1.267	6.00E-05	A_51_P268529	*Csad*	NM_144942	ref|Mus musculus cysteine sulfinic acid decarboxylase mRNA
7.49	1.265	0.00012	A_51_P158210	*Mcm2*	NM_008564	ref|Mus musculus minichromosome maintenance deficient 2 mitotin (S. cerevisiae) mRNA
8.56	1.260	1.00E-05	A_51_P118132	*Skil*	NM_011386	ref|Mus musculus SKI-like transcript variant 1 mRNA
8.30	1.257	0.00121	A_51_P191354	*Acot6*	ENSMUST00000056822	ens|Acyl-coenzyme A thioesterase 6 (Acyl-CoA thioesterase 6)(EC 3.1.2.-) [Source:UniProtKB/Swiss-Prot;Acc:Q32Q92]
10.09	1.254	2.00E-05	A_55_P1954266	*Zfp672*	NM_178761	ref|Mus musculus zinc finger protein 672 transcript variant 1 mRNA
14.03	1.251	0.00024	A_55_P1973809	*Hbb-b1*	NM_008220	ref|Mus musculus hemoglobin beta adult major chain mRNA
10.50	1.246	1.00E-04	A_55_P2177614	*Sfrs3*	NM_013663	ref|Mus musculus splicing factor arginine/serine-rich 3 mRNA
10.27	1.243	3.00E-05	A_55_P1962305	*Plac8*	NM_139198	ref|Mus musculus placenta-specific 8 mRNA
13.08	1.240	0.00016	A_55_P2003483	*Gldc*	NM_138595	ref|Mus musculus glycine decarboxylase mRNA
9.43	1.238	0.00016	A_55_P2033272	*Treh*	NM_021481	ref|Mus musculus trehalase (brush-border membrane glycoprotein) mRNA
7.74	1.236	8.00E-05	A_55_P1955309	*Zfp800*	NM_001081678	ref|Mus musculus zinc finger protein 800 mRNA
7.04	1.236	6.00E-04	A_51_P108581	*Adrbk2*	NM_177078	ref|Mus musculus adrenergic receptor kinase beta 2 transcript variant 1 mRNA
7.89	1.233	0.00032	A_55_P1997604	*Pla2g4a*	NM_008869	ref|Mus musculus phospholipase A2 group IVA (cytosolic calcium-dependent) mRNA
8.12	1.231	5.00E-05	A_55_P2004801	*Tacc3*	NM_001040435	ref|Mus musculus transforming acidic coiled-coil containing protein 3 mRNA
10.51	1.231	0	A_51_P396752	*Arl2bp*	NM_024191	ref|Mus musculus ADP-ribosylation factor-like 2 binding protein transcript variant 1 mRNA
8.57	1.229	0.00138	A_55_P1983773	*Birc5*	NM_001012273	ref|Mus musculus baculoviral IAP repeat-containing 5 transcript variant 3 mRNA

11.88	1.228	1.00E-05	A_55_P2003793	*Tspan3*	NM_019793	ref|Mus musculus tetraspanin 3 mRNA
8.65	1.224	1.00E-05	A_55_P2097259	*ENSMUST00000065640*	ENSMUST00000065640	ens|Zinc finger with UFM1-specific peptidase domain protein [Source:UniProtKB/Swiss-Prot;Acc:Q3T9Z9]
12.96	1.220	4.00E-05	A_55_P2038540	*Hbb-b2*	NM_016956	ref|Mus musculus hemoglobin beta adult minor chain mRNA
7.48	1.218	0.00111	A_51_P397296	*Marveld3*	NM_028584	ref|Mus musculus MARVEL (membrane-associating) domain containing 3 transcript variant 1 mRNA
7.12	1.216	1.00E-04	A_51_P108581	*Adrbk2*	NM_177078	ref|Mus musculus adrenergic receptor kinase beta 2 transcript variant 1 mRNA
10.99	1.215	0.00069	A_51_P392687	*Vim*	NM_011701	ref|Mus musculus vimentin mRNA
10.03	1.215	0.00088	A_51_P421140	*Tubb6*	NM_026473	ref|Mus musculus tubulin beta 6 mRNA
11.24	1.214	5.00E-05	A_51_P353252	*Mal2*	NM_178920	ref|Mus musculus mal T-cell differentiation protein 2 mRNA
8.15	1.212	0.00062	A_55_P1962918	*Mnda*	NM_001033450	ref|Mus musculus myeloid cell nuclear differentiation antigen mRNA
7.81	1.196	5.00E-05	A_51_P165914	*Zfp770*	NM_175466	ref|Mus musculus zinc finger protein 770 mRNA
11.74	1.194	3.00E-05	A_55_P1975420	*Dhx40*	NM_026191	ref|Mus musculus DEAH (Asp-Glu-Ala-His) box polypeptide 40 mRNA
9.34	1.193	1.00E-05	A_51_P134262	*1700052K11Rik*	NR_027956	ref|Mus musculus RIKEN cDNA 1700052K11 gene non-coding RNA
9.00	1.188	9.00E-05	A_66_P107585	*Taf2*	NM_001081288	ref|Mus musculus TAF2 RNA polymerase II TATA box binding protein (TBP)-associated factor mRNA
11.54	1.188	0	A_55_P1983177	*Acsl4*	NM_207625	ref|Mus musculus acyl-CoA synthetase long-chain family member 4 transcript variant 1 mRNA
7.03	1.187	3.00E-05	A_55_P1955308	*Sirpb1*	NM_001002898	ref|Mus musculus signal-regulatory protein beta 1 transcript variant 3 mRNA
8.76	1.185	0.00171	A_55_P2013823	*Gal3st1*	NM_016922	ref|Mus musculus galactose-3-O-sulfotransferase 1 (mRNA
7.95	1.182	6.00E-05	A_55_P1961335	*Ctsk*	NM_007802	ref|Mus musculus cathepsin K mRNA
7.34	1.181	2.00E-05	A_51_P150087	*Abhd10*	NM_172511	ref|Mus musculus abhydrolase domain containing 10 mRNA
10.40	1.177	1.00E-05	A_66_P121787	*Samd9l*	NM_010156	ref|Mus musculus sterile alpha motif domain containing 9-like mRNA
10.78	1.175	0.00035	A_55_P1964638	*Cxadr*	NM_001025192	ref|Mus musculus coxsackie virus and adenovirus receptor transcript variant 1 mRNA
8.48	1.175	3.00E-05	A_55_P2052062	*Cd200*	NM_010818	ref|Mus musculus CD200 antigen mRNA
14.94	1.174	0.00087	A_51_P110301	*C3*	NM_009778	ref|Mus musculus complement component 3 mRNA
8.99	1.173	0.00045	A_55_P2059382	*Arl6*	NM_019665	ref|Mus musculus ADP-ribosylation factor-like 6 mRNA
8.11	1.169	0.00016	A_55_P2119985	*Baiap2*	NM_130862	ref|Mus musculus brain-specific angiogenesis inhibitor 1-associated protein 2 transcript variant 2 mRNA
7.64	1.167	5.00E-04	A_52_P390944	*Chst3*	NM_016803	ref|Mus musculus carbohydrate (chondroitin 6/keratan) sulfotransferase 3 mRNA
7.16	1.165	0.00039	A_51_P452153	*2010001M09Rik*	NM_027222	ref|Mus musculus RIKEN cDNA 2010001M09 gene mRNA
9.44	1.157	1.00E-05	A_55_P2012296	*Gopc*	NM_053187	ref|Mus musculus golgi associated PDZ and coiled-coil motif containing mRNA
10.01	1.152	1.00E-05	A_55_P1989858	*Thrap3*	BC040346	gb|Mus musculus thyroid hormone receptor associated protein 3 mRNA (cDNA clone IMAGE:3498255) with apparent retained intron
10.38	1.152	3.00E-05	A_55_P2071271	*3110003A17Rik*	NM_028440	ref|Mus musculus RIKEN cDNA 3110003A17 gene mRNA
9.78	1.151	0.00016	A_51_P251357	*Ctps*	NM_016748	ref|Mus musculus cytidine 5'-triphosphate synthase mRNA
8.15	1.151	3.00E-05	A_55_P2020497	*Dcaf12l1*	NM_178739	ref|Mus musculus DDB1 and CUL4 associated factor 12-like 1 mRNA

8.58	1.149	0.00011	A_55_P2078460	*NAP111472-1*	NAP111472-1	Unknown
8.48	1.148	0.00049	A_55_P2126552	*Zdhhc13*	NM_028031	ref|Mus musculus zinc finger DHHC domain containing 13 mRNA
8.72	1.147	0.00025	A_52_P479262	*ENSMUST00000066153*	ENSMUST00000066153	ens|Collagen alpha3(VI) Precursor; Fragment [Source:UniProtKB/TrEMBL;Acc:Q9Z0I9]
7.88	1.147	0.00029	A_51_P257885	*Mmd2*	NM_175217	ref|Mus musculus monocyte to macrophage differentiation-associated 2 mRNA
7.46	1.146	4.00E-05	A_52_P481279	*Gm1060*	NM_001033460	ref|Mus musculus predicted gene 1060 mRNA
7.40	1.143	0.00015	A_55_P2068977	*Armcx3*	NM_027870	ref|Mus musculus armadillo repeat containing X-linked 3 mRNA
8.10	1.143	0.00033	A_55_P2061170	*Tbc1d2*	NM_198664	ref|Mus musculus TBC1 domain family member 2 mRNA
7.22	1.142	0.00012	A_51_P307741	*Cckar*	NM_009827	ref|Mus musculus cholecystokinin A receptor mRNA
7.58	1.139	7.00E-05	A_51_P363556	*Abi2*	NM_198127	ref|Mus musculus abl-interactor 2 mRNA
8.81	1.138	4.00E-05	A_55_P1978103	*Hisppd1*	NM_173760	ref|Mus musculus histidine acid phosphatase domain containing 1 mRNA
8.74	1.136	2.00E-04	A_51_P114878	*Ikbkap*	NM_026079	ref|Mus musculus inhibitor of kappa light polypeptide enhancer in B-cells kinase complex-associated protein mRNA
14.96	1.135	0.00179	A_51_P110301	*C3*	NM_009778	ref|Mus musculus complement component 3 mRNA
7.86	1.135	0.00059	A_51_P173709	*Gprc5b*	NM_022420	ref|Mus musculus G protein-coupled receptor family C group 5 member B mRNA
7.21	1.130	0.00012	A_52_P338066	*Ubd*	NM_023137	ref|Mus musculus ubiquitin D mRNA
7.40	1.130	0.00083	A_52_P625808	*Sf3b1*	NM_031179	ref|Mus musculus splicing factor 3b subunit 1 mRNA
9.26	1.130	1.00E-05	A_51_P511949	*Setd7*	NM_080793	ref|Mus musculus SET domain containing (lysine methyltransferase) 7 mRNA
8.72	1.127	3.00E-05	A_51_P193000	*Bbs4*	NM_175325	ref|Mus musculus Bardet-Biedl syndrome 4 (human) mRNA
8.30	1.126	0.00044	A_55_P2011341	*LOC100045268*	XM_001474162	ref|PREDICTED: Mus musculus similar to precursor (AA -28 to 232) mRNA
8.33	1.124	0.00054	A_51_P462428	*Galntl2*	ENSMUST00000022460	ens|Polypeptide N-acetylgalactosaminyltransferase-like protein 2 (EC 2.4.1.41)(Polypeptide GalNAc transferase-like protein 2)(pp-GaNTase-like protein 2)(GalNAc-T-like protein 2)(Protein-UDP acetylgalactosaminyltransferase-like protein 2)(UDP-GalNAc:polype
9.73	1.124	1.00E-05	A_52_P495104	*LOC100045753*	XM_001474871	ref|PREDICTED: Mus musculus similar to headcase homolog mRNA
7.03	1.122	8.00E-05	A_55_P2033041	*LOC100038947*	XM_001471956	ref|PREDICTED: Mus musculus similar to SIRP beta 1 cell surface protein mRNA
7.17	1.121	5.00E-05	A_55_P2174816	*5730601F06Rik*	NM_001082485	ref|Mus musculus RIKEN cDNA 5730601F06 gene transcript variant 1 mRNA
8.33	1.121	0.00033	A_52_P583458	*E2f3*	NM_010093	ref|Mus musculus E2F transcription factor 3 mRNA
10.63	1.119	4.00E-05	A_51_P360492	*Mcm6*	NM_008567	ref|Mus musculus minichromosome maintenance deficient 6 (MIS5 homolog S. pombe) (S. cerevisiae) mRNA
10.11	1.117	0.00096	A_55_P1998416	*Ifi47*	NM_008330	ref|Mus musculus interferon gamma inducible protein 47 mRNA
8.44	1.117	0.00011	A_55_P1981205	*Xrcc4*	NM_028012	ref|Mus musculus X-ray repair complementing defective repair in Chinese hamster cells 4 mRNA
8.23	1.117	0	A_51_P154842	*Oas1f*	NM_145153	ref|Mus musculus 2'-5' oligoadenylate synthetase 1F mRNA
10.56	1.115	0.00018	A_51_P169745	*Tuba1a*	NM_011653	ref|Mus musculus tubulin alpha 1A mRNA
8.52	1.112	0.00033	A_55_P2183597	*Tbc1d2*	NM_198664	ref|Mus musculus TBC1 domain family member 2 mRNA
10.72	1.111	0.0015	A_52_P38627	*Egf*	NM_010113	ref|Mus musculus epidermal growth factor mRNA

7.50	1.111	0.00165	A_66_P120603	*Trps1*	NM_032000	ref|Mus musculus trichorhinophalangeal syndrome I (human) mRNA
7.74	1.110	8.00E-05	A_55_P2116054	*Caprin1*	NM_016739	ref|Mus musculus cell cycle associated protein 1 transcript variant 1 mRNA
10.56	1.109	4.00E-05	A_52_P574697	*Khdrbs1*	NM_011317	ref|Mus musculus KH domain containing RNA binding signal transduction associated 1 mRNA
10.46	1.108	2.00E-05	A_51_P386810	*Gmppb*	NM_177910	ref|Mus musculus GDP-mannose pyrophosphorylase B mRNA
7.16	1.106	0.00053	A_51_P452629	*Tlr2*	NM_011905	ref|Mus musculus toll-like receptor 2 mRNA
12.61	1.106	6.00E-05	A_55_P1989452	*Nenf*	NM_025424	ref|Mus musculus neuron derived neurotrophic factor mRNA
14.74	1.104	0.00164	A_51_P110301	*C3*	NM_009778	ref|Mus musculus complement component 3 mRNA
8.30	1.103	5.00E-05	A_51_P442097	*Slc41a3*	NM_027868	ref|Mus musculus solute carrier family 41 member 3 transcript variant 1 mRNA
8.48	1.101	0.00156	A_51_P126437	*Enc1*	NM_007930	ref|Mus musculus ectodermal-neural cortex 1 mRNA
11.96	1.101	1.00E-04	A_55_P2123471	*Kpna2*	NM_010655	ref|Mus musculus karyopherin (importin) alpha 2 mRNA
11.09	1.101	7.00E-05	A_55_P2027278	*Gas2l1*	NM_030228	ref|Mus musculus growth arrest-specific 2 like 1 transcript variant alpha mRNA
9.79	1.101	5.00E-05	A_55_P2146177	*Cerk*	NM_145475	ref|Mus musculus ceramide kinase mRNA
10.11	1.099	1.00E-04	A_66_P118256	*Strn3*	AK040913	gb|Mus musculus adult male aorta and vein cDNA RIKEN full-length enriched library clone:A530044I19 product:nuclear autoantigen full insert sequence
8.76	1.098	8.00E-05	A_55_P2059904	*Chsy1*	NM_001081163	ref|Mus musculus chondroitin sulfate synthase 1 mRNA
9.11	1.097	4.00E-05	A_55_P1971889	*F3*	NM_010171	ref|Mus musculus coagulation factor III mRNA
16.62	1.094	0.00057	A_55_P1962299	*Hba-a2*	NM_001083955	ref|Mus musculus hemoglobin alpha adult chain 2 mRNA
9.86	1.090	0.00033	A_52_P638459	*Ccl5*	NM_013653	ref|Mus musculus chemokine (C-C motif) ligand 5 mRNA
8.81	1.088	0.00106	A_55_P1983448	*S100a4*	NM_011311	ref|Mus musculus S100 calcium binding protein A4 mRNA
11.56	1.086	0.00097	A_51_P391616	*Agxt2l1*	NM_027907	ref|Mus musculus alanine-glyoxylate aminotransferase 2-like 1 transcript variant 1 mRNA
8.39	1.085	0.00025	A_66_P124179	*Atp6v0d2*	NM_175406	ref|Mus musculus ATPase H+ transporting lysosomal V0 subunit D2 mRNA
11.53	1.083	2.00E-05	A_51_P434198	*Anapc4*	NM_024213	ref|Mus musculus anaphase promoting complex subunit 4 mRNA
14.91	1.082	0.00122	A_51_P462385	*G6pc*	NM_008061	ref|Mus musculus glucose-6-phosphatase catalytic mRNA
8.74	1.080	2.00E-04	A_51_P114878	*Ikbkap*	NM_026079	ref|Mus musculus inhibitor of kappa light polypeptide enhancer in B-cells kinase complex-associated protein mRNA
10.95	1.079	2.00E-05	A_66_P112853	*Eif1a*	NM_010120	ref|Mus musculus eukaryotic translation initiation factor 1A mRNA
9.03	1.078	5.00E-05	A_51_P196844	*Osbpl3*	NM_027881	ref|Mus musculus oxysterol binding protein-like 3 transcript variant 1 mRNA
9.33	1.078	0.00032	A_55_P2046509	*Amot*	NM_153319	ref|Mus musculus angiomotin mRNA
8.33	1.077	1.00E-05	A_51_P114878	*Ikbkap*	NM_026079	ref|Mus musculus inhibitor of kappa light polypeptide enhancer in B-cells kinase complex-associated protein mRNA
12.27	1.077	1.00E-05	A_55_P2000823	*Rbm39*	NM_133242	ref|Mus musculus RNA binding motif protein 39 mRNA
9.61	1.075	0.00036	A_55_P2108248	*Art4*	NM_026639	ref|Mus musculus ADP-ribosyltransferase 4 mRNA
12.45	1.075	4.00E-05	A_51_P122246	*Creld2*	NM_029720	ref|Mus musculus cysteine-rich with EGF-like domains 2 mRNA

10.48	1.072	7.00E-04	A_52_P257812	*Lpl*	NM_008509	ref|Mus musculus lipoprotein lipase mRNA
12.12	1.071	0.00021	A_55_P1984830	*Fgl1*	NM_145594	ref|Mus musculus fibrinogen-like protein 1 mRNA
7.52	1.071	0.00013	A_52_P49321	*Adamts9*	NM_175314	ref|Mus musculus a disintegrin-like and metallopeptidase (reprolysin type) with thrombospondin type 1 motif 9 mRNA
11.95	1.070	0.00019	A_51_P146149	*Napsa*	NM_008437	ref|Mus musculus napsin A aspartic peptidase mRNA
9.27	1.067	0.00022	A_55_P2169415	*Cgn*	NM_001037711	ref|Mus musculus cingulin mRNA
9.28	1.067	1.00E-04	A_51_P388298	*Mmachc*	NM_025962	ref|Mus musculus methylmalonic aciduria cblC type with homocystinuria mRNA
11.18	1.067	1.00E-05	A_52_P469381	*Comtd1*	NM_026965	ref|Mus musculus catechol-O-methyltransferase domain containing 1 mRNA
7.96	1.067	6.00E-05	A_65_P11306	*Gm4944*	XM_973961	ref|PREDICTED: Mus musculus predicted gene EG240038 mRNA
8.39	1.056	0.00022	A_51_P444437	*Ptgr1*	NM_025968	ref|Mus musculus prostaglandin reductase 1 mRNA
7.13	1.052	0.00025	A_51_P452153	*2010001M09Rik*	NM_027222	ref|Mus musculus RIKEN cDNA 2010001M09 gene mRNA
10.89	1.052	0.00043	A_55_P2046037	*Gm7083*	XM_001475231	ref|PREDICTED: Mus musculus predicted gene EG632248 mRNA
8.50	1.051	0.00056	A_55_P2119892	*Erbb4*	ENSMUST00000121473	ens|Receptor tyrosine-protein kinase erbB-4 Precursor (EC 2.7.10.1) [Source:UniProtKB/Swiss-Prot;Acc:Q61527]
12.80	1.051	0.00028	A_55_P2020577	*Pcolce*	NM_008788	ref|Mus musculus procollagen C-endopeptidase enhancer protein mRNA
10.31	1.051	5.00E-05	A_51_P200561	*4930506M07Rik*	NM_175172	ref|Mus musculus RIKEN cDNA 4930506M07 gene transcript variant 2 mRNA
7.12	1.050	0.00134	A_55_P2039541	*Arhgap15*	NM_153820	ref|Mus musculus Rho GTPase activating protein 15 transcript variant 1 mRNA
7.11	1.050	0.00052	A_55_P2002773	*Gm2942*	XM_001475175	ref|PREDICTED: Mus musculus hypothetical protein LOC100040747 mRNA
10.25	1.048	1.00E-05	A_55_P2043554	*Slc12a4*	NM_009195	ref|Mus musculus solute carrier family 12 member 4 mRNA
9.97	1.048	0.00083	A_55_P2022074	*Klf10*	NM_013692	ref|Mus musculus Kruppel-like factor 10 mRNA
12.46	1.047	6.00E-05	A_55_P2183015	*P2rx4*	NM_011026	ref|Mus musculus purinergic receptor P2X ligand-gated ion channel 4 mRNA
8.49	1.045	2.00E-05	A_51_P355040	*Nsun3*	ENSMUST00000063089	ens|Putative methyltransferase NSUN3 (EC 2.1.1.-)(NOL1/NOP2/Sun domain family member 3) [Source:UniProtKB/Swiss-Prot;Acc:Q8CCT7]
15.01	1.043	0.00192	A_51_P110301	*C3*	NM_009778	ref|Mus musculus complement component 3 mRNA
8.05	1.042	0.00023	A_52_P228236	*Tfrc*	NM_011638	ref|Mus musculus transferrin receptor mRNA
8.48	1.042	0.00131	A_55_P2003638	*Stxbp6*	NM_144552	ref|Mus musculus syntaxin binding protein 6 (amisyn) mRNA
7.38	1.04	8.00E-05	A_55_P2001198	*ENSMUST00000042146*	ENSMUST00000042146	ens|Syntaxin-18 [Source:UniProtKB/Swiss-Prot;Acc:Q8VDS8] [ENSMUST00000042146]
7.07	1.038	0.00104	A_55_P2335529	*4921531C22Rik*	AK076601	gb|Mus musculus adult male testis cDNA RIKEN full-length enriched library clone:4921531C22 product:hypothetical protein full insert sequence
7.34	1.036	0.00087	A_55_P2096933	*Cntln*	NM_177385	ref|Mus musculus centlein centrosomal protein transcript variant 2 mRNA
10.47	1.035	0.00025	A_55_P2007470	*Pdgfa*	NM_008808	ref|Mus musculus platelet derived growth factor alpha mRNA
7.25	1.035	5.00E-05	A_51_P452153	*2010001M09Rik*	NM_027222	ref|Mus musculus RIKEN cDNA 2010001M09 gene mRNA
10.75	1.034	0.00026	A_55_P2022211	*Plxdc2*	NM_026162	ref|Mus musculus plexin domain containing 2 mRNA
10.39	1.031	5.00E-05	A_55_P1969645	*Sdcbp*	NM_001098227	ref|Mus musculus syndecan binding protein transcript variant 1 mRNA

7.57	1.030	0.00015	A_55_P2178862	*2610101N10Rik*	NM_001114977	ref|Mus musculus RIKEN cDNA 2610101N10 gene transcript variant 1 mRNA
8.47	1.025	0.00088	A_51_P126437	*Enc1*	NM_007930	ref|Mus musculus ectodermal-neural cortex 1 mRNA
7.08	1.024	0.00093	A_52_P436447	*Slc25a35*	NM_028048	ref|Mus musculus solute carrier family 25 member 35 mRNA
10.16	1.022	1.00E-05	A_51_P349192	*2210013O21Rik*	NR_028432	ref|Mus musculus RIKEN cDNA 2210013O21 gene non-coding RNA
7.26	1.021	2.00E-04	A_51_P241667	*Prkdc*	NM_011159	ref|Mus musculus protein kinase DNA activated catalytic polypeptide mRNA
8.66	1.021	4.00E-05	A_51_P114878	*Ikbkap*	NM_026079	ref|Mus musculus inhibitor of kappa light polypeptide enhancer in B-cells kinase complex-associated protein mRNA
7.08	1.017	0.0018	A_55_P2033055	*Pdp1*	NM_001098230	ref|Mus musculus pyruvate dehyrogenase phosphatase catalytic subunit 1 nuclear gene encoding mitochondrial protein transcript variant 2 mRNA
7.58	1.012	0.00025	A_52_P228236	*Tfrc*	NM_011638	ref|Mus musculus transferrin receptor mRNA
9.92	1.011	0.00026	A_55_P2029842	*Hnrnpa1*	NM_001039129	ref|Mus musculus heterogeneous nuclear ribonucleoprotein A1 transcript variant 2 mRNA
11.11	1.005	0.00016	A_55_P2055557	*Sdsl*	NM_133902	ref|Mus musculus serine dehydratase-like mRNA
8.55	1.004	5.00E-05	A_55_P2106039	*Map3k6*	NM_016693	ref|Mus musculus mitogen-activated protein kinase kinase kinase 6 mRNA
8.68	1.004	0.00158	A_55_P2173892	*Isg20*	NM_020583	ref|Mus musculus interferon-stimulated protein transcript variant 1 mRNA
9.31	1.000	7.00E-04	A_51_P511482	*Ift57*	NM_028680	ref|Mus musculus intraflagellar transport 57 homolog (Chlamydomonas) mRNA

Table 88. All significantly down regulated genes in livers of female *Ahr* knockout by TCDD (25 µg/kg bw) identified by microarray analysis - mouse 5 days study. Selected parameters: A-value ≥ 7, log2 fc ≥ 1, p-value ≤ 0.05.

A	Log2 fc	p-value	Probe name	Gene name	Systematic name	Gene description
7.70	-4.345	0	A_52_P293682	*Gm7231*	XM_001477336	ref|PREDICTED: Mus musculus predicted gene EG638251 mRNA
8.58	-3.964	0	A_52_P218833	*Gm5584*	NM_001101534	ref|Mus musculus predicted gene 5584 mRNA
9.60	-3.712	0	A_55_P2113587	*ENSMUST00000107481*	ENSMUST00000107481	tc|MUP4_MOUSE (P11590) Major urinary protein 4 precursor partial (69%)
13.16	-3.561	0.00013	A_55_P1979904	*Mup9*	NM_001126319	ref|Mus musculus major urinary protein 9 mRNA
11.49	-3.482	9.00E-05	A_52_P412506	*Mup5*	NM_008649	ref|Mus musculus major urinary protein 5 mRNA
9.39	-3.459	0.00023	A_55_P1952507	*Gm5584*	NM_001101534	ref|Mus musculus predicted gene 5584 mRNA
10.14	-3.446	2.00E-05	A_55_P2033321	*ENSMUST00000107490*	ENSMUST00000107490	gb|uo03b07.y1 Sugano mouse liver mlia Mus musculus cDNA clone IMAGE:2582293 5' similar to gb:M16358 Mouse major urinary protein IV (MOUSE);
7.75	-3.385	0	A_55_P2103703	*LOC635091*	XM_001475400	ref|PREDICTED: Mus musculus similar to Predicted gene OTTMUSG00000007485 mRNA
9.76	-3.370	0	A_55_P2107223	*Gm6957*	NM_001081325	ref|Mus musculus predicted gene 6957 mRNA
10.23	-3.229	0	A_55_P2172532	*C730007P19Rik*	NM_009286	ref|Mus musculus RIKEN cDNA C730007P19 gene mRNA
10.75	-3.224	0.00079	A_55_P1952517	*Sult2a1*	NM_001111296	ref|Mus musculus sulfotransferase family 2A dehydroepiandrosterone (DHEA)-preferring member 1 mRNA
8.55	-3.218	0	A_55_P2046671	*CU104690.1*	XM_001477211	ref|PREDICTED: Mus musculus similar to Major urinary protein 1 mRNA
7.57	-3.182	0	A_52_P402127	*Mup9*	NM_001126319	ref|Mus musculus major urinary protein 9 mRNA
11.96	-3.160	0.00028	A_55_P2035029	*A_55_P2035029*	A_55_P2035029	Unknown
7.24	-3.019	1.00E-05	A_55_P2129449	*Sult3a1*	NM_020565	ref|Mus musculus sulfotransferase family 3A member 1 mRNA
12.02	-2.889	0.00121	A_55_P2051486	*Mup20*	NM_001012323	ref|Mus musculus major urinary protein 20 mRNA
7.10	-2.826	5.00E-05	A_52_P366803	*Cyp3a44*	NM_177380	ref|Mus musculus cytochrome P450 family 3 subfamily a polypeptide 44 mRNA
9.02	-2.800	1.00E-05	A_55_P2059586	*Fmo3*	NM_008030	ref|Mus musculus flavin containing monooxygenase 3 mRNA
7.13	-2.719	9.00E-05	A_55_P2116674	*A_55_P2116674*	A_55_P2116674	Unknown
12.62	-2.709	1.00E-04	A_55_P2010097	*Mup2*	NM_001045550	ref|Mus musculus major urinary protein 2 transcript variant 2 mRNA
7.67	-2.686	3.00E-05	A_55_P2061104	*Mup6*	NM_001081285	ref|Mus musculus major urinary protein 6 mRNA
8.47	-2.629	3.00E-05	A_55_P2004132	*Gm853*	NM_001034872	ref|Mus musculus predicted gene 853 mRNA
9.09	-2.592	0	A_51_P281333	*St3gal6*	NM_018784	ref|Mus musculus ST3 beta-galactoside alpha-23-sialyltransferase 6 mRNA
8.39	-2.588	0	A_55_P2075127	*Pax2*	NM_011037	ref|Mus musculus paired box gene 2 mRNA
8.46	-2.557	3.00E-05	A_52_P229981	*Osta*	NM_145932	ref|Mus musculus organic solute transporter alpha mRNA
7.55	-2.541	3.00E-05	A_52_P537827	*Wdr72*	NM_001033500	ref|Mus musculus WD repeat domain 72 mRNA
10.22	-2.515	1.00E-05	A_52_P289091	*Cyp2b13*	NM_007813	ref|Mus musculus cytochrome P450 family 2 subfamily b polypeptide 13 mRNA

9.93	-2.504	0.00119	A_55_P1989248	*Gm6168*	XM_885022	ref|PREDICTED: Mus musculus predicted gene EG620627 mRNA
10.45	-2.460	0	A_55_P2006008	*Serpinb1a*	NM_025429	ref|Mus musculus serine (or cysteine) peptidase inhibitor clade B member 1a mRNA
10.85	-2.396	0.00015	A_55_P1952512	*C730007P19Rik*	NM_009286	ref|Mus musculus RIKEN cDNA C730007P19 gene mRNA
10.55	-2.379	0	A_51_P269404	*Fmo3*	NM_008030	ref|Mus musculus flavin containing monooxygenase 3 mRNA
8.88	-2.339	0	A_52_P315976	*Tpm2*	NM_009416	ref|Mus musculus tropomyosin 2 beta mRNA
8.21	-2.324	0.00174	A_51_P333923	*Tspan1*	NM_133681	ref|Mus musculus tetraspanin 1 mRNA
9.71	-2.281	5.00E-05	A_55_P2079167	*Dnm1*	NM_010065	ref|Mus musculus dynamin 1 mRNA
11.15	-2.234	1.00E-05	A_55_P1960735	*Gdf15*	NM_011819	ref|Mus musculus growth differentiation factor 15 mRNA
7.23	-2.194	0.00095	A_51_P326685	*Lrtm1*	NM_176920	ref|Mus musculus leucine-rich repeats and transmembrane domains 1 mRNA
9.86	-2.185	0.00014	A_52_P595871	*Cyp1a2*	NM_009993	ref|Mus musculus cytochrome P450 family 1 subfamily a polypeptide 2 mRNA
10.33	-2.162	0.00111	A_51_P318830	*Syt10*	NM_018803	ref|Mus musculus synaptotagmin X mRNA
8.59	-2.146	8.00E-05	A_55_P1961466	*Dct*	NM_010024	ref|Mus musculus dopachrome tautomerase mRNA
9.86	-2.118	0.00064	A_55_P2048867	*Gm2922*	XM_001475122	ref|PREDICTED: Mus musculus hypothetical protein LOC100040715 mRNA
10.33	-2.111	0	A_55_P1983754	*Pcp4l1*	NM_025557	ref|Mus musculus Purkinje cell protein 4-like 1 mRNA
9.38	-2.056	1.00E-05	A_51_P224164	*Slc26a4*	NM_011867	ref|Mus musculus solute carrier family 26 member 4 mRNA
7.09	-2.012	0.00081	A_55_P2345853	*3830612M24*	AK028406	gb|Mus musculus 18 days pregnant adult female placenta and extra embryonic tissue cDNA RIKEN full-length enriched library clone:3830612M24 product:unclassifiable full insert sequence.
7.48	-2.012	0.00131	A_55_P2065919	*Macrod2*	ENSMUST00000110064	ens|MACRO domain-containing protein 2 [Source:UniProtKB/Swiss-Prot;Acc:Q3UYG8]
7.79	-2.004	0.00017	A_55_P2003053	*Dct*	NM_010024	ref|Mus musculus dopachrome tautomerase mRNA
8.100	-2.000	0.00079	A_55_P2065909	*Macrod2*	NM_001013802	ref|Mus musculus MACRO domain containing 2 transcript variant 1 mRNA
9.05	-1.973	0	A_55_P2121408	*Tpm2*	NM_009416	ref|Mus musculus tropomyosin 2 beta mRNA
8.51	-1.955	0.00032	A_55_P1973447	*LOC100045903*	XM_001475137	ref|PREDICTED: Mus musculus similar to Y box protein 2 mRNA
9.30	-1.948	0	A_55_P1963134	*Gm6135*	XM_895691	ref|PREDICTED: Mus musculus predicted gene EG620205 mRNA
7.80	-1.932	1.00E-05	A_55_P2007646	*Cryaa*	NM_013501	ref|Mus musculus crystallin alpha A mRNA
9.52	-1.900	7.00E-05	A_52_P1092823	*Irx1*	NM_010573	ref|Mus musculus Iroquois related homeobox 1 (Drosophila) mRNA
11.65	-1.858	0	A_66_P122086	*9030619P08Rik*	NM_001039720	ref|Mus musculus RIKEN cDNA 9030619P08 gene mRNA
9.92	-1.854	0	A_55_P2157586	*Gm4949*	XM_001478918	ref|PREDICTED: Mus musculus similar to glutamine synthetase mRNA
7.24	-1.836	8.00E-05	A_51_P466229	*Pdgfrl*	NM_026840	ref|Mus musculus platelet-derived growth factor receptor-like mRNA
9.46	-1.761	0	A_51_P164630	*Fitm1*	NM_026808	ref|Mus musculus fat storage-inducing transmembrane protein 1 mRNA
9.64	-1.750	0.00134	A_51_P468073	*Ggt1*	NM_008116	ref|Mus musculus gamma-glutamyltransferase 1 mRNA
9.49	-1.749	1.00E-05	A_55_P1955412	*Slc1a2*	NM_011393	ref|Mus musculus solute carrier family 1 (glial high affinity glutamate transporter) member 2 transcript variant 3 mRNA

7.50	-1.712	0.00094	A_52_P262219	*Fos*	NM_010234	ref|Mus musculus FBJ osteosarcoma oncogene mRNA
8.27	-1.703	0	A_55_P1994733	*ENSMUST00000027064*	ENSMUST00000027064	ens|Transmembrane protein 14A [Source:UniProtKB/Swiss-Prot;Acc:P56983]
7.49	-1.701	0.00037	A_52_P262219	*Fos*	NM_010234	ref|Mus musculus FBJ osteosarcoma oncogene mRNA
7.34	-1.689	5.00E-05	A_51_P469951	*Srgap3*	NM_080448	ref|Mus musculus SLIT-ROBO Rho GTPase activating protein 3 mRNA
10.89	-1.662	1.00E-05	A_55_P2046657	*Dio1*	NM_007860	ref|Mus musculus deiodinase iodothyronine type I mRNA
8.73	-1.641	0.00191	A_55_P2338200	*Glb1l2*	NM_153803	ref|Mus musculus galactosidase beta 1-like 2 mRNA
8.13	-1.633	0.00058	A_66_P106238	*Gm5106*	XM_001473563	ref|PREDICTED: Mus musculus predicted gene EG330031 mRNA
11.24	-1.631	0.00013	A_66_P101764	*ENSMUST00000066505*	ENSMUST00000066505	ens|Putative uncharacterized proteinMCG148307 ; [Source:UniProtKB/TrEMBL;Acc:Q8C950]
11.51	-1.626	1.00E-05	A_51_P498882	*Cyp2c37*	NM_010001	ref|Mus musculus cytochrome P450 family 2. subfamily c polypeptide 37 mRNA
9.60	-1.601	0	A_55_P2069907	*Acot3*	NM_134246	ref|Mus musculus acyl-CoA thioesterase 3 mRNA
9.93	-1.580	0.00061	A_55_P2121618	*Tox4*	NM_023434	ref|Mus musculus TOX high mobility group box family member 4 mRNA
7.94	-1.565	0.00099	A_55_P1958554	*Ar*	NM_013476	ref|Mus musculus androgen receptor mRNA
7.13	-1.554	0.00028	A_55_P2063937	*D630033A02Rik*	XM_001472939	ref|PREDICTED: Mus musculus RIKEN cDNA D630033A02 gene mRNA
9.14	-1.543	7.00E-05	A_55_P2039429	*Dio1*	NM_007860	ref|Mus musculus deiodinase iodothyronine type I mRNA
9.58	-1.537	0.00027	A_51_P107362	*Socs2*	NM_007706	ref|Mus musculus suppressor of cytokine signaling 2 transcript variant 1 mRNA
9.36	-1.536	0.00066	A_51_P134812	*Chac1*	NM_026929	ref|Mus musculus ChaC cation transport regulator-like 1 (E. coli) mRNA
11.08	-1.536	1.00E-05	A_52_P614777	*Sucnr1*	NM_032400	ref|Mus musculus succinate receptor 1 mRNA
8.57	-1.528	0.00049	A_55_P2165554	*ENSMUST00000099046*	ENSMUST00000099046	Unknown
9.83	-1.527	0.00117	A_51_P253481	*Ces1*	NM_021456	ref|Mus musculus carboxylesterase 1 mRNA
7.20	-1.523	3.00E-04	A_52_P99807	*Dpy19l3*	NM_178704	ref|Mus musculus dpy-19-like 3 (C. elegans) mRNA
10.96	-1.521	0	A_55_P2092501	*Med1*	NM_134027	ref|Mus musculus mediator complex subunit 1 transcript variant 2 mRNA
9.33	-1.519	2.00E-05	A_51_P418725	*Plekhf1*	NM_024413	ref|Mus musculus pleckstrin homology domain containing family F (with FYVE domain) member 1 mRNA
9.76	-1.518	9.00E-04	A_51_P249286	*Rgs16*	NM_011267	ref|Mus musculus regulator of G-protein signaling 16 mRNA
9.61	-1.513	7.00E-05	A_51_P304109	*Cyp2c39*	NM_010003	ref|Mus musculus cytochrome P450 family 2 subfamily c polypeptide 39 mRNA
8.98	-1.510	0.00099	A_55_P2093862	*ENSMUST00000099037*	ENSMUST00000099037	Unknown
10.27	-1.501	0	A_55_P2219059	*Lmnb2*	NM_010722	ref|Mus musculus lamin B2 mRNA
12.93	-1.495	3.00E-05	A_55_P2016842	*Me1*	NM_008615	ref|Mus musculus malic enzyme 1 NADP(+)-dependent cytosolic mRNA
9.59	-1.447	0.00029	A_51_P107362	*Socs2*	NM_007706	ref|Mus musculus suppressor of cytokine signaling 2 transcript variant 1 mRNA
11.81	-1.439	1.00E-05	A_51_P451588	*Plekhb1*	NM_013746	ref|Mus musculus pleckstrin homology domain containing family B (evectins) member 1 transcript variant 1 mRNA
7.94	-1.437	3.00E-05	A_55_P2007228	*Prkaca*	NM_008854	ref|Mus musculus protein kinase cAMP dependent catalytic alpha mRNA
9.28	-1.421	4.00E-05	A_55_P2071906	*ENSMUST00000108392*	ENSMUST00000108392	ens|Cytochrome P-450b (phenobarbital-inducible) Fragment [Source:UniProtKB/TrEMBL;Acc:Q61461]

8.00	-1.413	0.00036	A_55_P1978636	*ENSMUST00000099035*	ENSMUST00000099035	tc|Q4YHF0_PLABE (Q4YHF0) Pb-fam-2 protein (Fragment) partial (7%)
10.6	-1.404	1.00E-05	A_51_P185175	*Fkbp4*	NM_010219	ref|Mus musculus FK506 binding protein 4 mRNA
10.21	-1.398	0.00046	A_66_P108247	*Ucp3*	NM_009464	ref|Mus musculus uncoupling protein 3 (mitochondrial proton carrier) nuclear gene encoding mitochondrial protein mRNA
10.56	-1.397	5.00E-05	A_55_P2051094	*Rorc*	NM_011281	ref|Mus musculus RAR-related orphan receptor gamma mRNA
8.96	-1.391	3.00E-04	A_55_P2031676	*Gstm6*	NM_008184	ref|Mus musculus glutathione S-transferase mu 6 mRNA
8.02	-1.389	0	A_55_P1992164	*E130102H24Rik*	XM_001472210	ref|PREDICTED: Mus musculus RIKEN cDNA E130102H24 gene mRNA
8.67	-1.388	3.00E-05	A_51_P286488	*Ier3*	NM_133662	ref|Mus musculus immediate early response 3 mRNA
11.08	-1.37	1.00E-05	A_55_P2063312	*Mgll*	NM_001166250	ref|Mus musculus monoglyceride lipase transcript variant 4 mRNA
10.69	-1.368	0.00016	A_55_P2088440	*Arrdc2*	NM_027560	ref|Mus musculus arrestin domain containing 2 mRNA
7.05	-1.366	4.00E-05	A_55_P2136847	*Slc1a2*	NM_001077514	ref|Mus musculus solute carrier family 1 (glial high affinity glutamate transporter) member 2transcript variant 1 mRNA
7.31	-1.361	0.00032	A_51_P100573	*Map3k3*	NM_011947	ref|Mus musculus mitogen-activated protein kinase kinase kinase 3 mRNA
8.68	-1.360	9.00E-05	A_51_P245503	*Ugt2b1*	NM_152811	ref|Mus musculus UDP glucuronosyltransferase 2 family polypeptide B1 mRNA
11.04	-1.359	2.00E-05	A_51_P400366	*Rhbg*	NM_021375	ref|Mus musculus Rhesus blood group-associated B glycoprotein mRNA
10.24	-1.355	0.00011	A_51_P144531	*D630002G06Rik*	NM_172776	ref|Mus musculus RIKEN cDNA D630002G06 gene mRNA
11.18	-1.352	9.00E-04	A_55_P1974788	*Cfl1*	NM_007687	ref|Mus musculus cofilin 1 non-muscle mRNA
8.30	-1.340	3.00E-05	A_55_P2139587	*NAP092820-001*	NAP092820-001	Unknown
8.27	-1.339	7.00E-05	A_51_P514319	*Slc13a4*	NM_172892	ref|Mus musculus solute carrier family 13 (sodium/sulfate symporters) member 4 mRNA
8.42	-1.334	0.00041	A_55_P2004071	*Gm2058*	NM_001170345	ref|Mus musculus predicted gene 2058 mRNA
7.05	-1.331	0.00042	A_55_P2065249	*ENSMUST00000063239*	ENSMUST00000063239	ens|Putative uncharacterized protein [Source:UniProtKB/TrEMBL;Acc:Q9D605]
8.21	-1.330	0.00185	A_55_P2039532	*Pax8*	NM_011040	ref|Mus musculus paired box gene 8 mRNA
7.24	-1.328	8.00E-05	A_51_P475138	*Duox1*	NM_001099297	ref|Mus musculus dual oxidase 1 mRNA
7.65	-1.325	0.00031	A_55_P1955427	*Cux1*	NM_009986	ref|Mus musculus cut-like homeobox 1 transcript variant 1 mRNA
13.49	-1.323	1.00E-05	A_51_P334942	*Aldh1a1*	NM_013467	ref|Mus musculus aldehyde dehydrogenase family 1 subfamily A1 mRNA
12.23	-1.322	2.00E-05	A_51_P453043	*Aacs*	NM_030210	ref|Mus musculus acetoacetyl-CoA synthetase mRNA
9.45	-1.319	0.00071	A_55_P2138100	*ENSMUST00000099050*	ENSMUST00000099050	Unknown
12.19	-1.305	8.00E-04	A_55_P2158990	*Jun*	NM_010591	ref|Mus musculus Jun oncogene mRNA
9.05	-1.305	1.00E-05	A_55_P1979377	*Slc16a7*	NM_011391	ref|Mus musculus solute carrier family 16 (monocarboxylic acid transporters) member 7 mRNA
7.99	-1.303	1.00E-05	A_51_P469531	*Asna1*	NM_019652	ref|Mus musculus arsA arsenite transporter ATP-binding homolog 1 (bacterial) mRNA
8.62	-1.302	0.00047	A_55_P2114110	*Cadm4*	NM_153112	ref|Mus musculus cell adhesion molecule 4 mRNA
12.01	-1.301	1.00E-05	A_55_P2061338	*Slc16a11*	NM_153081	ref|Mus musculus solute carrier family 16 (monocarboxylic acid transporters) member 11 transcript variant 3 mRNA

9.93	-1.295	3.00E-05	A_55_P1961736	*Rcan2*	NM_207649	ref|Mus musculus regulator of calcineurin 2 transcript variant 1 mRNA
10.26	-1.289	0.00023	A_55_P2070976	*Gm6923*	XM_893647	ref|PREDICTED: Mus musculus predicted gene EG628855 mRNA
8.93	-1.286	1.00E-05	A_66_P105422	*Lonrf3*	NM_028894	ref|Mus musculus LON peptidase N-terminal domain and ring finger 3 mRNA
8.22	-1.264	0	A_55_P2123706	*Plekhb1*	NM_013746	ref|Mus musculus pleckstrin homology domain containing family B (evectins) member 1 transcript variant 1 mRNA
7.62	-1.262	4.00E-05	A_51_P406165	*Fam55b*	NM_030069	ref|Mus musculus family with sequence similarity 55 member B mRNA
9.48	-1.260	5.00E-05	A_55_P2037428	*Mogat1*	NM_026713	ref|Mus musculus monoacylglycerol O-acyltransferase 1 mRNA
7.63	-1.260	0.00011	A_52_P77093	*1600014C10Rik*	NM_028166	ref|Mus musculus RIKEN cDNA 1600014C10 gene transcript variant 2 mRNA
7.52	-1.259	0.00012	A_55_P2169124	*ENSMUST00000120540*	ENSMUST00000120540	ens|integral membrane transport protein UST1R [Source:RefSeq peptide;Acc:NP_795976]
9.36	-1.257	0.00054	A_55_P2035824	*Nr1i3*	NM_009803	ref|Mus musculus nuclear receptor subfamily 1 group I member 3 mRNA
10.40	-1.246	0.00036	A_55_P1966438	*Gstm2*	NM_008183	ref|Mus musculus glutathione S-transferase mu 2 mRNA
11.29	-1.245	1.00E-05	A_55_P2116290	*D4Ertd22e*	NM_001025608	ref|Mus musculus DNA segment Chr 4 ERATO Doi 22 expressed transcript variant 1 mRNA
9.93	-1.237	0.00045	A_55_P1957922	*Arrdc2*	NM_027560	ref|Mus musculus arrestin domain containing 2 mRNA
7.16	-1.233	0.00017	A_55_P2185185	*Tmem28*	NM_001081283	ref|Mus musculus transmembrane protein 28 mRNA
8.12	-1.232	0.00084	A_55_P2032770	*Inpp5e*	NM_033134	ref|Mus musculus inositol polyphosphate-5-phosphatase E mRNA
13.95	-1.225	5.00E-05	A_55_P2142146	*Glul*	NM_008131	ref|Mus musculus glutamate-ammonia ligase (glutamine synthetase) mRNA
8.06	-1.225	0.00018	A_66_P140507	*Lhpp*	NM_029609	ref|Mus musculus phospholysine phosphohistidine inorganic pyrophosphate phosphatase mRNA
10.56	-1.224	0.00043	A_51_P386648	*Glod5*	NM_027227	ref|Mus musculus glyoxalase domain containing 5 mRNA
8.32	-1.224	6.00E-05	A_55_P2040860	*Sunc1*	NM_177576	ref|Mus musculus Sad1 and UNC84 domain containing 1 mRNA
9.27	-1.223	0.00117	A_52_P423810	*ENSMUST00000062980*	ENSMUST00000062980	ens|Metallothionein-1 (MT-1)(Metallothionein-I)(MT-I) [Source:UniProtKB/Swiss-Prot;Acc:P02802]
11.33	-1.222	2.00E-05	A_55_P2038347	*Acot3*	NM_134246	ref|Mus musculus acyl-CoA thioesterase 3 mRNA
8.33	-1.221	0.00054	A_55_P2183914	*Gm7120*	NM_001039244	ref|Mus musculus predicted gene 7120 mRNA
7.52	-1.220	0.00034	A_52_P140881	*Slc26a10*	NM_177615	ref|Mus musculus solute carrier family 26 member 10 mRNA
8.26	-1.213	0.00025	A_55_P1994132	*Tmem184a*	ENSMUST00000110832	ens|Transmembrane protein 184A [Source:UniProtKB/Swiss-Prot;Acc:Q3UFJ6]
7.01	-1.205	0.00053	A_55_P2131163	*Sv2c*	AK173092	gb|Mus musculus mRNA for mKIAA1054 protein
7.50	-1.200	1.00E-05	A_51_P113182	*Lifr*	NM_013584	ref|Mus musculus leukemia inhibitory factor receptor transcript variant 1 mRNA
9.75	-1.198	0.00081	A_55_P2153783	*Fmo1*	NM_010231	ref|Mus musculus flavin containing monooxygenase 1 mRNA
8.85	-1.197	0	A_55_P2278775	*9130016M20Rik*	AK050221	gb|Mus musculus adult male liver tumor cDNA RIKEN full-length enriched library clone:C730027O05 product:unclassifiable full insert sequence
11.03	-1.195	0.00085	A_55_P2165091	*Acnat2*	NM_145368	ref|Mus musculus acyl-coenzyme A amino acid N-acyltransferase 2 mRNA
12.38	-1.194	0.00081	A_55_P2043531	*A_55_P2043531*	A_55_P2043531	Unknown
9.64	-1.194	6.00E-05	A_55_P2031671	*Gstm6*	NM_008184	ref|Mus musculus glutathione S-transferase mu 6 mRNA

10.10	-1.188	2.00E-05	A_55_P2035424	*Hpgd*	NM_008278	ref|Mus musculus hydroxyprostaglandin dehydrogenase 15 (NAD) mRNA
9.90	-1.186	1.00E-05	A_51_P406429	*Pdk1*	NM_172665	ref|Mus musculus pyruvate dehydrogenase kinase isoenzyme 1 nuclear gene encoding mitochondrial protein mRNA
10.33	-1.179	1.00E-05	A_55_P2070084	*Gm13151*	XM_984726	ref|PREDICTED: Mus musculus similar to crooked legs CG14938-PB mRNA
9.93	-1.177	0.00021	A_66_P124420	*NAP001637-001*	NAP001637-001	Unknown
13.33	-1.174	0.00121	A_55_P2171413	*Me1*	NM_008615	ref|Mus musculus malic enzyme 1 NADP(+)-dependent cytosolic mRNA
8.36	-1.174	2.00E-05	A_55_P2177513	*Chrna2*	NM_144803	ref|Mus musculus cholinergic receptor nicotinic alpha polypeptide 2 (neuronal) mRNA
8.63	-1.168	5.00E-05	A_55_P1973683	*Morn4*	NM_198108	ref|Mus musculus MORN repeat containing 4 mRNA
9.17	-1.166	6.00E-05	A_51_P462814	*Sars2*	NM_023637	ref|Mus musculus seryl-aminoacyl-tRNA synthetase 2 mRNA
9.59	-1.166	0.00073	A_55_P2038362	*Acot5*	NM_145444	ref|Mus musculus acyl-CoA thioesterase 5 mRNA
7.05	-1.165	0.00039	A_55_P2331974	*TC1653743*	TC1653743	Unknown
12.74	-1.161	0	A_55_P1963767	*Npr2*	NM_173788	ref|Mus musculus natriuretic peptide receptor 2 mRNA
10.04	-1.159	1.00E-05	A_55_P1997097	*Bod1*	NM_001024919	ref|Mus musculus biorientation of chromosomes in cell division 1 mRNA
10.16	-1.155	0.00024	A_55_P1988795	*Acss2*	NM_019811	ref|Mus musculus acyl-CoA synthetase short-chain family member 2 mRNA
8.50	-1.154	3.00E-05	A_55_P2181348	*Gm11378*	XM_001476139	ref|PREDICTED: Mus musculus hypothetical protein LOC100041312 mRNA
7.35	-1.151	0.00151	A_55_P2319020	*BB557941*	AK163349	gb|Mus musculus 2 cells egg cDNA RIKEN full-length enriched library clone:B020017L01 product:unclassifiable full insert sequence
9.21	-1.151	3.00E-04	A_55_P2127765	*Crp*	NM_007768	ref|Mus musculus C-reactive protein pentraxin-related mRNA
11.42	-1.151	0.00128	A_51_P316935	*8430408G22Rik*	NM_145980	ref|Mus musculus RIKEN cDNA 8430408G22 gene transcript variant 1 mRNA
7.13	-1.151	0.00019	A_51_P348672	*Zdhhc17*	NM_172554	ref|Mus musculus zinc finger DHHC domain containing 17 mRNA
12.17	-1.145	4.00E-05	A_55_P1970033	*Per1*	NM_011065	ref|Mus musculus period homolog 1 (Drosophila) transcript variant 1 mRNA
7.91	-1.145	3.00E-05	A_55_P2051384	*Ccdc88c*	NM_026681	ref|Mus musculus coiled-coil domain containing 88C mRNA
8.14	-1.143	0.00028	A_51_P340668	*Bcl9l*	NM_030256	ref|Mus musculus B-cell CLL/lymphoma 9-like mRNA
8.75	-1.142	0.00037	A_55_P2147136	*Akr1d1*	NM_145364	ref|Mus musculus aldo-keto reductase family 1 member D1 mRNA
9.23	-1.141	0.00041	A_52_P183524	*Tmem86b*	NM_023440	ref|Mus musculus transmembrane protein 86B mRNA
7.91	-1.141	0.00101	A_51_P136792	*Calcoco1*	NM_026192	ref|Mus musculus calcium binding and coiled coil domain 1 mRNA
14.26	-1.140	0.00057	A_55_P1966690	*Cyp2e1*	NM_021282	ref|Mus musculus cytochrome P450 family 2 subfamily e polypeptide 1 mRNA
7.81	-1.131	5.00E-05	A_55_P2035804	*Fzd8*	NM_008058	ref|Mus musculus frizzled homolog 8 (Drosophila) mRNA
8.63	-1.131	1.00E-05	A_52_P547662	*P2ry1*	NM_008772	ref|Mus musculus purinergic receptor P2Y G-protein coupled 1 mRNA
7.07	-1.131	7.00E-05	A_52_P35377	*Plagl2*	NM_018807	ref|Mus musculus pleiomorphic adenoma gene-like 2 mRNA
7.94	-1.130	0.00028	A_51_P176042	*Pklr*	NM_013631	ref|Mus musculus pyruvate kinase liver and red blood cell nuclear gene encoding mitochondrial protein transcript variant 1 mRNA
7.57	-1.125	0.00043	A_52_P157274	*Abi1*	NM_001077190	ref|Mus musculus abl-interactor 1 transcript variant 1 mRNA

9.26	-1.123	0.00031	A_52_P82765	*ENSMUST00000065861*	ENSMUST00000065861	ens|Testosterone 16a-hydroxylase type c Fragment [Source:UniProtKB/TrEMBL;Acc:Q61460]
10.4	-1.118	9.00E-04	A_55_P2000603	*Rag1ap1*	NM_009057	ref|Mus musculus recombination activating gene 1 activating protein 1 mRNA
9.08	-1.117	2.00E-05	A_52_P981697	*Zfp874*	NM_177712	ref|Mus musculus zinc finger protein 874 mRNA
14.41	-1.115	1.00E-05	A_51_P267063	*Ugt3a2*	NM_144845	ref|Mus musculus UDP glycosyltransferases 3 family polypeptide A2 mRNA
12.2	-1.112	0.00048	A_51_P502150	*Slc9a3r1*	NM_012030	ref|Mus musculus solute carrier family 9 (sodium/hydrogen exchanger) member 3 regulator 1 mRNA
9.05	-1.110	2.00E-04	A_65_P19089	*Esrrg*	NM_011935	ref|Mus musculus estrogen-related receptor gamma mRNA
12.43	-1.106	2.00E-05	A_52_P240796	*Rdh16*	NM_009040	ref|Mus musculus retinol dehydrogenase 16 mRNA
7.23	-1.098	9.00E-05	A_55_P2181602	*Calb1*	NM_009788	ref|Mus musculus calbindin 1 mRNA
11.98	-1.094	8.00E-05	A_51_P138044	*Foxo1*	NM_019739	ref|Mus musculus forkhead box O1 mRNA
9.44	-1.091	0.00048	A_55_P2130393	*Pnpla1*	NM_001034885	ref|Mus musculus patatin-like phospholipase domain containing 1 mRNA
9.92	-1.091	0.00037	A_51_P214107	*Tbc1d20*	NM_024196	ref|Mus musculus TBC1 domain family member 20 mRNA
11.26	-1.088	7.00E-05	A_51_P213691	*Scnn1a*	NM_011324	ref|Mus musculus sodium channel nonvoltage-gated 1 alpha mRNA
11.70	-1.088	0.00083	A_55_P2110290	*Gm10395*	XM_001472492	ref|PREDICTED: Mus musculus similar to D14Ertd449e protein transcript variant 1 mRNA
7.93	-1.087	0.00161	A_55_P2064965	*ENSMUST00000098392*	ENSMUST00000098392	ens|Putative uncharacterized protein [Source:UniProtKB/TrEMBL;Acc:Q3U3H4]
13.69	-1.084	9.00E-05	A_51_P430082	*Tst*	NM_009437	ref|Mus musculus thiosulfate sulfurtransferase mitochondrial nuclear gene encoding mitochondrial protein mRNA
7.32	-1.084	0.00076	A_51_P115626	*Shank3*	NM_021423	ref|Mus musculus SH3/ankyrin domain gene 3 mRNA
8.31	-1.077	0.00018	A_52_P63343	*Gm129*	NM_001033302	ref|Mus musculus predicted gene 129 mRNA
11.26	-1.076	1.00E-05	A_66_P139387	*Prlr*	NM_011169	ref|Mus musculus prolactin receptor mRNA
12.94	-1.075	0.00058	A_55_P2030183	*NAP112908-1*	NAP112908-1	tc|Q5T7C3_HUMAN (Q5T7C3) High-mobility group box 1 partial (83%)
7.33	-1.072	0.00115	A_55_P1964262	*Apol7a*	NM_029419	ref|Mus musculus apolipoprotein L 7a transcript variant 1 mRNA
8.45	-1.071	2.00E-04	A_66_P113268	*Mme*	NM_008604	ref|Mus musculus membrane metallo endopeptidase mRNA
11.07	-1.070	0.00026	A_55_P2062262	*Aspscr1*	NM_026877	ref|Mus musculus alveolar soft part sarcoma chromosome region candidate 1 (human) transcript variant 1 mRNA
13.25	-1.067	0.00053	A_55_P2030501	*Ppp2r4*	NM_138748	ref|Mus musculus protein phosphatase 2A regulatory subunit B (PR 53) mRNA
8.69	-1.065	0.00043	A_52_P52263	*D17Wsu92e*	NM_001044719	ref|Mus musculus DNA segment Chr 17 Wayne State University 92 expressed transcript variant 2 mRNA
7.78	-1.064	8.00E-04	A_55_P2295933	*Elmo3*	NM_172760	ref|Mus musculus engulfment and cell motility 3 ced-12 homolog (C. elegans) mRNA
10.12	-1.063	0.00037	A_55_P1966528	*Pmf1*	NM_025928	ref|Mus musculus polyamine-modulated factor 1 mRNA
9.63	-1.063	0.00014	A_55_P1995417	*1810031K17Rik*	NM_026977	ref|Mus musculus RIKEN cDNA 1810031K17 gene mRNA
11.63	-1.061	4.00E-05	A_55_P1999790	*Pkdcc*	NM_134117	ref|Mus musculus protein kinase domain containing cytoplasmic mRNA
7.46	-1.060	0.00014	A_55_P2149288	*Cmya5*	NM_023821	ref|Mus musculus cardiomyopathy associated 5 mRNA
7.14	-1.060	9.00E-05	A_55_P2044627	*Rnase10*	NM_029145	ref|Mus musculus ribonuclease RNase A family 10 (non-active) transcript variant 1 mRNA
11.01	-1.059	1.00E-05	A_55_P2088014	*Cdc42ep4*	NM_020006	ref|Mus musculus CDC42 effector protein (Rho GTPase binding) 4 transcript variant 1 mRNA
10.29	-1.058	0.00037	A_51_P442053	*Ptdss1*	NM_008959	ref|Mus musculus phosphatidylserine synthase 1 mRNA

11.19	-1.058	0.00097	A_55_P2116272	*Cyp2c38*	NM_010002	ref|Mus musculus cytochrome P450 family 2 subfamily c polypeptide 38 mRNA
8.98	-1.058	0.00025	A_52_P79639	*Vat1*	NM_012037	ref|Mus musculus vesicle amine transport protein 1 homolog (T californica) mRNA
9.93	-1.054	0.00058	A_55_P2025368	*Nkain1*	NM_025998	ref|Mus musculus Na+/K+ transporting ATPase interacting 1 mRNA
8.94	-1.049	0.00014	A_55_P2141938	*1810058I24Rik*	NR_027875	ref|Mus musculus RIKEN cDNA 1810058I24 gene transcript variant 1 non-coding RNA
9.67	-1.048	3.00E-05	A_55_P2367117	*Pitpnb*	NM_019640	ref|Mus musculus phosphatidylinositol transfer protein beta mRNA
11.64	-1.048	0.00064	A_55_P2055523	*Gm3160*	XM_001475214	ref|PREDICTED: Mus musculus similar to high-mobility group box 1 mRNA
7.55	-1.046	0.00022	A_55_P2068121	*Spag4l*	NM_029599	ref|Mus musculus sperm associated antigen 4-like mRNA
11.16	-1.044	5.00E-05	A_51_P293901	*Dhrs1*	NM_026819	ref|Mus musculus dehydrogenase/reductase (SDR family) member 1 mRNA
7.93	-1.042	6.00E-05	A_55_P2117984	*Vangl2*	NM_033509	ref|Mus musculus vang-like 2 (van gogh Drosophila) mRNA
10.30	-1.037	0.00105	A_52_P486322	*Fzr1*	NM_019757	ref|Mus musculus fizzy/cell division cycle 20 related 1 (Drosophila) mRNA
9.52	-1.034	0.00023	A_55_P2039289	*Hspb6*	NM_001012401	ref|Mus musculus heat shock protein alpha-crystallin-related B6 mRNA
7.18	-1.034	0.00029	A_55_P1994942	*Rorc*	NM_011281	ref|Mus musculus RAR-related orphan receptor gamma mRNA
9.37	-1.034	0.00074	A_51_P418908	*Larp1*	NM_028451	ref|Mus musculus La ribonucleoprotein domain family member 1 mRNA
10.20	-1.032	9.00E-05	A_66_P138976	*Lpin2*	NM_001164885	ref|Mus musculus lipin 2 transcript variant 1 mRNA
9.84	-1.032	0.00017	A_52_P561927	*Ncor1*	NM_011308	ref|Mus musculus nuclear receptor co-repressor 1 mRNA
10.79	-1.031	6.00E-05	A_55_P2120354	*Cib2*	NM_019686	ref|Mus musculus calcium and integrin binding family member 2 mRNA
7.27	-1.030	0.00041	A_55_P1997211	*Diras1*	NM_145217	ref|Mus musculus DIRAS family GTP-binding RAS-like 1 mRNA
7.57	-1.029	0.00014	A_66_P119074	*Tbc1d22b*	NM_198647	ref|Mus musculus TBC1 domain family member 22B mRNA
12.84	-1.028	0.001	A_55_P2025468	*Tst*	NM_009437	ref|Mus musculus thiosulfate sulfurtransferase mitochondrial nuclear gene encoding mitochondrial protein mRNA
8.03	-1.028	0.00074	A_55_P1985015	*Pard3*	NM_033620	ref|Mus musculus par-3 (partitioning defective 3) homolog (C. elegans) transcript variant 3 mRNA
10.24	-1.027	4.00E-05	A_52_P112651	*Lman2*	NM_025828	ref|Mus musculus lectin mannose-binding 2 mRNA
8.24	-1.026	0.00163	A_66_P136632	*1500003O03Rik*	NM_019769	ref|Mus musculus RIKEN cDNA 1500003O03 gene mRNA
14.42	-1.024	0.00011	A_52_P229972	*Slc22a1*	NM_009202	ref|Mus musculus solute carrier family 22 (organic cation transporter) member 1 mRNA
10.17	-1.022	0.00011	A_52_P516034	*Ptp4a1*	NM_011200	ref|Mus musculus protein tyrosine phosphatase 4a1 mRNA
8.55	-1.022	0.00018	A_51_P271984	*Tmem45b*	NM_144936	ref|Mus musculus transmembrane protein 45b mRNA
9.64	-1.021	9.00E-05	A_51_P453963	*9530008L14Rik*	NM_175417	ref|Mus musculus RIKEN cDNA 9530008L14 gene transcript variant 1 mRNA
8.19	-1.021	0.00154	A_52_P69558	*Gm8221*	XM_001475933	ref|PREDICTED: Mus musculus apolipoprotein L 3-like mRNA
10.5	-1.020	4.00E-05	A_55_P2177721	*Adra1b*	NM_007416	ref|Mus musculus adrenergic receptor alpha 1b mRNA
7.40	-1.020	0.00012	A_55_P2013645	*Tubg2*	NM_134028	ref|Mus musculus tubulin gamma 2 mRNA
13.3	-1.018	0.00021	A_55_P2052924	*Sepw1*	NM_009156	ref|Mus musculus selenoprotein W muscle 1 mRNA
8.00	-1.018	0.00019	A_52_P576049	*Inhbc*	NM_010565	ref|Mus musculus inhibin beta-C mRNA
8.73	-1.017	0.00038	A_52_P404363	*Cdc42bpb*	NM_183016	ref|Mus musculus CDC42 binding protein kinase beta mRNA

14.85	-1.012	0.00021	A_51_P162162	*Inmt*	NM_009349	ref|Mus musculus indolethylamine N-methyltransferase mRNA
7.00	-1.010	3.00E-04	A_55_P1991851	*Speg*	NM_001085370	ref|Mus musculus SPEG complex locus transcript variant 2 mRNA
8.83	-1.010	7.00E-04	A_51_P282837	*St14*	NM_011176	ref|Mus musculus suppression of tumorigenicity 14 (colon carcinoma) mRNA
14.29	-1.010	2.00E-05	A_51_P141535	*Oat*	NM_016978	ref|Mus musculus ornithine aminotransferase nuclear gene encoding mitochondrial protein mRNA
11.11	-1.005	0.00011	A_51_P192089	*2610028A01Rik*	NM_028228	ref|Mus musculus RIKEN cDNA 2610028A01 gene mRNA
7.81	-1.004	7.00E-04	A_51_P339380	*Setmar*	NM_178391	ref|Mus musculus SET domain and mariner transposase fusion gene mRNA
9.84	-1.003	4.00E-05	A_55_P2109922	*Gm2921*	XM_001474867	ref|PREDICTED: Mus musculus hypothetical protein LOC100040711 mRNA
9.84	-1.001	0.00039	A_55_P2123381	*Fga*	NM_010196	ref|Mus musculus fibrinogen alpha chain transcript variant 2 mRNA

Table 89. All significantly up regulated genes in hHeps after treatment with TCDD (10 nM) identified by microarray analysis. Selected parameters: A-value ≥ 7, log2 fc ≥ 1, p-value ≤ 0.05.

A	Log2 fc	p-value	Probe name	Gene name	Systemtatic name	Gene description
12.43	6.589	0	A_23_P209625	*CYP1B1*	NM_000104	ref|Homo sapiens cytochrome P450 family 1 subfamily B polypeptide 1 mRNA
12.73	5.368	0	A_23_P163402	*CYP1A1*	NM_000499	ref|Homo sapiens cytochrome P450 family 1 subfamily A polypeptide 1 mRNA
9.01	4.578	0	A_23_P165136	*LRRC25*	NM_145256	ref|Homo sapiens leucine rich repeat containing 25 mRNA
10.97	4.429	0	A_33_P3290343	*CYP1B1*	NM_000104	ref|Homo sapiens cytochrome P450 family 1 subfamily B polypeptide 1 mRNA
8.83	4.406	0	A_23_P207213	*ALDH3A1*	NM_000691	ref|Homo sapiens aldehyde dehydrogenase 3 family member A1 transcript variant 2 mRNA
10.10	4.197	0	A_33_P3238433	*ALDH3A1*	NM_001135168	ref|Homo sapiens aldehyde dehydrogenase 3 family member A1 transcript variant 1 mRNA
8.03	3.604	0	A_33_P3480395	*FLJ30901*	AK055463	gb|Homo sapiens cDNA FLJ30901 fis clone FEBRA2005778.
8.99	3.529	0	A_23_P26854	*ARHGAP44*	NM_014859	ref|Homo sapiens Rho GTPase activating protein 44 mRNA
9.76	3.259	0	A_33_P3397795	*C14orf135*	AK095489	gb|Homo sapiens cDNA FLJ38170 fis clone FCBBF1000024.
8.13	3.172	0	A_32_P49867	*LOC100507055*	NM_001195520	ref|Homo sapiens hypothetical LOC100507055 mRNA
10.23	3.106	0	A_23_P416581	*GNAZ*	NM_002073	ref|Homo sapiens guanine nucleotide binding protein (G protein) alpha z polypeptide mRNA
9.85	2.948	0	A_24_P157370	*IL17RB*	NM_018725	ref|Homo sapiens interleukin 17 receptor B mRNA
12.12	2.710	0	A_33_P3222762	*HULC*	NR_004855	ref|Homo sapiens highly up-regulated in liver cancer (non-protein coding) non-coding RNA
15.21	2.626	0	A_33_P3253747	*CYP1A2*	NM_000761	ref|Homo sapiens cytochrome P450 family 1 subfamily A polypeptide 2 mRNA
8.52	2.343	0	A_33_P3230990	*SCUBE1*	NM_173050	ref|Homo sapiens signal peptide CUB domain EGF-like 1 mRNA
11.3	2.311	0	A_23_P143845	*TIPARP*	NM_015508	ref|Homo sapiens TCDD-inducible poly(ADP-ribose) polymerase transcript variant 2 mRNA
11.27	2.291	0	A_23_P57910	*RTP3*	NM_031440	ref|Homo sapiens receptor (chemosensory) transporter protein 3 mRNA
8.74	2.276	0	A_33_P3734384	*LOC285957*	AK097526	gb|Homo sapiens cDNA FLJ40207 fis clone TESTI2020946
9.68	2.240	0	A_23_P41804	*NKD2*	NM_033120	ref|Homo sapiens naked cuticle homolog 2 (Drosophila) mRNA
8.99	2.159	0	A_23_P154806	*EPB41L1*	NM_012156	ref|Homo sapiens erythrocyte membrane protein band 4.1-like 1 transcript variant 1 mRNA
7.89	2.138	0	A_24_P335620	*SLC7A5*	NM_003486	ref|Homo sapiens solute carrier family 7 (amino acid transporter light chain L system) member 5 mRNA
8.85	2.137	0	A_23_P136355	*HHAT*	NM_018194	ref|Homo sapiens hedgehog acyltransferase transcript variant 1 mRNA
8.09	2.118	0	A_23_P257003	*PCSK5*	NM_006200	ref|Homo sapiens proprotein convertase subtilisin/kexin type 5 transcript variant 2 mRNA
7.15	2.078	0	A_23_P17673	*DNMT3L*	NM_013369	ref|Homo sapiens DNA (cytosine-5-)-methyltransferase 3-like transcript variant 1 mRNA
9.56	2.009	0	A_23_P75630	*APOA5*	NM_052968	ref|Homo sapiens apolipoprotein A-V transcript variant 1 mRNA
8.51	1.931	0	A_23_P116942	*LAG3*	NM_002286	ref|Homo sapiens lymphocyte-activation gene 3 mRNA
13.88	1.843	0	A_23_P94159	*FBXO25*	NM_183421	ref|Homo sapiens F-box protein 25 transcript variant 1 mRNA
10.18	1.830	0	A_23_P24723	*TMEM138*	NM_016464	ref|Homo sapiens transmembrane protein 138 transcript variant 1 mRNA

12.98	1.808	0	A_23_P421423	*TNFAIP2*	NM_006291	ref|Homo sapiens tumor necrosis factor alpha-induced protein 2 mRNA
7.31	1.758	0	A_23_P120125	*COLEC11*	NM_199235	ref|Homo sapiens collectin sub-family member 11 transcript variant 2 mRNA
15.22	1.750	2.00E-05	A_23_P42868	*IGFBP1*	NM_000596	ref|Homo sapiens insulin-like growth factor binding protein 1 mRNA
8.67	1.741	0.00032	A_23_P110777	*LECT2*	NM_002302	ref|Homo sapiens leukocyte cell-derived chemotaxin 2 mRNA
7.80	1.717	1.00E-05	A_23_P381489	*NCRNA00313*	NR_026863	ref|Homo sapiens non-protein coding RNA 313 non-coding RNA
11.35	1.713	0	A_23_P421032	*SEC14L4*	NM_174977	ref|Homo sapiens SEC14-like 4 (S. cerevisiae) transcript variant 1 mRNA
7.91	1.704	0	A_33_P3841368	*LOC286161*	AK091672	gb|Homo sapiens cDNA FLJ34353 fis clone FEBRA2011665
10.69	1.653	5.00E-05	A_24_P158089	*SERPINE1*	NM_000602	ref|Homo sapiens serpin peptidase inhibitor clade E (nexin plasminogen activator inhibitor type 1) member 1 transcript variant 1 mRNA
8.58	1.651	0	A_23_P259071	*AREG*	NM_001657	ref|Homo sapiens amphiregulin mRNA
11.48	1.643	0	A_23_P83110	*CDK5RAP2*	NM_018249	ref|Homo sapiens CDK5 regulatory subunit associated protein 2 transcript variant 1 mRNA
8.87	1.607	0	A_23_P103110	*MAFF*	NM_012323	ref|Homo sapiens v-maf musculoaponeurotic fibrosarcoma oncogene homolog F (avian) transcript variant 1 mRNA
10.75	1.585	8.00E-05	A_24_P158089	*SERPINE1*	NM_000602	ref|Homo sapiens serpin peptidase inhibitor clade E (nexin plasminogen activator inhibitor type 1) member 1 transcript variant 1 mRNA
9.58	1.569	0	A_23_P403335	*EXPH5*	NM_015065	ref|Homo sapiens exophilin 5 mRNA
10.63	1.544	5.00E-05	A_24_P158089	*SERPINE1*	NM_000602	ref|Homo sapiens serpin peptidase inhibitor clade E (nexin plasminogen activator inhibitor type 1) member 1 transcript variant 1 mRNA
9.08	1.530	0	A_23_P103110	*MAFF*	NM_012323	ref|Homo sapiens v-maf musculoaponeurotic fibrosarcoma oncogene homolog F (avian) transcript variant 1 mRNA
9.11	1.504	0	A_23_P103110	*MAFF*	NM_012323	ref|Homo sapiens v-maf musculoaponeurotic fibrosarcoma oncogene homolog F (avian) transcript variant 1 mRNA
10.45	1.482	9.00E-05	A_24_P158089	*SERPINE1*	NM_000602	ref|Homo sapiens serpin peptidase inhibitor clade E (nexin plasminogen activator inhibitor type 1) member 1 transcript variant 1 mRNA
9.01	1.482	1.00E-05	A_23_P103110	*MAFF*	NM_012323	ref|Homo sapiens v-maf musculoaponeurotic fibrosarcoma oncogene homolog F (avian) transcript variant 1 mRNA
10.92	1.481	0	A_33_P3341676	*MEF2A*	NM_001171894	ref|Homo sapiens myocyte enhancer factor 2A transcript variant 5 mRNA
14.34	1.468	2.00E-05	A_23_P52986	*VWCE*	NM_152718	ref|Homo sapiens von Willebrand factor C and EGF domains mRNA
9.88	1.467	0	A_23_P571	*SLC2A1*	NM_006516	ref|Homo sapiens solute carrier family 2 (facilitated glucose transporter) member 1 mRNA
8.47	1.465	5.00E-05	A_23_P60627	*ALOX15B*	NM_001141	ref|Homo sapiens arachidonate 15-lipoxygenase type B transcript variant d mRNA
11.15	1.461	0	A_23_P17065	*CCL20*	NM_004591	ref|Homo sapiens chemokine (C-C motif) ligand 20 transcript variant 1 mRNA
11.67	1.453	0	A_33_P3282394	*MLLT1*	NM_005934	ref|Homo sapiens myeloid/lymphoid or mixed-lineage leukemia (trithorax homolog Drosophila); translocated to 1 mRNA
9.03	1.453	0	A_23_P103110	*MAFF*	NM_012323	ref|Homo sapiens v-maf musculoaponeurotic fibrosarcoma oncogene homolog F (avian) transcript variant 1 mRNA
12.68	1.444	0	A_33_P3336622	*ALDH3A2*	NM_001031806	ref|Homo sapiens aldehyde dehydrogenase 3 family member A2 transcript variant 1 mRNA
10.02	1.437	1.00E-05	A_33_P3389060	*CDK5RAP2*	NM_018249	ref|Homo sapiens CDK5 regulatory subunit associated protein 2 transcript variant 1 mRNA
10.61	1.436	5.00E-05	A_24_P158089	*SERPINE1*	NM_000602	ref|Homo sapiens serpin peptidase inhibitor clade E (nexin plasminogen activator inhibitor type 1) member 1 transcript variant 1 mRNA

7.45	1.436	6.00E-05	A_23_P74799	*SLC25A24*	NM_213651	ref|Homo sapiens solute carrier family 25 (mitochondrial carrier; phosphate carrier) member 24 nuclear gene encoding mitochondrial protein transcript variant 2 mRNA
9.28	1.435	1.00E-05	A_33_P3214849	*KDELC2*	NM_153705	ref|Homo sapiens KDEL (Lys-Asp-Glu-Leu) containing 2 mRNA
9.07	1.427	0	A_23_P103110	*MAFF*	NM_012323	ref|Homo sapiens v-maf musculoaponeurotic fibrosarcoma oncogene homolog F (avian) transcript variant 1 mRNA
9.04	1.427	3.00E-05	A_23_P103110	*MAFF*	NM_012323	ref|Homo sapiens v-maf musculoaponeurotic fibrosarcoma oncogene homolog F (avian) transcript variant 1 mRNA
10.82	1.425	8.00E-05	A_24_P158089	*SERPINE1*	NM_000602	ref|Homo sapiens serpin peptidase inhibitor clade E (nexin plasminogen activator inhibitor type 1) member 1 transcript variant 1 mRNA
9.06	1.419	7.00E-05	A_33_P3682006	*ENST00000425189*	ENST00000425189	ens|non-protein coding RNA 118 [Source:HGNC Symbol;Acc:24155]
10.87	1.416	3.00E-05	A_24_P158089	*SERPINE1*	NM_000602	ref|Homo sapiens serpin peptidase inhibitor clade E (nexin plasminogen activator inhibitor type 1) member 1 transcript variant 1 mRNA
12.28	1.406	0	A_32_P180971	*LOC728323*	NR_024437	ref|Homo sapiens hypothetical LOC728323 non-coding RNA
10.73	1.403	8.00E-05	A_24_P158089	*SERPINE1*	NM_000602	ref|Homo sapiens serpin peptidase inhibitor clade E (nexin plasminogen activator inhibitor type 1) member 1 (SERPINE1) transcript variant 1 mRNA
10.61	1.402	3.00E-05	A_24_P158089	*SERPINE1*	NM_000602	ref|Homo sapiens serpin peptidase inhibitor clade E (nexin plasminogen activator inhibitor type 1) member 1 (SERPINE1) transcript variant 1 mRNA
11.28	1.400	0	A_23_P139704	*DUSP6*	NM_001946	ref|Homo sapiens dual specificity phosphatase 6 transcript variant 1 mRNA
10.99	1.392	0	A_23_P126075	*KCNK1*	NM_002245	ref|Homo sapiens potassium channel subfamily K member 1 mRNA
9.10	1.392	0	A_23_P103110	*MAFF*	NM_012323	ref|Homo sapiens v-maf musculoaponeurotic fibrosarcoma oncogene homolog F (avian) transcript variant 1 mRNA
9.85	1.386	5.00E-05	A_32_P524904	*C11orf86*	NM_001136485	ref|Homo sapiens chromosome 11 open reading frame 86 mRNA
9.05	1.385	1.00E-05	A_23_P431305	*FAM69B*	NM_152421	ref|Homo sapiens family with sequence similarity 69 member B mRNA
7.10	1.378	0	A_23_P161563	*RAB38*	NM_022337	ref|Homo sapiens RAB38 member RAS oncogene family mRNA
15.86	1.375	0	A_23_P16523	*GDF15*	NM_004864	ref|Homo sapiens growth differentiation factor 15 mRNA
12.46	1.371	0	A_23_P112531	*FAM102A*	NM_001035254	ref|Homo sapiens family with sequence similarity 102 member A transcript variant 1 mRNA
10.50	1.364	3.00E-05	A_23_P354387	*MYOF*	NM_013451	ref|Homo sapiens myoferlin transcript variant 1 mRNA
12.28	1.363	0	A_23_P112531	*FAM102A*	NM_001035254	ref|Homo sapiens family with sequence similarity 102 member A transcript variant 1 mRNA
12.58	1.363	0	A_23_P162142	*TSKU*	NM_015516	ref|Homo sapiens tsukushi small leucine rich proteoglycan homolog (Xenopus laevis) mRNA
10.45	1.358	6.00E-05	A_24_P158089	*SERPINE1*	NM_000602	ref|Homo sapiens serpin peptidase inhibitor clade E (nexin plasminogen activator inhibitor type 1) member 1 (SERPINE1) transcript variant 1 mRNA
12.37	1.355	0	A_23_P112531	*FAM102A*	NM_001035254	ref|Homo sapiens family with sequence similarity 102 member A transcript variant 1 mRNA
12.41	1.351	0	A_23_P112531	*FAM102A*	NM_001035254	ref|Homo sapiens family with sequence similarity 102 member A transcript variant 1 mRNA
12.37	1.351	0	A_23_P112531	*FAM102A*	NM_001035254	ref|Homo sapiens family with sequence similarity 102 member A transcript variant 1 mRNA
12.58	1.347	0	A_23_P112531	*FAM102A*	NM_001035254	ref|Homo sapiens family with sequence similarity 102 member A transcript variant 1 mRNA
12.61	1.341	0	A_23_P112531	*FAM102A*	NM_001035254	ref|Homo sapiens family with sequence similarity 102 member A transcript variant 1 mRNA
12.38	1.340	0	A_23_P112531	*FAM102A*	NM_001035254	ref|Homo sapiens family with sequence similarity 102 member A transcript variant 1 mRNA

12.30	1.340	0	A_23_P112531	*FAM102A*	NM_001035254	ref|Homo sapiens family with sequence similarity 102 member A transcript variant 1 mRNA
7.91	1.337	0	A_33_P3226650	*GSTA7P*	NR_033760	ref|Homo sapiens glutathione S-transferase alpha 7 pseudogene non-coding RNA
9.08	1.336	1.00E-05	A_23_P103110	*MAFF*	NM_012323	ref|Homo sapiens v-maf musculoaponeurotic fibrosarcoma oncogene homolog F (avian) transcript variant 1 mRNA
9.13	1.309	0	A_23_P66881	*RGS9*	NM_003835	ref|Homo sapiens regulator of G-protein signaling 9 transcript variant 1 mRNA
12.47	1.306	0	A_23_P112531	*FAM102A*	NM_001035254	ref|Homo sapiens family with sequence similarity 102 member A transcript variant 1 mRNA
12.88	1.301	0	A_23_P58036	*MCCC1*	NM_020166	ref|Homo sapiens methylcrotonoyl-CoA carboxylase 1 (alpha) nuclear gene encoding mitochondrial protein mRNA
8.96	1.296	4.00E-05	A_23_P103110	*MAFF*	NM_012323	ref|Homo sapiens v-maf musculoaponeurotic fibrosarcoma oncogene homolog F (avian) transcript variant 1 mRNA
9.99	1.293	3.00E-05	A_23_P342131	*CYBASC3*	NM_153611	ref|Homo sapiens cytochrome b ascorbate dependent 3 transcript variant 2 mRNA
13.49	1.291	0	A_33_P3357530	*SLC12A7*	NM_006598	ref|Homo sapiens solute carrier family 12 (potassium/chloride transporters) member 7 mRNA
10.40	1.289	0.00026	A_33_P3218960	*CACNA1H*	NM_021098	ref|Homo sapiens calcium channel voltage-dependent T type alpha 1H subunit transcript variant 1 mRNA
8.84	1.289	1.00E-05	A_23_P111724	*RUNDC3B*	NM_138290	ref|Homo sapiens RUN domain containing 3B transcript variant 1 mRNA
15.11	1.268	1.00E-05	A_33_P3360540	*AGPAT2*	NM_006412	ref|Homo sapiens 1-acylglycerol-3-phosphate O-acyltransferase 2 (lysophosphatidic acid acyltransferase beta) transcript variant 1 mRNA
9.51	1.268	0	A_32_P205637	*PARD6B*	NM_032521	ref|Homo sapiens par-6 partitioning defective 6 homolog beta (C. elegans) mRNA
10.41	1.262	0	A_23_P313389	*UGCG*	NM_003358	ref|Homo sapiens UDP-glucose ceramide glucosyltransferase mRNA
14.16	1.256	0	A_23_P118065	*HSD17B2*	NM_002153	ref|Homo sapiens hydroxysteroid (17-beta) dehydrogenase 2 mRNA
13.99	1.254	3.00E-05	A_33_P3245011	*DAK*	NM_015533	ref|Homo sapiens dihydroxyacetone kinase 2 homolog (S. cerevisiae) mRNA
13.05	1.253	0	A_33_P3336617	*ALDH3A2*	NM_000382	ref|Homo sapiens aldehyde dehydrogenase 3 family member A2 transcript variant 2 mRNA
9.07	1.251	0	A_23_P123402	*TRIM55*	NM_184086	ref|Homo sapiens tripartite motif containing 55 transcript variant 3 mRNA
14.20	1.244	0	A_23_P118065	*HSD17B2*	NM_002153	ref|Homo sapiens hydroxysteroid (17-beta) dehydrogenase 2 mRNA
14.17	1.244	0	A_23_P118065	*HSD17B2*	NM_002153	ref|Homo sapiens hydroxysteroid (17-beta) dehydrogenase 2 mRNA
11.07	1.243	0	A_24_P217234	*SLC3A1*	NM_000341	ref|Homo sapiens solute carrier family 3 (cystine dibasic and neutral amino acid transporters activator of cystine dibasic and neutral amino acid transport) member 1 mRNA
8.63	1.240	0	A_24_P256404	*ENST00000356370*	ENST00000356370	gb|Homo sapiens cDNA FLJ35883 fis clone TESTI2008929
7.67	1.240	1.00E-05	A_23_P74112	*IL28RA*	NM_170743	ref|Homo sapiens interleukin 28 receptor alpha (interferon lambda receptor) transcript variant 1 mRNA
14.19	1.236	0	A_23_P118065	*HSD17B2*	NM_002153	ref|Homo sapiens hydroxysteroid (17-beta) dehydrogenase 2 mRNA
14.27	1.235	0	A_23_P118065	*HSD17B2*	NM_002153	ref|Homo sapiens hydroxysteroid (17-beta) dehydrogenase 2 mRNA
14.33	1.233	0	A_23_P118065	*HSD17B2*	NM_002153	ref|Homo sapiens hydroxysteroid (17-beta) dehydrogenase 2 mRNA
14.30	1.232	0	A_23_P118065	*HSD17B2*	NM_002153	ref|Homo sapiens hydroxysteroid (17-beta) dehydrogenase 2 mRNA
14.36	1.230	0	A_23_P118065	*HSD17B2*	NM_002153	ref|Homo sapiens hydroxysteroid (17-beta) dehydrogenase 2 mRNA
11.61	1.226	0	A_23_P94921	*SLC20A2*	NM_006749	ref|Homo sapiens solute carrier family 20 (phosphate transporter) member 2 mRNA
14.29	1.222	0	A_23_P118065	*HSD17B2*	NM_002153	ref|Homo sapiens hydroxysteroid (17-beta) dehydrogenase 2 mRNA

14.22	1.222	0	A_23_P118065	*HSD17B2*	NM_002153	ref|Homo sapiens hydroxysteroid (17-beta) dehydrogenase 2 mRNA
9.68	1.218	0	A_24_P294124	*SERTAD2*	NM_014755	ref|Homo sapiens SERTA domain containing 2 mRNA
8.91	1.216	1.00E-05	A_23_P123402	*TRIM55*	NM_184086	ref|Homo sapiens tripartite motif containing 55 transcript variant 3 mRNA
7.38	1.211	0	A_24_P46093	*SLC6A6*	NM_003043	ref|Homo sapiens solute carrier family 6 (neurotransmitter transporter taurine) member 6 transcript variant 1 mRNA
7.70	1.201	2.00E-05	A_32_P175739	*HK2*	NM_000189	ref|Homo sapiens hexokinase 2 mRNA
8.64	1.201	8.00E-05	A_33_P3285580	*GLYCTK*	NM_145262	ref|Homo sapiens glycerate kinase transcript variant 1 mRNA [
8.92	1.201	0	A_23_P123402	*TRIM55*	NM_184086	ref|Homo sapiens tripartite motif containing 55 transcript variant 3 mRNA
11.19	1.197	0	A_33_P3334443	*FAM69A*	NM_001006605	ref|Homo sapiens family with sequence similarity 69 member A mRNA
7.40	1.196	0	A_33_P3419190	*AREG*	NM_001657	ref|Homo sapiens amphiregulin mRNA
12.66	1.185	0.00025	A_23_P127948	*ADM*	NM_001124	ref|Homo sapiens adrenomedullin mRNA
14.94	1.168	0	A_23_P60599	*UGT1A6*	NM_001072	ref|Homo sapiens UDP glucuronosyltransferase 1 family polypeptide A6 transcript variant 1 mRNA
9.11	1.163	8.00E-05	A_23_P123402	*TRIM55*	NM_184086	ref|Homo sapiens tripartite motif containing 55 transcript variant 3 mRNA
9.47	1.160	0.00024	A_32_P164246	*FOXQ1*	NM_033260	ref|Homo sapiens forkhead box Q1 mRNA
11.99	1.155	3.00E-05	A_23_P1682	*TMEM45B*	NM_138788	ref|Homo sapiens transmembrane protein 45B mRNA
7.04	1.154	1.00E-05	A_23_P102950	*RSPH1*	NM_080860	ref|Homo sapiens radial spoke head 1 homolog (Chlamydomonas) mRNA
10.37	1.149	0	A_23_P210708	*SIRPA*	NM_001040022	ref|Homo sapiens signal-regulatory protein alpha transcript variant 1 mRNA
7.93	1.149	0	A_24_P254278	*SLC23A2*	NM_203327	ref|Homo sapiens solute carrier family 23 (nucleobase transporters) member 2 transcript variant 2 mRNA
8.08	1.146	8.00E-05	A_33_P3414594	*NR1I3*	NM_001077474	ref|Homo sapiens nuclear receptor subfamily 1 group I member 3 transcript variant 8 mRNA
12.28	1.139	0	A_33_P3217983	*ACSL5*	NM_203380	ref|Homo sapiens acyl-CoA synthetase long-chain family member 5 transcript variant 3 mRNA
11.06	1.136	1.00E-05	A_23_P145786	*MLXIPL*	NM_032951	ref|Homo sapiens MLX interacting protein-like transcript variant 1 mRNA
8.97	1.124	2.00E-05	A_23_P123402	*TRIM55*	NM_184086	ref|Homo sapiens tripartite motif containing 55 transcript variant 3 mRNA
9.54	1.116	0.00025	A_32_P133395	*ENST00000442411*	ENST00000442411	ref|PREDICTED: Homo sapiens hypothetical LOC100507500 partial miscRNA
8.92	1.116	7.00E-05	A_23_P123402	*TRIM55*	NM_184086	ref|Homo sapiens tripartite motif containing 55 transcript variant 3 mRNA
12.72	1.112	0	A_33_P3327986	*A_33_P3327986*	A_33_P3327986	Unknown
8.99	1.102	0	A_23_P123402	*TRIM55*	NM_184086	ref|Homo sapiens tripartite motif containing 55 transcript variant 3 mRNA
13.16	1.100	0	A_23_P423197	*RXRA*	NM_002957	ref|Homo sapiens retinoid X receptor alpha mRNA
7.89	1.098	6.00E-05	A_23_P346673	*GPRC5C*	ENST00000392628	ens|G protein-coupled receptor family C group 5 member C [Source:HGNC Symbol;Acc:13309]
11.06	1.098	0.00014	A_33_P3257861	*SARDH*	NM_001134707	ref|Homo sapiens sarcosine dehydrogenase nuclear gene encoding mitochondrial protein transcript variant 2 mRNA
9.18	1.097	0	A_24_P154037	*IRS2*	NM_003749	ref|Homo sapiens insulin receptor substrate 2) mRNA
10.25	1.097	0	A_23_P128215	*SOCS2*	NM_003877	ref|Homo sapiens suppressor of cytokine signaling 2 mRNA
10.77	1.095	0	A_33_P3389728	*NR5A2*	NM_205860	ref|Homo sapiens nuclear receptor subfamily 5 group A member 2 transcript variant 1 mRNA
8.94	1.092	1.00E-05	A_33_P3372699	*SEC14L4*	NM_174977	ref|Homo sapiens SEC14-like 4 (S. cerevisiae) transcript variant 1 mRNA

8.45	1.085	0	A_33_P3245006	*DAK*	NM_015533	ref|Homo sapiens dihydroxyacetone kinase 2 homolog (S. cerevisiae) mRNA
9.09	1.080	1.00E-05	A_23_P123402	*TRIM55*	NM_184086	ref|Homo sapiens tripartite motif containing 55 transcript variant 3 mRNA
7.97	1.079	8.00E-05	A_23_P13772	*TBX3*	NM_016569	ref|Homo sapiens T-box 3 transcript variant 2 mRNA
12.75	1.079	2.00E-05	A_33_P3302075	*UGT1A8*	NM_019076	ref|Homo sapiens UDP glucuronosyltransferase 1 family polypeptide A8 mRNA
7.93	1.069	0	A_24_P583040	*C17orf67*	ENST00000397861	ens|chromosome 17 open reading frame 67 [Source:HGNC Symbol;Acc:27900]
8.48	1.065	0.00022	A_23_P146855	*MPPED1*	NM_001044370	ref|Homo sapiens metallophosphoesterase domain containing 1 mRNA
8.40	1.060	0.00023	A_23_P385861	*CDCA2*	NM_152562	ref|Homo sapiens cell division cycle associated 2 mRNA
9.89	1.048	0.00013	A_24_P37441	*PDK1*	NM_002610	ref|Homo sapiens pyruvate dehydrogenase kinase isozyme 1 nuclear gene encoding mitochondrial protein mRNA
9.20	1.047	4.00E-05	A_23_P257355	*OTC*	NM_000531	ref|Homo sapiens ornithine carbamoyltransferase nuclear gene encoding mitochondrial protein mRNA
9.77	1.046	6.00E-05	A_23_P319572	*NR1I3*	NM_001077482	ref|Homo sapiens nuclear receptor subfamily 1 group I member 3 transcript variant 1 mRNA
7.05	1.024	3.00E-05	A_23_P383819	*TBX3*	NM_016569	ref|Homo sapiens T-box 3 transcript variant 2 mRNA
11.03	1.021	0.00018	A_33_P3256858	*C14orf80*	NM_001134875	ref|Homo sapiens chromosome 14 open reading frame 80 transcript variant 1 mRNA
9.14	1.016	0.00018	A_24_P928052	*NRP1*	NM_003873	ref|Homo sapiens neuropilin 1 transcript variant 1 mRNA
9.15	1.012	3.00E-05	A_23_P123402	*TRIM55*	NM_184086	ref|Homo sapiens tripartite motif containing 55 transcript variant 3 mRNA
9.92	1.012	0	A_33_P3311371	*PDLIM2*	NM_198042	ref|Homo sapiens PDZ and LIM domain 2 (mystique) transcript variant 3 mRNA
8.97	1.010	4.00E-05	A_23_P123402	*TRIM55*	NM_184086	ref|Homo sapiens tripartite motif containing 55 transcript variant 3 mRNA
7.32	1.009	6.00E-05	A_23_P165989	*NEURL2*	NM_080749	ref|Homo sapiens neuralized homolog 2 (Drosophila) mRNA
9.18	1.000	0	A_33_P3418426	*SLC3A1*	NM_000341	ref|Homo sapiens solute carrier family 3 (cystine dibasic and neutral amino acid transporters activator of cystine dibasic and neutral amino acid transport) member 1 mRNA

Table 90. All significantly down regulated genes in hHeps after treatment with TCDD (10 nM) identified by microarray analysis. Selected parameters: A-value ≥ 7, log2 fc ≥ 1, p-value ≤ 0.05.

A	Log2 fc	p-value	Probe name	Gene name	Systemtatic name	Gene description
10.21	-1.825	0	A_23_P92161	*ARL14*	NM_025047	ref|Homo sapiens ADP-ribosylation factor-like 14 mRNA
8.34	-1.734	1.00E-05	A_33_P3342752	*ENST00000366873*	ENST00000366873	ens|calpain 8 [Source:HGNC Symbol;Acc:1485]
8.22	-1.488	0	A_23_P94782	*CAPN8*	NM_001143962	ref|Homo sapiens calpain 8 mRNA
7.53	-1.443	0.00022	A_23_P420551	*CIT*	NM_007174	ref|Homo sapiens citron (rho-interacting serine/threonine kinase 21) transcript variant 2 mRNA
10.61	-1.248	0	A_33_P3398331	*MMP24*	NM_006690	ref|Homo sapiens matrix metallopeptidase 24 (membrane-inserted) mRNA
9.47	-1.223	0	A_24_P405705	*SLC2A2*	NM_000340	ref|Homo sapiens solute carrier family 2 (facilitated glucose transporter) member 2 mRNA
9.28	-1.169	1.00E-05	A_23_P136978	*SRPX2*	NM_014467	ref|Homo sapiens sushi-repeat containing protein X-linked 2 mRNA
10.71	-1.156	0	A_23_P333029	*C8orf47*	NM_173549	ref|Homo sapiens chromosome 8 open reading frame 47 transcript variant 1 mRNA
8.53	-1.073	5.00E-05	A_23_P421401	*PDGFRB*	NM_002609	ref|Homo sapiens platelet-derived growth factor receptor beta polypeptide mRNA
9.48	-1.067	1.00E-04	A_23_P104798	*IL18*	NM_001562	ref|Homo sapiens interleukin 18 (interferon-gamma-inducing factor) mRNA
8.59	-1.063	3.00E-05	A_23_P2543	*CUX2*	NM_015267	ref|Homo sapiens cut-like homeobox 2 mRNA
12.82	-1.062	0	A_23_P331670	*PYGB*	NM_002862	ref|Homo sapiens phosphorylase glycogen; brain mRNA
9.38	-1.046	1.00E-05	A_23_P252052	*FILIP1L*	NM_182909	ref|Homo sapiens filamin A interacting protein 1-like transcript variant 1 mRNA
7.68	-1.039	0.00019	A_23_P122937	*ELMO1*	NM_014800	ref|Homo sapiens engulfment and cell motility 1 transcript variant 1 mRNA
8.87	-1.038	1.00E-05	A_23_P55251	*ITGA3*	NM_002204	ref|Homo sapiens integrin alpha 3 (antigen CD49C alpha 3 subunit of VLA-3 receptor) transcript variant a mRNA
9.80	-1.032	2.00E-05	A_23_P104798	*IL18*	NM_001562	ref|Homo sapiens interleukin 18 (interferon-gamma-inducing factor) mRNA
7.78	-1.031	0.00015	A_23_P122937	*ELMO1*	NM_014800	ref|Homo sapiens engulfment and cell motility 1 transcript variant 1 mRNA
9.52	-1.023	0.00014	A_23_P104798	*IL18*	NM_001562	ref|Homo sapiens interleukin 18 (interferon-gamma-inducing factor) mRNA
9.07	-1.021	0	A_33_P3247205	*MOSC1*	NM_022746	ref|Homo sapiens MOCO sulphurase C-terminal domain containing 1 nuclear gene encoding mitochondrial protein mRNA
9.89	-1.016	7.00E-05	A_33_P3226810	*TNFSF10*	NM_003810	ref|Homo sapiens tumor necrosis factor (ligand) superfamily member 10 transcript variant 1 mRNA

Table 91. All significantly up regulated genes in hHeps after treatment with 1-PnCDD (10 nM) identified by microarray analysis. Selected parameters: A-value ≥ 7, log2 fc ≥ 1, p-value ≤ 0.05.

A	Log2 fc	p-value	Probe name	Gene name	Systematic name	Gene description
12.43	5.462	0	A_23_P209625	*CYP1B1*	NM_000104	ref|Homo sapiens cytochrome P450 family 1 subfamily B polypeptide 1 mRNA
12.73	4.610	0	A_23_P163402	*CYP1A1*	NM_000499	ref|Homo sapiens cytochrome P450 family 1 subfamily A polypeptide 1 mRNA
9.01	4.026	0	A_23_P165136	*LRRC25*	NM_145256	ref|Homo sapiens leucine rich repeat containing 25 mRNA
10.97	3.892	0	A_33_P3290343	*CYP1B1*	NM_000104	ref|Homo sapiens cytochrome P450 family 1 subfamily B polypeptide 1 mRNA
8.99	3.572	0	A_23_P26854	*ARHGAP44*	NM_014859	ref|Homo sapiens Rho GTPase activating protein 44 mRNA
8.83	3.535	0	A_23_P207213	*ALDH3A1*	NM_000691	ref|Homo sapiens aldehyde dehydrogenase 3 family member A1 transcript variant 2 mRNA
8.03	3.268	0	A_33_P3480395	*FLJ30901*	AK055463	gb|Homo sapiens cDNA FLJ30901 fis clone FEBRA2005778
10.10	3.114	0	A_33_P3238433	*ALDH3A1*	NM_001135168	ref|Homo sapiens aldehyde dehydrogenase 3 family member A1 transcript variant 1 mRNA
9.85	2.815	0	A_24_P157370	*IL17RB*	NM_018725	ref|Homo sapiens interleukin 17 receptor B mRNA
8.13	2.732	0	A_32_P49867	*LOC100507055*	NM_001195520	ref|Homo sapiens hypothetical LOC100507055 mRNA
10.23	2.715	0	A_23_P416581	*GNAZ*	NM_002073	ref|Homo sapiens guanine nucleotide binding protein (G protein) alpha z polypeptide mRNA
11.30	2.606	0	A_23_P143845	*TIPARP*	NM_015508	ref|Homo sapiens TCDD-inducible poly(ADP-ribose) polymerase transcript variant 2 mRNA
11.27	2.534	0	A_23_P57910	*RTP3*	NM_031440	ref|Homo sapiens receptor (chemosensory) transporter protein 3 mRNA
12.12	2.442	0	A_33_P3222762	*HULC*	NR_004855	ref|Homo sapiens highly up-regulated in liver cancer (non-protein coding) non-coding RNA
8.52	2.344	0	A_33_P3230990	*SCUBE1*	NM_173050	ref|Homo sapiens signal peptide CUB domain EGF-like 1 mRNA
7.89	2.195	0	A_24_P335620	*SLC7A5*	NM_003486	ref|Homo sapiens solute carrier family 7 (amino acid transporter light chain L system) member 5 mRNA
9.76	2.069	0	A_33_P3397795	*C14orf135*	AK095489	gb|Homo sapiens cDNA FLJ38170 fis clone FCBBF1000024
15.21	2.064	0	A_33_P3253747	*CYP1A2*	NM_000761	ref|Homo sapiens cytochrome P450 family 1 subfamily A polypeptide 2 mRNA
9.68	2.022	0	A_23_P41804	*NKD2*	NM_033120	ref|Homo sapiens naked cuticle homolog 2 (Drosophila) mRNA
9.56	2.000	0	A_23_P75630	*APOA5*	NM_052968	ref|Homo sapiens apolipoprotein A-V transcript variant 1 mRNA
8.09	1.851	0	A_23_P257003	*PCSK5*	NM_006200	ref|Homo sapiens proprotein convertase subtilisin/kexin type 5 transcript variant 2 mRNA
8.58	1.697	0	A_23_P259071	*AREG*	NM_001657	ref|Homo sapiens amphiregulin mRNA
7.10	1.673	0	A_23_P161563	*RAB38*	NM_022337	ref|Homo sapiens RAB38 member RAS oncogene family mRNA
9.58	1.661	0	A_23_P403335	*EXPH5*	NM_015065	ref|Homo sapiens exophilin 5 mRNA
11.48	1.661	0	A_23_P83110	*CDK5RAP2*	NM_018249	ref|Homo sapiens CDK5 regulatory subunit associated protein 2 transcript variant 1 mRNA
8.74	1.658	0	A_33_P3734384	*LOC285957*	AK097526	gb|Homo sapiens cDNA FLJ40207 fis clone TESTI2020946
7.80	1.652	2.00E-05	A_23_P381489	*NCRNA00313*	NR_026863	ref|Homo sapiens non-protein coding RNA 313 non-coding RNA
8.51	1.634	0	A_23_P116942	*LAG3*	NM_002286	ref|Homo sapiens lymphocyte-activation gene 3 (LAG3) mRNA

8.99	1.601	2.00E-04	A_23_P154806	*EPB41L1*	NM_012156	ref|Homo sapiens erythrocyte membrane protein band 4.1-like 1 transcript variant 1 mRNA
8.85	1.599	3.00E-05	A_23_P136355	*HHAT*	NM_018194	ref|Homo sapiens hedgehog acyltransferase transcript variant 1 mRNA
7.40	1.583	0	A_33_P3419190	*AREG*	NM_001657	ref|Homo sapiens amphiregulin mRNA
9.06	1.566	2.00E-05	A_33_P3682006	*ENST00000425189*	ENST00000425189	ens|non-protein coding RNA 118 [Source:HGNC Symbol;Acc:24155]
14.34	1.418	4.00E-05	A_23_P52986	*VWCE*	NM_152718	ref|Homo sapiens von Willebrand factor C and EGF domains mRNA
11.15	1.407	0	A_23_P17065	*CCL20*	NM_004591	ref|Homo sapiens chemokine (C-C motif) ligand 20 transcript variant 1 mRNA
10.02	1.349	2.00E-05	A_33_P3389060	*CDK5RAP2*	NM_018249	ref|Homo sapiens CDK5 regulatory subunit associated protein 2 transcript variant 1 mRNA
7.04	1.347	0	A_23_P102950	*RSPH1*	NM_080860	ref|Homo sapiens radial spoke head 1 homolog (Chlamydomonas) mRNA
10.18	1.343	2.00E-05	A_23_P24723	*TMEM138*	NM_016464	ref|Homo sapiens transmembrane protein 138 transcript variant 1 mRNA
12.98	1.339	1.00E-04	A_23_P421423	*TNFAIP2*	NM_006291	ref|Homo sapiens tumor necrosis factor alpha-induced protein 2 mRNA
13.49	1.269	0	A_33_P3357530	*SLC12A7*	NM_006598	ref|Homo sapiens solute carrier family 12 (potassium/chloride transporters) member 7 mRNA
9.14	1.254	1.00E-05	A_24_P928052	*NRP1*	NM_003873	ref|Homo sapiens neuropilin 1 transcript variant 1 mRNA
11.48	1.242	1.00E-05	A_23_P64879	*KCNJ8*	NM_004982	ref|Homo sapiens potassium inwardly-rectifying channel subfamily J member 8 mRNA
11.01	1.241	5.00E-05	A_23_P108082	*CREB3L3*	NM_032607	ref|Homo sapiens cAMP responsive element binding protein 3-like 3 mRNA
11.35	1.237	4.00E-05	A_23_P421032	*SEC14L4*	NM_174977	ref|Homo sapiens SEC14-like 4 (S. cerevisiae) transcript variant 1 mRNA
9.97	1.223	0.00031	A_23_P75749	*GLYAT*	NM_201648	ref|Homo sapiens glycine-N-acyltransferase nuclear gene encoding mitochondrial protein transcript variant 1 mRNA
9.13	1.209	0	A_23_P66881	*RGS9*	NM_003835	ref|Homo sapiens regulator of G-protein signaling 9 transcript variant 1 mRNA
10.50	1.195	0.00016	A_23_P354387	*MYOF*	NM_013451	ref|Homo sapiens myoferlin (transcript variant 1 mRNA
12.68	1.191	0	A_33_P3336622	*ALDH3A2*	NM_001031806	ref|Homo sapiens aldehyde dehydrogenase 3 family member A2 transcript variant 1 mRNA
7.38	1.178	0	A_24_P46093	*SLC6A6*	NM_003043	ref|Homo sapiens solute carrier family 6 (neurotransmitter transporter taurine) member 6 transcript variant 1 mRNA
12.58	1.176	3.00E-05	A_23_P162142	*TSKU*	NM_015516	ref|Homo sapiens tsukushi small leucine rich proteoglycan homolog (Xenopus laevis) mRNA
9.38	1.158	0	A_23_P130376	*FAM38B*	NM_022068	ref|Homo sapiens family with sequence similarity 38 member B mRNA
9.05	1.153	8.00E-05	A_23_P431305	*FAM69B*	NM_152421	ref|Homo sapiens family with sequence similarity 69 member B mRNA
8.48	1.148	1.00E-05	A_33_P3314176	*FAM46C*	NM_017709	ref|Homo sapiens family with sequence similarity 46 member C mRNA
10.41	1.145	0	A_23_P313389	*UGCG*	NM_003358	ref|Homo sapiens UDP-glucose ceramide glucosyltransferase mRNA
12.88	1.142	0	A_23_P58036	*MCCC1*	NM_020166	ref|Homo sapiens methylcrotonoyl-CoA carboxylase 1 (alpha) nuclear gene encoding mitochondrial protein mRNA
7.91	1.136	2.00E-05	A_33_P3841368	*LOC286161*	AK091672	gb|Homo sapiens cDNA FLJ34353 fis clone FEBRA2011665
13.05	1.136	0	A_33_P3336617	*ALDH3A2*	NM_000382	ref|Homo sapiens aldehyde dehydrogenase 3 family member A2 transcript variant 2 mRNA
10.99	1.129	0	A_32_P46594	*LOC145837*	NR_026979	ref|Homo sapiens hypothetical LOC145837 non-coding RNA
9.28	1.123	0.00019	A_33_P3214849	*KDELC2*	NM_153705	ref|Homo sapiens KDEL (Lys-Asp-Glu-Leu) containing 2 mRNA
13.88	1.121	0	A_23_P94159	*FBXO25*	NM_183421	ref|Homo sapiens F-box protein 25 transcript variant 1 mRNA

9.68	1.118	0	A_24_P294124	*SERTAD2*	NM_014755	ref|Homo sapiens SERTA domain containing 2 mRNA
11.07	1.112	1.00E-05	A_24_P217234	*SLC3A1*	NM_000341	ref|Homo sapiens solute carrier family 3 (cystine dibasic and neutral amino acid transporters activator of cystine dibasic and neutral amino acid transport) member 1 mRNA
14.16	1.110	0	A_23_P118065	*HSD17B2*	NM_002153	ref|Homo sapiens hydroxysteroid (17-beta) dehydrogenase 2 mRNA
14.30	1.109	1.00E-05	A_23_P118065	*HSD17B2*	NM_002153	ref|Homo sapiens hydroxysteroid (17-beta) dehydrogenase 2 mRNA
8.64	1.102	0.00021	A_33_P3285580	*GLYCTK*	NM_145262	ref|Homo sapiens glycerate kinase transcript variant 1 mRNA
11.28	1.100	0	A_23_P139704	*DUSP6*	NM_001946	ref|Homo sapiens dual specificity phosphatase 6 transcript variant 1 mRNA
8.48	1.099	0.00016	A_23_P146855	*MPPED1*	NM_001044370	ref|Homo sapiens metallophosphoesterase domain containing 1 mRNA
10.85	1.092	0	A_24_P346431	*TNS3*	NM_022748	ref|Homo sapiens tensin 3 mRNA
7.85	1.086	0.00026	A_33_P3850216	*TRIM55*	NM_033058	ref|Homo sapiens tripartite motif containing 55 transcript variant 2 mRNA
10.39	1.085	0	A_23_P331895	*TTYH3*	NM_025250	ref|Homo sapiens tweety homolog 3 (Drosophila) mRNA
10.92	1.073	0	A_33_P3341676	*MEF2A*	NM_001171894	ref|Homo sapiens myocyte enhancer factor 2A transcript variant 5 mRNA
8.99	1.068	1.00E-05	A_23_P123402	*TRIM55*	NM_184086	ref|Homo sapiens tripartite motif containing 55 transcript variant 3 mRNA
11.71	1.067	1.00E-05	A_23_P127107	*CLRN3*	NM_152311	ref|Homo sapiens clarin 3 mRNA
12.28	1.054	5.00E-05	A_32_P180971	*LOC728323*	NR_024437	ref|Homo sapiens hypothetical LOC728323 non-coding RNA
13.87	1.048	1.00E-05	A_23_P386912	*UGT2B4*	NM_021139	ref|Homo sapiens UDP glucuronosyltransferase 2 family polypeptide B4 mRNA
9.77	1.047	6.00E-05	A_23_P319572	*NR1I3*	NM_001077482	ref|Homo sapiens nuclear receptor subfamily 1 group I member 3 transcript variant 1 mRNA
8.85	1.037	0.00012	A_24_P23625	*HS3ST3B1*	ENST00000360954	ens|heparan sulfate (glucosamine) 3-O-sulfotransferase 3B1 [Source:HGNC Symbol;Acc:5198]
14.94	1.035	1.00E-05	A_23_P60599	*UGT1A6*	NM_001072	ref|Homo sapiens UDP glucuronosyltransferase 1 family polypeptide A6 transcript variant 1 mRNA
14.20	1.032	0	A_23_P118065	*HSD17B2*	NM_002153	ref|Homo sapiens hydroxysteroid (17-beta) dehydrogenase 2 mRNA
9.18	1.018	0	A_33_P3418426	*SLC3A1*	NM_000341	ref|Homo sapiens solute carrier family 3 (cystine dibasic and neutral amino acid transporters activator of cystine dibasic and neutral amino acid transport) member 1 mRNA
14.36	1.015	1.00E-05	A_23_P118065	*HSD17B2*	NM_002153	ref|Homo sapiens hydroxysteroid (17-beta) dehydrogenase 2 mRNA
14.33	1.004	2.00E-05	A_23_P118065	*HSD17B2*	NM_002153	ref|Homo sapiens hydroxysteroid (17-beta) dehydrogenase 2 mRNA
11.67	1.000	0	A_33_P3282394	*MLLT1*	NM_005934	ref|Homo sapiens myeloid/lymphoid or mixed-lineage leukemia (trithorax homolog Drosophila); translocated to 1 mRNA

Table 92. All significantly down regulated genes in hHeps after treatment with 1-PnCDD (10 nM) identified by microarray analysis. Selected parameters: A-value ≥ 7, log2 fc ≤ -1, p-value ≤ 0.05.

A	Log2 fc	p-value	Probe name	Gene name	Systematic name	Gene description
8.43	-1.510	0.00013	A_24_P331704	*KRT80*	NM_182507	ref|Homo sapiens keratin 80 transcript variant 1 mRNA
9.55	-1.396	0	A_23_P104798	*IL18*	NM_001562	ref|Homo sapiens interleukin 18 (interferon-gamma-inducing factor) mRNA
8.34	-1.387	0.00012	A_33_P3342752	*ENST00000366873*	ENST00000366873	ens|calpain 8 [Source:HGNC Symbol;Acc:1485]
9.80	-1.354	0	A_23_P104798	*IL18*	NM_001562	ref|Homo sapiens interleukin 18 (interferon-gamma-inducing factor) mRNA
9.66	-1.342	0	A_23_P104798	*IL18*	NM_001562	ref|Homo sapiens interleukin 18 (interferon-gamma-inducing factor) mRNA
9.49	-1.291	0	A_23_P104798	*IL18*	NM_001562	ref|Homo sapiens interleukin 18 (interferon-gamma-inducing factor) mRNA
9.38	-1.276	0	A_23_P104798	*IL18*	NM_001562	ref|Homo sapiens interleukin 18 (interferon-gamma-inducing factor) mRNA
10.21	-1.271	2.00E-05	A_23_P92161	*ARL14*	NM_025047	ref|Homo sapiens ADP-ribosylation factor-like 14 mRNA
9.48	-1.265	1.00E-05	A_23_P104798	*IL18*	NM_001562	ref|Homo sapiens interleukin 18 (interferon-gamma-inducing factor) mRNA
10.61	-1.246	0	A_33_P3398331	*MMP24*	NM_006690	ref|Homo sapiens matrix metallopeptidase 24 (membrane-inserted) mRNA
9.52	-1.235	1.00E-05	A_23_P104798	*IL18*	NM_001562	ref|Homo sapiens interleukin 18 (interferon-gamma-inducing factor) mRNA
9.48	-1.234	8.00E-05	A_23_P104798	*IL18*	NM_001562	ref|Homo sapiens interleukin 18 (interferon-gamma-inducing factor) mRNA
9.58	-1.153	3.00E-05	A_23_P104798	*IL18*	NM_001562	ref|Homo sapiens interleukin 18 (interferon-gamma-inducing factor) mRNA
9.51	-1.126	0.00012	A_23_P104798	*IL18*	NM_001562	ref|Homo sapiens interleukin 18 (interferon-gamma-inducing factor) mRNA
9.47	-1.097	0	A_24_P405705	*SLC2A2*	NM_000340	ref|Homo sapiens solute carrier family 2 (facilitated glucose transporter) member 2 mRNA
8.53	-1.065	5.00E-05	A_23_P421401	*PDGFRB*	NM_002609	ref|Homo sapiens platelet-derived growth factor receptor beta polypeptide mRNA
10.71	-1.028	0	A_23_P333029	*C8orf47*	NM_173549	ref|Homo sapiens chromosome 8 open reading frame 47 transcript variant 1 mRNA
9.38	-1.026	1.00E-05	A_23_P252052	*FILIP1L*	NM_182909	ref|Homo sapiens filamin A interacting protein 1-like transcript variant 1 mRNA
7.24	-1.024	5.00E-05	A_33_P3354374	*LOC100507410*	NR_040018	ref|Homo sapiens hypothetical LOC100507410 transcript variant 1 non-coding RNA
8.22	-1.018	6.00E-05	A_23_P94782	*CAPN8*	NM_001143962	ref|Homo sapiens calpain 8 mRNA
8.63	-1.010	0	A_23_P202837	*CCND1*	NM_053056	ref|Homo sapiens cyclin D1 mRNA
8.47	-1.003	6.00E-05	A_23_P202837	*CCND1*	NM_053056	ref|Homo sapiens cyclin D1 mRNA

Table 93. All significantly up regulated genes in hHeps after treatment with 4-PnCDF (30 nM) identified by microarray analysis. Selected parameters: A-value ≥ 7, log2 fc ≥ 1, p-value ≤ 0.05.

A	Log2 fc	p-value	Probe name	Gene name	Systematic name	Gene description
12.43	5.963	0	A_23_P209625	*CYP1B1*	NM_000104	ref|Homo sapiens cytochrome P450 family 1 subfamily B polypeptide 1 mRNA
12.73	4.933	0	A_23_P163402	*CYP1A1*	NM_000499	ref|Homo sapiens cytochrome P450 family 1 subfamily A polypeptide 1 mRNA
9.01	4.315	0	A_23_P165136	*LRRC25*	NM_145256	ref|Homo sapiens leucine rich repeat containing 25 mRNA
10.97	4.107	0	A_33_P3290343	*CYP1B1*	NM_000104	ref|Homo sapiens cytochrome P450 family 1 subfamily B polypeptide 1 mRNA
8.99	3.929	0	A_23_P26854	*ARHGAP44*	NM_014859	ref|Homo sapiens Rho GTPase activating protein 44 mRNA
8.83	3.787	0	A_23_P207213	*ALDH3A1*	NM_000691	ref|Homo sapiens aldehyde dehydrogenase 3 family member A1 transcript variant 2 mRNA
8.03	3.696	0	A_33_P3480395	*FLJ30901*	AK055463	gb|Homo sapiens cDNA FLJ30901 fis clone FEBRA2005778
8.13	3.523	0	A_32_P49867	*LOC100507055*	NM_001195520	ref|Homo sapiens hypothetical LOC100507055 mRNA
10.1	3.406	0	A_33_P3238433	*ALDH3A1*	NM_001135168	ref|Homo sapiens aldehyde dehydrogenase 3 family member A1 transcript variant 1 mRNA
9.85	2.714	0	A_24_P157370	*IL17RB*	NM_018725	ref|Homo sapiens interleukin 17 receptor B mRNA
9.76	2.644	0	A_33_P3397795	*C14orf135*	AK095489	gb|Homo sapiens cDNA FLJ38170 fis clone FCBBF1000024
10.23	2.614	0	A_23_P416581	*GNAZ*	NM_002073	ref|Homo sapiens guanine nucleotide binding protein (G protein) alpha z polypeptide mRNA
11.27	2.471	0	A_23_P57910	*RTP3*	NM_031440	ref|Homo sapiens receptor (chemosensory) transporter protein 3 mRNA
12.12	2.445	0	A_33_P3222762	*HULC*	NR_004855	ref|Homo sapiens highly up-regulated in liver cancer (non-protein coding) non-coding RNA
8.52	2.292	0	A_33_P3230990	*SCUBE1*	NM_173050	ref|Homo sapiens signal peptide CUB domain EGF-like 1 mRNA
7.89	2.284	0	A_24_P335620	*SLC7A5*	NM_003486	ref|Homo sapiens solute carrier family 7 (amino acid transporter light chain L system) member 5 mRNA
15.21	2.231	0	A_33_P3253747	*CYP1A2*	NM_000761	ref|Homo sapiens cytochrome P450 family 1 subfamily A polypeptide 2 mRNA
11.30	2.193	0	A_23_P143845	*TIPARP*	NM_015508	ref|Homo sapiens TCDD-inducible poly(ADP-ribose) polymerase transcript variant 2 mRNA
7.09	2.169	9.00E-05	A_33_P3459365	*LOC339894*	NR_034007	ref|Homo sapiens hypothetical LOC339894 non-coding RNA
9.56	2.083	0	A_23_P75630	*APOA5*	NM_052968	ref|Homo sapiens apolipoprotein A-V transcript variant 1 mRNA
8.74	2.016	0	A_33_P3734384	*LOC285957*	AK097526	gb|Homo sapiens cDNA FLJ40207 fis clone TESTI2020946
8.09	1.973	0	A_23_P257003	*PCSK5*	NM_006200	ref|Homo sapiens proprotein convertase subtilisin/kexin type 5 transcript variant 2 mRNA
8.51	1.939	0	A_23_P116942	*LAG3*	NM_002286	ref|Homo sapiens lymphocyte-activation gene 3 mRNA
11.48	1.875	0	A_23_P83110	*CDK5RAP2*	NM_018249	ref|Homo sapiens CDK5 regulatory subunit associated protein 2 transcript variant 1 mRNA
7.88	1.874	2.00E-05	A_33_P3232504	*C9orf169*	NM_199001	ref|Homo sapiens chromosome 9 open reading frame 169 mRNA
8.99	1.857	3.00E-05	A_23_P154806	*EPB41L1*	NM_012156	ref|Homo sapiens erythrocyte membrane protein band 4.1-like 1 transcript variant 1 mRNA
7.15	1.851	2.00E-05	A_23_P17673	*DNMT3L*	NM_013369	ref|Homo sapiens DNA (cytosine-5-)-methyltransferase 3-like transcript variant 1 mRNA
12.98	1.843	0	A_23_P421423	*TNFAIP2*	NM_006291	ref|Homo sapiens tumor necrosis factor alpha-induced protein 2 mRNA

9.68	1.839	0	A_23_P41804	*NKD2*	NM_033120	ref|Homo sapiens naked cuticle homolog 2 (Drosophila) mRNA
7.64	1.834	3.00E-05	A_33_P3318668	*C9orf169*	NM_199001	ref|Homo sapiens chromosome 9 open reading frame 169 mRNA
8.85	1.810	1.00E-05	A_23_P136355	*HHAT*	NM_018194	ref|Homo sapiens hedgehog acyltransferase transcript variant 1 mRNA
9.06	1.726	1.00E-05	A_33_P3682006	*ENST00000425189*	ENST00000425189	ens|non-protein coding RNA 118 [Source:HGNC Symbol;Acc:24155]
10.18	1.723	0	A_23_P24723	*TMEM138*	NM_016464	ref|Homo sapiens transmembrane protein 138 transcript variant 1 mRNA
8.58	1.688	0	A_23_P259071	*AREG*	NM_001657	ref|Homo sapiens amphiregulin mRNA
10.02	1.684	0	A_33_P3389060	*CDK5RAP2*	NM_018249	ref|Homo sapiens CDK5 regulatory subunit associated protein 2 transcript variant 1 mRNA
7.40	1.632	0	A_33_P3419190	*AREG*	NM_001657	ref|Homo sapiens amphiregulin mRNA
7.80	1.621	2.00E-05	A_23_P381489	*NCRNA00313*	NR_026863	ref|Homo sapiens non-protein coding RNA 313 non-coding RNA
10.50	1.606	0	A_23_P354387	*MYOF*	NM_013451	ref|Homo sapiens myoferlin transcript variant 1 mRNA
11.15	1.564	0	A_23_P17065	*CCL20*	NM_004591	ref|Homo sapiens chemokine (C-C motif) ligand 20 transcript variant 1 mRNA
8.01	1.557	0.00027	A_23_P79803	*VSTM2L*	NM_080607	ref|Homo sapiens V-set and transmembrane domain containing 2 like mRNA
7.85	1.541	0	A_33_P3850216	*TRIM55*	NM_033058	ref|Homo sapiens tripartite motif containing 55 transcript variant 2 mRNA
9.14	1.540	0	A_24_P928052	*NRP1*	NM_003873	ref|Homo sapiens neuropilin 1 transcript variant 1 mRNA
9.58	1.535	0	A_23_P403335	*EXPH5*	NM_015065	ref|Homo sapiens exophilin 5 mRNA
7.10	1.523	0	A_23_P161563	*RAB38*	NM_022337	ref|Homo sapiens RAB38 member RAS oncogene family mRNA
11.28	1.467	0	A_23_P139704	*DUSP6*	NM_001946	ref|Homo sapiens dual specificity phosphatase 6 transcript variant 1 mRNA
8.47	1.418	7.00E-05	A_23_P60627	*ALOX15B*	NM_001141	ref|Homo sapiens arachidonate 15-lipoxygenase type B transcript variant d mRNA
13.49	1.416	0	A_33_P3357530	*SLC12A7*	NM_006598	ref|Homo sapiens solute carrier family 12 (potassium/chloride transporters) member 7 mRNA
9.28	1.414	1.00E-05	A_33_P3214849	*KDELC2*	NM_153705	ref|Homo sapiens KDEL (Lys-Asp-Glu-Leu) containing 2 mRNA
8.92	1.385	0	A_23_P123402	*TRIM55*	NM_184086	ref|Homo sapiens tripartite motif containing 55 transcript variant 3 mRNA
9.07	1.360	0	A_23_P123402	*TRIM55*	NM_184086	ref|Homo sapiens tripartite motif containing 55 transcript variant 3 mRNA
12.11	1.349	0.00029	A_23_P315364	*CXCL2*	NM_002089	ref|Homo sapiens chemokine (C-X-C motif) ligand 2 mRNA
9.18	1.313	0	A_33_P3418426	*SLC3A1*	NM_000341	ref|Homo sapiens solute carrier family 3 (cystine dibasic and neutral amino acid transporters activator of cystine dibasic and neutral amino acid transport) member 1 mRNA
8.97	1.311	0	A_23_P123402	*TRIM55*	NM_184086	ref|Homo sapiens tripartite motif containing 55 transcript variant 3 mRNA
10.41	1.309	0	A_23_P313389	*UGCG*	NM_003358	ref|Homo sapiens UDP-glucose ceramide glucosyltransferase mRNA
11.01	1.305	3.00E-05	A_23_P108082	*CREB3L3*	NM_032607	ref|Homo sapiens cAMP responsive element binding protein 3-like 3 mRNA
8.97	1.297	0	A_23_P123402	*TRIM55*	NM_184086	ref|Homo sapiens tripartite motif containing 55 transcript variant 3 mRNA
9.11	1.289	2.00E-05	A_23_P123402	*TRIM55*	NM_184086	ref|Homo sapiens tripartite motif containing 55 transcript variant 3 mRNA
8.91	1.288	0	A_23_P123402	*TRIM55*	NM_184086	ref|Homo sapiens tripartite motif containing 55 transcript variant 3 mRNA
8.85	1.276	1.00E-05	A_24_P23625	*HS3ST3B1*	ENST00000360954	ens|heparan sulfate (glucosamine) 3-O-sulfotransferase 3B1 [Source:HGNC Symbol;Acc:5198]

9.97	1.274	2.00E-04	A_23_P75749	*GLYAT*	NM_201648	ref|Homo sapiens glycine-N-acyltransferase nuclear gene encoding mitochondrial protein transcript variant 1 mRNA
8.92	1.273	0	A_23_P123402	*TRIM55*	NM_184086	ref|Homo sapiens tripartite motif containing 55 transcript variant 3 mRNA
7.91	1.267	1.00E-05	A_33_P3841368	*LOC286161*	AK091672	gb|Homo sapiens cDNA FLJ34353 fis clone FEBRA2011665
11.48	1.266	0	A_23_P64879	*KCNJ8*	NM_004982	ref|Homo sapiens potassium inwardly-rectifying channel subfamily J member 8 mRNA
9.15	1.263	0	A_23_P123402	*TRIM55*	NM_184086	ref|Homo sapiens tripartite motif containing 55 transcript variant 3 mRNA
9.38	1.251	0	A_23_P130376	*FAM38B*	NM_022068	ref|Homo sapiens family with sequence similarity 38 member B mRNA
8.64	1.249	5.00E-05	A_33_P3285580	*GLYCTK*	NM_145262	ref|Homo sapiens glycerate kinase transcript variant 1 mRNA
14.27	1.229	0	A_23_P118065	*HSD17B2*	NM_002153	ref|Homo sapiens hydroxysteroid (17-beta) dehydrogenase 2 mRNA
9.68	1.221	0	A_24_P294124	*SERTAD2*	NM_014755	ref|Homo sapiens SERTA domain containing 2 mRNA
14.16	1.216	0	A_23_P118065	*HSD17B2*	NM_002153	ref|Homo sapiens hydroxysteroid (17-beta) dehydrogenase 2 mRNA
14.33	1.208	0	A_23_P118065	*HSD17B2*	NM_002153	ref|Homo sapiens hydroxysteroid (17-beta) dehydrogenase 2 mRNA
9.05	1.207	5.00E-05	A_23_P431305	*FAM69B*	NM_152421	ref|Homo sapiens family with sequence similarity 69 member B mRNA
12.58	1.204	2.00E-05	A_23_P162142	*TSKU*	NM_015516	ref|Homo sapiens tsukushi small leucine rich proteoglycan homolog (Xenopus laevis) mRNA
14.22	1.203	0	A_23_P118065	*HSD17B2*	NM_002153	ref|Homo sapiens hydroxysteroid (17-beta) dehydrogenase 2 mRNA
14.36	1.202	0	A_23_P118065	*HSD17B2*	NM_002153	ref|Homo sapiens hydroxysteroid (17-beta) dehydrogenase 2 mRNA
14.30	1.202	0	A_23_P118065	*HSD17B2*	NM_002153	ref|Homo sapiens hydroxysteroid (17-beta) dehydrogenase 2 mRNA
14.17	1.199	0	A_23_P118065	*HSD17B2*	NM_002153	ref|Homo sapiens hydroxysteroid (17-beta) dehydrogenase 2 mRNA
9.99	1.193	9.00E-05	A_23_P342131	*CYBASC3*	NM_153611	ref|Homo sapiens cytochrome b ascorbate dependent 3 transcript variant 2 mRNA
9.13	1.192	0	A_23_P66881	*RGS9*	NM_003835	ref|Homo sapiens regulator of G-protein signaling 9 transcript variant 1 mRNA
10.92	1.180	0	A_33_P3341676	*MEF2A*	NM_001171894	ref|Homo sapiens myocyte enhancer factor 2A transcript variant 5 mRNA
8.99	1.180	0	A_23_P123402	*TRIM55*	NM_184086	ref|Homo sapiens tripartite motif containing 55 transcript variant 3 mRNA
9.01	1.169	0.00024	A_23_P103110	*MAFF*	NM_012323	ref|Homo sapiens v-maf musculoaponeurotic fibrosarcoma oncogene homolog F (avian) transcript variant 1 mRNA
7.62	1.166	1.00E-05	A_24_P13381	*TRPV4*	NM_147204	ref|Homo sapiens transient receptor potential cation channel subfamily V member 4 transcript variant 2 mRNA
11.07	1.163	1.00E-05	A_24_P217234	*SLC3A1*	NM_000341	ref|Homo sapiens solute carrier family 3 (cystine dibasic and neutral amino acid transporters activator of cystine dibasic and neutral amino acid transport) member 1 mRNA
7.05	1.159	1.00E-05	A_23_P383819	*TBX3*	NM_016569	ref|Homo sapiens T-box 3 transcript variant 2 mRNA
12.51	1.153	0	A_23_P99661	*ARHGEF40*	NM_018071	ref|Homo sapiens Rho guanine nucleotide exchange factor (GEF) 40 mRNA
7.91	1.147	1.00E-05	A_33_P3226650	*GSTA7P*	NR_033760	ref|Homo sapiens glutathione S-transferase alpha 7 pseudogene non-coding RNA
10.39	1.146	0	A_23_P331895	*TTYH3*	NM_025250	ref|Homo sapiens tweety homolog 3 (Drosophila) mRNA
9.10	1.144	4.00E-05	A_23_P103110	*MAFF*	NM_012323	ref|Homo sapiens v-maf musculoaponeurotic fibrosarcoma oncogene homolog F (avian) transcript variant 1 mRNA
7.32	1.144	1.00E-05	A_23_P165989	*NEURL2*	NM_080749	ref|Homo sapiens neuralized homolog 2 (Drosophila) mRNA

11.35	1.142	1.00E-04	A_23_P421032	*SEC14L4*	NM_174977	ref|Homo sapiens SEC14-like 4 (S. cerevisiae) transcript variant 1 mRNA
7.26	1.133	2.00E-05	A_23_P432573	*MRGPRF*	NM_145015	ref|Homo sapiens MAS-related GPR member F transcript variant 2 mRNA
7.01	1.125	2.00E-05	A_23_P212089	*NFKBIZ*	NM_031419	ref|Homo sapiens nuclear factor of kappa light polypeptide gene enhancer in B-cells inhibitor zeta transcript variant 1 mRNA
7.30	1.122	0.00024	A_32_P84242	*FAM169A*	NM_015566	ref|Homo sapiens family with sequence similarity 169 member A mRNA
9.09	1.115	0	A_23_P123402	*TRIM55*	NM_184086	ref|Homo sapiens tripartite motif containing 55 transcript variant 3 mRNA
14.19	1.114	0	A_23_P118065	*HSD17B2*	NM_002153	ref|Homo sapiens hydroxysteroid (17-beta) dehydrogenase 2 mRNA
13.05	1.108	0	A_33_P3336617	*ALDH3A2*	NM_000382	ref|Homo sapiens aldehyde dehydrogenase 3 family member A2 transcript variant 2 mRNA
14.29	1.106	0	A_23_P118065	*HSD17B2*	NM_002153	ref|Homo sapiens hydroxysteroid (17-beta) dehydrogenase 2 mRNA
14.20	1.105	0	A_23_P118065	*HSD17B2*	NM_002153	ref|Homo sapiens hydroxysteroid (17-beta) dehydrogenase 2 mRNA
7.17	1.101	1.00E-05	A_33_P3404316	*MIR100HG*	NR_024430	ref|Homo sapiens mir-100-let-7a-2 cluster host gene (non-protein coding) non-coding RNA
8.87	1.095	0.00032	A_23_P103110	*MAFF*	NM_012323	ref|Homo sapiens v-maf musculoaponeurotic fibrosarcoma oncogene homolog F (avian) transcript variant 1 mRNA
8.02	1.093	1.00E-05	A_33_P3620881	*LOC728218*	BC065757	gb|Homo sapiens cDNA clone IMAGE:4556546 partial cds
9.51	1.073	0	A_32_P205637	*PARD6B*	NM_032521	ref|Homo sapiens par-6 partitioning defective 6 homolog beta (C. elegans) mRNA
9.78	1.065	2.00E-05	A_23_P89431	*CCL2*	NM_002982	ref|Homo sapiens chemokine (C-C motif) ligand 2 mRNA
13.88	1.064	1.00E-05	A_23_P94159	*FBXO25*	NM_183421	ref|Homo sapiens F-box protein 25 transcript variant 1 mRNA
12.28	1.063	1.00E-05	A_23_P112531	*FAM102A*	NM_001035254	ref|Homo sapiens family with sequence similarity 102 member A transcript variant 1 mRNA
10.85	1.059	0	A_24_P346431	*TNS3*	NM_022748	ref|Homo sapiens tensin 3 mRNA
7.93	1.056	1.00E-05	A_24_P254278	*SLC23A2*	NM_203327	ref|Homo sapiens solute carrier family 23 (nucleobase transporters) member 2 transcript variant 2 mRNA
11.06	1.055	4.00E-05	A_23_P145786	*MLXIPL*	NM_032951	ref|Homo sapiens MLX interacting protein-like transcript variant 1 mRNA
7.38	1.054	2.00E-05	A_24_P46093	*SLC6A6*	NM_003043	ref|Homo sapiens solute carrier family 6 (neurotransmitter transporter taurine) member 6 transcript variant 1 mRNA
8.63	1.051	1.00E-05	A_24_P256404	*ENST00000356370*	ENST00000356370	gb|Homo sapiens cDNA FLJ35883 fis clone TESTI2008929
12.61	1.041	1.00E-05	A_23_P112531	*FAM102A*	NM_001035254	ref|Homo sapiens family with sequence similarity 102 member A transcript variant 1 mRNA
7.67	1.031	1.00E-04	A_23_P74112	*IL28RA*	NM_170743	ref|Homo sapiens interleukin 28 receptor alpha (interferon lambda receptor) transcript variant 1 mRNA
9.03	1.030	0.00021	A_23_P103110	*MAFF*	NM_012323	ref|Homo sapiens v-maf musculoaponeurotic fibrosarcoma oncogene homolog F (avian) transcript variant 1 mRNA
12.46	1.029	0	A_23_P112531	*FAM102A*	NM_001035254	ref|Homo sapiens family with sequence similarity 102 member A transcript variant 1 mRNA
10.60	1.029	6.00E-05	A_23_P112482	*AQP3*	NM_004925	ref|Homo sapiens aquaporin 3 (Gill blood group) mRNA
12.30	1.028	1.00E-05	A_23_P112531	*FAM102A*	NM_001035254	ref|Homo sapiens family with sequence similarity 102 member A transcript variant 1 mRNA
9.08	1.026	0.00021	A_23_P103110	*MAFF*	NM_012323	ref|Homo sapiens v-maf musculoaponeurotic fibrosarcoma oncogene homolog F (avian) transcript variant 1 mRNA
13.16	1.025	0	A_23_P423197	*RXRA*	NM_002957	ref|Homo sapiens retinoid X receptor alpha mRNA
9.07	1.023	0.00012	A_23_P103110	*MAFF*	NM_012323	ref|Homo sapiens v-maf musculoaponeurotic fibrosarcoma oncogene homolog F (avian) transcript variant 1 mRNA
12.37	1.021	9.00E-05	A_23_P112531	*FAM102A*	NM_001035254	ref|Homo sapiens family with sequence similarity 102 member A transcript variant 1 mRNA

12.47	1.021	0	A_23_P112531	*FAM102A*	NM_001035254	ref|Homo sapiens family with sequence similarity 102 member A transcript variant 1 mRNA
7.96	1.020	7.00E-05	A_23_P169039	*SNAI2*	NM_003068	ref|Homo sapiens snail homolog 2 (Drosophila) mRNA
11.61	1.016	3.00E-05	A_23_P94921	*SLC20A2*	NM_006749	ref|Homo sapiens solute carrier family 20 (phosphate transporter) member 2 mRNA
9.11	1.015	0.00015	A_23_P103110	*MAFF*	NM_012323	ref|Homo sapiens v-maf musculoaponeurotic fibrosarcoma oncogene homolog F (avian) transcript variant 1 mRNA
9.58	1.013	5.00E-05	A_23_P89431	*CCL2*	NM_002982	ref|Homo sapiens chemokine (C-C motif) ligand 2 mRNA
15.86	1.013	0	A_23_P16523	*GDF15*	NM_004864	ref|Homo sapiens growth differentiation factor 15 mRNA
12.44	1.013	1.00E-05	A_33_P3383233	*NDRG2*	NM_201535	ref|Homo sapiens NDRG family member 2 transcript variant 1 mRNA
9.77	1.009	9.00E-05	A_23_P319572	*NR1I3*	NM_001077482	ref|Homo sapiens nuclear receptor subfamily 1 group I member 3 transcript variant 1 mRNA
10.72	1.009	5.00E-05	A_23_P112482	*AQP3*	NM_004925	ref|Homo sapiens aquaporin 3 (Gill blood group) mRNA
11.67	1.009	0	A_33_P3282394	*MLLT1*	NM_005934	ref|Homo sapiens myeloid/lymphoid or mixed-lineage leukemia (trithorax homolog Drosophila); translocated to 1 mRNA
10.34	1.008	2.00E-05	A_23_P8240	*FAM50B*	NM_012135	ref|Homo sapiens family with sequence similarity 50 member B mRNA
12.38	1.005	1.00E-05	A_23_P112531	*FAM102A*	NM_001035254	ref|Homo sapiens family with sequence similarity 102 member A transcript variant 1 mRNA

Table 94. All significantly down regulated genes in hHeps after treatment with 4-PnCDF (30 nM) identified by microarray analysis. Selected parameters: A-value ≥ 7, log2 fc ≤ -1, p-value ≤ 0.05.

A	Log2 fc	p-value	Probe name	Gene name	Systematic name	Gene description
8.34	-1.536	3.00E-05	A_33_P3342752	*ENST00000366873*	ENST00000366873	ens|calpain 8 [Source:HGNC Symbol;Acc:1485]
8.43	-1.426	0.00025	A_24_P331704	*KRT80*	NM_182507	ref|Homo sapiens keratin 80 transcript variant 1 mRNA
8.53	-1.421	0	A_23_P421401	*PDGFRB*	NM_002609	ref|Homo sapiens platelet-derived growth factor receptor beta polypeptide mRNA
9.49	-1.317	0	A_23_P104798	*IL18*	NM_001562	ref|Homo sapiens interleukin 18 (interferon-gamma-inducing factor) mRNA
9.51	-1.297	2.00E-05	A_23_P104798	*IL18*	NM_001562	ref|Homo sapiens interleukin 18 (interferon-gamma-inducing factor) mRNA
9.66	-1.283	0	A_23_P104798	*IL18*	NM_001562	ref|Homo sapiens interleukin 18 (interferon-gamma-inducing factor) mRNA
9.80	-1.277	0	A_23_P104798	*IL18*	NM_001562	ref|Homo sapiens interleukin 18 (interferon-gamma-inducing factor) mRNA
10.71	-1.266	0	A_23_P333029	*C8orf47*	NM_173549	ref|Homo sapiens chromosome 8 open reading frame 47 transcript variant 1 mRNA
10.21	-1.238	3.00E-05	A_23_P92161	*ARL14*	NM_025047	ref|Homo sapiens ADP-ribosylation factor-like 14 mRNA
9.55	-1.224	0	A_23_P104798	*IL18*	NM_001562	ref|Homo sapiens interleukin 18 (interferon-gamma-inducing factor) mRNA
9.38	-1.223	0	A_23_P104798	*IL18*	NM_001562	ref|Homo sapiens interleukin 18 (interferon-gamma-inducing factor) mRNA
9.52	-1.180	3.00E-05	A_23_P104798	*IL18*	NM_001562	ref|Homo sapiens interleukin 18 (interferon-gamma-inducing factor) mRNA
10.61	-1.146	1.00E-05	A_33_P3398331	*MMP24*	NM_006690	ref|Homo sapiens matrix metallopeptidase 24 (membrane-inserted) mRNA
9.58	-1.107	5.00E-05	A_23_P104798	*IL18*	NM_001562	ref|Homo sapiens interleukin 18 (interferon-gamma-inducing factor) mRNA
9.48	-1.097	0.00028	A_23_P104798	*IL18*	NM_001562	ref|Homo sapiens interleukin 18 (interferon-gamma-inducing factor) mRNA
9.48	-1.090	8.00E-05	A_23_P104798	*IL18*	NM_001562	ref|Homo sapiens interleukin 18 (interferon-gamma-inducing factor) mRNA

Table 95. All significantly up regulated genes in hHeps after treatment with PCB 126 (100 nM) identified by microarray analysis. Selected parameters: A-value ≥ 7, log2 fc ≥ 1, p-value ≤ 0.05.

A	Log2 fc	p-value	Probe name	Gene name	Systematic name	Gene description
12.43	5.452	0	A_23_P209625	*CYP1B1*	NM_000104	ref|Homo sapiens cytochrome P450 family 1 subfamily B polypeptide 1 mRNA
12.73	4.713	0	A_23_P163402	*CYP1A1*	NM_000499	ref|Homo sapiens cytochrome P450 family 1 subfamily A polypeptide 1 mRNA
10.97	4.015	0	A_33_P3290343	*CYP1B1*	NM_000104	ref|Homo sapiens cytochrome P450 family 1 subfamily B polypeptide 1 mRNA
8.83	3.327	0	A_23_P207213	*ALDH3A1*	NM_000691	ref|Homo sapiens aldehyde dehydrogenase 3 family member A1 transcript variant 2 mRNA
9.01	3.185	0	A_23_P165136	*LRRC25*	NM_145256	ref|Homo sapiens leucine rich repeat containing 25 mRNA
8.99	3.090	0	A_23_P26854	*ARHGAP44*	NM_014859	ref|Homo sapiens Rho GTPase activating protein 44 mRNA
10.1	2.807	0	A_33_P3238433	*ALDH3A1*	NM_001135168	ref|Homo sapiens aldehyde dehydrogenase 3 family member A1 transcript variant 1 mRNA
15.21	2.190	0	A_33_P3253747	*CYP1A2*	NM_000761	ref|Homo sapiens cytochrome P450 family 1 subfamily A polypeptide 2 mRNA
8.13	2.106	1.00E-05	A_32_P49867	*LOC100507055*	NM_001195520	ref|Homo sapiens hypothetical LOC100507055 mRNA
10.23	1.907	0	A_23_P416581	*GNAZ*	NM_002073	ref|Homo sapiens guanine nucleotide binding protein (G protein) alpha z polypeptide mRNA
11.27	1.901	0	A_23_P57910	*RTP3*	NM_031440	ref|Homo sapiens receptor (chemosensory) transporter protein 3 mRNA
8.74	1.871	0	A_33_P3734384	*LOC285957*	AK097526	gb|Homo sapiens cDNA FLJ40207 fis clone TESTI2020946
9.76	1.844	0	A_33_P3397795	*C14orf135*	AK095489	gb|Homo sapiens cDNA FLJ38170 fis clone FCBBF1000024
8.58	1.766	0	A_23_P259071	*AREG*	NM_001657	ref|Homo sapiens amphiregulin mRNA
7.89	1.645	0	A_24_P335620	*SLC7A5*	NM_003486	ref|Homo sapiens solute carrier family 7 (amino acid transporter light chain L system) member 5 mRNA
7.40	1.639	0	A_33_P3419190	*AREG*	NM_001657	ref|Homo sapiens amphiregulin mRNA
12.12	1.496	8.00E-05	A_33_P3222762	*HULC*	NR_004855	ref|Homo sapiens highly up-regulated in liver cancer (non-protein coding) non-coding RNA
11.30	1.454	0	A_23_P143845	*TIPARP*	NM_015508	ref|Homo sapiens TCDD-inducible poly(ADP-ribose) polymerase transcript variant 2 mRNA
9.68	1.414	5.00E-05	A_23_P41804	*NKD2*	NM_033120	ref|Homo sapiens naked cuticle homolog 2 (Drosophila) mRNA
12.98	1.360	9.00E-05	A_23_P421423	*TNFAIP2*	NM_006291	ref|Homo sapiens tumor necrosis factor alpha-induced protein 2 mRNA
9.85	1.326	1.00E-05	A_24_P157370	*IL17RB*	NM_018725	ref|Homo sapiens interleukin 17 receptor B mRNA
9.56	1.313	0.00013	A_23_P75630	*APOA5*	NM_052968	ref|Homo sapiens apolipoprotein A-V transcript variant 1 mRNA
11.48	1.281	0	A_23_P83110	*CDK5RAP2*	NM_018249	ref|Homo sapiens CDK5 regulatory subunit associated protein 2 transcript variant 1 mRNA
8.51	1.230	3.00E-05	A_23_P116942	*LAG3*	NM_002286	ref|Homo sapiens lymphocyte-activation gene 3 mRNA
10.02	1.163	0.00011	A_33_P3389060	*CDK5RAP2*	NM_018249	ref|Homo sapiens CDK5 regulatory subunit associated protein 2 transcript variant 1 mRNA
9.58	1.134	1.00E-05	A_23_P403335	*EXPH5*	NM_015065	ref|Homo sapiens exophilin 5 mRNA
8.09	1.099	4.00E-05	A_23_P257003	*PCSK5*	NM_006200	ref|Homo sapiens proprotein convertase subtilisin/kexin type 5 transcript variant 2 mRNA
10.41	1.067	0	A_23_P313389	*UGCG*	NM_003358	ref|Homo sapiens UDP-glucose ceramide glucosyltransferase mRNA

8.98	1.030	0.00023	A_23_P52082	*INTS7*	NM_015434	ref|Homo sapiens integrator complex subunit 7 transcript variant 1 mRNA

Table 96. All significantly up regulated genes in HepG2 cells after treatment with TCDD (10 nM) identified by microarray analysis. Selected parameters: A-value ≥ 5, log2 fc ≥ 1, p-value ≤ 0.05.

A	Log2 fc	p-value	Probe name	Gene name	Systematic name	Gene description
10.68	5.003	0	A_23_P163402	*CYP1A1*	NM_000499	ref|Homo sapiens cytochrome P450 family 1 subfamily A polypeptide 1 mRNA
7.41	4.880	0	A_23_P51376	*NKAIN1*	NM_024522	ref|Homo sapiens Na+/K+ transporting ATPase interacting 1 mRNA
7.56	4.879	0	A_23_P165136	*LRRC25*	NM_145256	ref|Homo sapiens leucine rich repeat containing 25 mRNA
7.16	4.544	0	A_24_P253003	*WNT11*	NM_004626	ref|Homo sapiens wingless-type MMTV integration site family member 11 mRNA
6.25	4.505	0	A_23_P114883	*FMOD*	NM_002023	ref|Homo sapiens fibromodulin mRNA
7.78	4.402	0	A_23_P152791	*SLC16A6*	NM_004694	ref|Homo sapiens solute carrier family 16 member 6 (monocarboxylic acid transporter 7) transcript variant 2 mRNA
6.46	4.393	0	A_23_P114883	*FMOD*	NM_002023	ref|Homo sapiens fibromodulin mRNA
6.47	4.295	0	A_23_P114883	*FMOD*	NM_002023	ref|Homo sapiens fibromodulin mRNA
6.16	4.269	0	A_23_P114883	*FMOD*	NM_002023	ref|Homo sapiens fibromodulin mRNA
6.32	4.258	0	A_23_P114883	*FMOD*	NM_002023	ref|Homo sapiens fibromodulin mRNA
6.62	4.194	0	A_23_P114883	*FMOD*	NM_002023	ref|Homo sapiens fibromodulin mRNA
6.52	4.107	0	A_23_P114883	*FMOD*	NM_002023	ref|Homo sapiens fibromodulin mRNA
8.44	4.107	0	A_23_P130435	*LIM2*	NM_030657	ref|Homo sapiens lens intrinsic membrane protein 2 19kDa transcript variant 1 mRNA
6.15	4.100	0	A_23_P114883	*FMOD*	NM_002023	ref|Homo sapiens fibromodulin mRNA
5.63	3.989	1.00E-05	A_23_P358709	*AHRR*	NM_020731	ref|Homo sapiens aryl-hydrocarbon receptor repressor transcript variant 1 mRNA
6.35	3.981	0	A_23_P114883	*FMOD*	NM_002023	ref|Homo sapiens fibromodulin) mRNA
6.61	3.851	0	A_23_P114883	*FMOD*	NM_002023	ref|Homo sapiens fibromodulin mRNA
5.66	3.518	0	A_23_P209625	*CYP1B1*	NM_000104	ref|Homo sapiens cytochrome P450 family 1 subfamily B polypeptide 1 mRNA
6.60	3.499	0	A_23_P202658	*GSTP1*	NM_000852	ref|Homo sapiens glutathione S-transferase pi 1 mRNA
6.04	3.471	0	A_23_P421032	*SEC14L4*	NM_174977	ref|Homo sapiens SEC14-like 4 (S. cerevisiae) transcript variant 1 mRNA
7.85	3.469	0	A_23_P207213	*ALDH3A1*	NM_000691	ref|Homo sapiens aldehyde dehydrogenase 3 family member A1 transcript variant 2 mRNA
5.26	3.378	0	A_23_P165783	*MLPH*	NM_024101	ref|Homo sapiens melanophilin transcript variant 1 mRNA
7.45	3.323	0	A_33_P3222977	*TEKT5*	NM_144674	ref|Homo sapiens tektin 5 mRNA
8.66	3.319	0	A_33_P3238433	*ALDH3A1*	NM_001135168	ref|Homo sapiens aldehyde dehydrogenase 3 family member A1 transcript variant 1 mRNA
6.61	3.261	0	A_23_P202658	*GSTP1*	NM_000852	ref|Homo sapiens glutathione S-transferase pi 1 mRNA
6.26	3.254	0	A_23_P202658	*GSTP1*	NM_000852	ref|Homo sapiens glutathione S-transferase pi 1 mRNA
7.96	3.125	0	A_24_P115932	*GPR44*	NM_004778	ref|Homo sapiens G protein-coupled receptor 44 mRNA
6.49	3.077	0	A_23_P202658	*GSTP1*	NM_000852	ref|Homo sapiens glutathione S-transferase pi 1 mRNA

6.66	3.061	0	A_23_P202658	*GSTP1*	NM_000852	ref|Homo sapiens glutathione S-transferase pi 1 mRNA
6.36	3.056	0	A_23_P202658	*GSTP1*	NM_000852	ref|Homo sapiens glutathione S-transferase pi 1 mRNA
6.71	3.033	0	A_23_P202658	*GSTP1*	NM_000852	ref|Homo sapiens glutathione S-transferase pi 1 mRNA
7.73	3.025	0	A_23_P37410	*CYP19A1*	NM_031226	ref|Homo sapiens cytochrome P450 family 19 subfamily A polypeptide 1 transcript variant 2 mRNA
6.69	3.024	0	A_23_P202658	*GSTP1*	NM_000852	ref|Homo sapiens glutathione S-transferase pi 1 mRNA
7.07	3.015	0	A_23_P128215	*SOCS2*	NM_003877	ref|Homo sapiens suppressor of cytokine signaling 2 mRNA
5.54	2.999	0	A_33_P3365142	*GAD1*	NM_013445	ref|Homo sapiens glutamate decarboxylase 1 (brain 67kDa) transcript variant GAD25 mRNA
5.91	2.996	1.00E-05	A_33_P3346618	*LOC441179*	XR_112948	ref|PREDICTED: Homo sapiens hypothetical LOC441179 miscRNA
6.40	2.961	0	A_23_P202658	*GSTP1*	NM_000852	ref|Homo sapiens glutathione S-transferase pi 1 mRNA
11.42	2.915	0	A_33_P3360540	*AGPAT2*	NM_006412	ref|Homo sapiens 1-acylglycerol-3-phosphate O-acyltransferase 2 (lysophosphatidic acid acyltransferase beta) transcript variant 1 mRNA
6.48	2.896	0	A_23_P202658	*GSTP1*	NM_000852	ref|Homo sapiens glutathione S-transferase pi 1 mRNA
7.22	2.893	1.00E-05	A_23_P64721	*HCAR3*	NM_006018	ref|Homo sapiens hydroxycarboxylic acid receptor 3 mRNA
10.43	2.766	0	A_23_P408376	*HSPA12A*	NM_025015	ref|Homo sapiens heat shock 70kDa protein 12A mRNA
6.87	2.738	0	A_23_P354387	*MYOF*	NM_013451	ref|Homo sapiens myoferlin transcript variant 1 mRNA
7.46	2.686	0	A_24_P63019	*IL1R2*	NM_004633	ref|Homo sapiens interleukin 1 receptor type II transcript variant 1 mRNA
7.48	2.662	1.00E-05	A_23_P119916	*WNT6*	NM_006522	ref|Homo sapiens wingless-type MMTV integration site family member 6 mRNA
11.51	2.613	0	A_23_P138717	*RGS10*	NM_001005339	ref|Homo sapiens regulator of G-protein signaling 10 transcript variant 1 mRNA
8.28	2.595	0	A_24_P126210	*MRAP*	NM_178817	ref|Homo sapiens melanocortin 2 receptor accessory protein transcript variant 1 mRNA
6.28	2.566	2.00E-05	A_33_P3348224	*SEC14L6*	NM_001193336	ref|Homo sapiens SEC14-like 6 (S. cerevisiae) mRNA
7.66	2.540	0	A_23_P404667	*BIK*	NM_001197	ref|Homo sapiens BCL2-interacting killer (apoptosis-inducing) mRNA
6.84	2.524	2.00E-05	A_23_P112482	*AQP3*	NM_004925	ref|Homo sapiens aquaporin 3 (Gill blood group) mRNA
6.35	2.498	0	A_33_P3351371	*CYP19A1*	NM_031226	ref|Homo sapiens cytochrome P450 family 19 subfamily A polypeptide 1 transcript variant 2 mRNA
8.35	2.462	0	A_33_P3356406	*SOS1*	NM_005633	ref|Homo sapiens son of sevenless homolog 1 (Drosophila) mRNA
7.01	2.431	0	A_23_P112482	*AQP3*	NM_004925	ref|Homo sapiens aquaporin 3 (Gill blood group) mRNA
6.77	2.430	0	A_23_P112482	*AQP3*	NM_004925	ref|Homo sapiens aquaporin 3 (Gill blood group) mRNA
16.43	2.420	0	A_23_P42868	*IGFBP1*	NM_000596	ref|Homo sapiens insulin-like growth factor binding protein 1 mRNA
6.97	2.420	0	A_23_P112482	*AQP3*	NM_004925	ref|Homo sapiens aquaporin 3 (Gill blood group) mRNA
5.98	2.408	0	A_32_P49867	*LOC100507055*	NM_001195520	ref|Homo sapiens hypothetical LOC100507055 mRNA
8.38	2.389	0	A_23_P379649	*BMF*	NM_001003940	ref|Homo sapiens Bcl2 modifying factor transcript variant 1 mRNA
9.02	2.379	0	A_23_P128974	*BATF*	NM_006399	ref|Homo sapiens basic leucine zipper transcription factor ATF-like mRNA
5.49	2.367	7.00E-05	A_23_P166087	*RASSF2*	NM_014737	ref|Homo sapiens Ras association (RalGDS/AF-6) domain family member 2 transcript variant 1 mRNA

6.06	2.332	0	A_33_P3741022	*FLJ26484*	NR_033876	ref|Homo sapiens hypothetical LOC400619 non-coding RNA
6.95	2.328	0	A_23_P112482	*AQP3*	NM_004925	ref|Homo sapiens aquaporin 3 (Gill blood group) mRNA
7.02	2.309	5.00E-05	A_23_P12363	*ROR1*	NM_005012	ref|Homo sapiens receptor tyrosine kinase-like orphan receptor 1 transcript variant 1 mRNA
5.76	2.291	5.00E-05	A_33_P3243023	*ADRA1D*	NM_000678	ref|Homo sapiens adrenergic alpha-1D- receptor mRNA
7.03	2.277	0	A_23_P421423	*TNFAIP2*	NM_006291	ref|Homo sapiens tumor necrosis factor alpha-induced protein 2 mRNA
7.15	2.266	0	A_23_P112482	*AQP3*	NM_004925	ref|Homo sapiens aquaporin 3 (Gill blood group) mRNA
6.92	2.265	2.00E-05	A_23_P112482	*AQP3*	NM_004925	ref|Homo sapiens aquaporin 3 (Gill blood group) mRNA
6.83	2.243	0	A_23_P12363	*ROR1*	NM_005012	ref|Homo sapiens receptor tyrosine kinase-like orphan receptor 1 transcript variant 1 mRNA
7.01	2.239	0	A_23_P142878	*ATOH8*	NM_032827	ref|Homo sapiens atonal homolog 8 (Drosophila) mRNA
5.43	2.229	0.00049	A_23_P105012	*HRASLS2*	NM_017878	ref|Homo sapiens HRAS-like suppressor 2 mRNA
8.29	2.212	0	A_23_P35529	*MBL2*	NM_000242	ref|Homo sapiens mannose-binding lectin (protein C) 2 soluble mRNA
5.08	2.203	0	A_23_P105012	*HRASLS2*	NM_017878	ref|Homo sapiens HRAS-like suppressor 2 mRNA
7.00	2.179	1.00E-05	A_23_P112482	*AQP3*	NM_004925	ref|Homo sapiens aquaporin 3 (Gill blood group) mRNA
5.42	2.174	0	A_23_P105012	*HRASLS2*	NM_017878	ref|Homo sapiens HRAS-like suppressor 2 mRNA
6.94	2.173	0	A_23_P12363	*ROR1*	NM_005012	ref|Homo sapiens receptor tyrosine kinase-like orphan receptor 1 transcript variant 1 mRNA
6.35	2.151	5.00E-05	A_23_P112482	*AQP3*	NM_004925	ref|Homo sapiens aquaporin 3 (Gill blood group) mRNA
6.81	2.122	0.00026	A_23_P112482	*AQP3*	NM_004925	ref|Homo sapiens aquaporin 3 (Gill blood group) mRNA
5.33	2.118	0	A_33_P3371999	*TPPP*	NM_007030	ref|Homo sapiens tubulin polymerization promoting protein mRNA
9.36	2.096	0	A_23_P31407	*AGR2*	NM_006408	ref|Homo sapiens anterior gradient homolog 2 (Xenopus laevis) mRNA
9.49	2.066	0	A_23_P331928	*CD109*	NM_133493	ref|Homo sapiens CD109 molecule transcript variant 1 mRNA
6.92	2.057	0	A_23_P12363	*ROR1*	NM_005012	ref|Homo sapiens receptor tyrosine kinase-like orphan receptor 1 transcript variant 1 mRNA
9.34	2.054	0	A_23_P92042	*ITPR1*	NM_002222	ref|Homo sapiens inositol 145-trisphosphate receptor type 1 transcript variant 2 mRNA
5.22	2.046	5.00E-04	A_23_P105012	*HRASLS2*	NM_017878	ref|Homo sapiens HRAS-like suppressor 2 mRNA
6.93	2.037	0	A_23_P12363	*ROR1*	NM_005012	ref|Homo sapiens receptor tyrosine kinase-like orphan receptor 1 transcript variant 1 mRNA
8.27	2.016	0	A_23_P205370	*ASB2*	NM_016150	ref|Homo sapiens ankyrin repeat and SOCS box containing 2 transcript variant 2 mRNA
6.86	2.013	0	A_23_P12363	*ROR1*	NM_005012	ref|Homo sapiens receptor tyrosine kinase-like orphan receptor 1 transcript variant 1 mRNA
8.12	1.987	0	A_32_P108254	*FAM20A*	NM_017565	ref|Homo sapiens family with sequence similarity 20 member A transcript variant 1 mRNA
14.28	1.979	0	A_23_P106682	*EMP2*	NM_001424	ref|Homo sapiens epithelial membrane protein 2 mRNA
14.33	1.970	0	A_23_P106682	*EMP2*	NM_001424	ref|Homo sapiens epithelial membrane protein 2 mRNA
14.41	1.969	0	A_23_P106682	*EMP2*	NM_001424	ref|Homo sapiens epithelial membrane protein 2 mRNA
8.03	1.966	0	A_24_P88763	*LOXL3*	NM_032603	ref|Homo sapiens lysyl oxidase-like 3 mRNA
7.03	1.960	0	A_23_P12363	*ROR1*	NM_005012	ref|Homo sapiens receptor tyrosine kinase-like orphan receptor 1 transcript variant 1 mRNA

14.33	1.959	0	A_23_P106682	*EMP2*	NM_001424	ref|Homo sapiens epithelial membrane protein 2 mRNA
14.15	1.952	0	A_23_P106682	*EMP2*	NM_001424	ref|Homo sapiens epithelial membrane protein 2 mRNA
9.15	1.951	0	A_33_P3268472	*CTSC*	NM_001114173	ref|Homo sapiens cathepsin C transcript variant 3 mRNA
14.15	1.949	0	A_23_P87049	*SORL1*	NM_003105	ref|Homo sapiens sortilin-related receptor L(DLR class) A repeats containing mRNA
14.21	1.948	0	A_23_P106682	*EMP2*	NM_001424	ref|Homo sapiens epithelial membrane protein 2 mRNA
14.35	1.946	0	A_23_P106682	*EMP2*	NM_001424	ref|Homo sapiens epithelial membrane protein 2 mRNA
5.21	1.934	3.00E-05	A_23_P105012	*HRASLS2*	NM_017878	ref|Homo sapiens HRAS-like suppressor 2 mRNA
14.36	1.929	0	A_23_P106682	*EMP2*	NM_001424	ref|Homo sapiens epithelial membrane protein 2 mRNA
6.95	1.923	0	A_23_P12363	*ROR1*	NM_005012	ref|Homo sapiens receptor tyrosine kinase-like orphan receptor 1 transcript variant 1 mRNA
14.30	1.918	0	A_23_P106682	*EMP2*	NM_001424	ref|Homo sapiens epithelial membrane protein 2 mRNA
14.36	1.903	0	A_23_P106682	*EMP2*	NM_001424	ref|Homo sapiens epithelial membrane protein 2 mRNA
6.41	1.894	2.00E-05	A_23_P12363	*ROR1*	NM_005012	ref|Homo sapiens receptor tyrosine kinase-like orphan receptor 1 transcript variant 1 mRNA
10.65	1.891	0	A_23_P118065	*HSD17B2*	NM_002153	ref|Homo sapiens hydroxysteroid (17-beta) dehydrogenase 2 mRNA
10.42	1.883	0	A_23_P118065	*HSD17B2*	NM_002153	ref|Homo sapiens hydroxysteroid (17-beta) dehydrogenase 2 mRNA
13.94	1.878	0	A_33_P3210561	*A_33_P3210561*	A_33_P3210561	Unknown
10.51	1.873	0	A_23_P118065	*HSD17B2*	NM_002153	ref|Homo sapiens hydroxysteroid (17-beta) dehydrogenase 2 mRNA
5.38	1.873	0.00119	A_24_P105933	*VIPR1*	NM_004624	ref|Homo sapiens vasoactive intestinal peptide receptor 1 mRNA
7.13	1.872	0.00011	A_23_P121665	*SORCS2*	NM_020777	ref|Homo sapiens sortilin-related VPS10 domain containing receptor 2 mRNA
7.15	1.868	0.00081	A_23_P121665	*SORCS2*	NM_020777	ref|Homo sapiens sortilin-related VPS10 domain containing receptor 2 mRNA
6.15	1.866	0.00013	A_24_P237036	*TNFSF14*	NM_003807	ref|Homo sapiens tumor necrosis factor (ligand) superfamily member 14 transcript variant 1 mRNA
9.19	1.858	0	A_24_P658584	*SASH1*	NM_015278	ref|Homo sapiens SAM and SH3 domain containing 1 mRNA
16.42	1.851	0	A_23_P106844	*MT2A*	NM_005953	ref|Homo sapiens metallothionein 2A mRNA
10.64	1.842	0	A_23_P118065	*HSD17B2*	NM_002153	ref|Homo sapiens hydroxysteroid (17-beta) dehydrogenase 2 mRNA
10.43	1.837	0	A_23_P118065	*HSD17B2*	NM_002153	ref|Homo sapiens hydroxysteroid (17-beta) dehydrogenase 2 mRNA
10.42	1.835	0	A_23_P118065	*HSD17B2*	NM_002153	ref|Homo sapiens hydroxysteroid (17-beta) dehydrogenase 2 mRNA
5.31	1.830	3.00E-05	A_23_P105012	*HRASLS2*	NM_017878	ref|Homo sapiens HRAS-like suppressor 2 mRNA
5.54	1.829	2.00E-04	A_23_P105012	*HRASLS2*	NM_017878	ref|Homo sapiens HRAS-like suppressor 2 mRNA
7.32	1.827	0	A_33_P3253747	*CYP1A2*	NM_000761	ref|Homo sapiens cytochrome P450 family 1 subfamily A polypeptide 2 mRNA
10.08	1.821	0	A_23_P118065	*HSD17B2*	NM_002153	ref|Homo sapiens hydroxysteroid (17-beta) dehydrogenase 2 mRNA
10.62	1.821	0	A_23_P257003	*PCSK5*	NM_006200	ref|Homo sapiens proprotein convertase subtilisin/kexin type 5 transcript variant 2 mRNA
10.59	1.817	0	A_23_P118065	*HSD17B2*	NM_002153	ref|Homo sapiens hydroxysteroid (17-beta) dehydrogenase 2 mRNA
10.36	1.816	0	A_23_P118065	*HSD17B2*	NM_002153	ref|Homo sapiens hydroxysteroid (17-beta) dehydrogenase 2 mRNA

8.33	1.816	0	A_23_P343808	*SOS1*	NM_005633	ref|Homo sapiens son of sevenless homolog 1 (Drosophila) mRNA
9.92	1.815	0	A_33_P3215768	*GALNT6*	NM_007210	ref|Homo sapiens UDP-N-acetyl-alpha-D-galactosamine:polypeptide N-acetylgalactosaminyltransferase 6 (GalNAc-T6) mRNA [
12.47	1.805	0	A_23_P304682	*EMP2*	NM_001424	ref|Homo sapiens epithelial membrane protein 2 mRNA
11.26	1.799	0	A_33_P3336720	*HAMP*	NM_021175	ref|Homo sapiens hepcidin antimicrobial peptide mRNA
7.30	1.785	1.00E-04	A_23_P121665	*SORCS2*	NM_020777	ref|Homo sapiens sortilin-related VPS10 domain containing receptor 2 mRNA
10.32	1.775	0	A_23_P118065	*HSD17B2*	NM_002153	ref|Homo sapiens hydroxysteroid (17-beta) dehydrogenase 2 mRNA
6.62	1.769	0	A_23_P12363	*ROR1*	NM_005012	ref|Homo sapiens receptor tyrosine kinase-like orphan receptor 1 transcript variant 1 mRNA
5.57	1.761	7.00E-05	A_33_P3209591	*AQP3*	NM_004925	ref|Homo sapiens aquaporin 3 (Gill blood group) mRNA
10.16	1.759	0	A_23_P166823	*TNNC1*	NM_003280	ref|Homo sapiens troponin C type 1 (slow) mRNA
5.31	1.735	4.00E-05	A_23_P105012	*HRASLS2*	NM_017878	ref|Homo sapiens HRAS-like suppressor 2 mRNA
8.72	1.727	0	A_23_P104563	*CPT1A*	NM_001031847	ref|Homo sapiens carnitine palmitoyltransferase 1A (liver) nuclear gene encoding mitochondrial protein transcript variant 2 mRNA
8.92	1.726	0	A_23_P104563	*CPT1A*	NM_001031847	ref|Homo sapiens carnitine palmitoyltransferase 1A (liver) nuclear gene encoding mitochondrial protein transcript variant 2 mRNA
8.90	1.719	0	A_23_P104563	*CPT1A*	NM_001031847	ref|Homo sapiens carnitine palmitoyltransferase 1A (liver) nuclear gene encoding mitochondrial protein transcript variant 2 mRNA
9.26	1.719	0	A_23_P104563	*CPT1A*	NM_001031847	ref|Homo sapiens carnitine palmitoyltransferase 1A (liver) nuclear gene encoding mitochondrial protein transcript variant 2 mRNA
9.38	1.716	0	A_23_P50946	*RAMP1*	NM_005855	ref|Homo sapiens receptor (G protein-coupled) activity modifying protein 1 mRNA
7.09	1.716	0.00063	A_23_P121665	*SORCS2*	NM_020777	ref|Homo sapiens sortilin-related VPS10 domain containing receptor 2 mRNA
5.75	1.709	0.00025	A_23_P27306	*COLEC12*	NM_130386	ref|Homo sapiens collectin sub-family member 12 mRNA
7.17	1.703	0	A_24_P363100	*RGMB*	NM_001012761	ref|Homo sapiens RGM domain family member B mRNA
9.07	1.701	0	A_24_P340128	*P2RY8*	NM_178129	ref|Homo sapiens purinergic receptor P2Y G-protein coupled 8) mRNA
7.15	1.696	8.00E-05	A_23_P121665	*SORCS2*	NM_020777	ref|Homo sapiens sortilin-related VPS10 domain containing receptor 2 mRNA
9.43	1.696	0	A_23_P74112	*IL28RA*	NM_170743	ref|Homo sapiens interleukin 28 receptor alpha (interferon lambda receptor) transcript variant 1 mRNA
9.30	1.688	0	A_23_P104563	*CPT1A*	NM_001031847	ref|Homo sapiens carnitine palmitoyltransferase 1A (liver) nuclear gene encoding mitochondrial protein transcript variant 2 mRNA
9.18	1.683	0	A_23_P104563	*CPT1A*	NM_001031847	ref|Homo sapiens carnitine palmitoyltransferase 1A (liver) nuclear gene encoding mitochondrial protein transcript variant 2 mRNA
9.26	1.677	0	A_23_P104563	*CPT1A*	NM_001031847	ref|Homo sapiens carnitine palmitoyltransferase 1A (liver) nuclear gene encoding mitochondrial protein transcript variant 2 mRNA
8.91	1.675	0	A_23_P104563	*CPT1A*	NM_001031847	ref|Homo sapiens carnitine palmitoyltransferase 1A (liver) nuclear gene encoding mitochondrial protein transcript variant 2 mRNA
8.66	1.667	0	A_23_P431305	*FAM69B*	NM_152421	ref|Homo sapiens family with sequence similarity 69 member B mRNA

9.19	1.657	0	A_23_P104563	*CPT1A*	NM_001031847	ref|Homo sapiens carnitine palmitoyltransferase 1A (liver) nuclear gene encoding mitochondrial protein transcript variant 2 mRNA
10.69	1.652	0	A_24_P294124	*SERTAD2*	NM_014755	ref|Homo sapiens SERTA domain containing 2 mRNA
8.42	1.646	0	A_23_P23947	*MAP3K8*	NM_005204	ref|Homo sapiens mitogen-activated protein kinase kinase kinase 8 mRNA
8.35	1.634	0	A_24_P224488	*MAPT*	NM_016835	ref|Homo sapiens microtubule-associated protein tau transcript variant 1 mRNA
13.15	1.624	1.00E-05	A_23_P128919	*LGALS3*	NM_002306	ref|Homo sapiens lectin galactoside-binding soluble 3 transcript variant 1 mRNA
5.89	1.624	0	A_23_P147025	*RAB33A*	NM_004794	ref|Homo sapiens RAB33A member RAS oncogene family mRNA
6.80	1.621	1.00E-05	A_23_P121665	*SORCS2*	NM_020777	ref|Homo sapiens sortilin-related VPS10 domain containing receptor 2 mRNA
9.31	1.615	0	A_23_P104563	*CPT1A*	NM_001031847	ref|Homo sapiens carnitine palmitoyltransferase 1A (liver) nuclear gene encoding mitochondrial protein transcript variant 2 mRNA
10.89	1.615	0	A_23_P120863	*GAL3ST1*	NM_004861	ref|Homo sapiens galactose-3-O-sulfotransferase 1 mRNA
10.78	1.609	0	A_23_P120863	*GAL3ST1*	NM_004861	ref|Homo sapiens galactose-3-O-sulfotransferase 1 mRNA
10.43	1.607	0	A_23_P206661	*NQO1*	NM_000903	ref|Homo sapiens NAD(P)H dehydrogenase quinone 1 transcript variant 1 mRNA
10.74	1.605	0	A_23_P120863	*GAL3ST1*	NM_004861	ref|Homo sapiens galactose-3-O-sulfotransferase 1 mRNA
5.60	1.604	6.00E-05	A_33_P3382999	*PSAPL1*	NM_001085382	ref|Homo sapiens prosaposin-like 1 (gene/pseudogene) mRNA
7.51	1.589	0	A_33_P3358731	*PCSK5*	NM_006200	ref|Homo sapiens proprotein convertase subtilisin/kexin type 5 transcript variant 2 mRNA
15.00	1.588	0	A_23_P37983	*MT1B*	NM_005947	ref|Homo sapiens metallothionein 1B mRNA
13.76	1.585	0	A_23_P252783	*SLC2A8*	NM_014580	ref|Homo sapiens solute carrier family 2 (facilitated glucose transporter) member 8 mRNA
10.45	1.582	0	A_23_P120863	*GAL3ST1*	NM_004861	ref|Homo sapiens galactose-3-O-sulfotransferase 1 mRNA
8.85	1.578	0	A_33_P3368358	*NEDD9*	NM_182966	ref|Homo sapiens neural precursor cell expressed developmentally down-regulated 9 transcript variant 2 mRNA
10.77	1.577	0	A_23_P120863	*GAL3ST1*	NM_004861	ref|Homo sapiens galactose-3-O-sulfotransferase 1 mRNA
10.77	1.577	0	A_23_P120863	*GAL3ST1*	NM_004861	ref|Homo sapiens galactose-3-O-sulfotransferase 1 mRNA
10.69	1.576	0	A_23_P120863	*GAL3ST1*	NM_004861	ref|Homo sapiens galactose-3-O-sulfotransferase 1 mRNA
8.13	1.573	0	A_23_P254079	*STBD1*	NM_003943	ref|Homo sapiens starch binding domain 1 mRNA
9.25	1.572	0	A_24_P239606	*GADD45B*	NM_015675	ref|Homo sapiens growth arrest and DNA-damage-inducible beta mRNA
10.82	1.570	0	A_23_P120863	*GAL3ST1*	NM_004861	ref|Homo sapiens galactose-3-O-sulfotransferase 1 mRNA
5.24	1.568	0	A_33_P3355921	*LOC100130894*	NR_034083	ref|Homo sapiens hypothetical LOC100130894 non-coding RNA
6.01	1.567	1.00E-04	A_23_P80570	*AADAC*	NM_001086	ref|Homo sapiens arylacetamide deacetylase (esterase) mRNA
10.89	1.565	0	A_23_P120863	*GAL3ST1*	NM_004861	ref|Homo sapiens galactose-3-O-sulfotransferase 1 mRNA
6.44	1.563	1.00E-04	A_33_P3282683	*LOC100130027*	XR_110587	ref|PREDICTED: Homo sapiens hypothetical LOC100130027 partial miscRNA
10.75	1.562	0	A_23_P120863	*GAL3ST1*	NM_004861	ref|Homo sapiens galactose-3-O-sulfotransferase 1 mRNA
7.15	1.559	9.00E-05	A_23_P121665	*SORCS2*	NM_020777	ref|Homo sapiens sortilin-related VPS10 domain containing receptor 2 mRNA

6.73	1.554	1.00E-05	A_33_P3209279	*SASH1*	NM_015278	ref|Homo sapiens SAM and SH3 domain containing 1 mRNA
6.28	1.553	4.00E-05	A_23_P381172	*MRAP*	NM_206898	ref|Homo sapiens melanocortin 2 receptor accessory protein transcript variant 2 mRNA
15.20	1.548	0	A_23_P427703	*MT1L*	NR_001447	ref|Homo sapiens metallothionein 1L (gene/pseudogene) non-coding RNA
8.19	1.546	1.00E-05	A_23_P8801	*CYP3A5*	NM_000777	ref|Homo sapiens cytochrome P450 family 3 subfamily A polypeptide 5 transcript variant 1 mRNA
6.63	1.546	4.00E-05	A_23_P77756	*GALR2*	NM_003857	ref|Homo sapiens galanin receptor 2 mRNA
5.60	1.544	2.00E-04	A_23_P131036	*ENST00000443196*	ENST00000443196	gb|Homo sapiens cDNA clone IMAGE:4300770
12.80	1.539	0	A_23_P120883	*HMOX1*	NM_002133	ref|Homo sapiens heme oxygenase (decycling) 1 mRNA
10.50	1.537	0	A_23_P344555	*NEDD9*	NM_006403	ref|Homo sapiens neural precursor cell expressed developmentally down-regulated 9 transcript variant 1 mRNA
10.15	1.536	0	A_24_P254278	*SLC23A2*	NM_203327	ref|Homo sapiens solute carrier family 23 (nucleobase transporters) member 2 transcript variant 2 mRNA
12.41	1.531	0	A_23_P120883	*HMOX1*	NM_002133	ref|Homo sapiens heme oxygenase (decycling) 1 mRNA
12.89	1.530	0	A_23_P120883	*HMOX1*	NM_002133	ref|Homo sapiens heme oxygenase (decycling) 1 mRNA
5.86	1.526	0.00036	A_32_P4018	*ROR1*	ENST00000371079	ens|receptor tyrosine kinase-like orphan receptor 1 [Source:HGNC Symbol;Acc:10256]
10.95	1.524	0	A_33_P3282688	*LOC100130027*	XR_110587	ref|PREDICTED: Homo sapiens hypothetical LOC100130027 partial miscRNA
9.02	1.523	0	A_23_P103110	*MAFF*	NM_012323	ref|Homo sapiens v-maf musculoaponeurotic fibrosarcoma oncogene homolog F (avian) transcript variant 1 mRNA
14.68	1.522	0	A_24_P109214	*APOC1*	NM_001645	ref|Homo sapiens apolipoprotein C-I mRNA
12.74	1.519	0	A_23_P120883	*HMOX1*	NM_002133	ref|Homo sapiens heme oxygenase (decycling) 1 mRNA
6.01	1.518	1.00E-05	A_24_P222872	*UGT1A6*	NM_001072	ref|Homo sapiens UDP glucuronosyltransferase 1 family polypeptide A6 transcript variant 1 mRNA
8.59	1.515	0	A_23_P111583	*CD36*	NM_001001547	ref|Homo sapiens CD36 molecule (thrombospondin receptor) transcript variant 2 mRNA
12.40	1.515	0	A_23_P120883	*HMOX1*	NM_002133	ref|Homo sapiens heme oxygenase (decycling) 1 mRNA
12.72	1.515	0	A_23_P120883	*HMOX1*	NM_002133	ref|Homo sapiens heme oxygenase (decycling) 1 mRNA
12.75	1.513	0	A_23_P120883	*HMOX1*	NM_002133	ref|Homo sapiens heme oxygenase (decycling) 1 mRNA
12.85	1.511	0	A_23_P120883	*HMOX1*	NM_002133	ref|Homo sapiens heme oxygenase (decycling) 1 mRNA
12.76	1.503	0	A_23_P120883	*HMOX1*	NM_002133	ref|Homo sapiens heme oxygenase (decycling) 1 mRNA
12.55	1.502	0	A_24_P335620	*SLC7A5*	NM_003486	ref|Homo sapiens solute carrier family 7 (amino acid transporter light chain L system) member 5 mRNA
11.17	1.502	0	A_33_P3254460	*DLK2*	NM_206539	ref|Homo sapiens delta-like 2 homolog (Drosophila) transcript variant 2 mRNA
5.54	1.498	0.00021	A_23_P343398	*CCR7*	NM_001838	ref|Homo sapiens chemokine (C-C motif) receptor 7 mRNA
7.32	1.498	7.00E-05	A_23_P121665	*SORCS2*	NM_020777	ref|Homo sapiens sortilin-related VPS10 domain containing receptor 2 mRNA
9.13	1.494	0	A_23_P358917	*CYP3A7*	NM_000765	ref|Homo sapiens cytochrome P450 family 3 subfamily A polypeptide 7 mRNA
12.92	1.486	0	A_23_P120883	*HMOX1*	NM_002133	ref|Homo sapiens heme oxygenase (decycling) 1 mRNA
9.39	1.475	0	A_23_P103110	*MAFF*	NM_012323	ref|Homo sapiens v-maf musculoaponeurotic fibrosarcoma oncogene homolog F (avian) transcript variant 1 mRNA
8.50	1.469	0	A_23_P111583	*CD36*	NM_001001547	ref|Homo sapiens CD36 molecule (thrombospondin receptor) transcript variant 2 mRNA
8.48	1.468	0	A_23_P111583	*CD36*	NM_001001547	ref|Homo sapiens CD36 molecule (thrombospondin receptor) transcript variant 2 mRNA

15.05	1.466	0	A_33_P3399788	*SERPINA3*	NM_001085	ref|Homo sapiens serpin peptidase inhibitor clade A (alpha-1 antiproteinase antitrypsin) member 3 mRNA
8.96	1.466	0	A_23_P103110	*MAFF*	NM_012323	ref|Homo sapiens v-maf musculoaponeurotic fibrosarcoma oncogene homolog F (avian) transcript variant 1 mRNA
8.98	1.464	0	A_33_P3404588	*FGD4*	NM_139241	ref|Homo sapiens FYVE RhoGEF and PH domain containing 4 mRNA
8.49	1.460	0	A_23_P111583	*CD36*	NM_001001547	ref|Homo sapiens CD36 molecule (thrombospondin receptor) transcript variant 2 mRNA
8.96	1.460	0	A_23_P103110	*MAFF*	NM_012323	ref|Homo sapiens v-maf musculoaponeurotic fibrosarcoma oncogene homolog F (avian) transcript variant 1 mRNA
12.23	1.459	0	A_23_P44964	*FAM171A1*	NM_001010924	ref|Homo sapiens family with sequence similarity 171 member A1 mRNA
6.07	1.459	0	A_23_P17673	*DNMT3L*	NM_013369	ref|Homo sapiens DNA (cytosine-5-)-methyltransferase 3-like transcript variant 1 mRNA
8.50	1.458	0	A_23_P111583	*CD36*	NM_001001547	ref|Homo sapiens CD36 molecule (thrombospondin receptor) transcript variant 2 mRNA
13.33	1.455	0	A_33_P3244347	*PC*	NM_001040716	ref|Homo sapiens pyruvate carboxylase nuclear gene encoding mitochondrial protein transcript variant 3 mRNA
7.93	1.452	0	A_32_P57810	*RNF157*	NM_052916	ref|Homo sapiens ring finger protein 157 mRNA
10.52	1.451	2.00E-05	A_32_P160972	*C6orf115*	NM_021243	ref|Homo sapiens chromosome 6 open reading frame 115 mRNA
9.47	1.449	0	A_23_P103110	*MAFF*	NM_012323	ref|Homo sapiens v-maf musculoaponeurotic fibrosarcoma oncogene homolog F (avian) transcript variant 1 mRNA
6.99	1.447	0	A_33_P3229953	*EEF1A2*	NM_001958	ref|Homo sapiens eukaryotic translation elongation factor 1 alpha 2 mRNA
8.03	1.442	0	A_23_P111583	*CD36*	NM_001001547	ref|Homo sapiens CD36 molecule (thrombospondin receptor) transcript variant 2 mRNA
8.10	1.440	0	A_23_P111583	*CD36*	NM_001001547	ref|Homo sapiens CD36 molecule (thrombospondin receptor) transcript variant 2 mRNA
9.20	1.440	0	A_23_P103110	*MAFF*	NM_012323	ref|Homo sapiens v-maf musculoaponeurotic fibrosarcoma oncogene homolog F (avian) transcript variant 1 mRNA
9.44	1.439	0	A_23_P103110	*MAFF*	NM_012323	ref|Homo sapiens v-maf musculoaponeurotic fibrosarcoma oncogene homolog F (avian) transcript variant 1 mRNA
9.45	1.438	0	A_23_P103110	*MAFF*	NM_012323	ref|Homo sapiens v-maf musculoaponeurotic fibrosarcoma oncogene homolog F (avian) transcript variant 1 mRNA
9.28	1.434	0	A_23_P103110	*MAFF*	NM_012323	ref|Homo sapiens v-maf musculoaponeurotic fibrosarcoma oncogene homolog F (avian) transcript variant 1 mRNA
8.11	1.430	0	A_23_P111583	*CD36*	NM_001001547	ref|Homo sapiens CD36 molecule (thrombospondin receptor) transcript variant 2 mRNA
5.56	1.425	2.00E-04	A_23_P64611	*P2RY6*	NM_176798	ref|Homo sapiens pyrimidinergic receptor P2Y G-protein coupled 6 transcript variant 2 mRNA
9.95	1.423	0	A_24_P296508	*SLC43A2*	NM_152346	ref|Homo sapiens solute carrier family 43 member 2 mRNA
12.47	1.418	0	A_23_P63798	*KLF6*	NM_001300	ref|Homo sapiens Kruppel-like factor 6 transcript variant A mRNA
8.58	1.417	0	A_23_P111583	*CD36*	NM_001001547	ref|Homo sapiens CD36 molecule (thrombospondin receptor) transcript variant 2 mRNA
11.00	1.416	0	A_23_P130376	*FAM38B*	NM_022068	ref|Homo sapiens family with sequence similarity 38 member B mRNA
9.54	1.415	1.00E-05	A_23_P383819	*TBX3*	NM_016569	ref|Homo sapiens T-box 3 transcript variant 2 mRNA
5.94	1.412	0.00021	A_23_P39799	*LOXL3*	NM_032603	ref|Homo sapiens lysyl oxidase-like 3 mRNA
10.45	1.399	0	A_24_P158946	*FGD4*	NM_139241	ref|Homo sapiens FYVE RhoGEF and PH domain containing 4 mRNA
6.78	1.398	0	A_33_P3233906	*RAMP1*	NM_005855	ref|Homo sapiens receptor (G protein-coupled) activity modifying protein 1 mRNA
8.49	1.397	0	A_23_P111583	*CD36*	NM_001001547	ref|Homo sapiens CD36 molecule (thrombospondin receptor) transcript variant 2 mRNA
8.92	1.397	0	A_23_P69810	*AGPAT9*	NM_032717	ref|Homo sapiens 1-acylglycerol-3-phosphate O-acyltransferase 9 mRNA
9.37	1.394	0	A_23_P103110	*MAFF*	NM_012323	ref|Homo sapiens v-maf musculoaponeurotic fibrosarcoma oncogene homolog F (avian) transcript variant 1 mRNA

16.06	1.388	0	A_23_P16523	*GDF15*	NM_004864	ref|Homo sapiens growth differentiation factor 15 mRNA
7.80	1.387	0	A_23_P7562	*ACSL6*	NM_001009185	ref|Homo sapiens acyl-CoA synthetase long-chain family member 6 transcript variant 2 mRNA
7.21	1.386	4.00E-05	A_33_P3402868	*GRIN2D*	NM_000836	ref|Homo sapiens glutamate receptor ionotropic N-methyl D-aspartate 2D mRNA
7.37	1.378	1.00E-05	A_33_P3254708	*ARHGAP40*	NM_001164431	ref|Homo sapiens Rho GTPase activating protein 40 mRNA
10.74	1.374	0	A_23_P108082	*CREB3L3*	NM_032607	ref|Homo sapiens cAMP responsive element binding protein 3-like 3 mRNA
10.14	1.372	1.00E-05	A_23_P6771	*LMCD1*	NM_014583	ref|Homo sapiens LIM and cysteine-rich domains 1 mRNA
12.25	1.371	0	A_23_P67381	*SULT2A1*	NM_003167	ref|Homo sapiens sulfotransferase family cytosolic 2A dehydroepiandrosterone (DHEA)-preferring member 1 mRNA
5.01	1.368	0.00086	A_33_P3345534	*KRT14*	NM_000526	ref|Homo sapiens keratin 14 mRNA
9.09	1.360	0	A_33_P3298430	*FAM171A1*	NM_001010924	ref|Homo sapiens family with sequence similarity 171 member A1 mRNA
8.38	1.359	0.00012	A_33_P3289251	*LOC644727*	AK095971	gb|Homo sapiens cDNA FLJ38652 fis clone HHDPC2008843
12.83	1.355	2.00E-05	A_23_P94159	*FBXO25*	NM_183421	ref|Homo sapiens F-box protein 25 transcript variant 1 mRNA
12.79	1.351	0	A_23_P162918	*SERPINA3*	NM_001085	ref|Homo sapiens serpin peptidase inhibitor clade A (alpha-1 antiproteinase antitrypsin) member 3 mRNA
14.32	1.341	0	A_23_P2920	*SERPINA3*	NM_001085	ref|Homo sapiens serpin peptidase inhibitor clade A (alpha-1 antiproteinase antitrypsin) member 3 mRNA
5.75	1.338	2.00E-05	A_33_P3341474	*ZBTB38*	NM_001080412	ref|Homo sapiens zinc finger and BTB domain containing 38 mRNA
8.67	1.331	0	A_23_P166280	*ICOSLG*	ENST00000407780	ens|inducible T-cell co-stimulator ligand [Source:HGNC Symbol;Acc:17087]
10.24	1.330	0	A_24_P340066	*ELF4*	NM_001421	ref|Homo sapiens E74-like factor 4 (ets domain transcription factor) transcript variant 1 mRNA
6.87	1.329	1.00E-05	A_23_P129367	*CCDC135*	NM_032269	ref|Homo sapiens coiled-coil domain containing 135 mRNA
11.79	1.325	2.00E-05	A_23_P81898	*UBD*	NM_006398	ref|Homo sapiens ubiquitin D mRNA
14.29	1.319	0	A_33_P3350056	*MT1X*	NM_005952	ref|Homo sapiens metallothionein 1X mRNA
11.03	1.312	0	A_23_P46429	*CYR61*	NM_001554	ref|Homo sapiens cysteine-rich angiogenic inducer 61 mRNA
10.53	1.312	0	A_23_P13772	*TBX3*	NM_016569	ref|Homo sapiens T-box 3 transcript variant 2 mRNA
10.22	1.308	0	A_23_P324754	*KIAA1199*	NM_018689	ref|Homo sapiens KIAA1199 mRNA
10.54	1.307	1.00E-05	A_23_P67042	*MOCOS*	NM_017947	ref|Homo sapiens molybdenum cofactor sulfurase mRNA
9.34	1.306	0	A_24_P88850	*MRAS*	NM_012219	ref|Homo sapiens muscle RAS oncogene homolog transcript variant 1 mRNA
5.41	1.300	0.00051	A_33_P3211727	*FAM176B*	NM_018166	ref|Homo sapiens family with sequence similarity 176 member B mRNA
10.98	1.298	5.00E-05	A_33_P3294002	*A4GALT*	NM_017436	ref|Homo sapiens alpha 14-galactosyltransferase mRNA
7.66	1.296	4.00E-05	A_23_P65386	*OTUB2*	NM_023112	ref|Homo sapiens OTU domain ubiquitin aldehyde binding 2 mRNA
8.42	1.291	0	A_33_P3351150	*FAM38B*	NM_022068	ref|Homo sapiens family with sequence similarity 38 member B mRNA
12.75	1.288	0	A_23_P143143	*ID2*	NM_002166	ref|Homo sapiens inhibitor of DNA binding 2 dominant negative helix-loop-helix protein mRNA
9.16	1.285	7.00E-05	A_23_P19657	*LRP11*	NM_032832	ref|Homo sapiens low density lipoprotein receptor-related protein 11 mRNA
10.14	1.283	0	A_33_P3418158	*SLC2A8*	NM_014580	ref|Homo sapiens solute carrier family 2 (facilitated glucose transporter) member 8 mRNA

10.63	1.283	2.00E-05	A_23_P67042	*MOCOS*	NM_017947	ref|Homo sapiens molybdenum cofactor sulfurase mRNA
7.08	1.282	0	A_33_P3318117	*CYP3A7*	NM_000765	ref|Homo sapiens cytochrome P450 family 3 subfamily A polypeptide 7 mRNA
11.57	1.282	0	A_32_P180971	*LOC728323*	NR_024437	ref|Homo sapiens hypothetical LOC728323 non-coding RNA
6.78	1.281	4.00E-05	A_23_P397376	*MAF*	NM_001031804	ref|Homo sapiens v-maf musculoaponeurotic fibrosarcoma oncogene homolog (avian) transcript variant 2 mRNA
7.37	1.277	0	A_23_P342727	*STARD13*	NM_178006	ref|Homo sapiens StAR-related lipid transfer (START) domain containing 13 transcript variant alpha mRNA
11.07	1.276	0	A_33_P3767927	*NR3C1*	NM_001018077	ref|Homo sapiens nuclear receptor subfamily 3 group C member 1 (glucocorticoid receptor) transcript variant 5 mRNA
14.86	1.272	0	A_33_P3315314	*MT1H*	NM_005951	ref|Homo sapiens metallothionein 1H mRNA
6.84	1.271	0.00023	A_23_P121665	*SORCS2*	NM_020777	ref|Homo sapiens sortilin-related VPS10 domain containing receptor 2 mRNA
9.36	1.271	1.00E-05	A_24_P100551	*SH3RF1*	NM_020870	ref|Homo sapiens SH3 domain containing ring finger 1 mRNA
11.87	1.268	0	A_33_P3233841	*IL6ST*	NM_002184	ref|Homo sapiens interleukin 6 signal transducer (gp130 oncostatin M receptor) transcript variant 1 mRNA
10.66	1.266	0	A_32_P152437	*AKAP12*	NM_005100	ref|Homo sapiens A kinase (PRKA) anchor protein 12 transcript variant 1 mRNA
8.54	1.265	0	A_24_P107859	*SPRED1*	NM_152594	ref|Homo sapiens sprouty-related EVH1 domain containing 1 mRNA
11.64	1.262	0	A_32_P69368	*ID2*	NM_002166	ref|Homo sapiens inhibitor of DNA binding 2 dominant negative helix-loop-helix protein mRNA
5.45	1.260	0.00091	A_23_P70814	*C6orf123*	NR_026773	ref|Homo sapiens chromosome 6 open reading frame 123 non-coding RNA
10.62	1.258	1.00E-05	A_23_P67042	*MOCOS*	NM_017947	ref|Homo sapiens molybdenum cofactor sulfurase mRNA
9.96	1.256	0	A_23_P121527	*KLHL5*	NM_015990	ref|Homo sapiens kelch-like 5 (Drosophila) transcript variant 1 mRNA
11.35	1.255	8.00E-05	A_23_P116414	*PLA2G16*	NM_007069	ref|Homo sapiens phospholipase A2 group XVI transcript variant 1 mRNA
11.01	1.255	1.00E-05	A_23_P67042	*MOCOS*	NM_017947	ref|Homo sapiens molybdenum cofactor sulfurase mRNA
11.35	1.254	4.00E-05	A_23_P116414	*PLA2G16*	NM_007069	ref|Homo sapiens phospholipase A2 group XVI transcript variant 1 mRNA
9.13	1.252	2.00E-05	A_24_P48204	*SECTM1*	NM_003004	ref|Homo sapiens secreted and transmembrane 1 mRNA
6.14	1.249	0.00029	A_23_P206806	*ITGAL*	NM_002209	ref|Homo sapiens integrin alpha L (antigen CD11A (p180) lymphocyte function-associated antigen 1; alpha polypeptide) transcript variant 1 mRNA
11.46	1.249	5.00E-05	A_23_P116414	*PLA2G16*	NM_007069	ref|Homo sapiens phospholipase A2 group XVI transcript variant 1 mRNA
10.61	1.248	0	A_33_P3262020	*C8G*	NM_000606	ref|Homo sapiens complement component 8 gamma polypeptide (C8G) mRNA
9.04	1.248	7.00E-05	A_23_P502470	*IL6ST*	NM_002184	ref|Homo sapiens interleukin 6 signal transducer (gp130 oncostatin M receptor) transcript variant 1 mRNA
9.10	1.248	5.00E-05	A_23_P77415	*OSGIN1*	NM_013370	ref|Homo sapiens oxidative stress induced growth inhibitor 1 transcript variant 1 mRNA
8.24	1.248	0	A_32_P167471	*CLMN*	NM_024734	ref|Homo sapiens calmin (calponin-like transmembrane) mRNA
11.45	1.247	7.00E-05	A_23_P116414	*PLA2G16*	NM_007069	ref|Homo sapiens phospholipase A2 group XVI transcript variant 1 mRNA
9.95	1.242	0	A_23_P121527	*KLHL5*	NM_015990	ref|Homo sapiens kelch-like 5 (Drosophila) transcript variant 1 mRNA
11.49	1.240	3.00E-05	A_23_P116414	*PLA2G16*	NM_007069	ref|Homo sapiens phospholipase A2 group XVI transcript variant 1 mRNA
15.48	1.238	0	A_23_P54840	*MT1A*	NM_005946	ref|Homo sapiens metallothionein 1A mRNA

7.52	1.237	0	A_33_P3233843	*IL6ST*	NM_001190981	ref|Homo sapiens interleukin 6 signal transducer (gp130 oncostatin M receptor) transcript variant 3 mRNA
11.08	1.235	1.00E-05	A_23_P67042	*MOCOS*	NM_017947	ref|Homo sapiens molybdenum cofactor sulfurase mRNA
11.08	1.234	2.00E-05	A_23_P67042	*MOCOS*	NM_017947	ref|Homo sapiens molybdenum cofactor sulfurase mRNA
6.96	1.233	0	A_23_P24104	*PLAU*	NM_002658	ref|Homo sapiens plasminogen activator urokinase transcript variant 1 mRNA
13.33	1.230	0	A_33_P3236881	*C1orf15-NBL1*	NM_001204088	ref|Homo sapiens C1ORF15-NBL1 readthrough transcript variant 1 mRNA
11.12	1.230	1.00E-05	A_23_P67042	*MOCOS*	NM_017947	ref|Homo sapiens molybdenum cofactor sulfurase mRNA
7.67	1.229	0	A_33_P3420078	*LRP11*	ENST00000367368	ens|low density lipoprotein receptor-related protein 11 [Source:HGNC Symbol;Acc:16936]
17.03	1.228	0	A_23_P107653	*ETFB*	NM_001014763	ref|Homo sapiens electron-transfer-flavoprotein beta polypeptide transcript variant 2 mRNA
7.17	1.228	0.00011	A_24_P928052	*NRP1*	NM_003873	ref|Homo sapiens neuropilin 1 transcript variant 1 mRNA
8.23	1.223	0	A_33_P3216297	*NR3C1*	NM_001018077	ref|Homo sapiens nuclear receptor subfamily 3 group C member 1 (glucocorticoid receptor) transcript variant 5 mRNA
10.05	1.222	0	A_23_P121527	*KLHL5*	NM_015990	ref|Homo sapiens kelch-like 5 (Drosophila) transcript variant 1 mRNA
9.81	1.221	0	A_33_P3378556	*F11*	NM_000128	ref|Homo sapiens coagulation factor XI mRNA
17.05	1.220	0	A_23_P107653	*ETFB*	NM_001014763	ref|Homo sapiens electron-transfer-flavoprotein beta polypeptide transcript variant 2 mRNA
9.00	1.220	1.00E-05	A_23_P100654	*ZBTB4*	NM_020899	ref|Homo sapiens zinc finger and BTB domain containing 4 transcript variant 1 mRNA
11.34	1.219	6.00E-05	A_23_P116414	*PLA2G16*	NM_007069	ref|Homo sapiens phospholipase A2 group XVI transcript variant 1 mRNA
11.42	1.218	7.00E-05	A_23_P116414	*PLA2G16*	NM_007069	ref|Homo sapiens phospholipase A2 group XVI transcript variant 1 mRNA
13.89	1.216	0	A_23_P101208	*CYB5A*	NM_001914	ref|Homo sapiens cytochrome b5 type A (microsomal) transcript variant 2 mRNA
10.10	1.216	0	A_23_P121527	*KLHL5*	NM_015990	ref|Homo sapiens kelch-like 5 (Drosophila) transcript variant 1 mRNA
10.68	1.214	0	A_23_P162142	*TSKU*	NM_015516	ref|Homo sapiens tsukushi small leucine rich proteoglycan homolog (Xenopus laevis) mRNA
10.06	1.214	0	A_23_P121527	*KLHL5*	NM_015990	ref|Homo sapiens kelch-like 5 (Drosophila) (transcript variant 1 mRNA
8.46	1.211	0	A_23_P310483	*C8orf58*	NM_001013842	ref|Homo sapiens chromosome 8 open reading frame 58 transcript variant 1 mRNA
9.19	1.211	0	A_23_P100654	*ZBTB4*	NM_020899	ref|Homo sapiens zinc finger and BTB domain containing 4 transcript variant 1 mRNA
9.16	1.211	0	A_23_P100654	*ZBTB4*	NM_020899	ref|Homo sapiens zinc finger and BTB domain containing 4 transcript variant 1 mRNA
9.13	1.210	0	A_23_P100654	*ZBTB4*	NM_020899	ref|Homo sapiens zinc finger and BTB domain containing 4 transcript variant 1 mRNA
10.70	1.209	0	A_33_P3380417	*SLC25A30*	NM_001010875	ref|Homo sapiens solute carrier family 25 member 30 nuclear gene encoding mitochondrial protein mRNA
10.91	1.209	2.00E-05	A_23_P67042	*MOCOS*	NM_017947	ref|Homo sapiens molybdenum cofactor sulfurase mRNA
17.09	1.208	0	A_23_P107653	*ETFB*	NM_001014763	ref|Homo sapiens electron-transfer-flavoprotein beta polypeptide transcript variant 2 mRNA
10.14	1.208	0	A_23_P121527	*KLHL5*	NM_015990	ref|Homo sapiens kelch-like 5 (Drosophila) transcript variant 1 mRNA
8.29	1.207	9.00E-05	A_24_P158089	*SERPINE1*	NM_000602	ref|Homo sapiens serpin peptidase inhibitor clade E (nexin plasminogen activator inhibitor type 1) member 1 transcript variant 1 mRNA
7.60	1.206	0.00016	A_23_P119886	*GCKR*	NM_001486	ref|Homo sapiens glucokinase (hexokinase 4) regulator mRNA

14.71	1.206	0	A_23_P206724	*MT1E*	NM_175617	ref|Homo sapiens metallothionein 1E mRNA
8.91	1.206	0	A_23_P308305	*TTC39C*	NR_024232	ref|Homo sapiens tetratricopeptide repeat domain 39C transcript variant 3 non-coding RNA
8.39	1.205	5.00E-05	A_24_P158089	*SERPINE1*	NM_000602	ref|Homo sapiens serpin peptidase inhibitor clade E (nexin plasminogen activator inhibitor type 1) member 1 transcript variant 1 mRNA
11.05	1.204	1.00E-05	A_23_P67042	*MOCOS*	NM_017947	ref|Homo sapiens molybdenum cofactor sulfurase mRNA
11.05	1.202	6.00E-05	A_23_P116414	*PLA2G16*	NM_007069	ref|Homo sapiens phospholipase A2 group XVI transcript variant 1 mRNA
11.45	1.200	7.00E-05	A_23_P116414	*PLA2G16*	NM_007069	ref|Homo sapiens phospholipase A2 group XVI transcript variant 1 mRNA
8.85	1.199	0	A_33_P3233834	*IL6ST*	NM_001190981	ref|Homo sapiens interleukin 6 signal transducer (gp130 oncostatin M receptor) transcript variant 3 mRNA
17.02	1.195	0	A_23_P107653	*ETFB*	NM_001014763	ref|Homo sapiens electron-transfer-flavoprotein beta polypeptide transcript variant 2 mRNA
6.72	1.195	0.00018	A_23_P49145	*ZG16*	NM_152338	ref|Homo sapiens zymogen granule protein 16 homolog (rat) mRNA
16.73	1.193	0	A_23_P107653	*ETFB*	NM_001014763	ref|Homo sapiens electron-transfer-flavoprotein beta polypeptide transcript variant 2 mRNA
10.76	1.192	1.00E-05	A_23_P67042	*MOCOS*	NM_017947	ref|Homo sapiens molybdenum cofactor sulfurase mRNA
16.64	1.191	0	A_23_P107653	*ETFB*	NM_001014763	ref|Homo sapiens electron-transfer-flavoprotein beta polypeptide transcript variant 2 mRNA
10.14	1.191	0	A_23_P121527	*KLHL5*	NM_015990	ref|Homo sapiens kelch-like 5 (Drosophila) transcript variant 1 mRNA
16.66	1.190	0	A_23_P107653	*ETFB*	NM_001014763	ref|Homo sapiens electron-transfer-flavoprotein beta polypeptide transcript variant 2 mRNA
13.97	1.189	0	A_23_P101208	*CYB5A*	NM_001914	ref|Homo sapiens cytochrome b5 type A (microsomal) transcript variant 2 mRNA
6.80	1.188	0	A_33_P3227990	*MBP*	NM_001025101	ref|Homo sapiens myelin basic protein transcript variant 7 mRNA
12.64	1.186	0	A_23_P41314	*F11*	NM_000128	ref|Homo sapiens coagulation factor XI mRNA
11.81	1.184	0	A_33_P3399373	*TPRA1*	NM_001142646	ref|Homo sapiens transmembrane protein adipocyte asscociated 1 transcript variant 3 mRNA
13.92	1.181	0	A_23_P101208	*CYB5A*	NM_001914	ref|Homo sapiens cytochrome b5 type A (microsomal) transcript variant 2 mRNA
10.95	1.179	0.00012	A_23_P116414	*PLA2G16*	NM_007069	ref|Homo sapiens phospholipase A2 group XVI transcript variant 1 mRNA
9.41	1.178	0	A_23_P390068	*C19orf21*	NM_173481	ref|Homo sapiens chromosome 19 open reading frame 21 mRNA
11.12	1.176	1.00E-05	A_23_P61960	*ATP6V0E2*	NM_145230	ref|Homo sapiens ATPase H+ transporting V0 subunit e2 transcript variant 1 mRNA
16.58	1.173	0	A_23_P107653	*ETFB*	NM_001014763	ref|Homo sapiens electron-transfer-flavoprotein beta polypeptide transcript variant 2 mRNA
9.30	1.173	0	A_24_P402080	*MBP*	NM_001025100	ref|Homo sapiens myelin basic protein transcript variant 8 mRNA
13.92	1.171	0	A_23_P101208	*CYB5A*	NM_001914	ref|Homo sapiens cytochrome b5 type A (microsomal) transcript variant 2 mRNA
8.06	1.169	0	A_23_P111311	*AKAP12*	NM_144497	ref|Homo sapiens A kinase (PRKA) anchor protein 12 transcript variant 2 mRNA
6.59	1.168	0.00044	A_24_P13381	*TRPV4*	NM_147204	ref|Homo sapiens transient receptor potential cation channel subfamily V member 4 transcript variant 2 mRNA
16.94	1.167	0	A_23_P107653	*ETFB*	NM_001014763	ref|Homo sapiens electron-transfer-flavoprotein beta polypeptide transcript variant 2 mRNA
10.65	1.167	0	A_23_P72668	*SDPR*	NM_004657	ref|Homo sapiens serum deprivation response mRNA
9.25	1.167	4.00E-05	A_33_P3353791	*ITGA1*	NM_181501	ref|Homo sapiens integrin alpha 1 mRNA
10.05	1.165	0	A_33_P3231156	*ENST00000379816*	ENST00000379816	ens|metallothionein 1C pseudogene [Source:HGNC Symbol;Acc:7395]

8.44	1.165	1.00E-04	A_24_P158089	*SERPINE1*	NM_000602	ref|Homo sapiens serpin peptidase inhibitor clade E (nexin plasminogen activator inhibitor type 1) member 1 transcript variant 1 mRNA
10.69	1.161	1.00E-05	A_33_P3311371	*PDLIM2*	NM_198042	ref|Homo sapiens PDZ and LIM domain 2 (mystique) transcript variant 3 mRNA
10.07	1.158	0	A_23_P121527	*KLHL5*	NM_015990	ref|Homo sapiens kelch-like 5 (Drosophila) transcript variant 1 mRNA
8.20	1.157	0	A_33_P3841368	*LOC286161*	AK091672	gb|Homo sapiens cDNA FLJ34353 fis clone FEBRA2011665
7.37	1.157	2.00E-05	A_23_P24104	*PLAU*	NM_002658	ref|Homo sapiens plasminogen activator urokinase transcript variant 1 mRNA
17.01	1.156	0	A_23_P107653	*ETFB*	NM_001014763	ref|Homo sapiens electron-transfer-flavoprotein beta polypeptide transcript variant 2 mRNA
10.02	1.156	0	A_23_P121527	*KLHL5*	NM_015990	ref|Homo sapiens kelch-like 5 (Drosophila) transcript variant 1 mRNA
9.29	1.155	0	A_23_P25706	*CLMN*	NM_024734	ref|Homo sapiens calmin (calponin-like transmembrane) mRNA
10.29	1.154	0	A_24_P192914	*AMICA1*	NM_153206	ref|Homo sapiens adhesion molecule interacts with CXADR antigen 1 transcript variant 2 mRNA
10.10	1.152	0	A_23_P121527	*KLHL5*	NM_015990	ref|Homo sapiens kelch-like 5 (Drosophila) transcript variant 1 mRNA
9.16	1.152	0	A_23_P66948	*FAM59A*	NM_022751	ref|Homo sapiens family with sequence similarity 59 member A transcript variant 2 mRNA
9.81	1.147	0	A_33_P3313929	*CCR6*	NM_031409	ref|Homo sapiens chemokine (C-C motif) receptor 6 transcript variant 2 mRNA
5.61	1.146	0.00011	A_33_P3269924	*ENST00000535831*	ENST00000535831	ens|huntingtin interacting protein 1 related [Source:HGNC Symbol;Acc:18415]
6.03	1.145	0.00079	A_33_P3283480	*CTSC*	NM_148170	ref|Homo sapiens cathepsin C transcript variant 2 mRNA
13.41	1.144	0	A_33_P3294608	*MVP*	NM_017458	ref|Homo sapiens major vault protein transcript variant 1 mRNA
11.79	1.144	0	A_23_P83110	*CDK5RAP2*	NM_018249	ref|Homo sapiens CDK5 regulatory subunit associated protein 2 transcript variant 1 mRNA
10.02	1.141	0	A_23_P1102	*ACTA1*	NM_001100	ref|Homo sapiens actin alpha 1 skeletal muscle mRNA
8.50	1.138	9.00E-05	A_24_P158089	*SERPINE1*	NM_000602	ref|Homo sapiens serpin peptidase inhibitor clade E (nexin plasminogen activator inhibitor type 1) member 1 transcript variant 1 mRNA
14.12	1.138	0	A_23_P101208	*CYB5A*	NM_001914	ref|Homo sapiens cytochrome b5 type A (microsomal) transcript variant 2 mRNA
8.52	1.138	0	A_24_P17719	*KLHL5*	NM_015990	ref|Homo sapiens kelch-like 5 (Drosophila) transcript variant 1 mRNA
9.23	1.138	1.00E-05	A_23_P41804	*NKD2*	NM_033120	ref|Homo sapiens naked cuticle homolog 2 (Drosophila) mRNA
14.32	1.137	0	A_23_P101208	*CYB5A*	NM_001914	ref|Homo sapiens cytochrome b5 type A (microsomal) transcript variant 2 mRNA
13.77	1.134	0	A_23_P101208	*CYB5A*	NM_001914	ref|Homo sapiens cytochrome b5 type A (microsomal) transcript variant 2 mRNA
8.64	1.134	2.00E-05	A_33_P3240532	*RGL1*	NM_015149	ref|Homo sapiens ral guanine nucleotide dissociation stimulator-like 1 mRNA
7.63	1.133	0	A_23_P60599	*UGT1A6*	NM_001072	ref|Homo sapiens UDP glucuronosyltransferase 1 family polypeptide A6 transcript variant 1 mRNA
7.42	1.133	0	A_23_P24104	*PLAU*	NM_002658	ref|Homo sapiens plasminogen activator urokinase transcript variant 1 mRNA
9.78	1.132	0	A_33_P3402783	*A_33_P3402783*	A_33_P3402783	Unknown
14.32	1.131	0	A_23_P101208	*CYB5A*	NM_001914	ref|Homo sapiens cytochrome b5 type A (microsomal) transcript variant 2 mRNA
8.06	1.129	1.00E-05	A_33_P3333317	*OPTN*	NM_001008211	ref|Homo sapiens optineurin transcript variant 1 mRNA
14.30	1.128	0	A_23_P101208	*CYB5A*	NM_001914	ref|Homo sapiens cytochrome b5 type A (microsomal) transcript variant 2 mRNA

14.13	1.125	0	A_23_P101208	*CYB5A*	NM_001914	ref|Homo sapiens cytochrome b5 type A (microsomal) transcript variant 2 mRNA
7.85	1.124	0.00019	A_24_P158089	*SERPINE1*	NM_000602	ref|Homo sapiens serpin peptidase inhibitor clade E (nexin plasminogen activator inhibitor type 1) member 1 transcript variant 1 mRNA
6.67	1.124	1.00E-05	A_33_P3221989	*CACNB4*	NM_001005747	ref|Homo sapiens calcium channel voltage-dependent beta 4 subunit transcript variant 1 mRNA
10.37	1.124	0	A_23_P1102	*ACTA1*	NM_001100	ref|Homo sapiens actin alpha 1 skeletal muscle mRNA
9.19	1.124	0	A_23_P100654	*ZBTB4*	NM_020899	ref|Homo sapiens zinc finger and BTB domain containing 4 transcript variant 1 mRNA
6.68	1.118	3.00E-05	A_23_P27734	*NPAS1*	NM_002517	ref|Homo sapiens neuronal PAS domain protein 1 mRNA
8.37	1.117	6.00E-05	A_33_P3412438	*A_33_P3412438*	A_33_P3412438	Unknown
7.87	1.116	0.00025	A_23_P390518	*TNFRSF11A*	NM_003839	ref|Homo sapiens tumor necrosis factor receptor superfamily member 11a NFKB activator mRNA
9.15	1.112	4.00E-05	A_23_P122976	*GNAI1*	NM_002069	ref|Homo sapiens guanine nucleotide binding protein (G protein) alpha inhibiting activity polypeptide 1 mRNA
7.94	1.112	1.00E-05	A_23_P80503	*ROBO1*	NM_133631	ref|Homo sapiens roundabout axon guidance receptor homolog 1 (Drosophila) transcript variant 2 mRNA
9.76	1.109	0	A_33_P3287338	*IL6ST*	NM_001190981	ref|Homo sapiens interleukin 6 signal transducer (gp130 oncostatin M receptor) transcript variant 3 mRNA
8.07	1.108	2.00E-05	A_23_P348636	*FOXJ1*	NM_001454	ref|Homo sapiens forkhead box J1 mRNA
8.28	1.108	1.00E-05	A_23_P111311	*AKAP12*	NM_144497	ref|Homo sapiens A kinase (PRKA) anchor protein 12 transcript variant 2 mRNA
9.18	1.107	0	A_23_P100654	*ZBTB4*	NM_020899	ref|Homo sapiens zinc finger and BTB domain containing 4 transcript variant 1 mRNA
9.37	1.107	1.00E-05	A_23_P165989	*NEURL2*	NM_080749	ref|Homo sapiens neuralized homolog 2 (Drosophila) mRNA
9.29	1.104	0	A_23_P100654	*ZBTB4*	NM_020899	ref|Homo sapiens zinc finger and BTB domain containing 4 transcript variant 1 mRNA
7.94	1.104	1.00E-05	A_23_P111311	*AKAP12*	NM_144497	ref|Homo sapiens A kinase (PRKA) anchor protein 12 transcript variant 2 mRNA
8.26	1.103	0	A_32_P62211	*BX538057*	BX538057	gb|Homo sapiens mRNA; cDNA DKFZp686J1595 (from clone DKFZp686J1595)
10.43	1.101	1.00E-05	A_23_P1102	*ACTA1*	NM_001100	ref|Homo sapiens actin alpha 1 skeletal muscle mRNA
9.13	1.101	0	A_23_P100654	*ZBTB4*	NM_020899	ref|Homo sapiens zinc finger and BTB domain containing 4 transcript variant 1 mRNA
9.15	1.100	1.00E-05	A_23_P122976	*GNAI1*	NM_002069	ref|Homo sapiens guanine nucleotide binding protein (G protein) alpha inhibiting activity polypeptide 1 mRNA
8.98	1.100	1.00E-05	A_23_P122976	*GNAI1*	NM_002069	ref|Homo sapiens guanine nucleotide binding protein (G protein) alpha inhibiting activity polypeptide 1 mRNA
7.72	1.099	7.00E-05	A_23_P119886	*GCKR*	NM_001486	ref|Homo sapiens glucokinase (hexokinase 4) regulator mRNA
8.92	1.098	0	A_23_P100654	*ZBTB4*	NM_020899	ref|Homo sapiens zinc finger and BTB domain containing 4 transcript variant 1 mRNA
9.73	1.096	0	A_23_P385017	*G6PC*	NM_000151	ref|Homo sapiens glucose-6-phosphatase catalytic subunit mRNA
7.37	1.095	0.00075	A_24_P382187	*IGFBP4*	NM_001552	ref|Homo sapiens insulin-like growth factor binding protein 4 mRNA
9.05	1.095	3.00E-05	A_23_P122976	*GNAI1*	NM_002069	ref|Homo sapiens guanine nucleotide binding protein (G protein) alpha inhibiting activity polypeptide 1 mRNA
10.05	1.094	0	A_23_P82523	*ABCB1*	NM_000927	ref|Homo sapiens ATP-binding cassette sub-family B (MDR/TAP) member 1 mRNA
7.07	1.093	0	A_33_P3390656	*ACSL6*	NM_001009185	ref|Homo sapiens acyl-CoA synthetase long-chain family member 6 transcript variant 2 mRNA
10.46	1.092	1.00E-05	A_23_P1102	*ACTA1*	NM_001100	ref|Homo sapiens actin alpha 1 skeletal muscle mRNA
8.00	1.092	1.00E-05	A_23_P111311	*AKAP12*	NM_144497	ref|Homo sapiens A kinase (PRKA) anchor protein 12 transcript variant 2 mRNA

10.35	1.088	4.00E-04	A_23_P85015	*MAOB*	NM_000898	ref|Homo sapiens monoamine oxidase B nuclear gene encoding mitochondrial protein mRNA
7.33	1.084	1.00E-05	A_23_P24104	*PLAU*	NM_002658	ref|Homo sapiens plasminogen activator urokinase transcript variant 1 mRNA
7.74	1.081	6.00E-05	A_23_P119886	*GCKR*	NM_001486	ref|Homo sapiens glucokinase (hexokinase 4) regulator mRNA
7.69	1.081	1.00E-05	A_24_P36890	*RAP1GAP*	NM_002885	ref|Homo sapiens RAP1 GTPase activating protein transcript variant 3 mRNA
8.42	1.080	0	A_33_P3246505	*MAP3K8*	ENST00000375322	ens|mitogen-activated protein kinase kinase kinase 8 [Source:HGNC Symbol;Acc:6860]
10.23	1.078	1.00E-05	A_23_P1102	*ACTA1*	NM_001100	ref|Homo sapiens actin alpha 1 skeletal muscle mRNA
7.78	1.078	0	A_23_P119886	*GCKR*	NM_001486	ref|Homo sapiens glucokinase (hexokinase 4) regulator mRNA
14.20	1.078	0	A_23_P146798	*SEPHS2*	NM_012248	ref|Homo sapiens selenophosphate synthetase 2 mRNA
8.49	1.077	3.00E-05	A_24_P158089	*SERPINE1*	NM_000602	ref|Homo sapiens serpin peptidase inhibitor clade E (nexin plasminogen activator inhibitor type 1) member 1 transcript variant 1 mRNA
8.52	1.076	3.00E-05	A_24_P158089	*SERPINE1*	NM_000602	ref|Homo sapiens serpin peptidase inhibitor clade E (nexin plasminogen activator inhibitor type 1) member 1 transcript variant 1 mRNA
6.37	1.076	0.00045	A_33_P3225522	*OAS2*	NM_001032731	ref|Homo sapiens 2'-5'-oligoadenylate synthetase 2 69/71kDa transcript variant 3 mRNA
7.77	1.074	5.00E-05	A_23_P119886	*GCKR*	NM_001486	ref|Homo sapiens glucokinase (hexokinase 4) regulator mRNA
8.86	1.074	0	A_23_P416142	*DLG1*	NM_004087	ref|Homo sapiens discs large homolog 1 (Drosophila) transcript variant 2 mRNA
12.25	1.073	1.00E-04	A_23_P500300	*TRIM15*	NM_033229	ref|Homo sapiens tripartite motif containing 15 mRNA
10.54	1.070	0	A_32_P45168	*IL6ST*	NM_002184	ref|Homo sapiens interleukin 6 signal transducer (gp130 oncostatin M receptor) transcript variant 1 mRNA
9.66	1.069	8.00E-05	A_33_P3298024	*ABCC3*	NM_001144070	ref|Homo sapiens ATP-binding cassette sub-family C (CFTR/MRP) member 3 transcript variant 2 mRNA
8.89	1.068	5.00E-05	A_23_P122976	*GNAI1*	NM_002069	ref|Homo sapiens guanine nucleotide binding protein (G protein) alpha inhibiting activity polypeptide 1 mRNA
8.42	1.067	0	A_33_P3236102	*IER5L*	NM_203434	ref|Homo sapiens immediate early response 5-like mRNA
8.35	1.066	0	A_23_P111311	*AKAP12*	NM_144497	ref|Homo sapiens A kinase (PRKA) anchor protein 12 transcript variant 2 mRNA
13.84	1.065	0	A_23_P23996	*MAT1A*	NM_000429	ref|Homo sapiens methionine adenosyltransferase I alpha mRNA
10.43	1.065	0	A_23_P1102	*ACTA1*	NM_001100	ref|Homo sapiens actin alpha 1 skeletal muscle mRNA
7.07	1.065	0.00018	A_23_P24104	*PLAU*	NM_002658	ref|Homo sapiens plasminogen activator urokinase transcript variant 1 mRNA
10.42	1.065	0	A_33_P3389060	*CDK5RAP2*	NM_018249	ref|Homo sapiens CDK5 regulatory subunit associated protein 2 transcript variant 1 mRNA
10.31	1.065	0	A_32_P162150	*TAB3*	NM_152787	ref|Homo sapiens TGF-beta activated kinase 1/MAP3K7 binding protein mRNA
7.92	1.062	3.00E-05	A_24_P264943	*COMP*	NM_000095	ref|Homo sapiens cartilage oligomeric matrix protein mRNA
8.24	1.06	0.00018	A_24_P158089	*SERPINE1*	NM_000602	ref|Homo sapiens serpin peptidase inhibitor clade E (nexin plasminogen activator inhibitor type 1) member 1 transcript variant 1 mRNA
8.08	1.058	7.00E-05	A_24_P158089	*SERPINE1*	NM_000602	ref|Homo sapiens serpin peptidase inhibitor clade E (nexin plasminogen activator inhibitor type 1) member 1 transcript variant 1 mRNA
10.48	1.058	0	A_23_P1102	*ACTA1*	NM_001100	ref|Homo sapiens actin alpha 1 skeletal muscle mRNA
10.40	1.058	1.00E-05	A_23_P415401	*KLF9*	NM_001206	ref|Homo sapiens Kruppel-like factor 9 mRNA

7.81	1.058	3.00E-05	A_23_P119886	*GCKR*	NM_001486	ref|Homo sapiens glucokinase (hexokinase 4) regulator mRNA
5.31	1.058	0.00116	A_23_P215111	*ATP6V0A4*	NM_020632	ref|Homo sapiens ATPase H+ transporting lysosomal V0 subunit a4 transcript variant 1 mRNA
9.99	1.056	0	A_23_P1102	*ACTA1*	NM_001100	ref|Homo sapiens actin alpha 1 skeletal muscle mRNA
10.3	1.056	2.00E-05	A_23_P1102	*ACTA1*	NM_001100	ref|Homo sapiens actin alpha 1 skeletal muscle mRNA
13.95	1.056	0	A_33_P3311076	*CYB5A*	NM_001190807	ref|Homo sapiens cytochrome b5 type A (microsomal) transcript variant 3 mRNA
12.50	1.056	0	A_33_P3289296	*TMEM37*	NM_183240	ref|Homo sapiens transmembrane protein 37 mRNA
7.19	1.055	0	A_23_P394545	*KIAA1033*	NM_015275	ref|Homo sapiens KIAA1033 mRNA
7.88	1.052	1.00E-05	A_23_P119886	*GCKR*	NM_001486	ref|Homo sapiens glucokinase (hexokinase 4) regulator mRNA
7.80	1.051	2.00E-05	A_23_P119886	*GCKR*	NM_001486	ref|Homo sapiens glucokinase (hexokinase 4) regulator mRNA
14.11	1.051	0	A_23_P166459	*LGALS1*	NM_002305	ref|Homo sapiens lectin galactoside-binding soluble 1 mRNA
9.09	1.050	1.00E-05	A_23_P122976	*GNAI1*	NM_002069	ref|Homo sapiens guanine nucleotide binding protein (G protein) alpha inhibiting activity polypeptide 1 mRNA
10.25	1.047	1.00E-05	A_23_P1102	*ACTA1*	NM_001100	ref|Homo sapiens actin alpha 1 skeletal muscle mRNA
8.12	1.045	5.00E-05	A_23_P216679	*CDC14B*	NM_033331	ref|Homo sapiens CDC14 cell division cycle 14 homolog B (S. cerevisiae) transcript variant 2 mRNA
9.03	1.044	1.00E-05	A_23_P122976	*GNAI1*	NM_002069	ref|Homo sapiens guanine nucleotide binding protein (G protein) alpha inhibiting activity polypeptide 1 mRNA
9.47	1.043	0	A_23_P1043	*C1orf106*	NM_018265	ref|Homo sapiens chromosome 1 open reading frame 106 transcript variant 1 mRNA
7.43	1.042	1.00E-05	A_23_P24104	*PLAU*	NM_002658	ref|Homo sapiens plasminogen activator urokinase transcript variant 1 mRNA
9.63	1.034	0	A_23_P1043	*C1orf106*	NM_018265	ref|Homo sapiens chromosome 1 open reading frame 106 transcript variant 1 mRNA
9.70	1.033	2.00E-05	A_23_P406330	*SMAP2*	NM_022733	ref|Homo sapiens small ArfGAP2 transcript variant 1 mRNA
13.36	1.030	0	A_23_P30666	*TNFRSF21*	NM_014452	ref|Homo sapiens tumor necrosis factor receptor superfamily member 21 mRNA
7.52	1.025	0	A_33_P3226832	*F3*	NM_001993	ref|Homo sapiens coagulation factor III (thromboplastin tissue factor) transcript variant 1 mRNA
7.05	1.023	2.00E-05	A_23_P24104	*PLAU*	NM_002658	ref|Homo sapiens plasminogen activator urokinase transcript variant 1 mRNA
12.14	1.023	0	A_23_P160466	*SLC19A2*	NM_006996	ref|Homo sapiens solute carrier family 19 (thiamine transporter) member 2 mRNA
7.04	1.021	3.00E-05	A_33_P3258265	*SEMA6C*	NM_030913	ref|Homo sapiens sema domain transmembrane domain (TM) and cytoplasmic domain (semaphorin) 6C transcript variant 2 mRNA
8.95	1.020	0	A_33_P3268649	*SLC2A11*	NM_030807	ref|Homo sapiens solute carrier family 2 (facilitated glucose transporter) member 11 transcript variant 1 mRNA
8.93	1.019	2.00E-05	A_23_P122976	*GNAI1*	NM_002069	ref|Homo sapiens guanine nucleotide binding protein (G protein) alpha inhibiting activity polypeptide 1 mRNA
10.52	1.018	0.00015	A_33_P3280801	*LMO7*	NM_005358	ref|Homo sapiens LIM domain 7 transcript variant 1 mRNA
9.13	1.017	2.00E-05	A_23_P122976	*GNAI1*	NM_002069	ref|Homo sapiens guanine nucleotide binding protein (G protein) alpha inhibiting activity polypeptide 1 mRNA
8.16	1.017	3.00E-05	A_23_P111311	*AKAP12*	NM_144497	ref|Homo sapiens A kinase (PRKA) anchor protein 12 transcript variant 2 mRNA
9.75	1.014	0	A_33_P3283828	*CCDC154*	NM_001143980	ref|Homo sapiens coiled-coil domain containing 154 mRNA
9.26	1.012	0	A_23_P1043	*C1orf106*	NM_018265	ref|Homo sapiens chromosome 1 open reading frame 106 transcript variant 1 mRNA
8.53	1.011	0.00053	A_24_P158089	*SERPINE1*	NM_000602	ref|Homo sapiens serpin peptidase inhibitor clade E (nexin plasminogen activator inhibitor type 1) member 1

						transcript variant 1 mRNA
5.15	1.009	0.00054	A_33_P3238290	*FAM65C*	NM_080829	ref|Homo sapiens family with sequence similarity 65 member C mRNA
8.91	1.008	6.00E-05	A_23_P122976	*GNAI1*	NM_002069	ref|Homo sapiens guanine nucleotide binding protein (G protein) alpha inhibiting activity polypeptide 1 mRNA
8.43	1.008	0	A_23_P111311	*AKAP12*	NM_144497	ref|Homo sapiens A kinase (PRKA) anchor protein 12 transcript variant 2 mRNA
7.77	1.005	1.00E-05	A_23_P119886	*GCKR*	NM_001486	ref|Homo sapiens glucokinase (hexokinase 4) regulator mRNA
9.23	1.005	0	A_23_P1043	*C1orf106*	NM_018265	ref|Homo sapiens chromosome 1 open reading frame 106 transcript variant 1 mRNA
7.94	1.004	0	A_33_P3568387	*ASB4*	NM_016116	ref|Homo sapiens ankyrin repeat and SOCS box containing 4 transcript variant 1 mRNA
7.61	1.002	0.00106	A_23_P37942	*CLDN6*	NM_021195	ref|Homo sapiens claudin 6 mRNA

Table 97. All significantly down regulated genes in HepG2 cells after treatment with TCDD (10 nM) identified by microarray analysis. Selected parameters: A-value ≥ 5, log2 fc ≤ -1, p-value ≤ 0.05.

A	Log2 fc	p-value	Probe name	Gene name	Systematic name	Gene description
12.36	-2.305	0	A_32_P142440	*PCSK9*	NM_174936	ref|Homo sapiens proprotein convertase subtilisin/kexin type 9 mRNA
7.62	-1.819	0	A_23_P120243	*HOXD1*	NM_024501	ref|Homo sapiens homeobox D1 mRNA
11.36	-1.797	0	A_23_P24129	*DKK1*	NM_012242	ref|Homo sapiens dickkopf homolog 1 (Xenopus laevis) mRNA
10.98	-1.785	0	A_32_P196193	*PAQR9*	NM_198504	ref|Homo sapiens progestin and adipoQ receptor family member IX mRNA
7.68	-1.737	0	A_23_P120243	*HOXD1*	NM_024501	ref|Homo sapiens homeobox D1 mRNA
9.05	-1.715	0	A_24_P228550	*TUBB1*	NM_030773	ref|Homo sapiens tubulin beta 1 mRNA
7.77	-1.677	0	A_23_P120243	*HOXD1*	NM_024501	ref|Homo sapiens homeobox D1 mRNA
7.69	-1.662	0	A_23_P120243	*HOXD1*	NM_024501	ref|Homo sapiens homeobox D1 mRNA
8.70	-1.637	0	A_23_P63432	*RHBDL2*	NM_017821	ref|Homo sapiens rhomboid veinlet-like 2 (Drosophila) mRNA
7.75	-1.615	0	A_23_P120243	*HOXD1*	NM_024501	ref|Homo sapiens homeobox D1 mRNA
7.40	-1.585	0	A_23_P120243	*HOXD1*	NM_024501	ref|Homo sapiens homeobox D1 mRNA
9.65	-1.572	0	A_23_P109636	*LRIG1*	NM_015541	ref|Homo sapiens leucine-rich repeats and immunoglobulin-like domains 1 mRNA
10.12	-1.557	0	A_23_P109636	*LRIG1*	NM_015541	ref|Homo sapiens leucine-rich repeats and immunoglobulin-like domains 1 mRNA
10.02	-1.543	0	A_23_P109636	*LRIG1*	NM_015541	ref|Homo sapiens leucine-rich repeats and immunoglobulin-like domains 1 mRNA
9.91	-1.542	0	A_23_P109636	*LRIG1*	NM_015541	ref|Homo sapiens leucine-rich repeats and immunoglobulin-like domains 1 mRNA
10.00	-1.534	0	A_23_P109636	*LRIG1*	NM_015541	ref|Homo sapiens leucine-rich repeats and immunoglobulin-like domains 1 mRNA

6.72	-1.532	0	A_23_P94275	*DKK4*	NM_014420	ref|Homo sapiens dickkopf homolog 4 (Xenopus laevis) mRNA
7.97	-1.523	0	A_23_P120243	*HOXD1*	NM_024501	ref|Homo sapiens homeobox D1 mRNA
10.06	-1.518	0	A_23_P109636	*LRIG1*	NM_015541	ref|Homo sapiens leucine-rich repeats and immunoglobulin-like domains 1 mRNA
10.07	-1.488	0	A_23_P109636	*LRIG1*	NM_015541	ref|Homo sapiens leucine-rich repeats and immunoglobulin-like domains 1 mRNA
7.87	-1.487	0	A_23_P120243	*HOXD1*	NM_024501	ref|Homo sapiens homeobox D1 mRNA
9.05	-1.477	0	A_32_P46571	*RHBDL2*	NM_017821	ref|Homo sapiens rhomboid veinlet-like 2 (Drosophila) mRNA
7.61	-1.466	0	A_23_P120243	*HOXD1*	NM_024501	ref|Homo sapiens homeobox D1 mRNA
13.33	-1.453	0	A_23_P120902	*LGALS2*	NM_006498	ref|Homo sapiens lectin galactoside-binding soluble 2 mRNA
7.77	-1.450	0	A_23_P120243	*HOXD1*	NM_024501	ref|Homo sapiens homeobox D1 mRNA
13.39	-1.447	0	A_23_P120902	*LGALS2*	NM_006498	ref|Homo sapiens lectin galactoside-binding soluble 2 mRNA
13.29	-1.446	0	A_23_P120902	*LGALS2*	NM_006498	ref|Homo sapiens lectin galactoside-binding soluble 2 mRNA
9.90	-1.440	0	A_23_P109636	*LRIG1*	NM_015541	ref|Homo sapiens leucine-rich repeats and immunoglobulin-like domains 1 mRNA
13.42	-1.439	0	A_23_P120902	*LGALS2*	NM_006498	ref|Homo sapiens lectin galactoside-binding soluble 2 mRNA
13.37	-1.437	0	A_23_P120902	*LGALS2*	NM_006498	ref|Homo sapiens lectin galactoside-binding soluble 2 mRNA
13.26	-1.433	0	A_23_P120902	*LGALS2*	NM_006498	ref|Homo sapiens lectin galactoside-binding soluble 2 mRNA
13.40	-1.433	0	A_23_P120902	*LGALS2*	NM_006498	ref|Homo sapiens lectin galactoside-binding soluble 2 mRNA
9.47	-1.433	0	A_23_P109636	*LRIG1*	NM_015541	ref|Homo sapiens leucine-rich repeats and immunoglobulin-like domains 1 mRNA
13.12	-1.427	0	A_23_P120902	*LGALS2*	NM_006498	ref|Homo sapiens lectin galactoside-binding soluble 2 mRNA
12.98	-1.413	0	A_23_P120902	*LGALS2*	NM_006498	ref|Homo sapiens lectin galactoside-binding soluble 2 mRNA
13.17	-1.410	0	A_23_P120902	*LGALS2*	NM_006498	ref|Homo sapiens lectin galactoside-binding soluble 2 mRNA
9.57	-1.404	0	A_23_P109636	*LRIG1*	NM_015541	ref|Homo sapiens leucine-rich repeats and immunoglobulin-like domains 1 mRNA
7.36	-1.384	3.00E-04	A_23_P57709	*PCOLCE2*	NM_013363	ref|Homo sapiens procollagen C-endopeptidase enhancer 2 mRNA
9.16	-1.350	0	A_23_P122216	*LOX*	NM_002317	ref|Homo sapiens lysyl oxidase transcript variant 1 mRNA
9.61	-1.338	0	A_23_P122216	*LOX*	NM_002317	ref|Homo sapiens lysyl oxidase transcript variant 1 mRNA
8.30	-1.337	0	A_23_P421401	*PDGFRB*	NM_002609	ref|Homo sapiens platelet-derived growth factor receptor beta polypeptide mRNA
9.49	-1.316	0	A_23_P122216	*LOX*	NM_002317	ref|Homo sapiens lysyl oxidase transcript variant 1 mRNA
6.52	-1.314	1.00E-05	A_24_P237270	*ADORA2A*	NM_000675	ref|Homo sapiens adenosine A2a receptor mRNA
11.81	-1.295	0	A_24_P224727	*CEBPA*	NM_004364	ref|Homo sapiens CCAAT/enhancer binding protein (C/EBP) alpha mRNA
9.49	-1.292	1.00E-05	A_23_P122216	*LOX*	NM_002317	ref|Homo sapiens lysyl oxidase transcript variant 1 mRNA
9.51	-1.287	0	A_23_P122216	*LOX*	NM_002317	ref|Homo sapiens lysyl oxidase transcript variant 1 mRNA
7.12	-1.286	0	A_23_P8452	*LFNG*	NM_001040167	ref|Homo sapiens LFNG O-fucosylpeptide 3-beta-N-acetylglucosaminyltransferase transcript variant 1 mRNA
9.64	-1.283	2.00E-05	A_23_P122216	*LOX*	NM_002317	ref|Homo sapiens lysyl oxidase transcript variant 1 mRNA

9.53	-1.270	0	A_23_P122216	*LOX*	NM_002317	ref|Homo sapiens lysyl oxidase transcript variant 1 mRNA
7.45	-1.239	5.00E-05	A_24_P387875	*KCNJ10*	NM_002241	ref|Homo sapiens potassium inwardly-rectifying channel subfamily J member 10 mRNA
9.63	-1.228	0	A_23_P122216	*LOX*	NM_002317	ref|Homo sapiens lysyl oxidase transcript variant 1 mRNA
9.48	-1.224	1.00E-05	A_23_P122216	*LOX*	NM_002317	ref|Homo sapiens lysyl oxidase transcript variant 1 mRNA
8.20	-1.219	0	A_23_P154962	*RIMBP3*	NM_015672	ref|Homo sapiens RIMS binding protein 3 mRNA
8.24	-1.188	1.00E-05	A_33_P3263533	*SCN1A*	NM_001202435	ref|Homo sapiens sodium channel voltage-gated type I alpha subunit transcript variant 4 mRNA
6.94	-1.181	1.00E-05	A_23_P93141	*GSTA5*	NM_153699	ref|Homo sapiens glutathione S-transferase alpha 5 mRNA
8.11	-1.174	0	A_33_P3329974	*CGN*	NM_020770	ref|Homo sapiens cingulin mRNA
7.84	-1.170	0	A_23_P206359	*CDH1*	NM_004360	ref|Homo sapiens cadherin 1 type 1 E-cadherin (epithelial) mRNA
8.46	-1.168	1.00E-05	A_24_P131522	*ANTXR1*	NM_032208	ref|Homo sapiens anthrax toxin receptor 1 transcript variant 1 mRNA
11.11	-1.167	0	A_23_P76901	*PLEKHG3*	NM_015549	ref|Homo sapiens pleckstrin homology domain containing family G (with RhoGef domain) member 3 mRNA
8.46	-1.167	0	A_23_P391443	*PPM1H*	NM_020700	ref|Homo sapiens protein phosphatase Mg2+/Mn2+ dependent 1H mRNA
7.85	-1.166	0	A_23_P153964	*INHBB*	NM_002193	ref|Homo sapiens inhibin beta B mRNA
8.19	-1.157	2.00E-05	A_23_P206359	*CDH1*	NM_004360	ref|Homo sapiens cadherin 1 type 1 E-cadherin (epithelial) mRNA
11.40	-1.156	0	A_23_P383986	*CHST15*	NM_015892	ref|Homo sapiens carbohydrate (N-acetylgalactosamine 4-sulfate 6-O) sulfotransferase 15 transcript variant 1 mRNA
8.83	-1.152	2.00E-05	A_23_P19030	*ARSI*	NM_001012301	ref|Homo sapiens arylsulfatase family member I mRNA
8.19	-1.152	1.00E-05	A_23_P160336	*LEFTY1*	NM_020997	ref|Homo sapiens left-right determination factor 1 mRNA
9.60	-1.149	0	A_23_P200710	*PIK3C2B*	NM_002646	ref|Homo sapiens phosphoinositide-3-kinase class 2 beta polypeptide mRNA
9.09	-1.140	1.00E-05	A_23_P122216	*LOX*	NM_002317	ref|Homo sapiens lysyl oxidase transcript variant 1 mRNA
12.37	-1.139	4.00E-04	A_23_P19663	*CTGF*	NM_001901	ref|Homo sapiens connective tissue growth factor mRNA
7.78	-1.134	4.00E-05	A_23_P25396	*NR1H4*	NM_005123	ref|Homo sapiens nuclear receptor subfamily 1 group H member 4 transcript variant 3 mRNA
7.25	-1.123	0.00089	A_23_P218331	*CYB561*	NM_001017916	ref|Homo sapiens cytochrome b-561 transcript variant 2 mRNA
6.64	-1.123	0.00026	A_23_P15101	*TMC5*	NM_024780	ref|Homo sapiens transmembrane channel-like 5 transcript variant 3 mRNA
7.72	-1.118	1.00E-05	A_23_P206359	*CDH1*	NM_004360	ref|Homo sapiens cadherin 1 type 1 E-cadherin (epithelial) mRNA
8.11	-1.117	3.00E-05	A_23_P206359	*CDH1*	NM_004360	ref|Homo sapiens cadherin 1 type 1 E-cadherin (epithelial) mRNA
7.36	-1.115	2.00E-05	A_33_P3305288	*PAQR9*	NM_198504	ref|Homo sapiens progestin and adipoQ receptor family member IX mRNA
11.23	-1.108	0	A_33_P3304212	*PLEKHG3*	NM_015549	ref|Homo sapiens pleckstrin homology domain containing family G (with RhoGef domain) member 3 mRNA
8.18	-1.099	1.00E-05	A_23_P206359	*CDH1*	NM_004360	ref|Homo sapiens cadherin 1 type 1 E-cadherin (epithelial) mRNA
14.56	-1.086	5.00E-05	A_23_P330070	*TFPI*	NM_001032281	ref|Homo sapiens tissue factor pathway inhibitor (lipoprotein-associated coagulation inhibitor) transcript variant 2 mRNA
10.09	-1.076	0	A_23_P48997	*PSTPIP1*	NM_003978	ref|Homo sapiens proline-serine-threonine phosphatase interacting protein 1 mRNA

8.70	-1.075	9.00E-05	A_24_P261567	*GDPD5*	NM_030792	ref|Homo sapiens glycerophosphodiester phosphodiesterase domain containing 5 mRNA
8.22	-1.075	0	A_24_P383609	*NANOS1*	NM_199461	ref|Homo sapiens nanos homolog 1 (Drosophila) mRNA
7.06	-1.073	1.00E-05	A_23_P28224	*SCN1A*	NM_006920	ref|Homo sapiens sodium channel voltage-gated type I alpha subunit transcript variant 2 mRNA
6.13	-1.063	1.00E-05	A_33_P3394689	*SLC6A2*	NM_001172501	ref|Homo sapiens solute carrier family 6 (neurotransmitter transporter noradrenalin) member 2 transcript variant 2 mRNA
8.19	-1.055	1.00E-05	A_23_P206359	*CDH1*	NM_004360	ref|Homo sapiens cadherin 1 type 1 E-cadherin (epithelial) mRNA
8.04	-1.051	0	A_23_P372923	*FGFR1*	NM_001174066	ref|Homo sapiens fibroblast growth factor receptor 1 transcript variant 13 mRNA
6.28	-1.045	0.00011	A_33_P3610138	*LOC400568*	BC043554	gb|Homo sapiens cDNA clone IMAGE:5176687
9.74	-1.044	0	A_23_P30098	*ADH4*	NM_000670	ref|Homo sapiens alcohol dehydrogenase 4 (class II) pi polypeptide mRNA
12.18	-1.024	2.00E-05	A_23_P145644	*DDC*	NM_000790	ref|Homo sapiens dopa decarboxylase (aromatic L-amino acid decarboxylase) transcript variant 2 mRNA
7.70	-1.011	1.00E-05	A_24_P62505	*GLT25D2*	NM_015101	ref|Homo sapiens glycosyltransferase 25 domain containing 2 mRNA

Table 98. All significantly up regulated genes in hHeps after treatment with TCDD (10 nM) identified by microarray analysis - separate data processing. Selected parameters: A-value ≥ 5, log2 fc ≥ 1, p-value ≤ 0.05.

A	Log2 fc	p-value	Probe name	Gene name	Systematic name	Gene description
10.65	6.589	0	A_23_P209625	*CYP1B1*	NM_000104	ref|Homo sapiens cytochrome P450 family 1 subfamily B polypeptide 1 mRNA
10.63	5.368	0	A_23_P163402	*CYP1A1*	NM_000499	ref|Homo sapiens cytochrome P450 family 1 subfamily A polypeptide 1 mRNA
8.43	4.578	0	A_23_P165136	*LRRC25*	NM_145256	ref|Homo sapiens leucine rich repeat containing 25 mRNA
9.16	4.429	0	A_33_P3290343	*CYP1B1*	NM_000104	ref|Homo sapiens cytochrome P450 family 1 subfamily B polypeptide 1 mRNA
7.77	4.406	0	A_23_P207213	*ALDH3A1*	NM_000691	ref|Homo sapiens aldehyde dehydrogenase 3 family member A1 transcript variant 2 mRNA
9.37	4.197	0	A_33_P3238433	*ALDH3A1*	NM_001135168	ref|Homo sapiens aldehyde dehydrogenase 3 family member A1 transcript variant 1 mRNA
7.97	3.604	1.00E-05	A_33_P3480395	*FLJ30901*	AK055463	gb|Homo sapiens cDNA FLJ30901 fis clone FEBRA2005778
8.38	3.529	0	A_23_P26854	*ARHGAP44*	NM_014859	ref|Homo sapiens Rho GTPase activating protein 44 mRNA
9.71	3.259	0	A_33_P3397795	*C14orf135*	AK095489	gb|Homo sapiens cDNA FLJ38170 fis clone FCBBF1000024
7.57	3.172	0	A_32_P49867	*LOC100507055*	NM_001195520	ref|Homo sapiens hypothetical LOC100507055 mRNA
9.64	3.106	0	A_23_P416581	*GNAZ*	NM_002073	ref|Homo sapiens guanine nucleotide binding protein (G protein) alpha z polypeptide mRNA
9.09	2.948	0	A_24_P157370	*IL17RB*	NM_018725	ref|Homo sapiens interleukin 17 receptor B mRNA
11.94	2.710	0	A_33_P3222762	*HULC*	NR_004855	ref|Homo sapiens highly up-regulated in liver cancer (non-protein coding) non-coding RNA
13.05	2.626	0	A_33_P3253747	*CYP1A2*	NM_000761	ref|Homo sapiens cytochrome P450 family 1 subfamily A polypeptide 2 mRNA
6.31	2.518	1.00E-05	A_23_P379649	*BMF*	NM_001003940	ref|Homo sapiens Bcl2 modifying factor transcript variant 1 mRNA
8.35	2.343	2.00E-05	A_33_P3230990	*SCUBE1*	NM_173050	ref|Homo sapiens signal peptide CUB domain EGF-like 1 mRNA
6.38	2.324	5.00E-05	A_24_P48204	*SECTM1*	NM_003004	ref|Homo sapiens secreted and transmembrane 1 mRNA
10.44	2.311	0	A_23_P143845	*TIPARP*	NM_015508	ref|Homo sapiens TCDD-inducible poly(ADP-ribose) polymerase transcript variant 2 mRNA
10.93	2.291	0	A_23_P57910	*RTP3*	NM_031440	ref|Homo sapiens receptor (chemosensory) transporter protein 3 mRNA
7.24	2.276	0	A_33_P3734384	*LOC285957*	AK097526	gb|Homo sapiens cDNA FLJ40207 fis clone TESTI2020946
8.88	2.240	1.00E-05	A_23_P41804	*NKD2*	NM_033120	ref|Homo sapiens naked cuticle homolog 2 (Drosophila) mRNA
8.66	2.159	4.00E-05	A_23_P154806	*EPB41L1*	NM_012156	ref|Homo sapiens erythrocyte membrane protein band 4.1-like 1 transcript variant 1 mRNA
7.13	2.138	1.00E-05	A_24_P335620	*SLC7A5*	NM_003486	ref|Homo sapiens solute carrier family 7 (amino acid transporter light chain L system) member 5 mRNA
8.56	2.137	1.00E-05	A_23_P136355	*HHAT*	NM_018194	ref|Homo sapiens hedgehog acyltransferase transcript variant 1 mRNA
8.35	2.118	0	A_23_P257003	*PCSK5*	NM_006200	ref|Homo sapiens proprotein convertase subtilisin/kexin type 5 transcript variant 2 mRNA
6.79	2.078	3.00E-05	A_23_P17673	*DNMT3L*	NM_013369	ref|Homo sapiens DNA (cytosine-5-)-methyltransferase 3-like transcript variant 1 mRNA
9.94	2.009	1.00E-05	A_23_P75630	*APOA5*	NM_052968	ref|Homo sapiens apolipoprotein A-V transcript variant 1 mRNA
7.99	1.931	1.00E-05	A_23_P116942	*LAG3*	NM_002286	ref|Homo sapiens lymphocyte-activation gene 3 mRNA

6.00	1.883	1.00E-05	A_23_P416395	*STC2*	NM_003714	ref|Homo sapiens stanniocalcin 2 mRNA
5.75	1.861	2.00E-05	A_23_P79518	*IL1B*	NM_000576	ref|Homo sapiens interleukin 1 beta mRNA
13.46	1.843	0	A_23_P94159	*FBXO25*	NM_183421	ref|Homo sapiens F-box protein 25 transcript variant 1 mRNA
6.72	1.838	3.00E-05	A_23_P60990	*C2orf54*	NM_024861	ref|Homo sapiens chromosome 2 open reading frame 54 transcript variant 2 mRNA
9.53	1.830	3.00E-05	A_23_P24723	*TMEM138*	NM_016464	ref|Homo sapiens transmembrane protein 138 transcript variant 1 mRNA
7.47	1.717	0	A_23_P381489	*NCRNA00313*	NR_026863	ref|Homo sapiens non-protein coding RNA 313 non-coding RNA
7.67	1.704	0	A_33_P3841368	*LOC286161*	AK091672	gb|Homo sapiens cDNA FLJ34353 fis clone FEBRA2011665
8.01	1.651	4.00E-05	A_23_P259071	*AREG*	NM_001657	ref|Homo sapiens amphiregulin mRNA
11.35	1.643	0	A_23_P83110	*CDK5RAP2*	NM_018249	ref|Homo sapiens CDK5 regulatory subunit associated protein 2 transcript variant 1 mRNA
6.30	1.635	2.00E-05	A_23_P35529	*MBL2*	NM_000242	ref|Homo sapiens mannose-binding lectin (protein C) 2 soluble mRNA
6.09	1.584	5.00E-05	A_33_P3415240	*LOC730091*	NR_038387	ref|Homo sapiens hypothetical LOC730091 non-coding RNA
9.47	1.569	0	A_23_P403335	*EXPH5*	NM_015065	ref|Homo sapiens exophilin 5 mRNA
10.36	1.481	1.00E-05	A_33_P3341676	*MEF2A*	NM_001171894	ref|Homo sapiens myocyte enhancer factor 2A transcript variant 5 mRNA
11.11	1.453	0	A_33_P3282394	*MLLT1*	NM_005934	ref|Homo sapiens myeloid/lymphoid or mixed-lineage leukemia (trithorax homolog Drosophila); translocated to 1 mRNA
12.04	1.444	0	A_33_P3336622	*ALDH3A2*	NM_001031806	ref|Homo sapiens aldehyde dehydrogenase 3 family member A2 transcript variant 1 mRNA
8.76	1.435	0	A_33_P3214849	*KDELC2*	NM_153705	ref|Homo sapiens KDEL (Lys-Asp-Glu-Leu) containing 2 mRNA
10.42	1.400	0	A_23_P139704	*DUSP6*	NM_001946	ref|Homo sapiens dual specificity phosphatase 6 transcript variant 1 mRNA
8.16	1.392	7.00E-05	A_23_P103110	*MAFF*	NM_012323	ref|Homo sapiens v-maf musculoaponeurotic fibrosarcoma oncogene homolog F (avian) transcript variant 1 mRNA
6.94	1.378	1.00E-05	A_23_P161563	*RAB38*	NM_022337	ref|Homo sapiens RAB38 member RAS oncogene family mRNA
15.21	1.375	0	A_23_P16523	*GDF15*	NM_004864	ref|Homo sapiens growth differentiation factor 15 mRNA
11.96	1.371	3.00E-05	A_23_P112531	*FAM102A*	NM_001035254	ref|Homo sapiens family with sequence similarity 102 member A transcript variant 1 mRNA
9.67	1.364	1.00E-05	A_23_P354387	*MYOF*	NM_013451	ref|Homo sapiens myoferlin transcript variant 1 mRNA
11.92	1.363	4.00E-05	A_23_P112531	*FAM102A*	NM_001035254	ref|Homo sapiens family with sequence similarity 102 member A transcript variant 1 mRNA
11.84	1.351	5.00E-05	A_23_P112531	*FAM102A*	NM_001035254	ref|Homo sapiens family with sequence similarity 102 member A transcript variant 1 mRNA
12.02	1.351	4.00E-05	A_23_P112531	*FAM102A*	NM_001035254	ref|Homo sapiens family with sequence similarity 102 member A transcript variant 1 mRNA
12.13	1.347	4.00E-05	A_23_P112531	*FAM102A*	NM_001035254	ref|Homo sapiens family with sequence similarity 102 member A transcript variant 1 mRNA
12.20	1.341	2.00E-05	A_23_P112531	*FAM102A*	NM_001035254	ref|Homo sapiens family with sequence similarity 102 member A transcript variant 1 mRNA
12.04	1.340	3.00E-05	A_23_P112531	*FAM102A*	NM_001035254	ref|Homo sapiens family with sequence similarity 102 member A transcript variant 1 mRNA
11.95	1.340	4.00E-05	A_23_P112531	*FAM102A*	NM_001035254	ref|Homo sapiens family with sequence similarity 102 member A transcript variant 1 mRNA
8.21	1.337	1.00E-05	A_33_P3226650	*GSTA7P*	NR_033760	ref|Homo sapiens glutathione S-transferase alpha 7 pseudogene non-coding RNA
8.65	1.309	4.00E-05	A_23_P66881	*RGS9*	NM_003835	ref|Homo sapiens regulator of G-protein signaling 9 transcript variant 1 mRNA

12.11	1.306	5.00E-05	A_23_P112531	*FAM102A*	NM_001035254	ref|Homo sapiens family with sequence similarity 102 member A transcript variant 1 mRNA
12.63	1.301	2.00E-05	A_23_P58036	*MCCC1*	NM_020166	ref|Homo sapiens methylcrotonoyl-CoA carboxylase 1 (alpha) nuclear gene encoding mitochondrial protein mRNA
13.03	1.291	4.00E-05	A_33_P3357530	*SLC12A7*	NM_006598	ref|Homo sapiens solute carrier family 12 (potassium/chloride transporters) member 7 mRNA
6.92	1.277	2.00E-05	A_23_P102950	*RSPH1*	NM_080860	ref|Homo sapiens radial spoke head 1 homolog (Chlamydomonas) mRNA
8.98	1.268	3.00E-05	A_32_P205637	*PARD6B*	NM_032521	ref|Homo sapiens par-6 partitioning defective 6 homolog beta (C. elegans) mRNA
6.95	1.268	5.00E-05	A_23_P102950	*RSPH1*	NM_080860	ref|Homo sapiens radial spoke head 1 homolog (Chlamydomonas) mRNA
9.33	1.262	0	A_23_P313389	*UGCG*	NM_003358	ref|Homo sapiens UDP-glucose ceramide glucosyltransferase mRNA
13.35	1.256	1.00E-05	A_23_P118065	*HSD17B2*	NM_002153	ref|Homo sapiens hydroxysteroid (17-beta) dehydrogenase 2 mRNA
12.80	1.253	0	A_33_P3336617	*ALDH3A2*	NM_000382	ref|Homo sapiens aldehyde dehydrogenase 3 family member A2 transcript variant 2 mRNA
8.40	1.251	0	A_23_P123402	*TRIM55*	NM_184086	ref|Homo sapiens tripartite motif containing 55 transcript variant 3 mRNA
13.45	1.244	3.00E-05	A_23_P118065	*HSD17B2*	NM_002153	ref|Homo sapiens hydroxysteroid (17-beta) dehydrogenase 2 mRNA
13.79	1.244	2.00E-05	A_23_P118065	*HSD17B2*	NM_002153	ref|Homo sapiens hydroxysteroid (17-beta) dehydrogenase 2 mRNA
13.80	1.236	1.00E-05	A_23_P118065	*HSD17B2*	NM_002153	ref|Homo sapiens hydroxysteroid (17-beta) dehydrogenase 2 mRNA
13.86	1.235	1.00E-05	A_23_P118065	*HSD17B2*	NM_002153	ref|Homo sapiens hydroxysteroid (17-beta) dehydrogenase 2 mRNA
13.90	1.233	2.00E-05	A_23_P118065	*HSD17B2*	NM_002153	ref|Homo sapiens hydroxysteroid (17-beta) dehydrogenase 2 mRNA
13.57	1.232	4.00E-05	A_23_P118065	*HSD17B2*	NM_002153	ref|Homo sapiens hydroxysteroid (17-beta) dehydrogenase 2 mRNA
14.11	1.230	2.00E-05	A_23_P118065	*HSD17B2*	NM_002153	ref|Homo sapiens hydroxysteroid (17-beta) dehydrogenase 2 mRNA
11.29	1.226	5.00E-05	A_23_P94921	*SLC20A2*	NM_006749	ref|Homo sapiens solute carrier family 20 (phosphate transporter) member 2 mRNA
14.04	1.222	2.00E-05	A_23_P118065	*HSD17B2*	NM_002153	ref|Homo sapiens hydroxysteroid (17-beta) dehydrogenase 2 mRNA
13.38	1.222	2.00E-05	A_23_P118065	*HSD17B2*	NM_002153	ref|Homo sapiens hydroxysteroid (17-beta) dehydrogenase 2 mRNA
9.08	1.218	1.00E-05	A_24_P294124	*SERTAD2*	NM_014755	ref|Homo sapiens SERTA domain containing 2 mRNA
8.19	1.216	1.00E-05	A_23_P123402	*TRIM55*	NM_184086	ref|Homo sapiens tripartite motif containing 55 transcript variant 3 mRNA
8.18	1.201	2.00E-05	A_23_P123402	*TRIM55*	NM_184086	ref|Homo sapiens tripartite motif containing 55 transcript variant 3 mRNA
10.32	1.197	5.00E-05	A_33_P3334443	*FAM69A*	NM_001006605	ref|Homo sapiens family with sequence similarity 69 member A mRNA
7.06	1.196	3.00E-05	A_33_P3419190	*AREG*	NM_001657	ref|Homo sapiens amphiregulin mRNA
14.15	1.168	1.00E-05	A_23_P60599	*UGT1A6*	NM_001072	ref|Homo sapiens UDP glucuronosyltransferase 1 family polypeptide A6 transcript variant 1 mRNA
7.36	1.154	1.00E-05	A_23_P102950	*RSPH1*	NM_080860	ref|Homo sapiens radial spoke head 1 homolog (Chlamydomonas) mRNA
9.98	1.149	5.00E-05	A_23_P210708	*SIRPA*	NM_001040022	ref|Homo sapiens signal-regulatory protein alpha transcript variant 1 mRNA
11.86	1.139	4.00E-05	A_33_P3217983	*ACSL5*	NM_203380	ref|Homo sapiens acyl-CoA synthetase long-chain family member 5 transcript variant 3 mRNA
8.20	1.124	2.00E-05	A_23_P123402	*TRIM55*	NM_184086	ref|Homo sapiens tripartite motif containing 55 transcript variant 3 mRNA
8.20	1.116	1.00E-05	A_23_P123402	*TRIM55*	NM_184086	ref|Homo sapiens tripartite motif containing 55 transcript variant 3 mRNA
8.39	1.102	3.00E-05	A_23_P123402	*TRIM55*	NM_184086	ref|Homo sapiens tripartite motif containing 55 transcript variant 3 mRNA

12.95	1.100	0	A_23_P423197	*RXRA*	NM_002957	ref|Homo sapiens retinoid X receptor alpha mRNA
8.46	1.097	7.00E-05	A_24_P154037	*IRS2*	NM_003749	ref|Homo sapiens insulin receptor substrate 2 mRNA
9.61	1.097	2.00E-05	A_23_P128215	*SOCS2*	NM_003877	ref|Homo sapiens suppressor of cytokine signaling 2 mRNA
10.20	1.095	5.00E-05	A_33_P3389728	*NR5A2*	NM_205860	ref|Homo sapiens nuclear receptor subfamily 5 group A member 2 transcript variant 1 mRNA
7.23	1.069	3.00E-05	A_24_P583040	*C17orf67*	ENST00000397861	ens|chromosome 17 open reading frame 67 [Source:HGNC Symbol;Acc:27900]
10.25	1.015	8.00E-05	A_24_P141707	*INHBE*	NM_031479	ref|Homo sapiens inhibin beta E mRNA
9.52	1.012	1.00E-05	A_33_P3311371	*PDLIM2*	NM_198042	ref|Homo sapiens PDZ and LIM domain 2 (mystique) transcript variant 3 mRNA
8.23	1.010	5.00E-05	A_23_P123402	*TRIM55*	NM_184086	ref|Homo sapiens tripartite motif containing 55 transcript variant 3 mRNA

Table 99. All significantly down regulated genes in hHeps after treatment with TCDD (10 nM) identified by microarray analysis - separate data processing. Selected parameters: A-value ≥ 5, log2 fc ≤ -1, p-value ≤ 0.05.

A	Log2 fc	p-value	Probe name	Gene name	Systematic name	Gene description
8.52	-1.488	4.00E-05	A_23_P94782	*CAPN8*	NM_001143962	ref|Homo sapiens calpain 8 mRNA
6.92	-1.304	9.00E-05	A_33_P3278362	*ANKRD2*	NM_020349	ref|Homo sapiens ankyrin repeat domain 2 (stretch responsive muscle) transcript variant 1 mRNA
6.23	-1.261	1.00E-05	A_23_P215720	*CFTR*	NM_000492	ref|Homo sapiens cystic fibrosis transmembrane conductance regulator (ATP-binding cassette sub-family C member 7) mRNA
9.82	-1.223	1.00E-05	A_24_P405705	*SLC2A2*	NM_000340	ref|Homo sapiens solute carrier family 2 (facilitated glucose transporter) member 2 mRNA
10.71	-1.156	7.00E-05	A_23_P333029	*C8orf47*	NM_173549	ref|Homo sapiens chromosome 8 open reading frame 47 transcript variant 1 mRNA
12.64	-1.062	3.00E-05	A_23_P331670	*PYGB*	NM_002862	ref|Homo sapiens phosphorylase glycogen; brain mRNA
9.17	-1.038	3.00E-05	A_23_P55251	*ITGA3*	NM_002204	ref|Homo sapiens integrin alpha 3 (antigen CD49C alpha 3 subunit of VLA-3 receptor) transcript variant a mRNA
8.11	-1.034	1.00E-05	A_23_P122937	*ELMO1*	NM_014800	ref|Homo sapiens engulfment and cell motility 1 transcript variant 1 mRNA

IX.2 Curriculum Vitae

Christiane Lohr

Food Chemist

Academic Track Record

04/2009 - 10/2013	**University Kaiserslautern, Germany** Department of Chemistry PhD in Food Chemistry and Toxicology Supervisor: Prof. Dr. Dr. D. Schrenk Doctoral thesis: 'Effects of Polychlorinated Dibenzo-*p*-Dioxins, Polychlorinated Dibenzofurans, and Polychlorinated Biphenyls in Human Liver Cell Models (*in vitro*) and in Mice (*in vivo*)'

Education and Qualification

10/2004 - 03/2009	**University Kaiserslautern, Germany** Study of Food Chemistry Diploma Degree in Food Chemistry
10/2008 - 03/2009	**University Kaiserslautern, Germany** Institute of Food Chemistry and Toxicology Diploma thesis: 'Untersuchungen zur Mutagenität an ausgewählten Furocumarinen'
01/2008 - 04/2008	**University Kaiserslautern, Germany** Institute of Food Chemistry and Toxicology Research internship: 'Etablierung einer geeigneten Extraktionsmethode zur Bestimmung von Furocumarinen in Limetten & deren Zubereitungen'
08/1995 - 06/2004	**Gymnasium am Stadtgarten Saarlouis, Germany** University Entrance Qualification

Professional Experience and Advanced Training

11/2006 - 08/2008	**University Kaiserslautern, Germany** Department of Mechanical and Process Engineering Institute of Bioprocess Engineering Research assistant in Biotechnology
10/2009 - today	**German Society of Toxicology in DGPT (Deutsche Gesellschaft für Experimentelle und Klinische Pharmakologie und Toxikologie)** Advanced courses of Toxicology **Completed courses:** Food Toxicology Molecular Cell Toxicology

	Organ Toxicology and Pathology I + II Laboratory Animal Science I / Biostatistics Laboratory Animal Science II Clinical Toxicology Xenobiotic Metabolism / Toxicokinetics Immunotoxicology

Additional Skills

Language	German: native speaker English: fluent (spoken and written) Spanish: basic knowledge French: basic knowledge
Computer	Microsoft Office (Word, Excel, PowerPoint, Outlook) Origin, ChemDraw, GraphPad Instat, Adobe Photoshop, GIMP

Kaiserslautern, 25th of October 2013

IX.3 Poster Presentations and Publications

Poster Presentations

Lohr C., Gorgus E., Raquet N., Guth S., Schrenk D. (2009). Limettin und Furocumarine in citrus-haltigen Getränken. 38. Deutscher Lebensmittelchemiker Tag, Berlin.

Neser S., Lohr C., van Ede K. I., van Duursen M. B. M., van den Berg M., Andersson P. L., Schrenk D. (2011). Induction of CYP1A activity in *in vitro* models as a basis for derivation of systemic TEFs. Dioxin 2011, Brussels.

Lohr C., Neser S., Andresen K., Andersson P. L., Schrenk D. (2012). Untersuchung des Einflusses von TCDD und PCB 153 in humanen Zellsystemen mit Hilfe von Gesamtgenom-Microarrays. Arbeitstagung des Regionalverbandes Südwest der Lebensmittelchemischen Gesellschaft in der Gesellschaft Deutscher Chemiker, Kaiserslautern.

Lohr C., Neser S., Andresen K., Andersson P. L., Schrenk D. (2012). Whole genome microarray analysis of the effects of TCDD and PCB 153 in human hepatic cell models. 78. Jahrestagung der Deutschen Gesellschaft für Experimentelle und Klinische Pharmakologie und Toxikologie e. V., Dresden.

Neser S., Lohr C., Andresen K., van Ede K. I., van Duursen M. B. M., van den Berg M., Andersson P. L., Schrenk D. (2012). Gene regulating effects in mouse liver subsequent to treatment with selected dioxin-like compounds and PCB 153 using whole genome microarray analysis. 78. Jahrestagung der Deutschen Gesellschaft für Experimentelle und Klinische Pharmakologie und Toxikologie e. V., Dresden.

Publications

Gorgus E., Lohr C., Raquet N., Guth S., Schrenk D. (2010). Limettin and furocoumarins in beverages containing citrus juices or extracts. *Food and Chemical Toxicology*, 48(1):93-98.

Lohr C., Raquet N., Schrenk D. (2010). Application of the concept of relative photomutagenic potencies to selected furocoumarins in V79 cells. *Toxicology in Vitro*, 24(2):558-566.

Messer A., Nieborowski A., Strasser C., Lohr C., Schrenk D. (2011). Major furocoumarins in grapefruit juice I: Levels and urinary metabolite(s). *Food and Chemical Toxicology*, 49(12):3224-3231.

Messer A., Raquet N., Lohr C., Schrenk D. (2012). Major furocoumarins in grapefruit juice II: Phototoxicity, photogenotoxicity, and inhibitory potency vs. cytochrome P450 3A4 activity. *Food and Chemical Toxicology*, 50(3-4):756-760.

IX.4 Eidesstattliche Erklärung

Hiermit erkläre ich an Eides statt, dass ich die eingereichte Dissertation eigenständig verfaßt, die für die Arbeit benutzten Hilfsmittel und Quellen genannt und die Ergebnisse beteiligter Mitarbeiter sowie anderer Autoren klar gekennzeichnet habe. Ich habe weder die Dissertation oder Teile der Disseration als Prüfungsarbeit bei einem anderen Fachbereich eingereicht noch ein Promotionsverfahren bei einer anderen Hochschule beantragt.

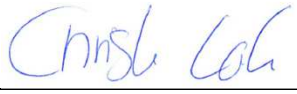

Kaiserslautern, 25. Oktober 2013 Christiane Lohr